TENDON STEM CELLS FROM BASIC BIOLOGY TO CLINICAL APPLICATION

EDITED BY: Zi Yin, Hongwei Ouyang, Gang Li and Ming Hao Zheng

PUBLISHED IN: Frontiers in Cell and Developmental Biology

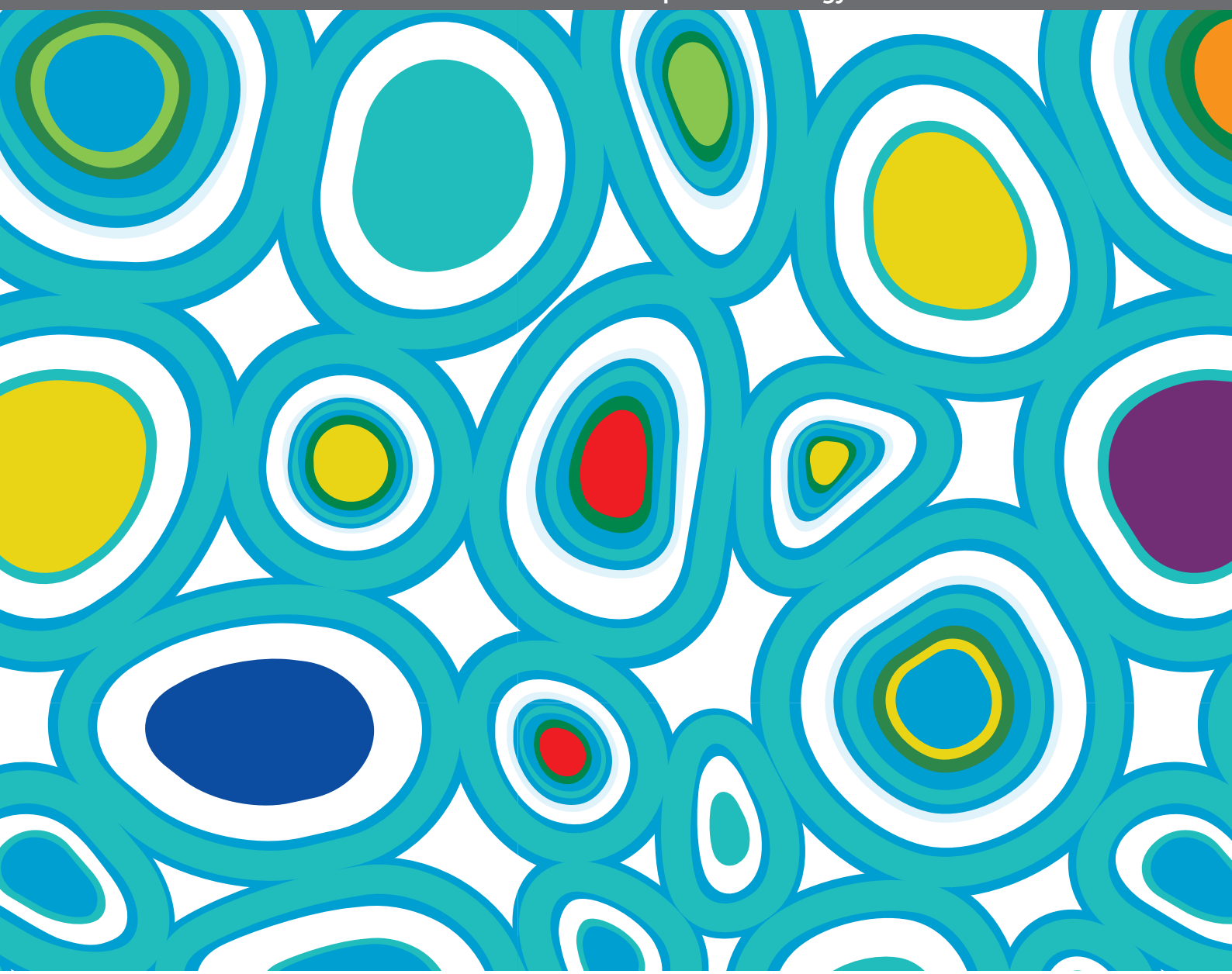

frontiers Research Topics

frontiers

ISSN 1664-8714
ISBN 978-2-83250-117-7
DOI 10.3389/978-2-83250-117-7

About Frontiers

Frontiers is more than just an open-access publisher of scholarly articles: it is a pioneering approach to the world of academia, radically improving the way scholarly research is managed. The grand vision of Frontiers is a world where all people have an equal opportunity to seek, share and generate knowledge. Frontiers provides immediate and permanent online open access to all its publications, but this alone is not enough to realize our grand goals.

Frontiers Journal Series

The Frontiers Journal Series is a multi-tier and interdisciplinary set of open-access, online journals, promising a paradigm shift from the current review, selection and dissemination processes in academic publishing. All Frontiers journals are driven by researchers for researchers; therefore, they constitute a service to the scholarly community. At the same time, the Frontiers Journal Series operates on a revolutionary invention, the tiered publishing system, initially addressing specific communities of scholars, and gradually climbing up to broader public understanding, thus serving the interests of the lay society, too.

Dedication to Quality

Each Frontiers article is a landmark of the highest quality, thanks to genuinely collaborative interactions between authors and review editors, who include some of the world's best academicians. Research must be certified by peers before entering a stream of knowledge that may eventually reach the public - and shape society; therefore, Frontiers only applies the most rigorous and unbiased reviews.
Frontiers revolutionizes research publishing by freely delivering the most outstanding research, evaluated with no bias from both the academic and social point of view. By applying the most advanced information technologies, Frontiers is catapulting scholarly publishing into a new generation.

What are Frontiers Research Topics?

Frontiers Research Topics are very popular trademarks of the Frontiers Journals Series: they are collections of at least ten articles, all centered on a particular subject. With their unique mix of varied contributions from Original Research to Review Articles, Frontiers Research Topics unify the most influential researchers, the latest key findings and historical advances in a hot research area! Find out more on how to host your own Frontiers Research Topic or contribute to one as an author by contacting the Frontiers Editorial Office: frontiersin.org/about/contact

TENDON STEM CELLS FROM BASIC BIOLOGY TO CLINICAL APPLICATION

Topic Editors:
Zi Yin, Zhejiang University, China
Hongwei Ouyang, Zhejiang University, China
Gang Li, The Chinese University of Hong Kong, China
Ming Hao Zheng, University of Western Australia, Australia

Citation: Yin, Z., Ouyang, H., Li, G., Zheng, M. H., eds. (2022). Tendon Stem Cells from Basic Biology to Clinical Application. Lausanne: Frontiers Media SA. doi: 10.3389/978-2-83250-117-7

Table of Contents

frontiers in Cell and Developmental Biology

ORIGINAL RESEARCH
published: 25 September 2020
doi: 10.3389/fcell.2020.570605

Higher BMP Expression in Tendon Stem/Progenitor Cells Contributes to the Increased Heterotopic Ossification in Achilles Tendon With Aging

*Guangchun Dai[1,2,3,4], Yingjuan Li[5], Junyan Liu[1,2,3,4], Cheng Zhang[1,2,3,4], Minhao Chen[1,2,3,4], Panpan Lu[1,2,3,4] and Yunfeng Rui[1,3,4,6]**

[1] Department of Orthopaedics, Zhongda Hospital, School of Medicine, Southeast University, Nanjing, China, [2] School of Medicine, Southeast University, Nanjing, China, [3] Orthopaedic Trauma Institute (OTI), Southeast University, Nanjing, China, [4] Trauma Center, Zhongda Hospital, Southeast University, Nanjing, China, [5] Department of Geriatrics, Zhongda Hospital, School of Medicine, Southeast University, Nanjing, China, [6] China Orthopedic Regenerative Medicine Group, Hangzhou, China

OPEN ACCESS

Edited by:
Hongwei Ouyang,
Zhejiang University, China

Reviewed by:
Jangho Kim,
Chonnam National University, South Korea
Johannes F. W. Greiner,
Bielefeld University, Germany

***Correspondence:**
Yunfeng Rui
ruiyunfeng@126.com

Specialty section:
This article was submitted to Stem Cell Research, a section of the journal Frontiers in Cell and Developmental Biology

Received: 08 June 2020
Accepted: 04 September 2020
Published: 25 September 2020

Citation:
Dai G, Li Y, Liu J, Zhang C, Chen M, Lu P and Rui Y (2020) Higher BMP Expression in Tendon Stem/Progenitor Cells Contributes to the Increased Heterotopic Ossification in Achilles Tendon With Aging. Front. Cell Dev. Biol. 8:570605. doi: 10.3389/fcell.2020.570605

Although the mineralization in tendon tissue has been reported in a series of aging and disease models, the underlying mechanisms remain unknown. This study aimed to describe the appearance of heterotopic ossification in rat Achilles tendon and further verify whether this tissue metaplasia is related to the enhanced osteogenic differentiation of tendon stem/progenitor cells (TSPCs) owing to the higher expression of bone morphogenetic proteins (BMP-2/4/7) with aging. The male SD rats, aged 4, 8, and 20 months (M), were used. The analyses of ossification and BMP expression in tendon were tested by radiological view (X-ray and CT), histological staining [hematoxylin and eosin (HE), Alcian blue, and Alizarin red], immunohistochemistry, and Western blot. The osteogenic differentiation potential and BMP expression of TSPCs were examined by Alizarin red S staining and real-time PCR. TSPCs were treated with BMP-2 or noggin, and the osteogenic differentiation potential was also examined. X-ray and CT showed the appearance of heterotopic ossification in tendon, and the volume and density of ossification was increased with aging. Histological staining showed the appearance of calcified region surrounded by chondrocyte-like cells and the increased osteogenesis-related gene and BMP expression in ossified tendon with aging. Moreover, the osteogenic differentiation potential and BMP expression in TSPCs isolated from ossified tendon were increased with aging. Additionally, BMP-2 increased the calcium nodule formation and osteogenesis-related gene expression in TSPCs. The addition of noggin inhibited BMP-induced enhancement of osteogenic differentiation. Thus, these findings suggested that the enhanced osteogenic differentiation of TSPCs contributes to the increased heterotopic ossification in aged tendon, which might be induced by the higher expression of BMPs with aging.

Keywords: aging, Achilles tendon, heterotopic ossification, tendon stem/progenitor cells, bone morphogenetic protein, osteogenic differentiation

INTRODUCTION

In our ever-aging population, a deep understanding of our musculoskeletal unit is of utmost importance. Age-related tendon disorders are one of the main causes for chronic pain, limited joint mobility, and tendon rapture among elderly patients. Heterotopic ossification has been reported in series models of injury and disease and plays an important role in uncommon conditions of tendon, including pathogenesis alterations (Rui et al., 2012b, 2013; Mao et al., 2019; Geng et al., 2020), which makes it as a vital target of tendon research. Moreover, a previous study has demonstrated that age-related tendon disorders is closely associated with the appearance of heterotopic ossification in tendon (Agabalyan et al., 2013). However, the underlying molecular mechanisms remain unclear and treatments are usually symptomatic.

Traditionally, tenocytes were considered the only cell present in tendon and played a critical role in tendon metabolism, repair, and regeneration. This hypothesis did not change until the isolation and identification of TSPCs in tendons, including mouse (Bi et al., 2007), human (Bi et al., 2007), rat (Rui et al., 2010), rabbit (Zhang and Wang, 2010), and fetal bovine (Yang et al., 2016). Although TSPCs represent a minor percentage of tendon cell compositions, these cells possess stem cell features such as self-renewal, clonogenicity, and multi-differentiation (Rui et al., 2010). After that, there was a substantial progress in the study of roles of TSPCs in tendon metabolism, repair, and regeneration. Compared with TSPCs isolated from healthy tendon, the proliferation of TSPCs isolated from collagenase-induced (CI) tendon injury model was significantly decreased, and the osteo-chondrogenic differentiation potential was increased, which might result in pathological ossification formation and failed tendon healing (Rui et al., 2013). Rui et al. (2011a) proposed that erroneous differentiation potential of TSPCs contributes to pathological alterations in calcified tendinopathy, which was consistent with the view of another study (Zhang X. et al., 2016). These findings supported the important role of altered TSPCs fate in pathological changes of chronic tendinopathy. During the aging process, TSPCs experienced an evident decrease in self-renewal and colony-forming ability and altered multi-differentiation capacity (Tan et al., 2012; Ruzzini et al., 2014; Dai et al., 2019; Li et al., 2019). TSPCs tended to differentiate into osteoblasts with over-passaging, which was a common cell senescence model *in vitro* (Tan et al., 2012). Ruzzini et al. (2014) indicated that aged TSPCs expressed higher levels of chondrogenic-related gene expression. Although there is no definite conclusion of these variations, the potential roles of altered TSPC differentiation capacity for age-related pathological changes in tendon were speculated (Dai et al., 2019; Li et al., 2019).

Ectopic expression of BMP-2/4/7 was detected in both clinical samples of tendinopathy (Rui et al., 2012b) and animal tendon injury model (Rui et al., 2013). The ectopic expression of BMPs was reported to facilitate non-tenogenic differentiation capacity of mesenchymal stem cells (MSCs) *in vitro*, including TSPCs (Lui, 2013; Zhang et al., 2019). BMPs might contribute to altered TSPCs' fate through enhancing osteogenic differentiation and impairing tenogenic differentiation ability (Rui et al., 2012a; Lui and Wong, 2013). Moreover, ectopic expression of BMPs was also detected in subacromial bursa of patients with chronic degeneration of rotator cuff, which might induce the occurrence of ectopic bone/cartilage and accelerate structural degeneration of rotator cuff (Neuwirth et al., 2006). Taken together, these factors stimulated the current study to further describe the appearance and trend of heterotopic ossification in aged tendon and verify that this tissue metaplasia is related to the enhanced osteogenic differentiation potential of TSPCs, which is induced by the higher expression of BMPs. Moreover, BMPs might be an ideal therapeutic target for prevention or inhibition of heterotopic ossification formation in tendon age-related disorders.

MATERIALS AND METHODS

Isolation and Culture of TSPCs

Animal experiments were approved by the Institutional Animal Care and Use Committee (IACUC) of the Southeast University School of Medicine. The procedures for TSPC isolation have been well established (Rui et al., 2010, 2011b). Briefly, the middle substance of Achilles tendon tissues per group was minced and digested with type I collagenase (3 mg/ml, Sigma-Aldrich, United States), and the cells were cultured in complete medium, which is low-glucose Dulbecco's modified Eagle's medium (LG-DMEM, Gibco, United States) containing 10% FBS, 100 U/ml penicillin, 100 mg/ml streptomycin, and 2 mM l-glutamine (Invitrogen, United States). TSPCs at passage 3 (P3) to P5 were used for all experiments. All experiments were repeated at least three times.

Radiological Evaluation

Radiological evaluation was performed as previously described (Qiao et al., 2020). The analysis of heterotopic calcification was assessed by X-ray radiography and CT (computed tomography) scanning in 4M (young), 8M (middle-aged), and 20M (aged) male SD rats, and the aging model mainly refers to previous studies (Xing et al., 2016; Rui et al., 2019). Thirty-six rats were euthanized with CO_2. X-ray radiography was performed with a Faxitron MX-20 X-ray machine at a voltage of 30 kV (Faxitron Bioptics, Wheeling, IL, United States). CT scans were acquired using a SkyScan 1176 radiograph microtomograph (BrukermicroCT, Kontich, Belgium) with an exposure time of 340 ms and a rotation step of 0.6°, a voltage of 65 kV, and a current of 385 μA. Reconstruction was performed with the NReconV.1.6.9.4 software using GPU acceleration. The ring artifact correction was fixed at 6, the smoothing was set at 1, the smoothing kernel was set at 2, and the beam hardening correction was set at 35%. After reconstruction, SkyScan CTAn (version: 1.13.8.1) was used for segmentation, registration, and quantification of all reconstructed images.

General Histology and Immunohistochemistry Staining

The sections of Achilles tendons were washed in PBS, fixed in buffered formalin and 100% ethanol, embedded in paraffin, cut longitudinally to 5-mm thick sections, and mounted on 3-aminopropyl-triethoxy-silane (Sigma-Aldrich, United States)-coated slides. After deparaffinization, the sections were stained with H&E, Alcian blue, and Alizarin red staining, according to standard techniques. Briefly, the sections were reacted with Harris hematoxylin for 5 min and eosin for 3 min in H&E staining; the sections were reacted for 12 min in Alcian blue (pH 2.5) and for 8 min in Alizarin red staining solution (G1027 and G1038; Servicebio, China); the calcified region was stained light blue by Alcian blue, while the mineralization was stained red by Alizarin red. Images were captured using a digital camera and Q-Capture Pro software (ver. 6.0 Media Cybernetics, Bethesda, United States). Immunohistochemistry staining was performed as previously described (Rui et al., 2012b), and primary antibodies against BMP-2, OPN and OCN (Proteintech, China), and Runx2 (Abcam, United States) were used. Goat anti-rabbit (Chemicon, Temecula, CA, United States) or goat anti-mouse horseradish peroxidase (HRP)-conjugated secondary antibodies (Millipore, Billerica, MA, United States), together with 3,30 diaminobenzidine tetrahydrochloride (DAKO, Glostrup, Denmark), were used for signal detection. The sections from different age points were stained in the same batch and examined under light and polarized microscopies (DMRXA2 and DMRB, Leica Microsystems Wetzlar GmbH, Germany). The assessors were blinded to the grouping of the samples.

Western Blot Assay

Western blot was performed to examine BMP-2/4/7 protein expression as previously described (Zhang J. et al., 2016). Achilles tendon from different age points was collected and protein was obtained from them. The protein was separated by 12% SDS-PAGE, transferred to PVDF membranes, and subsequently blocked in 5% fat-free milk for 2 h, followed by incubation with primary antibodies at 4°C overnight. All primary antibodies were from Bioworld Technology, Inc. Secondary antibody (Proteintech, China) conjugated with HRP was then applied. Finally, protein bands were detected with chemiluminescence (Beyotime, China). The protein expression levels assessed in this study was normalized to β -actin.

Osteogenic Differentiation Assay

The multi-differentiation methods of TSPCs were elaborated in previous studies (Rui et al., 2010; Shi et al., 2019). TSPCs (P3) isolated from ossified tendon were seeded at 4×10^3cells/cm^2 in 12-well plates and cultured in complete medium until confluence. Afterward, they were cultured in complete basal or osteogenic induction medium (OIM), which was complete basal medium supplemented with 1 nM dexamethasone, 50 mM ascorbic acid, and 20 mM β-glycerolphosphate (Sigma-Aldrich, United States) for 21 days to assess mRNA expression of Runx2, OPN, OCN, BMP2, BMP-4, and BMP-7 by qRT-PCR and calcium nodule formation by Alizarin red S staining.

Treatment of TSPCs With BMP-2 or Noggin

TSPCs isolated from ossified tendon aged 4M (abbreviated as Y-TSPC) and 8M and 20M (abbreviated as A-TSPC) were seeded at 4×10^3 cells/cm^2 in 12-well plates and cultured in complete medium until confluence. They were then cultured in OIM with or without recombinant human BMP-2 (rhBMP-2) (100 ng/ml; Solarbio, United States) (Rui et al., 2012a)/Noggin (0.25 μg/ml; Novoprotein, China) (Cho et al., 2005) for 7 days to assess mRNA expression of Runx2, OPN, and OCN by qRT-PCR and calcium nodule formation by Alizarin red S staining.

Quantitative Real-Time PCR (qRT-PCR) Assay

TSPCs were seeded at 4×10^3 cells/cm^2 in six-well plates and cultured in complete medium or OIM until the desired time. Then, TSPCs were harvested and homogenized for RNA extraction with the Rneasy mini kit (Qiagen GmbH, Hilden, Germany). The mRNA was reverse transcribed to cDNA by the First-Strand cDNA kit (Promega, Madison, WI, United States). One microliter of total cDNA of each sample was amplified in the final volume of 20 μl of reaction mixture containing Power SYBR Green PCR Master Mix (Invitrogen Corporation, Carlsbad, CA, United States) and specific primers for target gene using the ABI StepOne Plus system (Applied Biosystems, CA, United States) (**Supplementary Table S1**). Cycling conditions were denaturation at 95°C for 10 min, 45 cycles at 95°C for 20 s, optimal annealing temperature (**Supplementary Table S1**) for 20 s, 72°C for 30 s, and finally at 60–95°C with a heating rate of 0.1°C/s. β-actin was used as an endogenous control. The data were calculated using the $2^{-\Delta\Delta CT}$ formula.

DATA ANALYSIS

All data were presented as mean ± SD. Statistical analysis of the data was performed with SPSS (SPSS Inc, Chicago, IL, United States; version 22.0) using one-way ANOVA or unpaired Student's *t*-test. $P < 0.05$ was regarded as statistically significant.

RESULTS

Radiological Evaluation of Heterotopic Ossification in Achilles Tendon

X-ray showed the formation of heterotopic ossification, which was presented by visible radiopaque area in tendon (red arrows), and the visible radiopaque area was increased in size with aging (**Figures 1A–C**). CT sagittal view (**Figures 1D–F**), CT axial view (**Figures 1G–I**), and CT three-dimensional view (**Figures 1J–L**) also observed the visible radiopaque area (red arrows). Moreover, we calculated the volume and density of heterotopic ossification, and there was an increased trend in the volume (**Figure 1M**) and

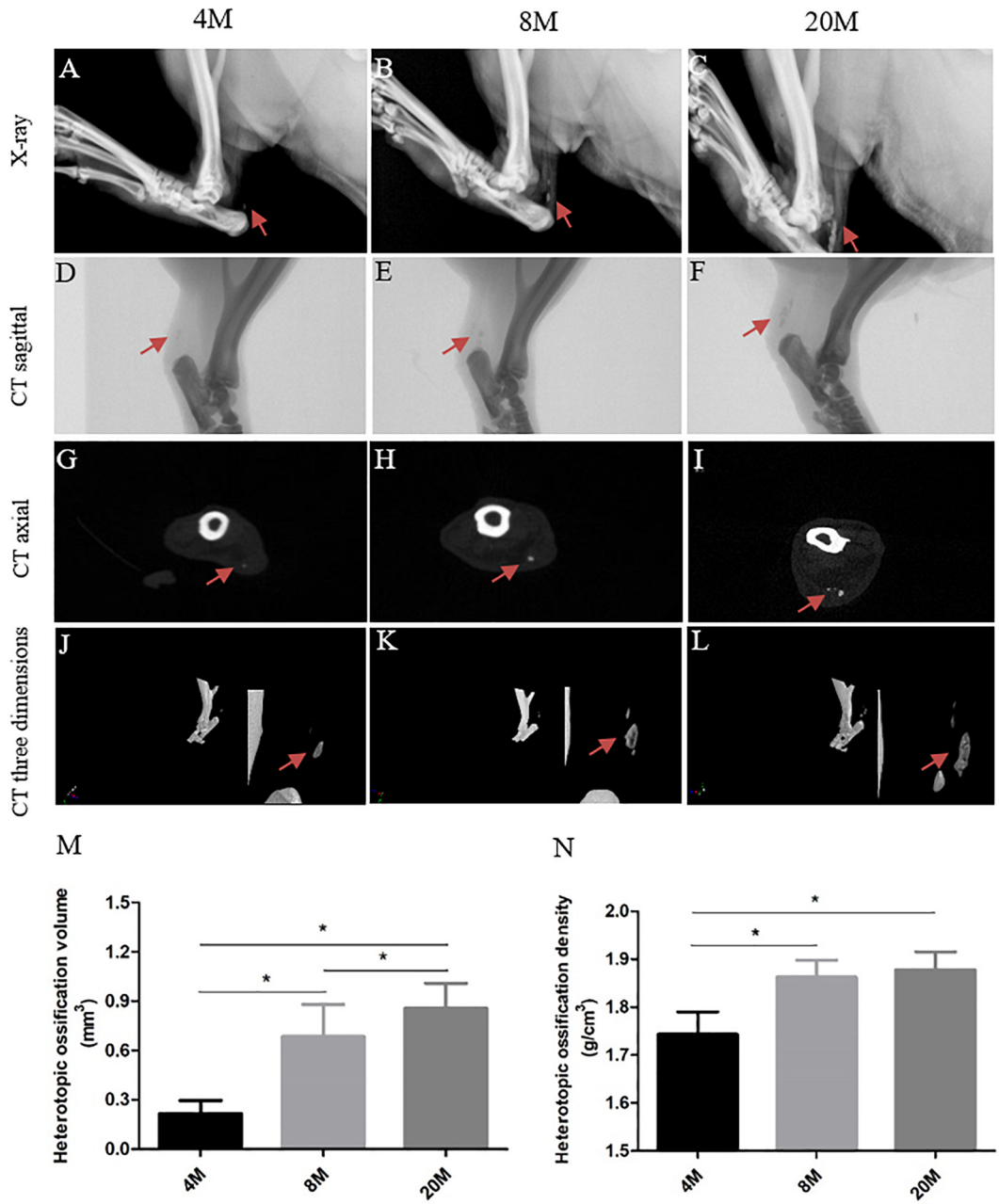

FIGURE 1 | Imaging evaluation of heterotopic ossification. Imaging evaluation of heterotopic ossification in rat Achilles tendon aged 4, 8, and 20 M. **(A–C)** Representative X-ray figures from rats aged 4, 8, and 20 M. The visible radiopaque area presents the heterotopic ossification formation in tendon, and red arrows show the ossification region. Representative CT sagittal view **(D–F)**, CT axial view **(G–I)**, and CT three-dimensional view **(J–L)** figures from rats aged 4, 8, and 20M. Statistical diagrams show the increased trend with age in the volume **(M)** and density **(N)** of heterotopic ossification. $^{*}P < 0.05$.

density with aging (**Figure 1N**), but not from the density between group aged 8M and group aged 20M.

Characterize Histological Alterations in Ossified Tendon With Aging

Next, we performed histology staining to characterize alterations in ossified tendon with aging. It was observed that tendon appeared to have degenerative changes with water content of tissue gradually decreasing, structure becoming tight, and color tending to slight yellow on gross observation (**Figures 2A–C**) during the natural aging process. H&E staining displayed degenerative characteristics, including the appearance of spontaneous ectopic calcified region (CR) surrounded by chondrocyte-like phenotype cells (black arrows) (**Figures 2I–K**), a decrease of crimp morphology, a decrease in cell number per

mm^2 (**Figures 2D–G**), and a more flattened cell nuclei shape (**Figures 2D–F,H**) with aging. Alcian blue (**Figures 2L–N**) and Alizarin red staining (**Figures 2O–Q**) showed the appearance of spontaneous ossification region, the accumulation of cartilaginous matrix by Alcian blue staining and calcium nodules formation by Alizarin red staining, and the ossification region stained by Alcian blue and Alizarin red was increased in size with aging.

The Osteogenesis-Related Genes Expression in Ossified Tendon Was Increased With Aging

Additionally, immunohistochemistry staining of Runx2, OPN, and OCN was to evaluate osteogenesis-related gene expression levels in ossified tendon with aging. At the age of 4M, weak expression of Runx2 was observed in the rounded tendon cells (black arrowhead) and calcific region matrix, while the expression of Runx2 surrounding the calcific matrix was very weak to undetectable throughout the tendon (**Figures 3A,A1**). Weak expression of OPN (**Figures 3E,E1**) and OCN (**Figures 3I,I1**) was also observed mainly in the rounded tendon cells (black arrowhead) and the calcific region matrix of tendon from the group aged 4M. At the age of 8M, there was moderate expression of Runx2 in the rounded tendon cells (black arrowhead), chondrocyte-like cells (black arrow), and calcific region, and the expression of Runx2 in the tendon cells and their surrounding matrix around the calcific region was weak (**Figures 3B,B1**). Increased expression of OPN (**Figures 3F,F1**) and OCN (**Figures 3J,J1**) was also observed mainly in the rounded tendon cells (black arrowhead), chondrocyte-like cells (black arrow), and calcific region matrix of tendon from the group aged 8M, and the expression of OPN and OCN in the tendon cells and their surrounding matrix around the calcific region was weak. At the age of 20M, there was intense expression of Runx2 (**Figures 3C,C1**), OPN (**Figures 3G,G1**), and OCN (**Figures 3K,K1**) in the rounded tendon cells (black arrowhead), chondrocyte-like cells (black arrow), and calcific region matrix, and the expression of these genes in the tendon cells and their surrounding matrix was moderate throughout the tendon. As shown in **Figures 3D,H,L**, semi-quantitative results showed that the expression levels of Runx2, OPN, and OCN were significantly increased with aging, but not from the OPN and OCN expression between the group aged 4M and the group aged 8M. Overall, the expression level of osteogenesis-related genes was increased with aging.

The Protein Expression of BMP-2/4/7 in Ossified Tendon Was Increased With Aging

Western blot assay showed the protein expression of BMP-2/4/7 in ossified tendon was increased with aging (**Figure 4A**). Quantitative analysis of the intensity showed that there was an increased trend of BMP-2/4/7 protein expression in ossified tendon with aging, but not from the BMP-4/7 expression between group aged 8M and group aged 20M (**Figures 4B–D**). Moreover, the BMP-2 expression was also detected by immunohistochemical staining. At the age of 4M, weak expression of BMP-2 was detected in the rounded tendon cells (black arrowhead) and calcific region matrix, while the expression of BMP-2 surrounding calcific matrix was very weak to undetectable (**Figures 4E,E1**). At the age of 8M, there was a moderate expression of BMP-2 in the rounded tendon cells (black arrowhead), chondrocyte-like cells (black arrow), and calcific region, and the expression of BMP-2 in tendon cells and their surrounding matrix around the calcific region was weak (**Figures 4F,F1**). At month 20, there was intense expression of BMP-2 in the rounded tendon cells (black arrowhead), chondrocyte-like cells (black arrow), and calcific region matrix, and the expression of BMP-2 in tendon cells and their surrounding matrix was moderate throughout the tendon (**Figures 4G,G1**). Semi-quantitative result of the intensity showed that the expression of BMP-2 was increased with aging (**Figure 4H**).

The Osteogenic Differentiation Potential of TSPCs Was Increased With Aging

At day 21, more alizarin red S (ARS)-positive calcium nodules were found in TSPCs cultured in OIM (**Figures 5H–M**) than basal medium (**Figures 5A–G**). Moreover, an increased trend of ARS-positive calcium of TSPCs with aging was observed in OIM (**Figures 5H–M**), and a slight increase of ARS-positive calcium of TSPCs with aging was observed in basal medium (**Figures 5A–G**). The quantification analysis showed that the TSPCs exhibited a significantly higher signal intensity of the calcium-bound ARS in induction medium than that in basal medium, and there was a significant increased trend with aging in induction medium (**Figure 5D**). In basal medium, there was an increased trend of signal intensity of the calcium-bound ARS between the group aged 4M and the group aged 20M (**Figure 5D**).

Moreover, the mRNA expression levels of Runx2, OPN, and OCN of TSPCs were remarkably upregulated after osteogenic induction compared with those in basal medium, but not the Runx2 expression of group aged 4M (**Figures 5N–P**). In OIM, the mRNA expression of Runx2, OPN, and OCN was significantly increased with aging apart from OPN expression between the group aged 4M and the group aged 8M (**Figures 5N–P**). At day 0, the expression of Runx2 was increased between the group aged 4M and the group aged 8M and between the group aged 4M and the group aged 20M, and the mRNA expression of OPN and OCN between the group aged 4M and the group aged 20M was also increased. Overall, these results showed that the osteogenic differentiation potential of TSPCs isolated from ossified tendon was upregulated with aging *in vitro*.

The BMP-2/4/7 Expression of TSPCs Was Increased With Aging

At day 0, there was a weak mRNA expression of BMP-2 in TSPCs aged 4M, and an increased trend of BMP-2 expression with aging was observed (**Figure 6A**). The mRNA expression of BMP-2 was significantly upregulated after osteogenic induction compared with that in basal medium, and the expression of BMP-2 was increased with aging (**Figure 6A**). At day 0, there

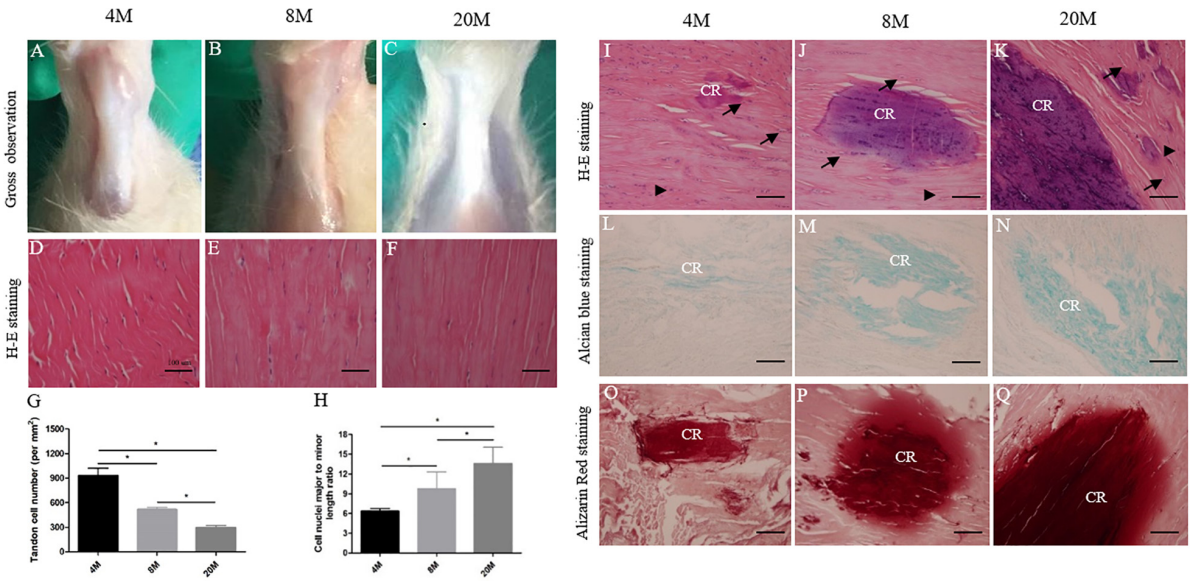

FIGURE 2 | Histological alterations in ossified tendon with aging. Histology analysis. **(A–C)** Gross observation of Achilles tendon from rats aged 4, 8, and 20 M. **(D–F)** Representative H&E images of Achilles tendon from rats aged 4, 8, and 20 M mainly focused on tendon cells' morphological appearance. Statistical diagrams show a decrease in cell number per mm^2 **(G)** and a more flattened cell nuclei shape **(H)** in aged Achilles tendon. Representative H&E **(I–K)**, Alcian blue **(L–N)**, and Alizarin red **(O–Q)** staining images of ossified tendon from rats aged 4, 8, and 20 M; the heterotopic ossification was observed and the ossified area size was increased with age. Arrowhead: rounded tendon cells; arrow: chondrocyte-like cells; CR, calcified region. Scale bar = 100 μm. $^*P < 0.05$.

was an increased mRNA expression level of BMP-4 between the group aged 4M and the group aged 20M (**Figure 6B**). Upon the influence of induction medium, the mRNA expression of BMP-4 was upregulated compared with that in basal medium, and the expression of BMP-4 was increased with aging but not between the group aged 8M and the group aged 20M (**Figure 6B**). Meanwhile, the mRNA expression of BMP-7 was increased with aging but not between the group aged 8M and the group aged 20M at day 0 (**Figure 6C**). Upon the influence of induction medium, the mRNA expression of BMP-7 was significantly upregulated compared with that in basal medium but not in the group aged 20M, and the mRNA expression of BMP-7 was increased with aging but not between the group aged 8M and the group aged 20M (**Figure 6C**). Overall, the mRNA expression of BMP-2/4/7 of TSPCs isolated from ossified tendon was increased with aging *in vitro*.

BMP-2 Stimulates the Osteogenic Differentiation Potential of Y-TSPCs

To explore the effect of BMP-2 on the osteogenic differentiation of Y-TSPCs isolated from ossified tendon aged 4M, TSPCs were treated with BMP-2 or noggin (a BMP signaling inhibitor which binds to BMPs). At day 7, stimulation with BMP-2 increased the ARS-positive calcium nodules of TSPCs (**Figures 7B,F**) compared with that in the control group (**Figures 7A,E**), and the calcium-bound ARS signal intensity in the BMP-2-treated group was significantly higher than that in the control group (**Figure 7D**). Moreover, the mRNA expression of osteogenesis-related genes in TSPCs, including Runx2, OPN, and OCN, was significantly higher than those in the control group after treatment with BMP-2 at day 7 (**Figures 7H–J**). Stimulation with BMP-2 plus noggin reduced the ARS-positive calcium nodules (**Figures 7C,G**), calcium-bound ARS signal intensity (**Figure 7D**), and the expression of Runx2, OPN, and OCN (**Figures 7H–J**) in TSPCs compared with those in the BMP-2-treated group. Overall, BMP-2 stimulates the osteogenic differentiation potential of TSPCs *in vitro*, and the addition of noggin inhibited BMP-2-induced potentiation of osteogenic differentiation.

Noggin Inhibits the Osteogenic Differentiation Potential of A-TSPCs

Then, noggin was used to inhibit the BMPs in A-TSPCs isolated from ossified tendon aged 8M and 20M. At day 7, Alizarin red S (ARS)-positive calcium nodules were found in TSPCs cultured in OIM (**Figures 8A,G**; **B,H**; and **D,J**), and stimulation with noggin reduced the ARS-positive calcium nodules of TSPCs aged 8M and 20M (**Figures 8C,I** and **8E,K**) compared with that in the control group (**Figures 8B,H** and **8D,J**), respectively, and the calcium-bound ARS signal intensity in the noggin-treated group was significantly lower than that in the control group (**Figure 8F**). Moreover, the mRNA expression of Runx2, OPN, and OCN in TSPCs was significantly lower than those in the control group after treatment with noggin at day 7 (**Figures 8L–N**), respectively. Overall, noggin inhibits the osteogenic differentiation potential of TSPCs aged 8M and 20M.

DISCUSSION

Our study firstly showed the appearance of heterotopic ossification in SD rat Achilles tendon and the increased trend

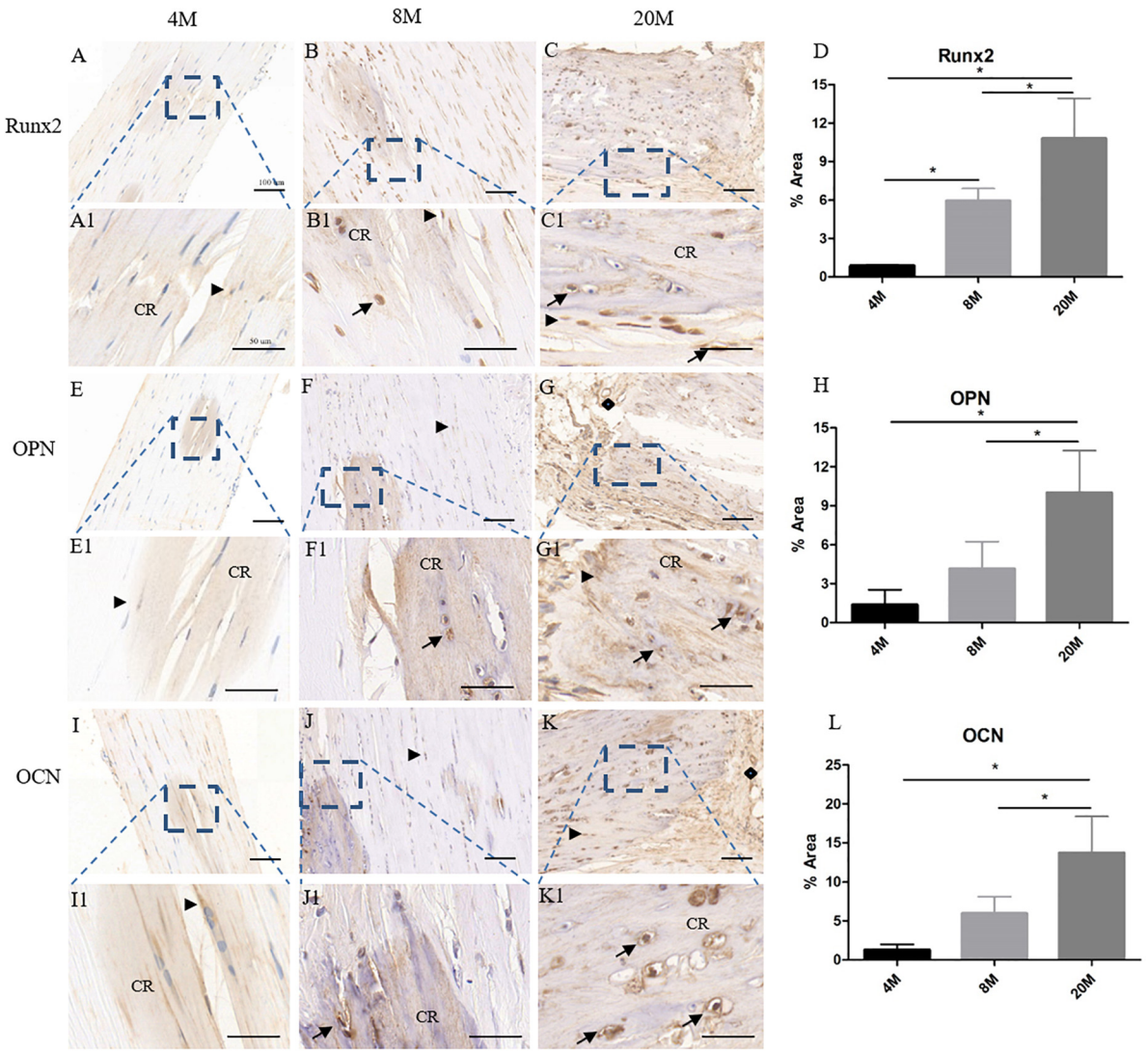

FIGURE 3 | The osteogenesis-related genes expression in ossified tendon was increased with aging. Immunohistochemistry (IHC) staining of osteogenesis-related gene markers in ossified tendon aged 4, 8, and 20 M. IHC staining results revealed higher expression level of Runx2 **(A–C,A1–C1)**, OPN **(E–G,E1–G1)**, and OCN **(I–K,I1–K1)** in aged tendon. An increased trend with age of Runx2 **(D)**, OPN **(H)**, and OCN **(L)** expression was observed in ossified tendon by semi-quantitative IHC assays. Arrowhead: rounded tendon cells; arrow: chondrocyte-like cells; CR, calcified region; rhombus: blood vessels. Scale bar = 100 μm **(A–C,E–G,I–K)**; Scale bar = 50 μm **(A1–C1,E1–G1,I1–K1)**. *$P < 0.05$.

of volume and density of ossification with aging. Moreover, the enhanced osteogenic differentiation potential of TSPCs isolated from ossified tendon might contribute to the heterotopic ossification, which is due to the higher expression of BMPs in TSPCs with aging.

Heterotopic ossification in tendon is a common clinical disease, often associated with tendon injury or surgery, or as a special manifestation of tendinopathy, and caused chronic pain and tendon rupture (Vaishya et al., 2019). In this study, we observed the appearance of heterotopic ossification in SD rat Achilles tendon, and the trend of volume and density of ossification was increased with aging. Heterotopic ossification of spinal ligament began in Tiptoe-walking mice at the age of 8 weeks, and the ossified area was increased with age (Liu et al., 2017). As shown in previous studies, heterotopic ossification is detrimental to normal healing of tendons and usually brings poor healing quality (Yee Lui et al., 2011; Rui et al., 2012b) and even accelerate other tissue aging progress (Pignolo et al., 2019). The healing ability of tendon tissues was decreased with aging (Tang et al., 2014; Dai et al., 2019), and heterotopic ossification is an important negative factor for tendon healing quality (Fang et al., 2014), indicating the occurrence of heterotopic ossification, and its increased trend in this study might cause the healing quality of aged tendon to weaken. Fang et al. (2014) showed that the choice of fetal fibroblasts as seed of tendon injury repair is better for the use of adult fibroblasts because of the decreased

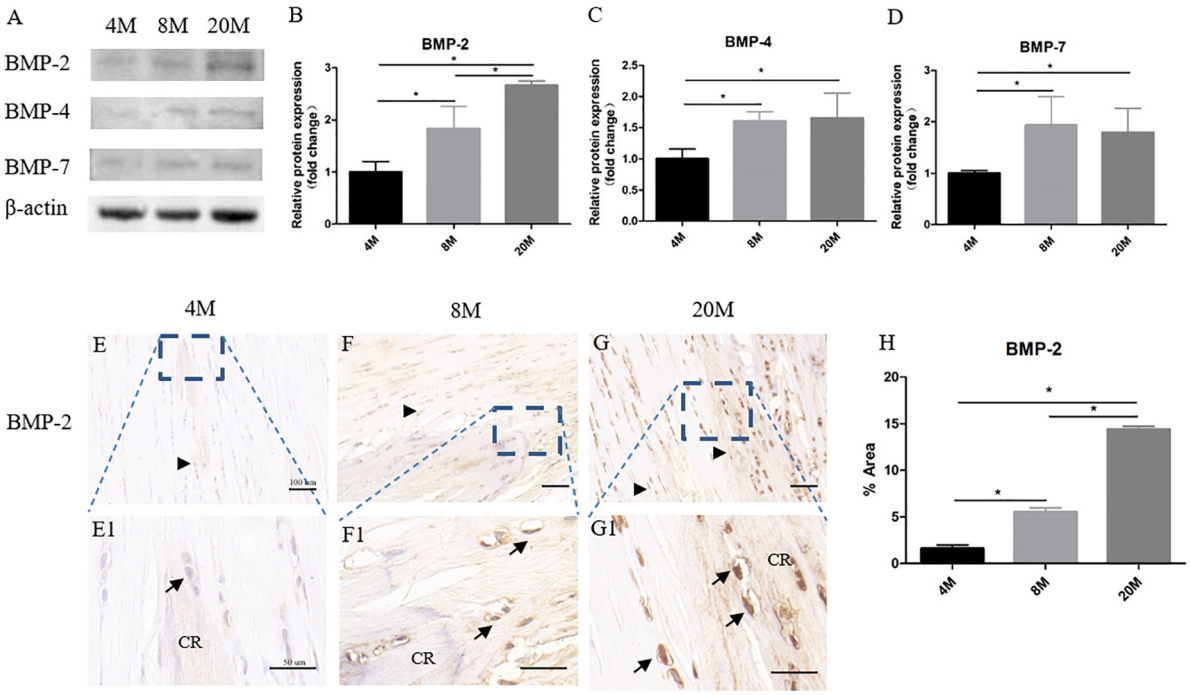

FIGURE 4 | The protein expression of BMP-2/4/7 in ossified tendon was increased with aging. The protein expression of BMP-2/4/7 in ossified tendon aged 4, 8, and 20 M. **(A)** The protein of BMP-2/4/7 was detected by Western blotting. The semi-quantitative results revealed the protein expression levels of BMP-2 **(B)**, BMP-4 **(C)**, and BMP-7 **(D)** were increased with age. **(E–G,E1–G1)** IHC staining of BMP-2 in ossified tendon. The semi-quantitative results showed that the expression level of BMP-2 was increased with age **(H)**. CR, calcified region; arrowhead: rounded tendon cells; arrow: chondrocyte-like cells. Scale bar = 100 μm **(E–G)**; Scale bar = 50 μm **(E1–G1)**. *$P < 0.05$.

formation of heterotopic ossification, which always undermines tendon regeneration efficacy; meanwhile, the healing quality is improved. Thus, this study further demonstrates the hypothesis that heterotopic ossification and its increased tendency are harmful to the tendon healing process. Heterotopic ossification is normally thought as an important reason for the increased tendon stiffness and the risk of tendon rupture (Wood et al., 2011). According to the results of this study, the formation of heterotopic ossification is highest in the group aged 20M, and it should have the highest rate of tendon rupture. However, some clinical etiology observation reported that the middle-aged group has the highest incidence of tendon rupture, and the injury rate may also be related to the higher force placed on tendon (Kubo et al., 2007a,b). Thus, comprehensive factors may lead to the occurrence of tendon injury, and the different roles of these factors need to be further studied.

Currently, scholars have studied the causes for heterotopic calcification in tendon but have not formed a convincing theory (Agabalyan et al., 2013). Compared with embryonic avian tendon, heterotopic ossification within adult tendon seems to be the result of an endochondral process driven by its cells (Agabalyan et al., 2013). Previous studies showed that the non-tenogenic differentiation potential of TSPCs might result in the formation of heterotopic calcification in chronic tendon disease or following tendon injury (Agabalyan et al., 2013; Rui et al., 2013; Fang et al., 2014; Shi et al., 2019). In addition, Dai et al. (2019) and Li et al. (2019) proposed an intimate relationship between tendon aging and TSPC senescence, and the altered TSPC differentiation fate might play an essential role in the pathological changes of aged tendon. Based on these factors, we thus assess the altered trend of TSPC osteogenic differentiation potential with aging. In this study, the osteogenic differentiation potential of TSPCs was increased with aging, which is consistent with the increased trend of heterotopic ossification in aged tendon. A study showed that the osteogenic differentiation capacity of fetal fibroblasts was lower than that in adult fibroblasts, which result in less spontaneous ectopic ossification during tendon repair process (Fang et al., 2014). Meanwhile, spinal-ligament heterotopic ossification began in Tiptoe-walking mice aged 8 weeks, and the ossified area was increased with age, Alizarin red S assay also showed a higher osteogenic potential of MSCs isolated from Tiptoe-walking mice compared with that in wild-type mice (Liu et al., 2017). These findings further demonstrated that the higher osteogenic differentiation potential of stem cell might be responsible for the formation of tissue heterotopic ossification. Moreover, the abnormal differentiation potential of stem cells resident in other tissues was also considered to be causes for tissue ectopic calcification, such as vascular (Speer et al., 2009) and skeleton (Lounev et al., 2009). Taken together, it is reasonable that the increased osteogenic differentiation capacity of TSPCs might play an important role in the process of heterotopic ossification formation in tendon with aging.

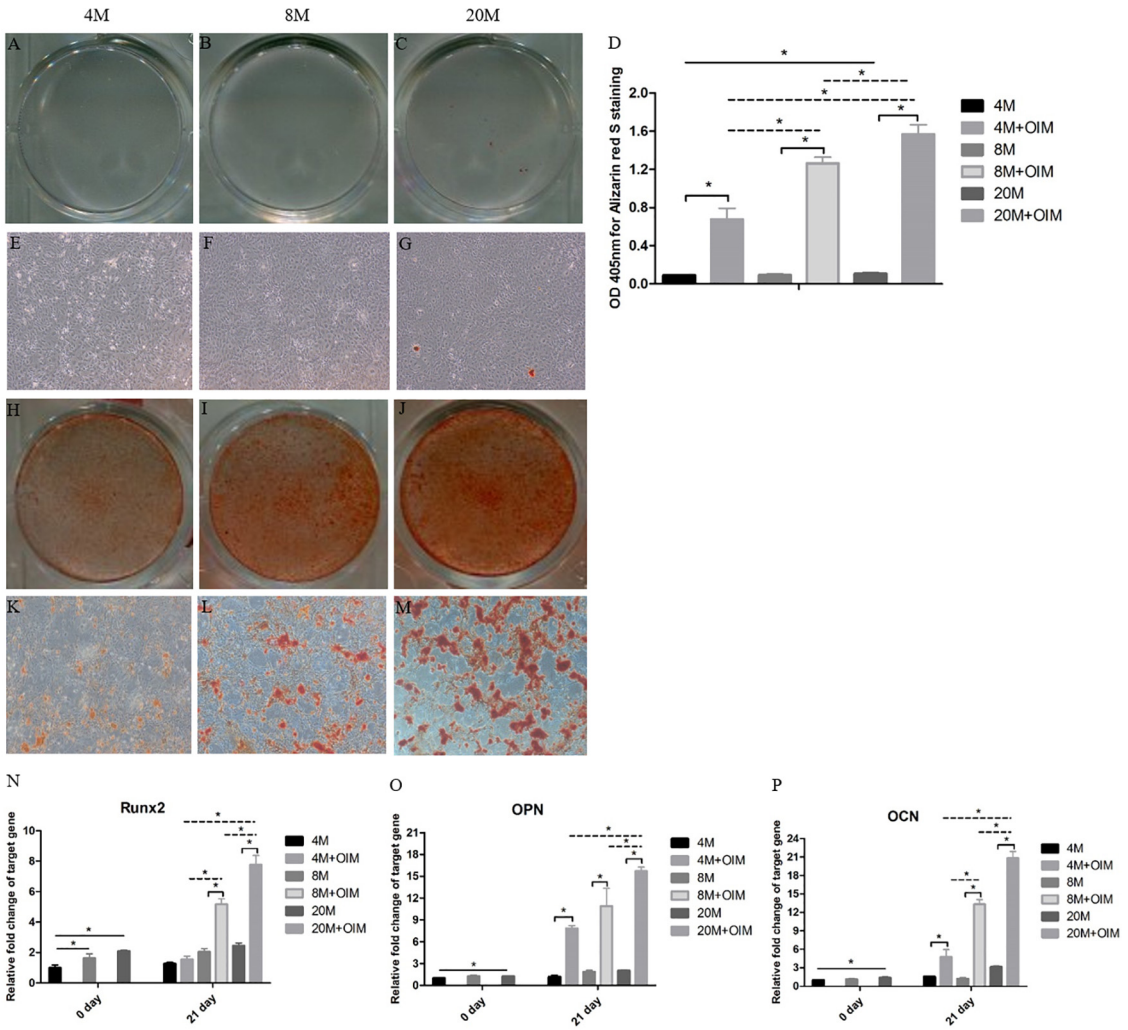

FIGURE 5 | The osteogenic differentiation potential of TSPCs was increased with aging. The osteogenic differentiation potential of TSPCs isolated from ossified tendon aged 4, 8, and 20 M. Obvious calcium deposition was seen in osteogenic induction medium **(H–M)**, but not in basic medium **(A–C,E–G)**. **(D)** Statistical diagrams show the quantization of bound Alizarin red S in TSPCs. **(J)** Statistical diagram shows the expression levels of osteogenesis-related genes measured by qRT-PCR, including Runx2 **(N)**, OPN **(O)**, and OCN **(P)**. Magnification × 1 **(A–C,H–J)** and × 40 **(E–G,K–M)**. $*P < 0.05$.

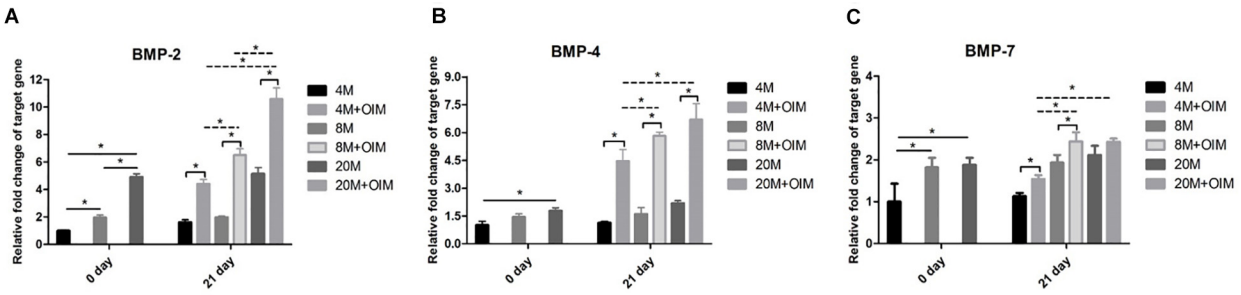

FIGURE 6 | The BMP-2/4/7 expression of TSPCs was increased with aging. The BMP-2/4/7 expression of TSPCs isolated from ossified tendon aged 4, 8, and 20 M. Statistical diagrams show the expression of target genes measured by qRT-PCR, including BMP-2 **(A)**, BMP-4 **(B)**, and BMP-7 **(C)**. $*P < 0.05$.

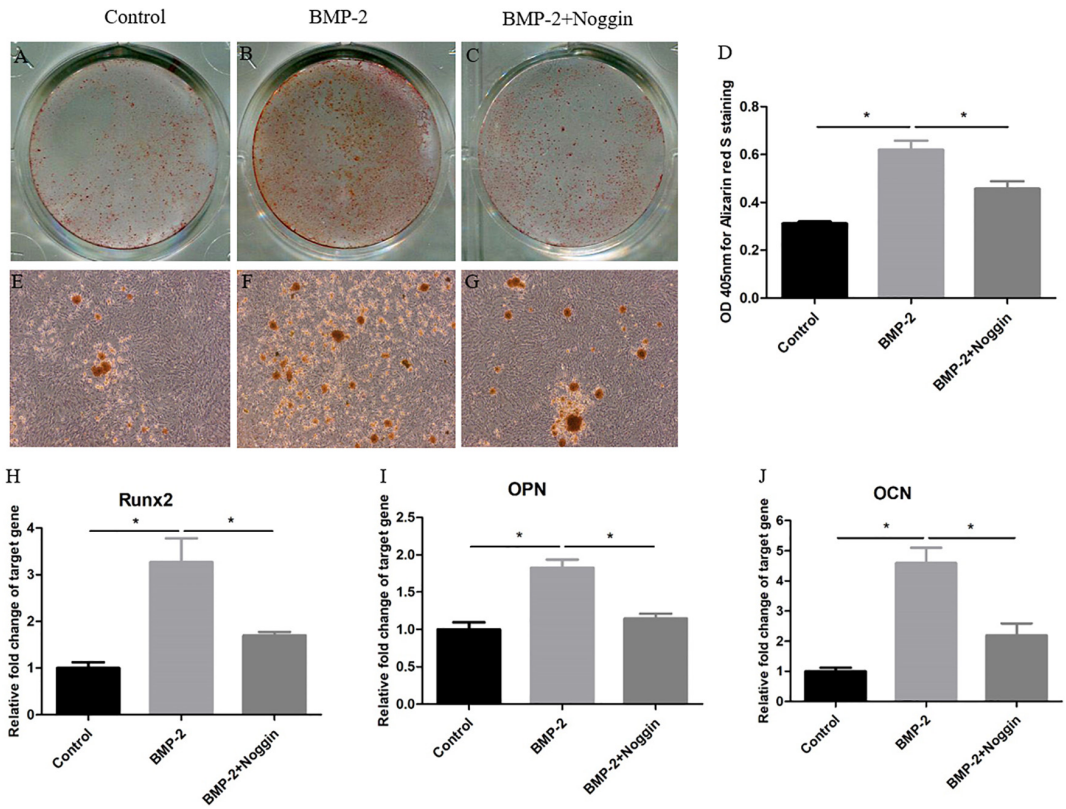

FIGURE 7 | BMP-2 stimulates the osteogenic differentiation of Y-TSPCs. Effect of BMP-2 on the osteogenic differentiation of Y-TSPCs isolated from ossified tendon aged 4M. Graphs show that BMP-2 stimulates osteogenic differentiation tendency of TSPCs **(A,B,E,F)** and noggin inhibited BMP-2-induced potentiation of osteogenic differentiation **(B,C,F,G)** at day 7 as indicated by Alizarin red S staining. Statistical diagrams show the quantification of the amount of Alizarin red S bound to the calcified deposits in TSPCs with BMP-2 or noggin stimulation at day 7 **(D)**. Statistical diagrams show the mRNA expression of Runx2 **(H)**, OPN **(I)**, and OCN **(J)** in TSPCs upon treatment with BMP-2 or noggin in vitro. Magnification × 1 **(A–C)** and ×40 **(E–G)**. $^*P < 0.05$.

The cytokines of BMP family, especially BMP-2/4/7, have been thought of as closely associated with tissue ectopic ossification formation and stem cell osteogenic differentiation potential. In the CI failed tendon healing animal model, chondrocyte phenotype and ossified region were observed (Lui et al., 2009), and the ectopic expression of BMP-2/4/7 was also observed around and in the chondrocyte-like cells and ossified region (Yee Lui et al., 2011), indicating the vital role of BMPs in the appearance of ectopic ossification, which was further corroborated by similar results observed in clinical specimens of tendinopathy (Rui et al., 2012b). In this study, the expression of BMP-2/4/7 in SD rat Achilles tendon was increased with aging, especially BMP-2, and its expression was consistent with the increased trend of heterotopic ossification and osteogenesis-related genes expression in tissue. Moreover, higher BMP-2 expression was observed around and in chondrocyte-like cells and ossified deposits, indicating that BMP-2 might account for the appearance of ectopic ossification in the overall process. BMP-2 was also responsible for the occurrence of ectopic ossification in the posterior longitudinal ligament (Harada et al., 2014), peripheral nerves (Olmsted-Davis et al., 2017), and rotator cuff (Neuwirth et al., 2006). In addition, stronger expression of BMP-2 and weaker expression of BMP-4/7 were observed in and around the chondrocyte-like cells and ossified region in ossified tendinopathy (Rui et al., 2012b), suggesting the possibility of BMP-2 playing a more vital role in this process. These results further confirmed the important role of BMP-2 in the occurrence of ectopic calcification in tendon, and BMP-2 might have been playing a key role throughout the process. However, another study showed that BMP-2 might not be involved in regulating the appearance of ossified area in the CI tendon injury model (Yee Lui et al., 2011); thus, more studies are needed to confirm the exact role of BMP-2. Moreover, BMP-4 also played a vital role in the heterotopic ossification formation after traumatic muscle injury (Kluk et al., 2012) and the idiopathic cutaneous ossification (Kim et al., 2008), and a similar role of BMP-7 in the formation of rotator cuff mineralization was observed (Neuwirth et al., 2006). Interestingly, in this study, the protein expression of BMP-4/7 in tendon between the group aged 8M and the group aged 20M was similar without significant difference as well as the gene expression of BMP-4/7 in TSPCs between the group aged 8M and the group aged 20M, indicating that BMP-4/7 might play an important role in the formation of ectopic ossification at the early stage and a weaker role at the late stage, which was corroborated

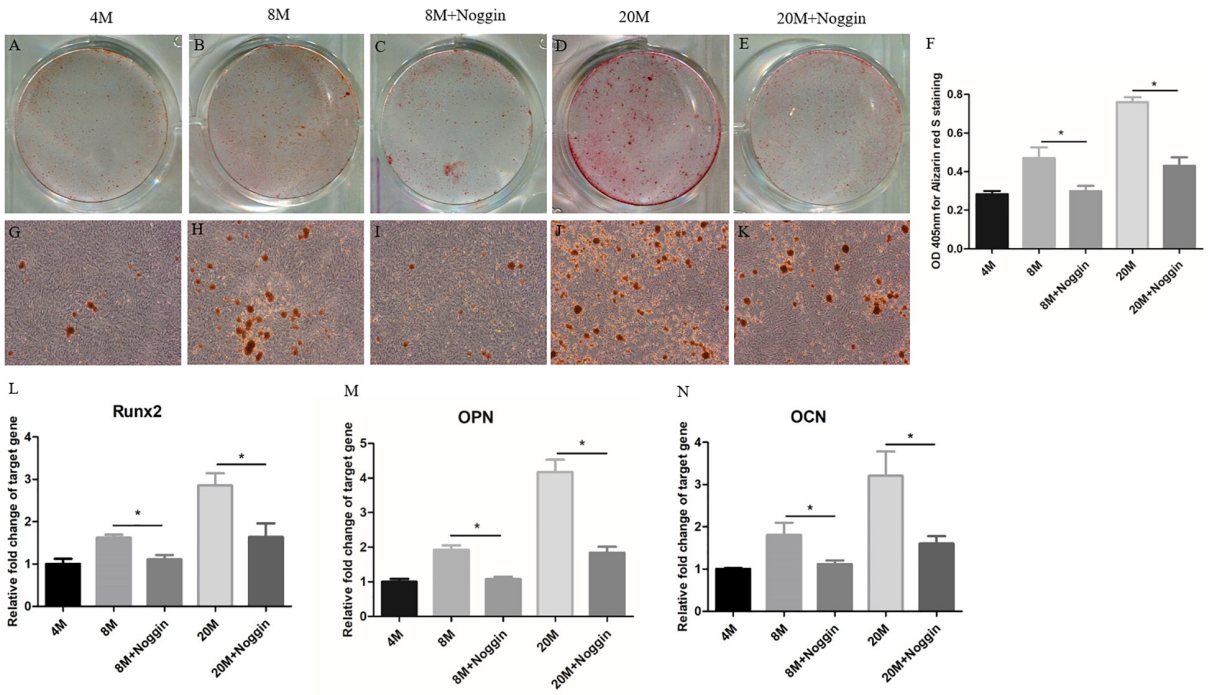

FIGURE 8 | Noggin inhibits the osteogenic differentiation of A-TSPCs. Effect of noggin on the osteogenic differentiation of A-TSPCs isolated from ossified tendon aged 8 and 20M. Graphs show that noggin inhibits osteogenic differentiation tendency of TSPCs at day 7 **(A–E,G–K)** as indicated by Alizarin red S staining. Statistical diagrams show the quantification of the amount of Alizarin red S bound to the calcified deposits in TSPCs with or without noggin stimulation at day 7 **(F)**. Statistical diagrams show the mRNA expression of Runx2 **(L)**, OPN **(M)**, and OCN **(N)** in TSPCs upon treatment with noggin *in vitro*. Magnification × 1 **(A–E)** and ×40 **(G–K)**. $^*P < 0.05$.

by similar results of the key role of BMP-7 at the early phase of heterotopic ossification formation after muscle injury (Li et al., 2019). Based on these findings, BMP-2 might play a vital role in the occurrence of ectopic calcification in tendon throughout the process, while BMP-4/7 might play an indispensable role at the early stage. Different kinds of BMP might play their respective roles at different periods of the heterotopic ossification formation process, and the intricate underlying mechanism still needs further research. Previous studies also showed that treatment with BMP-2 promotes osteo-chondrogenic differentiation of TSPCs *in vitro*, and when TSPCs were disposed with BMP-2 and then transplanted subcutaneously into immunocompromised mice, structures similar to osteotendinous junctions were formed (Bi et al., 2007), which were similar to the ectopic ossified structures observed in both the tendinopathy animal model (Lui et al., 2009) and human samples (Rui et al., 2012b). In this study, the expression levels of BMPs in TSPC was increased with aging and upon osteogenic induction, indicating the intimate relationship between BMP expression and osteogenic differentiation potential of TSPC. In addition, BMP-2 could increase the osteogenic differentiation potential of TSPCs in this study, and BMPs also regulated differentiation ability of other cell species, such as tenocytes (Sato et al., 1988), embryonic stem cells (Gunne-Braden et al., 2020), and MSCs (Zhang et al., 2019). At the same time, we have tested the effect of noggin on the osteogenic differentiation of TSPCs *in vitro*, and the results showed that the addition of noggin could inhibit BMP-induced enhancement of osteogenic differentiation of TSPCs. These findings demonstrated that BMPs might increase the osteogenic differentiation potential of TSPCs, which is responsible for the increased trend of heterotopic ossification formation in tendon with aging. Meanwhile, the osteogenic differentiation potential was declined when the activities of BMP signaling are inhibited. In this study, we have verified the inhibitory effect of noggin on the osteogenic differentiation of TSPCs *in vitro*; moreover, implantation of noggin gene or muscle-derived stem cells over-expressing noggin were also reported to inhibit heterotopic ossification formation induced by BMP-4 in animal models (Glaser et al., 2003; Hannallah et al., 2004). In addition, other molecules, such as TGF-β neutralizing antibody (Wang et al., 2018) and transferrin receptor 2 (Rauner et al., 2019), and some drugs, such as insulin (Zhang et al., 2014) and desloratadine (Kusano et al., 2020), could attenuate heterotopic ossification formation induced by BMPs. A previous study also showed that mTOR signaling modulator suppressed heterotopic ossification formation (Hino et al., 2018); metformin exerted a dual negative regulatory effect on mTOR and BMP signal, and it might inhibit heterotopic ossification through an mTOR-BMP crosstalk signaling network (Wu et al., 2019). Recently, synthetic retinoid agonists, as a new option, has shown promise because it inhibited BMP-mediated heterotopic ossification formation in animal models (Sinha et al., 2016), and retinoid agonist

therapy is being examined in patients with a rare, genetic form of heterotopic ossification (Lowery and Rosen, 2018). Thus, application of these factors might inhibit heterotopic ossification and promote tendon healing in tendinopathy and tendon injury models; further studies are needed to verify the effectiveness of these therapies for the management of heterotopic ossification formation during the tendon aging process. Although most of these strategies are at the stage of basic research, it is possible for them to enter clinical use when the distance between clinical medicine and basic research is resolved with more studies.

The limitation of this study is that the detailed signaling pathways of BMPs regulating the heterotopic ossification formation is not determined. Normally, BMP signaling mainly includes canonical SMAD signaling and non-SMAD signaling, and non-SMAD signaling is able to function by regulating SMAD signaling to form a crosstalk signaling network (Sanchez-Duffhues et al., 2015). A previous study showed that BMPs promote the osteogenic differentiation of TSPCs by phosphorylating SMAD in a failed tendon healing animal model (Lui and Wong, 2013), and SMAD was often a target of other cellular kinases, such as MAPK and GSK3-β, leading the crosstalk among these signals (Sanchez-Duffhues et al., 2015). Moreover, BMP-7 regulated the differentiation ability of MSC in the formation of heterotopic ossification of soft tissue through the Wnt/β-catenin pathway (Fu et al., 2017). In fibrodysplasia ossificans progressive disease, mTOR (Agarwal et al., 2016) and NF-κB/MAPK (Barruet et al., 2018) were related with the formation of muscle heterotopic ossification under crosstalk with BMP signaling, and BMPs together with SMAD, AKT, and mTOR/S6K signaling could prevent heterotopic ossification progress when the activity of PI3Kα was inhibited (Valer et al., 2019). RhoA-BMPs (Mu et al., 2013) and CGRP-SP-BMP-2 (Tuzmen et al., 2018) signaling also regulated heterotopic ossification progress in dystrophic muscle and Achilles tendon of mice, respectively. Additionally, BMP signaling pathway has crosstalk with Notch, FGF, and JAK/STAT signaling pathways in cell osteogenic differentiation potential and tissue ossification formation (Chen et al., 2012; Zhang et al., 2019, 2020). Thus, the factors from these signaling pathways might be involved in the formation of heterotopic ossification in aged tendon, and the detailed signaling pathways needed more studies. Moreover, Fang et al. (2014) have compared the form rate of heterotopic ossification with transplantation of mouse fetal or adult fibroblasts *in vivo*; thus, TSPCs isolated from different age points could be transplanted into nude mice to observe the formation of heterotopic ossification, which will further verify the hypothesis proposed in this study.

In summary, the appearance and the increased trend of heterotopic ossification were firstly reported in rat Achilles tendon with aging, and the enhanced osteogenic potential of TSPCs might contribute to the increased heterotopic ossification in aged tendon, which might be induced by the higher expression of BMPs in TSPCs with aging. These results might provide ideal prevention and treatment methods for heterotopic ossification in tendon, as well as other age-related tendon disorders.

DATA AVAILABILITY STATEMENT

All datasets generated for this study are included in the article/**Supplementary Material**.

ETHICS STATEMENT

The animal study was reviewed and approved by Institutional Animal Care and Use Committee (IACUC) in Southeast University School of Medicine.

AUTHOR CONTRIBUTIONS

GD and YR conceived and designed the study. GD, YL, JL, and CZ performed the majority part of the experiments. MC and PL provided help for the experiments. GD, JL, and CZ acquired and analyzed the data. GD and YR drafted and edited the manuscript. All the authors aided in revising this manuscript for intellectual content and approved the final version to be published.

FUNDING

This work was supported by the National Natural Science Foundation of China (81871812 and 81572187); the National Natural Science Foundation of China for Young Scholars (81201422); the Natural Science Foundation of Jiangsu Province for Young Scholars (BK2012334); the "Summit of the Six Top Talents" Program of Jiangsu Province (2013-WSW-054); the Jiangsu Provincial Medical Talent; The Project of Invigorating Health Care through Science, Technology and Education (ZDRCA2016083); and The Six Projects Sponsoring Talent Summits of Jiangsu Province, China (LGY2017099).

SUPPLEMENTARY MATERIAL

The Supplementary Material for this article can be found online at: https://www.frontiersin.org/articles/10.3389/fcell.2020.570605/full#supplementary-material

REFERENCES

Agabalyan, N. A., Evans, D. J., and Stanley, R. L. (2013). Investigating tendon mineralisation in the avian hindlimb: a model for tendon ageing, injury and disease *J. Anat.* 223, 262–277. doi: 10.1111joa.12078

Agarwal, S., Cholok, D., Loder, S., Li, J., Breuler, C., Chung, M. T., et al. (2016). mTOR inhibition and BMP signaling act synergistically to reduce muscle fibrosis and improve myofiber regeneration. *JCI Insight* 1:e89805. doi: 10.1172/jci.insight.89805

Barruet, E., Morales, B. M., Cain, C. J., Ton, A. N., Wentworth, K. L., Chan, T. V., et al. (2018). NF-kappaB/MAPK activation underlies ACVR1-mediated inflammation in human heterotopic ossification. *JCI Insight* 3:e122958. doi: 10.1172/jci.insight.122958

Bi, Y., Ehirchiou, D., Kilts, T. M., Inkson, C. A., Embree, M. C., Sonoyama, W., et al. (2007). Identification of tendon stem/progenitor cells and the role of the extracellular matrix in their niche. *Nat. Med.* 13, 1219–1227. doi: 10.1038/nm1630

Chen, G., Deng, C., and Li, Y. P. (2012). TGF-beta and BMP signaling in osteoblast differentiation and bone formation. *Int. J. Biol. Sci.* 8, 272–288. doi: 10.7150/ijbs.2929

Cho, H. H., Park, H. T., Kim, Y. J., Bae, Y. C., Suh, K. T., and Jung, J. S. (2005). Induction of osteogenic differentiation of human mesenchymal stem cells by histone deacetylase inhibitors. *J. Cell. Biochem.* 96, 533–542. doi: 10.1002/jcb.20544

Dai, G. C., Li, Y. J., Chen, M. H., Lu, P. P., and Rui, Y. F. (2019). Tendon stem/progenitor cell ageing: modulation and rejuvenation. *World J. Stem Cells* 11, 677–692. doi: 10.4252/wjsc.v11.i9.677

Fang, Z., Zhu, T., Shen, W. L., Tang, Q. M., Chen, J. L., Yin, Z., et al. (2014). Transplantation of fetal instead of adult fibroblasts reduces the probability of ectopic ossification during tendon repair. *Tissue Eng. Part A* 20, 1815–1826. doi: 10.1089/ten.TEA.2013.0296

Fu, H. D., Wang, H. R., and Li, D. H. (2017). BMP-7 accelerates the differentiation of rabbit mesenchymal stem cells into cartilage through the Wnt/beta-catenin pathway. *Exp. Ther. Med.* 14, 5424–5428. doi: 10.3892/etm.2017.5210

Geng, Y., Zhao, X., Xu, J., Zhang, X., Hu, G., Fu, S. C., et al. (2020). Overexpression of mechanical sensitive miR-337-3p alleviates ectopic ossification in rat tendinopathy model via targeting IRS1 and Nox4 of tendon-derived stem cells. *J. Mol. Cell. Biol.* 12, 305–317. doi: 10.1093/jmcb/mjz030

Glaser, D. L., Economides, A. N., Wang, L., Liu, X., Kimble, R. D., Fandl, J. P., et al. (2003). In vivo somatic cell gene transfer of an engineered Noggin mutein prevents BMP4-induced heterotopic ossification. *J. Bone Joint Surg. Am.* 85, 2332–2342. doi: 10.2106/00004623-200312000-00010

Gunne-Braden, A., Sullivan, A., Gharibi, B., Sheriff, R. S. M., Maity, A., Wang, Y. F., et al. (2020). GATA3 mediates a fast, irreversible commitment to BMP4-driven differentiation in human embryonic stem cells. *Cell Stem Cell* 26, 693.e9–706.e9. doi: 10.1016/j.stem.2020.03.005

Hannallah, D., Peng, H., Young, B., Usas, A., Gearhart, B., and Huard, J. (2004). Retroviral delivery of Noggin inhibits the formation of heterotopic ossification induced by BMP-4, demineralized bone matrix, and trauma in an animal model. *J. Bone Joint Surg. Am.* 86, 80–91. doi: 10.2106/00004623-200401000-00013

Harada, Y., Furukawa, K., Asari, T., Chin, S., Ono, A., Tanaka, T., et al. (2014). Osteogenic lineage commitment of mesenchymal stem cells from patients with ossification of the posterior longitudinal ligament. *Biochem. Biophys. Res. Commun.* 443, 1014–1020. doi: 10.1016/j.bbrc.2013.12.080

Hino, K., Zhao, C., Horigome, K., Nishio, M., Okanishi, Y., Nagata, S., et al. (2018). / An mTOR signaling modulator suppressed heterotopic ossification of fibrodysplasia ossificans progressiva. *Stem Cell Rep.* 11, 1106–1119. doi: 10.1016/j.stemcr.2018.10.007

Kim, S. Y., Choi, H. Y., Myung, K. B., and Choi, Y. W. (2008). The expression of molecular mediators in the idiopathic cutaneous calcification and ossification. *J. Cutan Pathol.* 35, 826–831. doi: 10.1111/j.1600-0560.2007.00904.x

Kluk, M. W., Ji, Y., Shin, E. H., Amrani, O., Onodera, J., Jackson, W. M., et al. (2012). Fibroregulation of mesenchymal progenitor cells by BMP-4 after traumatic muscle injury. *J. Orthop. Trauma* 26, 693–698. doi: 10.1097/BOT.0b013e3182712adf

Kubo, K., Ishida, Y., Komuro, T., Tsunoda, N., Kanehisa, H., and Fukunaga, T. (2007a). Age-related differences in the force generation capabilities and tendon extensibilities of knee extensors and plantar flexors in men. *J. Gerontol. A Biol. Sci. Med. Sci.* 62, 1252–1258. doi: 10.1093/gerona/62.11.1252

Kubo, K., Morimoto, M., Komuro, T., Tsunoda, N., Kanehisa, H., and Fukunaga, T. (2007b). Age-related differences in the properties of the plantar flexor muscles and tendons. *Med. Sci. Sports Exerc.* 39, 541–547. doi: 10.1249/01.mss.0000247006.24965.74

Kusano, T., Nakatani, M., Ishiguro, N., Ohno, K., Yamamoto, N., Morita, M., et al. (2020). Desloratadine inhibits heterotopic ossification by suppression of BMP2-Smad1/5/8 signaling. *J. Orthop. Res.* [Epub ahead of print]. doi: 10.1002/jor.24625

Li, L., Jiang, Y., Lin, H., Shen, H., Sohn, J., Alexander, P. G., et al. (2019). Muscle injury promotes heterotopic ossification by stimulating local bone morphogenetic protein-7 production. *J. Orthop. Translat.* 18, 142–153. doi: 10.1016/j.jot.2019.06.001

Li, Y., Dai, G., Shi, L., Lin, Y., Chen, M., Li, G., et al. (2019). The potential roles of tendon stem/progenitor cells in tendon aging. *Curr. Stem Cell Res. Ther.* 14, 34–42. doi: 10.2174/1574888X13666181017112233

Liu, X., Kumagai, G., Wada, K., Tanaka, T., Asari, T., Oishi, K., et al. (2017). High osteogenic potential of adipose- and muscle-derived mesenchymal stem cells in spinal-ossification model mice. *Spine* 42, E1342–E1349. doi: 10.1097/BRS.0000000000002266

Lounev, V. Y., Ramachandran, R., Wosczyna, M. N., Yamamoto, M., Maidment, A. D., Shore, E. M., et al. (2009). Identification of progenitor cells that contribute to heterotopic skeletogenesis. *J. Bone Joint Surg. Am.* 91, 652–663. doi: 10.2106/JBJS.H.01177

Lowery, J. W., and Rosen, V. (2018). Bone morphogenetic protein-based therapeutic approaches. *Cold Spring Harb. Perspect. Biol.* 10:a022327. doi: 10.1101/cshperspect.a022327

Lui, P. P. (2013). Histopathological changes in tendinopathy–potential roles of BMPs? *Rheumatology* 52, 2116–2126. doi: 10.1093/rheumatology/ket165

Lui, P. P., Fu, S. C., Chan, L. S., Hung, L. K., and Chan, K. M. (2009). Chondrocyte phenotype and ectopic ossification in collagenase-induced tendon degeneration. *J. Histochem. Cytochem.* 57, 91–100. doi: 10.1369/jhc.2008.952143

Lui, P. P., and Wong, Y. (2013). Higher BMP/Smad sensitivity of tendon-derived stem cells (TDSCs) isolated from the collagenase-induced tendon injury model: possible mechanism for their altered fate in vitro. *BMC Musculoskelet. Disord.* 14:248. doi: 10.1186/1471-2474-14-248

Mao, D., Mi, J., Pan, X., Li, F., and Rui, Y. (2019). Tamoxifen inhibits the progression of trauma-induced heterotopic ossification in mice. *Med. Sci. Monit.* 25, 7872–7881. doi: 10.12659/MSM.916733

Mu, X., Usas, A., Tang, Y., Lu, A., Wang, B., Weiss, K., et al. (2013). RhoA mediates defective stem cell function and heterotopic ossification in dystrophic muscle of mice. *FASEB J.* 27, 3619–3631. doi: 10.1096/fj.13-233460

Neuwirth, J., Fuhrmann, R. A., Veit, A., Aurich, M., Stonans, I., Trommer, T., et al. (2006). Expression of bioactive bone morphogenetic proteins in the subacromial bursa of patients with chronic degeneration of the rotator cuff. *Arthritis Res. Ther.* 8:R92. doi: 10.1186/ar1965

Olmsted-Davis, E. A., Salisbury, E. A., Hoang, D., Davis, E. L., Lazard, Z., Sonnet, C., et al. (2017). Progenitors in Peripheral Nerves Launch Heterotopic Ossification. *Stem Cells Transl. Med.* 6, 1109–1119. doi: 10.1002/sctm.16-0347

Pignolo, R. J., Wang, H., and Kaplan, F. S. (2019). Fibrodysplasia ossificans progressiva (FOP): a segmental progeroid syndrome. *Front. Endocrinol.* 10:908. doi: 10.3389/fendo.2019.00908

Qiao, W., Yu, S., Sun, H., Chen, L., Wang, R., Wu, X., et al. (2020). 1,25-Dihydroxyvitamin D insufficiency accelerates age-related bone loss by increasing oxidative stress and cell senescence. *Am. J. Transl. Res.* 12, 507–518.

Rauner, M., Baschant, U., Roetto, A., Pellegrino, R. M., Rother, S., Salbach-Hirsch, J., et al. (2019). Transferrin receptor 2 controls bone mass and pathological bone formation via BMP and Wnt signaling. *Nat. Metab.* 1, 111–124. doi: 10.1038/s42255-018-0005-8

Rui, Y. F., Chen, M. H., Li, Y. J., Xiao, L. F., Geng, P., Wang, P., et al. (2019). CTGF attenuates tendon-derived stem/progenitor cell aging. *Stem Cells Int.* 2019:6257537. doi: 10.1155/2019/6257537

Rui, Y. F., Lui, P. P., Chan, L. S., Chan, K. M., Fu, S. C., and Li, G. (2011a). Does erroneous differentiation of tendon-derived stem cells contribute to the pathogenesis of calcifying tendinopathy? *Chin. Med. J.* 124, 606–610.

Rui, Y. F., Lui, P. P., Ni, M., Chan, L. S., Lee, Y. W., and Chan, K. M. (2011b). Mechanical loading increased BMP-2 expression which promoted osteogenic differentiation of tendon-derived stem cells. *J. Orthop. Res.* 29, 390–396. doi: 10.1002/jor.21218

Rui, Y. F., Lui, P. P., Lee, Y. W., and Chan, K. M. (2012a). Higher BMP receptor expression and BMP-2-induced osteogenic differentiation in tendon-derived stem cells compared with bone-marrow-derived mesenchymal stem cells. *Int. Orthop.* 36, 1099–1107. doi: 10.1007/s00264-011-1417-1

Rui, Y. F., Lui, P. P., Rolf, C. G., Wong, Y. M., Lee, Y. W., and Chan, K. M. (2012b). Expression of chondro-osteogenic BMPs in clinical samples of patellar tendinopathy. *Knee Surg. Sports Traumatol. Arthrosc.* 20, 1409–1417. doi: 10.1007/s00167-011-1685-8

Rui, Y. F., Lui, P. P., Li, G., Fu, S. C., Lee, Y. W., and Chan, K. M. (2010). Isolation and characterization of multipotent rat tendon-derived stem cells. *Tissue Eng. Part A* 16, 1549–1558. doi: 10.1089/ten.TEA.2009.0529

Rui, Y. F., Lui, P. P., Wong, Y. M., Tan, Q., and Chan, K. M. (2013). Altered fate of tendon-derived stem cells isolated from a failed tendon-healing animal model of tendinopathy. *Stem Cells Dev.* 22, 1076–1085. doi: 10.1089/scd.2012.0555

Ruzzini, L., Abbruzzese, F., Rainer, A., Longo, U. G., Trombetta, M., Maffulli, N., et al. (2014). Characterization of age-related changes of tendon stem cells from adult human tendons. *Knee Surg. Sports Traumatol. Arthrosc.* 22, 2856–2866. doi: 10.1007/s00167-013-2457-4

Sanchez-Duffhues, G., Hiepen, C., Knaus, P., and Ten Dijke, P. (2015). Bone morphogenetic protein signaling in bone homeostasis. *Bone* 80, 43–59. doi: 10.1016/j.bone.2015.05.025

Sato, K., Miura, T., and Iwata, H. (1988). Cartilaginous transdifferentiation of rat tenosynovial cells under the influence of bone morphogenetic protein in tissue culture. *Clin. Orthop. Relat. Res.* 236, 233–239.

Shi, L., Li, Y. J., Dai, G. C., Lin, Y. C., Li, G., Wang, C., et al. (2019). Impaired function of tendon-derived stem cells in experimental diabetes mellitus rat tendons: implications for cellular mechanism of diabetic tendon disorder. *Stem Cell Res. Ther.* 10:27. doi: 10.1186/s13287-018-1108-6

Sinha, S., Uchibe, K., Usami, Y., Pacifici, M., and Iwamoto, M. (2016). Effectiveness and mode of action of a combination therapy for heterotopic ossification with a retinoid agonist and an anti-inflammatory agent. *Bone* 90, 59–68. doi: 10.1016/j.bone.2016.02.008

Speer, M. Y., Yang, H. Y., Brabb, T., Leaf, E., Look, A., Lin, W. L., et al. (2009). Smooth muscle cells give rise to osteochondrogenic precursors and chondrocytes in calcifying arteries. *Circ. Res.* 104, 733–741. doi: 10.1161/CIRCRESAHA.108.183053

Tan, Q., Lui, P. P., and Rui, Y. F. (2012). Effect of in vitro passaging on the stem cell-related properties of tendon-derived stem cells-implications in tissue engineering. *Stem Cells Dev.* 21, 790–800. doi: 10.1089/scd.2011.0160

Tang, Q. M., Chen, J. L., Shen, W. L., Yin, Z., Liu, H. H., Fang, Z., et al. (2014). Fetal and adult fibroblasts display intrinsic differences in tendon tissue engineering and regeneration. *Sci. Rep.* 4:5515. doi: 10.1038/srep05515

Tuzmen, C., Verdelis, K., Weiss, L., and Campbell, P. (2018). Crosstalk between substance P and calcitonin gene-related peptide during heterotopic ossification in murine achilles tendon. *J. Orthop. Res.* 36, 1444–1455. doi: 10.1002/jor.23833

Vaishya, R., Maduka, C. O., Agarwal, A. K., Vijay, V., and Vaish, A. (2019). Heterotopic ossification of tendo achilles: an uncommon clinical entity. *J. Orthop. Case Rep.* 9, 45–47. doi: 10.13107/jocr.2250-0685.1364

Valer, J. A., Sanchez-de-Diego, C., Gamez, B., Mishina, Y., Rosa, J. L., and Ventura, F. (2019). Inhibition of phosphatidylinositol 3-kinase alpha (PI3Kalpha) prevents heterotopic ossification. *EMBO Mol. Med.* 11:e10567. doi: 10.15252/emmm.201910567

Wang, X., Li, F., Xie, L., Crane, J., Zhen, G., Mishina, Y., et al. (2018). Inhibition of overactive TGF-beta attenuates progression of heterotopic ossification in mice. *Nat. Commun.* 9:551. doi: 10.1038/s41467-018-02988-5

Wood, L. K., Arruda, E. M., and Brooks, S. V. (2011). Regional stiffening with aging in tibialis anterior tendons of mice occurs independent of changes in collagen fibril morphology. *J. Appl. Physiol.* 111, 999–1006. doi: 10.1152/japplphysiol.00460.2011

Wu, J., Ren, B., Shi, F., Hua, P., and Lin, H. (2019). BMP and mTOR signaling in heterotopic ossification: does their crosstalk provide therapeutic opportunities? *J. Cell Biochem.* 120, 12108–12122. doi: 10.1002/jcb.28710

Xing, Y., Sun, W., Wang, Y., Gao, F., and Ma, H. (2016). Mutual inhibition of insulin signaling and PHLPP-1 determines cardioprotective efficiency of Akt in aged heart. *Aging* 8, 873–888. doi: 10.18632/aging.100933

Yang, J., Zhao, Q., Wang, K., Liu, H., Ma, C., Huang, H., et al. (2016). Isolation and biological characterization of tendon-derived stem cells from fetal bovine. *In Vitro Cell Dev. Biol. Anim.* 52, 846–856. doi: 10.1007/s11626-016-0043-z

Yee Lui, P. P., Wong, Y. M., Rui, Y. F., Lee, Y. W., Chan, L. S., and Chan, K. M. (2011). Expression of chondro-osteogenic BMPs in ossified failed tendon healing model of tendinopathy. *J. Orthop Res.* 29, 816–821. doi: 10.1002/jor.21313

Zhang, B., Yang, L., Zeng, Z., Feng, Y., Wang, X., Wu, X., et al. (2020). Leptin potentiates BMP9-induced osteogenic differentiation of mesenchymal stem cells through the activation of JAK/STAT signaling. *Stem Cells Dev.* 29, 498–510. doi: 10.1089/scd.2019.0292

Zhang, J., and Wang, J. H. (2010). Characterization of differential properties of rabbit tendon stem cells and tenocytes. *BMC Musculoskelet Disord.* 11:10. doi: 10.1186/1471-2474-11-10

Zhang, J., Xiong, J., Fang, L., Lu, Z., Wu, M., Shi, L., et al. (2016). The protective effects of human umbilical cord mesenchymal stem cells on damaged ovarian function: a comparative study. *Biosci. Trends* 10, 265–276. doi: 10.5582/bst.2016.01125

Zhang, J., Zhao, Y., Hou, X., Chen, B., Xiao, Z., Han, J., et al. (2014). The inhibition effects of insulin on BMP2-induced muscle heterotopic ossification. *Biomaterials.* 35, 9322–9331. doi: 10.1016/j.biomaterials.2014.07.056

Zhang, L., Luo, Q., Shu, Y., Zeng, Z., Huang, B., Feng, Y., et al. (2019). Transcriptomic landscape regulated by the 14 types of bone morphogenetic proteins (BMPs) in lineage commitment and differentiation of mesenchymal stem cells (MSCs). *Genes Dis.* 6, 258–275. doi: 10.1016/j.gendis.2019.03.008

Zhang, X., Lin, Y. C., Rui, Y. F., Xu, H. L., Chen, H., Wang, C., et al. (2016). Therapeutic roles of tendon stem/progenitor cells in tendinopathy. *Stem Cells Int.* 2016:4076578. doi: 10.1155/2016/4076578

Conflict of Interest: The authors declare that the research was conducted in the absence of any commercial or financial relationships that could be construed as a potential conflict of interest.

frontiers in Cell and Developmental Biology

ORIGINAL RESEARCH
published: 11 February 2021
doi: 10.3389/fcell.2021.629274

Melatonin Promotes Heterotopic Ossification Through Regulation of Endothelial-Mesenchymal Transition in Injured Achilles Tendons in Rats

Jie Zhang[1,2†], Jiajun Tang[1,2†], Jie Liu[1,2†], Bo Yan[1,2], Bin Yan[1,2], Minjun Huang[1,2], Zhongmin Zhang[3] and Liang Wang[1,2]**

[1] Department of Orthopedics, The Third Affiliated Hospital, Southern Medical University, Guangzhou, China, [2] Academy of Orthopedics, Guangzhou, China, [3] Division of Spine Surgery, Department of Orthopedics, Nanfang Hospital, Southern Medical University, Guangzhou, China

OPEN ACCESS

Edited by:
Zi Yin,
Zhejiang University, China

Reviewed by:
Heng Feng,
Center for Excellence in Molecular Cell Science, Shanghai Institute of Biochemistry and Cell Biology, Chinese Academy of Sciences, China
Gianandrea Pasquinelli,
University of Bologna, Italy

***Correspondence:**
Zhongmin Zhang
nfzzm@163.com
Liang Wang
liang091@aliyun.com

† These authors have contributed equally to this work

Specialty section:
This article was submitted to Stem Cell Research, a section of the journal Frontiers in Cell and Developmental Biology

Received: 14 November 2020
Accepted: 25 January 2021
Published: 11 February 2021

Citation:
Zhang J, Tang J, Liu J, Yan B, Yan B, Huang M, Zhang Z and Wang L (2021) Melatonin Promotes Heterotopic Ossification Through Regulation of Endothelial-Mesenchymal Transition in Injured Achilles Tendons in Rats. Front. Cell Dev. Biol. 9:629274. doi: 10.3389/fcell.2021.629274

Although heterotopic ossification (HO) has been reported to be a common complication of the posttraumatic healing process, the underlying mechanism remains unknown. Endothelial-mesenchymal transition (EndMT) is known to play a role in HO, and our recent study observed that neuroendocrine signals can promote HO by modulating EndMT. Melatonin, a neuroendocrine hormone secreted mainly by the pineal gland, has been documented to perform its function in the skeletal system. This study aimed at describing the expression of melatonin during the formation of HO in rat models of Achilles tendon injury and to further investigate its role in regulating EndMT in HO. Histological staining revealed the expression of melatonin throughout the formation of heterotopic bone in injured Achilles tendons, and the serum melatonin levels were increased after the initial injury. Double immunofluorescence showed that the MT2 melatonin receptor was notably expressed at the sites of injury. Micro-CT showed the enhancement of heterotopic bone volume and calcified areas in rats treated with melatonin. Additionally, our data showed that melatonin induced EndMT in primary rat aortic endothelial cells (RAOECs), which acquired traits including migratory function, invasive function and EndMT and MSC marker gene and protein expression. Furthermore, our data exhibited that melatonin promoted the osteogenic differentiation of RAOECs undergoing EndMT *in vitro*. Importantly, inhibition of the melatonin-MT2 pathway by using the MT2 selective inhibitor 4-P-PDOT inhibited melatonin-induced EndMT and osteogenesis both *in vivo* and *in vitro*. In conclusion, these findings demonstrated that melatonin promoted HO through the regulation of EndMT in injured Achilles tendons in rats, and these findings might provide additional directions for the management of HO.

Keywords: heterotopic ossification, melatonin, EndMT, osteogenesis, neuroendocrine

INTRODUCTION

Heterotopic ossification (HO) is a pathological process within the formation of mature bony tissues in extraskeletal sites, including joints, skeletal muscles and surrounding tissues, such as fascia and tendons (Meyers et al., 2019). HO can be conceptualized as aberrant tissue repair and is a devastating complication that is common in the healing processes of traumatic injuries, such as fractures, total hip arthroplasties, severe burns and spinal cord injuries (Li and Tuan, 2020). Unfortunately, this pathological phenomenon is also observed in a rare genetic disorder known as fibrodysplasia ossificans progressiva (FOP), which is caused by a gain-of-function mutation in the bone morphogenetic protein (BMP) type I receptor ACVR1 (Shore et al., 2006). The effectiveness of conservative treatments, such as NSAIDs and radiotherapy, is limited, and correction of HO relies on invasive surgeries; however, surgeries may lead to the postoperative recurrence of HO. Thus, there is an urgent need to gain knowledge about the mechanisms underlying aberrant repair and to develop a novel preventive treatment for HO.

The mechanisms of HO formation at sites of injury remain largely unclear. Currently, it is believed that the development of ectopic bone ossification is closely associated with the abnormal differentiation of mesenchymal stem cells (MSCs) at injured sites. MSCs from injured sites differentiate into osteoblasts or chondrocytes instead of differentiating into muscle or tendon cells due to the modulation of various signals or cytokines (Loder et al., 2018). Previous studies have reported that tendon-derived stem cells (TDSCs) (Jiang et al., 2017), hematopoietic stem cells and myofibroblasts are considered candidates for potential osteogenic cell types (Zhang et al., 2016). In a recent study, vascular endothelial cells that undergo the endothelial-mesenchymal transition (EndMT) process were found to play a role in HO formation in injured Achilles tendons in rats (Zhang et al., 2019). EndMT begins when endothelial cells delaminate from the organized cell layer and invade the underlying tissue, causing the loss of endothelial-specific markers, including vascular endothelial cadherin (VE-cadherin), cluster of differentiation 31 (CD31), tyrosine kinase with immunoglobulin-like and EGF-like 1 (Tie-1), and the gain of mesenchymal-specific markers, such as vimentin, neural cadherin (N-cadherin) and fibroblast-specific protein 1 (FSP-1). Increasing evidence now demonstrates that, in addition to its known functions in the cardiovascular system and cancer progression (Potenta et al., 2008), EndMT also plays a role in skeletal repair events (Piera-Velazquez et al., 2011; Medici and Olsen, 2012). Many reports have suggested that under pathological conditions, vascular endothelial cells that undergo EndMT are able to acquire the differentiation potential of mesenchymal stem-like cells, and these endothelial-derived MSC-like cells contribute to HO formation by differentiating into chondrocytes and osteoblasts (Medici et al., 2010; Medici and Olsen, 2012; Zhang et al., 2016). Recently, in a rat model of Achilles tendon injury, we observed the conversion of vascular endothelial cells into MSC-like cells through BMP-4- or TGF-β2-induced EndMT (Zhang et al., 2019). Furthermore, these newly formed cells represented the dedifferentiation of endothelial cells into a stem cell phenotype, and cells of this phenotype can subsequently redifferentiate into osteoblasts and chondrocytes and contribute to HO formation. Although we confirmed the critical effect of EndMT on HO formation, illustrating the underlying regulatory mechanism of EndMT in HO formation remains challenging.

Current studies hold the view that the effect of neuroendocrine signals in regulating the abnormal differentiation of MSCs at injured sites is one of the vital factors that affects the pathogenesis of HO formation (Gugala et al., 2018; Huang et al., 2018). A recent study demonstrated that Neurotrophin-3, with its neuroendocrine characteristics, can modulate the EndMT process in HO formation in rats (Zhang et al., 2019), suggesting that neuroendocrine cytokines can participate in the regulation of EndMT. Melatonin (*N*-acetyl-5-methoxytryptamine) is a neuroendocrine hormone that is secreted mainly by the pineal gland in mammals and is also expressed in other tissues, such as the ovary, testis, gut, and placenta (Fan et al., 2020). Many studies have demonstrated that melatonin regulates a variety of physiological activities, including the circadian cycle, oxidative stress and neuroendocrine processes, either through melatonin receptor 1A (MT1)/melatonin receptor 1B (MT2) or by acting directly as an antioxidant in cells (Majidinia et al., 2018). Currently, studies have focused on the role of melatonin in the skeletal system and have shown that melatonin is a key factor in regulating the osteogenic differentiation of various MSCs. A previous study reported that melatonin is capable of promoting the osteogenic differentiation and mineralization of MC3T3-E1 cells under hypoxic conditions via the activation of PKD/p38 pathways (Jang-Ho Son et al., 2014). In addition, melatonin showed a capacity to enhance the osteoblastic differentiation of human mandibular bone or iliac bone cells *in vitro* and to increase the volume of newly formed cortical bone of mice femora (Satomura et al., 2007). Moreover, melatonin enhanced the BMP-4-induced osteogenesis and increased the expression of osteogenic markers, especially Osterix, which is an essential transcription factor for the differentiation of C2C12 cells from preosteoblasts into mature osteoblasts (Han et al., 2017). Furthermore, a recent study demonstrated that the serum levels of melatonin are increased in ankylosing spondylitis (AS) patients, especially in those presenting with spinal bone ossification (Li et al., 2020). These previous studies have described the function of melatonin in osteogenesis or bone formation; however, few reports have elucidated the relationship between melatonin and HO formation. Importantly, our previous study indicates the effect of neuroendocrine signals such as Neurotrophin-3 on HO formation via EndMT modulation. Therefore, this study, as an extension of our previous research, focuses on the ability of melatonin to promote HO formation by inducing vascular endothelial cells to undergo EndMT in rats with Achilles tendon injuries.

MATERIALS AND METHODS

Rat Achilles Tendon Injury Model and Melatonin Intervention Treatment

To investigate the roles of melatonin in the formation of ectopic bone in Achilles tendon injuries, a rat model of Achilles tendon injury was used, as we previously described (Zhang et al., 2019). These experiments were approved by the Ethical Committee for Animal Research (IAC1907001). At 4, 8, and 12 weeks after the operation, some rats ($n = 6$/time point) were euthanized, and their limbs were collected for gene expression and histological analyses of melatonin. A control group was euthanized ($n = 6$) as well. Additionally, for the HO formation study, the remaining rats were randomly divided into another four groups: the normal control, HO control, melatonin, and melatonin+4-P-PDOT groups ($n = 6$/group). The rats received a daily intraperitoneal injection of melatonin (50 μg/kg) (R&D Systems, Tocris Bioscience, Cat. #3550) for 12 weeks, and 4-P-PDOT (1 mg/kg) (R&D Systems, Tocris Bioscience, Cat. #1034) was also intraperitoneally administered daily. All the rats in the HO control group were administered a saline vehicle weekly. Twelve weeks after the Achilles tenotomy, all the rats were euthanized, and their limbs were collected for further study.

Analysis of Serum Melatonin Levels in Rats With Achilles Tendon Injuries

Blood samples from rats with Achilles tendon injuries were acquired and centrifuged (2,000 rpm; 10 min; 4°C). Plasma fractions were stored at −80°C. The serum concentration of melatonin was determined using the ELISA Kit for melatonin (Rat: Cloud-Clone Corp. CEA908Ge) according to the manufacturer's instructions.

Micro-CT Analysis

HO volume was measured *in vivo* by micro-CT scanning (μCT 80, Scanco Medical, Bruttisellen, Zürich, Switzerland) of limbs from the experimental and control groups. The specimens was made a mean 20-μm thick slice. 60 kV and 150 μA were set for scanning. 3D images were reconstructed by the Micro-CT system software package, and the HO volume was calculated.

Histological Analysis and Melatonin Immunohistochemistry

Specimens were collected from the rats with Achilles tendon injuries in the experimental and control groups, and the specimens were fixed, decalcified, dehydrated and processed for paraffin embedding, and cut into 4 μm thick slices. To describe HO, HE (Sigma-Aldrich, St. Louis, MI, United States), Safranin O and Fast Green (Sigma-Aldrich) (SOFG) staining were performed. The percentages of the calcified areas in the series sections were quantified by ImageJ software. After deparaffinization and rehydration, the sections were treated with 200 mg/ml proteinase K (Sigma–Aldrich) for 15 min at 37°C to unmask the antigen. The sections for immunohistochemistry (IHC) analysis were treated with 3% hydrogen peroxide for 15 min and then blocked with 1% goat serum at room temperature for 1 h. Then, the sections were immunostained with primary antibodies against melatonin (1:100, Abcam, ab203346) for IHC.

MT1 and MT2 Melatonin Receptor Immunofluorescence Analysis in Rat Achilles Tendons

To investigate the primary receptor through which melatonin exerts its biological effect during HO formation, MT1 (1:100, Abclonal, A13030), MT2 (1:100, Abcam, ab203346), CD31 (1:100, Abcam, ab24590), SOX9 (1:100, Abcam, ab185966), and OCN (1:100, Abcam, ab13420) antibodies were used for immunofluorescence (IF). After incubation at 4°C overnight, a species-matched Alexa Fluor 488-, Alexa Fluor 594- or HRP-labeled secondary antibody was used (1:500) at 37°C for 1 h. For IHC, DAB (ZSGB-Bio, Beijing, China) was used as the chromogen, and hematoxylin was used for counterstaining. For IF, the sections were stained with DAPI (Roche Applied Science, Indianapolis, IN, United States). All the samples were observed under a microscope.

Rat Aortic Endothelial Cell Isolation and Identification

To examine the effect of melatonin on EndMT, rat aortic endothelial cells (RAOECs) were isolated from SD rats as previously described (Zhang et al., 2019). The intact aorta was excised, a 6-0 suture was fixed on one end of the aorta and the inner surface of the aorta was flipped to the outside by drawing the suture through the lumen of the blood vessel with a blunt no. 5 suture needle. The turnover aorta was then cultured in endothelial cell medium (ECM) (ScienCell, Carlsbad, CA, United States) at 37°C under 5% CO_2. The medium was refreshed every other day. After 1 week, the adherent cells were observed under a microscope. The adherent cells were identified as endothelial cells by IF staining with CD31 and Tie-1 antibodies (1: 100, Abcam, ab27851). Third passage endothelial cells were collected for further researches.

CCK-8 Proliferation Assay

RAOECs were seeded at 1,000 cells/well in 96-well plates and treated with melatonin (10 ng/ml), BMP-4 (100 ng/ml), and TGF-β2 (100 ng/ml), respectively, for 48 h. Then, the cell number was determined using a CCK-8 proliferation assay kit (CCK-8, Dojindo, Japan) according to the instructions. The number of viable cells in each well was measured at an absorbance wavelength of 450 nm.

The Induction of EndMT and Osteogenesis of RAOECs

For EndMT induction, RAOECs were cultured within melatonin (10 ng/ml), BMP-4 (100 ng/ml), and TGF-β2 (100 ng/ml) (R&D Systems) for 2 weeks. For osteogenesis, RAOECs were then cultured in osteogenic medium within 50 μmol/L ascorbic acid, 0.1 μmol/L dexamethasone, and 10 mmol/L β-glycerol phosphate

(Sigma–Aldrich) after EndMT induction for another 2 weeks. For the functional study of melatonin, MT2 melatonin receptor inhibitor 4-P-PDOT (25 ng/ml) was added after the treatment of melatonin in RAOECs.

Scratch Assay and Transwell Migration/Invasion Assay

The migratory ability of RAOECs after undergoing EndMT was measured by scratch and transwell migration/invasion assays. Cells were plated and a scratch was made in the cell monolayer with a P200 pipette tip for the scratch assay. The cells were then incubated in 5% CO_2 at 37°C and photographed for up to 48 h. Closure of the scratch area was analyzed by Image-Pro Plus 6.0, and the scratch healing rate was quantified by the percent change in the scratch area. For the transwell migration and invasion assay, we seeded cells in the upper chamber, and the lower chambers were filled with low-serum ECM medium. After 48 h, the non-migrated cells were removed, and the migrated and invasive cells on the lower side of the membrane were stained with crystal violet. Images of four random sections were captured.

Flow Cytometry

RAOECs were stained in a FACS buffer composed of PBS, 2% FCS, and 2 mM EDTA on ice for 20 min with the following specific antibodies: CD90 (Abacm, ab225), CD44 (Abacm, ab157107), CD31 (R&D Systems, AF3628), and CD105 (Abacm, ab2529). Flow cytometry was conducted on a BD Fortessa apparatus using FACSDiva software (BD Biosciences).

ALP and ARS Cell Staining

To examine the potential effect of melatonin on osteogenic calcification activity, RAOECs were washed with PBS and fixed with 4% paraformaldehyde for 30 min after osteogenesis induction. ALP staining to detect osteogenesis was performed with cells cultured in osteogenic medium for 14 days according to ALP kit (Sigma-Aldrich). For Alizarin red staining, the cells were cultured for 21 days and then stained with 2% Alizarin red S staining solution (pH 4.2; Sigma-Aldrich) for 30 min at 37°C to visualize matrix calcification in the culture medium.

Quantitative RT-PCR Gene Expression Analyses

Quantitative RT-PCR assays were used to analyze the effect of the treatments on the expression of regulatory genes in Achilles tendons or the cells from the cell culture experiments described above. Total RNA was extracted with TRIzol reagent (Life Technologies, Grand Island, NY, United States). cDNA was synthesized with the TaKaRa PrimeScript RT Reagent Kit (Takara Biotechnology Co. Ltd., Shija, Japan). Quantitative RT-PCR was performed using the TaKaRa SYBR Premix Ex Taq II kit according to the instructions (Takara). The primers were purchased from Shanghai Biological Engineering, the sequences are provided in **Supplementary Table 1**. The relative gene expression was calculated using the $2^{-\Delta\Delta CT}$ method (Kenneth and Livak, 2001).

Western Blot Analyses

Western blot assays were used to analyze the effect of the treatments on the expression of regulatory genes in cells from the cell culture experiments described above. RAOEC lysates were collected and prepared for western blot analysis. We incubated the blots with primary antibodies (1,000-fold dilution) against VE-cadherin (Abcam, ab205336), Tie-1 (Abcam, ab27851), CD31 (Abcam, ab24590), N-cadherin (Abcam, ab76011), FSP-1 (Abcam, ab68124), Vimentin (Abcam, ab92547), OSX (Abacm, ab209484), OPN (Abacm, ab8448), Runx2 (CST, 12556S), OCN (Abcam, ab13420), and GAPDH (ZSGB-Bio, China) overnight at 4°C, followed by incubation with an anti-IgG horseradish peroxidase-conjugated secondary antibody (1:4000) for 1 h. Chemiluminescence was detected using an enhanced chemiluminescence (ECL) system. GAPDH served as the loading control.

Statistical Analysis

For comparisons of two groups, significance was calculated by 2-tailed Student's *t*-test. For comparisons of more than two groups, significance was calculated by 1-way ANOVA using SPSS 20.0 software (SPSS Inc., Chicago, IL, United States). A *P*-value of <0.05 was considered to be statistically significant.

RESULTS

Melatonin in HO Formation in Rats With Achilles Tendon Injuries

To determine the mechanism of HO pathogenesis, we examined surgical specimens from the rat model of Achilles tenotomy and identified these specimens histologically as being at an early stage of injury (4 weeks after the operation), osteogenesis stage (4–8 weeks after the operation) and mature stage (8–12 weeks after the operation). HE and SOFG staining of the HO specimens revealed cartilage layers adjacent to cancellous bone and bone marrow 8 weeks after the operation, while 12 weeks after the initial operation, large, well-developed cancellous bone and bone marrow were observed [**Figures 1A(a–h)**]. These histological staining results reveal a typical endochondral ossification process of HO formation in the injured Achilles tendons.

To investigate the role of melatonin in HO formation, we used an ELISA kit to examine the level of melatonin in the sera of the model rats at the indicated time points during HO formation, and normal rats were used as a control. Compared to the normal control rats, the model rats exhibited elevated serum levels of melatonin from 4 to 12 weeks, and the highest expression was observed 8 weeks after the operation (**Figure 1C**). Subsequently, to localize the expression of melatonin, we conducted IHC staining of melatonin during HO formation. Melatonin-positive cells were rarely found in the normal Achilles tendons [**Figure 1A(i)**], while in the injured Achilles tendons, melatonin-positive cells were observed from 4 to 12 weeks during ectopic bone formation [**Figures 1A(j–l),B**]; this result was consistent with

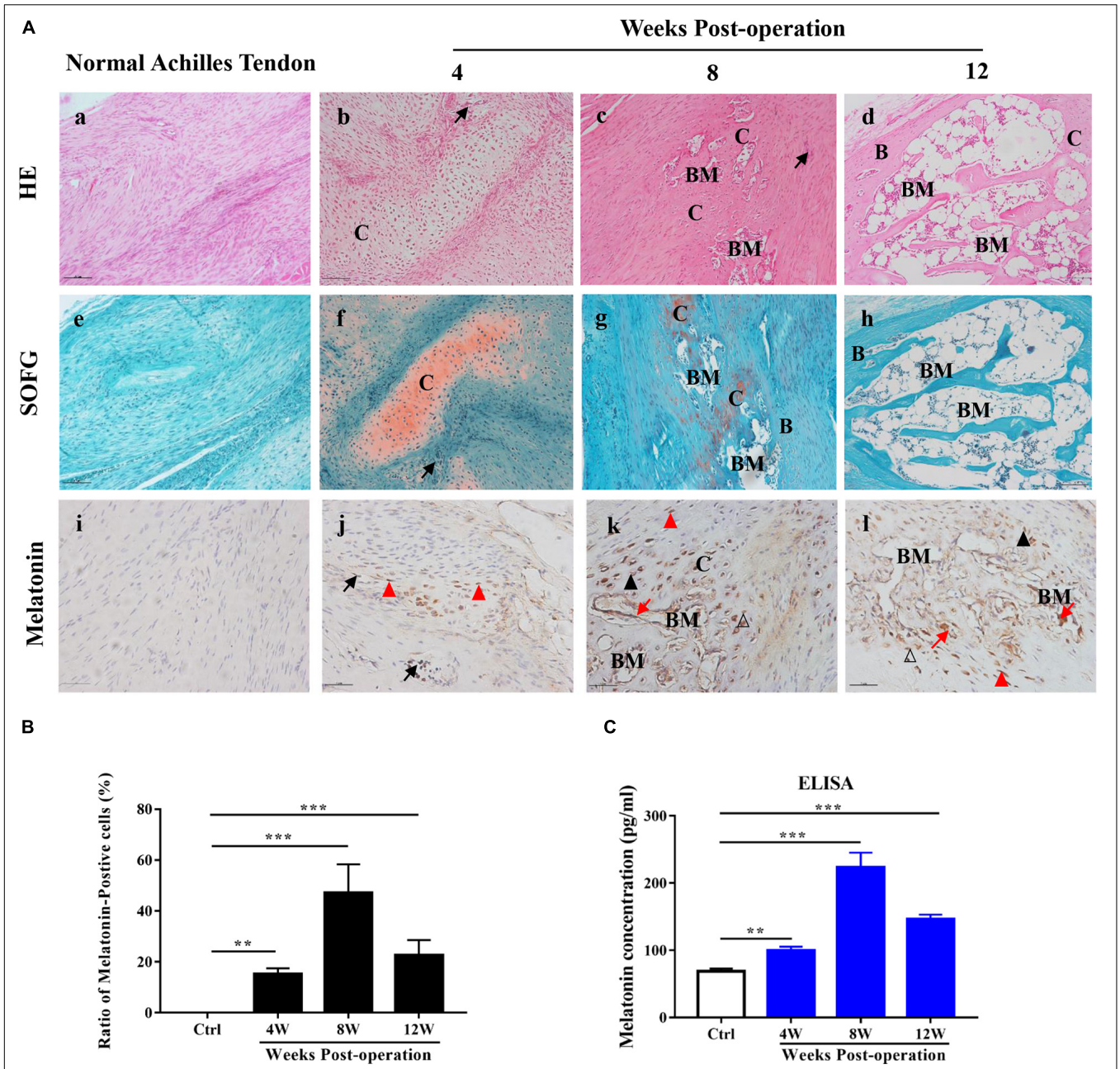

FIGURE 1 | Melatonin in HO formation in rats with Achilles tendon injuries. **(A)** HE and SOFG staining of normal Achilles tendons **(a,e)** and HO specimens at 4, 8, and 12 weeks after the operation **(b–d,f–h)**. The occurrence of HO was seen at 8 weeks after the operation. Proteoglycan (red) and ectopic bone (green). Immunohistochemical staining of melatonin (brown) in normal Achilles tendons **(i)** and HO specimens at 4, 8, and 12 weeks after the operation **(j–l)**. IHC showed that melatonin was expressed in vascular endothelial cells, infiltrating mesenchymal cells, chondrocytes, osteoblasts and newly formed bone marrow cells. B, bone; BM, bone marrow; C, cartilage; Me, mesenchyme, black arrows point to vessel endothelial cells, red triangles point to infiltrating mesenchymal cells, black triangles point to chondrocytes, blank triangles point to osteoblasts and red arrows point to newly formed bone marrow cells. Scale bar, 10 μm. **(B)** The number of melatonin-positive cells in injured Achilles tendon specimens at the indicated time points. **(C)** Serum concentrations of melatonin from normal rats or rats with Achilles tendon injuries at different time points. The data represent the mean ± SD. $^{**}P < 0.01$, $^{***}P < 0.001$ *versus* the normal control.

the ELISA results. Additionally, melatonin was observed in vascular endothelial cells, in infiltrating mesenchymal cells at 4 weeks [**Figure 1A(j)**] and in chondrocytes, osteoblasts, and some newly formed bone marrow cells from 8 to 12 weeks [**Figures 1A(k,l)**]. These findings demonstrate that melatonin is important for HO formation and that melatonin might contribute to the different stages of HO formation in injured Achilles tendons.

Roles of the MT1 and MT2 Melatonin Receptors Throughout HO Formation in Injured Achilles Tendons

Heterotopic ossification formation in injured Achilles tendons is a process of endochondral ossification. Consequently, we identified the different stages of HO formation by conducting IFC on specimens from experimental rats; we used a CD31 antibody to represent the angiogenesis stage, a SOX9 antibody to represent the chondrogenesis stage and an OCN antibody to represent the osteogenesis stage (**Figures 2A–C**). The results showed that high numbers of CD31-positive cells were observed 4 weeks after the operation, while SOX9- and OCN-positive cells were mainly observed 8 and 12 weeks after the operation in the injured Achilles tendon; these results were in line with the histological analyses shown in **Figure 1A**. To investigate the roles of the MT1 and MT2 melatonin receptors in HO formation in injured Achilles tendons, specific IFC antibodies against MT1 and MT2 were used to stain the different melatonin receptors in specimens from rats with Achilles tendon injuries at 4, 8, and 12 weeks after the operation (**Figures 2A–C**). The data revealed that MT2-positive cells were more prominent at every indicated time point after the operation than MT1-positive cells (**Figures 2A–F**), suggesting a primary effect of the MT2 melatonin receptor on HO formation. Furthermore, to illustrate the potential relationship between the MT1/MT2 melatonin receptors and vascular endothelial cells, chondrocytes and osteoblasts in the progression of HO formation in injured Achilles tendons, we then performed double-labeling IFC staining on specimens from rats with Achilles tendon injuries (**Figures 2A–C**). The data showed the colocalization of melatonin with the vascular endothelial marker CD31, the chondrogenic marker SOX9 and the osteogenic marker OCN near the injured Achilles tendons, suggesting that melatonin receptors play a role in endochondral ossification in the injured Achilles tendon. These data suggest that melatonin and the MT2 melatonin receptor participate in HO formation in injured Achilles tendons.

Effect of the Melatonin-MT2 Pathway on HO Formation in Injured Achilles Tendons

To evaluate the effect of the melatonin-MT2 pathway on HO formation *in vivo*, both melatonin and the MT2 receptor selective inhibitor 4-P-PDOT were administered to rats with Achilles tendon injuries, and we saline treatment and normal rats were used as controls. Micro–CT and HE staining were conducted to assess ectopic bone occurrence in rats with Achilles tendon injuries 12 weeks after surgery. The data show that compared with the normal control and saline treatments, the administration of melatonin to the rats with Achilles tendon injuries clearly increased the HO bone volume and calcified area, whereas melatonin combined with 4-P-PDOT treatment exerted a rescue effect on HO formation, showing a significant reduction in ectopic bone and calcified area (**Figure 3A**). In addition, quantitative analysis of the bone volume and calcified HO area suggested that compared with the normal control and saline treatment, melatonin significantly increased both the bone volume and calcified area of the injured Achilles tendons (**Figures 3B,C**). The results show that melatonin treatment significantly promotes HO formation, and inhibition of the melatonin-MT2 pathway suppresses HO formation in injured Achilles tendons.

Role of Melatonin in EndMT of RAOECs

As previously described, BMP-4 and TGF-β2 are identified as the inducer of EndMT (Zhang et al., 2019), which is associated with HO formation (Sun et al., 2016). Therefore, we induced EndMT in primary RAOECs by treatment with BMP-4 and TGF-β2 and investigated the effects of melatonin on endothelial- and mesenchymal-specific marker expression during EndMT. Initially, The morphology identification as well as IFC staining with CD31 and Tie-1 antibodies was carried out to identify the primary cells (**Figure 4A**). To evaluate the efficacy of melatonin treatment as well as to determine the suitable concentration, RAOECs were treated with 1, 10, 100, and 200ng/ml of melatonin as well as BMP-4 (100 ng/ml), and TGF-β2 (100 ng/ml), respectively, for 96 h in preliminary experiments (**Supplementary Figure 1B**). For the formal study, the CCK-8 assay showed that primary RAOECs exhibited no significant difference in cell proliferation after 48 h of culture in the presence of melatonin, BMP-4 and TGF-β2 (**Figure 4B**); these results suggest that stimulation with 10 ng/ml melatonin and 100 ng/ml BMP-4 and TGF-β2 did not cause toxic effects on the growth of RAOECs. We next performed scratch, transwell and invasion and migration assays to evaluate the effect of melatonin on cell motility. Compared with the control group, the melatonin-treated group exhibited notably enhanced scratch closure after 48 h of treatment, and the data showed that the cells in the BMP-4 and TGF-β2 treatment groups exhibited migration capacity similar to those in the melatonin treatment group (**Figures 4C,D**). Furthermore, we confirmed the effect of melatonin on the migration ability of RAOECs by conducting transwell and invasion assays. The data showed similar results to those of the scratch assay (**Figures 4E,F**).

Subsequently, assessment of the expression of EndMT markers by quantitative RT-PCR and western blotting with protein quantification analysis suggested that treatment with melatonin, BMP-4 and TGF-β2 for 2 weeks downregulated the endothelial markers VE-cadherin, Tie-1 and CD31 and upregulated the mesenchymal markers N-cadherin, FSP-1 and vimentin at both the gene and protein levels (**Figures 5A–C**); these results indicated that melatonin can induce EndMT in RAOECs. To determine whether RAOECs acquire a stem cell–like phenotype after EndMT induction, flow cytometry was performed to examine the co-expression of the specific markers for endothelial cells (including CD31 and CD105) as well as mesenchymal cells (including CD44 and CD90). The data showed that the cells in control group were positive for CD31 and CD105 but negative for CD44 and CD90. Furthermore, compared to the control-treated cells, the melatonin-treated cells expressed not only the endothelial markers CD31 and CD105

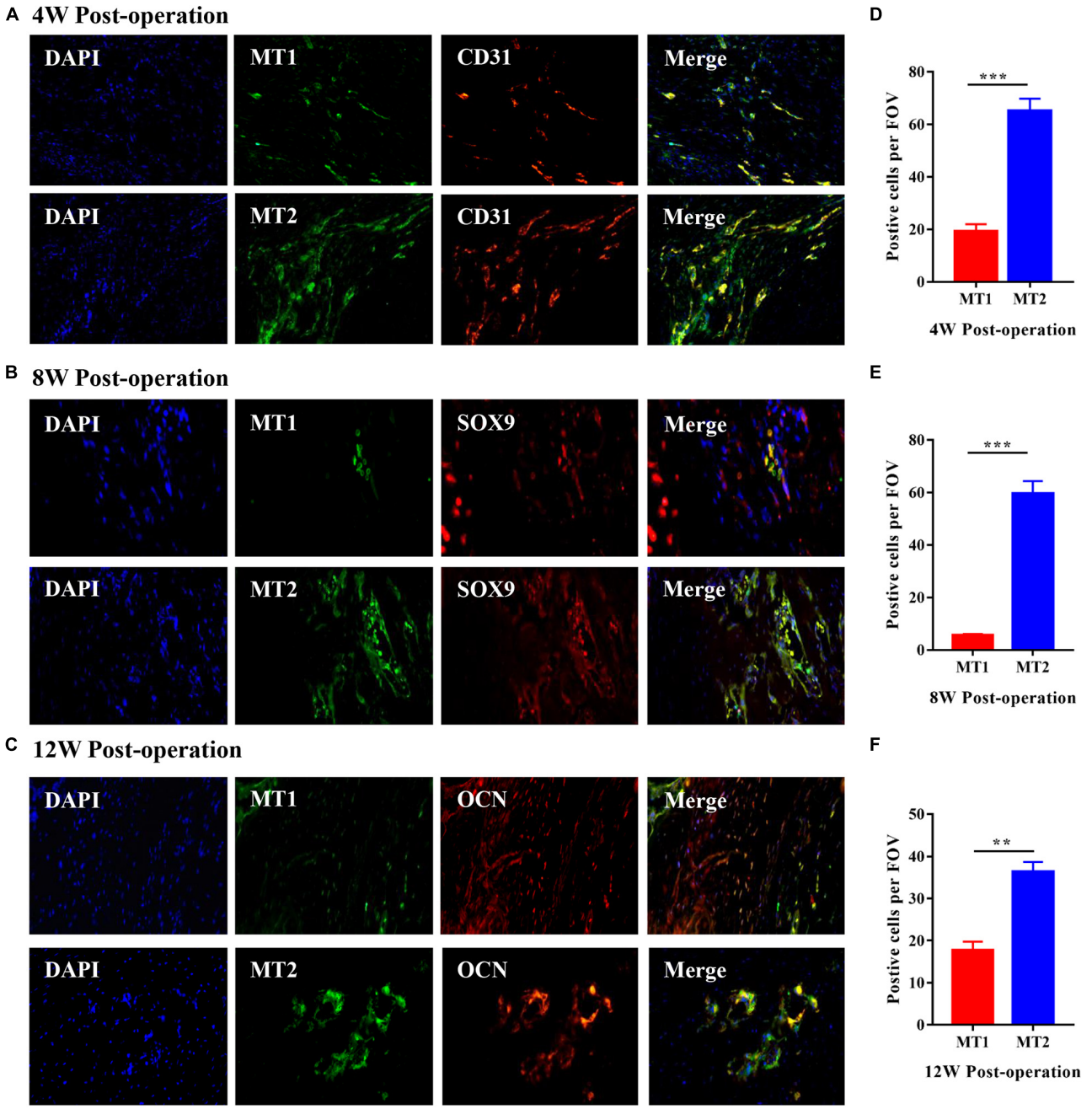

FIGURE 2 | Roles of the MT1 and MT2 melatonin receptors throughout HO formation in injured Achilles tendons. **(A)** IFC analysis of HO specimens of injured Achilles tendons at 4 weeks after the operation with antibodies specific for the vascular endothelial marker CD31 (red), the MT1 melatonin receptor (green) and the MT2 melatonin receptor (green). Images show the coexpression of CD31 and MT1 (upper) and the coexpression of CD31 and MT2 (bottom). **(B)** IFC analysis of HO specimens from injured Achilles tendons at 8 weeks after the operation with antibodies specific for the chondrogenic marker SOX9 (red), the MT1 melatonin receptor (green) and the MT2 melatonin receptor (green). Images show the coexpression of SOX9 and MT1 (upper) and the coexpression of SOX9 and MT2 (bottom). **(C)** IFC analysis of HO specimens from injured Achilles tendons at 12 weeks after the operation with antibodies specific for the osteogenic marker OCN (red), the MT1 melatonin receptor (green) and the MT2 melatonin receptor (green). Images show the coexpression of OCN and MT1 (upper) and the coexpression of OCN and MT2 (bottom). Blue represents nuclear DAPI staining. Scale bar, 20 μm. **(D–F)** The number of MT2-positive cells was higher than that of MT1-positive cells at the indicated time points. The data represent the mean ± SD. $^{**}P < 0.01$, $^{***}P < 0.001$ *versus* the MT1 group.

but also the classic mesenchymal markers CD44 and CD90, and obvious expression of these markers was also observed in the BMP-4- and TGF-β2-treated cells (**Figure 5D**). Taken together, these data suggest that melatonin can induce EndMT and acquisition of a mesenchymal stem-like phenotype in EndMT-induced RAOECs.

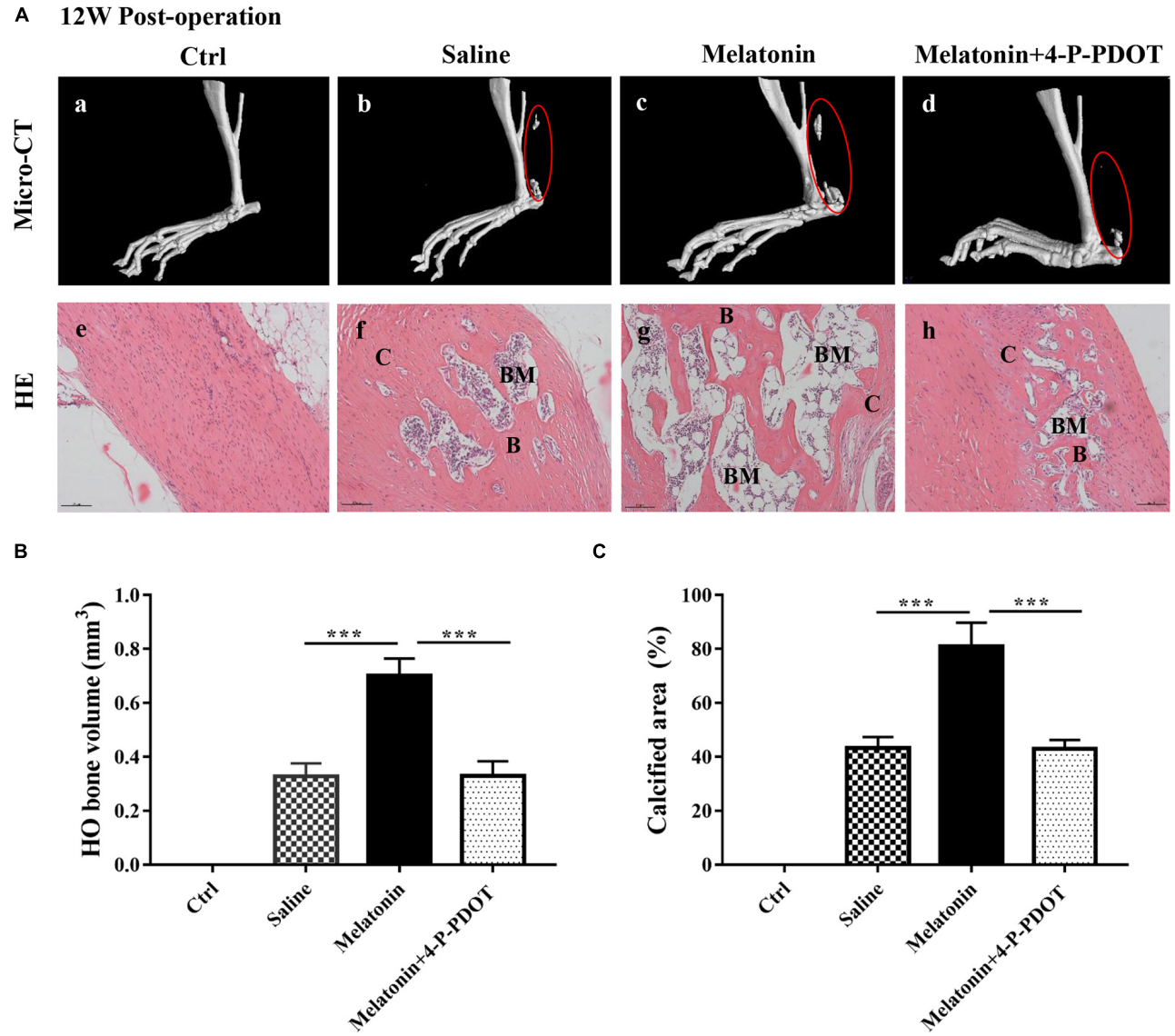

FIGURE 3 | Effect of the melatonin-MT2 pathway on HO formation in injured Achilles tendons. **(A)** Micro-CT scans of HO formation in specimens from Achilles tendons from normal rats **(a)**, saline-treated rats **(b)**, melatonin-treated rats **(c)**, and melatonin- and 4-P-PDOT-treated rats **(d)** at 12 weeks after the operation. HE staining of normal and injured Achilles tendons and heterotopic ossification from the different groups mentioned above. B, bone; BM, bone marrow; C, cartilage, black arrows: blood vessels, black triangles: chondrocytes. The dashed line of the SOFG-stained sections shows the newly formed heterotopic bone. Scale bar, 100 μm. **(B)** HO volume (mm^3) at injured Achilles tendons at 12 weeks. **(C)** Quantitative histological analyses of the proportions (%) of calcified areas at injured Achilles tendons at 12 weeks. The data represent the mean ± SD. ***$P < 0.001$ *versus* the saline control group or the melatonin group.

Effect of Melatonin on Osteogenesis in EndMT-Induced RAOECs

To further investigate the effect of melatonin on HO formation, we next assessed the osteogenesis ability of melatonin-treated RAOECs *in vitro*. RAOECs were cultured with melatonin, BMP-4 and TGF-β2 for 2 weeks to induce EndMT, and then, these cells were induced to undergo osteogenic differentiation for another 3 weeks. As shown by cell staining, melatonin markedly increased ALP and Alizarin Red staining compared to the control treatment, and higher ALP and Alizarin Red staining absorbance was observed in the melatonin-treated cells. Similarly, BMP-4 and TGF-β2 led to a marked increase in ALP and Alizarin Red staining and absorbance (**Figure 6A**). Then, the osteogenic potential of the EndMT-induced RAOECs was confirmed by western blot with protein quantification analysis and quantitative RT-PCR, and the results showed an enhancement of osteogenesis-related genes and proteins, such as OSX, OPN, RUNX2, and OCN, in the melatonin treatment group (**Figures 6B–D**). Similar gene and protein expression patterns were observed in the BMP-4 and TGF-β2 treatment groups. In contrast, neither cell staining nor these osteogenic markers were detected in the control group. These results show that melatonin

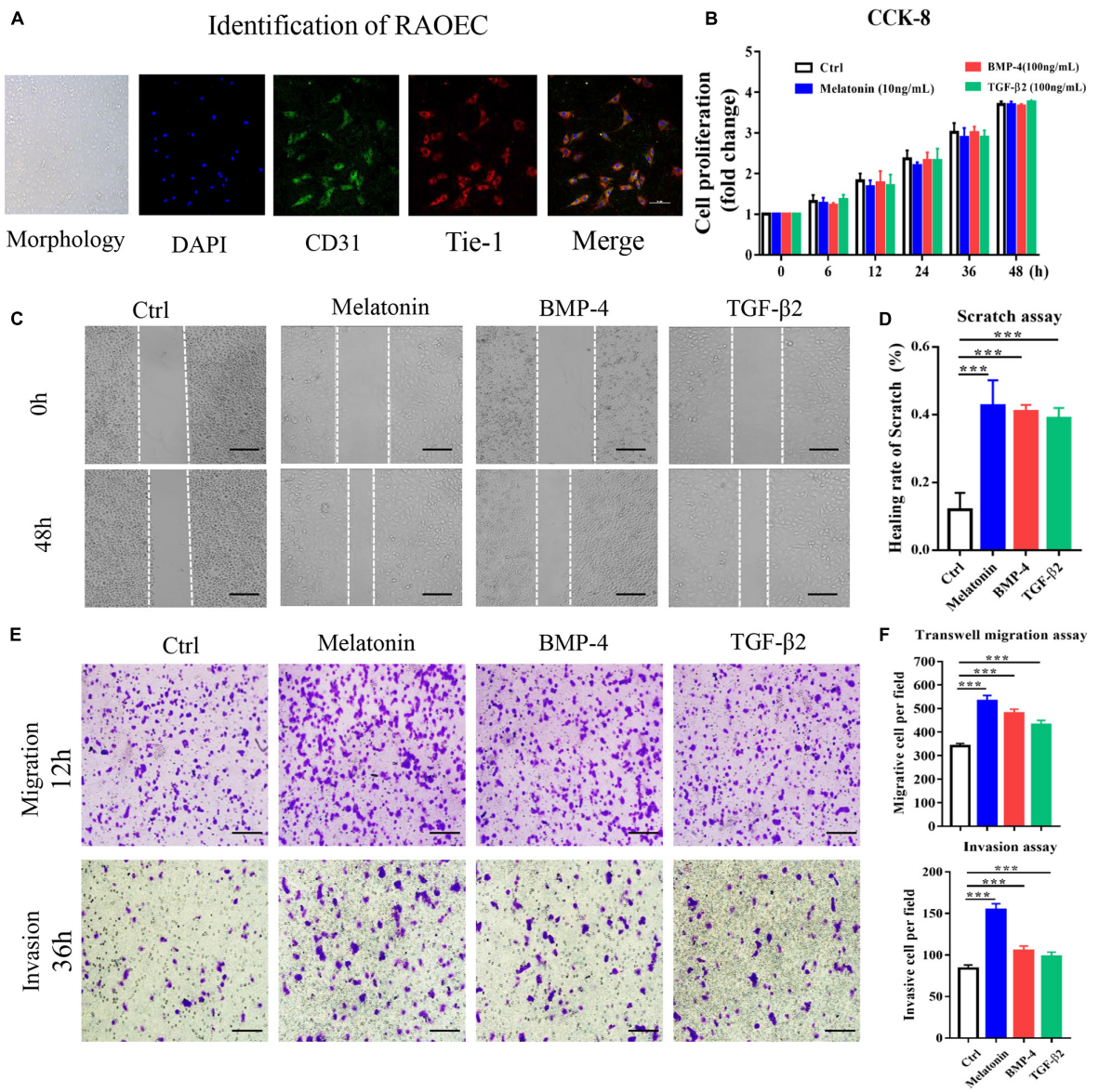

FIGURE 4 | Melatonin induces EndMT in RAOECs. Primary RAOECs were cultured with melatonin, BMP-4 or TGF-β2 for 48 h. **(A)** The morphology of primary RAOECs and identification of primary RAOECs with CD31 and Tie-1 antibodies by IFC. Scale bar, 20 μm. **(B)** Cell viability was assessed by the CCK-8 assay. **(C)** Migratory function was evaluated by scratch, transwell and invasion migration assays **(E)** with quantitative analysis **(D,F)**. Images of the scratch, transwell and invasion migration assays, showing that melatonin increased RAOEC migration compared with the control treatment. Scale bar, 50 μm. The data represent the mean ± SD. ***P < 0.001 *versus* the control group.

may contribute to the heterotopic bone formation associated with EndMT, confirming the osteogenic effect of melatonin on EndMT-induced RAOECs.

Role of the Melatonin-MT2 Pathway in the Induction of EndMT

To explore the role of the melatonin-MT2 pathway in the induction of EndMT during HO formation, 4-P-PDOT, a selective inhibitor of the MT2 melatonin receptor, was utilized and the expression of EndMT markers in RAOECs was analyzed. The quantitative RT-PCR results showed that 4-P-PDOT rescued the effect of melatonin on EndMT in RAOECs, upregulating the endothelial-specific genes (VE-cadherin, Tie-1, and CD31) and downregulating the mesenchymal-specific genes (N-cadherin, FSP-1, and vimentin) induced by melatonin (**Figure 7A**). Similarly, western blot with protein quantification analysis demonstrated that 4-P-PDOT reversed the downregulation of endothelial-specific proteins and the upregulation of mesenchymal-specific proteins induced by melatonin (**Figures 7B,C**). In addition, IFC staining illustrated that 4-P-PDOT inhibited the melatonin-induced expression of

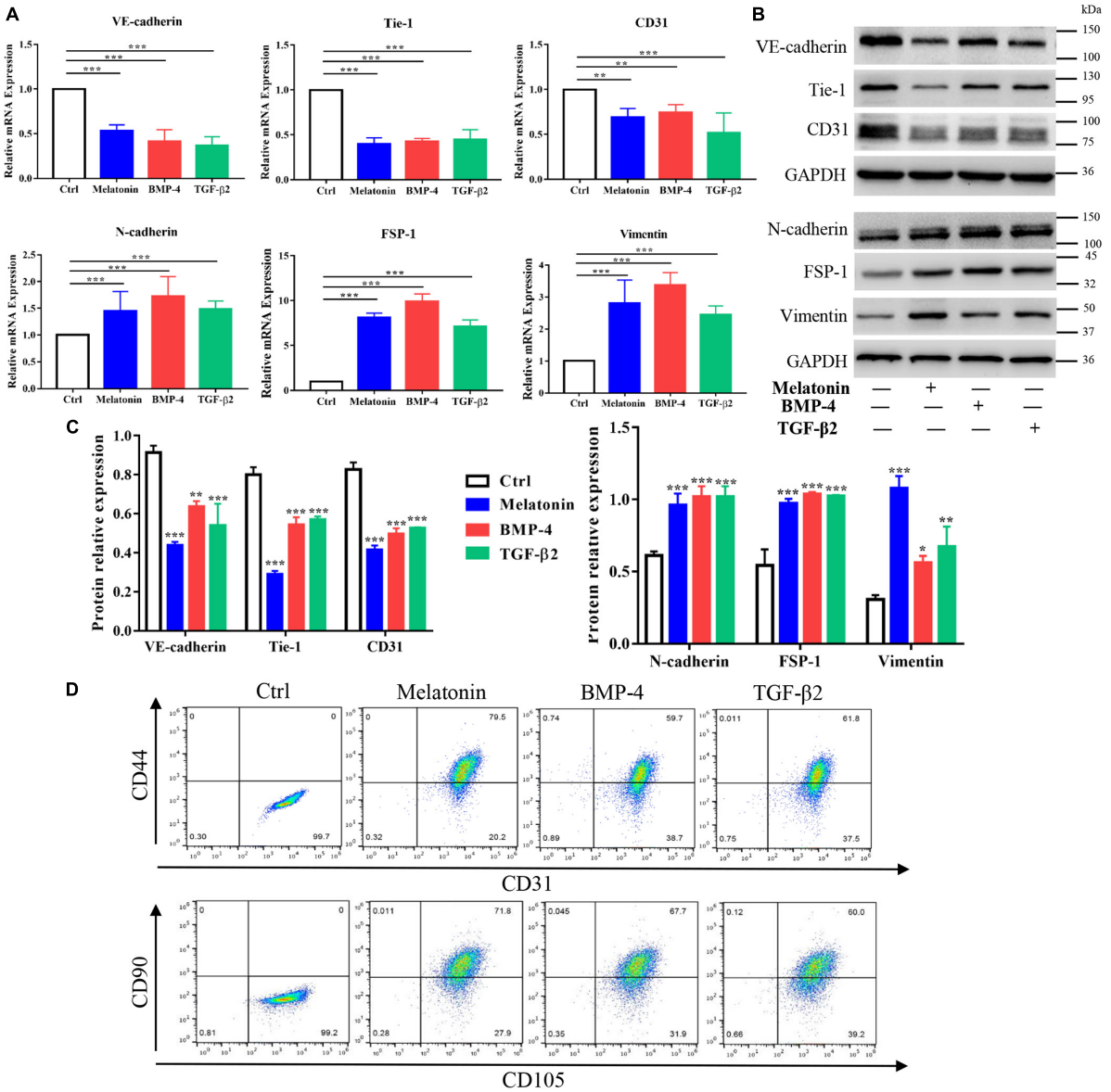

FIGURE 5 | Role of melatonin in EndMT of RAOECs. Primary RAOECs were cultured with melatonin, BMP-4 or TGF-β2 for 2 weeks. **(A)** Total RNA was extracted for quantitative RT-PCR. Quantitative RT-PCR showed that melatonin downregulated the expression of the endothelial markers VE-cadherin, Tie-1, and CD31 and upregulated the expression of the mesenchymal markers N-cadherin, FSP-1 and vimentin. **(B,C)** Protein lysates were extracted for western blot and protein quantification analysis, and the data showed results similar to those of quantitative RT-PCR. **(D)** Flow cytometry results showed the co-expression of CD31 and CD44 as well as CD105 and CD90 in RAOECs cultured with melatonin, BMP-4 or TGF-β2. The data represent the mean ± SD. $^{*}P < 0.05$, $^{**}P < 0.01$, $^{***}P < 0.001$ *versus* the control group.

the MSC marker CD44 (**Figure 7D**). Taken together, these results demonstrate that inhibition of the melatonin-MT2 pathway could suppress melatonin-induced EndMT in RAOECs.

Inhibition of the Melatonin-MT2 Pathway Suppressed Osteogenesis in EndMT-Induced RAOECs

To further examine the effect of melatonin on osteogenesis in EndMT-induced RAOECs, the cells were treated with both melatonin and 4-P-PDOT. The cell staining data showed that the effect of melatonin in increasing ALP and Alizarin Red staining was inhibited by 4-P-PDOT, leading to a marked reduction in the ALP and Alizarin Red staining absorbance (**Figure 8A**). Moreover, to determine the role of 4-P-PDOT in melatonin-accelerated osteogenesis *in vitro*, the expression of osteogenic markers was evaluated by quantitative RT-PCR and western blot. The data demonstrated that 4-P-PDOT significantly decreased the melatonin-induced high expression of OSX, OPN, RUNX2, and OCN at both the gene and protein levels (**Figures 8B,C**).

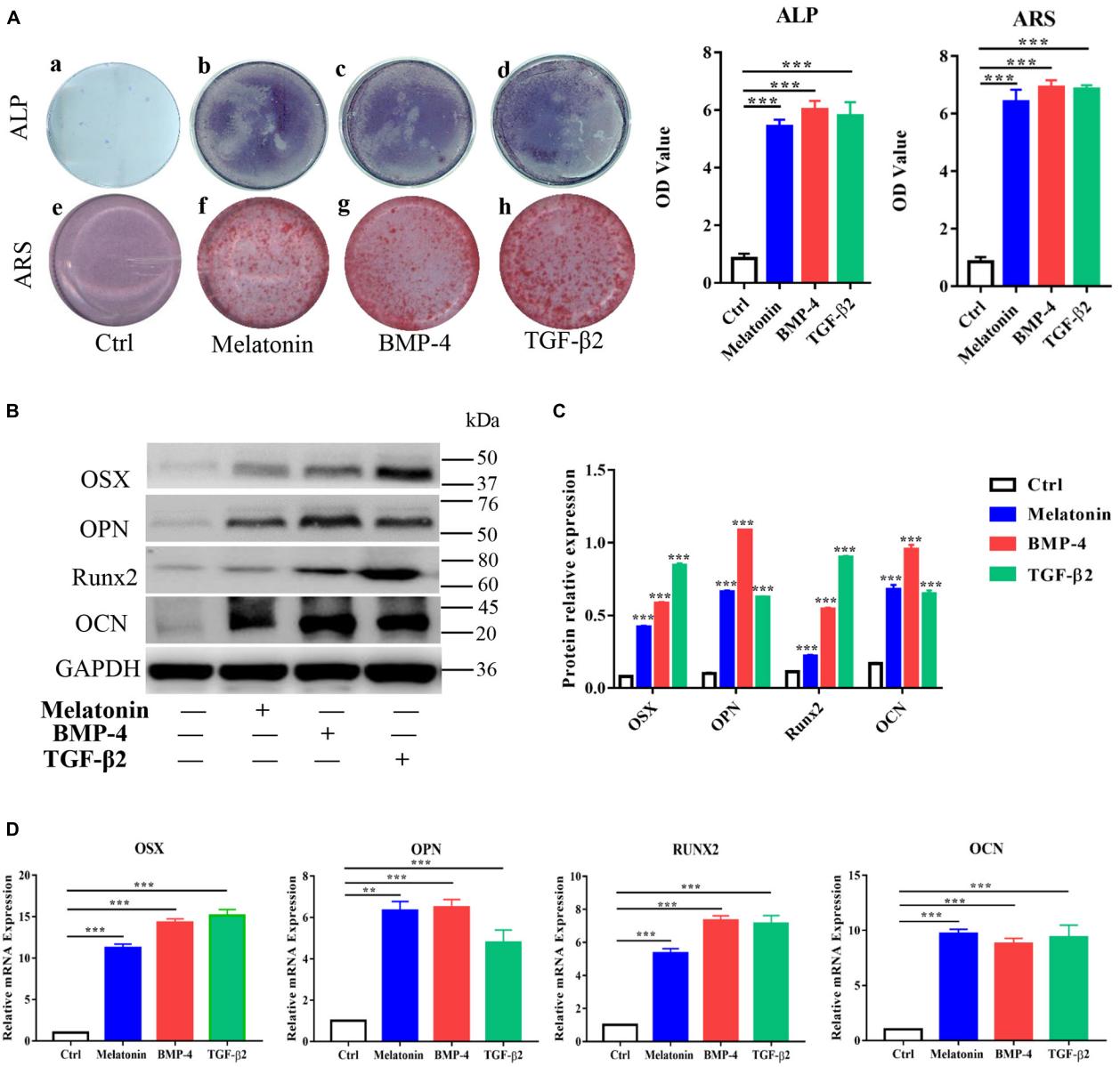

FIGURE 6 | Effect of melatonin on osteogenesis of EndMT-induced RAOECs. Primary RAOECs were induced to undergo EndMT for 2 weeks and further induced to undergo osteogenic differentiation for another 3 weeks. **(A)** Cells in the experimental and control groups were stained with ALP and Alizarin Red. **(B)** Western blot with quantification analysis **(C,D)** quantitative RT-PCR both showed that melatonin enhanced the expression of the osteogenic markers OSX, OPN, Runx2, and OCN. The data represent the mean ± SD. $^{**}P < 0.01$, $^{***}P < 0.001$ *versus* the control group.

Taken together, these data suggest that the effect of melatonin on osteogenesis in EndMT-induced RAOECs can be inhibited by the MT2-specific inhibitor 4-P-PDOT, demonstrating that inhibition of the melatonin-MT2 pathway can suppress HO formation *in vitro*.

DISCUSSION

Although pathological analysis has revealed that heterotopic ossification is a process of endochondral bone formation, the underlying cellular and molecular events leading to HO formation remain unclear. Our previous study showed that endothelial-mesenchymal transition (EndMT) plays a role in HO formation in rats with Achilles tendon injuries (Zhang et al., 2019). Heterotopic bone specimens from rats with posttraumatic HO in their Achilles tendons showed the coexpression of the endothelial marker Tie-1 with the osteogenic differentiation marker OCN, suggesting that the osteoblasts in heterotopic lesions are of endothelial origin. In addition, our data showed that osteoblasts from normal bone tissue do not stain positive for endothelial markers, suggesting that the osteoblasts in

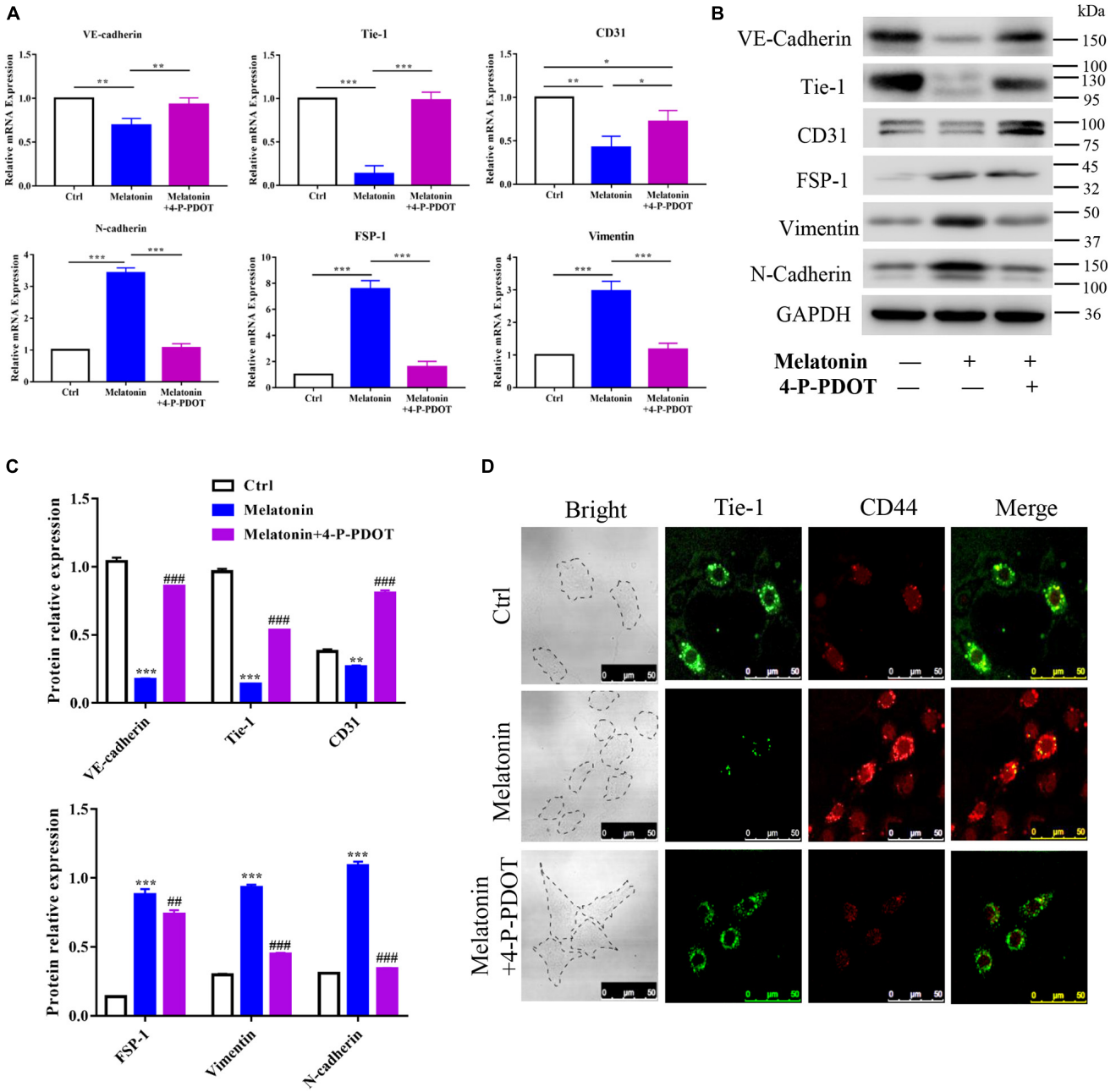

FIGURE 7 | Role of the melatonin-MT2 pathway in the induction of EndMT. Primary RAOECs were induced to undergo EndMT with melatonin in the presence or absence of 4-P-PDOT for 2 weeks. **(A,B)** Quantitative RT-PCR and western blot with protein quantification **(C)** analyses showed that 4-P-PDOT reversed the melatonin-induced expression of endothelial markers and mesenchymal markers. **(D)** IFC staining also showed a reduction in the expression of MSC markers in the melatonin- and 4-P-PDOT-treated group. The data represent the mean ± SD. $^{*}P < 0.05$, $^{**}P < 0.01$, and $^{***}P < 0.001$ *versus* the control group and melatonin group. $^{\#\#}P < 0.01$, $^{\#\#\#}P < 0.001$ versus the melatonin group.

HO are generated via EndMT. Furthermore, our previous study showed that neuroendocrine signaling factors, such as Neurotrophin-3, and other cytokines, such as BMP-4 and TGF-β2, induce EndMT in RAOECs by driving the transition from vascular endothelial cells into mesenchymal stem-like cells and promoting the gene and protein expression of EndMT and MSC markers. In the current study, the molecular mechanism by which melatonin participates in the EndMT during HO formation in rats with Achilles tendon injuries was investigated. First, we demonstrated the expression of melatonin on surgical specimens from a rat model of Achilles tenotomy-induced posttraumatic HO formation. Subsequently, we identified the role of the MT2 receptor in HO formation. Additionally, we illustrated that melatonin induced the EndMT of RAOECs

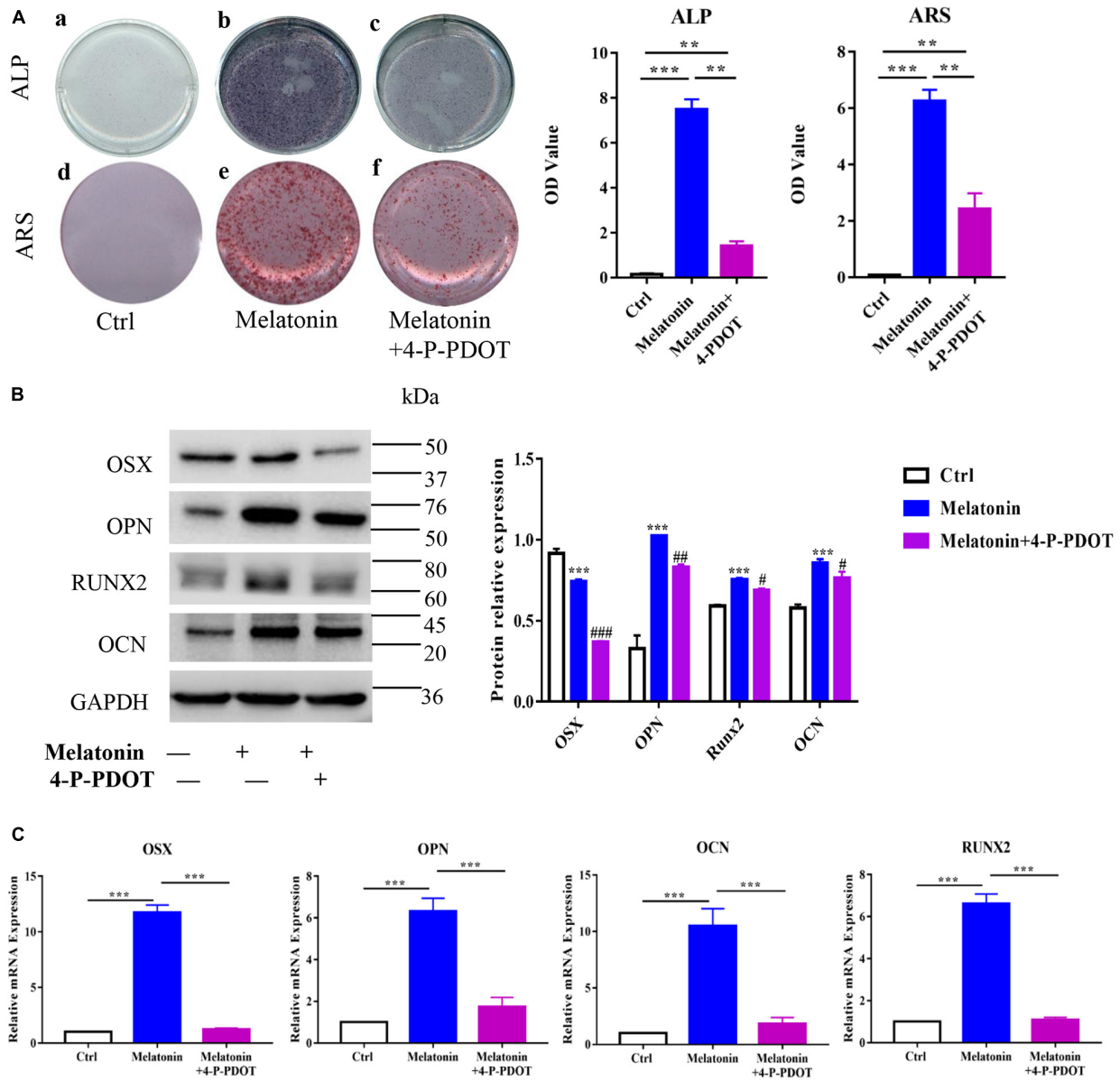

FIGURE 8 | Inhibition of the melatonin-MT2 pathway suppressed the osteogenesis of EndMT-induced RAOECs. **(A)** The rescue effect of 4-P-PDOT on melatonin-induced osteogenesis was observed by ALP and Alizarin Red staining. **(B,C)** Western blot with protein quantification and quantitative RT-PCR showed that 4-P-PDOT reversed the melatonin-induced expression of osteogenic differentiation markers. The data represent the mean ± SD. $^{**}P < 0.01$, $^{***}P < 0.001$ *versus* the control group and melatonin group. $^{\#}P < 0.05$, $^{\#\#}P < 0.01$, and $^{\#\#\#}P < 0.001$ versus the melatonin group.

and enhanced the osteogenic differentiation potential of MSC-like cells generated by EndMT. Furthermore, inhibition of the melatonin-MT2 pathway suppressed the role of melatonin in enhancing EndMT and osteogenic differentiation of EndMT-generated MSC-like cells.

Melatonin is a neuroendocrine molecule that is produced by the pineal gland and other organs and has been shown to exert a broad range of biological effects, including antioxidant, anti-inflammation, oncostatic, and circadian and endocrine rhythm regulatory effects (Hill et al., 2015; Mortezaee and Khanlarkhani, 2018; Ikegame et al., 2019). Recently, an increasing number of studies have reported that melatonin exerts a potent regulatory effect on the viability, proliferation and differentiation of various types of stem cells, such as MSCs, endothelial progenitor cells (EPCs) and induced pluripotent stem cells (iPSCs) (Luchetti et al., 2014). Due to its broad spectrum of effects, melatonin can regulate the differentiation of MSCs into osteogenic, chondrogenic and other lineages, opening up novel avenues for exploring its functions in the skeletal system. Previous studies have shown the effect of melatonin in promoting the osteoblastic mineralization and differentiation of MC3T3-E1 cells by increasing ALP activity and ALP, OSX, and OCN transcription

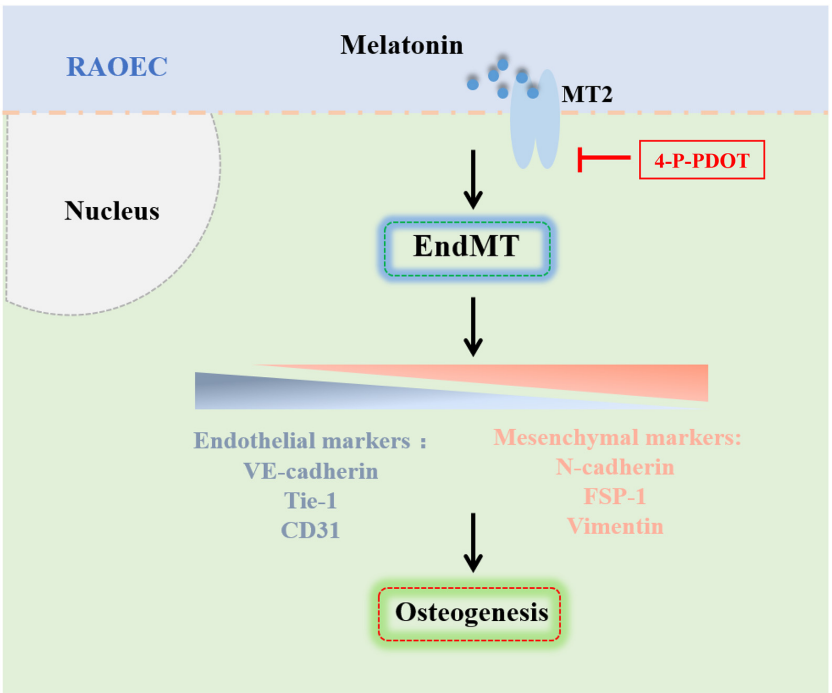

FIGURE 9 | Schematic representation of the mechanism by which melatonin promotes HO formation by regulating EndMT through the MT2 receptor pathway. Melatonin promotes HO formation by inducing EndMT and generating vascular endothelial-derived MSC-like cells through the MT2 melatonin receptor pathway.

levels in hypoxic environments, and the selective antagonist of melatonin receptors strikingly inhibits these effects (Jang-Ho Son et al., 2014; Son et al., 2017). Similarly, studies have shown that melatonin notably rescues the osteogenic differentiation of BMSCs by impairing the senescence of BMSCs caused by iron overload and preventing the reduction of cell proliferation (Yang et al., 2017a,b). Furthermore, enhancement in bone mass and facilitation of new bone growth were reported as positive functions of melatonin in the skeletal system (Majidinia et al., 2018). Although these previous studies investigated and reported the stimulatory effect of melatonin on osteogenic differentiation, the role of melatonin in aberrant bone tissue repair, especially in HO formation, remains largely unknown. In the present study, we observed that melatonin expression was markedly induced during the formation of heterotopic bone at the site of injured Achilles tendons. Melatonin was localized to vascular endothelial cells, chondrocytes, osteoblasts and some newly formed bone marrow cells at the injured sites. In addition, ELISA kits showed that melatonin expression in the serum was upregulated in a time-dependent manner at the early stage of osteogenesis and downregulated at the late stage of HO formation. These results illustrated that melatonin participates in HO formation in injured Achilles tendons in rats. While a previous study showed that higher serum levels of melatonin were observed in AS patients with spinal bone ossification formed (Li et al., 2020), our data showed that administration of melatonin led to increased heterotopic bone volume and calcified areas at the sites of injured Achilles tendons, suggesting that melatonin can accelerate HO formation. With these findings, we speculated that melatonin may play an important role in HO formation; however, the precise mechanisms and signaling pathways involved in this process remain unclear.

It has been suggested that the classic pathway through which melatonin exerts most its physiological effects is the receptor-dependent pathway (Luchetti et al., 2014). Melatonin receptor (MT), a member of the G protein-coupled receptor (GPCR) family, consists of two subtypes in mammals, MT1 and MT2 (Lacoste et al., 2015). Melatonin activates the coupled G protein by binding to the MT receptors, leading to the activation of many critical downstream signaling pathways. In addition to the central nervous system, MT receptors are also widely expressed in other tissues, including the skin, gonads and gastrointestinal tract (Stazi et al., 2020). Increasing evidence has shown that the MT2 melatonin receptor mediates the effect of melatonin on osteoblastic differentiation and bone mass regulation, while inactivation of MT1 does not affect bone mass (Sharan et al., 2017; Maria et al., 2018). Therefore, to investigate whether melatonin receptors were responsible for the effect of melatonin on HO formation in rats with Achilles tendon injuries, we measured the expression of the MT1 and MT2 melatonin receptors on surgical specimens from the experimental rats. Our data showed that melatonin receptors, including MT1 and MT2, were expressed at the sites of injured Achilles tendons throughout HO formation. Furthermore, we analyzed the expression of the MT1 and MT2 melatonin receptors over a time course and found that the MT2 melatonin receptor was more highly induced than the MT1 melatonin receptor at every stage of HO formation. These results supported the primary role of the MT2 melatonin

receptor in HO formation in injured Achilles tendons, which was consistent with previous findings about the dominant effect of the MT2 melatonin receptor in bone. Additionally, our double-labeling immunostaining studies revealed the colocalization of the MT1 and MT2 melatonin receptors with the vascular endothelial marker CD31, the chondrogenic differentiation marker SOX9 and the osteogenic differentiation marker OCN in injured Achilles tendons during HO formation, suggesting that melatonin receptors, especially the MT2 melatonin receptor, mediate the effects of melatonin in modulating HO formation in rats with Achilles tendon injuries.

Previous studies have confirmed the role of EndMT in traumatic HO formation and showed the osteogenic differentiation ability of endothelial-derived MSC-like cells generated by EndMT (Lounev et al., 2009; Medici et al., 2010); however, none of these studies elucidated the underlying mechanisms of EndMT regulation. Neuroendocrine signals, which are regarded as potential mediators of EndMT (Salisbury et al., 2011; Lazard et al., 2015), have been shown to be associated with the bone system as they regulate the viability, proliferation and differentiation of osteoblasts (Takeda and Karsenty, 2008). Stimulatory actions of melatonin in the regulation of bone formation have been reported in various studies (Luchetti et al., 2014; Altındal and Gümüşderelioğlu, 2016; Pytka et al., 2017). However, precise details revealing the regulatory mechanism of melatonin in EndMT during HO formation are lacking. In the current study our data showed that similar to BMP-4 and TGF-β2, melatonin induced the transition from vascular endothelial cells into mesenchymal cells by altering the cellular migratory and invasive functions. Melatonin induced the expression of mesenchymal cell markers and inhibited the expression of vascular endothelial cell markers. These data suggested that melatonin can induce EndMT. Furthermore, vascular endothelial cells that underwent melatonin-induced EndMT notably expressed MSC markers, such as CD44 and CD90, confirming that EndMT can generate mesenchymal stem-like cells. Subsequently, the present study showed that melatonin promoted the osteogenic differentiation of mesenchymal stem-like cells generated by EndMT by increasing the expression of OSX, RUNX2, and OCN at both the gene and protein levels; these data indicate that melatonin can promote HO formation by mediating EndMT. Taken together, the current study identified for the first time the profound role of melatonin in EndMT and HO formation.

To further illustrate the underlying signaling pathway by which melatonin participates in the HO formation associated with EndMT, we selected the MT2 melatonin receptor-specific inhibitor 4-P-PDOT for use in these studies. 4-P-PDOT, which has been shown to be an MT2-specific antagonist (Juszczak et al., 2014), was used to block the function of melatonin. As shown in our data, treatment with 4-P-PDOT not only suppressed the increase in heterotopic bone volume at injured Achilles tendons but also attenuated the effect of melatonin on inducing EndMT and promoting osteogenic differentiation. Treatment with 4-P-PDOT reversed the melatonin-induced EndMT by upregulating endothelial markers and downregulating mesenchymal and MSC markers at both the gene and protein levels in RAOECs *in vitro*. For osteogenesis, 4-P-PDOT reduced the melatonin-induced osteogenic differentiation by regulating gene and protein expression and inhibited mineralization in RAOECs. Additionally, 4-P-PDOT reversed the melatonin-induced acceleration of HO formation in rats with Achilles tendon injuries. Taken together, our data suggested an effect of the melatonin-MT2 pathway on HO formation both *in vivo* and *in vitro* and revealed that inhibition of the melatonin-MT2 pathway by 4-P-PDOT could suppress the induction of EndMT and HO formation in injured Achilles tendons. These findings may provide a novel preventive therapy for HO management.

Although we have identified a role of melatonin in EndMT on HO formation, in addition to vascular endothelial cells, melatonin has been reported to regulate the differentiation of a variety of MSCs at sites of injury. Therefore, further studies should be conducted to identify other candidate MSCs that are responsible for the formation of HO. Additionally, according to our data, the expression of melatonin was rarely found in normal Achilles tendons compared to injured Achilles tendons, suggesting that melatonin may not be generated and secreted near normal Achilles tendons. Thus, further research should focus on the potential sources of melatonin during HO formation at injured Achilles tendons. Moreover, the effects of melatonin on EndMT may be controversial according to a recent study (Liu et al., 2018). Liu et al. (2018) have demonstrated that melatonin could attenuate EndMT of GEnCs in diabetic nephropathy. Within this controversy, we may consider the different effects of melatonin on EndMT may be caused by the different biological pathway that melatonin plays its effects. Previous study has revealed that melatonin regulates various of physiological activities either through melatonin receptors (including MT1, MT2, or MT3) or by acting directly as an antioxidant in cells. The impairment of diabetic nephropathy was mainly related with oxidative stress injury, thus Liu et al. have suggested that melatonin's antioxidant activity might be useful in treating diabetes and attenuating diabetic nephropathy, and reported that melatonin could attenuate EndMT of GEnCs. In addition, accumulating studies (Elbe et al., 2014; Onk et al., 2016; Winiarska et al., 2016) have supported the idea that melatonin has antioxidant and anti-inflammation activities in diabetic nephropathy. Based on these data and evidence, we believed that melatonin, which may play its direct antioxidant, attenuated EndMT of GEnCs in diabetic nephropathy. On the contrary, our data supported the primary role of the MT2 melatonin receptor in HO formation in injured Achilles tendons, which was consistent with previous findings about the dominant effect of the MT2 melatonin receptor in bone. Moreover, inhibition of melatonin-MT2 pathway both suppressed the EndMT induction and HO formation. Taken together, we believed that melatonin could promote EndMT in RAOECs through its MT2 melatonin receptor in HO formation of Achilles tendons injury rats. In addition, our main strength was that we utilized simple and repeatable rat models of Achilles tenotomy to illustrate the effects of melatonin on EndMT during HO, as well as the potential mechanisms. More importantly, we identified the role of the MT2 melatonin receptor in melatonin-induced EndMT and HO formation.

In summary, our analysis of rat models of Achilles tenotomy demonstrated that melatonin enhanced HO formation by promoting the osteogenic differentiation of vascular endothelial-derived MSC-like cells, which were generated by melatonin-induced EndMT. Inhibition of the melatonin-MT2 pathway could suppress EndMT induction and HO formation. Taken together, these findings illustrated the role and underlying mechanism of melatonin in the pathogenesis of HO formation (**Figure 9**), and these findings are expected to provide new strategies and targets for the clinical prevention and treatment of HO.

DATA AVAILABILITY STATEMENT

The original contributions generated for this study are included in the article/**Supplementary Material**, further inquiries can be directed to the corresponding author/s.

ETHICS STATEMENT

These experiments were approved by the Ethical Committee for Animal Research (IAC1907001).

AUTHOR CONTRIBUTIONS

JZ, ZZ, and LW contributed to the study conception and design. Material preparation and data acquisition were performed by JL and JT. JZ, BiY, and BoY performed the experiments. JZ, MH, and LW contributed to the data analysis and interpretation. The first draft of the manuscript was written by JZ, ZZ, and LW. All authors approved the submitted version and agreed to be personally accountable for the authors own contributions and manuscript contents.

FUNDING

The study was supported by grants from the National Natural Science Foundation of China (81874013) and Natural Science Foundation of Guangdong Province (2019A1515011887).

SUPPLEMENTARY MATERIAL

The Supplementary Material for this article can be found online at: https://www.frontiersin.org/articles/10.3389/fcell.2021.629274/full#supplementary-material

REFERENCES

Altındal, D. Ç, and Gümüşderelioğlu, M. (2016). Melatonin releasing PLGA micro/nanoparticles and their effect on osteosarcoma cells. *J. Microencapsul.* 33, 53–63. doi: 10.3109/02652048.2015.115901

Elbe, H., Vardi, N., Esrefoglu, M., Ates, B., Yologlu, S., and Taskapan, C. (2014). Amelioration of streptozotocin-induced diabetic nephropathy by melatonin, quercetin, and resveratrol in rats. *Hum. Exp. Toxicol.* 34, 100–113. doi: 10.1177/0960327114531995

Fan, C., Feng, J., Tang, C., Zhang, Z., Feng, Y., Duan, W., et al. (2020). Melatonin suppresses ER stress-dependent proapoptotic effects via AMPK in bone mesenchymal stem cells during mitochondrial oxidative damage. *Stem Cell Res. Ther.* 11, 442. doi: 10.1186/s13287-020-01948-5

Gugala, Z., Olmsted-Davis, E. A., Xiong, Y., Davis, E. L., and Davis, A. R. (2018). Trauma-induced heterotopic ossification regulates the blood-nerve barrier. *Front. Neurol.* 9:108. doi: 10.3389/fneur.2018.00408

Han, Y., Kim, Y. M., Kim, H. S., and Lee, K. Y. (2017). Melatonin promotes osteoblast differentiation by regulating Osterix protein stability and expression. *Sci. Rep.* 7, 5716. doi: 10.1038/s41598-017-06304-x

Hill, S., Belancio, V., Dauchy, R., Xiang, S., Brimer, S., Mao, L., et al. (2015). Melatonin: an inhibitor of breast cancer. *Endocr. Relat. Cancer* 22, R183–R204. doi: 10.1530/ERC-15-0030

Huang, H., Cheng, W. X., Hu, Y. P., Chen, J. H., Zheng, Z. T., and Zhang, P. (2018). Relationship between heterotopic ossification and traumatic brain injury: why severe traumatic brain injury increases the risk of heterotopic ossification. *J. Orthop. Transl.* 12, 16–25. doi: 10.1016/j.jot.2017.10.002

Ikegame, M., Hattori, A., Tabata, M. J., Kitamura, K. I., Tabuchi, Y., Furusawa, Y., et al. (2019). Melatonin is a potential drug for the prevention of bone loss during space flight. *J. Pineal Res.* 67, e12594. doi: 10.1111/jpi.12594

Jiang, H., Chen, Y., Chen, G., Tian, X., Tang, J., Luo, L., et al. (2017). Leptin accelerates the pathogenesis of heterotopic ossification in rat tendon tissues via mTORC1 signaling. *J. Cell Physiol.* 233, 1017–1028. doi: 10.1002/jcp.25955

Juszczak, M., Roszczyk, M., Kowalczyk, E., and Stempniak, B. (2014). The influence od melatonin receptors antagonists, luzindole and 4-phenyl-2-propionamidotetralin (4-P-PDOT), on melatonin-dependent vasopressin and adrenocorticotropic hormone (ACTH) release from the rat hypothalamo-hypophysial system. In vitro and in vivo studies. *J. Physiol. Pharmacol.* 65, 777–784.

Kenneth, J., and Livak, T. D. S. (2001). Analysis of relative gene expression data using RealTime quantitative PCR and the 2-DDCT method. *Methods* 25, 402–408. doi: 10.1006/meth.2001.126

Lacoste, B., Angeloni, D., Dominguez-Lopez, S., Calderoni, S., Mauro, A., Fraschini, F., et al. (2015). Anatomical and cellular localization of melatonin MT1 and MT2 receptors in the adult rat brain. *J. Pineal Res.* 58, 397–417. doi: 10.1111/jpi.12224

Lazard, Z. W., Olmsted-Davis, E. A., Salisbury, E. A., Gugala, Z., Sonnet, C., Davis, E. L., et al. (2015). Osteoblasts have a neural origin in heterotopic ossification. *Clin. Orthop. Relat. Res.* 473, 2790–2806. doi: 10.1007/s11999-015-4323-9

Li, L., and Tuan, R. S. (2020). Mechanism of traumatic heterotopic ossification: in search of injury-induced osteogenic factors. *J. Cell Mol. Med.* 24, 11046–11055. doi: 10.1111/jcmm.15735

Li, Y., Cui, X., Li, Z., Jia, Q., Jiang, L., Zhang, Z., et al. (2020). High melatonin levels are related to spinal ossification in patients with ankylosing spondylitis. *Mod. Rheumatol.* 30, 373–378. doi: 10.1080/14397595.2019.1601854

Liu, F., Zhang, S., Xu, R., Gao, S., and Yin, J. (2018). Melatonin attenuates endothelial-to-mesenchymal transition of glomerular endothelial cells via regulating miR-497/ROCK in diabetic nephropathy. *Kidney Blood Press Res.* 43, 1425–1436. doi: 10.1159/000493380

Loder, S. J., Agarwal, S., Chung, M. T., Cholok, D., Hwang, C., Visser, N., et al. (2018). Characterizing the circulating cell populations in traumatic heterotopic ossification. *Am. J. Pathol.* 188, 2464–2473. doi: 10.1016/j.ajpath.2018.07.014

Lounev, V. Y., Ramachandran, R., Wosczyna, M. N., Yamamoto, M., Maidment, A. D., Shore, E. M., et al. (2009). Identification of progenitor cells that contribute to heterotopic skeletogenesis. *J. Bone Joint Surg. Am.* 91, 652–663. doi: 10.2106/JBJS.H.01177

Luchetti, F., Canonico, B., Bartolini, D., Arcangeletti, M., Ciffolilli, S., Murdolo, G., et al. (2014). Melatonin regulates mesenchymal stem cell differentiation: a review. *J. Pineal Res.* 56, 382–397. doi: 10.1111/jpi.12133

Majidinia, M., Reiter, R. J., Shakouri, S. K., Mohebbi, I., Rastegar, M., Kaviani, M., et al. (2018). The multiple functions of melatonin in regenerative medicine. *Ageing Res. Rev.* 45, 33–52. doi: 10.1016/j.arr.2018.04.003

Maria, S., Samsonraj, R. M., Munmun, F., Glas, J., Silvestros, M., Kotlarczyk, M. P., et al. (2018). Biological effects of melatonin on osteoblast/osteoclast cocultures, bone, and quality of life: implications of a role for MT2 melatonin receptors, MEK1/2, and MEK5 in melatonin-mediated osteoblastogenesis. *J. Pineal Res.* 64:e12465. doi: 10.1111/jpi.12465

Medici, D., and Olsen, B. R. (2012). The role of endothelial-mesenchymal transition in heterotopic ossification. *J Bone Miner Res.* 27, 1619–1622. doi: 10.1002/jbmr.1691

Medici, D., Shore, E. M., Lounev, V. Y., Kaplan, F. S., Kalluri, R., and Olsen, B. R. (2010). Conversion of vascular endothelial cells into multipotent stem-like cells. *Nat. Med.* 16, 1400–1406. doi: 10.1038/nm.2252

Meyers, C., Lisiecki, J., Miller, S., Levin, A., Fayad, L., Ding, C., et al. (2019). Heterotopic ossification: a comprehensive review. *JBMR Plus* 34, e10172. doi: 10.1002/jbm4.10172

Mortezaee, K., and Khanlarkhani, N. (2018). Melatonin application in targeting oxidative-induced liver injuries: a review. *J. Cell Physiol.* 233, 4015–4032. doi: 10.1002/jcp.26209

Onk, D., Onk, O. A., Turkmen, K., Erol, H. S., Ayazoglu, T. A., Keles, O. N., et al. (2016). Melatonin attenuates contrast-induced nephropathy in diabetic rats: the role of Interleukin-33 and oxidative stress. *Mediators Inflamm.* 2016:9050828. doi: 10.1155/2016/9050828

Piera-Velazquez, S., Li, Z., and Jimenez, S. A. (2011). Role of endothelial-mesenchymal transition (EndoMT) in the pathogenesis of fibrotic disorders. *Am. J. Pathol.* 179, 1074–1080. doi: 10.1016/j.ajpath.2011.06.001

Potenta, S., Zeisberg, E., and Kalluri, R. (2008). The role of endothelial-to-mesenchymal transition in cancer progression. *Br. J. Cancer* 99, 1375–1379. doi: 10.1038/sj.bjc.6604662

Pytka, K., Młyniec, K., Podkowa, K., Podkowa, A., Jakubczyk, M., Żmudzka, E., et al. (2017). The role of melatonin, neurokinin, neurotrophic tyrosine kinase and glucocorticoid receptors in antidepressant-like effect. *Pharmacol. Rep.* 69, 546–554. doi: 10.1016/j.pharep.2017.01.026

Salisbury, E., Rodenberg, E., Sonnet, C., Hipp, J., Gannon, F. H., Vadakkan, T. J., et al. (2011). Sensory nerve induced inflammation contributes to heterotopic ossification. *J. Cell Biochem.* 112, 2748–2758. doi: 10.1002/jcb.23225

Satomura, K., Tobiume, S., Tokuyama, R., Yamasaki, Y., Kudoh, K., Maeda, E., et al. (2007). Melatonin at pharmacological doses enhances human osteoblastic differentiation in vitro and promotes mouse cortical bone formation in vivo. *J. Pineal Res.* 42, 231–239. doi: 10.1111/j.1600-079X.2006.00410.x

Sharan, K., Lewis, K., Furukawa, T., and Yadav, V. K. (2017). Regulation of bone mass through pineal-derived melatonin-MT2 receptor pathway. *J. Pineal Res.* 63, e12423. doi: 10.1111/jpi.12423

Shore, E., Xu, M., Feldman, G., Fenstermacher, D., Cho, T., Choi, I., et al. (2006). A recurrent mutation in the BMP type I receptor ACVR1 causes inherited and sporadic fibrodysplasia ossificans progressiva. *Nat. Genet.* 38, 525–527. doi: 10.1038/ng1783

Son, J., Park, B., Kim, I., Sung, I., Cho, Y., Kim, J., et al. (2017). A novel combination treatment to stimulate bone healing and regeneration under hypoxic conditions: photobiomodulation and melatonin. *Lasers Med. Sci.* 32, 533–541. doi: 10.1007/s10103-017-2145-6

Son, J.-H., Cho, Y.-C., Sung, I.-Y., Kim, I.-R., Park, B.-S., and Kim, Y.-D. (2014). Melatonin promotes osteoblast differentiation and mineralization of MC3T3-E1 cells under hypoxic conditions through activation of PKD/p38 pathways. *J. Pineal Res.* 57, 385–392. doi: 10.1111/jpi.12177

Stazi, M., Negro, S., Megighian, A., D'Este, G., Solimena, M., Jockers, R., et al. (2020). Melatonin promotes regeneration of injured motor axons via MT receptors. *J. Pineal Res.* 70:e12695. doi: 10.1111/jpi.12695

Sun, Y., Cai, J., Yu, S., Chen, S., Li, F., and Fan, C. (2016). MiR-630 inhibits endothelial-mesenchymal transition by targeting slug in traumatic heterotopic ossification. *Sci. Rep.* 6, 22729. doi: 10.1038/srep22729

Takeda, S., and Karsenty, G. (2008). Molecular bases of the sympathetic regulation of bone mass. *Bone* 42, 837–840. doi: 10.1016/j.bone.2008.01.005

Winiarska, K., Dzik, J. M., Labudda, M., Focht, D., Sierakowski, B., Owczarek, A., et al. (2016). Melatonin nephroprotective action in Zucker diabetic fatty rats involves its inhibitory effect on NADPH oxidase. *J. Pineal Res.* 60, 109–117. doi: 10.1111/jpi.12296

Yang, F., Li, Y., Yan, G., Liu, T., Feng, C., Gong, R., et al. (2017a). Inhibition of iron overload-induced apoptosis and necrosis of bone marrow mesenchymal stem cells by melatonin. *Oncotarget* 8, 31626–31637. doi: 10.18632/oncotarget.16382

Yang, F., Yang, L., Li, Y., Yan, G., Feng, C., Liu, T., et al. (2017b). Melatonin protects bone marrow mesenchymal stem cells against iron overload-induced aberrant differentiation and senescence. *J. Pineal Res.* 63, e12422. doi: 10.1111/jpi.12422

Zhang, C., Zhang, Y., Zhong, B., and Luo, C. F. (2016). SMAD7 prevents heterotopic ossification in a rat Achilles tendon injury model via regulation of endothelial-mesenchymal transition. *FEBS J.* 283, 1275–1285. doi: 10.1111/febs.13667

Zhang, J., Wang, L., Cao, H., Chen, N., Yan, B., Ao, X., et al. (2019). Neurotrophin-3 acts on the endothelial-mesenchymal transition of heterotopic ossification in rats. *J. Cell Mol. Med.* 23, 2595–2609. doi: 10.1111/jcmm.14150

Conflict of Interest: The authors declare that the research was conducted in the absence of any commercial or financial relationships that could be construed as a potential conflict of interest.

frontiers in Cell and Developmental Biology

REVIEW
published: 18 February 2021
doi: 10.3389/fcell.2021.631272

Tendon Stem/Progenitor Cell Subpopulations and Their Implications in Tendon Biology

*Zizhan Huang[1,2,3], Zi Yin[3,4,5], Jialu Xu[6], Yang Fei[1,2,3], Boon Chin Heng[7], Xuesheng Jiang[8], Weishan Chen[1,2] and Weiliang Shen[1,2,3,4,5]**

[1] Department of Orthopedic Surgery, The Second Affiliated Hospital, School of Medicine, Zhejiang University, Hangzhou, China, [2] Orthopedics Research Institute, Zhejiang University, Hangzhou, China, [3] Institute of Sports Medicine, Zhejiang University, Hangzhou, China, [4] Dr. Li Dak Sum and Yip Yio Chin Center for Stem Cell and Regenerative Medicine, Zhejiang University, Hangzhou, China, [5] China Orthopedic Regenerative Medicine (CORMed), Hangzhou, China, [6] Department of Infectious Diseases, The First Affiliated Hospital, Wenzhou Medical University, Wenzhou, China, [7] School of Stomatology, Peking University, Beijing, China, [8] Department of Orthopedic Surgery, Huzhou Hospital, Zhejiang University, Huzhou, China

OPEN ACCESS

Edited by:
Simone Pacini, University of Pisa, Italy

Reviewed by:
Chavaunne T. Thorpe, Royal Veterinary College (RVC), United Kingdom
Denitsa Docheva, University Medical Center Regensburg, Germany

***Correspondence:**
Weiliang Shen
wlshen@zju.edu.cn

Specialty section:
This article was submitted to Stem Cell Research, a section of the journal Frontiers in Cell and Developmental Biology

Received: *19 November 2020*
Accepted: *27 January 2021*
Published: *18 February 2021*

Citation:
Huang Z, Yin Z, Xu J, Fei Y, Heng BC, Jiang X, Chen W and Shen W (2021) Tendon Stem/Progenitor Cell Subpopulations and Their Implications in Tendon Biology. Front. Cell Dev. Biol. 9:631272. doi: 10.3389/fcell.2021.631272

Tendon harbors a cell population that possesses stem cell characteristics such as clonogenicity, multipotency and self-renewal capacity, commonly referred to as tendon stem/progenitor cells (TSPCs). Various techniques have been employed to study how TSPCs are implicated in tendon development, homeostasis and healing. Recent advances in single-cell analysis have enabled much progress in identifying and characterizing distinct subpopulations of TSPCs, which provides a more comprehensive view of TSPCs function in tendon biology. Understanding the mechanisms of physiological and pathological processes regulated by TSPCs, especially a particular subpopulation, would greatly benefit treatment of diseased tendons. Here, we summarize the current scientific literature on the various subpopulations of TSPCs, and discuss how TSPCs can contribute to tissue homeostasis and pathogenesis, as well as examine the key modulatory signaling pathways that determine stem/progenitor cell state. A better understanding of the roles that TSPCs play in tendon biology may facilitate the development of novel treatment strategies for tendon diseases.

Keywords: tendon stem/progenitor cells, subpopulation, niche, healing, TGFβ

INTRODUCTION

Tendon tissues have a hierarchical structure with unique mechanical properties, and serve to connect embryologically distinct musculoskeletal tissues, bone and muscle, and mainly function to transmit mechanical forces to enable skeletal locomotion. Tendons consist of fibrillar arrangement where type I collagen form fibrils, fibrils assemble into fibers, and then fibers assemble into fascicles (Nourissat et al., 2015). Bundles of fascicles form the fascicular matrix (FM) (Zhang et al., 2019). Endotenon or interfascicular matrix (IFM), a connective tissue compartment envelops each

fascicle and is encompassed by the epitenon, which is covered by another layer of connective tissue, paratenon (Zhang et al., 2019). Together, the epitenon and paratenon are called peritenon (Mienaltowski et al., 2014). Tendon proper, refers to the remaining tendon tissue that comprises both FM and IFM after removing the peritenon (Mienaltowski et al., 2013; Zhang et al., 2019; **Figure 1**).

Tendon injuries remains a formidable challenge in the clinic, as disrupted tendon structure compromises tendon function and may lead to flawed healing, such as heterotopic ossification (HO) (Agarwal et al., 2016; Millar et al., 2017). Although surgical treatment can restore tendon tissue integrity, the injured tendon often cannot revert back to pre-injury conditions because of scar formation and fibrosis, which leads to higher risks of re-rupture (Andarawis-Puri et al., 2015). Multiple therapeutic modalities have been proposed to treat the disease such as platelet-rich plasma, hyaluronic acid, corticosteroid injection and so on (Osti et al., 2015; Frizziero et al., 2019; Kaux et al., 2019). Amongst these, stem cell-based treatment shows great promise, and tendon-derived stem cells (TDSCs) have aroused much interest due to their origin (Schneider et al., 2018).

Tendon stem cells (TSCs), commonly referred to as tendon stem/progenitor cells (TSPCs) due to their heterogeneity, exhibit varying propensities in differentiation potential. When these cells were first discovered, they were defined by their clonogenicity, self-renewal potential and multipotency (Bi et al., 2007). Since then, TSPCs have attracted a lot of attention because current treatment modalities for tendon diseases often fail to yield a satisfactory outcome. TSPCs play key roles in tendon development, homeostasis and healing (Bi et al., 2007). Transplantation of exogenous stem cells or activation of the endogenous population has already shown pro-regenerative effects on injured or diseased tendons (Schneider et al., 2018). Investigating the role of TSPCs in tendon biology is critical for unveiling the peculiar characteristics of tendon tissues. Better understanding and in-depth analysis of their identities, interaction with the local niche and involvement in the reparative process could promote optimized manipulation of TSPCs and hasten progress of future clinical applications.

Advancement in high-throughput sequencing and lineage tracing has made isolation and identification of distinct tendon stem cell subpopulations tangible, which further reveals distinct properties of TSPCs (Yin et al., 2016; Harvey et al., 2019). Other state-of-the-art technologies including genetic models and three-dimensional imaging, provide a means of dissecting the role of TSPCs in physiological and pathological processes of tendon tissues. Moreover, accumulating scientific evidence support the key roles of the TGFβ superfamily in determining the lineage fate of TSPCs (Tan et al., 2020).

This review will primarily focus on: (1) different subpopulations of TSPCs, (2) an overview of how TSPCs maintain tendon integrity, (3) the role of the TGFβ superfamily in regulating TSPCs lineage fate. We would like to address the latest discoveries of the emerging roles of TSPCs in tendon biology and pathology. Under most circumstances, TSCs, tendon progenitor cells (TPCs) or TDSCs should be included within the generic term of TSPCs.

SUBPOPULATIONS OF TSPCs

Niches of TSPCs

Stem cell niches dynamically orchestrate cell behavior and cell fate thorough physical interaction and regulatory factors. The native environment is critical for maintaining the stemness of TSPCs due to their topography and biological properties (Ning et al., 2015). Inherent topographical patterns, biochemical composition and biomechanical properties of native tendon matrix could facilitate homogeneous distribution and alignment, promote proliferation, and favor tenogenic phenotype instead of non-tenogenic differentiation of TSPCs (Yin et al., 2013; Ning et al., 2015).

Biglycan (Bgn) and fibromodulin, two critical extracellular matrix (ECM) components, have been shown to be crucial in regulating the lineage fate of TSPCs, since their depletion in double knock-out animal led instead to bone-like tissues being formed (Bi et al., 2007). Biglycan also enhances proliferation and tenogenic differentiation of TSPCs (Bi et al., 2007). Tenomodulin (Tnmd), a transmembrane glycoprotein with cleavable C-terminus localized on the ECM, is essential for adhesion to collagen I, and maintaining the self-renewal capacity, cell senescence and matrix remodeling capacity of TSPCs (Dex et al., 2017; Yin et al., 2019). But TSPCs still possess the multipotency after loss of tenomodulin (Alberton et al., 2015). Decellularized tendon matrix are superior in promoting proliferation and preserving stemness of TSPCs than other engineered biomaterial, which confirms the supportive role of tendon ECM in TSPCs maintenance (Zhang et al., 2011). Tendon ECM also favors the tenogenic disposition of TSPCs, which could be attributed to the niche signals of the tendon matrix (Yin et al., 2013). Alteration to ECM composition is frequently observed in tendinopathy, and aberrant differentiation of TSPCs could be induced by inflammatory and biomechanical cues, which accounts for the regulatory roles of local niches and their functions in tendinopathy (Xu and Murrell, 2008; Zhang and Wang, 2010c). The cellular component is critical in constituting the microenvironment as well, since non-stem/progenitor cells could secret paracrine factors to regulate the differentiation of TSPCs (Lee et al., 2015).

Perivascular regions have often been proposed as a potential niche for TSPCs. An early study had found that cells in the perivascular niche express stem cell-like characteristics (Tempfer et al., 2009). In fact, predominantly perivascular CD146-positive cells have been identified to constitute a fraction of the whole stem/progenitor population (Lee et al., 2015). CD146 is a commonly used marker to identify pericyte population (Gumucio et al., 2020). By utilizing Monocle pseudotime analysis, recent research has confirmed that pericytes form a part of the TSPCs population (De Micheli et al., 2020). Moreover, Xu et al., have reported a P75 (p75 neurotrophin receptor) expressing cell subpopulation with stem cell characteristics within the perivascular regions which could proliferate within the peritenon

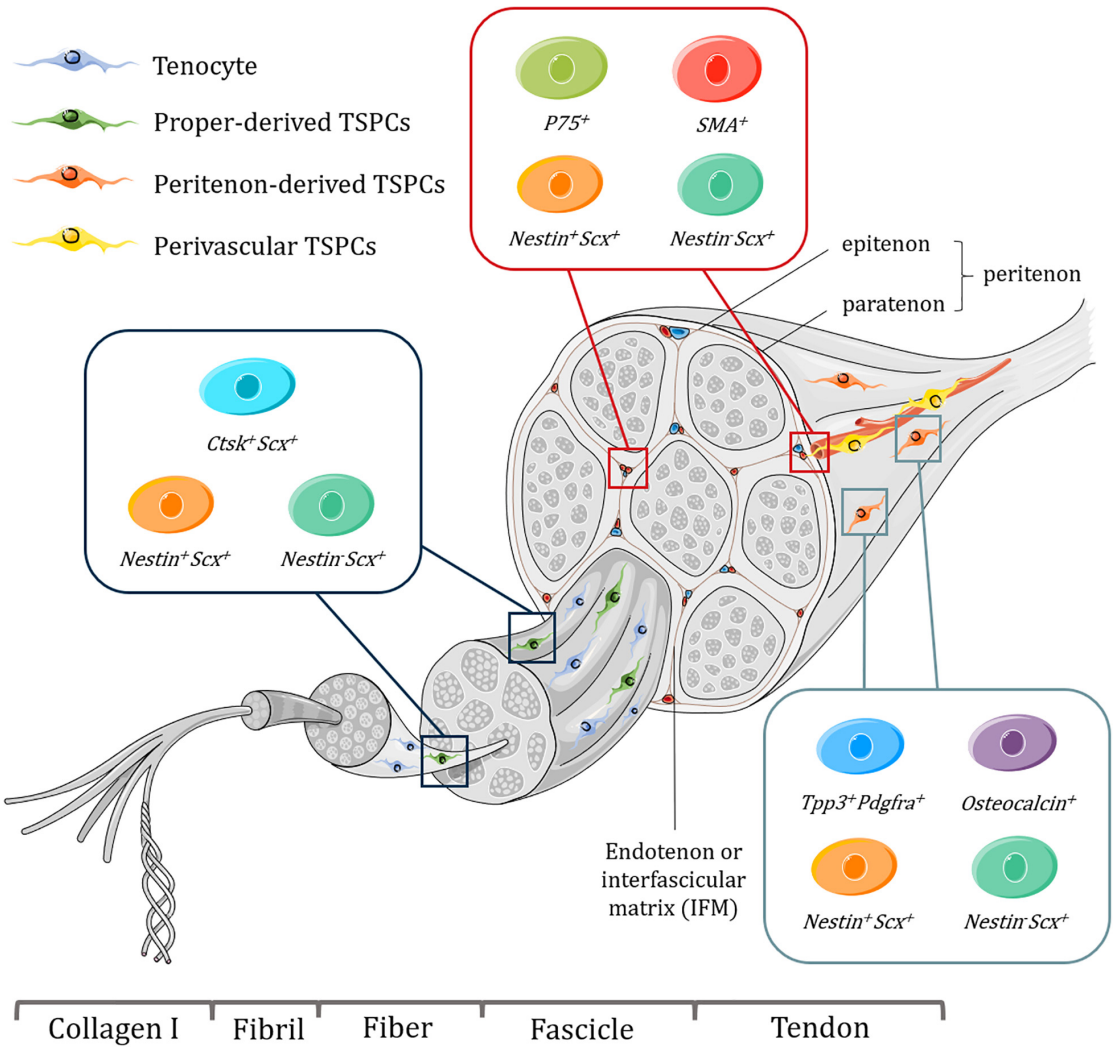

FIGURE 1 | Schematic representation of tendon hierarchical structure and various subpopulations of TSPCs with specific markers harvested from different niches, including tendon proper, peritenon and perivascular region. Tenocytes are aligned between fibers. It should be noted that some of these subpopulations might overlap with each other and perivascular TSPCs may be present in endotenon as well as the peritenon. What's more, the exact location of proper-derived TSPCs is not well determined. Figures were produced using Servier Medical Art (https://smart.servier.com/).

and migrate to interstitial space in response to injury (Xu et al., 2015). Finally, single-cell surface proteomics identified a perivascular niche where a tendon cell cluster expressed high levels of CD90 and CD146 (Kendal et al., 2020). Taken together, these results support the perivascular areas as a tendon stem cell niche.

In general, tendon stem cell niche is essential for TSPCs to maintain their properties and determine tenogenic fate.

Early Insight of the Presence of Subpopulations Within the TSPCs Niche

Initial study had observed that TSPCs isolated from tendon proper actually consist of various phenotypes with heterogenous proliferation and differentiation capacities (Bi et al., 2007). The TSPCs' lines of quadra-potential cells (i.e., tenogenesis, chondrogenesis, osteogenesis, and adipogenesis), yielded the highest expression levels of Scleraxis (Scx) and Mohawk (Mkx), probably suggesting their optimal tenogenic lineage commitment (Rajpar and Barrett, 2020). TSPCs derived from different anatomical origins at different developmental stages also exhibited distinct response to bioactive molecules, suggesting the heterogenicity of TSPCs (Brown et al., 2014). In addition, TSPCs extracted from discrete locations, in both the endotenon and peritenon, have different capabilities to form tendon-like construct (Mienaltowski et al., 2014).

Traditionally, TSPCs have been isolated from the tendon proper (Bi et al., 2007; Rui et al., 2010). However, cell population from the peritenon has been demonstrated to be capable of multipotent differentiation and migration (Cadby et al., 2014).

They expressed higher amounts of progenitor cell markers including CD45, CD90, CD105, and Oct-4, and despite their relatively lower proportions, peritenon-derived stem/progenitor cells have higher proliferative capacity (Mienaltowski et al., 2013; Cadby et al., 2014). Upon labeling stem cells with Iododeoxyuridine (IdU), more label-retaining stem cells were found in the peritenon than in mid-substances, particularly at the perivascular region (Tan et al., 2013). Cells from the peritenon would activate Scleraxis expression in response to mechanical loading and could form primitive tendons *in vitro* (Mendias et al., 2012; Mienaltowski et al., 2013). Furthermore, following tendon injury, cells from the surrounding peritenon would proliferate, migrate and contribute to tenogenesis (Dyment et al., 2013; Tan et al., 2013; Sakabe et al., 2018). These phenomena are a reminder that TSPCs constitute heterogenous groups of cells with distinct characteristics.

Recent Identification of Subpopulations Within the TSPCs Niche

The confirmation and lineage mapping of distinct TSPC subpopulations have been achieved by lineage tracing and single-cell sequencing (**Figure 1**). Early attempts at understanding the origin and identity of resident tendon progenitors mainly depend on lineage-tracing and alpha smooth muscle actin (αSMA) labeling revealed that SMA^+ Scx^+ cells located within the tendon mid-substance as an amplifying resident progenitor population that contribute to postnatal growth and healing (Dyment et al., 2014). Thus SMA^+ cells could be a source of TSPCs. In a later study, Harvey et al. (2019) proposed that SMA^+ cells are not TSPCs, as they did not convert to tenocytes with longitudinally aligned collagen matrix with second harmonic generation signals. However, a significant fraction of the SMA^+ population did turn on Scx expression, which is a hallmark for tenogenesis (Dyment et al., 2014).

During the reparative process, diverse subpopulations of TSPCs could also be noticed, as TSPCs integrated into the injury site and they mainly constituted two subpopulations, with or without surface marker CD105 (Asai et al., 2014). The CD105-positive subpopulation perform better with regard to expressing Scx and avoiding chondroid degenerative lesions than the CD105-negative subpopulation (Asai et al., 2014). However, their specific origin is unclear.

Since then, intense efforts have been made to characterize subtleties within the tendon stem cell population. Our understanding of subpopulations of resident TSPCs has been improved greatly as potent single-cell sequencing method emerges and render a panoramic view of their composition. An important finding is that a $nestin^+$ subpopulation of TSPCs, which is more capable of self-renewal and tenogenic differentiation than the $nestin^-$ subpopulation, has been identified by single-cell analysis and is involved in the development and endogenous repair of tendon tissues (Yin et al., 2016). The majority of the $nestin^+$ subpopulation reside in the endotenon and peritenon, particularly within the perivascular area (Yin et al., 2016). Additionally, nestin has been shown to be essential for maintaining the tenocyte-lineage phenotype and reparative capacities of TSPCs (Yin et al., 2016).

Transcriptome profiles revealed that peritenon harbors a collection of cell population and might be an abundant source of TSPCs (Mienaltowski et al., 2019). Indeed, Osteocalcin-expressing cells whose proliferation and differentiation are regulated by Hedgehog (Hh) signaling, have been found in the peritenon, demonstrating stem/progenitor cell properties comparable to TSPCs isolated from the mid-substance (Wang et al., 2017).

Tubulin polymerization-promoting protein family member 3 (Tppp3) is the first discovered molecular marker that is expressed in the developing epitenon and paratenon (Staverosky et al., 2009). Recently, a paratenon-derived cell cluster expressing both Tppp3 and platelet-derived growth factor receptor alpha (Pdgfra) has been identified as a novel subpopulation of tendon stem cells by utilizing single-cell transcriptomics, which are capable of self-renewal and generating *de novo* tenocytes (Harvey et al., 2019). Tppp3+Pdgfra+ cells dwell in the tendon sheath and are present from embryo to adulthood (Harvey et al., 2019). Unlike previously described TSPCs, the Tppp3+Pdgfra+ subpopulation express high levels of CD34 and rarely Scx (Harvey et al., 2019).

Tendon sheathes normally envelop areas of tendon fibers subjected to high levels of friction, and are conventionally believed to function as lubrication during movement. The pool and regenerative potential of tendon sheath stem/progenitor cells could add extra protection for vulnerable tendon.

The proper-derived and peritenon-derived stem/progenitor cells showed some differences. Proper-derived progenitors have greater potential in forming tendon-like structures compared to peritenon-derived progenitors (Mienaltowski et al., 2014). The peritenon-derived population has also been shown to secrete stimulatory factors that regulate tendon-related gene expression, such as Scx, Tnmd and Bgn (Mienaltowski et al., 2014). Furthermore, tendon proper-derived stem cells expressed genes related to cartilage and chondrocyte development, while peritenon-derived stem cells expressed genes related to positive regulation of endothelial cell proliferation and angiogenesis (Mienaltowski et al., 2019).

Recently, a report noted that the rat model to study tendon biology possess a different hierarchical structure compared to larger species, which lacks the structure of fascicle and hence the structure of endotenon (Lee and Elliott, 2019). Considering this, the TSPCs niche found in murine model might be different from that of larger species and future researchers should be cautious about animal model choice when they attempt to locate TSPCs niche in a more detailed scale.

Potential New Source of TSPCs Subpopulations

A previous study has shown some evidence that adjoining tissues might provide a pool of stem/progenitor cells for tendon maintenance. The expanded SMA^+ cells with negative Scx expression were initially present within surrounding structures (i.e., retinaculum and periosteum), then they migrated to the paratenon and later differentiated into the tenogenic lineage in response to injury, which indicates that adjacent paratendinous structures may serve as reservoirs of TSPCs (Dyment et al., 2014).

Recently, a research based on the zebra fish model demonstrated that progenitors from neighboring tissues are able to regenerate well-organized tendons after total ablation of embryonic tendon cells (Niu et al., 2020). At the surrounding cartilage or muscle attachment site, sox10$^+$ perichondral cells and nkx2.5$^+$ cells could generate a pool of progenitors capable of coordinating tendon regeneration (Niu et al., 2020). Since zebrafish tendons are structurally, molecularly and mechanically similar to mammalian tendons, the regenerative mechanism might shed light on the potential existence of adjoining tissues-derived stem cell subpopulations. Indeed, a recent study has defined an interstitial Scx$^+$ cell subpopulations capable of tenogenic differentiation in adult skeletal muscles by single-cell analysis, which suggests a potential reservoir for tendon regeneration (Giordani et al., 2019). Furthermore, Hic1 successfully defined a subpopulation of vasculature-related Scx positive cells expressing Col22a1 within the peritenon near the myotendinous junction (MTJ), and they share unique but overlapping transcriptional properties with that of tendon progenitors (Scott et al., 2019). This very subpopulation is found to expand and are present within the tendon after muscle injury (Scott et al., 2019).

In tendon tissues, clusters of *ITGA7*$^+$ cells, which are highly similar to those smooth muscle-mesenchymal cells found in muscle are situated around vessels and they also express surface markers CD90 and CD146 (Giordani et al., 2019; Kendal et al., 2020). Actually, developmental evidence suggests that TGFβ signaling emanating from muscles and cartilage are critical for tendon progenitors recruitment, implicating the cross-talk between different tissues of the musculoskeletal system (Pryce et al., 2009). Scx$^+$Sox9$^+$ progenitors give rise to the junction between the cartilage and tendon (Blitz et al., 2013; Sugimoto et al., 2013). The aforementioned evidences corroborate that musculoskeletal tissues might contain respective stem/progenitor populations. Future studies could investigate whether bone or muscle tissues from human or mouse contain a reserve cell population that share something in common with TSPCs, and which could restore functional tendon after injury. These efforts may provide novel cell sources for developing cell-based treatment.

The Need for Novel Biomarkers to Trace TSPCs Subpopulations

Scx alone labels most but not all tendon cells (Sakabe et al., 2018). Besides Scx, tendon cells also express S100a4 which may help mark subsets of resident tendon stem cells, as S100a4 combined with Scx, label distinct but overlapping tendon cell subpopulations during homeostasis and healing (Best and Loiselle, 2019). Recent single-cell sequencing and Cellular Indexing of Transcriptomes and Epitopes by Sequencing (CITE-seq) results unveiled other previously unidentified tendon cell populations (De Micheli et al., 2020; Kendal et al., 2020). Canonical tenogenic markers Scx, Mkx and tenomodulin were only observed to be expressed in a subset of tenocytes and not necessarily co-expressed, which suggests great heterogenicity in tendon cells with different origins or functions (De Micheli et al., 2020). Characterization and classification of TSPCs by reliable and definitive markers are strongly needed to further map their distinct subpopulations and biological functions in tendon, because current markers including Oct-4, Nanog, Sox2, CD44 and Sca-1 are not very specific for labeling TSPCs (Tan et al., 2013; **Table 1**). Specific surface markers are also required to better isolate, sort and purify TSPCs, and thus to achieve better clinical applications.

Hierarchically-expressed markers that can reveal the origin and development of stem/progenitor cells might be uncovered. TSPCs exhibit different characteristics on the spatiotemporal scale, which might correlate to specific stages of development (Chen et al., 2016). Combined single-cell RNA sequencing with genetic-based lineage tracing, stemness markers and spatial information would enable us to better understand the various subpopulations, their characteristics and functions *in vivo* and sequential stem cell states. Elucidation of how different subpopulations contribute to regeneration and most importantly the role that they play in yielding non-functional scar formation and heterotopic ossification, might enable formulation of more targeted strategies to improve tendon healing.

It must however be noted that viable markers for the identification of TSPCs *in vitro* are not necessarily useful for tracking TSPCs *in situ*. Tendon tissues across the body and between different species differ in architecture, biomechanics and transcriptome (Disser et al., 2020). Much caution should be exercised in classifying TSPCs subpopulations, considering the influence of different cell sources and contamination. More specific markers would allow precise fate-mapping of ambiguous stem/progenitor populations. A more specific culture system should be developed, as the traditional culture system fails to maintain the phenotype of TSPCs (Yan et al., 2018; Zhang et al., 2018).

TSPCs IN TENDON BIOLOGY

TSPCs Participate in Tendon Homeostasis

Tendon maintenance involves not only its extracellular matrix, but also the cells that reside within it. The cell-ECM interaction is essential for maintaining tendon homeostasis as ECM could generate cell signals that regulate proliferation, differentiation, adhesion and migration (Screen et al., 2015). Although TSPCs were previously thought to be dormant in healthy adult tendon without injury, the shifted postnatal cell turnover activity of tendon unveiled the possibility of resident tendon stem/progenitor population participating in the homeostatic renewal mechanism (Runesson et al., 2013; Grinstein et al., 2019). A recent study showed a transitional cell division rate and dynamic tendon-related gene expression in postnatal tendon tissues (Grinstein et al., 2019). In fact, TSPCs are capable of adjusting gene expression and modifying ECM in response to different mechanical loadings, which favors the expression of tenocyte-related genes at moderate levels (Zhang and Wang, 2010b). The *in vivo* roles of TSPCs within intact tendon remain largely elusive since most studies investigating TSPCs activity are

TABLE 1 | Niches and Markers of TSPCs.

Species	Anatomical location	Niches	Markers	References
Human	Hamstring tendon	Not determined	Tnmd, Stro1, CD146, CD44, CD90	Bi et al., 2007
Human	Hamstring tendon	Not determined	CD44, CD146, Stro1, αSMA, Tnmd	Ruzzini et al., 2014
Human	Supraspinatus tendon	Perivascular region	Musashi1, Nestin, Scx, SMA, Prominin1/CD133, Col I, Col III, Smad8, CD29, CD44	Tempfer et al., 2009
Human	Supraspinatus tendon	Not determined	CD90, CD105, CD73	Menon et al., 2018
Human	Patellar tendon	Tendon proper	CD44, CD73, CD90, CD105	Lee et al., 2012
Human	Achilles tendon	Not determined	CD105, CD90, CD44, CD146	Yin et al., 2010
Human	Achilles tendon	Not determined	CD73, CD90, CD105, Stro1, CD146, CD44, Musashi1	Kohler et al., 2013
Human	Achilles tendon	Not determined	Nestin, Scx, CD146, CD44, CD90	Yin et al., 2016
Human	Achilles tendon	Not determined	CD44, CD90	Hu et al., 2017
Human	Achilles tendon	Not determined	CD44, CD29, CD105, CD90	Qin et al., 2020
Mouse	Patellar tendon	Tendon proper	Comp, Scx, Sca1, Tenascin C, Col I, CD90.2, CD44, Sox9, Runx2	Bi et al., 2007
Mouse	Patellar tendon	Peritenon	Tppp3, Pdgfra, CD34	Harvey et al., 2019
Mouse	Achilles tendon	Tendon proper	Sca1, CD90.2, CD44, Tnmd, Scx, nucleostemin	Mienaltowski et al., 2013
Mouse	Achilles tendon	Peritenon	Sca1, CD90.2, CD44, endomucin, CD133, nucleostemin, Musashi1	Mienaltowski et al., 2013
Mouse	Achilles tendon	Not determined	CD29, CD44, CD49e, Sca1	Asai et al., 2014
Mouse	Achilles tendon	Tendon proper	Nestin, Scx, CD146, CD105, CD90, CD44, CD29, CD51	Yin et al., 2016
Mouse	Achilles tendon	Tendon proper	Fmod, Mkx, Gdf5, Scx, Thbs4, Wnt10a	Mienaltowski et al., 2019
Mouse	Achilles tendon	Peritenon	Prominin1/CD133	Mienaltowski et al., 2019
Mouse	Achilles tendon	Tendon proper	Ctsk, Nestin, Sca-1, CD44, CD105, CD24, CD200	Feng et al., 2020
Mouse	Tail tendon	Not determined	CD146, CD105, CD90.2, CD73, CD44, Sca1, Nestin, Nanog	Alberton et al., 2015
Mouse	Tail tendon	Not determined	CD90.2, Sca1	Liu et al., 2017
Mouse	Tibialis Anterior Tendon	Peritenon	Osteocalcin	Wang et al., 2017
Mouse	Limb tendon	Peritenon	Sca1, CD34, CD44	Tan et al., 2020
Rat	Flexor tendon	Tendon proper	CD44, CD90, Tenascin C, Tnmd, Aggrecan, αSMA	Rui et al., 2010
Rat	Patellar tendon	Tendon proper	Nucleostemin, Scx, Tnmd, Oct4, SSEA4, CD44, CD90.1	Zhou et al., 2010
Rat	Patellar tendon	Tendon proper	CD73, CD90, Scx, Tnmd	Tan et al., 2012
Rat	Patellar tendon	Not determined	CD146, CD44, Sca1, Scx, Tnmd, Smad8, Oct4, Nanog, Sox2, nucleostemin	Tan et al., 2013
Rat	Patellar Tendon	Perivascular region	CD29, CD90, P75, Vimentin, Sox10, Snail	Xu et al., 2015
Rat	Achilles tendon	Not determined	Nucleostemin, Oct 3/4, Dyn2	Runesson et al., 2015
Rat	Achilles tendon	Not determined	CD29, CD44, CD90	Chen et al., 2016
Rat	Achilles tendon	Tendon proper	CD90, CD73, nucleostemin	Guo et al., 2016
Rat	Achilles tendon	Not determined	CD44, Stro1	Hu et al., 2016
Rabbit	Patellar tendon and Achilles tendon	Tendon proper	Oct4, SSEA4, nucleostemin	Zhang and Wang, 2010a
Horse	Superficial digital flexor tendon	Tendon proper	Scx, CD90, CD105, Oct4	Cadby et al., 2014
Horse	Superficial digital flexor tendon	Peritenon	CD45, CD90, CD105, Oct4	Cadby et al., 2014
Horse	Superficial digital flexor tendon	Tendon proper	CD44, CD90, CD29	Durgam et al., 2019

conducted in the context of injury or ex vivo models. Further exploration into their *in vivo* activities is needed.

TSPCs Plays an Essential Role in Tendon Regeneration

The origin or source of cells that contribute to the tendon healing process have not been fully elucidated. TSPCs from both the tendon proper and surrounding peritenon are known to participate in the process of tendon repair, representing the intrinsic and extrinsic response to tendon injuries (Bi et al., 2007; Harvey et al., 2019). Intrinsic recruitment of Scx^+ cells are critical for restoring tendon, which accounts for the superior regeneration observed in neonates compared to adults, since adult Scx^+ cells are not mobilized properly and transdifferentiate into ectopic cartilage (Howell et al., 2017). A $nestin^+Scx^+$ subpopulation would be recruited to the injury site within a short time period (Yin et al., 2016). TSPCs are supposed to differentiate into the tenogenic-lineage in response to tendon injury. As expected, at 14 days post-injury, Scx-positive lineage cells have been integrated into the aligned bridging tissues that connect two ends of transected sites (Best and Loiselle, 2019).

The paratenon transforms from a quiescent state to an active state, generating multiple cell layers and bridging the wound site and cells within it, which would turn on expression of tenogenic markers, such as Scx (Dyment et al., 2013). The cells from the periphery of the struts would also express Scx, which indicates a possible Scx-negative stem cell subpopulation (Dyment et al., 2013). Following injury, an expanded SMA^+ population within paratenon would form a collagenous bridge and permeate nearby tendon struts where high level tenascin-C could be detected as they remodel the tendon body (Dyment et al., 2014). The collagen fibers of the bridge would transform from loose and thin to dense and thick as time progresses (Dyment et al., 2014). There are almost no Scx-positive lineage cells, which indicates the origin of tendon proper, exhibiting αSMA staining in normal tendon and bridging scar tissues (Howell et al., 2017; Best and Loiselle, 2019).

Furthermore, sheath osteocalcin-expressing stem/progenitor cells will congregate at the injury site, differentiate into tenocytes, and engender fiber-like structures, during which activated Hh signaling is critical for the reparative capacity of sheath stem/progenitor cells (Wang et al., 2017; **Table 2**).

The majority of the $Tppp3^+$ lineage inhabits the paratenon sheath and mostly remain quiescent in the homeostatic state (Harvey et al., 2019). Likewise, once tendon is injured, $Tppp3^+Pdgfra^+$ cells would migrate and infiltrate the mid-substance to repair the damaged region, where they differentiate into tenocytes and lose their stem cell signature (Harvey et al., 2019). $Tppp3^+Pdgfra^+$ stem cells left within sheath would proliferate and maintain their proportions (Harvey et al., 2019). During the healing process, PDGFRα signaling is indispensable for tenogenic differentiation of the $Tppp3^+Pdgfra^+$ subpopulation, but not necessary for their Scx expression (Harvey et al., 2019). Also, a small fraction of this subpopulation might contribute to fibrosis during tendon healing (Harvey et al., 2019). Inflammation is a vital part of the tendon healing process which could eventually impact the reparative outcome. TSPCs were demonstrated to play a regulatory role during inflammation and remodeling when encountering acute tendon injuries by upregulating IL-10 and TIMP-3 via the JNK/STAT signaling pathway (Tarafder et al., 2017). Inflammation could determine the fate of TSPCs as inflammatory signaling and mediators were shown to have effects on TSPCs (Hu et al., 2016). Abnormal upregulation of HIF-2α in proinflammatory milieu directs TSPCs commitment into osteochondral-lineage (Hu et al., 2016). Prostaglandin E_2 decreases the proliferation capacity of TSPCs, and induces their non-tenogenic differentiation (Zhang and Wang, 2010c). IL-1β

TABLE 2 | Behaviors of tendon cells during regeneration.

Tendon cell populations	Events	References
Paratenon cells	3 d.p.i. Cells proliferate and produce tenascin-C and fibromodulin 7 d.p.i. Migrate toward the lesion and express Scx and smooth muscle actin alpha, maintain tenascin-C and fibromodulin expression 14 d.p.i. Bridge the lesion	Dyment et al., 2013
SMA^+ cells	7 d.p.i. Partly Migrate from adjacent structure, expanded in the paratenon and synthesize collagen in paratenon bridge 14 d.p.i. Extend over the lesion, infiltrate adjacent region to remodel and mostly differentiate into Scx^+ cells; Bridge formed 35 d.p.i. Reduced SMA^+Scx^+ cells	Dyment et al., 2014
$P75^+$ cells	0–7 d.p.i. Cells proliferate 2 d.p.i. Capillaries formed; contact with endothelial cells in the peg and socket arrangement; detached from basal lamina encasement; deposit ECM 28 d.p.i. Cell number decreases	Xu et al., 2015
$Nestin^+Scx^+$ cells	7 d.p.i. Accumulated at the injury site 7–21 d.p.i. Cell number decreased	Yin et al., 2016
$Osteocalcin^+$ cells	14 d.p.i. Migrate to lesion; Express Mkx 45 d.p.i. Form tendon-fiber-like construct, Mkx. Scx, ECM components significantly upregulated	Wang et al., 2017
$Tppp3^+Pdgfra^+$ cells	3–14 d.p.i. Migrate to lesion 3–7 d.p.i. Turn on Scx 14 d.p.i. Located deep within mid-substance 1–14 d.p.i. Primarily proliferate, peak at 7 d.p.i., cease at 28 d.p.i.	Harvey et al., 2019
Scx^+ lineage cells	0–2 d.p.i No Scx^+. Present within the scar tissue 14 d.p.i. Present at the injury site 21 d.p.i. Specific to the tendon stubs and form aligned bridging region of the scar tissue	Sakabe et al., 2018; Best and Loiselle, 2019

d.p.i., days post injury.

could promote the motility of TSPCs and also cause phenotype loss of TSPCs, which is associated with altered expression of tendon-related genes (Zhang et al., 2015; Chen et al., 2019; Wang et al., 2019b). Altogether, these evidences reveal a dynamic interplay between inflammation and TSPCs.

Notably, the proportions of TSPCs subpopulations vary according to tendon tissue types, which might determine the corresponding reparative outcome (Dyment et al., 2014; Harvey et al., 2019). Also, different populations display distinct regional and temporal expressions during the reparative process, whereby Oct3/4 positive cells are enriched at the injury site and nucleostemin positive cells are dispersed throughout tendon (Runesson et al., 2015).

It is also worth noting that embryonic and early postnatal tendons regenerate better than late postnatal tendons, which may be caused by the differences between embryonic and postnatal TSPCs (Beredjiklian et al., 2003; Howell et al., 2017). After inflammatory stimuli treatment, embryonic and postnatal tendon cells share similar tenogenic commitment but the latter upregulate expression of inflammatory mediators and catabolic enzymes (Li J. et al., 2019). TSPCs from embryo reside in a mechanically different tendon compared with TSPCs from postnatal stage and during development embryonic TSPCs become more tenogenesis guided (Nguyen et al., 2018). Additionally, mechanical loading alone hardly regulates the behavior of embryonic TSPCs while it can change the dynamic of postnatal TSPCs (Zhang et al., 2010; Brown et al., 2014).

In general, TSPCs would migrate to the injury site, proliferate and express tendon-related, pluripotency and pericyte-related markers to modulate tendon healing and remodeling (Tan et al., 2013). Also, exosomes from TSPCs are capable of regulating matrix metabolism and promoting tenogenesis of TSPCs, which could further boost tendon healing (Wang et al., 2019a; **Figure 2**).

Accumulating scientific evidence shows that the treatment of TSPCs combined with proper delivery vehicle could promote tendon regeneration (Shen et al., 2012; Lui et al., 2014; Komatsu et al., 2016; Zhang et al., 2018). These validate the potential therapeutic efficacy of stem-cell based treatment. Investigating the mechanism that drives the switch from the quiescent to active state of TSPCs could benefit translational application. Spatiotemporal distribution and cellular dynamics of different subpopulations during the reparative process should be addressed, which will help us develop more precise manipulation of stem-cell based therapy to overcome the clinical barriers.

TSPCs in Tendon Pathology

TSPCs from tendinopathic tissues exhibit altered characteristics, such as proliferation and differentiation capacity (Kim et al., 2018; Chang et al., 2020). The tendinopathic region showed strong expression of MKX and GLI1, protein product of the Hh target gene, indicating that Hh signaling is activated (Wang et al., 2017). The expression of higher collagen III to collagen I ratio is observed in a TSPCs phenotype, which is a pattern usually seen in tendinopathy (Rajpar and Barrett, 2020). Additionally, general factors related to tendinopathy also reshape TSPCs (Scott et al., 2015; Ranger et al., 2016). Hyperglycemia decreases the proliferation capacity of TSPCs as well as promotes

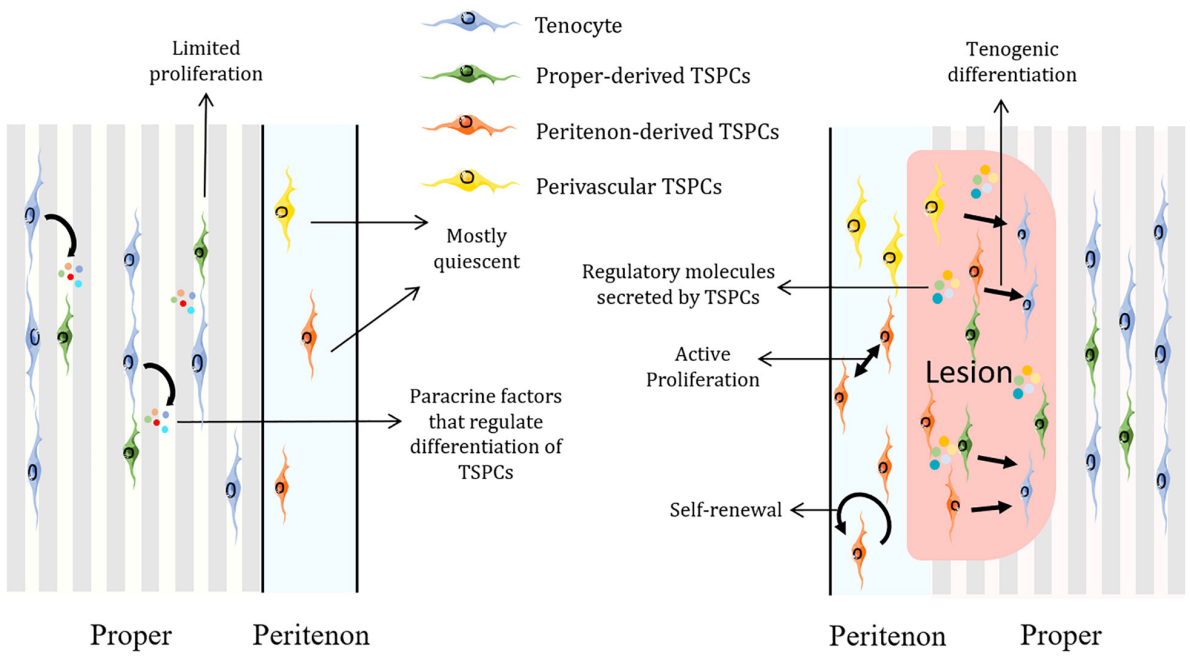

FIGURE 2 | Schematic representation of how TSPCs are implicated in tendon homeostasis and regeneration. TSPCs remain mostly dormant in homeostatic state and surrounding non-stem/progenitor cells could secret factors to regulate their differentiation. Upon injury, TSPCs would be activated and mobilized. TSPCs self-renew, proliferate, migrate to the lesion and differentiate into tenocytes as well as modify the inflammatory process by increasing regulatory molecules such as IL-10. Figures were produced using Servier Medical Art (https://smart.servier.com/).

their osteochondrogenic differentiation potential (Shi et al., 2019). High cholesterol not only inhibits tendon-related gene expressions in TSPCs but also initiates their apoptosis and autophagy (Li K. et al., 2019; Li et al., 2020).

Scx^+ lineage progenitor cells have been recognized as the origin of ectopic bone formation (Dey et al., 2016; Agarwal et al., 2017). Rigorous studies on various subpopulations of TSPCs deepen our understanding of the elusive mechanism of tendon pathological healing. A Cathepsin K (Ctsk) expressing TSPCs subpopulation present at mid-substance had been identified, which contribute to heterotopic ossification (Feng et al., 2020). Ctsk is a proven marker of osteoclasts, periosteal stem cells and perichondrial progenitors (Nakamura et al., 2007; Yang et al., 2013; Debnath et al., 2018). $Ctsk^+Scx^+$ TSPCs possess great self-renewal capacity and differentiation potentials with enriched progenitor cell markers (Feng et al., 2020). The depletion of the Suppressor of fused followed by activation of Hh signaling would trigger subsequent chondrogenesis and osteogenesis of $Ctsk^+Scx^+$ TSPCs (Feng et al., 2020).

Aging has also been revealed as a contributor to the altered properties of TSPCs (Zhou et al., 2010). TSPCs isolated from aged or degenerated tendon exhibit early sign of senescence and shifted transcriptomic profiling with impaired self-renewal and clonogenic ability (Kohler et al., 2013; Ruzzini et al., 2014). Besides, aged TSPCs show reduced migratory capacity, slower actin turnover, and dysregulated gene expressions related to cell-matrix interactions (Kohler et al., 2013). These effects are at least partly caused by augmented Rho-associated protein kinases (ROCK), inhibition of which could restore the phenotype of aged TSPCs to one similar to young TSPCs (Kohler et al., 2013; Kiderlen et al., 2019). Additionally, downregulation of nuclear regulator CITED2 and Aquaporin 1(AQP1) are also reported to be correlated with TSPCs aging (Hu et al., 2017; Chen et al., 2020). Functionally incompetent aged TSPCs will assemble into a less cell-populated, poorly organized and biomechanically inferior three-dimensional tendon organoids (Yan et al., 2020). With advancing age, osteogenic differentiation potential and BMP expression are enhanced in TSPCs, which consequently contribute to increased heterotopic ossification in tendons (Dai et al., 2020). These researches confirm the profound effects of aging on the phenotype of TSPCs and explain the higher incidence of tendon disorders in elderly population (Gumucio et al., 2014).

Generally, TSPCs display shifted properties in tendon diseases and account for key processes in pathogenesis. How TSPCs transform and transdifferentiate under pathological conditions need to be addressed utilizing single-cell sequencing and lineage tracing, so as to identify diseases-specific TSPCs phenotype and develop more targeted therapeutic strategies.

Major Roles of TGFβ Superfamily Signaling in TSPCs

The TGF superfamily include Transforming Growth Factor-beta (TGFβ), Bone Morphogenetic Proteins (BMPs), and Growth/differentiation Factor (GDF). The ligand-receptor model charting cell-interaction found that the TGFβ family and their ligands were among the most abundantly expressed growth factors within tendon tissues, indicating their significant roles in tendon biology (De Micheli et al., 2020).

TGFβ signaling enables tenocytes to retain a stable cellular phenotype (Theiss et al., 2015; Tan et al., 2020). TSPCs treated with TGFβ2 tend to undergo tenogenesis as TGFβ2 treatment increase both Col1a and Scx expression (Guerquin et al., 2013; Brown et al., 2014; Havis et al., 2014; Liu et al., 2015). It was reported that Mkx regulates tenogenesis by directly activating TGFβ2 in TSPCs (Liu et al., 2015). Additionally, transcription of EGR1 also directs tenogenic differentiation partially via TGFβ2 signaling (Guerquin et al., 2013). Endogenous microRNA MiR-378a could bind to TGFβ2, suppressing tenogenic differentiation of TSPCs and impeding tendon healing (Liu et al., 2019).

Transcriptome analysis reveals that during the developmental process of mouse limbs, TGFβ is the most predominant signaling pathway in tendon cells and shows the highest upregulation of TGFβ in differentiated tenocytes, as compared with TSPCs (Havis et al., 2014). TGFβ/SMAD2/3 signaling is required for Scx expression in undifferentiated tendon progenitors and essential for tendon development, which might regulate later recruitment of tendon cells (Pryce et al., 2009; Havis et al., 2016). Other than serving as a potent inducer of Scleraxis expression and a strong recruiter of tendon progenitors, TGFβ also maintained Scx expression of TSPCs *in vitro* (Asai et al., 2014; Feng et al., 2020). Additionally, TGFβ balance the expression of Sox9 and Scx expression within a pool of progenitor cells and thus modulate their chondrogenic and tenogenic differentiation (Blitz et al., 2013; Sugimoto et al., 2013).

After abrogation of TGFβ signaling, committed and functional tendon cells lost their differentiation markers and revert to a more stem/progenitor cell-like state, acquiring expression of stem cell markers such as Sca-1 and CD44 (Tan et al., 2020). Immediately after reintroduction of the TGFβ type II receptor, the mutant cells are able to recover differentiated fate (Tan et al., 2020). Nevertheless, a mere loss of TGFβ signaling alone is not sufficient to induce tendon cell dedifferentiation, since the microenvironment may also participate in the process (Tan et al., 2020). As is the case of early embryonic development, continuous TGFβ signaling with external factors is essential for tendon progenitors to undergo commitment to the tendon cell fate (Pryce et al., 2009). TGFβ would also be released in response to mechanical forces and thus modulate ECM production and sensory projections of tenocytes (Subramanian et al., 2018). All in all, TGFβ acts to maintain tenocyte morphology and differentiation fate (Subramanian et al., 2018; Tan et al., 2020).

CD105 has been marked to be a coreceptor of the TGFβ superfamily (Sakamoto et al., 2020). CD105-negative TSPCs collected from the injury site exhibited a stronger chondrogenic ability than the CD105-postive subpopulation, which are closely related to activated TGFβ/BMP signaling (Asai et al., 2014). Transforming Growth Factor B Induced Gene Human Clone 3 (βig-h3), an extracellular matrix protein induced by TGFβ, were found to be upregulated in Achilles tendon HO (Zhang et al., 2020). βig-h3 could bind to TSPCs and inhibit their attachment to collagen I, as well as accelerate the condensation

of TSPCs and promote mesenchymal chondrogenesis (Zhang et al., 2020). Inhibition of TGFβ effectively attenuates HO progression at multiple stages (Wang et al., 2018). Amelioration of HO progression could also be achieved by inhibiting Hh signaling (Feng et al., 2020). However, Hh signaling promotes tendon healing by inducing Mkx and Collagen I expression of tendon sheath stem cell through the TGFβ pathway (Wang et al., 2017).These evidences show the complicated roles of TGFβ signaling in the context of TSPCs.

BMP signaling is critical to TSPCs. A complete ECM niche mediates TSPC fate by BMP signaling (Bi et al., 2007). The absence of biglycan and fibromodulin increased sensitivity of TSPCs to BMP2, and consequently promote osteochondrogenic differentiation (Bi et al., 2007). BMP2 could stimulate non-tenogenic differentiation of TSPCs and elevated BMPs are observed in tendinopathic samples (Rui et al., 2011, 2012, 2013). Scleraxis-lineage cells contribute to all stages of heterotopic ossification of tendon and hyperactive BMP receptor has been shown to be involved in the process of chondrogenesis (Dey et al., 2016; Agarwal et al., 2017). BMP signaling has also been shown to contribute to enthesis development in mouse embryos (Blitz et al., 2009). BMP signaling is active in zebrafish Sternohyoideus tendon formation and regeneration (Niu et al., 2020). Pharmacological or genetic inhibition of BMP signaling have been demonstrated to reduce the number of tendon cells and impede the attachment progenitor cells being recruited and becoming tendon cells (Niu et al., 2020).

GDF signaling exerts effects on TSPCs as well. Growth/differentiation factor 5 (GDF5) labeled progenitor population also participate in tendon formation as they extend from the tendon proper to enthesis (Dyment et al., 2014). GDF5 promotes the transition of TSPCs toward tenocytes (Holladay et al., 2016).

In general, members of the TGFβ superfamily are essential molecular regulators of the orchestrated differentiation of tendon progenitors and tendon formation (**Figure 3**).

CONCLUDING REMARKS AND FUTURE DIRECTIONS

Tendon stem/progenitor cells are heterogenous and consist of several distinct but overlapping subpopulations. They are actively involved in tendon development, homeostasis and pathogenesis. Significantly, various members of the TGFβ superfamily play multiple roles in regulating TSPCs. Cutting-edge technology such as single-cell sequencing, multi-omics analyses and three-dimensional imaging, could provide researchers more potent tools to define and determine the dynamics and functions of the various TSPCs subpopulations. A full illustrative map would greatly benefit the development of more effective cell-based therapies and likely enable precision medicine.

Future studies could explore how TSPCs interact with neighboring cells, and the tissue environment to establish properly patterned tendon tissue and influence the regenerative process. Identifying other undiscovered TSPCs subpopulations and which of these is responsible for certain physiological or pathological process, are of great importance as well.

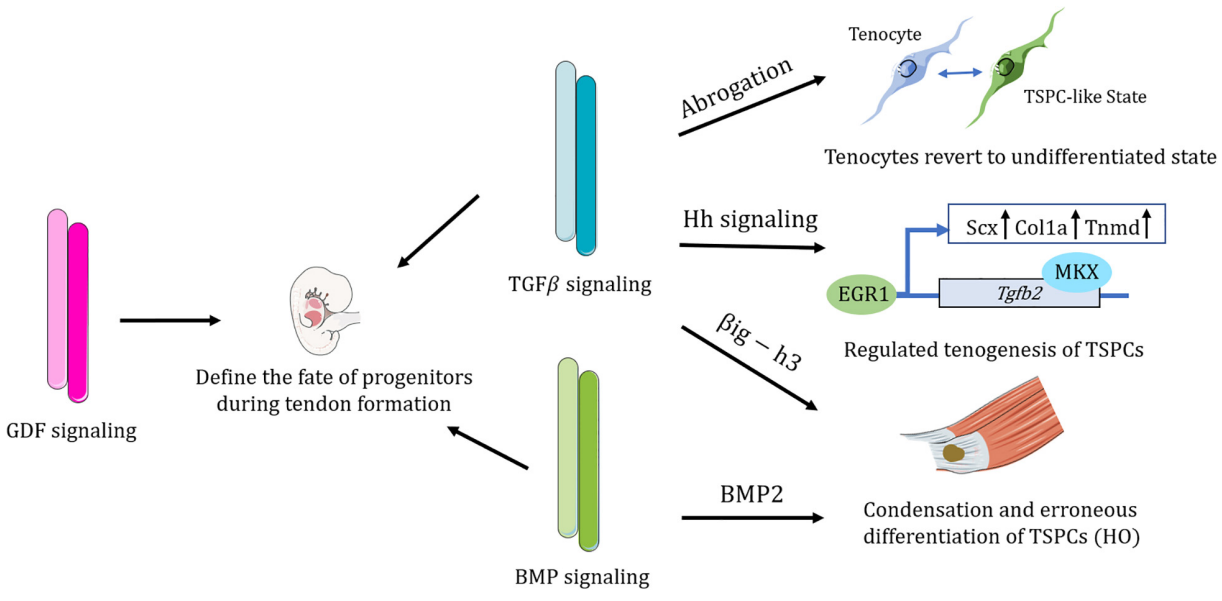

FIGURE 3 | Schematic representation of the complex regulatory roles of the TGFβ superfamily in TSPCs. TGFβ signaling has been shown to maintain the differentiated fate of tenocytes, without which tenocytes would revert to a more TSPC-like state. TGFβ signaling directs distinct lineage commitment of TSPCs by different mechanisms. BMP signaling contributes to erroneous differentiation of TSPCs. TGFβ superfamily members, including TGFβ signaling, BMP signaling, and GDF signaling are all vital in defining the fate of tendon progenitors during tendon formation. Figures were produced using Servier Medical Art (https://smart.servier.com/).

Scientists could also elucidate more specific roles of the TGF-β superfamily and thus design corresponding strategies to address the clinical challenges brought by tendon rupture or tendinopathy.

AUTHOR CONTRIBUTIONS

ZH: original draft writing. ZY: conception and design. JX: visualization. YF: table preparation. BH, WC, and WS: review and editing draft. XJ: referenced manuscript analysis. All authors contributed to the article and approved the submitted version.

FUNDING

This work was supported by the National Key Research and Development Program of China (2017YFA0104900), the NSFC grants (81874019), the Zhejiang Provincial Natural Science Foundation of China (LR20H060002), and the Fundamental Research Funds for the Central Universities (2019QNA7040).

REFERENCES

Agarwal, S., Loder, S., Brownley, C., Cholok, D., Mangiavini, L., Li, J., et al. (2016). Inhibition of Hif1α prevents both trauma-induced and genetic heterotopic ossification. *Proc. Natl. Acad. Sci.* 113, E338–E347. doi: 10.1073/pnas.1515397113

Agarwal, S., Loder, S. J., Cholok, D., Peterson, J., Li, J., Breuler, C., et al. (2017). Scleraxis-lineage cells contribute to ectopic bone formation in muscle and tendon. *Stem Cells* 35, 705–710. doi: 10.1002/stem.2515

Alberton, P., Dex, S., Popov, C., Shukunami, C., Schieker, M., and Docheva, D. (2015). Loss of tenomodulin results in reduced self-renewal and augmented senescence of tendon stem/progenitor cells. *Stem Cells Dev.* 24, 597–609. doi: 10.1089/scd.2014.0314

Andarawis-Puri, N., Flatow, E. L., and Soslowsky, L. J. (2015). Tendon basic science: development, repair, regeneration, and healing. *J. Orthop. Res.* 33, 780–784. doi: 10.1002/jor.22869

Asai, S., Otsuru, S., Candela, M. E., Cantley, L., Uchibe, K., Hofmann, T. J., et al. (2014). Tendon progenitor cells in injured tendons have strong chondrogenic potential: the CD105-negative subpopulation induces chondrogenic degeneration. *Stem Cells* 32, 3266–3277. doi: 10.1002/stem.1847

Beredjiklian, P. K., Favata, M., Cartmell, J. S., Flanagan, C. L., Crombleholme, T. M., and Soslowsky, L. J. (2003). Regenerative versus reparative healing in tendon: a study of biomechanical and histological properties in fetal sheep. *Ann. Biomed. Eng.* 31, 1143–1152. doi: 10.1114/1.1616931

Best, K. T., and Loiselle, A. E. (2019). Scleraxis lineage cells contribute to organized bridging tissue during tendon healing and identify a subpopulation of resident tendon cells. *FASEB J.* 33, 8578–8587. doi: 10.1096/fj.201900130RR

Bi, Y., Ehirchiou, D., Kilts, T. M., Inkson, C. A., Embree, M. C., Sonoyama, W., et al. (2007). Identification of tendon stem/progenitor cells and the role of the extracellular matrix in their niche. *Nat. Med.* 13, 1219–1227. doi: 10.1038/nm1630

Blitz, E., Sharir, A., Akiyama, H., and Zelzer, E. (2013). Tendon-bone attachment unit is formed modularly by a distinct pool of Scx- and Sox9-positive progenitors. *Development* 140, 2680–2690. doi: 10.1242/dev.093906

Blitz, E., Viukov, S., Sharir, A., Shwartz, Y., Galloway, J. L., Pryce, B. A., et al. (2009). Bone ridge patterning during musculoskeletal assembly is mediated through SCX regulation of Bmp4 at the tendon-skeleton junction. *Dev. Cell* 17, 861–873. doi: 10.1016/j.devcel.2009.10.010

Brown, J. P., Finley, V. G., and Kuo, C. K. (2014). Embryonic mechanical and soluble cues regulate tendon progenitor cell gene expression as a function of developmental stage and anatomical origin. *J. Biomech.* 47, 214–222. doi: 10.1016/j.jbiomech.2013.09.018

Cadby, J. A., Buehler, E., Godbout, C., van Weeren, P. R., and Snedeker, J. G. (2014). Differences between the cell populations from the peritenon and the tendon core with regard to their potential implication in tendon repair. *PLoS One* 9:e92474. doi: 10.1371/journal.pone.0092474

Chang, W., Callan, K. T., and Dragoo, J. L. (2020). The behavior of tendon progenitor cells from tendinopathic tendons: implications for treatment. *Tissue Eng. Part A* 26, 38–46. doi: 10.1089/ten.TEA.2019.0042

Chen, J., Zhang, W., Liu, Z., Zhu, T., Shen, W., Ran, J., et al. (2016). Characterization and comparison of post-natal rat Achilles tendon-derived stem cells at different development stages. *Sci. Rep.* 6:22946. doi: 10.1038/srep22946

Chen, M., Li, Y., Xiao, L., Dai, G., Lu, P., Wang, Y., et al. (2020). AQP1 modulates tendon stem/progenitor cells senescence during tendon aging. *Cell Death Dis.* 11:193. doi: 10.1038/s41419-020-2386-3

Chen, Y., Xie, Y., Liu, M., Hu, J., Tang, C., Huang, J., et al. (2019). Controlled-release curcumin attenuates progression of tendon ectopic calcification by regulating the differentiation of tendon stem/progenitor cells. *Mater. Sci. Eng. C Mater. Biol. Appl.* 103:109711. doi: 10.1016/j.msec.2019.04.090

Dai, G., Li, Y., Liu, J., Zhang, C., Chen, M., Lu, P., et al. (2020). Higher BMP expression in tendon stem/progenitor cells contributes to the increased heterotopic ossification in Achilles tendon with aging. *Front. Cell Dev. Biol.* 8:570605. doi: 10.3389/fcell.2020.570605

De Micheli, A. J., Swanson, J. B., Disser, N. P., Martinez, L. M., Walker, N. R., Oliver, D. J., et al. (2020). Single-cell transcriptomic analyses identifies extensive heterogeneity in the cellular composition of mouse Achilles tendons. *Am. J. Physiol. Cell Physiol.* 319, C885–C894. doi: 10.1152/ajpcell.00372.2020

Debnath, S., Yallowitz, A. R., McCormick, J., Lalani, S., Zhang, T., Xu, R., et al. (2018). Discovery of a periosteal stem cell mediating intramembranous bone formation. *Nature* 562, 133–139. doi: 10.1038/s41586-018-0554-8

Dex, S., Alberton, P., Willkomm, L., Söllradl, T., Bago, S., Milz, S., et al. (2017). Tenomodulin is required for tendon endurance running and collagen I fibril adaptation to mechanical load. *EBioMedicine* 20, 240–254. doi: 10.1016/j.ebiom.2017.05.003

Dey, D., Bagarova, J., Hatsell, S. J., Armstrong, K. A., Huang, L., Ermann, J., et al. (2016). Two tissue-resident progenitor lineages drive distinct phenotypes of heterotopic ossification. *Sci. Transl. Med.* 8:366ra163. doi: 10.1126/scitranslmed.aaf1090

Disser, N. P., Ghahramani, G. C., Swanson, J. B., Wada, S., Chao, M. L., Rodeo, S. A., et al. (2020). Widespread diversity in the transcriptomes of functionally divergent limb tendons. *J. Physiol.* 598, 1537–1550. doi: 10.1113/JP279646

Durgam, S. S., Altmann, N. N., Coughlin, H. E., Rollins, A., and Hostnik, L. D. (2019). Insulin enhances the in Vitro osteogenic capacity of flexor tendon-derived progenitor cells. *Stem Cells Int.* 2019:1602751. doi: 10.1155/2019/1602751

Dyment, N. A., Hagiwara, Y., Matthews, B. G., Li, Y., Kalajzic, I., and Rowe, D. W. (2014). Lineage tracing of resident tendon progenitor cells during growth and natural healing. *PLoS One* 9:e96113. doi: 10.1371/journal.pone.0096113

Dyment, N. A., Liu, C. F., Kazemi, N., Aschbacher-Smith, L. E., Kenter, K., Breidenbach, A. P., et al. (2013). The paratenon contributes to scleraxis-expressing cells during patellar tendon healing. *PLoS One* 8:e59944. doi: 10.1371/journal.pone.0059944

Feng, H., Xing, W., Han, Y., Sun, J., Kong, M., Gao, B., et al. (2020). Tendon-derived cathepsin K-expressing progenitor cells activate hedgehog signaling to drive heterotopic ossification. *J. Clin. Investig.* 130, 6354–6365. doi: 10.1172/JCI132518

Frizziero, A., Oliva, F., Vittadini, F., Vetrano, M., Bernetti, A., Giordan, N., et al. (2019). Efficacy of ultrasound-guided hyaluronic acid injections in Achilles and patellar tendinopathies: a prospective multicentric clinical trial. *Muscles Ligaments Tendons J.* 9, 305–313. doi: 10.32098/mltj.03.2019.01

Giordani, L., He, G. J., Negroni, E., Sakai, H., Law, J. Y. C., Siu, M. M., et al. (2019). High-dimensional single-cell cartography reveals novel skeletal muscle-resident cell populations. *Mol. Cell* 74, 609–621.e6. doi: 10.1016/j.molcel.2019.02.026

Grinstein, M., Dingwall, H. L., O'Connor, L. D., Zou, K., Capellini, T. D., and Galloway, J. L. (2019). A distinct transition from cell growth to physiological homeostasis in the tendon. *Elife* 8:e48689. doi: 10.7554/eLife.48689

Guerquin, M. J., Charvet, B., Nourissat, G., Havis, E., Ronsin, O., Bonnin, M. A., et al. (2013). Transcription factor EGR1 directs tendon differentiation and promotes tendon repair. *J. Clin. Investig.* 123, 3564–3576. doi: 10.1172/JCI67521

Gumucio, J. P., Korn, M. A., Saripalli, A. L., Flood, M. D., Phan, A. C., Roche, S. M., et al. (2014). Aging-associated exacerbation in fatty degeneration and infiltration after rotator cuff tear. *J. Shoulder Elb. Surg.* 23, 99–108. doi: 10.1016/j.jse.2013.04.011

Gumucio, J. P., Schonk, M. M., Kharaz, Y. A., Comerford, E., and Mendias, C. L. (2020). Scleraxis is required for the growth of adult tendons in response to mechanical loading. *JCI Insight* 5:e138295. doi: 10.1172/jci.insight.138295

Guo, J., Chan, K. M., Zhang, J. F., and Li, G. (2016). Tendon-derived stem cells undergo spontaneous tenogenic differentiation. *Exp. Cell Res.* 341, 1–7. doi: 10.1016/j.yexcr.2016.01.007

Harvey, T., Flamenco, S., and Fan, C. M. (2019). A Tppp3+Pdgfra+ tendon stem cell population contributes to regeneration and reveals a shared role for PDGF signalling in regeneration and fibrosis. *Nat. Cell Biol.* 21, 1490–1503. doi: 10.1038/s41556-019-0417-z

Havis, E., Bonnin, M. A., Esteves de Lima, J., Charvet, B., Milet, C., and Duprez, D. (2016). TGFβ and FGF promote tendon progenitor fate and act downstream of muscle contraction to regulate tendon differentiation during chick limb development. *Development* 143, 3839–3851. doi: 10.1242/dev.136242

Havis, E., Bonnin, M. A., Olivera-Martinez, I., Nazaret, N., Ruggiu, M., Weibel, J., et al. (2014). Transcriptomic analysis of mouse limb tendon cells during development. *Development* 141, 3683–3696. doi: 10.1242/dev.108654

Holladay, C., Abbah, S. A., O'Dowd, C., Pandit, A., and Zeugolis, D. I. (2016). Preferential tendon stem cell response to growth factor supplementation. *J. Tissue Eng. Regen. Med.* 10, 783–798. doi: 10.1002/term.1852

Howell, K., Chien, C., Bell, R., Laudier, D., Tufa, S. F., Keene, D. R., et al. (2017). Novel model of tendon regeneration reveals distinct cell mechanisms underlying regenerative and fibrotic tendon healing. *Sci. Rep.* 7:45238. doi: 10.1038/srep45238

Hu, C., Zhang, Y., Tang, K., Luo, Y., Liu, Y., and Chen, W. (2017). Downregulation of CITED2 contributes to TGFβ-mediated senescence of tendon-derived stem cells. *Cell Tissue Res.* 368, 93–104. doi: 10.1007/s00441-016-2552-1

Hu, J. J., Yin, Z., Shen, W. L., Xie, Y. B., Zhu, T., Lu, P., et al. (2016). Pharmacological regulation of in situ tissue stem cells differentiation for soft tissue calcification treatment. *Stem Cells* 34, 1083–1096. doi: 10.1002/stem.2306

Kaux, J. F., Dardenne, N., Deroisy, R., Samson, A., Roberjot, M., Croisier, J. L., et al. (2019). Comparison between platelet-rich plasma injections and hyaluronic acid injections in the treatment of patellar tendinopathies: a randomized trial. *Muscles Ligaments Tendons J.* 9, 322–327.

Kendal, A. R., Layton, T., Al-Mossawi, H., Appleton, L., Dakin, S., Brown, R., et al. (2020). Multi-omic single cell analysis resolves novel stromal cell populations in healthy and diseased human tendon. *Sci. Rep.* 10:13939. doi: 10.1038/s41598-020-70786-5

Kiderlen, S., Polzer, C., Rädler, J. O., Docheva, D., Clausen-Schaumann, H., and Sudhop, S. (2019). Age related changes in cell stiffness of tendon stem/progenitor cells and a rejuvenating effect of ROCK-inhibition. *Biochem. Biophys. Res. Commun.* 509, 839–844. doi: 10.1016/j.bbrc.2019.01.027

Kim, S. J., Song, D. H., and Kim, S. J. (2018). Characteristics of tendon derived stem cells according to different factors to induce the tendinopathy. *J. Cell. Physiol.* 233, 6196–6206. doi: 10.1002/jcp.26475

Kohler, J., Popov, C., Klotz, B., Alberton, P., Prall, W. C., Haasters, F., et al. (2013). Uncovering the cellular and molecular changes in tendon stem/progenitor cells attributed to tendon aging and degeneration. *Aging Cell* 12, 988–999. doi: 10.1111/acel.12124

Komatsu, I., Wang, J. H. C., Iwasaki, K., Shimizu, T., and Okano, T. (2016). The effect of tendon stem/progenitor cell (TSC) sheet on the early tendon healing in a rat Achilles tendon injury model. *Acta Biomater.* 42, 136–146. doi: 10.1016/j.actbio.2016.06.026

Lee, A. H., and Elliott, D. M. (2019). Comparative multi-scale hierarchical structure of the tail, plantaris, and Achilles tendons in the rat. *J. Anat.* 234, 252–262. doi: 10.1111/joa.12913

Lee, C. H., Lee, F. Y., Tarafder, S., Kao, K., Jun, Y., Yang, G., et al. (2015). Harnessing endogenous stem/progenitor cells for tendon regeneration. *J. Clin. Invest.* 125, 2690–2701. doi: 10.1172/JCI81589

Lee, W. Y. W., Lui, P. P. Y., and Rui, Y. F. (2012). Hypoxia-mediated efficient expansion of human tendon-derived stem cells in vitro. *Tissue Eng. Part A* 18, 484–498. doi: 10.1089/ten.TEA.2011.0130

Li, J., Stoppato, M., Schiele, N. R., Graybeal, K. L., Nguyen, P. K., and Kuo, C. K. (2019). Embryonic and postnatal tendon cells respond differently to interleukin-1β. *Ann. N. Y. Acad. Sci.* 1442, 118–127. doi: 10.1111/nyas.14013

Li, K., Deng, G., Deng, Y., Chen, S., Wu, H., Cheng, C., et al. (2019). High cholesterol inhibits tendon-related gene expressions in tendon-derived stem cells through reactive oxygen species-activated nuclear factor-κB signaling. *J. Cell. Physiol.* 234, 18017–18028. doi: 10.1002/jcp.28433

Li, K., Deng, Y., Deng, G., Chen, P., Wang, Y., Wu, H., et al. (2020). High cholesterol induces apoptosis and autophagy through the ROS-activated AKT/FOXO1 pathway in tendon-derived stem cells. *Stem Cell Res. Ther.* 11:131. doi: 10.1186/s13287-020-01643-5

Liu, H., Zhang, C., Zhu, S., Lu, P., Zhu, T., Gong, X., et al. (2015). Mohawk promotes the tenogenesis of mesenchymal stem cells through activation of the TGFβ signaling pathway. *Stem Cells* 33, 443–455. doi: 10.1002/stem.1866

Liu, Y., Feng, L., Xu, J., Yang, Z., Wu, T., Zhang, J., et al. (2019). MiR-378a suppresses tenogenic differentiation and tendon repair by targeting at TGF-β2. *Stem Cell Res. Ther.* 10:108. doi: 10.1186/s13287-019-1216-y

Liu, Y., Xu, J., Xu, L., Wu, T., Sun, Y., Lee, Y. W., et al. (2017). Cystic fibrosis transmembrane conductance regulator mediates tenogenic differentiation of tendon-derived stem cells and tendon repair: accelerating tendon injury healing by intervening in its downstream signaling. *FASEB J.* 31, 3800–3815. doi: 10.1096/fj.201601181R

Lui, P. P. Y., Kong, S. K., Lau, P. M., Wong, Y. M., Lee, Y. W., Tan, C., et al. (2014). Allogeneic tendon-derived stem cells promote tendon healing and suppress immunoreactions in hosts: in vivo model. *Tissue Eng. Part A* 20, 2998–3009. doi: 10.1089/ten.TEA.2013.0713

Mendias, C. L., Gumucio, J. P., Bakhurin, K. I., Lynch, E. B., and Brooks, S. V. (2012). Physiological loading of tendons induces scleraxis expression in epitenon fibroblasts. *J. Orthop. Res.* 30, 606–612. doi: 10.1002/jor.21550

Menon, A., Creo, P., Piccoli, M., Bergante, S., Conforti, E., Banfi, G., et al. (2018). Chemical activation of the hypoxia-inducible factor reversibly reduces tendon stem cell proliferation, inhibits their differentiation, and maintains cell undifferentiation. *Stem Cells Int.* 2018:9468085. doi: 10.1155/2018/9468085

Mienaltowski, M. J., Adams, S. M., and Birk, D. E. (2013). Regional differences in stem cell/progenitor cell populations from the mouse achilles tendon. *Tissue Eng. Part A* 19, 199–210. doi: 10.1089/ten.TEA.2012.0182

Mienaltowski, M. J., Adams, S. M., and Birk, D. E. (2014). Tendon proper- and peritenon-derived progenitor cells have unique tenogenic properties. *Stem Cell Res. Ther.* 5:86. doi: 10.1186/scrt475

Mienaltowski, M. J., Cánovas, A., Fates, V. A., Hampton, A. R., Pechanec, M. Y., Islas-Trejo, A., et al. (2019). Transcriptome profiles of isolated murine Achilles tendon proper- and peritenon-derived progenitor cells. *J. Orthop. Res.* 37, 1409–1418. doi: 10.1002/jor.24076

Millar, N. L., Murrell, G. A. C., and McInnes, I. B. (2017). Inflammatory mechanisms in tendinopathy – towards translation. *Nat. Rev. Rheumatol.* 13, 110–122. doi: 10.1038/nrrheum.2016.213

Nakamura, T., Imai, Y., Matsumoto, T., Sato, S., Takeuchi, K., Igarashi, K., et al. (2007). Estrogen prevents bone loss via estrogen receptor alpha and induction of Fas ligand in osteoclasts. *Cell* 130, 811–823. doi: 10.1016/j.cell.2007.07.025

Nguyen, P. K., Pan, X. S., Li, J., and Kuo, C. K. (2018). Roadmap of molecular, compositional, and functional markers during embryonic tendon development. *Connect. Tissue Res.* 59, 495–508. doi: 10.1080/03008207.2018.1511710

Ning, L. J., Zhang, Y. J., Zhang, Y., Qing, Q., Jiang, Y. L., Yang, J. L., et al. (2015). The utilization of decellularized tendon slices to provide an inductive microenvironment for the proliferation and tenogenic differentiation of stem cells. *Biomaterials* 52, 539–550. doi: 10.1016/j.biomaterials.2015.02.061

Niu, X., Subramanian, A., Hwang, T. H., Schilling, T. F., and Galloway, J. L. (2020). Tendon cell regeneration is mediated by attachment site-resident progenitors and BMP signaling. *Curr. Biol.* 30, 3277–3292.e5. doi: 10.1016/j.cub.2020.06.016

Nourissat, G., Berenbaum, F., and Duprez, D. (2015). Tendon injury: from biology to tendon repair. *Nat. Rev. Rheumatol.* 11, 223–233. doi: 10.1038/nrrheum.2015.26

Osti, L., Buda, M., Buono, A. D., Osti, R., and Massari, L. (2015). Clinical evidence in the treatment of rotator cuff tears with hyaluronic acid. *Muscles Ligaments Tendons J.* 5, 270–275. doi: 10.11138/mltj/2015.5.4.270

Pryce, B. A., Watson, S. S., Murchison, N. D., Staverosky, J. A., Dünker, N., and Schweitzer, R. (2009). Recruitment and maintenance of tendon progenitors by TGFbeta signaling are essential for tendon formation. *Development* 136, 1351–1361. doi: 10.1242/dev.027342

Qin, S., Wang, W., Liu, Z., Hua, X., Fu, S., Dong, F., et al. (2020). Fibrochondrogenic differentiation potential of tendon-derived stem/progenitor cells from human patellar tendon. *J. Orthop. Translat.* 22, 101–108. doi: 10.1016/j.jot.2019.08.006

Rajpar, I., and Barrett, J. G. (2020). Multi-differentiation potential is necessary for optimal tenogenesis of tendon stem cells. *Stem Cell Res. Ther.* 11:152. doi: 10.1186/s13287-020-01640-8

Ranger, T. A., Wong, A. M., Cook, J. L., and Gaida, J. E. (2016). Is there an association between tendinopathy and diabetes mellitus? a systematic review with meta-analysis. *Br. J. Sports Med.* 50, 982–989. doi: 10.1136/bjsports-2015-094735

Rui, Y. F., Lui, P. P. Y., Li, G., Fu, S. C., Lee, Y. W., and Chan, K. M. (2010). Isolation and characterization of multipotent rat tendon-derived stem cells. *Tissue Eng. Part A* 16, 1549–1558. doi: 10.1089/ten.TEA.2009.0529

Rui, Y. F., Lui, P. P. Y., Ni, M., Chan, L. S., Lee, Y. W., and Chan, K. M. (2011). Mechanical loading increased BMP-2 expression which promoted osteogenic differentiation of tendon-derived stem cells. *J. Orthop. Res.* 29, 390–396. doi: 10.1002/jor.21218

Rui, Y. F., Lui, P. P. Y., Rolf, C. G., Wong, Y. M., Lee, Y. W., and Chan, K. M. (2012). Expression of chondro-osteogenic BMPs in clinical samples of patellar tendinopathy. *Knee Surg. Sports Traumatol. Arthrosc.* 20, 1409–1417. doi: 10.1007/s00167-011-1685-8

Rui, Y. F., Lui, P. P. Y., Wong, Y. M., Tan, Q., and Chan, K. M. (2013). BMP-2 stimulated non-tenogenic differentiation and promoted proteoglycan deposition of tendon-derived stem cells (TDSCs) in vitro. *J. Orthop. Res.* 31, 746–753. doi: 10.1002/jor.22290

Runesson, E., Ackermann, P., Brisby, H., Karlsson, J., and Eriksson, B. I. (2013). Detection of slow-cycling and stem/progenitor cells in different regions of rat Achilles tendon: response to treadmill exercise. *Knee Surg. Sports Traumatol. Arthrosc.* 21, 1694–1703. doi: 10.1007/s00167-013-2446-7

Runesson, E., Ackermann, P., Karlsson, J., and Eriksson, B. I. (2015). Nucleostemin- and Oct 3/4-positive stem/progenitor cells exhibit disparate anatomical and temporal expression during rat Achilles tendon healing. *BMC Musculoskelet. Disord.* 16:212. doi: 10.1186/s12891-015-0658-3

Ruzzini, L., Abbruzzese, F., Rainer, A., Longo, U. G., Trombetta, M., Maffulli, N., et al. (2014). Characterization of age-related changes of tendon stem cells from adult human tendons. *Knee Surg. Sports Traumatol. Arthrosc.* 22, 2856–2866. doi: 10.1007/s00167-013-2457-4

Sakabe, T., Sakai, K., Maeda, T., Sunaga, A., Furuta, N., Schweitzer, R., et al. (2018). Transcription factor scleraxis vitally contributes to progenitor lineage direction in wound healing of adult tendon in mice. *J. Biol. Chem.* 293, 5766–5780. doi: 10.1074/jbc.RA118.001987

Sakamoto, R., Kajihara, I., Miyauchi, H., Maeda-Otsuka, S., Yamada-Kanazawa, S., Sawamura, S., et al. (2020). Inhibition of endoglin exerts antitumor effects through the regulation of non-smad TGF-β signaling in Angiosarcoma. *J. Invest. Dermatol.* 140, 2060–2072. doi: 10.1016/j.jid.2020.01.031

Schneider, M., Angele, P., Jarvinen, T. A. H., and Docheva, D. (2018). Rescue plan for Achilles: therapeutics steering the fate and functions of stem cells in tendon wound healing. *Adv. Drug Deliv. Rev.* 129, 352–375. doi: 10.1016/j.addr.2017.12.016

Scott, A., Zwerver, J., Grewal, N., de Sa, A., Alktebi, T., Granville, D. J., et al. (2015). Lipids, adiposity and tendinopathy: is there a mechanistic link? critical review. *Br. J. Sports Med.* 49, 984–988. doi: 10.1136/bjsports-2014-093989

Scott, R. W., Arostegui, M., Schweitzer, R., Rossi, F. M. V., and Underhill, T. M. (2019). Hic1 defines quiescent mesenchymal progenitor subpopulations with distinct functions and fates in skeletal muscle regeneration. *Cell Stem Cell* 25, 797–813. doi: 10.1016/j.stem.2019.11.004

Screen, H. R. C., Berk, D. E., Kadler, K. E., Ramirez, F., and Young, M. F. (2015). Tendon functional extracellular matrix. *J. Orthop. Res.* 33, 793–799. doi: 10.1002/jor.22818

Shen, W., Chen, J., Yin, Z., Chen, X., Liu, H., Heng, B. C., et al. (2012). Allogenous tendon stem/progenitor cells in silk scaffold for functional shoulder repair. *Cell Transplant.* 21, 943–958. doi: 10.3727/096368911X627453

Shi, L., Li, Y. J., Dai, G. C., Lin, Y. C., Li, G., Wang, C., et al. (2019). Impaired function of tendon-derived stem cells in experimental diabetes mellitus rat tendons: implications for cellular mechanism of diabetic tendon disorder. *Stem Cell Res. Ther.* 10:27. doi: 10.1186/s13287-018-1108-6

Staverosky, J. A., Pryce, B. A., Watson, S. S., and Schweitzer, R. (2009). Tubulin polymerization-promoting protein family member 3, Tppp3, is a specific marker of the differentiating tendon sheath and synovial joints. *Dev. Dyn.* 238, 685–692. doi: 10.1002/dvdy.21865

Subramanian, A., Kanzaki, L. F., Galloway, J. L., and Schilling, T. F. (2018). Mechanical force regulates tendon extracellular matrix organization and tenocyte morphogenesis through TGFbeta signaling. *Elife* 7:e38069. doi: 10.7554/eLife.38069

Sugimoto, Y., Takimoto, A., Akiyama, H., Kist, R., Scherer, G., Nakamura, T., et al. (2013). Scx+/Sox9+ progenitors contribute to the establishment of the junction between cartilage and tendon/ligament. *Development* 140, 2280–2288. doi: 10.1242/dev.096354

Tan, G. K., Pryce, B. A., Stabio, A., Brigande, J. V., Wang, C., Xia, Z., et al. (2020). Tgfβ signaling is critical for maintenance of the tendon cell fate. *eLife* 9:e52695. doi: 10.7554/eLife.52695

Tan, Q., Lui, P. P. Y., and Lee, Y. W. (2013). In vivo identity of tendon stem cells and the roles of stem cells in tendon healing. *Stem Cells Dev.* 22, 3128–3140. doi: 10.1089/scd.2013.0073

Tan, Q., Lui, P. P. Y., and Rui, Y. F. (2012). Effect of in vitro passaging on the stem cell-related properties of tendon-derived stem cells-implications in tissue engineering. *Stem Cells Dev.* 21, 790–800. doi: 10.1089/scd.2011.0160

Tarafder, S., Chen, E., Jun, Y., Kao, K., Sim, K. H., Back, J., et al. (2017). Tendon stem/progenitor cells regulate inflammation in tendon healing JNK and STAT3 signaling. *FASEB J.* 31, 3991–3998. doi: 10.1096/fj.201700071R

Tempfer, H., Wagner, A., Gehwolf, R., Lehner, C., Tauber, M., Resch, H., et al. (2009). Perivascular cells of the supraspinatus tendon express both tendon- and stem cell-related markers. *Histochem. Cell Biol.* 131, 733–741. doi: 10.1007/s00418-009-0581-5

Theiss, F., Mirsaidi, A., Mhanna, R., Kümmerle, J., Glanz, S., Bahrenberg, G., et al. (2015). Use of biomimetic microtissue spheroids and specific growth factor supplementation to improve tenocyte differentiation and adaptation to a collagen-based scaffold in vitro. *Biomaterials* 69, 99–109. doi: 10.1016/j.biomaterials.2015.08.013

Wang, X., Li, F., Xie, L., Crane, J., Zhen, G., Mishina, Y., et al. (2018). Inhibition of overactive TGF-β attenuates progression of heterotopic ossification in mice. *Nat. Commun.* 9:551. doi: 10.1038/s41467-018-02988-5

Wang, Y., He, G., Guo, Y., Tang, H., Shi, Y., Bian, X., et al. (2019a). Exosomes from tendon stem cells promote injury tendon healing through balancing synthesis and degradation of the tendon extracellular matrix. *J. Cell. Mol. Med.* 23, 5475–5485. doi: 10.1111/jcmm.14430

Wang, Y., He, G., Tang, H., Shi, Y., Kang, X., Lyu, J., et al. (2019b). Aspirin inhibits inflammation and scar formation in the injury tendon healing through regulating JNK/STAT-3 signalling pathway. *Cell Prolif.* 52:e12650. doi: 10.1111/cpr.12650

Wang, Y., Zhang, X., Huang, H., Xia, Y., Yao, Y., Mak, A. F. T., et al. (2017). Osteocalcin expressing cells from tendon sheaths in mice contribute to tendon repair by activating Hedgehog signaling. *eLife* 6:e30474. doi: 10.7554/eLife.30474

Xu, W., Sun, Y., Zhang, J., Xu, K., Pan, L., He, L., et al. (2015). Perivascular-derived stem cells with neural crest characteristics are involved in tendon repair. *Stem Cells Dev.* 24, 857–868. doi: 10.1089/scd.2014.0036

Xu, Y., and Murrell, G. A. (2008). The basic science of tendinopathy. *Clin. Orthop. Relat. Res.* 466, 1528–1538. doi: 10.1007/s11999-008-0286-4

Yan, Z., Yin, H., Brochhausen, C., Pfeifer, C. G., Alt, V., and Docheva, D. (2020). Aged tendon stem/progenitor cells are less competent to form 3D tendon organoids due to cell autonomous and matrix production deficits. *Front. Bioeng. Biotech.* 8:406. doi: 10.3389/fbioe.2020.00406

Yan, Z., Yin, H., Nerlich, M., Pfeifer, C. G., and Docheva, D. (2018). Boosting tendon repair: interplay of cells, growth factors and scaffold-free and gel-based carriers. *J. Exp. Orthop*. 5:1. doi: 10.1186/s40634-017-0117-1

Yang, W., Wang, J., Moore, D. C., Liang, H., Dooner, M., Wu, Q., et al. (2013). Ptpn11 deletion in a novel progenitor causes metachondromatosis by inducing hedgehog signalling. *Nature* 499, 491–495. doi: 10.1038/nature12396

Yin, H., Caceres, M. D., Yan, Z., Schieker, M., Nerlich, M., and Docheva, D. (2019). Tenomodulin regulates matrix remodeling of mouse tendon stem/progenitor cells in an ex vivo collagen I gel model. *Biochem. Biophys. Res. Commun*. 512, 691–697. doi: 10.1016/j.bbrc.2019.03.063

Yin, Z., Chen, X., Chen, J. L., Shen, W. L., Hieu Nguyen, T. M., Gao, L., et al. (2010). The regulation of tendon stem cell differentiation by the alignment of nanofibers. *Biomaterials* 31, 2163–2175. doi: 10.1016/j.biomaterials.2009.11.083

Yin, Z., Chen, X., Zhu, T., Hu, J. J., Song, H. X., Shen, W. L., et al. (2013). The effect of decellularized matrices on human tendon stem/progenitor cell differentiation and tendon repair. *Acta Biomater*. 9, 9317–9329. doi: 10.1016/j.actbio.2013.07.022

Yin, Z., Hu, J. J., Yang, L., Zheng, Z. F., An, C. R., Wu, B. B., et al. (2016). Single-cell analysis reveals a nestin tendon stem/progenitor cell population with strong tenogenic potentiality. *Sci. Adv*. 2:e1600874. doi: 10.1126/sciadv.1600874

Zhang, C., Zhang, E., Yang, L., Tu, W., Lin, J., Yuan, C., et al. (2018). Histone deacetylase inhibitor treated cell sheet from mouse tendon stem/progenitor cells promotes tendon repair. *Biomaterials* 172, 66–82. doi: 10.1016/j.biomaterials.2018.03.043

Zhang, C., Zhu, J., Zhou, Y., Thampatty, B. P., and Wang, J. H. C. (2019). Tendon stem/progenitor cells and their interactions with extracellular matrix and mechanical loading. *Stem Cells Int*. 2019:3674647. doi: 10.1155/2019/3674647

Zhang, J., Li, B., and Wang, J. H. C. (2011). The role of engineered tendon matrix in the stemness of tendon stem cells in vitro and the promotion of tendon-like tissue formation in vivo. *Biomaterials* 32, 6972–6981. doi: 10.1016/j.biomaterials.2011.05.088

Zhang, J., Pan, T., Liu, Y., and Wang, J. H. C. (2010). Mouse treadmill running enhances tendons by expanding the pool of tendon stem cells (TSCs) and TSC-related cellular production of collagen. *J. Orthop. Res*. 28, 1178–1183. doi: 10.1002/jor.21123

Zhang, J., and Wang, J. H. C. (2010a). Characterization of differential properties of rabbit tendon stem cells and tenocytes. *BMC. Musculoskele. Disord*. 11:10. doi: 10.1186/1471-2474-11-10

Zhang, J., and Wang, J. H. C. (2010b). Mechanobiological response of tendon stem cells: implications of tendon homeostasis and pathogenesis of tendinopathy. *J. Orthop. Res*. 28, 639–643. doi: 10.1002/jor.21046

Zhang, J., and Wang, J. H. C. (2010c). Production of PGE(2) increases in tendons subjected to repetitive mechanical loading and induces differentiation of tendon stem cells into non-tenocytes. *J. Orthop. Res*. 28, 198–203. doi: 10.1002/jor.20962

Zhang, K., Asai, S., Yu, B., and Enomoto-Iwamoto, M. (2015). IL-1beta irreversibly inhibits tenogenic differentiation and alters metabolism in injured tendon-derived progenitor cells in vitro. *Biochem. Biophys. Res. Commun*. 463, 667–672. doi: 10.1016/j.bbrc.2015.05.122

Zhang, Q., Zhang, Y., Yan, M., Zhu, K., Su, Q., Pan, J., et al. (2020). βig-h3 enhances chondrogenesis via promoting mesenchymal condensation in rat Achilles tendon heterotopic ossification model. *Aging* 12, 7030–7041. doi: 10.18632/aging.103060

Zhou, Z., Akinbiyi, T., Xu, L., Ramcharan, M., Leong, D. J., Ros, S. J., et al. (2010). Tendon-derived stem/progenitor cell aging: defective self-renewal and altered fate. *Aging Cell* 9, 911–915. doi: 10.1111/j.1474-9726.2010.00598.x

Conflict of Interest: The authors declare that the research was conducted in the absence of any commercial or financial relationships that could be construed as a potential conflict of interest.

frontiers in Cell and Developmental Biology

ORIGINAL RESEARCH
published: 29 March 2021
doi: 10.3389/fcell.2021.650250

Inhibition of JAK-STAT Signaling Pathway Alleviates Age-Related Phenotypes in Tendon Stem/Progenitor Cells

Minhao Chen[1,2,3], Longfei Xiao[1,2,3], Guangchun Dai[1,2,3], Panpan Lu[1,2,3], Yuanwei Zhang[1,2,3], Yingjuan Li[4], Ming Ni[5] and Yunfeng Rui[1,2,3,6]**

[1] Department of Orthopaedics, Zhongda Hospital, School of Medicine, Southeast University, Nanjing, China, [2] Orthopaedic Trauma Institute (OTI), Southeast University, Nanjing, China, [3] Trauma Center, Zhongda Hospital, School of Medicine, Southeast University, Nanjing, China, [4] Department of Geriatrics, Zhongda Hospital, School of Medicine, Southeast University, Nanjing, China, [5] Department of Orthopedics, The First Medical Center, Chinese PLA General Hospital, Beijing, China, [6] China Orthopedic Regenerative Medicine Group, Hangzhou, China

OPEN ACCESS

Edited by:
Zi Yin,
Zhejiang University, China

Reviewed by:
Weiliang Shen,
Zhejiang University, China
Can Zhang,
Hunan University, China

***Correspondence:**
Yunfeng Rui
ruiyunfeng@126.com
Ming Ni
niming301@163.com

Specialty section:
This article was submitted to Stem Cell Research, a section of the journal Frontiers in Cell and Developmental Biology

Received: 06 January 2021
Accepted: 23 February 2021
Published: 29 March 2021

Citation:
Chen M, Xiao L, Dai G, Lu P, Zhang Y, Li Y, Ni M and Rui Y (2021) Inhibition of JAK-STAT Signaling Pathway Alleviates Age-Related Phenotypes in Tendon Stem/Progenitor Cells. Front. Cell Dev. Biol. 9:650250. doi: 10.3389/fcell.2021.650250

Diminished regeneration or healing capacity of tendon occurs during aging. It has been well demonstrated that tendon stem/progenitor cells (TSPCs) play a vital role in tendon maintenance and repair. Here, we identified an accumulation of senescent TSPCs in tendon tissue with aging. In aged TSPCs, the activity of JAK-STAT signaling pathway was increased. Besides, genetic knockdown of JAK2 or STAT3 significantly attenuated TSPC senescence in aged TSPCs. Pharmacological inhibition of JAK-STAT signaling pathway with AG490 similarly attenuated cellular senescence and senescence-associated secretory phenotype (SASP) of aged TSPCs. In addition, inhibition of JAK-STAT signaling pathway also restored the age-related dysfunctions of TSPCs, including self-renewal, migration, actin dynamics, and stemness. Together, our findings reveal the critical role of JAK-STAT signaling pathway in the regulation of TSPC aging and suggest an ideal therapeutic target for the age-related tendon disorders.

Keywords: tendon-derived stem/progenitor cells, tendon aging, senescence, JAK-STAT signaling pathway, AG490

INTRODUCTION

Tendon aging is characterized by time-dependent declines in structural, compositional, and functional properties (Zaseck et al., 2016; Marqueti et al., 2018). Aged tendon is more prone to tendon disorder, such as tendon tear, re-tear, and tendinopathy. Due to the limited endogenous repair capacity of aged tendon, the restoration of injured tendon is still a major clinical challenge. Currently, stem cell-based strategies to restore the original property of injured tendon are being investigated. Tendon tissue contains terminally differentiated tenocytes and a small resident tendon stem cell population, known as tendon stem/progenitor cells (TSPCs). TSPCs showed standard mesenchymal stem cell (MSC) characteristics, including self-renewal, clonogenicity, and multilineage differentiation potential; TSPCs also express classical MSC surface antigens and tendon lineage genes (Bi et al., 2007; Lui and Wong, 2019). TSPCs are essential for effective repair, regeneration, and maintenance of tendon. Previous studies have demonstrated that TSPCs features

alter during tendon aging; aged TSPCs premature entry into senescence and exhibit profound self-renewal, migration, and tenogenic differentiation deficits (Kohler et al., 2013; Yin et al., 2020). These age-related changes of TSPCs led to impaired tendon healing and regeneration capacity (Dai et al., 2019; Li et al., 2019). Although the link between TSPCs and tendon aging has been well recognized, the specific mechanisms underlying age-related TSPC dysfunction remain incompletely clarified.

The Janus kinase-signal transducer and activator of transcription (JAK-STAT) signaling pathway is a cytokine-stimulated signal transduction pathway and involves in various biological processes, including differentiation, immune regulation, proliferation, and hematopoiesis (Herrera and Bach, 2019; Salas et al., 2020). Studies have also demonstrated that JAK-STAT signaling pathway plays a vital role in stem cell aging. In satellite cells, increased JAK-STAT signaling pathway impairs muscle regeneration during aging, and JAK-STAT signaling inhibition enhances satellite cell expansion, muscle repair, and functional performance (Price et al., 2014). Xu et al. (2015b) reported that inhibition of JAK-STAT signaling pathway attenuates the senescence-associated secretory phenotype (SASP) in aged preadipocytes and umbilical vein endothelial cells; JAK-STAT inhibition also decreases age-related inflammation and frailty. Doles et al. (2012) showed that increased JAK-STAT signaling inhibits hair follicle stem cell function in aged mice. In addition, our previous study has demonstrated that JAK-STAT signaling pathway is activated in TSPCs of Achilles tendon from aged rats (Chen et al., 2020). Therefore, these findings prompted us to investigate the specific role of the JAK-STAT signaling pathway in TSPC aging and age-related dysfunction.

In the present study, we confirm that senescent TSPCs accumulate in tendon tissue with aging. We showed that increased JAK-STAT signaling induces TSPC senescence. Inhibition of JAK-STAT signaling pathway attenuates cell senescence and SASP in aged TSPCs. Moreover, JAK-STAT inhibitor restored the age-related dysfunction of self-renewal, migration, and stemness. Our findings provide insights into the possible contribution of senescent TSPCs to age-related tendon disorder. JAK-STAT signaling pathway could be an ideal therapeutic target to antagonize tendon aging.

MATERIALS AND METHODS

TSPC Isolation and Culture

For TSPC isolation and culture, 4- and 20-month-old male Sprague-Dawley rats were used ($n = 10$). Rat TSPCs were isolated from young and aged Achilles tendons as previously described (Rui et al., 2010). All experimental procedures were approved by the Animal Research Ethics Committee of Southeast University. Briefly, the Achilles tendons were minced and digested with type I collagenase (3 mg/ml; Sigma-Aldrich), then gently passed through 70 μm cell strainers (Becton Dickinson) to obtain single-cell suspensions. The cells were cultured in Dulbecco's modified essential medium (DMEM), supplemented with 10% fetal bovine serum, and 1% penicillin-streptomycin (all from Gibco) at 5% CO_2 (37°C). Fresh culture medium was changed every 3 days. Cells from passages 2–6 were used for the experiments.

Cell Transfection

JAK2-siRNA and STAT3-siRNA were designed and synthetized from GenePharma (Shanghai, China). The sequence of JAK2-siRNA was as follows: GCACAUCAGAAUGGUGAUATT (sense: 5′-3′), UAUCACCAUUCUGAUGUGCTT (anti-sense: 5′-3′). The sequence of STAT3-siRNA was as follows: GGCAUUCGGAAAGUAUUGUTT (sense: 5′-3′), ACAAUACUUUCCGAAUGCCTT (anti-sense: 5′-3′). When cells reached 50% confluence, they were transfected with siRNAs using the jetPRIME transfection reagent (Polyplus) according to the manufacturer's protocol. At 48 h after transfection, the cells were harvested and used for subsequent assays.

RNA Sequencing

The RNA sequencing was performed by Beijing CapitalBio Corporation (Beijing, China) as previously described (Chen et al., 2020). The libraries were generated using NEBNext Ultra RNA Library Prep Kit for Illumina and sequenced on the Illumina HiSeq 2500 platform. For data analysis, genes with fold change ≥ 2 and P-value < 0.05 were recognized as to be significantly differentially expressed genes. Clustering analysis and heat map construction were performed with Cluster 3.0 software. For gene set enrichment analysis (GSEA, Broad Institute), the significant difference was verified using the normalized enrichment score (NES) and false discovery rate (FDR).

Quantitative RT-PCR

Total RNA of the TSPCs was extracted using MiniBEST universal RNA extraction kit (Takara) according to the manufacturer's instructions. The First-Strand cDNA kit (Promega) was used to synthesize cDNA from mRNA. Each PCR reaction was conducted in a 20-μl reaction mixture containing 1 μl of total cDNA, Power SYBR Green PCR Master Mix (Invitrogen), and specific primers. Quantitative RT-PCR was performed using the ABI Step-One Plus system. The cycling parameters were as follows: 95°C for 10 min, followed by 45 cycles at 95°C for 20 s, optimal annealing temperature for 20 s, 72°C for 30 s, and finally 60–95°C in increments of 0.1°C/s. The relative expression of each target gene was normalized with β-actin gene. Relative gene expression fold change was calculated with $2^{-\Delta\Delta Ct}$ method. The primers used for PCR are listed in **Supplementary Table 1**.

Western Blotting

Total protein of the TSPCs was extracted in cold RIPA lysis buffer (Keygen biotech), and the protein concentration was measured using BCA protein assay kit (Thermo Scientific). A total of 30 μg of protein was electrophoresed on SDS-PAGE. After electrotransfer onto PVDF membrane (Millipore), the membranes were blocked with PBST containing 5% non-fat dry milk for 1 h at room temperature. The membranes were then incubated with primary antibody against JAK2 (Proteintech), p-JAK2 (Abcam), STAT3 (Proteintech), p-STAT3 (Abcam),

$p16^{INK4A}$ (Beyotime Biotechnology), cyclin D1 (Bioworld), cyclin B1 (Proteintech), and GAPDH (Proteintech) at 4°C overnight. After washing with PBST, the membranes were incubated with secondary antibody and immunoreactive bands were visualized with ECL reagents (Keygen biotech).

β-Galactosidase Staining

β-Galactosidase staining was performed with the senescence-associated β-galactosidase staining kit (Sigma). TSPCs were plated in 12-well plates and incubated for 48 h; cells were then washed with PBS and fixed in 4% paraformaldehyde for 15 min. Next, cells were incubated with staining mixture for 16 h at 37°C. The percentage of positive cells was calculated by counting at least 300 cells in six microscopic fields. Images were captured using an Olympus inverted phase contrast microscope.

Cell Cycle Analysis

Analysis of cell cycle distribution was assessed using the cell cycle detection kit (Keygen Biotech). The TSPCs were cultured for 24 h before being trypsinized and detached. Cells were then fixed in 70% ethanol overnight at 4°C. After being washed, the ethanol-fixed cells were incubated with RNase A and propidium iodine for 30 min. The cell cycle distributions were analyzed on flow cytometry (Becton-Dickinson) using Cell Quest software.

Colony Forming Unit Assays

Tendon stem/progenitor cells were seeded at a density of 2, 5, and 10 cells/cm^2 in six-well plates respectively and cultured for 10 days to form colonies. Cells were fixed in 4% paraformaldehyde for 15 min and stained with 0.5% crystal violet for counting the number of colonies. Colony forming unit (CFU) efficiency was calculated as follows: counted colonies/number of inoculated cells × 100.

EdU Detection

For EdU detection, the EdU Cell Proliferation Kit with Alexa Fluor 594 (Beyotime Biotechnology) was used according to the manufacturer's protocol. Briefly, cultured TSPCs were incubated with 10 μM EdU for 5 h, then fixed in 4% paraformaldehyde for 15 min at room temperature. After being washed, cells were permeabilized with 0.3% Triton X-100 for 10 min, then cells were stained with click additive solution for 30 min. Immunofluorescence was visualized using a Nikon Ts2R fluorescence microscope.

CCK-8 Assay

Cell proliferation was measured using the Cell Counting Kit-8 (CCK-8, Keygen biotech) assay. TSPCs were seeded at a density of 3,000 cells/well in 96-well plates and cultured for 0, 24, 48, and 72 h, respectively. The cells were then treated with 10 μl of CCK-8 reagent and incubated for 2 h at 37°C. The absorbance value of each well was measured at 450 nm.

Population Doubling Time Assay

Population doubling time (PDT) was calculated using the formula $\log_2 [N_c/N_0]$, where N_c is the total cell number at confluence and N_0 is the number of inoculated cells.

TSPCs Migration Assay

A scratch assay was used to measure TSPC migration. TSPCs were seeded in six-well plates and grown to confluence. The cell layer was then scratched with a sterile pipette tip and incubated for 16 h. Images were captured using an Olympus inverted phase contrast microscope. Cell velocity was quantified by scratch length and scratch bridging time.

Investigation of Actin Dynamics

For actin dynamics analysis, TSPCs were seeded in six-well plates and incubated for 48 h. Cells were then treated with 0.4 μM latrunculin A (Sigma Aldrich) for 0, 15, 30, and 60 min, respectively. Next, cells were fixed in 4% paraformaldehyde for 15 min at room temperature. After being washed, cells were permeabilized with 0.1% Triton X-100 for 10 min, then cells were stained with Alexa Flour 546 phalloidin (Thermo Scientific) for 1 h at room temperature. Immunofluorescence was visualized using a Nikon Ts2R fluorescence microscope.

Statistical Analysis

All data are plotted as mean ± SEM. Unpaired *t*-test was used for comparisons between two groups, and one-way analysis of variance (ANOVA) followed by Tukey's *post hoc* test was used for multiple comparisons. $P < 0.05$ were considered to be statistically significant. Each experiment had three replicates per condition, and the experiment was performed three times.

RESULTS

TSPCs Exhibit a Senescent Phenotype With Advancing Age

To characterize the senescent phenotype in TSPCs, we isolated TSPCs from Achilles tendon of 4-month-old (Y-TSPC) and 20-month-old (A-TSPC) Sprague-Dawley rats. We first performed RNA sequencing on young and aged TSPCs; we found substantial changes in transcriptome. The results showed 2,142 upregulated mRNAs and 2,455 downregulated mRNAs in aged TSPCs (**Figure 1A**). In addition, we observed increased in the number of β-galactosidase (β-gal)-positive senescent cells in aged TSPCs (**Figures 1B,C**). This was coupled with a significant upregulation of senescence-associated marker $p16^{INK4A}$ in aged TSPCs (**Figures 1D,E**). Cell cycle arrest is an important indication of cellular senescence (Gorgoulis et al., 2019); we next investigated cell cycle phase distribution of TSPCs. The results revealed an accumulation of aged TSPCs in G1 phase, with a reduced number of cells in the S and G2/M phases (**Figure 1F**). Moreover, we investigated the expressions of some representative SASP genes, including interleukin (IL)6, matrix metalloproteinase (MMP)9, and C-X-C motif chemokine ligand 12 (CXCL12), and the results showed that these SASP gene levels were highly increased in aged TSPCs (**Figures 1G–I**). Collectively, our findings suggested that the aged tendon contains an increased proportion of senescent TSPCs, which could induce tissular and cellular dysfunction.

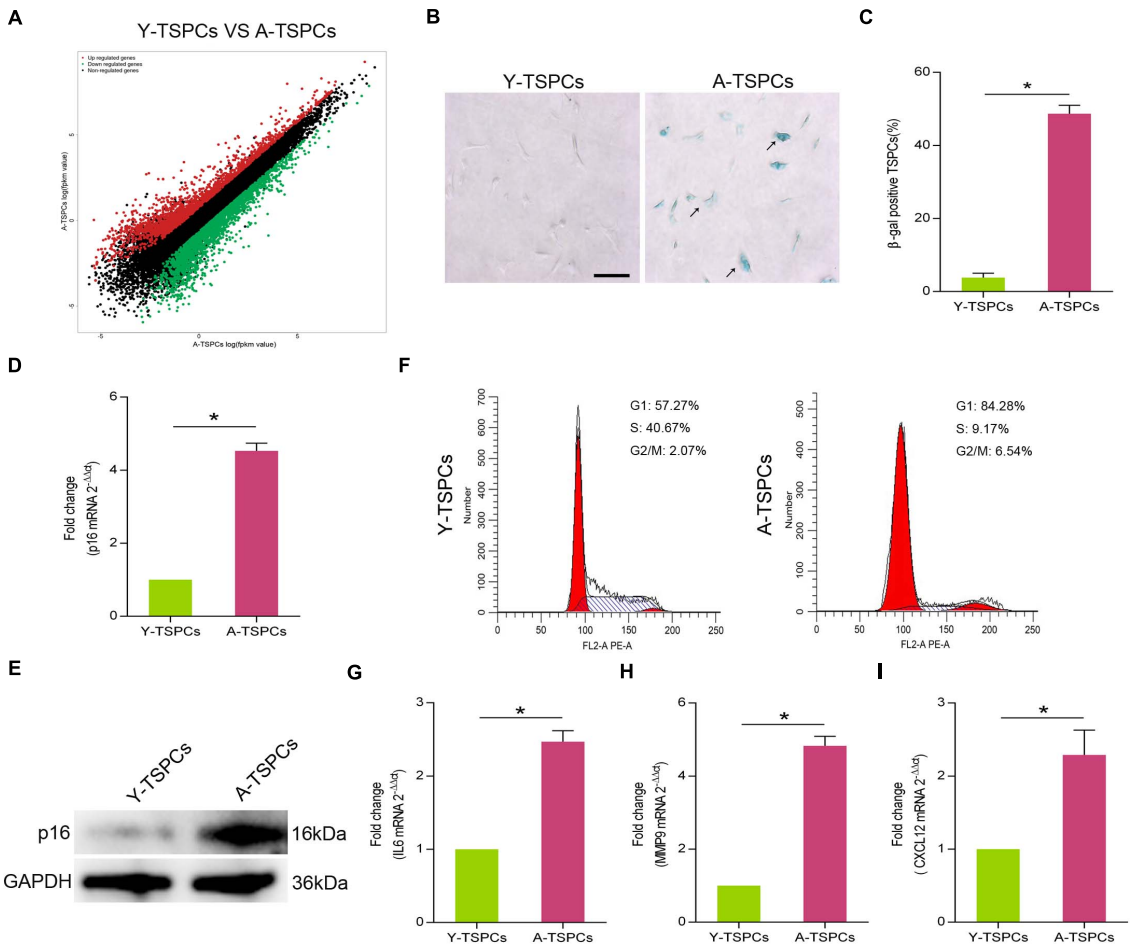

FIGURE 1 | The TSPCs from aged Achilles tendon showed senescence characteristics. **(A)** RNA-seq analysis of young and aged TSPCs. Scatter plot represents fpkm values for genes expressed in young and aged TSPCs. Red dots show the upregulated and green dots show the downregulated genes (fold change ≥ 2). **(B,C)** β-gal staining for the senescent cells in young and aged TSPCs. Scale bars: 100 μm. **(D)** Relative mRNA levels of $p16^{INK4A}$ in young and aged TSPCs were investigated by qRT-PCR. **(E)** Western blotting for the $p16^{INK4A}$ protein levels in young and aged TSPCs. **(F)** The cell cycle distribution of TSPCs was measured by flow cytometry. **(G–I)** qRT-PCR for SASP gene (IL6, MMP9, and CXCL12) expressions in young and aged TSPCs. *$P < 0.05$ compared with young group.

JAK-STAT Signaling Pathway Is Activated in Aged TSPCs

We analyzed gene sets using the Kyoto encyclopedia of genes and genomes (KEGG) suite in Gene set enrichment analysis (GSEA) to identify enriched signaling pathways in young and aged TSPCs. The GSEA KEGG analysis showed a significant decrease in enrichment of genes associated with JAK-STAT signaling pathway in aged TSPCs (**Figure 2A**). To study the activity of JAK-STAT signaling pathway in aged TSPCs, we investigated the expressions of p-JAK2 and p-STAT3 in young and aged TSPCs, and the result showed that the protein levels of p-JAK2 and p-STAT3 were notably increased in aged TSPCs (**Figure 2B**). Moreover, we examined the expressions of some representative genes involved in JAK-STAT signaling pathway, and we found significant higher levels of JAK-STAT activators (Egfr, Ar, and IL6ST), JAK-STAT coactivators (JunD, Cebpd, and Fos), and JAK-STAT targets (Bcl2, Pim1, and Myc) in TSPCs from aged rat relative to young rat (**Figures 2C–E**). We next treated young TSPCs with interferon-γ (IFN-γ), an activating cytokine of JAK-STAT signaling pathway. The results showed that IFN-γ treatment increased the percentage of β-gal-positive senescent cells (**Figures 2F,G**), as well as the expression of $p16^{INK4A}$ in young TSPCs (**Figures 2H,I**). Cell cycle analysis revealed that IFN-γ treatment induced G1 arrest in young TSPCs (**Figure 2J**). Moreover, IFN-γ treatment also increased the mRNA levels of IL6, MMP9, and CXCL12 in young TSPCs (**Figures 2K–M**). These results indicated that the activity of JAK-STAT signaling pathway is increased with age, which might be associated with the senescence of TSPCs.

Inhibition of JAK-STAT Signaling Pathway Attenuates TSPC Senescence

To investigate the specific role of JAK-STAT signaling pathway in TSPC senescence, we treated aged TSPCs with JAK2-siRNA or STAT3-siRNA. The transfection efficiency was detected by Western blotting and qRT-PCR (**Figures 3A–D**). Our

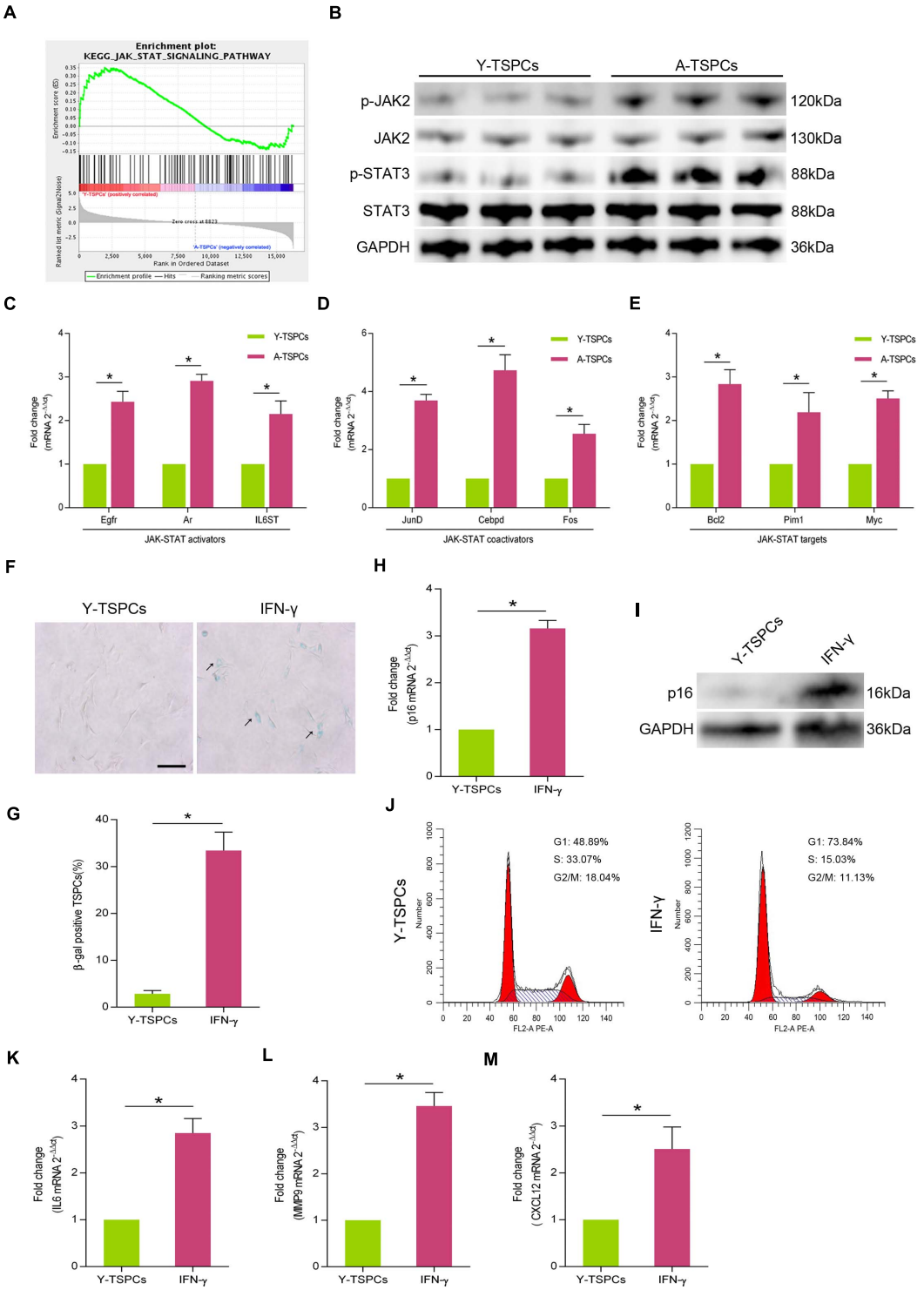

FIGURE 2 | The activity of JAK-STAT signaling pathway is increased with age. **(A)** GSEA plots showed a gene set related to JAK-STAT pathway. **(B)** Western blotting for the p-JAK2, JAK2, p-STAT3, and STAT3 protein levels in young and aged TSPCs. **(C–E)** Relative mRNA levels of JAK-STAT activators (Egfr, Ar, and IL6ST), JAK-STAT coactivators (JunD, Cebpd, and Fos), and JAK-STAT targets (Bcl2, Pim1, and Myc) in young and aged TSPCs were validated by qRT-PCR. **(F,G)** β-gal staining for the senescent cells in young TSPCs upon IFN-γ (100 ng/ml, 24 h) treatment. Scale bars: 100 μm. **(H)** qRT-PCR for the $p16^{INK4A}$ mRNA levels in young TSPCs upon IFN-γ treatment for 8 h. **(I)** Western blotting for the $p16^{INK4A}$ protein levels in young TSPCs after treatment with IFN-γ (100 ng/ml, 8 h). **(J)** Flow cytometry analysis was used to measure the cell cycle distribution of young TSPCs after IFN-γ treatment for 48 h. **(K–M)** qRT-PCR for SASP genes (IL6, MMP9, and CXCL12) expressions in young TSPCs upon IFN-γ treatment for 8 h. $^*P < 0.05$ compared with the young group.

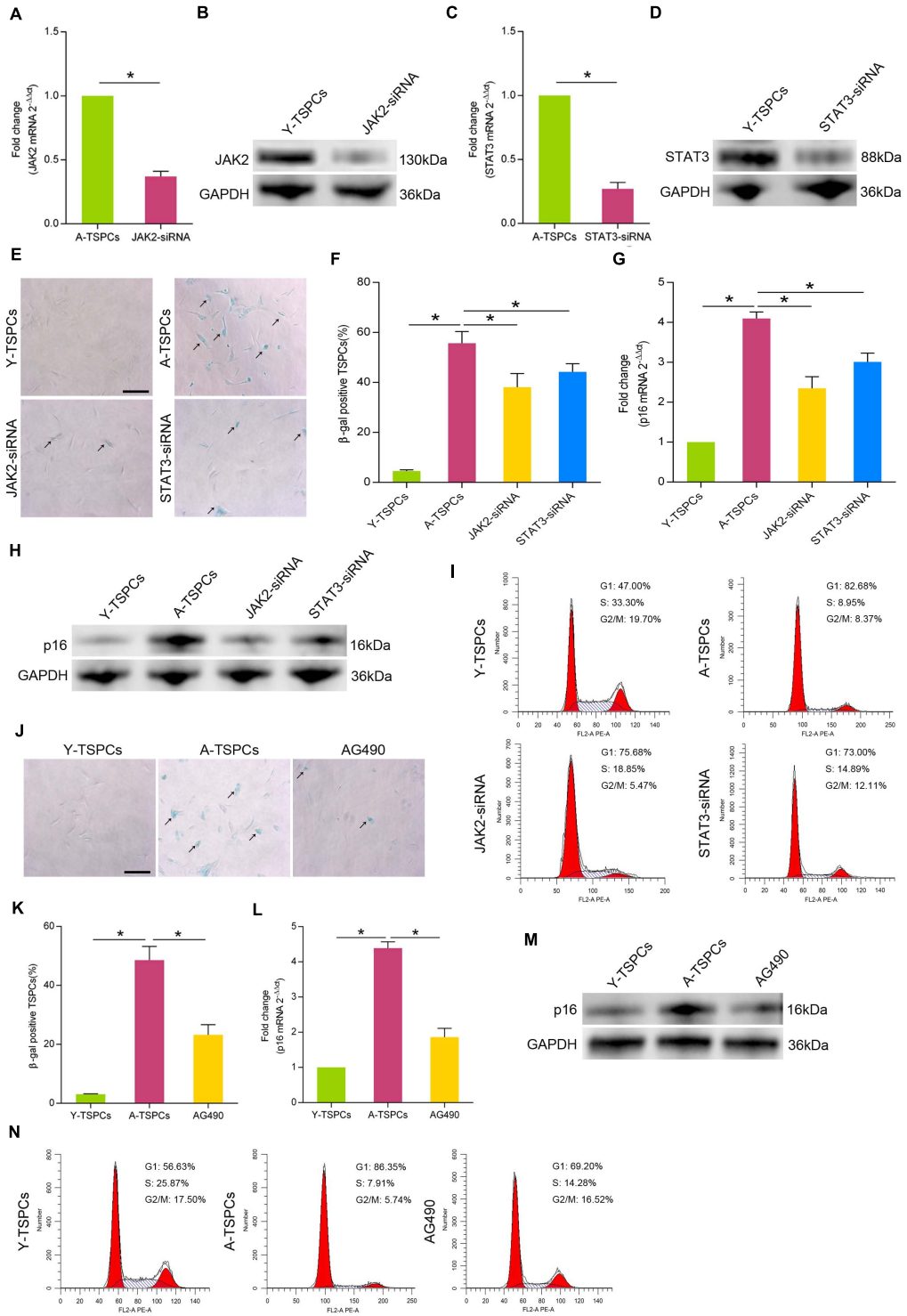

FIGURE 3 | Inhibition of JAK-STAT signaling pathway inhibits cellular senescence. **(A,B)** The transfection efficiency of JAK2-siRNA was explored by qRT-PCR and Western blotting in aged TSPCs. **(C,D)** The expression of STAT3 mRNA and protein was measured by qRT-PCR and Western blotting in aged TSPCs after treatment with STAT3-siRNA. **(E,F)** β-gal staining for the senescent cells in aged TSPCs upon JAK2-siRNA or STAT3-siRNA treatment. Scale bars: 100 μm. **(G,H)** The expression of $p16^{INK4A}$ mRNA and protein was measured by qRT-PCR and Western blotting. **(I)** The cell cycle distribution of TSPCs was measured by flow cytometry after JAK2-siRNA/STAT3-siRNA treatment. **(J,K)** β-gal staining for the senescent cells in aged TSPCs after treatment with AG490 treatment (100 μM, 24 h). Scale bars: 100 μm. **(L,M)** The $p16^{INK4A}$ level was investigated by qRT-PCR and Western blotting in young, aged, and aged AG490-treated TSPCs. **(N)** Cell cycle analysis of aged TSPCs after AG490 treatment for 48 h. *$P < 0.05$ compared with the young or aged group.

results showed that treatment with JAK2-siRNA or STAT3-siRNA significantly reduced the β-gal-positive senescent cells in aged TSPCs (**Figures 3E,F**). Besides, JAK2-siRNA or STAT3-siRNA treatment also decreased the $p16^{INK4A}$ level of aged TSPCs (**Figures 3G,H**). Cell cycle analysis revealed that the accumulation of aged TSPCs at G1 phase was rescued after JAK2 or STAT3 knockdown (**Figure 3I**). In addition, we also treated aged TSPCs with the JAK-STAT signaling pathway inhibitor AG490. Notably, AG490 treatment showed an attenuated senescent phenotype, as indicated by reduced β-gal-positive senescent cells (**Figures 3J,K**) and $p16^{INK4A}$ level (**Figures 3L,M**), as well as the accumulation of G1 phase (**Figure 3N**). Together, these findings further indicated that the JAK-STAT signaling pathway plays an essential role in regulating TSPC senescence.

JAK-STAT Signaling Pathway Inhibitor Suppresses the SASP in Aged TSPCs

Given that the inhibition of JAK-STAT signaling pathway could attenuate cellular senescence in aged TSPCs, we examined whether inhibiting the JAK-STAT pathway blunts the SASP gene expressions. Using qRT-PCR, we investigated the expressions of some representative SASP genes, including IL6, IL1B, MMP3, MMP9, and CXCL12. The results showed that these SASP gene expressions were significantly increased in aged TSPCs (**Figures 4A–E**), which suggested that TSPCs exhibit a SASP upon becoming senescent. Meanwhile, AG490 treatment reduced the SASP gene levels of aged TSPCs (**Figures 4A–E**). Collectively, our findings indicated that the capacity of JAK-STAT signaling pathway inhibitor suppresses the SASP in aged TSPCs.

AG490 Restores the Self-Renewal Deficit of Aged TSPCs

To investigate the role of JAK-STAT signaling pathway in TSPC self-renewal, we treated aged TSPCs with AG490. The results showed that AG490 significantly increased the colony number and CFU efficiency in the aged TSPCs compared with the young TSPCs (**Figures 5A,B**). We next measured the percentage of proliferating cells after incubation with 5-ethynyl-2′-deoxyuridine (EdU), and AG490 treatment increased the percentage of EdU-positive senescent cells in aged TSPCs (**Figures 5C,D**). Moreover, the PDT and CCK-8 assay also demonstrated the ability of AG490 to enhance the proliferative potential of aged TSPCs (**Figures 5E,F**). To further explore the changes at molecular level, we investigated the expressions of cell proliferation-related proteins in TSPCs, and we found that the expressions of cyclin D1 and cyclin B were significantly reduced in aged TSPCs, while the reduced levels of these proteins were rescued after AG490 treatment (**Figure 5G**). Together, our results suggested that inhibition of JAK-STAT signaling pathway improves the self-renewal ability of aged TSPCs.

Inhibition of JAK-STAT Signaling Pathway Promotes Migration and Actin Dynamics of Aged TSPCs

Tendon stem/progenitor cell migration is required for tendon-healing process. We tested if JAK-STAT signaling pathway suppression improves the migration deficit of aged TSPCs. We performed a scratch assay to mimic wound closure, and the result showed that the migration speed and distance of aged TSPCs were slower than young TSPCs, while AG490 restores the migration deficit of aged TSPCs (**Figures 6A–C**). Since the turnover rate of the actin cytoskeleton is important for cell migration, we performed phalloidin staining to compare the actin dynamics by treating TSPCs with latrunculin A in a time-dependent manner. We observed a slower rate of actin turnover in aged TSPCs compared with the young TSPCs, and AG490 significantly reduced the F-actin content in aged TSPCs, which suggested that AG490 increases actin turnover of aged TSPCs (**Figure 6D**). Collectively, these results indicated that inhibition of JAK-STAT signaling pathway restores the migration deficit and improves actin dynamics of aged TSPCs.

AG490 Promotes Stemness and Tendon-Related Marker Expressions of Aged TSPCs

To study the role of JAK-STAT signaling pathway in the stemness of TSPCs, we investigated the expressions of some representative stem cell markers, including Nanog, Oct-4, Sca-1, and Ssea-1. The results revealed that these markers were reduced in aged TSPCs, which suggested that aging suppresses the stemness of TSPCs, and AG490 treatment reverses the inhibitory effect of aging on stemness in aged TSPCs (**Figures 7A–D**). Given the ability of AG490 to promote stemness of aged TSPCs, we next investigated the role of JAK-STAT signaling pathway in tenogenic differentiation of TSPCs. We examined the mRNA levels of the key tendon-related marker, including Tnmd, Scx, Col1A1, Nestin, and Dcn, and these markers were significantly downregulated in aged TSPCs, which suggested a lower tenogenic differentiation capacity of aged TSPCs. In addition, AG490 treatment could increase the expressions of the tendon-related markers in aged TSPCs (**Figures 7E–I**). Together, these findings indicated a critical role of JAK-STAT signaling pathway in stemness and tenogenic differentiation of TSPCs.

DISCUSSION

Tendon stem/progenitor cell function declines with age. Our study showed that TSPCs isolated from aged tendon exhibit a senescent phenotype, as evidenced by increased expression of senescence-associated marker ($p16^{INK4A}$, β-gal), cell cycle arrest, and SASP. Cellular senescence is a cell state related to various physiological processes and a series of age-related diseases (Gorgoulis et al., 2019). The accumulation of senescent cells in aged TSPCs not only offer new insights into the biological mechanisms of TSPCs aging but also indicate that age-related TSPC dysfunction could be linked to the pathological changes of aged tendon. In the present study, we demonstrated that activation of the JAK-STAT signaling pathway is closely correlated with TSPC senescence. The JAK-STAT signaling pathway is an important intracellular pathway and has been shown to play a vital role in aging (Shen-Orr et al., 2016; Lenhart et al., 2019). As JAK-STAT signaling pathway is

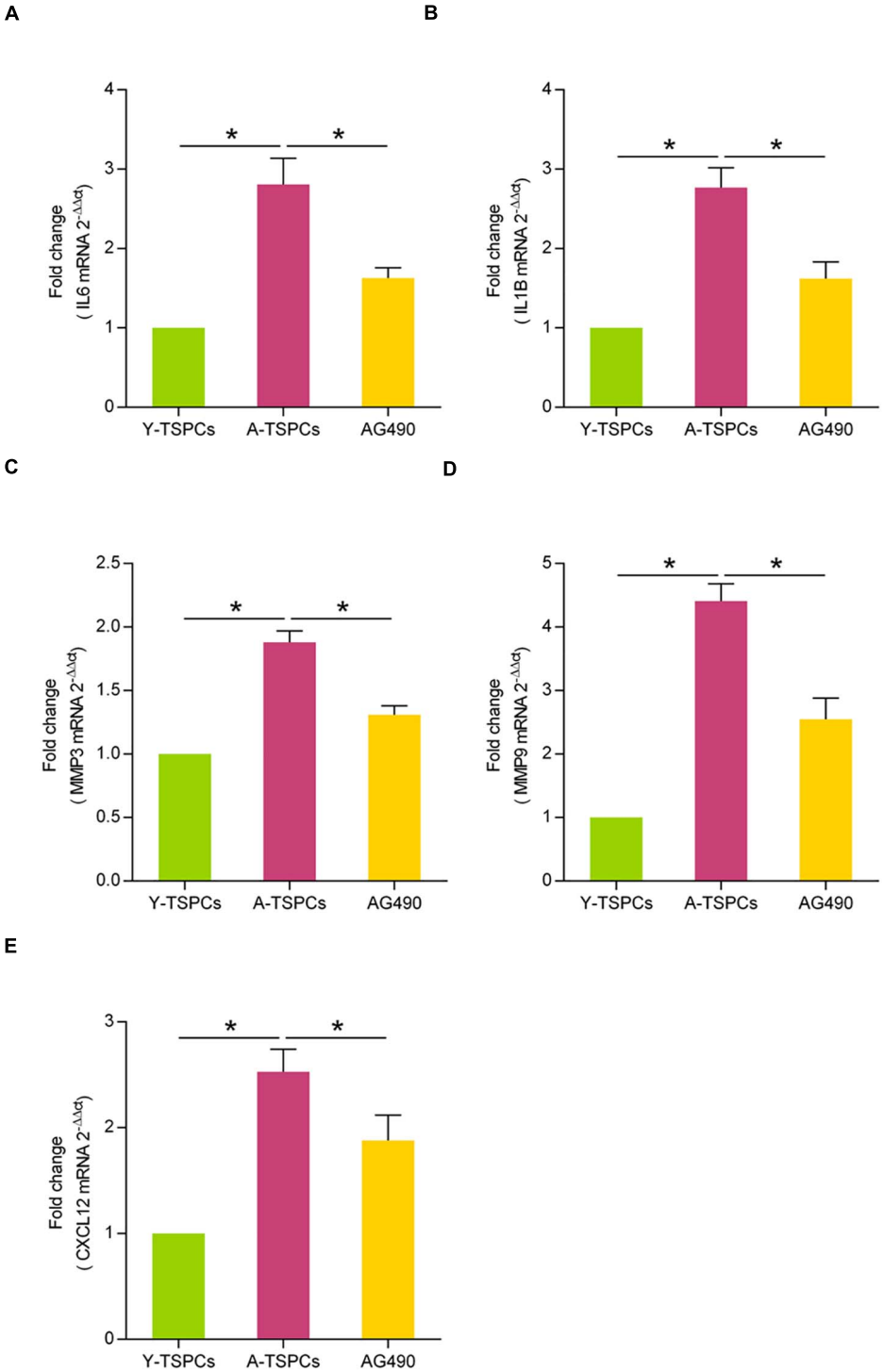

FIGURE 4 | AG490 inhibits the SASP expression in aged TSPCs. **(A–E)** Relative mRNA levels of representative SASP genes (IL6, IL1B, MMP3, MMP9, and CXCL12) in young, aged, and aged AG490-treated TSPCs were investigated by qRT-PCR. *$P < 0.05$ compared with the young or aged group.

frequently activated during the aging process, JAK inhibitors are being widely used to alleviate age-related dysfunction (Tierney et al., 2014; Qin et al., 2016; Verstovsek et al., 2017). These findings raise the possibility that inhibition of the JAK-STAT signaling is a potentially promising strategy for antagonizing TSPC aging. Consistent with this possibility, we treated aged TSPCs with inhibitors of the JAK-STAT signaling pathway JAK2-siRNA, STAT3-siRNA, and AG490; notably, treatment

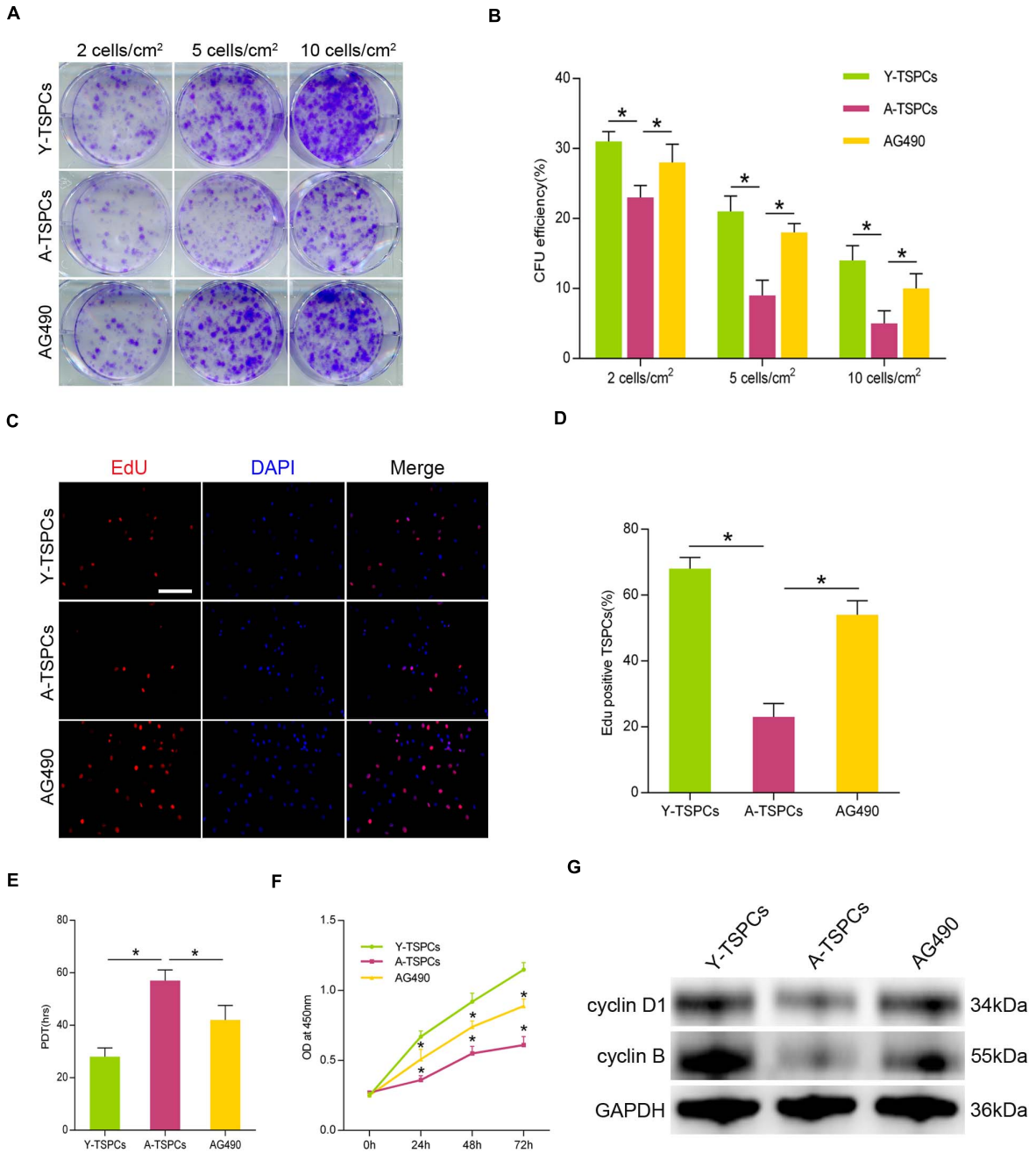

FIGURE 5 | Inhibition of JAK-STAT signaling pathway increases aged TSPC self-renewal. **(A)** Colony forming unit (CFU) assay showed multiple TSPC colonies stained with crystal violet at three densities. **(B)** Colony forming efficiency of young, aged, and aged AG490-treated TSPCs. **(C,D)** Representative images for EdU staining and EdU incorporation was quantified as EdU$^+$ cells/total cells. Scale bar: 50 μm. **(E,F)** Cell proliferation was investigated by population doubling time (PDT) assay and CCK-8 assay. **(G)** The protein levels of cyclin D1 and cyclin B were analyzed by Western blotting. *$P < 0.05$ compared with the young or aged group.

with these inhibitors significantly attenuated TSPC senescence, highlighting the role of JAK-STAT signaling pathway in TSPCs. In contrary, treatment of young TSPCs with activating cytokine of JAK-STAT signaling pathway IFN-γ promoted premature senescence of young TSPCs. Collectively, the role of JAK-STAT signaling pathway in promoting senescence may represent a new mechanism in TSPC aging.

A hallmark of aging is chronic sterile inflammation, and increased pro-inflammatory cytokines and cytokines are closely associated with age-related diseases (Lopez-Otin et al., 2013; Tchkonia et al., 2013; Xu et al., 2015b). Studies have demonstrated that inflammation is also associated with tendon aging, and chronic, low-grade inflammation can damage tendon structure (Gaida et al., 2009; Dakin et al., 2012). Senescent cells exhibit a

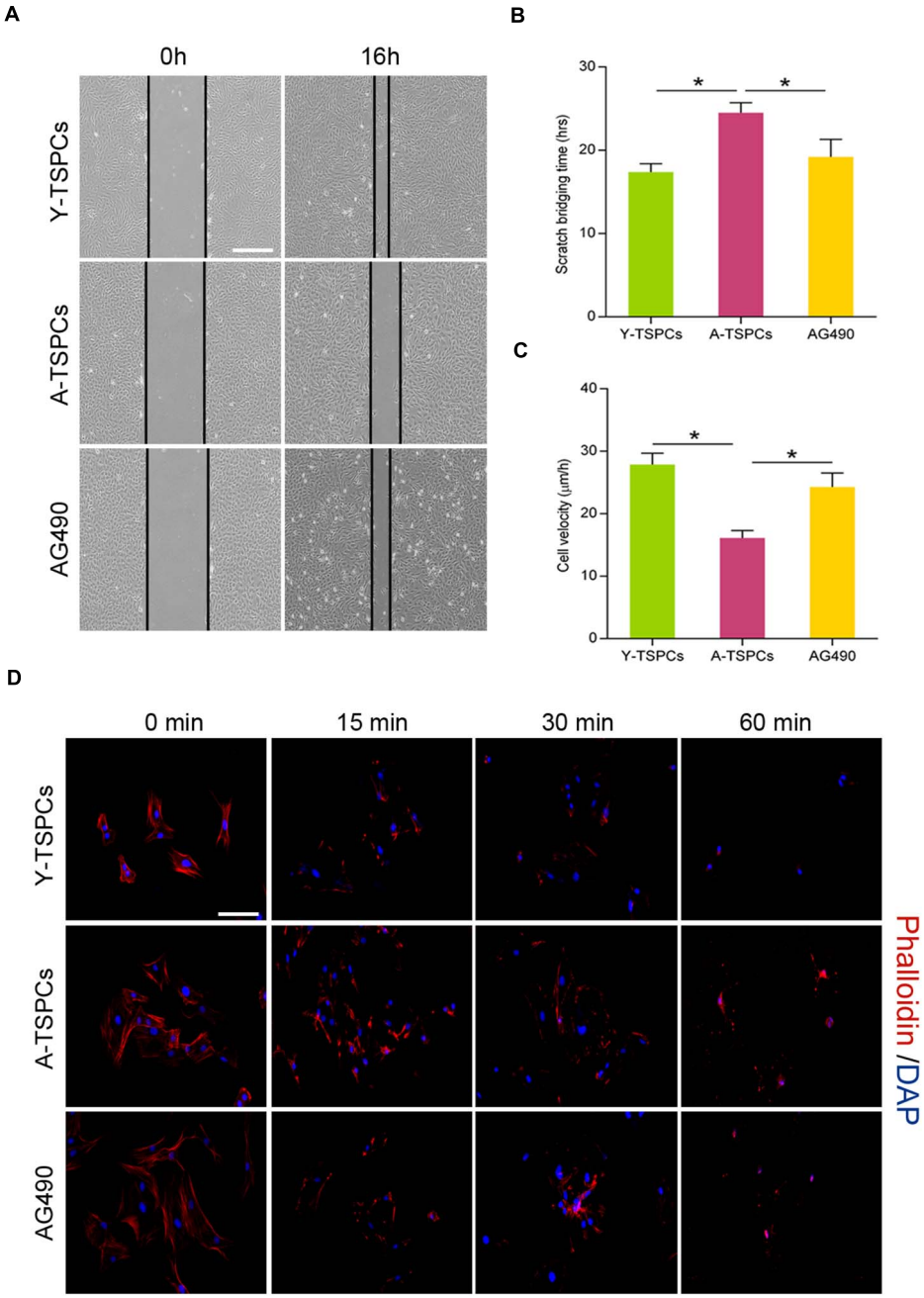

FIGURE 6 | AG490 enhances aged TSPC migration and actin dynamics. **(A)** Representative scratch assay of young, aged, and aged AG490-treated TSPCs. Scale bar: 200 μm. **(B,C)** TSPC migration rate was calculated by scratch bridging time and cell velocity. **(D)** Phalloidin staining for F-actin in young, aged, and aged AG490-treated TSPCs at each time point after latrunculin A treatment. Scale bar: 20 μm. *$P < 0.05$ compared with the young or aged group.

SASP, and the SASP contains large amounts of pro-inflammatory cytokines, matrix metalloproteinases, and chemokines and contributes to persistent chronic inflammation (Coppe et al., 2010a,b; Franceschi and Campisi, 2014). Therefore, the harmful and pro-aging effects of senescent cells are partly due to the SASP. Previous studies have reported that preadipocytes, endothelial cells, and omental adipose tissue cells develop a SASP with aging (Xu et al., 2015a, 2018). In the present study, a robust pattern of SASP induction is shown in aged TSPCs, which suggests the possibility that senescent TSPCs promotes tendon aging. Studies have demonstrated that the JAK-STAT signaling pathway mediates numerous pro-inflammatory cytokine expressions (Yu et al., 2009; Xu et al., 2015b; Salas et al., 2020). Inhibition of JAK-STAT signaling pathway seems to be an ideal choice for suppressing SASP; consistent with this possibility, we also showed that JAK inhibitor AG490 decreased the SASP in aged TSPCs.

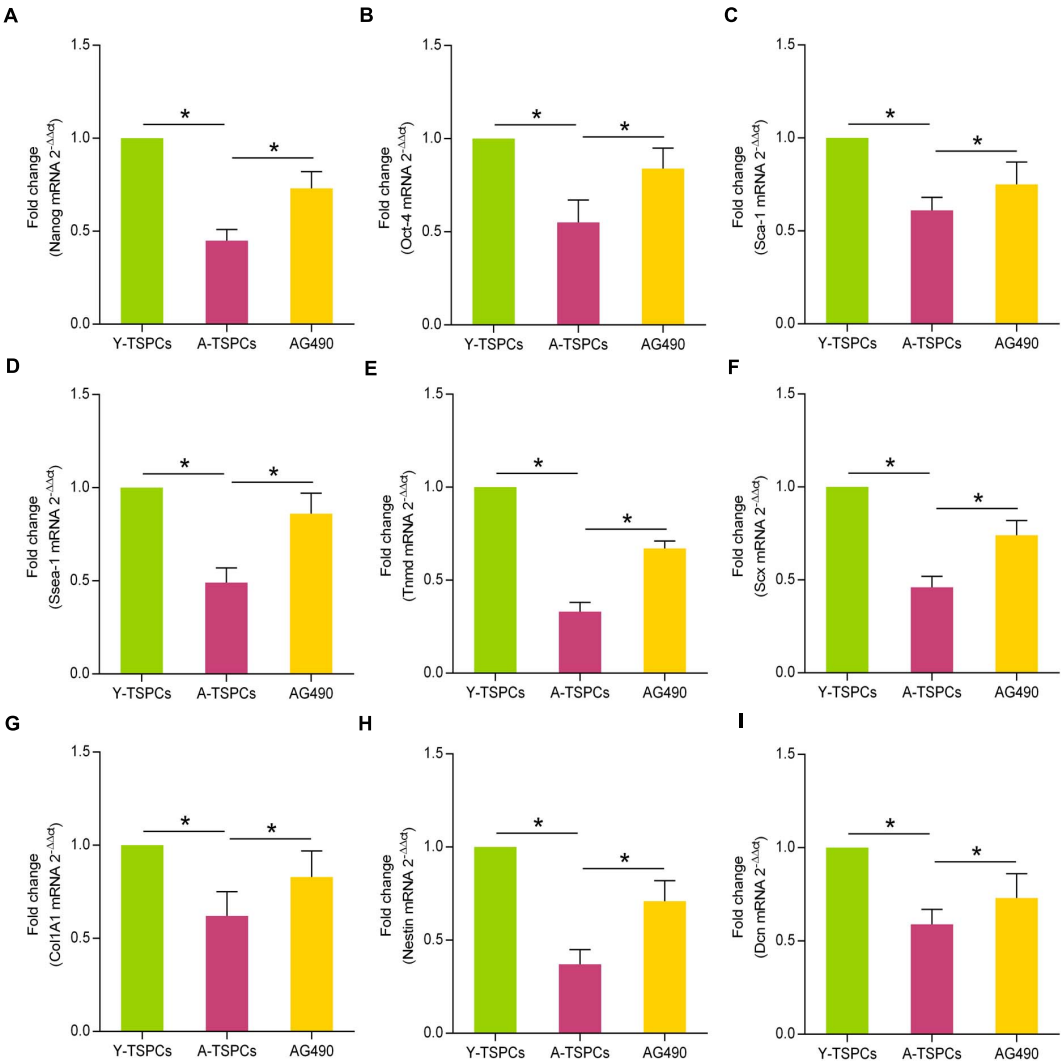

FIGURE 7 | AG490 increases the expressions of stem cell markers and tendon-related genes in aged TSPCs. **(A–D)** Relative mRNA levels of stem cell markers (Nanog, Oct-4, Sca-1, and Ssea-1) in young, aged, and aged AG490-treated TSPCs were investigated by qRT-PCR. **(E–I)** qRT-PCR for the tendon-related genes (Tnmd, Scx, Col1A1, Nestin, and Dcn) upon AG490 treatment. *$P < 0.05$ compared with the young or aged group.

Thus, our results suggested that the JAK-STAT signaling pathway plays a vital role in the SASP and could be an ideal target for alleviating SASP during tendon aging.

Self-renewal ability is a critical property of stem cell to regulate tissue regeneration and homeostasis (Alberton et al., 2015). TSPCs self-renew to maintain a pool of healthy stem cells (Zhang and Wang, 2010). TSPCs exhibit a reduced self-renewal during tendon aging, which may be the key mechanism for ineffective self-renewal and impaired tendon regeneration capacity (Kohler et al., 2013; Zhang and Wang, 2015; Chen et al., 2020). Consistent with previous studies, our results also showed an attenuated self-renewal ability in aged TSPCs, as evidenced by decreased clonogenic potential and proliferation. It has been reported that JAK-STAT signaling pathway plays an important role in stem cell self-renewal, and appropriate levels of JAK-STAT signaling pathway are required for stem cell maintenance and self-renewal (Tulina and Matunis, 2001; Flaherty et al., 2010). In the present study, we reported that inhibition of JAK-STAT signaling pathway significantly enhanced clonogenic capacity and proliferative rate of aged TSPCs, supporting a potential therapeutic role of JAK-STAT signaling pathway in self-renewal of aged TSPCs.

Studies have shown that aged TSPCs exhibit marked reduction in cell migration and actin dynamics of TSPC during tendon aging (Kohler et al., 2013; Popov et al., 2015). Here, we demonstrated that JAK-STAT signaling pathway inhibitor significantly promoted migration and actin dynamics of aged TSPCs. These findings are in line with a benefit effect of JAK-STAT signaling pathway inhibitor in cell migration and actin dynamics as several studies reported (Tu et al., 2012; Ji et al., 2017). Migration is an important repair-mediating TSPC function, enabling TSPCs to move toward and repair

damaged tendon tissues (Dekoninck and Blanpain, 2019). Thus, by improving migration deficit in aged TSPCs, inhibition of JAK-STAT signaling pathway may provide a more effective treatment strategy for age-related tendon disorders. Besides, given that the actin cytoskeleton and its dynamics are vital for cell migration (Rottner and Stradal, 2011), the lower rate of actin turnover offers a possible explanation for the migration deficit in aged TSPCs. Therefore, the enhanced migratory capacity of aged TSPCs may be associated with the improved actin dynamics after JAK-STAT signaling pathway inhibitor treatment.

Differentiation capacity is another key property of TSPCs regulating tendon regeneration and homeostasis (Bi et al., 2007). TSPCs express pluripotency-related factors (Shi et al., 2017; Liu et al., 2018), but their expression decreased with age (Zhang and Wang, 2015). In the present study, we showed that the expressions of Nanog, Oct-4, Sca-1, and Ssea-1 were reduced in aged TSPCs. Nanog and Ssea-1 are involved in the maintenance of stemness in undifferentiated embryonic stem cells (Cui et al., 2004; Pan and Thomson, 2007). Oct-4 is essential for maintaining pluripotency in stem cells (Pesce and Scholer, 2001). Sca-1 is widely recognized as a stem cell marker (Raghuvanshi et al., 2010). Thus, the reduced expressions of these stem cell markers in aged TSPCs observed here indicated that aging suppresses the stemness of TSPCs. In addition, studies have demonstrated that JAK-STAT signaling pathway plays an essential role in stem cell differentiation (Lin et al., 2010; Tanaka et al., 2018). Here, we found that inhibition of JAK-STAT signaling pathway increased these stem cell markers in aged TSPCs, which suggested a vital role of JAK-STAT signaling pathway in TSPC stemness. We next used several tendon-related markers (Tnmd, Scx, Col1A1, Nestin, and Dcn) to investigate the potential role of JAK-STAT signaling pathway in the tenogenic differentiation ability of TSPCs. These tendon-related markers have been shown to be reduced in aged TSPCs, which suggested an impaired tenogenic differentiation ability of aged TSPCs (Zhang et al., 2016; Han et al., 2017). Moreover, inhibition of JAK-STAT signaling pathway restored the age-related reduction of these tendon-related markers in aged TSPCs. Therefore, our results also showed a critical role of JAK-STAT signaling pathway in tenogenic differentiation of TSPCs.

CONCLUSION

In summary, our study suggested that aberrant JAK-STAT signaling pathway is an important contributor to TSPC senescence during tendon aging. Inhibition of JAK-STAT signaling pathway attenuated cellular senescence and SASP in aged TSPCs. In addition, inhibition of JAK-STAT signaling pathway also restored the age-related reduction of self-renewal, migration, actin dynamics, and stemness in TSPCs. Our findings suggested a promising therapeutic target for age-related tendon disorders.

DATA AVAILABILITY STATEMENT

The datasets presented in this study can be found in online repositories. The names of the repository/repositories and accession number(s) can be found here: NCBI BioProject PRJNA701067, https://www.ncbi.nlm.nih.gov/bioproject/PRJNA701067.

ETHICS STATEMENT

The animal study was reviewed and approved by Animal Experimentation Ethics Committee, School of Medicine, Southeast University. Written informed consent was obtained from the owners for the participation of their animals in this study.

AUTHOR CONTRIBUTIONS

YR, MN, and MC designed the experiments. MC, LX, GD, PL, and YZ performed the experiments. YL and MN performed the statistical analysis. MC and YR wrote the manuscript. All authors read and approved the final manuscript.

FUNDING

This work was supported by the National Natural Science Foundation of China (81572187 and 81871812); Jiangsu Provincial Medical Talent, The Project of Invigorating Health Care through Science, Technology, and Education (ZDRCA2016083); the Six Projects Sponsoring Talent Summits of Jiangsu Province, China (LGY2017099); and a grant from the Beijing Municipal Natural Science Foundation (7192194).

SUPPLEMENTARY MATERIAL

The Supplementary Material for this article can be found online at: https://www.frontiersin.org/articles/10.3389/fcell.2021.650250/full#supplementary-material

REFERENCES

Alberton, P., Dex, S., Popov, C., Shukunami, C., Schieker, M., and Docheva, D. (2015). Loss of tenomodulin results in reduced self-renewal and augmented senescence of tendon stem/progenitor cells. *Stem Cells Dev.* 24, 597–609. doi: 10.1089/scd.2014.0314

Bi, Y., Ehirchiou, D., Kilts, T. M., Inkson, C. A., Embree, M. C., Sonoyama, W., et al. (2007). Identification of tendon stem/progenitor cells and the role of the extracellular matrix in their niche. *Nat. Med.* 13, 1219–1227. doi: 10.1038/nm1630

Chen, M., Li, Y., Xiao, L., Dai, G., Lu, P., Wang, Y., et al. (2020). AQP1 modulates tendon stem/progenitor cells senescence during tendon aging. *Cell Death Dis.* 11:193.

Coppe, J. P., Desprez, P. Y., Krtolica, A., and Campisi, J. (2010a). The senescence-associated secretory phenotype: the dark side of tumor suppression. *Annu. Rev. Pathol.* 5, 99–118. doi: 10.1146/annurev-pathol-121808-102144

Coppe, J. P., Patil, C. K., Rodier, F., Krtolica, A., Beausejour, C. M., Parrinello, S., et al. (2010b). A human-like senescence-associated secretory phenotype is conserved in mouse cells dependent on physiological oxygen. *PLoS One* 5:e9188. doi: 10.1371/journal.pone.0009188

Cui, L., Johkura, K., Yue, F., Ogiwara, N., Okouchi, Y., Asanuma, K., et al. (2004). Spatial distribution and initial changes of SSEA-1 and other cell adhesion-related molecules on mouse embryonic stem cells before and during differentiation. *J. Histochem. Cytochem.* 52, 1447–1457. doi: 10.1369/jhc.3a6241.2004

Dai, G. C., Li, Y. J., Chen, M. H., Lu, P. P., and Rui, Y. F. (2019). Tendon stem/progenitor cell ageing: modulation and rejuvenation. *World J. Stem Cells* 11, 677–692. doi: 10.4252/wjsc.v11.i9.677

Dakin, S. G., Dudhia, J., Werling, N. J., Werling, D., Abayasekara, D. R., and Smith, R. K. (2012). Inflamm-aging and arachadonic acid metabolite differences with stage of tendon disease. *PLoS One* 7:e48978. doi: 10.1371/journal.pone.0048978

Dekoninck, S., and Blanpain, C. (2019). Stem cell dynamics, migration and plasticity during wound healing. *Nat. Cell Biol.* 21, 18–24. doi: 10.1038/s41556-018-0237-6

Doles, J., Storer, M., Cozzuto, L., Roma, G., and Keyes, W. M. (2012). Age-associated inflammation inhibits epidermal stem cell function. *Genes Dev.* 26, 2144–2153. doi: 10.1101/gad.192294.112

Flaherty, M. S., Salis, P., Evans, C. J., Ekas, L. A., Marouf, A., Zavadil, J., et al. (2010). chinmo is a functional effector of the JAK/STAT pathway that regulates eye development, tumor formation, and stem cell self-renewal in Drosophila. *Dev. Cell* 18, 556–568. doi: 10.1016/j.devcel.2010.02.006

Franceschi, C., and Campisi, J. (2014). Chronic inflammation (inflammaging) and its potential contribution to age-associated diseases. *J. Gerontol. A Biol. Sci. Med. Sci.* 69(Suppl. 1), S4–S9.

Gaida, J. E., Alfredson, L., Kiss, Z. S., Wilson, A. M., Alfredson, H., and Cook, J. L. (2009). Dyslipidemia in achilles tendinopathy is characteristic of insulin resistance. *Med. Sci. Sports Exerc.* 41, 1194–1197. doi: 10.1249/mss.0b013e31819794c3

Gorgoulis, V., Adams, P. D., Alimonti, A., Bennett, D. C., Bischof, O., Bishop, C., et al. (2019). Cellular senescence: defining a path forward. *Cell* 179, 813–827. doi: 10.1016/j.cell.2019.10.005

Han, W., Wang, B., Liu, J., and Chen, L. (2017). The p16/miR-217/EGR1 pathway modulates age-related tenogenic differentiation in tendon stem/progenitor cells. *Acta Biochim. Biophys. Sin.* 49, 1015–1021. doi: 10.1093/abbs/gmx104

Herrera, S. C., and Bach, E. A. (2019). JAK/STAT signaling in stem cells and regeneration: from Drosophila to vertebrates. *Development* 146:dev167643. doi: 10.1242/dev.167643

Ji, J., Wu, Y., Meng, Y., Zhang, L., Feng, G., Xia, Y., et al. (2017). JAK-STAT signaling mediates the senescence of bone marrow-mesenchymal stem cells from systemic lupus erythematosus patients. *Acta Biochim. Biophys. Sin.* 49, 208–215. doi: 10.1093/abbs/gmw134

Kohler, J., Popov, C., Klotz, B., Alberton, P., Prall, W. C., Haasters, F., et al. (2013). Uncovering the cellular and molecular changes in tendon stem/progenitor cells attributed to tendon aging and degeneration. *Aging Cell* 12, 988–999. doi: 10.1111/acel.12124

Lenhart, K. F., Capozzoli, B., Warrick, G. S. D., and Dinardo, S. (2019). Diminished Jak/STAT signaling causes early-onset aging defects in stem cell cytokinesis. *Curr. Biol.* 29:e253.

Li, Y., Dai, G., Shi, L., Lin, Y., Chen, M., Li, G., et al. (2019). The potential roles of tendon stem/progenitor cells in tendon aging. *Curr. Stem Cell Res. Ther.* 14, 34–42. doi: 10.2174/1574888x13666181017112233

Lin, G., Xu, N., and Xi, R. (2010). Paracrine unpaired signaling through the JAK/STAT pathway controls self-renewal and lineage differentiation of drosophila intestinal stem cells. *J. Mol. Cell Biol.* 2, 37–49. doi: 10.1093/jmcb/mjp028

Liu, Q., Zhu, Y., Amadio, P. C., Moran, S. L., Gingery, A., and Zhao, C. (2018). Isolation and characterization of multipotent turkey tendon-derived stem cells. *Stem Cells Int.* 2018:3697971.

Lopez-Otin, C., Blasco, M. A., Partridge, L., Serrano, M., and Kroemer, G. (2013). The hallmarks of aging. *Cell* 153, 1194–1217.

Lui, P. P. Y., and Wong, C. M. (2019). Biology of tendon stem cells and tendon in aging. *Front. Genet.* 10:1338.

Marqueti, R. C., Durigan, J. L. Q., Oliveira, A. J. S., Mekaro, M. S., Guzzoni, V., Aro, A. A., et al. (2018). Effects of aging and resistance training in rat tendon remodeling. *FASEB J.* 32, 353–368. doi: 10.1096/fj.201700543r

Pan, G., and Thomson, J. A. (2007). Nanog and transcriptional networks in embryonic stem cell pluripotency. *Cell Res.* 17, 42–49. doi: 10.1038/sj.cr.7310125

Pesce, M., and Scholer, H. R. (2001). Oct-4: gatekeeper in the beginnings of mammalian development. *Stem Cells* 19, 271–278. doi: 10.1634/stemcells.19-4-271

Popov, C., Kohler, J., and Docheva, D. (2015). Activation of EphA4 and EphB2 reverse signaling restores the age-associated reduction of self-renewal, migration, and actin turnover in human tendon stem/progenitor cells. *Front. Aging Neurosci.* 7:246.

Price, F. D., Von Maltzahn, J., Bentzinger, C. F., Dumont, N. A., Yin, H., Chang, N. C., et al. (2014). Inhibition of JAK-STAT signaling stimulates adult satellite cell function. *Nat. Med.* 20, 1174–1181. doi: 10.1038/nm.3655

Qin, H., Buckley, J. A., Li, X., Liu, Y., Fox, T. H., Meares, G. P., et al. (2016). Inhibition of the JAK/STAT pathway protects against alpha-synuclein-induced neuroinflammation and dopaminergic neurodegeneration. *J. Neurosci.* 36, 5144–5159. doi: 10.1523/jneurosci.4658-15.2016

Raghuvanshi, S., Sharma, P., Singh, S., Van Kaer, L., and Das, G. (2010). Mycobacterium tuberculosis evades host immunity by recruiting mesenchymal stem cells. *Proc. Natl. Acad. Sci. U.S.A.* 107, 21653–21658. doi: 10.1073/pnas.1007967107

Rottner, K., and Stradal, T. E. (2011). Actin dynamics and turnover in cell motility. *Curr. Opin. Cell Biol.* 23, 569–578. doi: 10.1016/j.ceb.2011.07.003

Rui, Y. F., Lui, P. P., Li, G., Fu, S. C., Lee, Y. W., and Chan, K. M. (2010). Isolation and characterization of multipotent rat tendon-derived stem cells. *Tissue Eng. Part A* 16, 1549–1558. doi: 10.1089/ten.tea.2009.0529

Salas, A., Hernandez-Rocha, C., Duijvestein, M., Faubion, W., Mcgovern, D., Vermeire, S., et al. (2020). JAK-STAT pathway targeting for the treatment of inflammatory bowel disease. *Nat. Rev. Gastroenterol. Hepatol.* 17, 323–337. doi: 10.1038/s41575-020-0273-0

Shen-Orr, S. S., Furman, D., Kidd, B. A., Hadad, F., Lovelace, P., Huang, Y. W., et al. (2016). Defective signaling in the JAK-STAT pathway tracks with chronic inflammation and cardiovascular risk in aging humans. *Cell Syst.* 3:e374.

Shi, Y., Zhou, K., Zhang, W., Zhang, Z., Zhou, G., Cao, Y., et al. (2017). Microgrooved topographical surface directs tenogenic lineage specific differentiation of mouse tendon derived stem cells. *Biomed. Mater.* 12:015013. doi: 10.1088/1748-605x/12/1/015013

Tanaka, Y., Yasugi, T., Nagayama, M., Sato, M., and Ei, S. I. (2018). JAK/STAT guarantees robust neural stem cell differentiation by shutting off biological noise. *Sci. Rep.* 8:12484.

Tchkonia, T., Zhu, Y., Van Deursen, J., Campisi, J., and Kirkland, J. L. (2013). Cellular senescence and the senescent secretory phenotype: therapeutic opportunities. *J. Clin. Invest.* 123, 966–972. doi: 10.1172/jci64098

Tierney, M. T., Aydogdu, T., Sala, D., Malecova, B., Gatto, S., Puri, P. L., et al. (2014). STAT3 signaling controls satellite cell expansion and skeletal muscle repair. *Nat. Med.* 20, 1182–1186. doi: 10.1038/nm.3656

Tu, B., Du, L., Fan, Q. M., Tang, Z., and Tang, T. T. (2012). STAT3 activation by IL-6 from mesenchymal stem cells promotes the proliferation and metastasis of osteosarcoma. *Cancer Lett.* 325, 80–88. doi: 10.1016/j.canlet.2012.06.006

Tulina, N., and Matunis, E. (2001). Control of stem cell self-renewal in Drosophila spermatogenesis by JAK-STAT signaling. *Science* 294, 2546–2549. doi: 10.1126/science.1066700

Verstovsek, S., Mesa, R. A., Gotlib, J., Gupta, V., Dipersio, J. F., Catalano, J. V., et al. (2017). Long-term treatment with ruxolitinib for patients with myelofibrosis: 5-year update from the randomized, double-blind, placebo-controlled, phase 3 COMFORT-I trial. *J. Hematol. Oncol.* 10:55.

Xu, M., Palmer, A. K., Ding, H., Weivoda, M. M., Pirtskhalava, T., White, T. A., et al. (2015a). Targeting senescent cells enhances adipogenesis and metabolic function in old age. *Elife* 4:e12997.

Xu, M., Pirtskhalava, T., Farr, J. N., Weigand, B. M., Palmer, A. K., Weivoda, M. M., et al. (2018). Senolytics improve physical function and increase lifespan in old age. *Nat. Med.* 24, 1246–1256. doi: 10.1038/s41591-018-0092-9

Xu, M., Tchkonia, T., Ding, H., Ogrodnik, M., Lubbers, E. R., Pirtskhalava, T., et al. (2015b). JAK inhibition alleviates the cellular senescence-associated secretory phenotype and frailty in old age. *Proc. Natl. Acad. Sci. U.S.A.* 112, E6301–E6310.

Yin, H., Strunz, F., Yan, Z., Lu, J., Brochhausen, C., Kiderlen, S., et al. (2020). Three-dimensional self-assembling nanofiber matrix rejuvenates aged/degenerative human tendon stem/progenitor cells. *Biomaterials* 236:119802. doi: 10.1016/j.biomaterials.2020.119802

Yu, H., Pardoll, D., and Jove, R. (2009). STATs in cancer inflammation and immunity: a leading role for STAT3. *Nat. Rev. Cancer* 9, 798–809. doi: 10.1038/nrc2734

Zaseck, L. W., Miller, R. A., and Brooks, S. V. (2016). Rapamycin attenuates age-associated changes in tibialis anterior tendon viscoelastic properties. *J. Gerontol. A Biol. Sci. Med. Sci.* 71, 858–865. doi: 10.1093/gerona/glv307

Zhang, J., and Wang, J. H. (2010). Characterization of differential properties of rabbit tendon stem cells and tenocytes. *BMC Musculoskelet. Disord.* 11:10.

Zhang, J., and Wang, J. H. (2015). Moderate exercise mitigates the detrimental effects of aging on tendon stem cells. *PLoS One* 10:e0130454. doi: 10.1371/journal.pone.0130454

Zhang, J., Yuan, T., and Wang, J. H. (2016). Moderate treadmill running exercise prior to tendon injury enhances wound healing in aging rats. *Oncotarget* 7, 8498–8512. doi: 10.18632/oncotarget.7381

Conflict of Interest: The authors declare that the research was conducted in the absence of any commercial or financial relationships that could be construed as a potential conflict of interest.

frontiers in Cell and Developmental Biology

ORIGINAL RESEARCH
published: 07 April 2021
doi: 10.3389/fcell.2021.654084

Hepatocyte Growth Factor-Induced Tendon Stem Cell Conditioned Medium Promotes Healing of Injured Achilles Tendon

Zenan Zhang†, Yutian Li†, Tingting Zhang, Manyu Shi, Xin Song, Shulong Yang, Hengchen Liu, Mingzhao Zhang, Qingbo Cui and Zhaozhu Li**

Department of Pediatric Surgery, The Second Affiliated Hospital of Harbin Medical University, Harbin, China

Tendon repair is a medical challenge. Our present study investigated the effectiveness of acellular therapy consisting of conditioned medium (CM) of tendon stem cells (TSCs) induced with hepatocyte growth factor (HGF) in promoting the healing of injured Achilles tendon in a rat model. Proteomic analysis of soluble substances in the CM was performed using an array chip, and bioinformatic analysis was carried out to evaluate interactions among the factors. The effects of CM on viability and migratory capacity of tendon fibroblasts derived from rats with ruptured Achilles tendon were evaluated with the Cell Counting Kit 8 and wound healing assay, respectively. The expression of extracellular matrix (ECM)-related protein was assessed by western blotting. Rats with Achilles tendon injury were treated with CM by local injection for 2 weeks, and the organization of tendon fibers at the lesion site was evaluated by hematoxylin and eosin and Masson's trichrome staining of tissue samples. The deposition and degradation of ECM proteins and the expression of inflammatory factors at the lesion site were evaluated by immunohistochemistry and immunofluorescence. Biomechanical testing was carried out on the injured tendons to assess functional recovery. There were 12 bioactive molecules in the CM, with HGF as the hub of the protein–protein interaction network. CM treatment enhanced the viability and migration of tendon fibroblasts, altered the expression of ECM proteins, promoted the organization of tendon fibers, suppressed inflammation and improved the biomechanics of the injured Achilles tendon. These results suggest that HGF stimulates the secretion of soluble secretory products by TSCs and CM promotes the repair and functional recovery of ruptured Achilles tendon. Thus, HGF-induced TSC CM has therapeutic potential for the treatment of tendinopathy.

Keywords: tendon stem cell, hepatocyte growth factor, conditioned medium, paracrine, acellular therapy, tendon repair

OPEN ACCESS

Edited by:
Hongwei Ouyang,
Zhejiang University, China

Reviewed by:
Hong-Bin Lu,
Central South University, China
Wenguo Cui,
Shanghai Jiao Tong University, China

****Correspondence:***
Zhaozhu Li
zhaozhu247@163.com
Qingbo Cui
cuiqingbocqb@163.com

† These authors have contributed equally to this work and share first authorship

Specialty section:
This article was submitted to Stem Cell Research, a section of the journal Frontiers in Cell and Developmental Biology

Received: *15 January 2021*
Accepted: *15 March 2021*
Published: *07 April 2021*

Citation:
Zhang Z, Li Y, Zhang T, Shi M, Song X, Yang S, Liu H, Zhang M, Cui Q and Li Z (2021) Hepatocyte Growth Factor-Induced Tendon Stem Cell Conditioned Medium Promotes Healing of Injured Achilles Tendon. Front. Cell Dev. Biol. 9:654084. doi: 10.3389/fcell.2021.654084

INTRODUCTION

Tendons are prone to injury through tearing or rupture as they are overstretched during physical activity (Kannus and Natri, 1997). Because of the inefficiency of the natural healing process, the formation of scar tissue is almost inevitable (Rhatomy et al., 2020). Moreover, spontaneously recovered tendons often exhibit substandard biomechanical properties and are susceptible to

reinjury (Gaspar et al., 2015). Thus, unqualified repair can lead to long-term pain, discomfort, mobility impairment, and disability (Olsson et al., 2011; Gaspar et al., 2015; Braunstein et al., 2018). Various physical and biological interventions have been developed to improve the healing of injured tendons. For example, many stem cell (SC) types including mesenchymal (M)SCs derived from bone marrow (i.e., BMSCs) (Sharma and Snedeker, 2010; Yin et al., 2016; Veronesi et al., 2017), adipose tissue (Lee et al., 2017) and umbilical cord (Marmotti et al., 2018) were found to be effective in promoting tendon repair owing to their self-renewal capacity and multidifferentiation potential.

Stem cell-based treatments have certain limitations such as the short survival and tumorigenic potential of transplanted cells, local swelling, and undesirable spontaneous differentiation. Acellular therapies have been used to minimize these risks. Cultured MSCs promoted tissue regeneration through a paracrine mechanism involving the secretion of various factors (Vizoso et al., 2017). The resultant conditioned medium (CM) constituted a microenvironment that was conducive to the growth of SCs and contained soluble proteins, bioactive molecules, growth factors, and extracellular vesicles (EVs) or exosomes (Pawitan, 2014). BMSC CM was shown to promote tenocyte proliferation and reduce the levels of pro-inflammatory factors (Shimode et al., 2007; Chen et al., 2018). The effectiveness of BMSC-derived molecules in promoting tendon repair has been confirmed by other studies (Gissi et al., 2020; Yu et al., 2020). Tendon (T)SCs are a type of MSC found in tendon fascicles (Bi et al., 2007). Because of their strong tendency to differentiate into tenocytes (Zhang and Wang, 2010) and their secretion of trophic factors (Fu et al., 2017), TSCs have been used extensively in tendon repair and regeneration. Although there are some researches based on CM of TSCs, few studies to date have systematically analyzed the soluble components of TSC CM.

Conditioned medium can be modified to achieve a desired effect. Inflammation-stimulated or interferon γ-primed SC-derived EVs were shown to attenuate inflammation (Harting et al., 2018; Shen et al., 2020). It is possible that TSC CM can be similarly primed by specific biomolecules. In order to make the engineered TSC CM have the effect of promoting tissue healing, hepatocyte growth factor (HGF) can be used as an inducer. HGF, a typical paracrine growth factor, is mainly secreted by mesenchymal cells (Fukushima et al., 2018). It had an antifibrotic effect (Moon et al., 2019; Oka et al., 2019; Xie et al., 2019; Ma et al., 2020) and positive effects on tissue regeneration (Boldyreva et al., 2019; Choi J.S. et al., 2019; Choi W. et al., 2019) together with angiogenesis (Beilmann et al., 2004). Besides, it was thought to be a key factor in maintaining the stemness of hBMSCs (Cao et al., 2020) and MSC-EVs that encapsulated with HGF enhanced the barrier function of microvascular endothelial cells (Wang et al., 2017).

We speculate that CM of TSCs induced with HGF can promote tissue repair and functional recovery of a ruptured tendon. We tested our hypothesis with tendon fibroblasts for *in vitro* experiments and a rat model of Achilles tendon injury for *in vivo* investigations. Our results demonstrate that HGF-induced TSC CM is a novel acellular therapy that can facilitate the healing of injured tendon.

MATERIALS AND METHODS

Isolation and Culture of TSCs

Tendon stem cells were isolated from Sprague-Dawley rats and cultured according to procedures described in our previous study (Zhang et al., 2020). Achilles tendons that were free of peritendinous tissues were harvested from euthanized rats. To reduce blood contamination, the samples were thoroughly washed with sterile phosphate-buffered saline (PBS) (Solarbio, Beijing, China). After digestion with trypsin (Beyotime, Shanghai, China), the specimens were cut into 1-mm^3 blocks and were immersed in low-glucose Dulbecco's Modified Eagle's Medium (LG-DMEM) (Gibco, Grand Island, NY, United States) containing 3% w/v collagenase type I (Invitrogen, Carlsbad, CA, United States) and 4% w/v neutral proteinase (PeproTech, Rocky Hill, NJ, United States). The samples were incubated with gentle horizontal shaking for 1.5 h at 37°C, then passed through a 70-μm filter to obtain a single-cell suspension. After centrifugation, the cell pellet was resuspended in complete medium composed of LG-DMEM, fetal bovine serum (Biological Industries, Beit HaEmek, Israel) and penicillin plus streptomycin (Beyotime). The primary cells were cultured in T25 flasks in a humid environment with 5% CO_2 at 37°C. The medium was changed for the first time on day 5 and replaced every 2 or 3 days thereafter. When they reached 80% confluence, the attached cells were released by trypsinization, identified and expanded for use in experiments.

Preparation of CM

The following six TSC CM were prepared: CM1, LG-DMEM only; CM2, LG-DMEM with TSCs; CM3, LG-DMEM with 10 ng/ml HGF (PeproTech) + TSCs; CM4, LG-DMEM with 20 ng/ml HGF + TSCs; CM5, LG-DMEM with 40 ng/ml HGF + TSCs; and CM6, LG-DMEM with 80 ng/ml HGF + TSCs. The same number of TSCs were used in each preparation. After 24 h of culture, the supernatant from CM2–6 was collected and centrifuged, and the new supernatant was filtered to remove cell debris. The filtrate was divided into 2 equal parts. One portion was used in *in vitro* experiments and the other was concentrated using 3-kDa ultrafiltration centrifuge tubes (Millipore, Billerica, MA, United States) at 6000 × *g* for 1 h at 4°C for *in vivo* studies.

Proteome Profiler Array and Bioinformatic Analysis

Based on cytokine antibody chip technology, the proteomic analyses of the soluble components of CM2–6 were conducted. All experimental procedures referred to the instruction of a Rat XL Cytokine Array Kit (R&D Systems, Minneapolis, MN, United States). A 1.5 ml solution containing 1.0 ml CM (i.e., the preparations described in section "Preparation of CM") was dropped onto the surface of a blocked array chip. After overnight incubation at 4°C, the array chip was rinsed with washing buffer and then incubated with 1.5 ml diluted Detection Antibody Cocktail for 1 h at room temperature with gentle shaking. After washing, the array was incubated with horseradish peroxidase (HRP)–streptavidin for 30 min. Immunoreactive

spots were detected with the Chemi Reagent Mix and the soluble secretory products of TSC were identified. By comparing the gray values of the corresponding spots on different array chips, the regulatory effect of HGF on the paracrine of TSC was verified. The experimental results were analyzed by cluster analysis and a protein–protein interaction (PPI) network was constructed using STRING v11.0[1]. The protein pairs with parameters of interaction relationships greater than 0.7 were listed.

Ruptured Achilles Tendon Model

Male Sprague-Dawley rats weighing 160–180 g were purchased from the Laboratory Animal Center of Harbin Medical University. Animal experiments were carried out in accordance with the National Institutes of Health (NIH) Guide for the Care and Use of Laboratory Animals, and were approved by the Ethics Committee of Harbin Medical University. Proper biosafety measurements were also adopted.

To establish the complete Achilles tendon rupture model, amputation was performed at the midpoint of the calcaneal insertion and musculotendinous junction with a sharp surgical knife. The injured tendon was reconstructed by double-cross suturing with a 4-0 Vicryl absorbable suture (Johnson & Johnson, New Brunswick, NJ, United States) under a microscope. The skin incision was closed and reinforced with biological tissue glue (B. Braun, Melsungen, Germany). The rats were freely fed with food and water after they recovered from anesthesia. After 2 weeks, the naturally healed tendons of six rats were harvested for the isolation of tendon fibroblasts and all the other 63 rats used for *in vivo* experiments were sacrificed for sample harvest. Fifty one of the 63 rats were treated with CM2-6 (Group A–E). The condensed CM (0.1 ml) was postoperatively administered by local injection three times per week for 14 days. The other 12 rats (Group F) were left untreated as a control. The specific animal amount for each experiment was preciously introduced below.

Isolation and Culture of Tendon Fibroblasts

The harvested naturally healed tendons were rinsed with cold sterile PBS. After mincing the tissue into 1- to 2-mm^3 pieces, an explant culture was established to obtain primary cells. The composition of the culture medium and schedule for medium changes were the same as described for TSC culture. Third-generation long fusiform cells were used for *in vitro* experiments.

Cell Counting Kit (CCK)-8

Tendon fibroblasts (1×10^4) were seeded in a 96-well plate. After overnight incubation, the culture medium was replaced with 100 μl of CM1–6. The effect of CM on cell viability was evaluated with the CCK-8 assay (Dojindo, Kumamoto, Japan) according to the manufacturer's instructions. The absorbance at 450 nm was measured at five time points (2, 4, 8, 12, and 24 h). The experiment was performed in triplicate and the data were averaged. Results for groups treated with CM2–6 are presented relative to the values for the CM1-treated group.

[1]https://string-db.org/

Wound Healing Assay

As in our previous study (Han et al., 2019), tendon fibroblasts were cultured in 6-well plates. When the cells reached 100% confluence, a sterile 200-μl pipette tip and ruler were used to draw a smooth scratch mark across the bottom of each well. After washing off the scraped cells with sterile PBS, 2 ml CM was added to each well. Photos were obtained with an optical microscope (Olympus, Tokyo, Japan) at five time points (0, 12, 24, 48, and 60 h). The cell migration rate at each time point was calculated based on the corresponding acellular zone at 0 h.

Western Blotting

Tendon fibroblasts were cultured with CM for 24 h, then lysed in precooled radioimmunoprecipitation assay buffer (Solarbio) supplemented with phenylmethylsulfonyl fluoride (Beyotime) for 30 min. Cell debris was cleared by centrifugation at 12,000 × *g* for 20 min at 4°C. The total protein concentration was determined with the BCA Protein Assay Reagent kit (Beyotime). The protein samples were diluted with 5 × sodium dodecyl sulfate loading buffer (Beyotime) and 20 μg protein per lane was electrophoretically separated on a 10% polyacrylamide gel (Beyotime). The proteins were transferred to polyvinylidene difluoride membranes and blocked with 5% non-fat dry milk (BD Biosciences, Franklin Lakes, NJ, United States) for 2 h at room temperature. Then, the membranes were separately probed overnight at 4°C with primary antibodies against collagen (COL)III (1:500), fibronectin (1:2000), matrix metalloproteinase (MMP)-1 (1:2000), MMP-9 (1:500) (all from Abcam, Cambridge, United Kingdom) and β-actin (1:1000) (WanleiBio, Shenyang, China). The membranes were rinsed with Tris-buffered saline (Solarbio) with 0.1% Tween-20 (Solarbio) and then incubated with the appropriate HRP-conjugated secondary antibodies (Boster Bio, Wuhan, China) for 1.5 h at room temperature. Protein bands were visualized using enhanced chemiluminescence substrate reagent (HaiGene, Harbin, China). The gray value was quantified with ImageJ software (NIH, Bethesda, MD, United States).

Immunohistochemistry Analysis

Extracellular matrix (ECM) organization at the tendon lesion site following CM treatment was evaluated by immunohistochemistry. Tendon specimens (1 cm long) harvested from 15 CM treated rats (n = 3) and 3 untreated ones were immediately immersed in 4% paraformaldehyde solution (BioSharp, Hefei, China). After dehydration through a graded alcohol series, samples were embedded in paraffin and serial sections of the tissue blocks were cut at a thickness of 5 μm parallel to the long axis of the tendons on a microtome (Leica, Wetzlar, Germany). After antigen retrieval, tissue sections mounted on glass slides were treated with 3% hydrogen peroxide to quench endogenous peroxidase activity, blocked with 10% goat serum (Solarbio) for 15 min at room temperature and incubated overnight at 4°C with primary antibodies against COLIII (1:100), fibronectin (1:100), α-smooth muscle actin (SMA) (1:100), MMP-2 (1:100), MMP-9 (1:100), tissue inhibitor of metalloproteinase (TIMP)-1 (1:100), and vascular endothelial growth factor (VEGF) (1:100) (all from Abcam). The slides

were then incubated in the dark with species-specific secondary antibodies. Diaminobenzidine (Solarbio) was used to visualize the bound antibody complex. After dehydrating the sections and covering the slides with glass coverslips, the sections were examined and photographed under a microscope (Olympus) mounted with a camera. Positive signals were quantified with ImageJ software.

Histological Analysis

Tendon samples were harvested from 15 CM treated rats ($n = 3$). Normal tendons were also collected. After dehydration and embedding in paraffin, the samples were also cut into 5-mm thickness serial sections. Then, the slices were stained with hematoxylin and eosin (H&E) and Masson's trichrome and observed under a light microscope. The organization of tendon fibers was evaluated according to a previously described parallel fiber alignment scoring method (Jiang et al., 2016) by investigators who were blinded to group assignment. The scoring scale was as follows: 0, 0–25% parallel fiber alignment; 1, 25–50%; 2, 50–75%; and 3, 75%–100%.

Immunofluorescence Analysis

The expression of the pro-inflammatory cytokine interleukin (IL)-6 and anti-inflammatory cytokine IL-10 was detected by immunofluorescence analysis. The sample collection was same as the description in section "Immunohistochemistry analysis". Tendon tissue samples were embedded in optimal cutting temperature compound and frozen serial sections were cut at a thickness of 10 μm. After antigen retrieval, the sections were blocked with 10% goat serum for 15 min at room temperature, then incubated overnight at 4°C with primary antibodies against IL-6 (1:100) and IL-10 (1:100) (both from Abcam), followed by Cy3-conjugated goat anti-rabbit IgG (Beyotime) for 60 min at room temperature. Nuclei were stained with DAPI (Beyotime). Images were acquired under a fluorescence microscope (Olympus), and the area of positive signal was determined using ImageJ software.

Biomechanical Testing

We evaluated the effectiveness of the CM with the greatest therapeutic effect in all the above experiments [sections "Cell Counting Kit (CCK)-8," "Wound healing assay," "Western blotting," "Immunohistochemistry analysis," "Histological analysis," and "Immunofluorescence analysis"] in promoting functional recovery in the rat model of Achilles tendon rupture. Eighteen tendon-calcaneal complexes were carefully dissected from six CM treated rats, six naturally healed rats, and six intact animals (i.e., without injury). They were used for biomechanical testing as previously described (Chamberlain et al., 2019). Briefly, the transverse diameter (TD) and anteroposterior diameter (AD) of the healed sections were measured with electronic vernier calipers. The tissue sample's cross-sectional area (S) was approximated as an oval, and was calculated with the equation $S = \pi TD \times AD/4$. A universal tensile testing machine (Hengruijin, Jinan, China) was used for testing. The proximal muscle wrapped in a piece of 100 × sandpaper and the distal naked paw were affixed to the two testing clamps. An axial 0.1 N preload was applied along the long axis of the tendon, with elongation at a speed of 5 mm/min. The maximum tensile load was recorded. Stiffness and Young's modulus were calculated based on the linear slope of the strain–stress curve.

Statistical Analysis

Data are presented as mean ± SD. Differences between groups were evaluated by one-way analysis of variance (ANOVA) followed by Tukey's *post hoc* test if necessary or by two-way ANOVA using Prism v8.3.0 software (GraphPad, La Jolla, CA, United States). $P < 0.05$ was considered statistically significant.

RESULTS

Characterization of TSCs

Primary TSCs were spindle-shaped, reaching 40–50% confluence on Day 10 after seeding (**Figure 1A**). The parts stained by crystal violet were the cell colonies (**Figure 1B**). Flow cytometry analysis revealed that 99.7% of cells expressed the cell surface marker cluster of differentiation (CD) 90 and 99.1% expressed CD44. Meanwhile, only 3.9% and 7.4% expressed CD11 and CD106, respectively (**Figure 1C**). TSCs had multi-differentiation potential, as determined by the detection of lipid droplets (**Figure 1D**), mineralized nodules (**Figure 1E**), and acid mucopolysaccharide (**Figure 1F**).

Proteomic Analysis of CM and PPIs of Soluble Bioactive Molecules

A total of 12 molecules were detected in the CM2 with the proteome profiler antibody array. HGF contained in the CM3–6 were depleted from the culture medium after 24 h of culture. As a result, it caused variations in the concentrations of CM components but no generation of new products (**Figure 2A**). Almost all the secretion of these bioactive molecules can be inhibited by a high concentration of HGF (i.e., CM6 with 80 ng/ml HGF). Compared with CST3, CCL2, Serpin E1, VEGFa, MMP-2, and WISP-1, the concentration variations of LGALS3, NOV, and TNFRSF11b were sensitive to the dose of HGF. While, only when the concentration of HGF was 40 mg/ml, the contents of IGFRP-6, IGFBP-3, and SPP1 changed obviously (**Figure 2B**). PPIs of the 12 molecules are shown in **Figure 2C**. HGF interacted with 6 proteins. SPP1, CCL2, and MMP-2 interacted with eight proteins. In maximum, there were 10 PPIs for VEGFa. WISP-1 only interacted with MMP-2 but not with other proteins; the same was true for IGFBP-6 and IGFBP-3, NOV and VEGFa. The strength of the interactions are shown in **Figure 2D**. LGALS3, IGFBP-3, IGFBP-6, NOV, and WISP-1 had a low degree of interaction (<0.7), whereas HGF and VEGFa, VEGFa and Serpin E1, HGF and Serpin E1, MMP-2 and VEGFa, CST3 and SPP1 showed strong interactions (>0.9).

CM Promotes the Viability and Migration of Tendon Fibroblasts

Conditioned medium treatment had no effect on the viability of tendon fibroblasts at 2, 4, 8, and 12 h, but the viability was

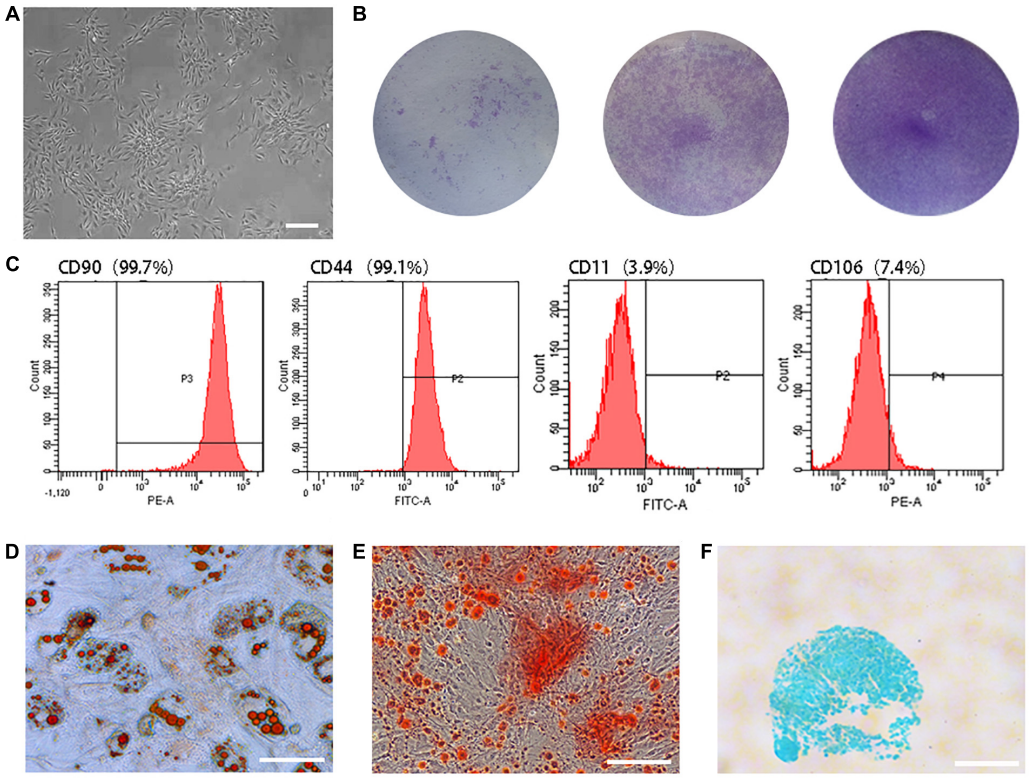

FIGURE 1 | Characterization of TSCs. **(A)** Primary TSCs were spindle-shaped and reached 40–50% confluence on Day 10 after seeding. **(B)** After 7 days of culture, cell colonies were visualized by crystal violet staining. The initial seeding densities were 1×10^3, 1×10^4, and 1×10^5 per well, respectively. **(C)** Flow cytometry analysis revealed that 99.7% of cells expressed CD90 and 99.1% expressed CD44. Meanwhile, only 3.9% and 7.4% expressed CD11 and CD106. **(D)** Lipid droplets were observed by oil red O staining after adipogenic differentiation induction of TSCs. **(E)** Mineralized nodules were observed by alizarin red staining after osteogenic differentiation induction of TSCs. **(F)** Acid mucopolysaccharide was observed by Alcian blue staining after chondrogenic differentiation induction of TSCs. All bars: 200 μm.

doubled at 24 h. No statistical significance was observed among CM2-6 (**Figure 3A**). Likewise, CM accelerated the migration of tendon fibroblasts (**Figures 3B,C**). The effect showed a dose-dependent relationship with the concentration of HGF. Obviously, the wound closure of the fibroblasts with CM1-5 increased gradually. The maximum rate of migration was observed with CM5 (64.48% ± 0.80% wound closure after 60 h). When the concentration of HGF reached at 80 ng/ml (i.e., CM6), no further increase of wound closure was observed. In fact, it yielded a result similar to that obtained with CM4.

CM Alters ECM Composition and Promotes Angiogenesis

In vitro experiment, MMP-2 and MMP-9 were upregulated following the application of CM (**Figures 4A,D,E**). The expression of MMP-2 was highest in tendon fibroblasts treated with CM5 and CM6 compared to the other CM formulations, with no difference between the two groups. Similar results were obtained for MMP-9, which showed the highest expression in the CM5-treated group. With the increase of HGF concentration, their expressions of COLIII and fibronectin decreased (**Figures 4A–C**). All the above results, upregulated MMPs and downregulated ECM components, were verified *in vivo* experiment by immunohistochemistry (**Figures 5A,B,D,E**). Although theirs levels were lower than that of Group F, the expression of α-SMA was increased among experimental groups treated with CM2-6 (**Figure 5C**). Meanwhile, the expression of TIMP-1 first decreased and then increased with increasing concentrations of HGF (**Figure 5F**). The turning point came at Group D. VEGF, which promotes angiogenesis, was upregulated in the presence of CM, with the highest level detected in tissues treated with CM6 (i.e., Group E) (**Figure 5G**).

CM Promotes the Orderly Arrangement of Tendon Fibers

The effect of CM on tendon fiber alignment was evaluated by histological analysis. Achilles tendon tissue sections treated with CM5 and CM6 (i.e., Group D and Group E) showed a much more regular and compact alignment of collagen fibers compared to those treated with CM2 and CM3 (i.e., Group A and Group B), which had disorganized fibers (**Figure 6A**). Samples treated with CM4 (i.e., Group C) had an intermediate phenotype. These results were also confirmed by the fiber alignment score, which

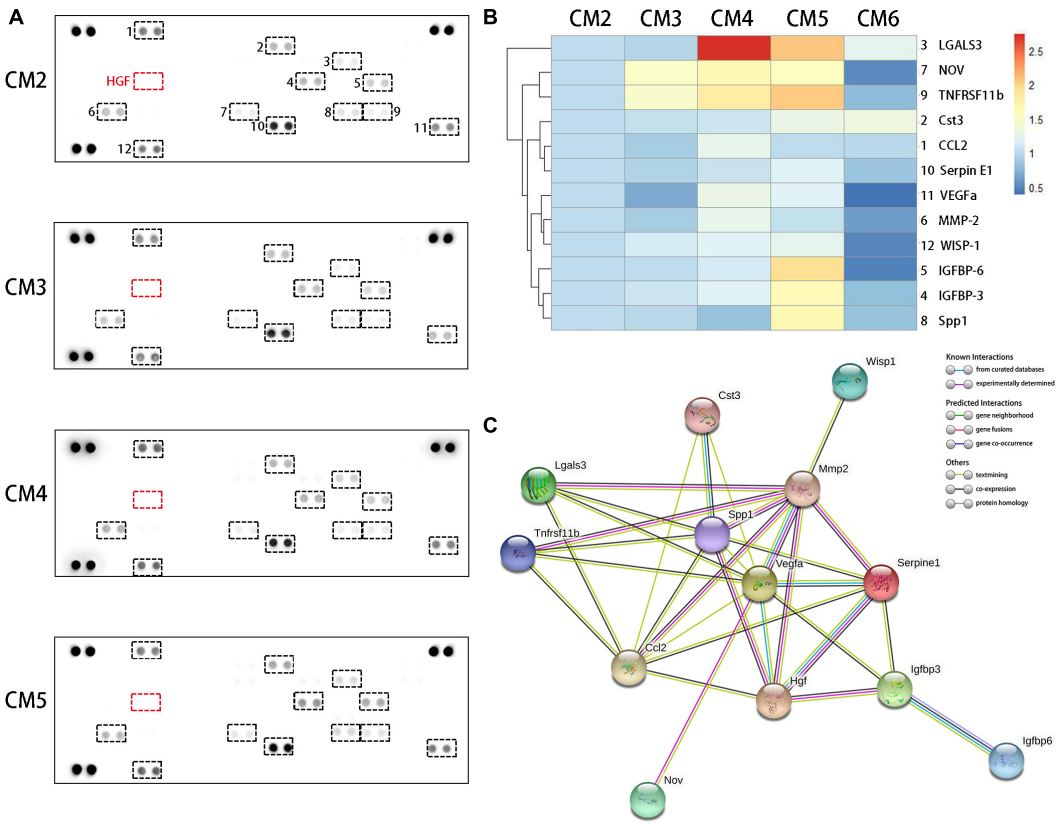

D

NO.	Protein 1	Protein 2	The parameter of interactive relationships
1	HGF	VEGFa	0.985
2	VEGFa	Serpin E1	0.973
3	HGF	Serpin E1	0.965
4	MMP-2	VEGFa	0.964
5	Cst3	Spp1	0.959
6	CCL2	Serpin E1	0.826
7	Spp1	VEGFa	0.785
8	CCL2	VEGFa	0.768
9	Spp1	TNFRSF11b	0.757
10	CCL2	MMP-2	0.751
11	CCL2	Spp1	0.744
12	MMP-2	Spp1	0.706

FIGURE 2 | Proteomic analysis of CM and PPIs of soluble bioactive molecules. **(A)** A total of 12 molecules were detected in the CM2 with the proteome profiler antibody array. The concentrations of soluble bioactive molecules can be modified by HGF. **(B)** A cluster analysis result was shown by a heat map. Compared with CST3, CCL2, Serpin E1, VEGFa, MMP-2, and WISP-1, the concentration variations of LGALS3, NOV, and TNFRSF11b were sensitive to the dose of HGF. While, only when the concentration of HGF was 40 mg/ml, the contents of IGFRP-6, IGFBP-3, and SPP1 changed obviously. **(C)** PPIs network of the 12 proteins detected in TSC CM and HGF. Known interactions are indicated by light blue (weak) or purple (strong) lines. **(D)** Protein pairs with interaction score > 0.7. HGF and VEGFa, VEGFa and Serpin E1, HGF and Serpin E1, MMP-2 and VEGFa, CST3 and SPP1 showed strong interactions (>0.9).

was higher for samples treated with CM5 and CM6 than for the other three groups (**Figure 6B**).

CM Suppresses Inflammation in Injured Tendon

IL-6 level was highest in rats with Achilles tendon injury that were left untreated (Group F) and decreased with CM treatment (**Figure 7A**). The capacities of inhibiting pro-inflammatory cytokine expression in Group A and Group B (i.e., treatments with CM2 and CM3) were weaker than those in Group C, Group D, and Group E. However, the difference between Group C and Group D was not statistically significant (**Figure 7B**). The opposite trend was observed for IL-10, which showed the lowest expression in Group F (**Figure 7C**). With the treatment of CM, anti-inflammatory cytokine expressions increased. The effect was greater at higher concentration of HGF. It maximized in Group D. When it came to Group E, no further increase

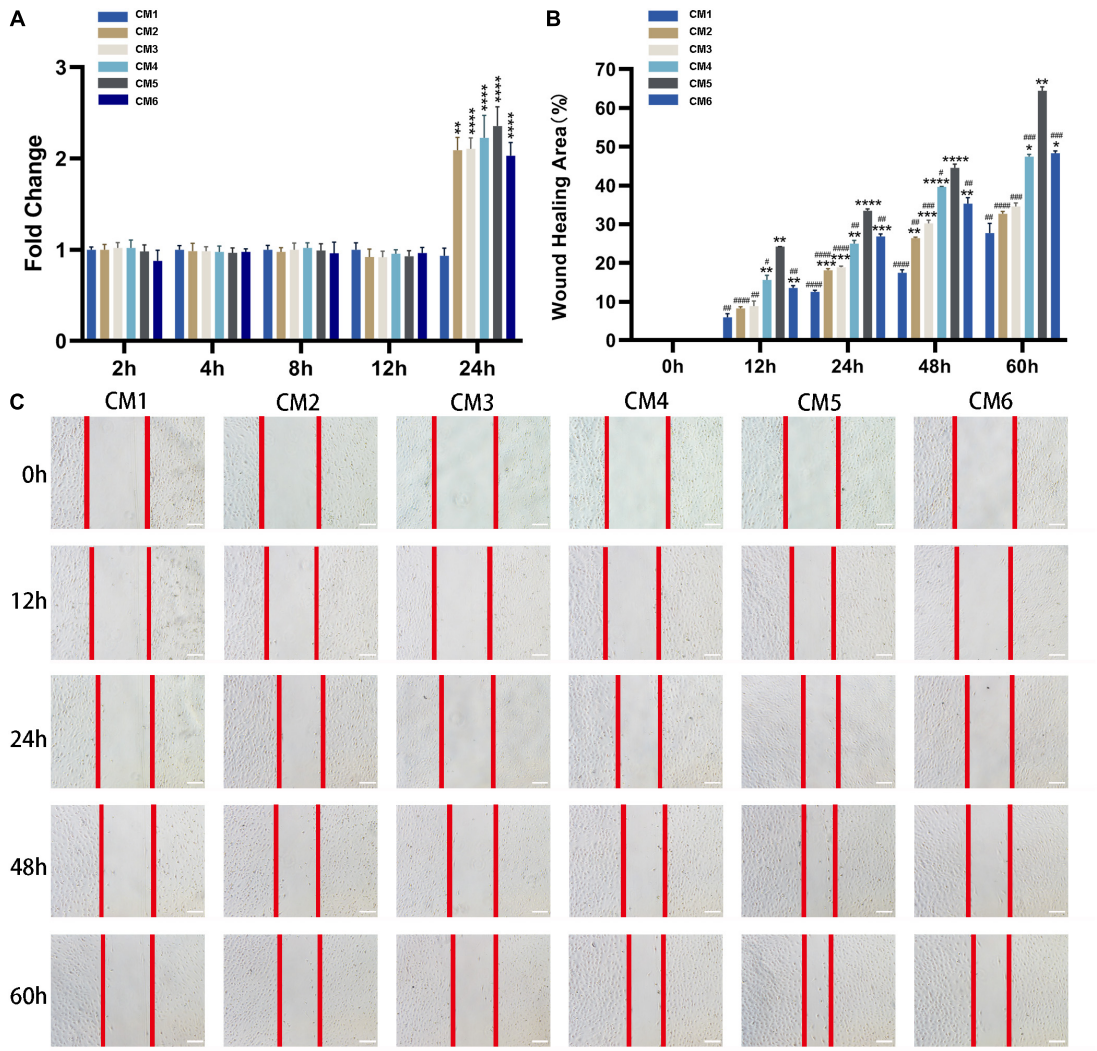

FIGURE 3 | CM promotes the viability and migration of tendon fibroblasts. **(A)** Cell viability was evaluated with CCK-8. CM treatment had no effect on the viability of tendon fibroblasts at 2, 4, 8, and 12 h, but the viability was doubled at 24 h. The effect was independent of HGF concentration. **(B,C)** The migration of tendon fibroblasts was evaluated with the wound healing assay. Red lines indicate the migration front. The wound closure of the fibroblasts with CM1-5 increased gradually. The maximum rate of migration was observed with CM5. No further increase of wound closure was observed with CM6. Bars: 200 μm. *, versus CM1. * means $p < 0.05$, ** means $p < 0.01$, *** means $p < 0.001$, **** means $p < 0.0001$. #, versus CM5. # means $p < 0.05$, ## means $p < 0.01$, ### means $p < 0.001$, #### means $p < 0.0001$.

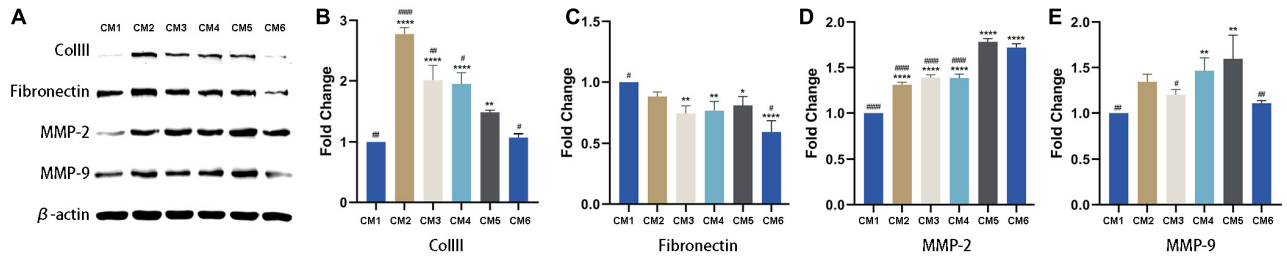

FIGURE 4 | Expression of ECM-related factors detected by western blotting. **(A)** COLIII, fibronectin, MMP-2 and MMP-9 levels were detected by western blotting. β-actin served as the loading control. **(B,C)** Quantitative analysis result of COLIII and fibronectin. With the increase of HGF concentration, their expressions decreased. **(D,E)** Quantitative analysis result of MMP-2 and MMP-9. They were upregulated following the applications of CMs. *, versus CM1. * means $p < 0.05$, ** means $p < 0.01$, **** means $p < 0.0001$. #, versus CM5. # means $p < 0.05$, ## means $p < 0.01$, #### means $p < 0.0001$.

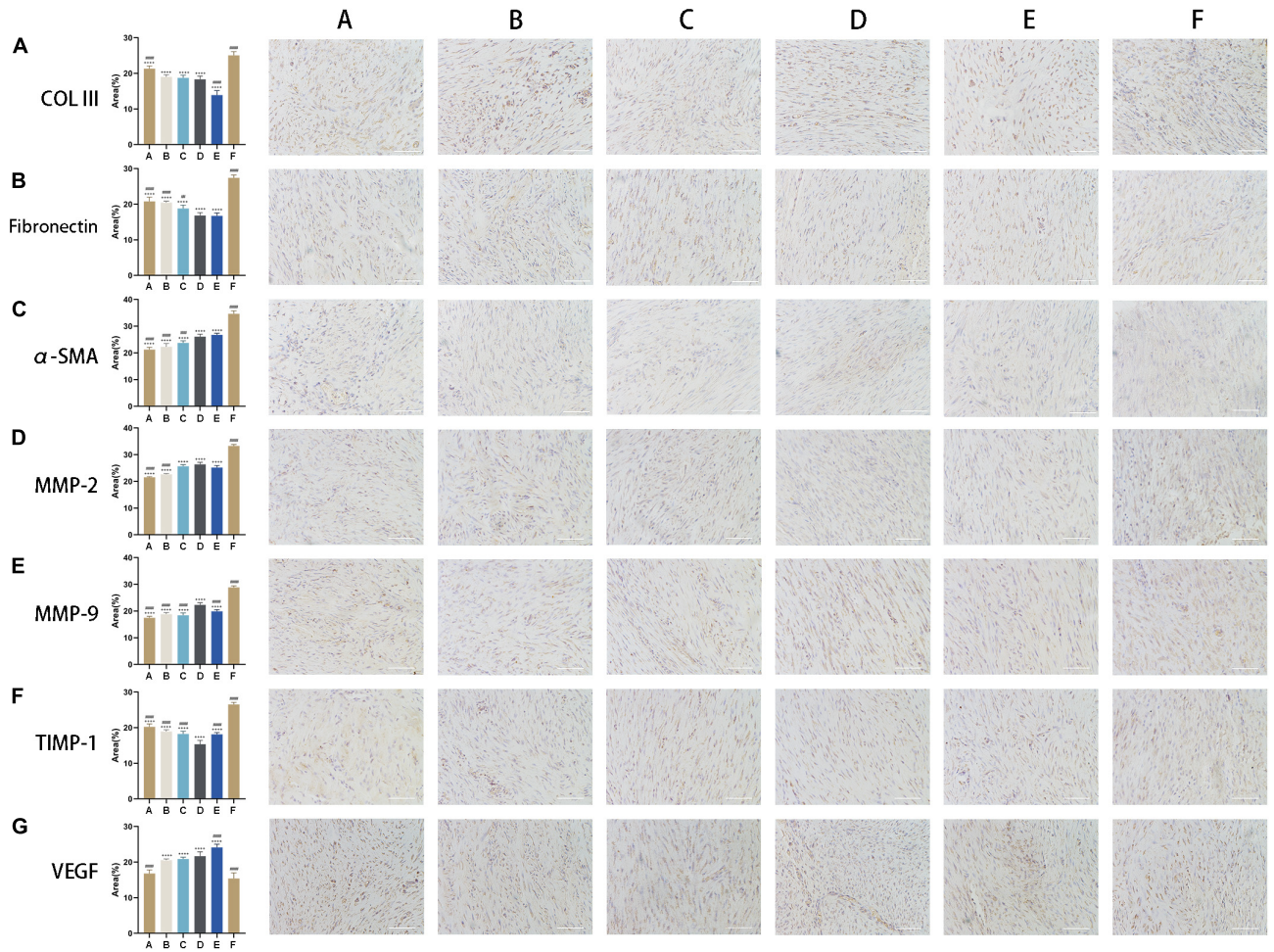

FIGURE 5 | CM alters ECM composition and promotes angiogenesis. **(A,B)** Expression levels of COLIII and fibronectin. With the increase of HGF concentration, their expressions decreased. **(C)** Expression level of α-SMA. Its expression increased following the applications of CMs. **(D,E)** Expression levels of MMP-2 and MMP-9. With the increase of HGF concentration, their expressions increased. **(F)** Expression level of TIMP-1. Its expression first decreased and then increased. The turning point came at Group D. **(G)** Expression level of VEGF. It was upregulated in the presence of CM, with the highest level detected in cells treated with CM6. Bars: 200 μm. #, versus D. ## means $p < 0.01$, ### means $p < 0.001$, #### means $p < 0.0001$. +, versus F. ++++ means $p < 0.0001$.

of anti-inflammatory cytokine expression was observed. In contrast, it dropped to the same value as that in Group B (**Figure 7D**).

CM Enhances the Biomechanical Properties of Injured Achilles Tendon

Based on the above results, tendons from Group D (i.e., treatment with CM5) were used for biomechanical testing. Healed tendon from Group D and F had a cross-sectional area nearly three times that of uninjured tissue (**Figures 8A,B**). Although there was functional improvement after CM treatment, the maximum tensile load was still lower than normal tendon (**Figure 8C**), corresponding to 60% recovery. What was worse, naturally healed tendons in Group F only recovered 30% of the normal maximum tensile load. The stiffness and Young's modulus of samples in Group D and Group F were still far less than that of normal tissues. There were also no differences between CM treated tendons and naturally healed ones (**Figures 8D,E**).

DISCUSSION

The results of our study confirmed the secretory function of TSCs: the CM produced after 24 h of culture contained more than 12 bioactive molecules, including those were known to promote tissue healing or exert anti-inflammatory and antifibrotic effects. Specifically, C–C motif chemokine ligand (CCL)2 stimulated macrophage chemotaxis. CST3 was shown to alleviate tissue fibrosis in kidney and lung (Kim et al., 2018a,b). LGALS3, also known as galectin-3, functioned as a regulatory molecule at various stages of inflammation from acute to chronic as well as in tissue fibrogenesis (Henderson and Sethi, 2009). MMP-2 was involved in ECM remodeling. SPP1 played an important role in the production of collagen and the resolution of inflammation

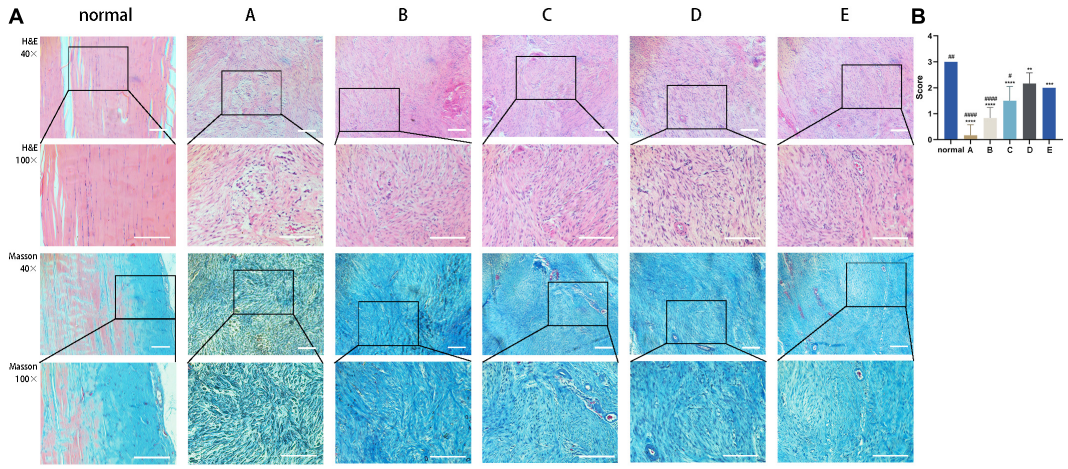

FIGURE 6 | CM promotes the orderly arrangement of tendon fibers. **(A)** Sections of healed tendon tissue stained with H&E and Masson's trichrome were observed by light microscopy at 40× and 100× magnification. Achilles tendon tissue sections treated with CM5 and CM6 (i.e., Group D and Group E) showed a much more regular and compact alignment of collagen fibers compared to the other groups. **(B)** Histogram of fiber alignment score. With the increase of HGF concentration, tendon fibers arranged orderly. Bars: 500 μm. *, versus normal. ** means $p < 0.01$, *** means $p < 0.001$, **** means $p < 0.0001$. #, versus D. # means $p < 0.05$, ## means $p < 0.01$, #### means $p < 0.0001$.

(Ruberti et al., 2018; Bevan et al., 2020). Serpin E1 regulated tissue homeostasis and promoted wound healing by inhibiting plasmin-mediated MMP activation (Flevaris and Vaughan, 2017). VEGF mediated angiogenesis. Thus, the combined presence of these factors in TSC CM had a positive effect on tendon healing. Our results also showed that the levels of these factors in the CM varied with HGF concentration. Based on the results of the bioinformatic analysis, we inferred that HGF regulated the secretory activity of TSCs. The PPI network of secreted molecules revealed strong connections between HGF and VEGFa (0.985) and between HGF and Serpin E1 (0.965), which were consistent with previous reports (Chang et al., 2013; Su et al., 2013). HGF might stimulate the release of VEGFa and Serpin E1, which interacted with or activate the release of MMP-2, CCL2 and SPP1. SPP1 then induced the expression of tumor necrosis factor receptor superfamily member (TNFRSF)11b and CST3. Owing to the complexity of the PPIs involving HGF, the 5 TSC CMs (i.e., CM2-6) tested in our study had distinct therapeutic effects.

Tissue repair is a complex process (Leong et al., 2020) that consists of three stages: inflammation, proliferation, and remodeling (Thankam et al., 2018). Inflammation occurs in the early stage of tissue damage and can lead to increased vascular permeability, neovascularization and local recruitment of inflammatory cells. Suppressing this response is beneficial for the healing of injured tendons (Blomgran et al., 2017; Chamberlain et al., 2019; Shi et al., 2019). Macrophages play an important role in this process (Hays et al., 2008; Millar et al., 2017). M1- and M2-polarized macrophages respectively mediate inflammation and its resolution. The switch from the former to the latter stimulates tendon tissue repair (Manning et al., 2015). IL-6—a pro-inflammatory cytokine associated with macrophage activation (Munder et al., 1998)—was used as a marker in our study along with the anti-inflammatory cytokine IL-10, which could stimulate M2 polarization of macrophages. The ratio of M1- to M2-polarized macrophages depends on cues in the microenvironment (Gordon and Martinez, 2010). Upon treatment with TSC CM, IL-6 was downregulated and IL-10 was upregulated at the lesion site, suggesting that CM modulated the inflammatory response by inducing macrophage phenotype switching. Thus, like EVs or exosomes isolated from some SC types (Shen et al., 2020; Shi et al., 2019), TSC CM can also attenuate the early inflammatory response.

Rat BMSC CM and the secretome of human MSCs were shown to enhance the viability of tenocytes and stimulate cell migration (Chen et al., 2018; Sevivas et al., 2018). This is in agreement with our observations. Given that fibroblasts would fill with the lesion during tendon repair, tendon fibroblasts extracted from the defect site were used as the target cells in our *in vitro* experiments. The TSC CM enhanced cell viability at 24 h and promoted cell migration up to 60 h. Thus, local CM injection every 2 or 3 days may be an effective strategy to promote tendon repair.

Tissue repair involves a balance between ECM deposition and degradation. MMPs play an important role in the latter in cooperation with TIMPs. Ciprofloxacin induced MMP-2 expression in tendon (Tsai et al., 2011) while exosomes from TSCs inhibited the expression of MMP-3 and increased that of TIMP-3 (Wang et al., 2019). In our study, the expressions of MMP-2 and MMP-9 were gradually upregulated while TIMP-1 had an opposite tendency after the treatments with CM2-5, indicating that there was a balance in MMPs and TIMPs. Collagen (e.g., COLIII) and non-collagenous glycoproteins (e.g., fibronectin) are the main components of ECM. COLIII accounted for around 10% of the total collagen in tendon tissue and excessive amounts could result in scar formation (Tsai et al., 2006; Xu et al., 2018). With the increasing activity of MMP-2 and MMP-9 in each experimental group, the expression of COLIII and fibronectin was decreased gradually. This outcome benefited the injured tendon remodeling. α-SMA was a marker of myofibroblasts,

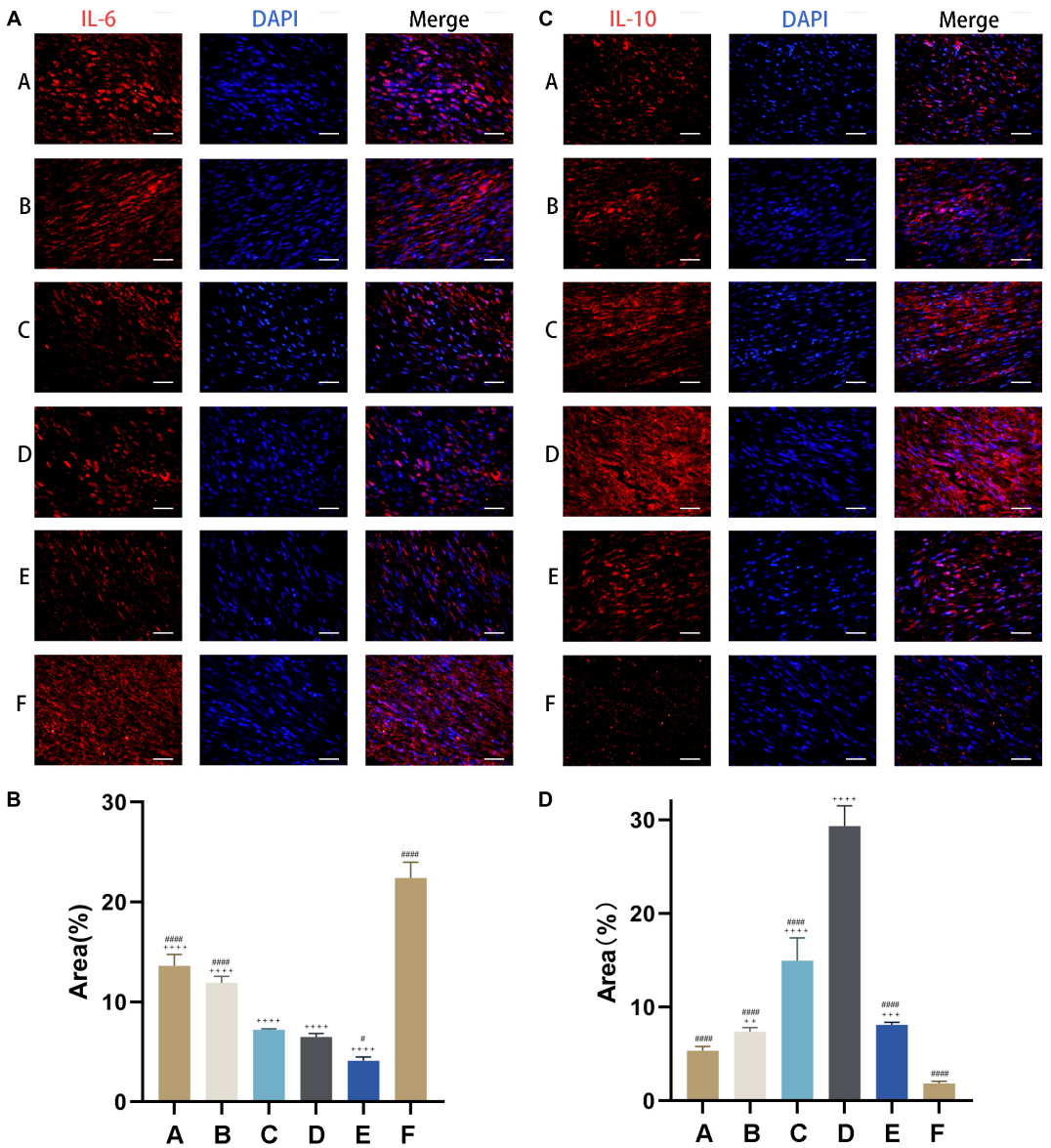

FIGURE 7 | CM suppresses inflammation in injured tendon. **(A)** Expression of the pro-inflammatory cytokine IL-6 (red) was detected by immunocytochemistry. Nuclei were stained with DAPI (blue). CM held the capacity of inhibiting pro-inflammatory cytokine expression. **(B)** Quantitative analysis of IL-6 expression levels based on the area of positive signal. **(C)** Expression of the anti-inflammatory cytokine IL-10 (red) was detected by immunocytochemistry. Nuclei were stained with DAPI (blue). CM held the capacity of promoting anti-inflammatory cytokine expression. **(D)** Quantitative analysis of IL-10 expression levels based on the area of positive signal. Bars: 50 μm. #, versus D. # means $p < 0.05$, #### means $p < 0.0001$. +, versus F. ++ means $p < 0.01$, +++ means $p < 0.001$, ++++ means $p < 0.0001$.

which were derived from activated fibroblasts (Sun et al., 2019). It has a pair of opposite physiology effects. The negative side, excessive myofibroblasts lead to scar formation. The expressions of α-SMA in CM treated groups were much lower than that in control group, indicating that CM can inhibit the formation of scar. The positive side, myofibroblasts contribute to wound contraction. Our results showed that the level of α-SMA in experimental groups was increased along with the increase of HGF concentration. That is to say that higher dose of HGF posts more obvious effect on tissue repair. In addition, early angiogenesis promoted tissue repair (Chamberlain et al., 2019); VEGF, a marker of angiogenesis, was upregulated at the lesion site following treatment with CM, which likely contributed to tendon repair in our model.

The ultimate goal of tendon healing is functional restoration, as determined by the ability to resume normal activities without experiencing pain or recurrence of the injury. Load bearing by the Achilles tendon in rat was increased by TSC exosome injection (Wang et al., 2019); and stiffness and Young's modulus were improved following application of EV-educated macrophages (Chamberlain et al., 2019). We found that the maximum tensile load that could be borne by healed Achilles tendon was increased

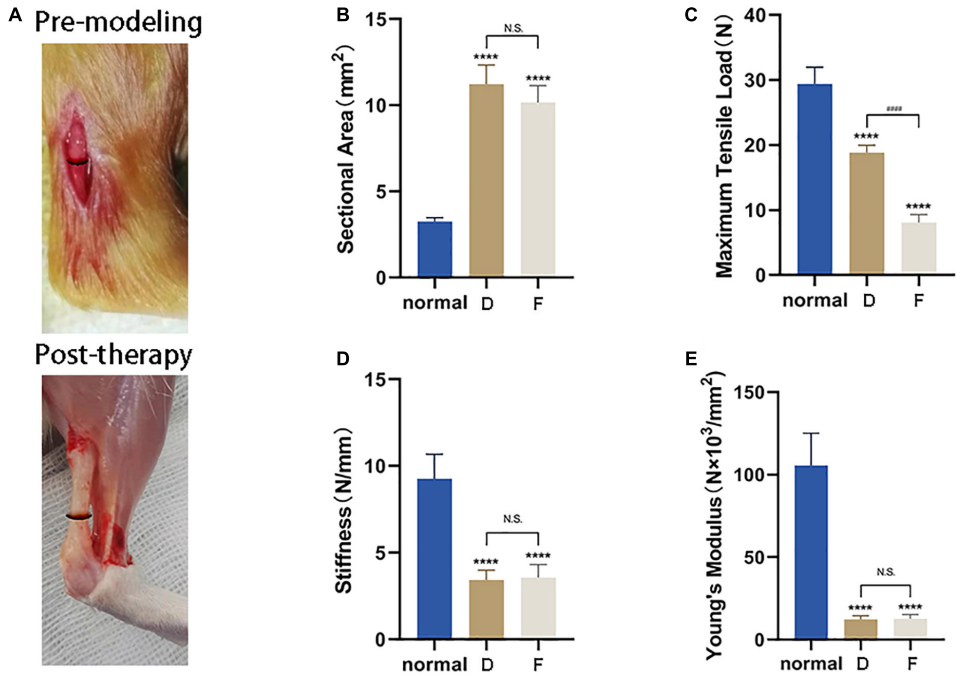

FIGURE 8 | CM enhances the biomechanical properties of injured Achilles tendon. **(A)** Lesion area before and after tendon repair. **(B)** Healed tendon from Group D and F had a cross-sectional area nearly three times that of uninjured tissue. **(C)** After CM treatment, functional improvement of the maximum tensile load was still lower than in normal tendon, corresponding to 60% recovery. **(D)** The stiffness of samples in Group D and Group F were still far less than that of normal tissues. There were no differences between the two experimental groups. **(E)** Recovery of Young's modulus of samples was same as that of stiffness. *, versus normal. **** means $p < 0.0001$; #, D versus F, #### means $p < 0.0001$.

by CM5 treatment. This was in line with our observation that the tendon tissue of CM5-treated rats had a much more parallel and dense arrangement of fibers. There are two possible explanations for why there were no improvements in stiffness and Young's modulus in our study. The change in stress may not have adapted to the rapid tendon displacement—that is, the slope of the strain–stress curve is not sufficiently large. Alternatively, the enlargement of the cross-sectional area of the healed lesion site may have dispersed the tensile force. Therefore, rehabilitation training should be carried out reasonably after treatment with HGF-induced TSC CM. Meanwhile, there is a risk that the healed Achilles tendon could re-rupture.

The results of our study demonstrate that the therapeutic effects of TSC CM varied with HGF concentration; 40 ng/ml HGF showed maximal effectiveness in terms of stimulating cell migration, modulating ECM and inflammation, and restoring tendon fiber alignment and biomechanical properties. A limitation of our study is that we do not carry out long-term observations of tissue remodeling following CM treatment. Additionally, a more detailed investigation of the mechanisms underlying the therapeutic effects of CM is warranted. Whether the therapeutic effect of HGF-induced TSC CM is mediated by exosome needs a further study. Nonetheless, HGF-induced TSC CM treatment enhanced the viability and migration of tendon fibroblasts, altered the expression of ECM proteins, promoted the organization of tendon fibers, suppressed inflammation and improved the biomechanics of the injured Achilles tendon.

CONCLUSION

These results suggest that HGF stimulates the secretion of soluble secretory products by TSCs and CM promotes the repair and functional recovery of ruptured Achilles tendon. Thus, HGF-induced TSC CM has therapeutic potential for the treatment of tendinopathy.

DATA AVAILABILITY STATEMENT

The original contributions presented in the study are included in the article. Further inquiries can be directed to the corresponding author.

ETHICS STATEMENT

The animal study was reviewed and approved by the Ethics Committee of Harbin Medical University.

AUTHOR CONTRIBUTIONS

ZZ and YL contributed equally to this work and shared first authorship. ZZ, QC, and ZL conceived this study. ZZ, YL, TZ, and XS conducted all the experiments and data analyses. MS participated in data curation and statistical analysis. SY, HL, and MZ provided the experimental technical guidance. ZZ

finished the original draft. YL, QC, and ZL gave text revision and edition. All the authors read the final manuscript.

FUNDING

The authors gratefully acknowledged funds from the National Natural Science Foundation of China (81572117 and 81871837) and the Research & Practice Innovation Program of Harbin Medical University (YJSKYCX2018-59HYD).

ACKNOWLEDGMENTS

The contributions of the Scientific Research Center of the Second Affiliated Hospital of Harbin Medical University and Key Laboratory of Engineering Dielectrics and Its Application of Ministry of Education in Harbin University of Science and Technology were highly appreciated. Thanks to the staff who have aided the efforts of us, especially Weichao Zhang, Dong Wang, and Yuping Yue.

REFERENCES

Beilmann, M., Birk, G., and Lenter, M. C. (2004). Human primary co-culture angiogenesis assay reveals additive stimulation and different angiogenic properties of VEGF and HGF. *Cytokine* 26, 178–185. doi: 10.1016/j.cyto.2004.03.003

Bevan, L., Lim, Z. W., Venkatesh, B., Riley, P. R., Martin, P., and Richardson, R. J. (2020). Specific macrophage populations promote both cardiac scar deposition and subsequent resolution in adult zebrafish. *Cardiovasc. Res*. 116, 1357–1371. doi: 10.1093/cvr/cvz221

Bi, Y., Ehirchiou, D., Kilts, T. M., Inkson, C. A., Embree, M. C., Sonoyama, W., et al. (2007). Identification of tendon stem/progenitor cells and the role of the extracellular matrix in their niche. *Nat Med*. 13, 1219–1227. doi: 10.1038/nm1630

Blomgran, P., Hammerman, M., and Aspenberg, P. (2017). Systemic corticosteroids improve tendon healing when given after the early inflammatory phase. *Sci. Rep*. 7:12468. doi: 10.1038/s41598-017-12657-0

Boldyreva, M. A., Shevchenko, E. K., Molokotina, Y. D., Makarevich, P. I., Beloglazova, I. B., Zubkova, E. S., et al. (2019). Transplantation of adipose stromal cell sheet producing hepatocyte growth factor induces pleiotropic effect in ischemic skeletal muscle. *Int. J. Mol. Sci*. 20:3088. doi: 10.3390/ijms20123088

Braunstein, M., Baumbach, S. F., Boecker, W., Carmont, M. R., and Polzer, H. (2018). Development of an accelerated functional rehabilitation protocol following minimal invasive Achilles tendon repair. *Knee Surg. Sports Traumatol. Arthrosc*. 26, 846–853. doi: 10.1007/s00167-015-3795-1

Cao, Z., Xie, Y., Yu, L., Li, Y., and Wang, Y. (2020). Hepatocyte growth factor (HGF) and stem cell factor (SCF) maintained the stemness of human bone marrow mesenchymal stem cells (hBMSCs) during long-term expansion by preserving mitochondrial function via the PI3K/AKT, ERK1/2, and STAT3 signaling pathways. *Stem Cell Res. Ther*. 11:329. doi: 10.1186/s13287-020-01830-4

Chamberlain, C. S., Clements, A., Kink, J. A., Choi, U., Baer, G. S., Halanski, M. A., et al. (2019). Extracellular vesicle-educated macrophages promote early Achilles tendon healing. *Stem Cells* 37, 652–662. doi: 10.1002/stem.2988

Chang, C. P., Chio, C. C., Cheong, C. U., Chao, C. M., Cheng, B. C., and Lin, M. T. (2013). Hypoxic preconditioning enhances the therapeutic potential of the secretome from cultured human mesenchymal stem cells in experimental traumatic brain injury. *Clin. Sci*. 124, 165–176. doi: 10.1042/CS20120226

Chen, Q., Liang, Q., Zhuang, W., Zhou, J., Zhang, B., Xu, P., et al. (2018). Tenocyte proliferation and migration promoted by rat bone marrow mesenchymal stem cell-derived conditioned medium. *Biotechnol. Lett*. 40, 215–224. doi: 10.1007/s10529-017-2446-7

Choi, J. S., Ryu, H. A., Cheon, S. H., and Kim, S. W. (2019). Human adipose derived stem cells exhibit enhanced liver regeneration in acute liver injury by controlled releasing hepatocyte growth factor. *Cell. Physiol. Biochem*. 52, 935–950. doi: 10.33594/000000065

Choi, W., Lee, J., Lee, J., Lee, S. H., and Kim, S. (2019). Hepatocyte growth factor regulates macrophage transition to the M2 phenotype and promotes murine skeletal muscle regeneration. *Front. Physiol*. 10:914. doi: 10.3389/fphys.2019.00914

Flevaris, P., and Vaughan, D. (2017). The role of plasminogen activator inhibitor type-1 in fibrosis. *Semin. Thromb. Hemost*. 43, 169–177. doi: 10.1055/s-0036-1586228

Fu, Y., Karbaat, L., Wu, L., Leijten, J., Both, S. K., and Karperien, M. (2017). Trophic effects of mesenchymal stem cells in tissue regeneration. *Tissue Eng. Part B Rev*. 23, 515–528. doi: 10.1089/ten.TEB.2016.0365

Fukushima, T., Uchiyama, S., Tanaka, H., and Kataoka, H. (2018). Hepatocyte growth factor activator: a proteinase linking tissue injury with repair. *Int. J. Mol. Sci*. 19, 3435. doi: 10.3390/ijms19113435

Gaspar, D., Spanoudes, K., Holladay, C., Pandit, A., and Zeugolis, D. (2015). Progress in cell-based therapies for tendon repair. *Adv. Drug Deliv. Rev*. 84, 240–256. doi: 10.1016/j.addr.2014.11.023

Gissi, C., Radeghieri, A., Antonetti Lamorgese Passeri, C., Gallorini, M., Calciano, L., Oliva, F., et al. (2020). Extracellular vesicles from rat-bone-marrow mesenchymal stromal/stem cells improve tendon repair in rat Achilles tendon injury model in dose-dependent manner: a pilot study. *PLoS One* 15:e0229914. doi: 10.1371/journal.pone.0229914

Gordon, S., and Martinez, F. O. (2010). Alternative activation of macrophages: mechanism and functions. *Immunity* 32, 593–604. doi: 10.1016/j.immuni.2010.05.007

Han, P., Cui, Q., Lu, W., Yang, S., Shi, M., Li, Z., et al. (2019). Hepatocyte growth factor plays a dual role in tendon-derived stem cell proliferation, migration, and differentiation. *J. Cell. Physiol*. 234, 17382–17391. doi: 10.1002/jcp.28360

Harting, M. T., Srivastava, A. K., Zhaorigetu, S., Bair, H., Prabhakara, K. S., Toledano Furman, N. E., et al. (2018). Inflammation-stimulated mesenchymal stromal cell-derived extracellular vesicles attenuate inflammation. *Stem Cells* 36, 79–90. doi: 10.1002/stem.2730

Hays, P. L., Kawamura, S., Deng, X. H., Dagher, E., Mithoefer, K., Ying, L., et al. (2008). The role of macrophages in early healing of a tendon graft in a bone tunnel. *J. Bone Joint Surg. Am*. 90, 565–579. doi: 10.2106/JBJS.F.00531

Henderson, N. C., and Sethi, T. (2009). The regulation of inflammation by galectin-3. *Immunol. Rev*. 230, 160–171. doi: 10.1111/j.1600-065X.2009.00794.x

Jiang, D., Gao, P., Lin, H., and Geng, H. (2016). Curcumin improves tendon healing in rats: a histological, biochemical, and functional evaluation. *Connect. Tissue Res*. 57, 20–27. doi: 10.3109/03008207.2015.1087517

Kannus, P., and Natri, A. (1997). Etiology and pathophysiology of tendon ruptures in sports. *Scand. J. Med. Sci. Sports* 7, 107–112. doi: 10.1111/j.1600-0838.1997.tb00126.x

Kim, Y. I., Shin, H. W., Chun, Y. S., Cho, C. H., Koh, J., Chung, D. H., et al. (2018a). Epithelial cell-derived cytokines CST3 and GDF15 as potential therapeutics for pulmonary fibrosis. *Cell Death Dis*. 9:506. doi: 10.1038/s41419-018-0530-0

Kim, Y. I., Shin, H. W., Chun, Y. S., and Park, J. W. (2018b). CST3 and GDF15 ameliorate renal fibrosis by inhibiting fibroblast growth and activation. *Biochem. Biophys. Res. Commun*. 500, 288–295. doi: 10.1016/j.bbrc.2018.04.061

Lee, S. Y., Kwon, B., Lee, K., Son, Y. H., and Chung, S. G. (2017). Therapeutic mechanisms of human adipose derived mesenchymal stem cells in a rat tendon injury model. *Am. J. Sports Med*. 45, 1429–1439. doi: 10.1177/0363546517689874

Leong, N. L., Kator, J. L., Clemens, T. L., James, A., Enamoto-Iwamoto, M., and Jiang, J. (2020). Tendon and ligament healing and current approaches to tendon and ligament regeneration. *J. Orthop. Res*. 38, 7–12. doi: 10.1002/jor.24475

Ma, J., Yan, X., Lin, Y., and Tan, Q. (2020). Hepatocyte growth factor secreted from human adipose-derived stem cells inhibits fibrosis in hypertrophic scar fibroblasts. *Curr. Mol. Med*. 20, 558–571. doi: 10.2174/1566524020666200106095745

Manning, C. N., Martel, C., Sakiyama-Elbert, S. E., Silva, M. J., Shah, S., Gelberman, R. H., et al. (2015). Adipose-derived mesenchymal stromal cells modulate

tendon fibroblast responses to macrophage-induced inflammation in vitro. *Stem Cell Res. Ther*. 6:74. doi: 10.1186/s13287-015-0059-4

Marmotti, A., Peretti, G. M., Mattia, S., Mangiavini, L., de Girolamo, L., Viganò, M., et al. (2018). Pulsed electromagnetic fields improve tenogenic commitment of umbilical cord-derived mesenchymal stem cells: a potential strategy for tendon repair – an in vitro study. *Stem Cells Int*. 2018, 9048237. doi: 10.1155/2018/9048237

Millar, N. L., Murrell, G. A., and McInnes, I. B. (2017). Inflammatory mechanisms in tendinopathy – towards translation. *Nat. Rev. Rheumatol*. 13, 110–122. doi: 10.1038/nrrheum.2016.213

Moon, S. H., Lee, C. M., Park, S. H., and Jin Nam, M. (2019). Effects of hepatocyte growth factor gene-transfected mesenchymal stem cells on dimethylnitrosamine-induced liver fibrosis in rats. *Growth Factors* 37, 105–119. doi: 10.1080/08977194.2019.1652399

Munder, M., Eichmann, K., and Modolell, M. (1998). Alternative metabolic states in murine macrophages reflected by the nitric oxide synthase/arginase balance: competitive regulation by CD4+ T cells correlates with Th1/Th2 phenotype. *J. Immunol*. 160, 5347–5354.

Oka, M., Sekiya, S., Sakiyama, R., Shimizu, T., and Nitta, K. (2019). Hepatocyte growth factor-secreting mesothelial cell sheets suppress progressive fibrosis in a rat model of CKD. *J. Am. Soc. Nephrol*. 30, 261–276. doi: 10.1681/ASN.2018050556

Olsson, N., Nilsson-Helander, K., Karlsson, J., Eriksson, B. I., Thomée, R., Faxén, E., et al. (2011). Major functional deficits persist 2 years after acute Achilles tendon rupture. *Knee Surg. Sports Traumatol. Arthrosc*. 19, 1385–1393. doi: 10.1007/s00167-011-1511-3

Pawitan, J. A. (2014). Prospect of stem cell conditioned medium in regenerative medicine. *BioMed. Res. Int*. 2014:965849. doi: 10.1155/2014/965849

Rhatomy, S., Prasetyo, T. E., Setyawan, R., Soekarno, N. R., Romaniyanto, F., Sedjati, A., et al. (2020). Prospect of stem cells conditioned medium (secretome) in ligament and tendon healing: a systematic review. *Stem Cells Transl. Med*. 9, 895–902. doi: 10.1002/sctm.19-0388

Ruberti, S., Bianchi, E., Guglielmelli, P., Rontauroli, S., Barbieri, G., Tavernari, L., et al. (2018). Involvement of MAF/SPP1 axis in the development of bone marrow fibrosis in PMF patients. *Leukemia* 32, 438–449. doi: 10.1038/leu.2017.220

Sevivas, N., Teixeira, F. G., Portugal, R., Direito-Santos, B., Espregueira-Mendes, J., Oliveira, F. J., et al. (2018). Mesenchymal stem cell secretome improves tendon cell viability in vitro and tendon-bone healing in vivo when a tissue engineering strategy is used in a rat model of chronic massive rotator cuff tear. *Am. J. Sports Med*. 46, 449–459. doi: 10.1177/0363546517735850

Sharma, R. I., and Snedeker, J. G. (2010). Biochemical and biomechanical gradients for directed bone marrow stromal cell differentiation toward tendon and bone. *Biomaterials* 31, 7695–7704. doi: 10.1016/j.biomaterials.2010.06.046

Shen, H., Yoneda, S., Abu-Amer, Y., Guilak, F., and Gelberman, R. H. (2020). Stem cell-derived extracellular vesicles attenuate the early inflammatory response after tendon injury and repair. *J. Orthop. Res*. 38, 117–127. doi: 10.1002/jor.24406

Shi, Z., Wang, Q., and Jiang, D. (2019). Extracellular vesicles from bone marrow-derived multipotent mesenchymal stromal cells regulate inflammation and enhance tendon healing. *J. Transl. Med*. 17:211. doi: 10.1186/s12967-019-1960-x

Shimode, K., Iwasaki, N., Majima, T., Funakoshi, T., Sawaguchi, N., Onodera, T., et al. (2007). Bone marrow stromal cells act as feeder cells for tendon fibroblasts through soluble factors. *Tissue Eng*. 13, 333–341. doi: 10.1089/ten.2006.0079

Su, G. H., Sun, Y. F., Lu, Y. X., Shuai, X. X., Liao, Y. H., Liu, Q. Y., et al. (2013). Hepatocyte growth factor gene-modified bone marrow-derived mesenchymal stem cells transplantation promotes angiogenesis in a rat model of hindlimb ischemia. *J. Huazhong Univ. Sci. Technolog. Med. Sci*. 33, 511–519. doi: 10.1007/s11596-013-1151-6

Sun, Y., Chen, W., Hao, Y., Gu, X., Liu, X., Cai, J., et al. (2019). Stem cell-conditioned medium promotes graft remodeling of midsubstance and intratunnel incorporation after anterior cruciate ligament reconstruction in a rat model. *Am. J. Sports Med*. 47, 2327–2337. doi: 10.1177/0363546519859324

Thankam, F. G., Roesch, Z. K., Dilisio, M. F., Radwan, M. M., Kovilam, A., Gross, R. M., et al. (2018). Association of inflammatory responses and ECM disorganization with HMGB1 upregulation and NLRP3 inflammasome activation in the injured rotator cuff tendon. *Sci. Rep*. 8:8918. doi: 10.1038/s41598-018-27250-2

Tsai, W. C., Hsu, C. C., Chen, C. P., Chang, H. N., Wong, A. M., Lin, M. S., et al. (2011). Ciprofloxacin up-regulates tendon cells to express matrix metalloproteinase-2 with degradation of type I collagen. *J. Orthop. Res*. 29, 67–73. doi: 10.1002/jor.21196

Tsai, W. C., Pang, J. H., Hsu, C. C., Chu, N. K., Lin, M. S., and Hu, C. F. (2006). Ultrasound stimulation of types I and III collagen expression of tendon cell and upregulation of transforming growth factor beta. *J. Orthop. Res*. 24, 1310–1316. doi: 10.1002/jor.20130

Veronesi, F., Salamanna, F., Tschon, M., Maglio, M., Nicoli Aldini, N., and Fini, M. (2017). Mesenchymal stem cells for tendon healing: what is on the horizon? *J. Tissue Eng. Regen. Med*. 11, 3202–3219. doi: 10.1002/term.2209

Vizoso, F. J., Eiro, N., Cid, S., Schneider, J., and Perez-Fernandez, R. (2017). Mesenchymal stem cell secretome: toward cell-free therapeutic strategies in regenerative medicine. *Int. J. Mol. Sci*. 18:1852. doi: 10.3390/ijms18091852

Wang, H., Zheng, R., Chen, Q., Shao, J., Yu, J., and Hu, S. (2017). Mesenchymal stem cells microvesicles stabilize endothelial barrier function partly mediated by hepatocyte growth factor (HGF). *Stem Cell Res. Ther*. 8:211. doi: 10.1186/s13287-017-0662-7

Wang, Y., He, G., Guo, Y., Tang, H., Shi, Y., Bian, X., et al. (2019). Exosomes from tendon stem cells promote injury tendon healing through balancing synthesis and degradation of the tendon extracellular matrix. *J. Cell. Mol. Med*. 23, 5475–5485. doi: 10.1111/jcmm.14430

Xie, M., Wan, J., Zhang, F., Zhang, R., Zhou, Z., and You, D. (2019). Influence of hepatocyte growth factor-transfected bone marrow-derived mesenchymal stem cells towards renal fibrosis in rats. *Indian J. Med. Res*. 149, 508–516. doi: 10.4103/ijmr.IJMR_1527_16

Xu, K., Sun, Y., Kh Al-Ani, M., Wang, C., Sha, Y., Sung, K. P., et al. (2018). Synergistic promoting effects of bone morphogenetic protein 12/connective tissue growth factor on functional differentiation of tendon derived stem cells and patellar tendon window defect regeneration. *J. Biomech*. 66, 95–102. doi: 10.1016/j.jbiomech.2017.11.004

Yin, Z., Guo, J., Wu, T. Y., Chen, X., Xu, L. L., Lin, S. E., et al. (2016). Stepwise differentiation of mesenchymal stem cells augments tendon-like tissue formation and defect repair in vivo. *Stem Cells Transl. Med*. 5, 1106–1116. doi: 10.5966/sctm.2015-0215

Yu, H., Cheng, J., Shi, W., Ren, B., Zhao, F., Shi, Y., et al. (2020). Bone marrow mesenchymal stem cell-derived exosomes promote tendon regeneration by facilitating the proliferation and migration of endogenous tendon stem/progenitor cells. *Acta Biomater*. 106, 328–341. doi: 10.1016/j.actbio.2020.01.051

Zhang, J., and Wang, J. H. (2010). Characterization of differential properties of rabbit tendon stem cells and tenocytes. *BMC Musculoskelet. Disord*. 11:10. doi: 10.1186/1471-2474-11-10

Zhang, M., Liu, H., Cui, Q., Han, P., Yang, S., Shi, M., et al. (2020). Tendon stem cell-derived exosomes regulate inflammation and promote the high-quality healing of injured tendon. *Stem Cell Res. Ther*. 11:402. doi: 10.1186/s13287-020-01918-x

Conflict of Interest: The authors declare that the research was conducted in the absence of any commercial or financial relationships that could be construed as a potential conflict of interest.

frontiers in Cell and Developmental Biology

ORIGINAL RESEARCH
published: 27 April 2021
doi: 10.3389/fcell.2021.651583

Enhancement of Migration and Tenogenic Differentiation of Macaca Mulatta Tendon-Derived Stem Cells by Decellularized Tendon Hydrogel

*Liang-Ju Ning[1†], Ya-Jing Zhang[1†], Yan-Jing Zhang[1,2], Min Zhu[1], Wei Ding[1], Yan-Lin Jiang[1], Yi Zhang[2], Jing-Cong Luo[1] and Ting-Wu Qin[1]**

[1] Laboratory of Stem Cell and Tissue Engineering, Orthopedic Research Institute, State Key Laboratory of Biotherapy and Cancer Center, West China Hospital, Sichuan University and Collaborative Innovation Center of Biotherapy, Chengdu, China, [2] Core Facility of West China Hospital, Sichuan University, Chengdu, China

OPEN ACCESS

Edited by:
Zi Yin,
Zhejiang University, China

Reviewed by:
Jiajie Hu,
Zhejiang University, China
Jie Zhu,
Northwest A&F University, China

***Correspondence:**
Ting-Wu Qin
tingwuqin@hotmail.com

† These authors have contributed equally to this work and share first authorship

Specialty section:
This article was submitted to Stem Cell Research, a section of the journal Frontiers in Cell and Developmental Biology

Received: 10 January 2021
Accepted: 06 April 2021
Published: 27 April 2021

Citation:
Ning L-J, Zhang Y-J, Zhang Y-J, Zhu M, Ding W, Jiang Y-L, Zhang Y, Luo J-C and Qin T-W (2021) Enhancement of Migration and Tenogenic Differentiation of Macaca Mulatta Tendon-Derived Stem Cells by Decellularized Tendon Hydrogel. Front. Cell Dev. Biol. 9:651583. doi: 10.3389/fcell.2021.651583

Decellularized tendon hydrogel from human or porcine tendon has been manufactured and found to be capable of augmenting tendon repair *in vivo*. However, no studies have clarified the effect of decellularized tendon hydrogel upon stem cell behavior. In the present study, we developed a new decellularized tendon hydrogel (T-gel) from Macaca mulatta, and investigated the effect of T-gel on the proliferation, migration and tenogenic differentiation of Macaca mulatta tendon-derived stem cells (mTDSCs). The mTDSCs were first identified to have universal stem cell characteristics, including clonogenicity, expression of mesenchymal stem cell and embryonic stem cell markers, and multilineage differentiation potential. Decellularization of Macaca mulatta Achilles tendons was confirmed to be effective by histological staining and DNA quantification. The resultant T-gel exhibited highly porous structure or similar nanofibrous structure and approximately swelling ratio compared to the collagen gel (C-gel). Interestingly, stromal cell-derived factor-1 (SDF-1) and fibromodulin (Fmod) inherent in the native tendon extracellular matrix (ECM) microenvironment were retained and the values of SDF-1 and Fmod in the T-gel were significantly higher than those found in the C-gel. Compared with the C-gel, the T-gel was found to be cytocompatible with NIH-3T3 fibroblasts and displayed good histocompatibility when implanted into rat subcutaneous tissue. More importantly, it was demonstrated that the T-gel supported the proliferation of mTDSCs and significantly promoted the migration and tenogenic differentiation of mTDSCs compared to the C-gel. These findings indicated that the T-gel, with its retained nanofibrous structure and some bioactive factors of native tendon ECM microenvironment, represents a promising hydrogel for tendon regeneration.

Keywords: decellularized tendon, hydrogel, ECM microenvironment, Macaca mulatta, tendon-derived stem cells, migration, differentiation

INTRODUCTION

Tendinopathy, also called tendinosis, is often caused by overuse or sudden stress on a tendon. Evidence from clinical and animal studies showed histopathological changes associated with tendinopathy, including degeneration and disorganization of collagen fibers, increased cellularity, as well as minimal inflammation (Khan et al., 1999; Soslowsky et al., 2000). Subsequent studies demonstrated that tendinopathy weakened the mechanical and material properties of the tendon (Arya and Kulig, 2010), and the progression of tendon fatigue damage accumulation leaded to collagen fiber rupture and eventual tendon full-thickness tearing with higher loading (Neviaser et al., 2012), which illustrated the progression from tendinopathy to full-thickness tearing. The current treatment options for tendinopathy focused on exercise-based physical therapy, other physical therapy modalities (such as ultrasound and low-level laser therapy), growth factors and stem cell treatment, and so on (Andres and Murrell, 2008). Among them, growth factors (de Vos et al., 2010; Kaux and Crielaard, 2013; Carr et al., 2015) and stem cell (Chong et al., 2007; Yuksel et al., 2016) treatments have attracted growing interest.

Extracellular matrix (ECM) hydrogels from decellularized tissues have been widely utilized to deliver exogenous stem cells (Viswanath et al., 2017; Yuan et al., 2017; Bai et al., 2019), growth factors (Seif-Naraghi et al., 2012; Xu et al., 2016; Liu et al., 2019) or other bioactive molecules for tissue repair and regeneration, which was demonstrated to support cell viability and function and enhance retention and delivery of growth factors. Besides, ECM hydrogels provide advantages such as injectability, regulable mechanical properties, good processibility as well as the ability to fill an irregularly shaped space (Wolf et al., 2012; Pati et al., 2015; Lin et al., 2018). Promisingly, previous work demonstrated that hydrogels formed from enzymatically degraded and solubilized ECM retained some of the components and bioactivity of the intact ECM (Wolf et al., 2012; Wu et al., 2015; Wang et al., 2016; Lin et al., 2018), and their degradation caused the release of many bioactive components, such as cryptic peptides, which are contribute to endogenous cell recruiting and tissue remodeling (Agrawal et al., 2011a,b). Recently, Ungerleider et al. (2020) reported that tissue specific muscle ECM hydrogel improved skeletal muscle regeneration *in vivo* over non-matched tissue source, which suggested ECM choice is a crucial consideration for optimal tissue regeneration.

Decellularized tendon ECM as a tissue-specific bioscaffold has been widely accepted as an ideal substrate for tendon regeneration. We previously developed a new and mild decellularization protocol, including physical methods and enzymatic solutions for processing canine Achilles tendons, and produced a 300 μm-thick sheet-like scaffold of decellularized tendon slices (DTSs), which retained more than 93% of fibromodulin (Fmod) and biglycan (Bgn) as well as four growth factors (TGF-β1, IGF-1, VEGF, and CTGF) of the native tendon (Ning et al., 2012). Also, the DTSs that maintained the native tendon ECM microenvironment cues, promoted stem cell proliferation and tenogenic differentiation (Ning et al., 2015). Three-dimensional (3D) collagen scaffold supplemented with tendon ECM was found to significantly increase proliferation and tenogenic differentiation of human adipose-derived stem cells (Yang et al., 2013). Promisingly, an injectable tendon hydrogel from decellularized human tendon were designed and found to hold the distinctive composition specific for tendon ECM, and displayed good biocompatibility (Farnebo et al., 2014). Then, this decellularized tendon hydrogel was demonstrated to be capable of augmenting tendon repair in rat Achilles tendon injury model as well as chronic rotator cuff injury model (Kim et al., 2014; Crowe et al., 2016). However, no studies have clarified the effect of decellularized tendon hydrogel upon stem cell behavior.

Due to their highly similar to humans in terms of genetics and physiology, the rhesus monkeys (Macaca mulatta) have become the most widely used non-human primate in basic and applied biomedical research (Gibbs et al., 2007). In this study, we developed a new decellularized tendon hydrogel (T-gel) from Macaca mulatta, and investigated the effect of T-gel on the proliferation, migration and tenogenic differentiation of Macaca mulatta tendon-derived stem cells (mTDSCs).

MATERIALS AND METHODS

Macaca Mulatta TDSCs Isolation, Culture, and Identification

The Achilles tendons were harvested from adult Macaca mulatta within 2 h of euthanasia, which were gathered from the West China-Frontier Pharma Tech (Chengdu, China). The isolation of mTDSCs was performed according to our previously published protocol (Ning et al., 2015). Using the same protocol, we isolated and cultured mTDSCs from Macaca mulatta Achilles tendons. Fresh culture medium consisting of Dulbecco's modified Eagle's medium (DMEM, Gibco) supplemented with 20% fetal bovine serum (FBS), 100 μg/ml streptomycin, 100 U/ml penicillin and 2 mM L-glutamine (all from Invitrogen, Carlsbad, CA), was changed every other day. Cells at passage 3 (P3) were utilized in the subsequent experiments.

To determine the self-renewal potential of mTDSCs, the cells were seeded at 500 cells or 1,000 cells in 25-cm^2 flasks to form colonies. After 10 days, the cell colonies were stained using 0.5% crystal violet (Sigma). The number of all colonies with diameters >2 mm was counted.

For flow cytometry analysis of cell surface antigens, mTDSCs (5×10^5) were incubated with 1 μg of phycoerythrin (PE)-Cy^{TM}7-conjugated mouse anti-human CD73, APC-conjugated mouse anti-human CD90, PE-conjugated mouse anti-human CD105 (BD), PE-conjugated mouse anti-human CD105 (BD) or FITC-conjugated mouse anti-human CD34 (Santa Cruz Biotechnology) and CD45 (BD) for 30 min at 4°C. After washing with phosphate-buffered saline (PBS) by centrifugation at 1,200 rpm for 5 min, the stained cells were resuspended in 200 μl of ice-cold PBS and detected by the Cytomics FC500 MCL Flow Cytometer (Beckman Coulter).

Immunofluorescent staining was performed to examine the following stem cell markers: Nanog, octamer-binding transcription factor 4 (Oct-4) and stage-specific embryonic antigen-1 (SSEA-1). mTDSCs (2×10^4) were seeded on the

24×24 mm^2 glass coverslips and cultured with growth medium for 3 days. The cells were then fixed in 4% paraformaldehyde for 15 min at room temperature and permeabilized with 0.5% Triton X-100. Fixed cells were washed with PBS and blocked for 30 min with 1% BSA, and then incubated with primary antibody at 4°C overnight. The primary antibodies and the titers used were as follows: rabbit anti-human Nanog (1:50, Abcam), rabbit anti-human Oct-4 (1:50, Abcam), or mouse anti-human SSEA-1 (1:50, Millpore). After washing the cells with PBS, Cy3-conjugated goat anti-rabbit IgG secondary antibody (1:200) was applied to Nanog and Oct-4 and Alexa Fluor® 488-conjugated goat anti-mouse IgG antibody (1:50) (all from Jackson ImmunoResearch Laboratories, PA) was used for SSEA-1 at room temperature for 1 h. Finally, the nuclei were counter-stained with 4,6-diamidino-2-phenylindole (DAPI, Sigma). The images were observed and taken with fluorescence microscopy (Olympus, Japan).

The multidifferentiation potential of mTDSCs was tested *in vitro* for the osteogenic, adipogenic, and chondrogenic lineages as described previously (Ning et al., 2015). For osteogenic differentiation, mTDSCs (3×10^3/cm^2) were cultured in basic growth medium (containing 10% FBS, 100 μg/ml streptomycin and 100 U/ml penicillin in DMEM- low glucose) plus 0.1 μM dexamethasone, 10 mM b-glycerol phosphate, and 100 μg/ml ascorbic acid for 28 days. For adipogenic differentiation, mTDSCs (5×10^3/cm^2) were cultured in adipogenic induction medium consisting of basic growth medium supplemented with 0.5 μM dexamethasone, 50 μM indomethacin, 50 μM isobutylmethylxanthine (IBMX) and 10 μg/ml insulin for 14 days. For chondrogenic differentiation, a pellet culture system was used (Rui et al., 2010). mTDSCs (3×10^5) were pelleted into a micromass by centrifugation at 1,200 rpm for 10 min in a 15-ml conical polypropylene tube and cultured in chondrogenic induction medium consisting of basic growth medium added with 0.1 μM dexamethasone, 10 ng/ml TGF-β3, 40 μg/ml proline, 100 μg/ml sodium pyruvate, 50 μg/ml ascorbate 2-phosphate and 1% ITS + Premix (BD) for 21 days. To determine the osteogenesis, adipogenesis and chondrogenesis of mTDSCs, Alizarin Red S, Oil Red O and Safranin O/Fast Green staining were performed, respectively.

Preparation of the T-gel

The DTSs from Macaca mulatta Achilles tendons were prepared using our previously published protocol (Ning et al., 2012). In brief, the harvested Achilles tendons were firstly trimmed into segments roughly 2 cm in length and then subjected to repetitive freeze/thaw treatment, frozen section with a 300 μm thickness, as well as nuclease treatment for 12 h at 37°C. The tendon segments were only performed to longitudinally sliced into thicknesses of 300 μm, as native tendon slices (NTSs). Finally, all tendon slices were washed three times with PBS for 30 min each. The decellularization effectiveness were determined by hematoxylin and eosin (H&E) and DAPI staining, as well as DNA quantification assays.

The T-gel was prepared using a previously published protocol with some modifications (Farnebo et al., 2014). Lyophilized DTSs were cryomilled using a Mixer Mill (Retsch, MM400, Germany) after precooled in liquid nitrogen for 5 min. The milled DTSs powder was digested in a solution of 1 mg/ml pepsin (Sigma) in 0.02 M HCl such that the final concentration of decellularized tendon pre-gel was 20 or 30 mg/ml. The DTSs powder was digested for 24 h at 4°C under constant stirring. While cooled on ice, the pH was neutralized to 7.4 by adding 0.2 M NaOH (1/10 of original digest volume), and salt concentration was adjusted by adding 10 × PBS (1/10 of final neutralized volume). Then, the final mixture (pre-gel) was allowed to gel formation for 1 h at 37°C. Rat-tail tendon collagen type I gel (C-gel, 2 mg/ml; Shengyou, China) was prepared according to the manufacturer's instruction and served as the control in this study.

Characterization of the T-gel

The microstructure of the T-gel and C-gel was visualized by scanning electron microscopy (SEM) (ZEISS EVO10, Germany). After gelation, the gel samples were directly freeze-dried at -70°C for 24 h or immediately fixed in 2.5% glutaraldehyde at 4°C for 24 h. The freeze-dried gel samples were mounted on aluminum stubs and coated with gold, then observed with SEM. The glutaraldehyde-fixed gel samples were dehydrated in graded ethanol (50, 70, 90, and 100% ethanol) for 2 h at each concentration, and then were conducted to critical point drying. After coating with gold, the gel samples were examined with SEM.

The equilibrium swelling ratios of the T-gel and C-gel were determined by the classical gravimetric method. Both gels ($n = 3$ per group) were immersed in PBS (pH = 7.4) at 37°C for 24 h to ensure that all the gels reached their equilibrium swelling states. The equilibrium swelling ratios of the different gels were calculated according to our previous work (Wang et al., 2016) by equation: swelling ratio (%) = (Ww—Wi)/Ww × 100, where Ww and Wi are the weights of the hydrogels in the equilibrium swelling state and initial gelling state, respectively.

The bioactive factors retained in the T-gel and C-gel were measured by enzyme-linked immunosorbent assay (ELISA). Soluble molecules were extracted from the T-gel and C-gel ($n = 6$ for each group) using the Radio Immunoprecipitation Assay (RIPA) Lysis Buffer (Beyotime, China) with protease inhibitor cocktail and homogenized by the High-Throughput Tissue Automatic Grinding Machine (Servicebio, China). The extracted lysates were centrifuged at 10,000 rpm for 20 min at 4°C and then the supernatant was collected. ELISA measures were performed to detect IGF-1, SDF-1 and Fmod according to the manufacturer's instructions (IGF-1 and SDF-1, Multisciences Biotech, China; Fmod, DLdevelop, China). All samples were normalized by per ml gel.

The *in vitro* cytotoxicity of the T-gel and C-gel was evaluated using the Live/Dead staining and the cell counting kit-8 (CCK-8, Dojindo, Japan) assay. For Live/Dead staining assay, a 96-well plate was coated with 50 μl pre-T-gel or pre-C-gel ($n = 4$ for each group), then incubated at 37°C in 5% CO_2 for 1 h. After washing with PBS, the NIH-3T3 fibroblasts were seeded on gel-coated plates at a concentration of 4×10^3 cells/well and cultured with basic growth medium. After 1, 3, and 5 days of culture, cell viability was confirmed using a fluorescent live/dead viability/cytotoxicity kit (Thermo Fisher Scientific, United States) according to the manufacturer's protocol. Live and dead cells

were observed with a phase contrast fluorescence inverted microscope (Nikon, Japan). Meanwhile, at each time point, cell proliferation was assessed using the CCK-8 assay according to the manufacturer's protocol. After incubation at 37°C for 1.5 h, the absorbance was measured at 450 nm via a Multiskan FC® Microplate Photometer (Thermo Fisher Scientific, United States). Cell number was correlated to optical density (OD).

Twenty male Sprague Dawley (SD) rats (7–8 weeks old, 250–310 g) were used to evaluate the histocompatibility of the T-gel and C-gel *in vivo*. All animal procedures were approved by the Sichuan University Animal Care and Use Committee. After anesthesia, 1 ml of pre-T-gel or pre-C-gel were injected directly into the subcutaneous tissue of rats along the dorsal midline. At 3, 7, 14, and 28 days of post-injection, five rats for each time point were euthanized. The implant/skin tissue constructs were harvested and immediately fixed in 10% neutral buffered formalin for histological evaluation using H&E and Masson's Trichrome staining. The host response to the implants was quantitatively assessed by measuring the number of inflammatory cells, including macrophages, lymphocytes, neutrophils, eosinophils, and so on. High magnification images (400×) were obtained from four randomly selected fields in each sample under a light microscope (Olympus, Japan). At each time point, the number of inflammatory cells in five different tissue samples ($n = 5$) was measured and normalized to the gel area.

Functional Evaluation of the T-gel

Cell viability and proliferation were determined by the Live/Dead staining and CCK-8 assay. Briefly, a 96-well plate was coated with the C-gel and T-gel prior to seeding mTDSCs at a density of 4×10^3 cells/well. The cell viability of mTDSCs seeded on the C-gel and T-gel over a period of 7 days was determined using the Live/Dead staining. Cell proliferation was assessed quantitatively at 1, 3, 5, and 7 days using the CCK-8 assay.

A Transwell chemotactic migration model (pore size: 8 μm, Corning, United States) was used to assess the migration capacity of mTDSCs mediated by the C-gel and T-gel. After serum-starving for 24 h, 200 μl of mTDSCs suspension (5×10^4 cells/ml) was placed within the upper chamber, and 1 ml DMEM containing 10% FBS was added to 200 μl of C-gel or T-gel coated lower chamber. After 24 or 48 h of incubation, the cells that migrated to the lower side of the membrane were fixed and dyed by DAPI (Sigma). The number of migrated cells was counted in five randomly selected fields (100×) in each well.

For tenogenic differentiation analysis, the expression of tendon-related markers at the mRNA level was tested in mTDSCs cultured on the T-gel and C-gel in basic growth medium for 3, 7, or 14 days. At each time point, total RNA was isolated by lysis in TRIzol (Life Technologies). First-strand cDNA was synthesized with oligo (dT) primers using a cDNA synthesis kit (Promega) according to the manufacturer's instructions. Quantification of mRNA expression was performed specific for scleraxis (SCX), tenomodulin (TNMD), tenascin-C (TNC), collagen types I (COL I) and III (COL III) using the Step One Plus Real-Time PCR System (Life Technologies) and values normalized to GAPDH and presented as $2^{-\Delta\Delta Ct}$. All primers were designed using primer 5.0 and are summarized in **Table 1**.

Statistical Analysis

Data were presented as mean ± standard deviation (SD). A two-tailed Student's *t*-test or one-way analysis of variance (ANOVA) with a *post hoc* Dunnett's T3 test wherever applicable, was used for statistical analysis. Differences were considered statistically significant at $P < 0.05$.

RESULTS

Identification and Characterization of mTDSCs

During the primary culture and continuous passage culture, mTDSCs mainly showed two different types of morphologies: fibroblast-like morphology and cobblestone-like morphology (**Figure 1A**). The colony-forming assay showed that colonies that had formed from single cells after 10 days of culture were visualized using crystal violet staining (**Figures 1B,C**). About 4% of mTDSCs at P3 were able to form colonies. The results of flow cytometric analysis indicated that these cells expressed a set of classic mesenchymal stem cell (MSC) markers, including CD73, CD90 and CD105 (**Figure 1D**). They were negative for the hematopoietic stem cell marker CD34 and for the leukocyte marker CD45, thus verifying the absence of contaminating hematopoietic cells (**Figure 1D**). Immunofluorescent staining of these cells showed that mTDSCs were positive for embryonic stem cells marker, such as Nanog, Oct-4 and SSEA-1 (**Figure 1E**). The potential of mTDSCs to undergo osteogenesis, adipogenesis, and chondrogenesis was tested (**Figure 1F**). When mTDSCs were cultured in osteogenic medium for 28 days, Alizarin-red S positive calcium nodules were found in osteogenic induction group only but not in control group, in which mTDSCs were cultured in basic growth medium without osteogenic supplements. Lipid droplets were observed after adipogenic induction of mTDSCs for 14 days as indicated by Oil-red O staining whereas this was not observed in the control group.

TABLE 1 | List of primer sequences utilized for real-time Polymerase Chain Reaction.

Genes	5′-3′	Primer sequences	Production size (bp)
GAPDH	Forward	TGACCTGCCGTCTGGAAA	138
	Reverse	GGGTGTCGCTGTTGAAGT	
SCX	Forward	CGAGAACACCCAGCCCAAAC	105
	Reverse	GCCACCTCCTAACTGCGAAT	
TNMD	Forward	TCAGTGATTTGGGTCCCAGC	218
	Reverse	GGGACCACCCACTGTTCATT	
TNC	Forward	TTTCCCAGACAGATAACAGC	197
	Reverse	AGCAGAAACTCCAATCCC	
COLI	Forward	GACATCCCACCAATCACCT	118
	Reverse	CGTCATCGCACAACACCTT	
COLIII	Forward	CAGGGAACAACTTGATGG	140
	Reverse	AGTGGGATGAAGCAGAGC	

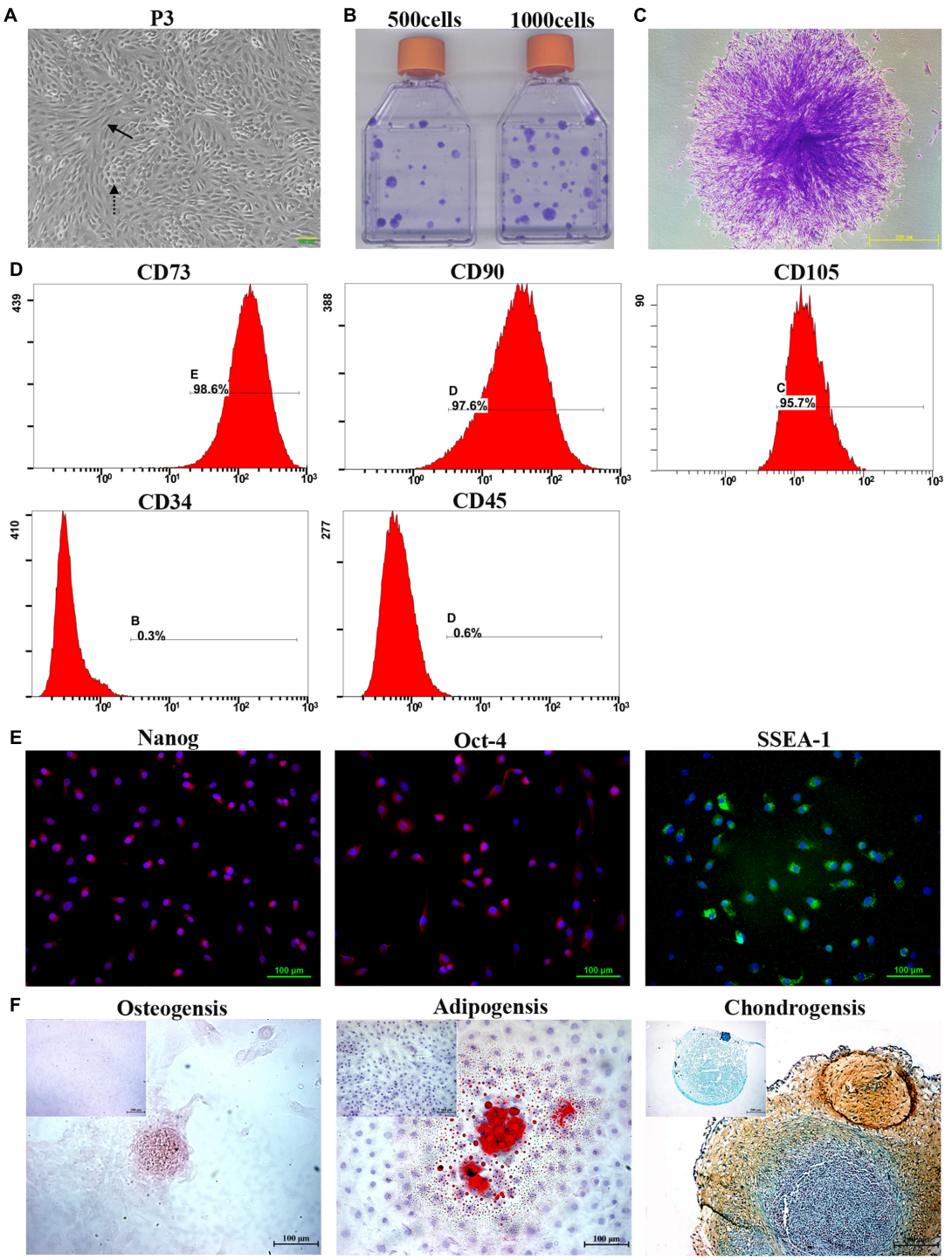

FIGURE 1 | Isolation and characterization of mTDSCs. **(A)** Morphology of mTDSCs at P3. These cells were fibroblast-like morphology (solid arrow) or cobblestone-like morphology (dotted arrow). **(B)** Crystal violet staining of colonies formed by mTDSCs. **(C)** Representative image of a single clone. **(D)** Flow cytometry analysis of the expression of cell surface markers related to MSCs, hematopoietic stem cells, and endothelial cells on mTDSCs. **(E)** Immunofluorescent staining of stem cell markers for mTDSCs. Scale bar = 100 μm. **(F)** Multidifferentiation potential of mTDSCs toward osteogenesis (Scale bar = 100 μm), adipogenesis (Scale bar = 100 μm) and chondrogenesis (Scale bar = 200 μm) *in vitro*, as evidenced by Alizarin Red, Oil Red O, and Safranin O/Fast Green staining respectively. The upper left corner inset shows the mTDSCs in basic growth medium without such a multidifferentiation potential.

After culturing in chondrogenic induction medium for 21 days, the micromass formed by mTDSCs were stained positive for glycosaminoglycan (GAG)-rich matrix with Safranin O/Fast Green staining, which were negative in the control group. These data suggested that mTDSCs had multidifferentiation potential.

Preparation and Characterization of the T-gel

Prior to preparation of the T-gel, the Achilles tendons from adult Macaca mulatta were subjected to complete decellularization. H&E staining of the tendon slices before and after decellularization demonstrated that preservation of the native tendon collagen structure while removing the cellular components (**Figure 2A**). DAPI staining also indicated an absence of nuclei in the DTSs. By comparison, abundant nuclear materials were observed in the NTSs (**Figure 2A**). DNA quantification assay indicated the residual DNA content was significantly reduced in the DTSs (28.62 $\pm$ 3.11 ng/mg) as compared with that in the NTSs (174.70 $\pm$ 13.42 ng/mg), which further demonstrated efficient removal of DNA from the native tendon (**Figure 2B**).

A typical process for the production of T-gel is presented in **Figure 3**. The T-gel from decellularized tendon ECM was successfully prepared at 20 or 30 mg/ml concentration, which was determined to be injectable through a syringe with a 25 G needle. Specially, the higher concentrated T-gel (30 mg/ml) showed a stiffer structure and more stable gel-forming ability compared to the lower concentrated (20 mg/ml) T-gel. Therefore, 30 mg/ml T-gel was used in the following experiments.

For freeze-dried samples, SEM images of cross section of both gels exhibited an interconnected and highly porous structure. Notably, the C-gel showed interlaced lamellar and the T-gel showed alveolate (**Figure 4A**). For glutaraldehyde-fixed samples, SEM analysis revealed that both the C-gel and T-gel exhibited similar nanoscale collagen features (**Figure 4A**), with assembled nanofibers that were 87.77 $\pm$ 9.12 nm and 74.30 $\pm$ 5.33 nm in diameter, respectively.

The swelling ratio of the C-gel and T-gel is shown in **Figure 4B**. The T-gel showed a slightly lower swelling ratio than the C-gel, and no statistical significance was found between the two groups ($P > 0.05$).

The retention of the bioactive factors naturally existing in native tendon was demonstrated by the ELISA measures of protein extractions from the C-gel and T-gel. No detectable IGF-1 was found in the C-gel and T-gel (data not shown). SDF-1 and Fmod were present in the T-gel, while no detectable Fmod was present in the C-gel. The values of SDF-1 and Fmod in the T-gel were significantly higher than those in the C-gel (**Figure 4C**).

The Live/Dead staining indicated that the majority of NIH-3T3 fibroblasts cultured on the surface of the C-gel and T-gel were viable, with few dead cells from 1 to 5 days (**Figure 5A**). However, fibroblasts cultured on the C-gel-coated plates showed more obvious increases in cell number than those on the T-gel-coated plates. Interestingly, fibroblasts were observed to infiltrate into the T-gel and tended to grow as cell clusters. The CCK-8 assay also verified significant lower cell viability of fibroblasts in the T-gel-coated group, as compared with that in the C-gel-coated group ($P < 0.05$, **Figure 5B**). Nonetheless, both groups showed cell number significantly increased with time in culture ($P < 0.05$, **Figure 5B**).

Histologically, at 3 days after injection, a large number of inflammatory cells appeared around the C-gel and T-gel, indicating that both gels elicited a moderate degree inflammatory response (**Figure 6A**). Quantitatively, the average inflammatory cells density in the T-gel group was significantly higher than that in the C-gel group at this time point (C-gel: 602.62 $\pm$ 65.68/mm^2 vs. T-gel: 978.17 $\pm$ 95.36/mm^2, $P < 0.05$, **Figure 6B**). At 7 days, numerous inflammatory cells, including macrophages, lymphocytes, neutrophils and eosinophils, infiltrated into the gel implants (**Figure 6A**). The number of inflammatory cells showed slight increase in the C-gel group but obvious decrease in the T-gel group. However, no significant differences in the average inflammatory cells density between the two groups were detected (C-gel: 659.39 $\pm$ 61.08/mm^2 vs. T-gel: 703.06 $\pm$ 73.48/mm^2, $P > 0.05$, **Figure 6B**). By 14 days, the infiltration of inflammatory cells gradually decreased and a small number of spindle-shaped fibroblasts were observed (**Figure 6A**). The average inflammatory cells density decreased to 510.92 $\pm$ 59.99/mm^2 and 563.32 $\pm$ 81.91/mm^2 for the C-gel and T-gel, respectively ($P > 0.05$, **Figure 6B**). By 28 days, the inflammatory reaction was basically eliminated along with the increase of fibroblasts (**Figure 6A**), and the number of inflammatory cells further decreased to 329.69 $\pm$ 92.44/mm^2 and 342.79 $\pm$ 71.00/mm^2 for the C-gel and T-gel, respectively ($P > 0.05$, **Figure 6B**). Besides, Masson's Trichrome staining indicated no fibrous capsule formation at the interface between tissues and the gels (**Figure 7**). Both gels showed faint blue staining. The C-gel degraded more quickly than T-gel during the period of 28 days and tended to be much looser. Taken together, the T-gel did not elicit a significant immune response as compared to the C-gel with excellent biocompatibility.

Functional Evaluation of the T-gel

As shown in **Figure 8A**, mTDSCs were well attached on the surface of the C-gel or T-gel-coated plates after 1 day of culture. From 1 to 7 days, Live/Dead staining displayed negligible cell death on the C-gel and T-gel. Furthermore, both groups showed evident increase in cell number with time in culture. The CCK-8 assay indicated that significant lower cell viability of mTDSCs cultured on the surface of the T-gel at all time points, as compared with that of the C-gel ($P < 0.05$, **Figure 8B**). However, it's worth noting that the number of mTDSCs from 1 to 7 days significantly increased with time ($P < 0.05$, **Figure 8B**). Overall, these results validated that the T-gel was able to support the survival and proliferation of mTDSCs.

DAPI staining of the migrated mTDSCs showed relatively more nuclei in the T-gel group than in the C-gel group at 24 or 48 h (**Figure 9A**). The semi-quantitative results of our Transwell migration assay revealed that the number of migrated mTDSCs in the T-gel group was significantly higher than that in the C-gel group at both time points (**Figure 9B**). In short, these results demonstrated the T-gel promoted the migration of mTDSCs.

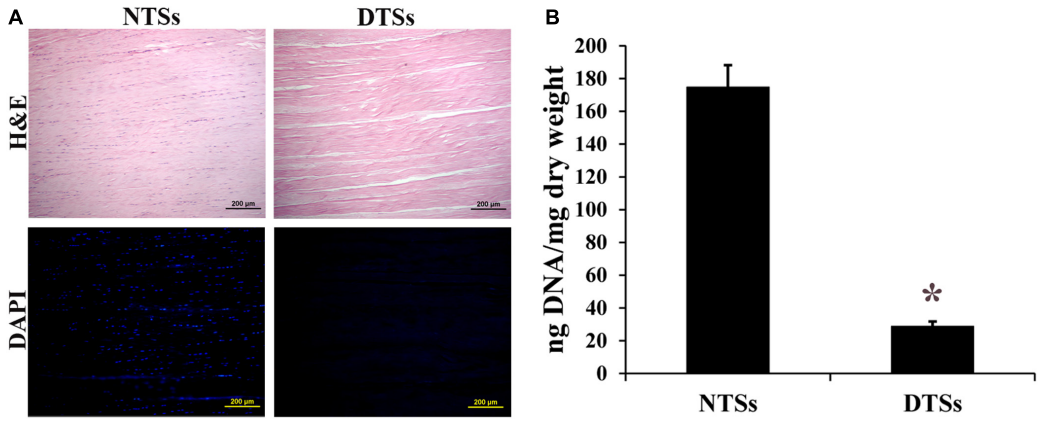

FIGURE 2 | Assessment of decellularization effectiveness. **(A)** H&E staining and DAPI staining of the NTSs and DTSs. Scale bar = 200 μm. **(B)** PicoGreen analysis of residual DNA content in the NTSs and DTSs. *Signifies a *P*-value of <0.05 as compared to the NTSs.

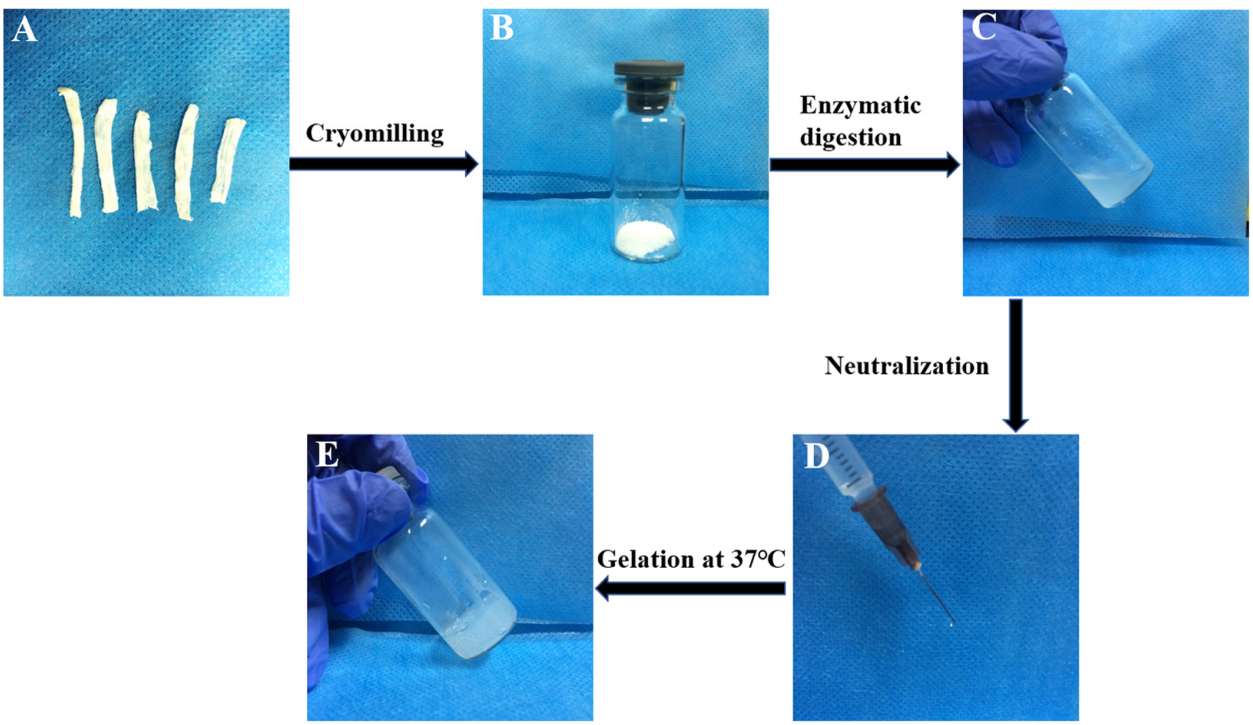

FIGURE 3 | A typical process for the production of the T-gel from decellularized tendon ECM. The DTSs **(A)** were cryomilled to form powder **(B)**, subjected to enzymatic digestion **(C)**, and then neutralized **(D)** after dissolution, and incubated at 37°C to form the T-gel **(E)**.

Gene expression of mTDSCs cultured on the C-gel or T-gel-coated plates was quantified at the mRNA level by RT-qPCR. The expression of SCX was significantly up-regulated in mTDSCs cultured on the T-gel-coated group compared to those on the C-gel-coated group at 7 days but not at 3 or 14 days (**Figure 10A**). The expression of TNMD was significantly enhanced in mTDSCs cultured on the T-gel-coated group at 7 or 14 days when compared to those on the C-gel-coated group, and no significant difference was found at 3 days (**Figure 10B**). Though there was no significant difference between two groups at 3 or 7 days, the expression of TNC, COLI and COL III was elevated significantly at 14 days in mTDSCs cultured on the T-gel-coated group (**Figures 10C–E**). As a whole, these data indicated that the T-gel was capable of promoting tenogenic differentiation of mTDSCs.

DISCUSSION

The current study focused on demonstrating that the T-gel support the proliferation of mTDSCs and significantly promote

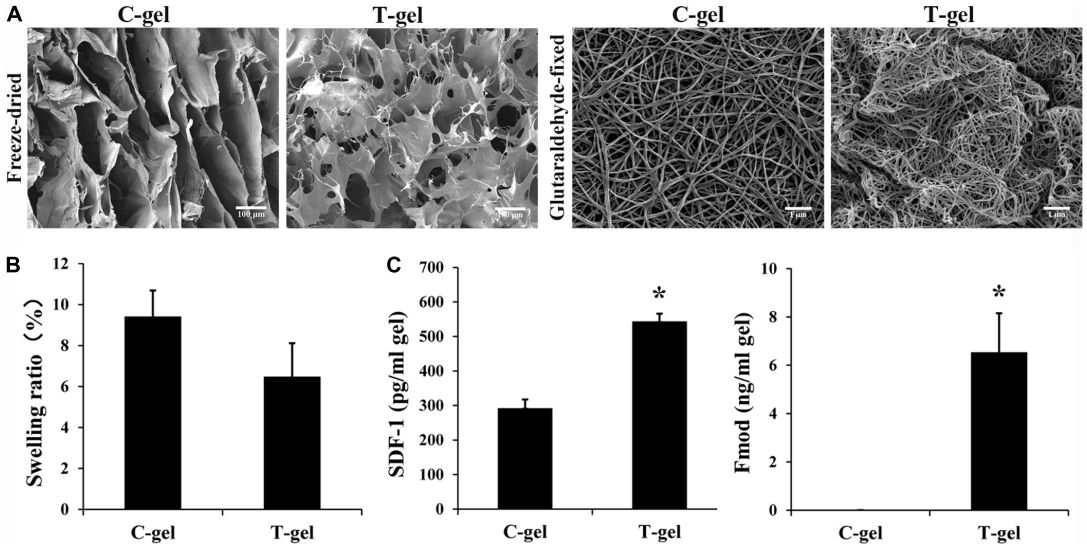

FIGURE 4 | Analysis of microstructure, retained bioactive factors and equilibrium swelling properties of the C-gel and T-gel. **(A)** Representative SEM micrographs of the C-gel and T-gel. Scale bar = 100 μm for freeze-dried samples and Scale bar = 1 μm for glutaraldehyde-fixed samples. **(B)** Swelling ratios of the C-gel and T-gel. **(C)** The content of SDF-1 and Fmod in the C-gel and T-gel as measured by ELISA. *Signifies a *P*-value of <0.05 as compared to the C-gel.

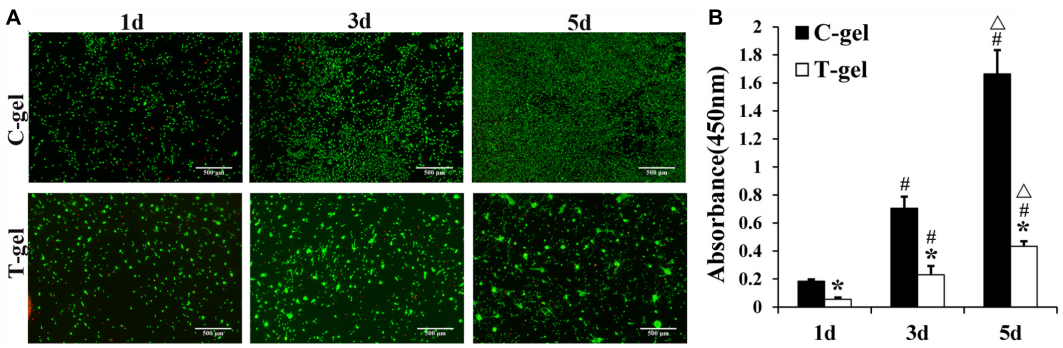

FIGURE 5 | Cytotoxicity analysis of the C-gel and T-gel. **(A)** Live/Dead staining of NIH 3T3 fibroblasts seeded on the C-gel and T-gel at 1, 3, and 5 days by fluorescence microscopy (green, live cells; red, dead cells). Scale bar = 500 μm. **(B)** The cytotoxicity of the C-gel and T-gel using NIH-3T3 fibroblasts cultured for 1, 3, and 5 days as determined by the CCK-8 assay. *Signifies a *P*-value of<0.05 as compared to the C-gel; #, signifies a *P*-value of <0.05 as compared to 1 day for each gel; △, signifies a *P*-value of <0.05 as compared to 3 days for each gel.

the migration and tenogenic differentiation of mTDSCs compared to the C-gel. The isolated mTDSCs were first identified to have universal MSC characteristics. The DTSs from Macaca mulatta were verified to be thoroughly decellularized and the resultant T-gel exhibited highly porous structure or similar nanofibrous structure and approximately swelling ratio compared to the C-gel. More importantly, the T-gel was confirmed to retain some native tendon ECM bioactive factors, such as SDF-1 and Fmod. Furthermore, the T-gel was found to be cytocompatible with NIH-3T3 fibroblasts and displayed good histocompatibility when implanted into rat subcutaneous tissue. Collectively, these findings illustrate the effect of T-gel with nanofibrous structure and some bioactive factors of native tendon ECM microenvironment on the proliferation, migration and tenogenic differentiation of mTDSCs, as well as suggest the potential of the T-gel for treatment of tendinopathy or tendon repair and regeneration.

TDSCs, also described as tendon stem/progenitor cells (TSPCs), were isolated and identified for the first time in 2007 (Bi et al., 2007). After that, TDSCs, as a new member in MSC families, the roles of which in tendon metabolism, repair and regeneration have been studied extensively. Since 2007, TDSCs from human (Bi et al., 2007), mouse (Bi et al., 2007), rabbit (Zhang and Wang, 2010), rat (Rui et al., 2010), horse (Lovati et al., 2011), fetal bovine (Yang et al., 2016), and pig (Yang et al., 2018) were isolated and identified successively. In this study, we first isolated, identified, and used mTDSCs to explore the effect of T-gel on the proliferation, migration and tenogenic differentiation of stem cells. Our data demonstrated that the isolated tendon-derived cells from Macaca mulatta possessed universal MSC

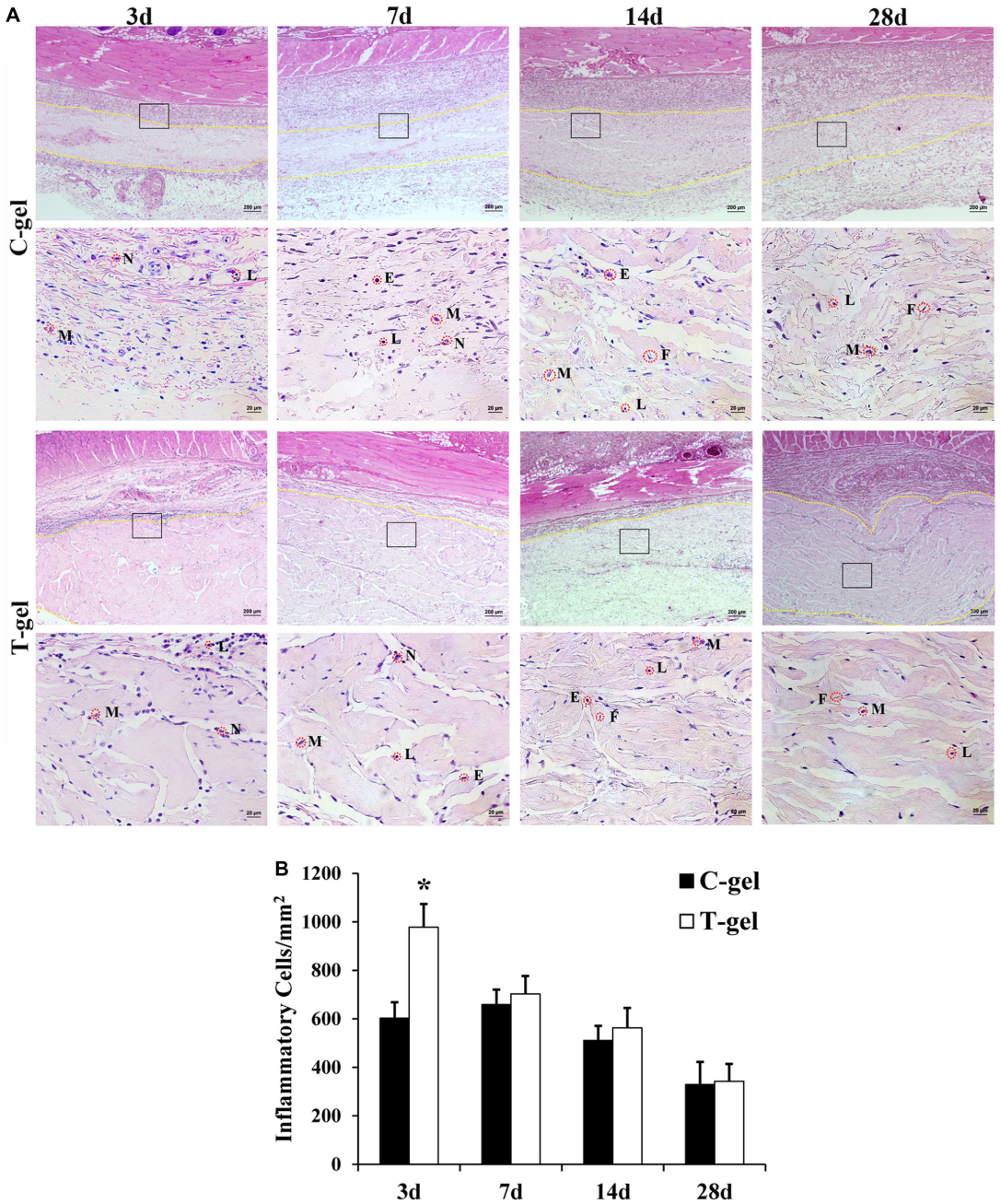

FIGURE 6 | Histocompatibility evaluation of the C-gel and T-gel. **(A)** Histological appearance of tissue response to the C-gel and T-gel at 3, 7, 14, and 28 days post subcutaneous implantation in a rat model as revealed by H&E staining. Images in the bottom panels (Scale bar = 20 μm) are higher resolution images of the areas boxed in the images of top panels (Scale bar = 200 μm). M, macrophage; N, neutrophil; L, lymphocyte; E, eosinophil; F, fibroblast. **(B)** Semiquantitative evaluation of tissue response to the C-gel and T-gel at each time point. Total inflammatory cells were counted with H&E staining in five randomly selected 400× field-of-view and reported as average number per mm^2. *Signifies a *P*-value of <0.05 as compared to the C-gel.

characteristics, including clonogenicity, the expression of stem cell markers and multidifferentiation potential. As far as we know, this is the first work that isolated and characterized Macaca mulatta TDSCs *in vitro*. The isolation and identification of mTDSCs are highly necessary as Macaca mulatta is highly similar to humans in terms of genetics and physiology and is the most widely used non-human primate in basic and applied biomedical research (Gibbs et al., 2007). Therefore, mTDSCs provide an attractive tool to study the physiological mechanism of tendinopathy and the basic tendon biology.

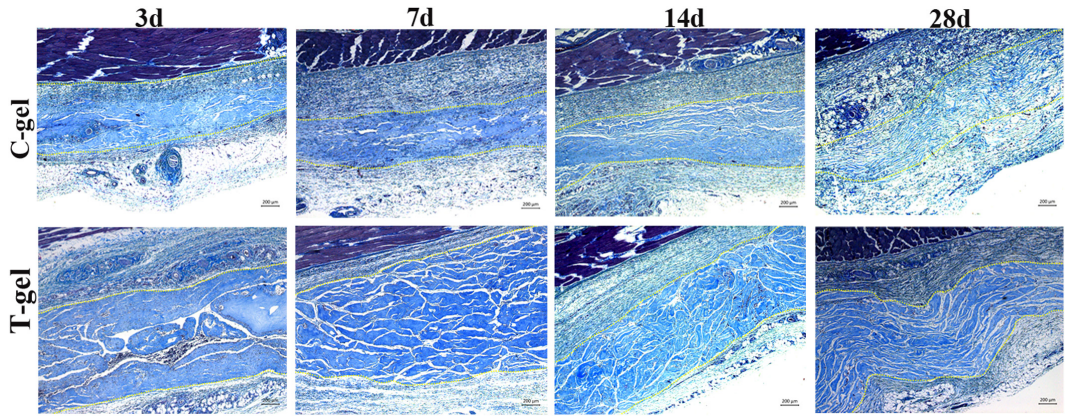

FIGURE 7 | Masson's Trichrome staining of the C-gel and T-gel at 3, 7, 14, and 28 days post subcutaneous implantation. Scale bar = 200 μm.

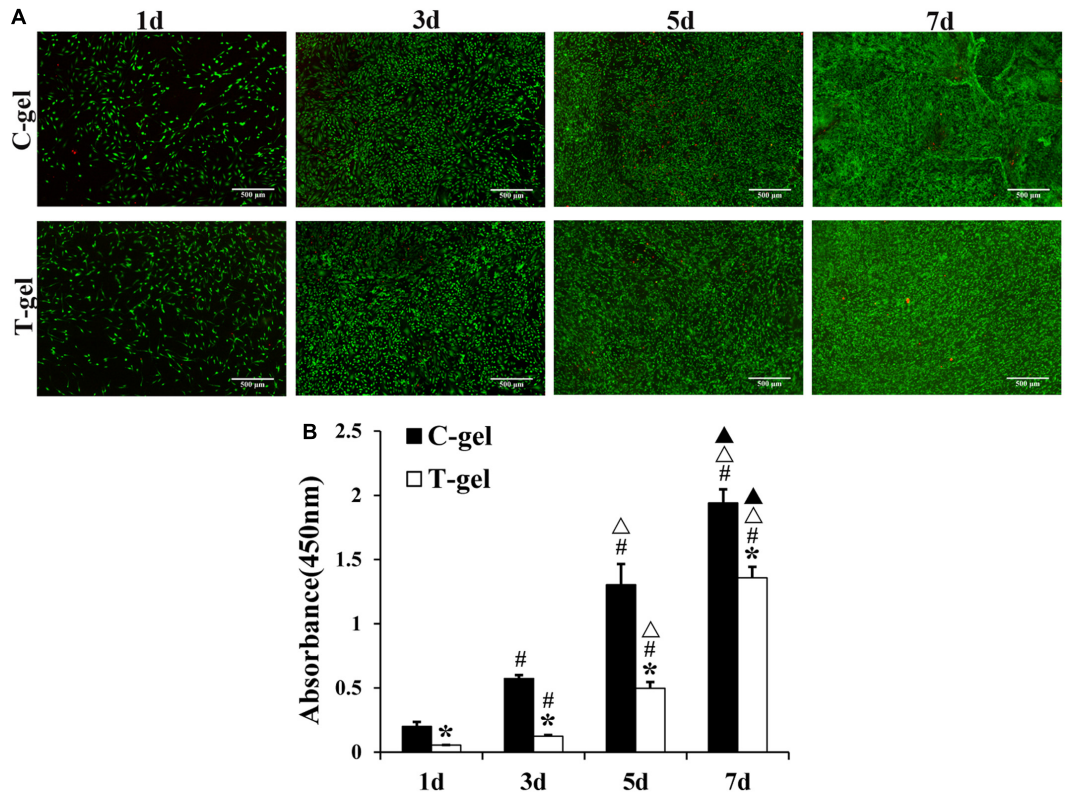

FIGURE 8 | Cell proliferation assays of the C-gel and T-gel. **(A)** Live/Dead staining of mTDSCs seeded on the C-gel and T-gel at 1, 3, 5, and 7 days by fluorescence microscopy (green, live cells; red, dead cells). Scale bar = 500 μm. **(B)** Cell proliferation of mTDSCs cultured on the C-gel and T-gel for 1, 3, 5, and 7 days as determined by the CCK-8 assay. *, signifies a *P*-value of <0.05 as compared to the C-gel; #, signifies a *P*-value of <0.05 as compared to 1 day for each gel; △, signifies a *P*-value of <0.05 as compared to 3 days for each gel; ▲, signifies a *P*-value of <0.05 as compared to 5 days for each gel.

In the present study, the DTSs from Macaca mulatta Achilles tendons were fabricated using our previously established protocol (Ning et al., 2012), i.e., repetitive freeze/thaw, frozen section in combination with nuclease treatment 12 h, which was proved to be a mild and effective decellularization method and preserve almost all of the native tendon ECM microenvironment cues, after decellularization (Ning et al., 2015). The results of the current study showed that such decellularization method was effective for removal of the cellular and nuclear materials as evidenced by H&E staining and DAPI staining. DNA quantification assay also indicated such decellularization treatment significantly reduced the remaining

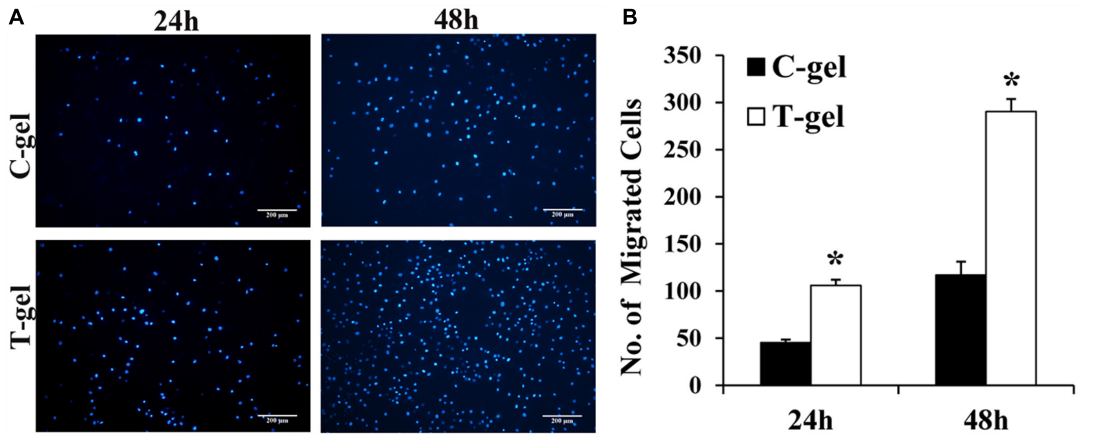

FIGURE 9 | Cell migration assays of the C-gel and T-gel. **(A)** Representative fluorescence staining of the migrated mTDSCs for each group. Scale bar = 200 μm. **(B)** The semi-quantitative results of the number of the migrated mTDSCs for each group. *Signifies a *P*-value of <0.05 as compared to the C-gel.

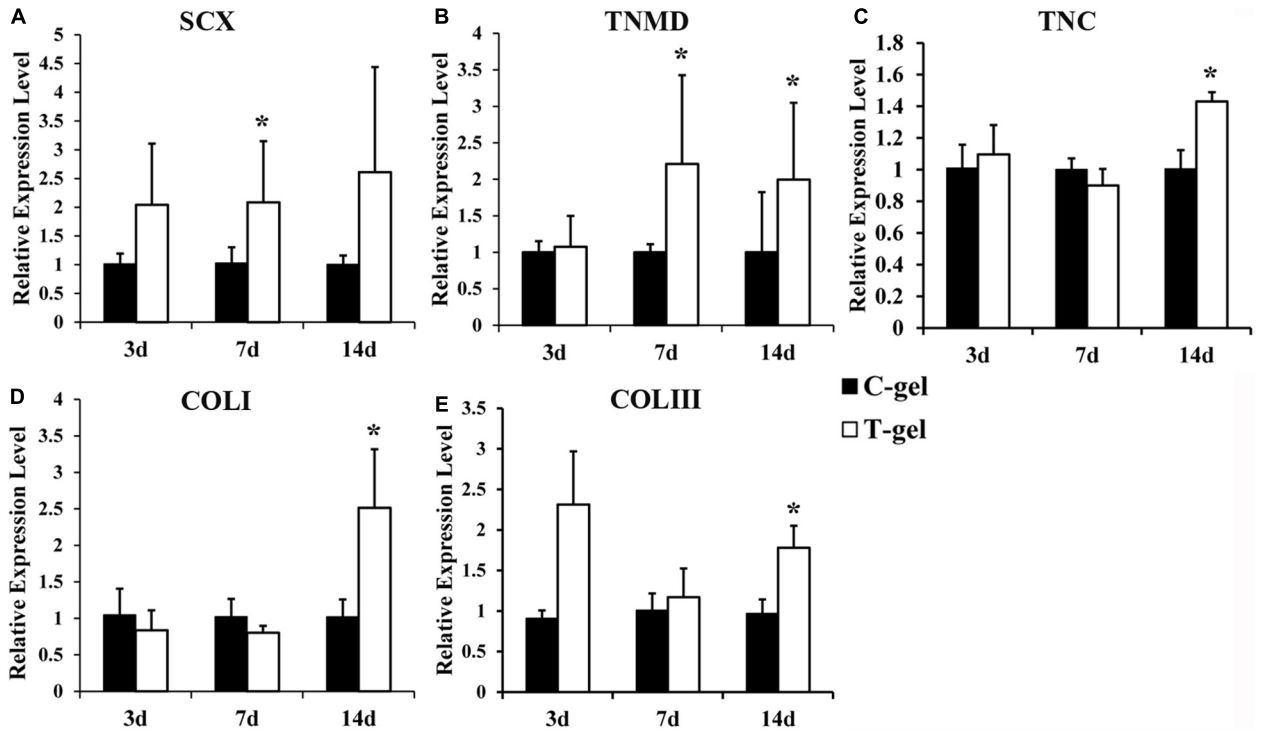

FIGURE 10 | Cell differentiation assays of the C-gel and T-gel. **(A–E)** RT-qPCR analysis of tendon-related gene expressions of the mTDSCs seeded on the C-gel and T-gel at different time points. Gene expression levels are normalized to the housekeeping gene, GAPDH. *Signifies a *P*-value of <0.05 as compared to the C-gel.

DNA content. Previous studies showed repeated and intensive chemical decellularization of the porcine nerve significantly reduced DNA content but resulted in significant loss of ECM components, which led to the difficulty of hydrogel formation at 37°C (Lin et al., 2018). Lin et al. (2018) believed it was necessary to maintain the DNA content of porcine decellularized nerve matrix hydrogel between 40 and 50 ng/mg to ensure low immunogenicity and ease of gelatinization. However, our study showed it was easy to gelatinize when the DNA content of DTSs for preparation of the T-gel was only 28.62 ± 3.11 ng/mg. This discrepancy may be attributed to different tissue sources, different decellularization methods and different preparation process of ECM hydrogels.

ECM hydrogel formation is a collagen-based self-assembly process that is partly regulated by the presence of GAGs, proteoglycans, and other ECM proteins (Brightman et al., 2000; Saldin et al., 2017). In the present study, purified collagen type I from rat-tail was selected as the control due to the following

reasons: (1) collagen type I is the most abundant and best studied collagen, and is also the main ECM component of tendons (Gelse, 2003); (2) collagen type I hydrogel possesses excellent biocompatibility, often used as three-dimensional substrates for cell culture *in vitro* and causes a very limited inflammatory reaction *in vivo* (Nöth et al., 2007; Antoine et al., 2014). After decellularization and solubilization treatments, the resultant T-gel samples that have been directly freeze-dried exhibited an interconnected and highly porous structure, which is closely similar to the C-gel, but not identical. More specifically, the C-gel showed interlaced lamellas while the T-gel showed alveolates. However, when the gel samples were fixed with glutaraldehyde and dehydrated by gradient alcohol, both the C-gel and T-gel exhibited similar nanoscale collagen features, with assembled nanofibers that were 87.77 ± 9.12 nm and 74.30 ± 5.33 nm in diameter, respectively. Our results are consistent with Brightman et al. (2000) who concluded that the fibrils of purified collagen type I exhibited a larger diameter compared to those of interstitial ECM. Liang et al. (2015) also reported that the average fiber diameter of collagen hydrogels was slightly higher than that of porcine small intestine submucosa ECM hydrogels (114 ± 4 nm vs. 105 ± 10 nm). Kreger et al. (2010) found the fiber structure data of collagen type I hydrogels at concentration above 3 mg/ml was notably absent. Antoine et al. (2014) stated that no research has been reported that present fiber structure analysis of collagen hydrogels when the collagen concentration exceeded 4 mg/ml, except for one article (Cross et al., 2010), which presented fiber structure images inconsistent with other publications. In this study, the concentration of C-gel was determined to be 2 mg/ml, which is also the maximum concentration recommended by the manufacturer. In fact, the nanofibrous structure has been demonstrated to promote stem cell differentiation (Zeng et al., 2014). In the present study, we speculated the significantly enhanced tenogenic differentiation of mTDSCs in the T-gel group is most likely caused by the bioactive factors retained in the T-gel, but we didn't exclude the possible contribution of nanofibrous structure feature for the tenogenic differentiation of mTDSCs.

The T-gel developed in the present study retained some bioactive factors of native tendon ECM microenvironment, such as SDF-1 and Fmod. Unfortunately, no detectable IGF-1 was found in the C-gel and T-gel. However, our previous study demonstrated that more than 93% IGF-1 in native tendon was preserved in the canine DTSs using the same decellularization protocol (Ning et al., 2012). Hence, the loss of IGF-1 may be caused by the process of preparing the T-gel. As we all known, the loss of bioactive factors is almost inevitable in the process of preparing ECM hydrogels. Lin et al. (2018) found the loss of bioactive factors during the process of preparing the porcine decellularized nerve matrix hydrogel may lead to the suboptimal repair effect in rat sciatic nerve defect model. Encouragingly, our results from ELISA data indicated that the values of SDF-1 and Fmod in the T-gel were significantly higher than those found in the C-gel, which may account for higher ability of the T-gel to promote the migration and tenogenic differentiation of mTDSCs compared to that of C-gel. In the current study, we selected IGF-1, SDF-1 and Fmod for analysis because they may play important roles in promoting the proliferation, migration and tenogenic differentiation of stem cells. IGF-1, as one of insulin-like growth factors, has been demonstrated to regulate survival, proliferation, and differentiation of many types of cells, including stem cells (Bendall et al., 2007; Huat et al., 2014). SDF-1, as one of the most representative homing factors, has been extensively proved to stimulate stem cell homing (Shimode et al., 2009; Theiss et al., 2011; Chen et al., 2015) and migration (Jung et al., 2013; Park et al., 2017). Fmod, as one of critical components of TDSCs niches (Bi et al., 2007), was found to promote rat Achilles tendon repair *in vivo* and *in vitro* by gene delivery (Delalande et al., 2015). Our study also proved that soluble Fmod at an appropriate concentration can induce the tenogenic differentiation of TDSCs *in vitro* while inhibiting the chondrogenic and osteogenic differentiation of TDSCs (unpublished data). It should be pointed out that three representative bioactive factors were selected to detect in this study. There should be some other bioactive factors in the T-gel, which also may influence the migration and tenogenic differentiation of mTDSCs.

To apply the T-gel as a carrier of cells or growth factors or directly used for tendon repair and regeneration, the cytotoxicity and histocompatibility of T-gel were evaluated. As expected, the C-gel as a commercial product specifically used for 2D and 3D cell cultures showed excellent cytocompatibility. The results of Live/Dead staining revealed that the majority of NIH-3T3 fibroblasts were viable in a time-frame of 5 days when cultured on the surface of both gels. Yet, fibroblasts cultured on the surface of the C-gel showed more obvious increases in cell number than those on surface of the T-gel. The CCK-8 test also displayed a similar trend. It must be admitted that the cytocompatibility of the T-gel was indeed inferior to that of the C-gel, suggesting that the method of preparing the T-gel need to be further optimized. After all, the DTSs were demonstrated to facilitate the proliferation of NIH-3T3 fibroblasts in our previous study (Ning et al., 2012). Nonetheless, compared with the C-gel, the T-gel was deemed to be cytocompatible with NIH-3T3 fibroblasts because the number of viable cells within the T-gel from 1 to 5 days was significantly increased with time. Interestingly, NIH-3T3 fibroblasts were observed to infiltrate into the T-gel and tended to grow as cell clusters. Labuschagne et al. (2019) found that cell clustering-induced metabolic switch promotes metastatic capacity. Hence, we speculated NIH-3T3 fibroblasts infiltrated into the T-gel with the formation of cell clusters, which led to decreased cellular proliferation and increased antioxidant defense. Hopefully, when implanted into rat subcutaneous tissue, the T-gel, as good as the C-gel, displayed good histocompatibility. Both gels invoked just a moderate degree of inflammation at early time points. Along with the degradation of both gels, the inflammation reaction gradually subsided over time. In addition, the two types of gels, especially the C-gel, significantly degraded over time. This is consistent with the findings from previous study which reported the collagen carrier is absorbed within 1 month after injection (Lemperle et al., 2010). Collectively, these results demonstrated that the T-gel was biocompatible.

The mechanisms of the ECM hydrogels mediating cell behavior are not fully understood. Saldin et al. (2017) came up with the native ECM microenvironment signals that are

preserved during production of a tissue-specific ECM hydrogel may markedly affect cell viability, proliferation, migration, morphology, differentiation and phenotype. Unlike hydrogels formed by single ECM component, ECM hydrogels preserve most of the biochemical complexity of native ECM, which may regulate stem cells fate in a tissue-specific manner. To our knowledge, no studies have clarified the effect of decellularized tendon hydrogel upon stem cell behavior, involving the proliferation, migration and tenogenic differentiation. In the current study, although not as good as the C-gel, the T-gel was found to support the proliferation of mTDSCs, as evidenced by the high cell viability and very obvious proliferation of mTDSCs on the surface of the T-gel in a time-frame of 7 days. What needs to be pointed out is that we used the same detection methods including the Live/Dead staining and CCK-8 assay to evaluate the cytotoxicity of T-gel and the effect of T-gel on stem cell proliferation, respectively. An interesting finding is that mTDSCs seeded on the surface of the T-gel showed higher vitality and faster proliferation than NIH-3T3 fibroblasts. Further research is needed to determine the underlying causes. Another encouragingly, consistent with the results from ELISA data, the results of our Transwell analysis and RT-qPCR analysis revealed that the T-gel significantly promote the migration and tenogenic differentiation of mTDSCs compared to the C-gel, respectively. More specifically, in comparison with the C-gel, the T-gel with significant higher value of SDF-1 markedly promote the migration of mTDSCs at both time points, which is in accordance with the findings of Chen et al. (2015) who found the addition of SDF-1 to the radially oriented collagen scaffold further accelerated the migration of bone marrow-derived MSCs. As expected, the T-gel as a tendon-specific ECM hydrogel, which retained nanofibrous structure and some bioactive factors (SDF-1, Fmod et al) of native tendon ECM microenvironment, significantly promoted tenogenic differentiation of mTDSCs based on the tendon-related gene expressions. SCX, as a well-known tendon marker, was significantly up-regulated in the T-gel group compared to that in the C-gel group at 7 days. Although a previous study suggested that the expression of SCX was not specific for adult tendon (Jelinsky et al., 2010), SCX was still often selected as one of tendon-related markers in many studies (Yang et al., 2013; Czaplewski et al., 2014; Yin et al., 2016). It has been reported that SCX positively regulates the expression of TNMD (Shukunami et al., 2006). Consistently, the significantly up-regulated expression of TNMD in the T-gel group was found at 7 and 14 days. TNC, as an ECM glycoprotein, is known to be existing in native tendon and involved in the regulation of collagen fibrillogenesis (Burk et al., 2014). Though TNC was found to be expressed in diverse cell types and its upregulation is also explicitly related to non-musculoskeletal diseases (Brellier et al., 2009), it was also frequently used as an additional tenogenic differentiation marker (Kuo and Tuan, 2008; Yang et al., 2013). In this study, we found that the T-gel significantly up-regulated the expression of TNC at 14 days compared to the C-gel. Additionally, the expressions of other two tendon-related markers COL I and COL III were also significantly higher in the T-gel group at 14 days. In summary, the T-gel was verified to promote the tenogenic differentiation of mTDSCs.

There are several limitations in this study. First, the method of preparing the T-gel needs to be further optimized to obtain excellent cytocompatibility as good as the commercialized C-gel and ensure a long shelf life for potential clinical use. Second, although there may be many different types of bioactive factors preserved in the T-gel, only three representative factors including IGF-1, SDF-1 and Fmod were investigated. In future study, we should pay attention to more kinds of bioactive factors. Third, an *in vivo* study is needed to verify the effectiveness of the T-gel for promoting tendon healing.

In conclusion, our study demonstrates that TDSCs derived from Macaca mulatta have universal MSC characteristics and the T-gel derived from Macaca mulatta decellularized tendon is capable of supporting the proliferation of mTDSCs as well as promoting the migration and tenogenic differentiation of mTDSCs. Our findings indicated that the T-gel, with its retained nanofibrous structure and some bioactive factors of native tendon ECM microenvironment, represents a promising hydrogel for tendon regeneration.

DATA AVAILABILITY STATEMENT

The original contributions presented in the study are included in the article/supplementary material, further inquiries can be directed to the corresponding author/s.

ETHICS STATEMENT

The animal study was reviewed and approved by the Institutional Animal Care and Use Committee (IACUC) in Sichuan University.

AUTHOR CONTRIBUTIONS

L-JN and Ya-JZ conceived the study and performed the majority part of the experiments and data interpretation, drafted and edited the manuscript. Yan-JZ and MZ provided help for the experiments. WD provided resources and J-CL provided help for the investigation. T-WQ conceived and designed the study, and critically reviewed the manuscript. All authors have read and approved the final submitted manuscript.

FUNDING

This work was supported by the Grants from National Natural Science Foundation of China (32071348, 31870968, and 31600783) and Science and Technology Plan of Sichuan Province (2018SZ0044).

REFERENCES

Agrawal, V., Kelly, J., Tottey, S., Daly, K. A., Johnson, S. A., Siu, B. F., et al. (2011a). An isolated cryptic peptide influences osteogenesis and bone remodeling in an adult mammalian model of digit amputation. *Tissue Eng. Part A* 17, 3033–3044. doi: 10.1089/ten.tea.2011.0257

Agrawal, V., Tottey, S., Johnson, S. A., Freund, J. M., Siu, B. F., and Badylak, S. F. (2011b). Recruitment of progenitor cells by an extracellular matrix cryptic peptide in a mouse model of digit amputation. *Tissue Eng. Part A* 17, 2435–2443. doi: 10.1089/ten.TEA.2011.0036

Andres, B. M., and Murrell, G. A. C. (2008). Treatment of tendinopathy: what works, what does not, and what is on the horizon. *Clin. Orthop. Relat. Res.* 466, 1539–1554. doi: 10.1007/s11999-008-0260-1

Antoine, E. E., Vlachos, P. P., and Rylander, M. N. (2014). Review of collagen i hydrogels for bioengineered tissue microenvironments: characterization of mechanics, structure, and transport. *Tissue Eng. Part B Rev.* 20, 683–696. doi: 10.1089/ten.teb.2014.0086

Arya, S., and Kulig, K. (2010). Tendinopathy alters mechanical and material properties of the Achilles tendon. *J. Appl. Physiol. (1985)* 108, 670–675. doi: 10.1152/japplphysiol.00259.2009

Bai, R., Tian, L., Li, Y., Zhang, J., Wei, Y., and Jin, Z. (2019). Combining ECM hydrogels of cardiac bioactivity with stem cells of high cardiomyogenic potential for myocardial repair. *Stem Cells Int.* 2019, 6708435. doi: 10.1155/2019/6708435

Bendall, S. C., Stewart, M. H., Menendez, P., George, D., Vijayaragavan, K., Werbowetski-Ogilvie, T., et al. (2007). IGF and FGF cooperatively establish the regulatory stem cell niche of pluripotent human cells in vitro. *Nature* 448, 1015–1021. doi: 10.1038/nature06027

Bi, Y., Ehirchiou, D., Kilts, T. M., Inkson, C. A., Embree, M. C., Sonoyama, W., et al. (2007). Identification of tendon stem/progenitor cells and the role of the extracellular matrix in their niche. *Nat. Med.* 13, 1219–1227. doi: 10.1038/nm1630

Brellier, F., Tucker, R. P., and Chiquet-Ehrismann, R. (2009). Tenascins and their implications in diseases and tissue mechanics. *Scand. J. Med. Sci. Sports* 19, 511–519. doi: 10.1111/j.1600-0838.2009.00916.x

Brightman, A. O., Rajwa, B. P., Sturgis, J. E., McCallister, M. E., Robinson, J. P., and Voytik-Harbin, S. L. (2000). Time-lapse confocal reflection microscopy of collagen fibrillogenesis and extracellular matrix assembly in vitro. *Biopolymers* 54, 222–234. doi: 10.1002/1097-0282(200009)54:3<222::AID-BIP80<3.0.CO;2-K

Burk, J., Gittel, C., Heller, S., Pfeiffer, B., Paebst, F., Ahrberg, A. B., et al. (2014). Gene expression of tendon markers in mesenchymal stromal cells derived from different sources. *BMC Res. Notes* 7:826. doi: 10.1186/1756-0500-7-826

Carr, A. J., Murphy, R., Dakin, S. G., Rombach, I., Wheway, K., Watkins, B., et al. (2015). Platelet-rich plasma injection with arthroscopic acromioplasty for chronic rotator cuff tendinopathy: a randomized controlled trial. *Am. J. Sports Med.* 43, 2891–2897. doi: 10.1177/0363546515608485

Chen, P., Tao, J., Zhu, S., Cai, Y., Mao, Q., Yu, D., et al. (2015). Radially oriented collagen scaffold with SDF-1 promotes osteochondral repair by facilitating cell homing. *Biomaterials* 39, 114–123. doi: 10.1016/j.biomaterials.2014.10.049

Chong, A. K., Ang, A. D., Goh, J. C., Hui, J. H., Lim, A. Y., Lee, E. H., et al. (2007). Bone marrow-derived mesenchymal stem cells influence early tendon-healing in a rabbit Achilles tendon model. *J. Bone Joint Surg. Am.* 89, 74–81. doi: 10.2106/JBJS.E.01396

Cross, V. L., Zheng, Y., Won, C. N., Verbridge, S. S., Sutermaster, B. A., Bonassar, L. J., et al. (2010). Dense type I collagen matrices that support cellular remodeling and microfabrication for studies of tumor angiogenesis and vasculogenesis in vitro. *Biomaterials* 31, 8596–8607. doi: 10.1016/j.biomaterials.2010.07.072

Crowe, C. S., Chiou, G., McGoldrick, R., Hui, K., Pham, H., Hollenbeck, E., et al. (2016). In vitro characteristics of porcine tendon hydrogel for tendon regeneration. *Ann. Plast. Surg.* 77, 47–53. doi: 10.1097/SAP.0000000000000361

Czaplewski, S. K., Tsai, T. L., Duenwald-Kuehl, S. E., Vanderby, R. J., and Li, W. J. (2014). Tenogenic differentiation of human induced pluripotent stem cell-derived mesenchymal stem cells dictated by properties of braided submicron fibrous scaffolds. *Biomaterials* 35, 6907–6917. doi: 10.1016/j.biomaterials.2014.05.006

de Vos, R. J., van Veldhoven, P. L., Moen, M. H., Weir, A., Tol, J. L., and Maffulli, N. (2010). Autologous growth factor injections in chronic tendinopathy: a systematic review. *Br. Med. Bull.* 95, 63–77. doi: 10.1093/bmb/ldq006

Delalande, A., Gosselin, M. P., Suwalski, A., Guilmain, W., Leduc, C., Berchel, M., et al. (2015). Enhanced Achilles tendon healing by fibromodulin gene transfer. *Nanomedicine* 11, 1735–1744. doi: 10.1016/j.nano.2015.05.004

Farnebo, S., Woon, C. Y., Schmitt, T., Joubert, L. M., Kim, M., Pham, H., et al. (2014). Design and characterization of an injectable tendon hydrogel: a novel scaffold for guided tissue regeneration in the musculoskeletal system. *Tissue Eng. Part A* 20, 1550–1561. doi: 10.1089/ten.TEA.2013.0207

Gelse, K. (2003). Collagens—structure, function, and biosynthesis. *Adv. Drug Deliv. Reviews.* 55, 1531–1546. doi: 10.1016/j.addr.2003.08.002

Gibbs, R. A., Rogers, J., Katze, M. G., Bumgarner, R., Weinstock, G. M., Mardis, E. R., et al. (2007). Evolutionary and biomedical insights from the rhesus macaque genome. *Science* 316, 222–234. doi: 10.1126/science.1139247

Huat, T. J., Khan, A. A., Pati, S., Mustafa, Z., Abdullah, J. M., and Jaafar, H. (2014). IGF-1 enhances cell proliferation and survival during early differentiation of mesenchymal stem cells to neural progenitor-like cells. *BMC Neurosci.* 15:91. doi: 10.1186/1471-2202-15-91

Jelinsky, S. A., Archambault, J., Li, L., and Seeherman, H. (2010). Tendon-selective genes identified from rat and human musculoskeletal tissues. *J. Orthop. Res.* 28, 289–297. doi: 10.1002/jor.20999

Jung, Y., Kim, J. K., Shiozawa, Y., Wang, J., Mishra, A., Joseph, J., et al. (2013). Recruitment of mesenchymal stem cells into prostate tumours promotes metastasis. *Nat. Commun.* 4:1795. doi: 10.1038/ncomms2766

Kaux, J. F., and Crielaard, J. M. (2013). Platelet-rich plasma application in the management of chronic tendinopathies. *Acta Orthop. Belg.* 79, 10–15.

Khan, K. M., Cook, J. L., Bonar, F., Harcourt, P., and Astrom, M. (1999). Histopathology of common tendinopathies. Update and implications for clinical management. *Sports Med.* 27, 393–408. doi: 10.2165/00007256-199927060-00004

Kim, M. Y., Farnebo, S., Woon, C. Y. L., Schmitt, T., Pham, H., and Chang, J. (2014). Augmentation of tendon healing with an injectable tendon hydrogel in a rat Achilles tendon model. *Plast. Reconstr. Surg.* 133, 645e–653e. doi: 10.1097/PRS.0000000000000106

Kreger, S. T., Bell, B. J., Bailey, J., Stites, E., Kuske, J., Waisner, B., et al. (2010). Polymerization and matrix physical properties as important design considerations for soluble collagen formulations. *Biopolymers* 93, 690–707. doi: 10.1002/bip.21431

Kuo, C. K., and Tuan, R. S. (2008). Mechanoactive tenogenic differentiation of human mesenchymal stem cells. *Tissue Eng. Part A* 14, 1615–1627. doi: 10.1089/ten.tea.2006.0415

Labuschagne, C. F., Cheung, E. C., Blagih, J., Domart, M., and Vousden, K. H. (2019). Cell clustering promotes a metabolic switch that supports metastatic colonization. *Cell Metab.* 30, 720–734. doi: 10.1016/j.cmet.2019.07.014

Lemperle, G., Knapp, T. R., Sadick, N. S., and Lemperle, S. M. (2010). ArteFill® permanent injectable for soft tissue augmentation: I. Mechanism of action and injection techniques. *Aesthet. Plast. Surg.* 34, 264–272. doi: 10.1007/s00266-009-9413-1

Liang, R., Yang, G., Kim, K. E., D'Amore, A., Pickering, A. N., and Zhang, C. (2015). Positive effects of an extracellular matrix hydrogel on rat anterior cruciate ligament fibroblast proliferation and collagen mRNA expression. *J. Orthop. Translat.* 3, 114–122. doi: 10.1016/j.jot.2015.05.001

Lin, T., Liu, S., Chen, S., Qiu, S., Rao, Z., Liu, J., et al. (2018). Hydrogel derived from porcine decellularized nerve tissue as a promising biomaterial for repairing peripheral nerve defects. *Acta Biomater.* 73, 326–338. doi: 10.1016/j.actbio.2018.04.001

Liu, C., Jin, Z., Ge, X., Zhang, Y., and Xu, H. (2019). Decellularized annulus fibrosus Matrix/Chitosan hybrid hydrogels with basic fibroblast growth factor for annulus fibrosus tissue engineering. *Tissue Eng. Part A* 25, 1605–1613. doi: 10.1089/ten.TEA.2018.0297

Lovati, A. B., Corradetti, B., Lange, C. A., Recordati, C., Bonacina, E., Bizzaro, D., et al. (2011). Characterization and differentiation of equine tendon-derived progenitor cells. *J. Biol. Regul. Homeost. Agents* 25, S75–S84.

Neviaser, A., Andarawis-Puri, N., and Flatow, E. (2012). Basic mechanisms of tendon fatigue damage. *J. Shoulder Elbow Surg.* 21, 158–163. doi: 10.1016/j.jse.2011.11.014

Ning, L. J., Zhang, Y. J., Zhang, Y., Qing, Q., Jiang, Y. L., Yang, J. L., et al. (2015). The utilization of decellularized tendon slices to provide an inductive microenvironment for the proliferation and tenogenic differentiation of stem cells. *Biomaterials* 52, 539–550. doi: 10.1016/j.biomaterials.2015.02.061

Ning, L. J., Zhang, Y., Chen, X. H., Luo, J. C., Li, X. Q., Yang, Z. M., et al. (2012). Preparation and characterization of decellularized tendon slices for tendon tissue engineering. *J. Biomed. Mater. Res. Part A* 100, 1448–1456. doi: 10.1002/jbm.a.34083

Nöth, U., Rackwitz, L., Heymer, A., Weber, M., Baumann, B., Steinert, A., et al. (2007). Chondrogenic differentiation of human mesenchymal stem cells in collagen type I hydrogels. *J. Biomed. Mater. Res. Part A* 83, 626–635. doi: 10.1002/jbm.a.31254

Park, S., Jang, H., Kim, B. S., Hwang, C., Jeong, G. S., and Park, Y. (2017). Directional migration of mesenchymal stem cells under an SDF-1α gradient on a microfluidic device. *PLoS One* 12:e184595. doi: 10.1371/journal.pone.0184595

Pati, F., Song, T. H., Rijal, G., Jang, J., Kim, S. W., and Cho, D. W. (2015). Ornamenting 3D printed scaffolds with cell-laid extracellular matrix for bone tissue regeneration. *Biomaterials* 37, 230–241. doi: 10.1016/j.biomaterials.2014.10.012

Rui, Y. F., Lui, P. P., Li, G., Fu, S. C., Lee, Y. W., and Chan, K. M. (2010). Isolation and characterization of multipotent rat tendon-derived stem cells. *Tissue Eng. Part A* 16, 1549–1558. doi: 10.1089/ten.TEA.2009.0529

Saldin, L. T., Cramer, M. C., Velankar, S. S., White, L. J., and Badylak, S. F. (2017). Extracellular matrix hydrogels from decellularized tissues: structure and function. *Acta Biomater.* 49, 1–15. doi: 10.1016/j.actbio.2016.11.068

Seif-Naraghi, S. B., Horn, D., Schup-Magoffin, P. J., and Christman, K. L. (2012). Injectable extracellular matrix derived hydrogel provides a platform for enhanced retention and delivery of a heparin-binding growth factor. *Acta Biomater.* 8, 3695–3703. doi: 10.1016/j.actbio.2012.06.030

Shimode, K., Iwasaki, N., Majima, T., Funakoshi, T., Sawaguchi, N., Onodera, T., et al. (2009). Local upregulation of stromal cell-derived factor-1 after ligament injuries enhances homing rate of bone marrow stromal cells in rats. *Tissue Eng. Part A* 15, 2277–2284. doi: 10.1089/ten.tea.2008.0224

Shukunami, C., Takimoto, A., Oro, M., and Hiraki, Y. (2006). Scleraxis positively regulates the expression of tenomodulin, a differentiation marker of tenocytes. *Dev. Biol.* 298, 234–247. doi: 10.1016/j.ydbio.2006.06.036

Soslowsky, L. J., Thomopoulos, S., Tun, S., Flanagan, C. L., Keefer, C. C., Mastaw, J., et al. (2000). Neer Award 1999. Overuse activity injures the supraspinatus tendon in an animal model: a histologic and biomechanical study. *J. Shoulder Elbow Surg.* 9, 79–84. doi: 10.1067/mse.2000.101962

Theiss, H. D., Vallaster, M., Rischpler, C., Krieg, L., Zaruba, M. M., and Brunner, S. (2011). Dual stem cell therapy after myocardial infarction acts specifically by enhanced homing via the SDF-1/CXCR4 axis. *Stem Cell Res.* 7, 244–255. doi: 10.1016/j.scr.2011.05.003

Ungerleider, J. L., Dzieciatkowska, M., Hansen, K. C., and Christman, K. L. (2020). Tissue specific muscle extracellular matrix hydrogel improves skeletal muscle regeneration in vivo over non-matched tissue source. *bioRxiv*. doi: 10.1101/2020.06.30.181164

Viswanath, A., Vanacker, J., Germain, L., Leprince, J. G., Diogenes, A., Shakesheff, K. M., et al. (2017). Extracellular matrix-derived hydrogels for dental stem cell delivery. *J. Biomed. Mater. Res A* 105, 319–328. doi: 10.1002/jbm.a.35901

Wang, W., Zhang, X., Chao, N., Qin, T., Ding, W., Zhang, Y., et al. (2016). Preparation and characterization of pro-angiogenic gel derived from small intestinal submucosa. *Acta Biomater.* 29, 135–148. doi: 10.1016/j.actbio.2015.10.013

Wolf, M. T., Daly, K. A., Brennan-Pierce, E. P., Johnson, S. A., Carruthers, C. A., D'Amore, A., et al. (2012). A hydrogel derived from decellularized dermal extracellular matrix. *Biomaterials* 33, 7028–7038. doi: 10.1016/j.biomaterials.2012.06.051

Wu, J., Ding, Q., Dutta, A., Wang, Y., Huang, Y., Weng, H., et al. (2015). An injectable extracellular matrix derived hydrogel for meniscus repair and regeneration. *Acta Biomater.* 16, 49–59. doi: 10.1016/j.actbio.2015.01.027

Xu, H., Tian, F., Lu, C., Xu, J., Fan, Z., Yang, J.-J., et al. (2016). Thermo-sensitive hydrogels combined with decellularised matrix deliver bFGF for the functional recovery of rats after a spinal cord injury. *Sci. Rep.* 6:38332. doi: 10.1038/srep38332

Yang, G., Rothrauff, B. B., Lin, H., Gottardi, R., Alexander, P. G., and Tuan, R. S. (2013). Enhancement of tenogenic differentiation of human adipose stem cells by tendon-derived extracellular matrix. *Biomaterials* 34, 9295–9306. doi: 10.1016/j.biomaterials.2013.08.054

Yang, J., Zhao, Q., Wang, K., Liu, H., Ma, C., Huang, H., et al. (2016). Isolation and biological characterization of tendon-derived stem cells from fetal bovine. *In Vitro Cell. Dev. Biol. Anim.* 52, 846–856. doi: 10.1007/s11626-016-0043-z

Yang, J., Zhao, Q., Wang, K., Ma, C., Liu, H., Liu, Y., et al. (2018). Isolation, culture and biological characteristics of multipotent porcine tendon-derived stem cells. *Int. J. Mol. Med.* 41, 3611–3619. doi: 10.3892/ijmm.2018.3545

Yin, Z., Guo, J., Wu, T. Y., Chen, X., Xu, L. L., Lin, S. E., et al. (2016). Stepwise differentiation of mesenchymal stem cells augments tendon-like tissue formation and defect repair in vivo. *Stem Cells Transl. Med.* 5, 1106–1116. doi: 10.5966/sctm.2015-0215

Yuan, X., Wei, Y., Villasante, A., Ng, J. J. D., Arkonac, D. E., Chao, P. G., et al. (2017). Stem cell delivery in tissue-specific hydrogel enabled meniscal repair in an orthotopic rat model. *Biomaterials* 132, 59–71. doi: 10.1016/j.biomaterials.2017.04.004

Yuksel, S., Gulec, M. A., Gultekin, M. Z., Adanir, O., Caglar, A., Beytemur, O., et al. (2016). Comparison of the early period effects of bone marrow-derived mesenchymal stem cells and platelet-rich plasma on the Achilles tendon ruptures in rats. *Connect Tissue Res.* 57, 360–373. doi: 10.1080/03008207.2016.1189909

Zeng, C. G., Xiong, Y., Xie, G. Y., Dong, P., and Quan, D. P. (2014). Fabrication and evaluation of PLLA multichannel conduits with nanofibrous microstructure for the differentiation of NSCs in vitro. *Tissue Eng. Part A* 20, 1038–1048. doi: 10.1089/ten.tea.2013.0277

Zhang, J., and Wang, J. H. (2010). Characterization of differential properties of rabbit tendon stem cells and tenocytes. *BMC Musculoskelet Disord.* 11:10. doi: 10.1186/1471-2474-11-10

Conflict of Interest: The authors declare that the research was conducted in the absence of any commercial or financial relationships that could be construed as a potential conflict of interest.

frontiers in Cell and Developmental Biology

ORIGINAL RESEARCH
published: 03 June 2021
doi: 10.3389/fcell.2021.654397

The Scleraxis Transcription Factor Directly Regulates Multiple Distinct Molecular and Cellular Processes During Early Tendon Cell Differentiation

*Han Liu[1], Jingyue Xu[1], Yu Lan[1,2,3,4], Hee-Woong Lim[4,5] and Rulang Jiang[1,2,4]**

[1] Division of Developmental Biology, Cincinnati Children's Hospital Medical Center, Cincinnati, OH, United States, [2] Division of Plastic Surgery, Cincinnati Children's Hospital Medical Center, Cincinnati, OH, United States, [3] Department of Surgery, University of Cincinnati College of Medicine, Cincinnati, OH, United States, [4] Department of Pediatrics, University of Cincinnati College of Medicine, Cincinnati, OH, United States, [5] Division of Biomedical Informatics, Cincinnati Children's Hospital Medical Center, Cincinnati, OH, United States

OPEN ACCESS

Edited by:
Hongwei Ouyang, Zhejiang University, China

Reviewed by:
Lin Junxin, Zhejiang University, China
Alice Huang, Icahn School of Medicine at Mount Sinai, United States

***Correspondence:**
Rulang Jiang
Rulang.Jiang@cchmc.org

Specialty section:
This article was submitted to Stem Cell Research, a section of the journal Frontiers in Cell and Developmental Biology

Received: *16 January 2021*
Accepted: *05 May 2021*
Published: *03 June 2021*

Citation:
Liu H, Xu J, Lan Y, Lim H-W and Jiang R (2021) The Scleraxis Transcription Factor Directly Regulates Multiple Distinct Molecular and Cellular Processes During Early Tendon Cell Differentiation. Front. Cell Dev. Biol. 9:654397. doi: 10.3389/fcell.2021.654397

Proper development of tendons is crucial for the integration and function of the musculoskeletal system. Currently little is known about the molecular mechanisms controlling tendon development and tendon cell differentiation. The transcription factor Scleraxis (Scx) is expressed throughout tendon development and plays essential roles in both embryonic tendon development and adult tendon healing, but few direct target genes of Scx in tendon development have been reported and genome-wide identification of Scx direct target genes *in vivo* has been lacking. In this study, we have generated a Scx^{Flag} knockin mouse strain, which produces fully functional endogenous Scx proteins containing a 2xFLAG epitope tag at the carboxy terminus. We mapped the genome-wide Scx binding sites in the developing limb tendon tissues, identifying 12,097 high quality Scx regulatory *cis*-elements in-around 7,520 genes. Comparative analysis with previously reported embryonic tendon cell RNA-seq data identified 490 candidate Scx direct target genes in early tendon development. Furthermore, we characterized a new *Scx* gene-knockout mouse line and performed whole transcriptome RNA sequencing analysis of E15.5 forelimb tendon cells from $Scx^{-/-}$ embryos and control littermates, identifying 68 genes whose expression in the developing tendon tissues significantly depended on Scx function. Combined analysis of the ChIP-seq and RNA-seq data yielded 32 direct target genes that required Scx for activation and an additional 17 target genes whose expression was suppressed by Scx during early tendon development. We further analyzed and validated Scx-dependent tendon-specific expression patterns of a subset of the target genes, including *Fmod*, *Kera*, *Htra3*, *Ssc5d*, *Tnmd*, and *Zfp185*, by *in situ* hybridization and real-time quantitative polymerase chain reaction assays. These results provide novel insights into the molecular mechanisms mediating Scx function in tendon development and homeostasis. The ChIP-seq and RNA-seq data provide a rich resource for aiding design of further studies of the

mechanisms regulating tendon cell differentiation and tendon tissue regeneration. The Scx^{Flag} mice provide a valuable new tool for unraveling the molecular mechanisms involving Scx in the protein interaction and gene-regulatory networks underlying many developmental and disease processes.

Keywords: bHLH, cell differentiation, ChIP-seq, CRISPR, RNA-seq, Scx, tendon development

INTRODUCTION

Tendons and ligaments are specialized connective tissues densely packed with collagen fibers, composed primarily of type I collagen fascicles with several other collagens, elastin, and various proteoglycans making up the remainder of the extracellular matrix (ECM) surrounding the resident tenocytes (Birch et al., 2013; Davis et al., 2013). Tendons connect skeletal muscles to bones and transmit mechanical forces generated from muscle contraction whereas the ligaments align bones within joints and reinforce their stability and flexibility. Many musculoskeletal diseases involve injuries and tissue degeneration in tendons and ligaments (Yang et al., 2013; Nourissat et al., 2015). Although it is expected that many genes and molecular pathways are shared during the processes of tendon development and tendon healing/regeneration, the molecular mechanisms controlling tendon development, including specification of tendon progenitor cells from mesenchymal stem cells, migration to local domains and differentiation into mature tenocytes, secretion of ECM molecules and organization of fibrils and fibers into tendon bundles, are not well understood. With the development and wide application of gene knockout technologies, thousands of mutant mouse lines carrying loss-of-function mutations in individual genes have been generated and analyzed in the last 30 years. However, only loss of function of the Scleraxis (Scx) transcription factor and TGFβ signaling led to severe disruption of tendon development whereas mice deficient in several other genes individually or in combination, including genes encoding the Mohawk (Mkx) transcription factor, the early growth response (EGR) 1 and 2 transcription factors, various proteoglycans, and tenomodulin, exhibited mild postnatal tendon defects (Docheva et al., 2005; Murchison et al., 2007; Kilts et al., 2009; Pryce et al., 2009; Ito et al., 2010; Liu et al., 2010; Lejard et al., 2011; Dourte et al., 2013; Guerquin et al., 2013; Dunkman et al., 2014; Delgado Caceres et al., 2018; Shukunami et al., 2018). While these data suggest that the tendon developmental processes are well orchestrated with built-in compensatory regulatory mechanisms (Delgado Caceres et al., 2018), better understanding of the molecular mechanisms controlling tendon development and tendon cell differentiation will be instrumental for the development of effective methods for tendon repair and regeneration.

Scleraxis is a basic helix-loop-helix (bHLH) transcription factor that is expressed in early embryonic tendon progenitor cells and stays strongly expressed throughout tendon cell differentiation into mature tenocytes (Cserjesi et al., 1995; Schweitzer et al., 2001). Mice homozygous for *Scx* null mutation exhibit severe hypoplasia or complete absence of force transmitting tendons, while the muscle anchoring tendons and ligaments are less affected (Murchison et al., 2007; Shukunami et al., 2018). Further studies showed that Scx function is not required for tendon progenitor cell initiation but is crucial for tendon cell differentiation (Murchison et al., 2007). Studies in mouse and chick embryos showed that TGFβ and FGF signaling pathways are essential for induction of tendon progenitor cells by activating expression of *Scx* and other tendon genes (Kuo et al., 2008; Pryce et al., 2009; Hasson, 2011; Havis et al., 2016). Moreover, a recent study demonstrated that Scx function is also required for adult tendons in response to mechanical loading (Gumucio et al., 2020). How Scx regulates tendon cell differentiation is still unclear. Currently very few genes, including *Col1a1* and *Tnmd*, have been identified as potential direct target genes of Scx in tenocytes primarily through *in vitro* functional analysis of putative Scx-binding promoter elements (Shukunami et al., 2006, 2018; Lejard et al., 2007), whereas large scale identification of Scx direct transcriptional target genes during tendon cell differentiation *in vivo* is still lacking.

In this study, we first generated a novel Scx^{Flag} knockin mouse line, which expresses the endogenous Scx protein with a 2xFLAG epitope tag at the carboxy terminus, through CRISPR/cas9-mediated genome editing. Using the Scx^{Flag} mice, we mapped the genome-wide Scx binding sites in embryonic tendon progenitors and differentiating tendon cells using chromatin immunoprecipitation followed by high throughput DNA sequencing, which mapped high quality Scx-binding sites in the promoter and/or enhancer regions in 7,520 genes. Furthermore, we characterized a new *Scx* gene-knockout mouse resource that is accessible to the wide biomedical research community and performed whole transcriptome RNA sequencing analysis of early differentiating limb tendons in $Scx^{-/-}$ and wildtype littermates. These ChIP-seq and RNA-seq datasets provide a rich resource for further studies of the molecular mechanisms regulating tendon formation and tendon cell differentiation. Combined analyses of the ChIP-seq and RNA-seq data provide novel insights into the molecular mechanisms mediating Scx regulation of tendon cell differentiation.

MATERIALS AND METHODS

Mice

Scx-GFP transgenic mice (Pryce et al., 2007) were generously provided by Dr. Ronen Schweitzer (Shriners Hospitals for Children, Portland, Oregon). To generate Scx^{Flag} knock-in mice, pretested guide RNAs targeting the genomic sequence containing the endogenous Scx translational STOP codon

were co-injected with a single-stranded oligonucleotide donor template (**Figure 1A**) and humanized *Cas9* mRNAs into zygotes of B6D2F1 (C57BL/6 X DBA2) mice. Genome-modified founder mice were identified by using polymerase chain reaction (PCR) assay and crossed to CD-1 mice to generate $Scx^{Flag/+}$ hemizygous mice. Genotypically verified G1 $Scx^{Flag/+}$ hemizygous mice were intercrossed to generate $Scx^{Flag/Flag}$ homozygous mice. $Scx^{+/-}$ mutant mice were purchased from the Mutant Mouse Research and Resource Center at the University of California Davis (KOMP catalog#13478). All mouse strains were maintained by crossing to CD-1 wildtype mice (Charles River, Stock# 022), or by intercrossing between siblings. All animal procedures were approved by the Institutional Animal Care and Use Committee (IACUC) at Cincinnati Children's Hospital Medical Center (CCHMC). The mice were housed in AAALAC accredited barrier housing conditions at CCHMC.

Histology, *in situ* Hybridization, and Immunofluorescent Staining

Mice were euthanized at predetermined stage and embryos were collected in cold PBS, fixed in 4% PFA overnight, washed in PBS for 3 times and processed to 100% methanol (for whole mount *in situ* hybridization), or paraffin for section (for histology staining and section *in situ* hybridization). Histology staining and *in situ* hybridization procedures were performed as previously described (Liu et al., 2013, 2015). *In situ* probe templates were amplified by PCR from total cDNA sample of E13.5 wildtype forelimbs. Antisense RNA probes were synthesized from templates using T7 RNA polymerase (Promega catalog# P2075). Immunofluorescent staining was performed as previously described (Xu et al., 2014). The primary antibodies used include anti-Sox9 (Santa Cruz, catalog# sc-20095, 1:25 dilution) and anti-FLAG antibody (Sigma, catalog# F1804, 1:50 dilution). The secondary antibodies were Alexa Fluor 568-conjugated goat anti-mouse IgG (H + L) and Alexa Fluor 488-conjugated goat anti-rabbit IgG (H + L) [(Thermo Fisher Scientific, Waltham, MA, United States), catalog# A11004 and A27034, 1:500 dilution].

Skeletal Preparations

Mice were euthanized at postnatal day 0, heated at 65°C in distilled water for 3 min, and de-skinned manually. Whole de-skinned embryos were stained in Alcian Blue solution (15 mg Alcian Blue dissolved in 20 ml glacial acetic acid plus 80 ml 95%

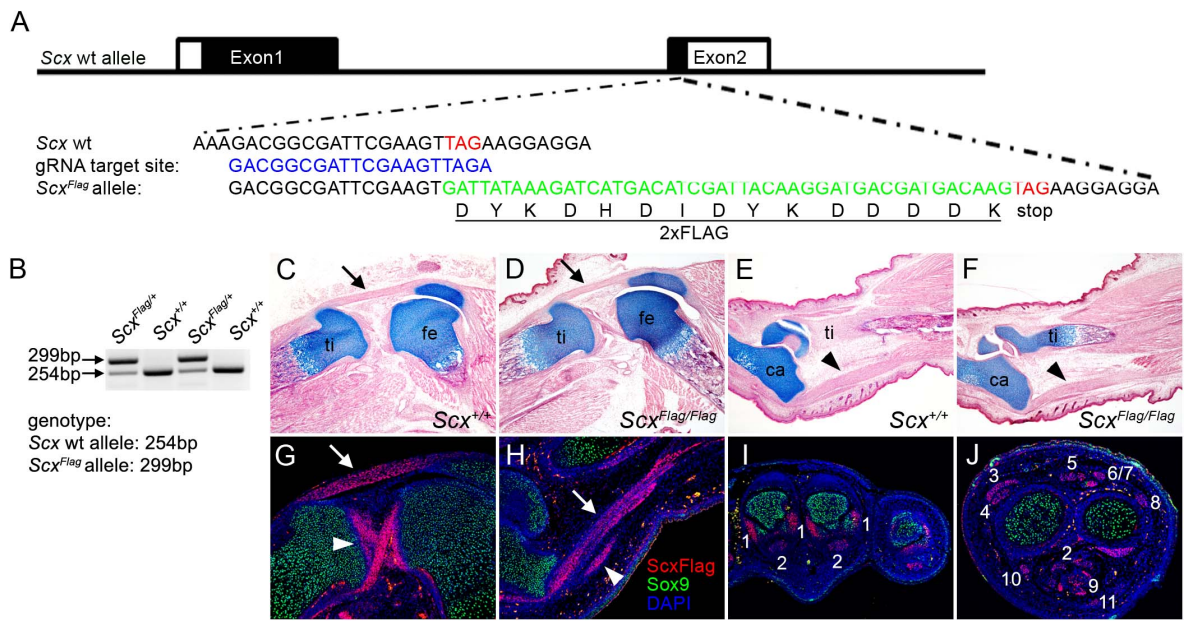

FIGURE 1 | Generation of Scx^{Flag} mice. **(A)** Schematics of the strategy for generating Scx^{Flag} mice using the CRISPR/CAS9 approach. The top row shows the genomic organization of the mouse *Scx* locus. The two exons are boxed with coding regions filled in black and untranslated regions in white. The second row shows the sequence around the translation STOP codon (TAG, labeled in red font). The third row shows the selected guide RNA target site sequence. The fourth row shows part of the correctly edited Scx^{Flag} allele sequence containing the insertion of the 2xFLAG coding sequence (in green font) immediately 5′ to the STOP codon. The fifth row shows the amino acid sequence of the 2xFLAG tag. **(B)** PCR genotyping result from a litter of $Scx^{Flag/+}$ mouse intercross. **(C–F)** Images of HE and alcian blue-stained longitudinal sections through the middle of the knee **(C,D)** and ankle **(E,F)** of E18.5 wildtype **(C,E)** and $Scx^{Flag/Flag}$ **(D,F)** embryos. Arrow in panels **(C,D)** point to patellar tendon. Arrowheads in panels **(E,F)** point to Achilles tendon. ca, calcaneus; fe, femur; ti, tibia. **(G–J)** immunofluorescent staining of sections through the knee **(G)**, ankle **(H)**, forelimb autopod **(I)**, and forelimb zeugopod **(J)** regions of E16.5 $Scx^{Flag/+}$ embryos. Immunofluorescence of Sox9 is shown in green color, Immunofluorescence of the FLAG epitope is shown in red color, and DAPI counterstaining of cellular nuclei is shown in blue color. Arrow in panels **G,H** points to patellar and Achilles tendons, respectively. Arrowhead in panel **(G)** point to the cruciate ligaments, whereas arrowhead in panel **(H)** point to a smaller tendon next to the Achilles. The numbers in panels **(I,J)** mark distinct forelimb tendons as: 1 - Collateral Ligament Metacarpophalangeal joint; 2 - Flexor Digitorium Profundus; 3 - Extensor Pollicis; 4 - Extensor Carpi Radialis Longus; 5 - Extensor Digitorium Communis; 6 - Extensor Digiti Quarti; 7 - Extensor Digiti Quinti; 8 - Extensor Carpi Ulnaris; 9 - Flexor Digitorium Sublimis; 10 - Flexor Carpi Radialis; 11 - Palmaris Longus.

ethanol) for 48–72 h, re-fixed in 100% ethanol for 24 h, and stained in Alizarin Red solution (50 mg Alizarin Red dissolved in 2% KOH) for 24 h. The samples were transferred into 50% glycerol solution for imaging and long term storage.

Body Weight Measurement and Statistical Analysis

Mice were weighed at post-natal day 21. Body weights of 10 $Scx^{+/+}$, 19 $Scx^{+/-}$, and 12 $Scx^{-/-}$ mice were collected and processed for statistical analysis. To compare the body weight differences among the three genotypes, we used one-way ANOVA followed by Turkey's multiple comparison posttest. *P* value less than 0.05 was considered statistically significant and marked as *. *P* value less than 0.01 was marked as **, whereas *P* value less than 0.001 was marked as *** when applicable.

ChIP-seq and Data Analysis

Three biological repeats, each containing 10 pairs of forelimbs from E13.5 $Scx^{Flag/Flag}$ embryos, were collected for chromatin immunoprecipitation (ChIP) analysis as previously described (Xu et al., 2020). Briefly, DNA/protein complexes were extracted and incubated with the anti-FLAG antibody (Sigma, catalog# F1804). Sequencing libraries were generated using the ThruPLEX DNA sequencing kit (Rubicon Genomics). Sequencing was performed on Illumina NextSeq500. ChIP-seq reads were aligned to UCSC mouse genome 10 mm using STAR aligner (ver. 2.7.4) (Dobin et al., 2013). To match the sequencing depth across samples, aligned reads were down-sampled to 30 million. After deduplication, peaks were called for each Scx ChIP-seq dataset using HOMER (Hypergeometric Optimization of Motif EnRichment) (v4.11) (Heinz et al., 2010) against a matching input sample. To identify reproducible and unified Scx peaks, we performed second round differential analysis comparing Scx samples versus input samples anchoring on all the detected Scx peaks. First, Scx peaks from the three biological replicates were pooled and merged into a preliminary peak set. Second, read counts were measured in all the Scx ChIP samples and input samples within the peak set. Finally, exact test was performed using EdgeR (Robinson et al., 2010) comparing Scx ChIP and input samples. Final Scx peaks were defined by $\log_2$ fold-change ($\log_2$FC) over input > 2 and FDR < 0.01. *De novo* motif analysis of the Scx peaks was performed within a 200 bp window using Homer (v4.11) (Heinz et al., 2010) with default options. Peak-gene association analysis was performed utilizing the online GREAT (Genomic Regions Enrichment of Annotations Tool) program (version 4.0) (McLean et al., 2010). Gene regulatory domains utilized for region annotation were defined as minimum 5 kb upstream and 1 kb downstream of the gene transcription start site (TSS), and extended in both directions to the nearest gene's basal domain but no more than the maximum extension of 1000 kb in one direction ("Basal plus extension" option)[1]. The ChIP-seq raw data have been deposited into the National Center for Biotechnology Information Gene Expression Omnibus database (NCBI GEO Accession Number GSE173428).

[1]http://great.stanford.edu

Fluorescence-Activating Cell Sorting (FACS)

E15.5 embryonic forelimbs were dissected from embryos of $Scx^{+/-}$; *Scx-GFP* female crossed with $Scx^{+/-}$; *Scx-GFP* male mice. The freshly dissected embryonic forelimbs were digested with the trypsin−EDTA solution (Invitrogen) at 37°C for 4 min. After inactivation of trypsin with DMEM containing 10% FBS, cells were dissociated by pipetting. The dissociated limb cells were suspended in PBS with 2% FBS and 10 mM EDTA, and filtered through a 40 μm nylon cell strainer (BD Falcon, 352340). GFP^+ cells from each sample were isolated using BD FACSAria II.

RNA−Seq and Data Analysis

RNA-seq were carried out using FACS isolated GFP^+ cells from the forelimb tissues of three $Scx^{-/-}$ embryos and three littermate controls at E15.5. Total RNAs were extracted from FACS isolated E15.5 forelimb GFP^+ cells using the Qiagen RNeasy Micro Kit (Qiagen catalog# 74004). cDNA amplification was carried out using the Ovation RNA-Seq System V2 kit (Tecan Genomics Inc.). The sequencing libraries were made using the Nextera XT DNA Library Prep kit (Illumina), and sequenced using Illumina NovaSeq 6000 for 75 bp paired-end reads. RNA-seq reads were aligned to UCSC mouse genome 10 mm using STAR aligner (v2.7.4) (Dobin et al., 2013). Read counts for each gene were measured using FeatureCounts in the subread package (v1.6.2) (Liao et al., 2014). To avoid sex-specific bias in the analysis, genes in chromosome Y were discarded. In addition, RUVseq (RUVs, k = 1) (Risso et al., 2014) was applied to account for sex-specific contribution to the gene expression profiles and to identify sex-independent gene expression changes upon *Scx* deletion. Principal component analysis was applied to normalized FPKM (fragment per kilobase of transcript per million mapped reads) and log-transformed count data. Differential gene expression analysis was performed using DESeq2 (Love et al., 2014). Differentially expressed genes were identified by FDR < 0.05. Gene ontology (GO) analysis was performed using the online ToppGene tools[2] (Chen et al., 2009). Hierarchical clustering of the differential gene expression profiles was performed using Pearson correlation coefficient of log-transformed gene expression level (FPKM) as similarity measure under Ward's criterion. Clustering heatmap was visualized in z-score. The RNA-seq data have been deposited into the National Center for Biotechnology Information Gene Expression Omnibus database (NCBI GEO Accession Number GSE173428).

Quantitative RT-PCR

E13.5 and E15.5 $Scx^{-/-}$ mutant and wildtype control forelimb samples were collected. Total RNAs were extracted using the Qiagen RNeasy Micro Kit (Qiagen catalog# 74004), and reverse transcribed using SuperScript™ III First-Strand Synthesis System (Thermo Fisher Scientific, Waltham, MA, United States catalog# 18080051). At each stage, at least 5 samples per genotype were used for quantitative RT-PCR. Relative mRNA levels were

[2]https://toppgene.cchmc.org

normalized to that of *Hprt* mRNAs. Student's *t* test was used for pairwise comparison. $P < 0.05$ was considered significantly different. *P* value less than 0.05 was considered statistically significant and marked as *. *P* value less than 0.01 was marked as **, whereas *P* value less than 0.001 was marked as *** when applicable.

RESULTS

Generation of a Novel *Scx^{Flag}* Mouse Line and Genome-Wide Mapping of Endogenous Scx Binding Sites in the Tendon Progenitor Cells *in vivo*

No specific antibody for the Scx protein that allows direct analysis of endogenous Scx-binding at target genes has been reported. To facilitate direct and specific analysis of endogenous Scx protein activity, we used the CRISPR/Cas9-mediated genome editing strategy (Cong et al., 2013; Scott and Hu, 2019) to insert a well-characterized 2xFLAG epitope tag at the carboxy terminus of the endogenous Scx protein in mice (**Figure 1A**). Detailed description of the procedures for generating the *Scx^{Flag}* founder mice is provided in the Materials and Methods section. The *Scx$^{Flag/+}$* founder mice were crossed to wildtype CD1 mice and the G1 *Scx$^{Flag/+}$* hemizygous progenies (**Figure 1B**) were sequence-verified for correct integration and germ-line transmission of the *Scx^{Flag}* allele as designed. The *Scx$^{Flag/+}$* mice were then intercrossed to generate *Scx$^{Flag/Flag}$* homozygous mice, which were born at expected Mendelian ratio and did not display any phenotypic difference from their hemizygous or wildtype littermates (**Figures 1C–F**). Immunofluorescent staining of sections of mouse embryos using an anti-FLAG antibody (Sigma, catalog# F1804) showed that the Scx-FLAG fusion protein was strongly and specifically expressed in both tendons and ligaments (**Figures 1G–J**), consistent with previously reported patterns of expression of endogenous *Scx* mRNAs and of the transgenic Scx-GFP reporter activity (Murchison et al., 2007; Pryce et al., 2007; Watson et al., 2009). Since the *Scx$^{Flag/Flag}$* homozygous mice do not have any phenotypic abnormality, the insertion of the FLAG epitope tag at the carboxy-terminus of the endogenous Scx protein did not affect Scx function, providing a valuable new tool for direct analysis of endogenous Scx function during development, tissue homeostasis, and injury repair.

To investigate Scx-mediated transcriptional regulation during early tendon development, we dissected forelimbs from E13.5 *Scx$^{Flag/Flag}$* embryos and performed ChIP-seq experiments in triplicates using the anti-FLAG antibody (Sigma, catalog# F1804). Analysis of the ChIP-seq data identified 12,097 highly enriched Scx-associated chromatin regions (ChIP-seq peaks) (**Figures 2A,B**). About 77% (9,272 of 12,097) of the Scx ChIP-seq peaks were located in intronic or intergenic regions associated with one or two genes in the immediate vicinity within 500 kb from the gene's transcription start site (TSS), whereas only about 14% (1,670 of 12,097) of the Scx-binding sites were located within gene promoter regions (**Figures 2A–C**). *De novo* motif analysis revealed that the most enriched endogenous Scx-binding domain contains a core sequence C-A-G/T-A/C-T-G (**Figure 2D**), which was present in >45% of the ChIP-seq peak regions and matches the Scx-binding core sequence previously determined by electrophoresis mobility shift assays (Shukunami et al., 2018). The second most enriched motif, which is present in 15.8% of the ChIP-seq peaks, contains a core sequence that matches the consensus binding motif of the Nfat family transcription factors, TGGAAA (Yu et al., 2015; Klein-Hessling et al., 2017; **Figure 2D**). It has been reported that Scx and Nfatc4, a member of the Nfat family, act cooperatively to regulate the transcription of *Col1a1* in tendon fibroblast cells (Lejard et al., 2007). The significant enrichment of the Nfat binding motif in the Scx ChIP-seq peaks indicate that Scx and Nfat family proteins act together to regulate expression of many genes during tendon development.

Genomic Regions Enrichment of Annotations Tool analysis of the ChIP-seq data recovered 7,520 genes associated with the Scx-binding genomic regions. To gain insight into Scx-mediated transcriptional regulation during early tendon development, we compared the ChIP-seq data with the previously reported RNA-seq data analyzing transcriptome profiles of developing mouse hindlimb tendons (Liu et al., 2015). We found that high quality Scx ChIP-seq peaks were detected in 490 of the 970 genes whose expression was upregulated by more than 1.5-fold in Scx-GFP^{+} cells during early tendon cell differentiation in the mouse hindlimb from E13.5 to E15.5 (**Figure 2E**). GO analysis showed that this group is highly enriched with genes playing roles in "extracellular matrix organization," "collagen fibril organization," and "connective tissue development" (**Figure 2F**), consistent with a major role of Scx in regulating tendon formation.

Characterization of a New *Scx* Mutant Mouse Resource

Whereas several distinct *Scx* mutant mouse lines have been reported (Murchison et al., 2007; Yoshimoto et al., 2017; Shukunami et al., 2018), none of these are available to the wide biomedical research community through the Mutant Mouse Resource Centers. On the other hand, the United States National Institutes of Health-funded Knock-out Mouse Project (KOMP) Consortium has generated a *Scx*-knockout mouse line [C57BL/6N-*Scx$^{tm1.1(KOMP)Vlcg}$/MbpMmucd*] and made available through the Mouse Biology Program at the University of California Davis, but the tendon developmental defects in mice homozygous for this particular *Scx* knockout allele has not been described. We obtained the C57BL/6N-*Scx$^{tm1.1(KOMP)Vlcg}$/MbpMmucd* mouse line and established a breeding colony. The *Scx$^{tm1.1(KOMP)}$* allele (abbreviated as *Scx^{-}* in the rest of the report) contains an insertion of the VelociGene ZEN-Ub1 LacZ reporter cassette replacing the entire protein-coding sequences from the translation start site in Exon-1 to 56 bp 3′ to the translation STOP codon in Exon-2 of the *Scx* gene (**Figure 3A**). We confirmed the structure and correct integration of the *lacZ* reporter cassette at the *Scx* locus through Sanger sequencing of genomic PCR products. However, no specific beta-galactosidase reporter

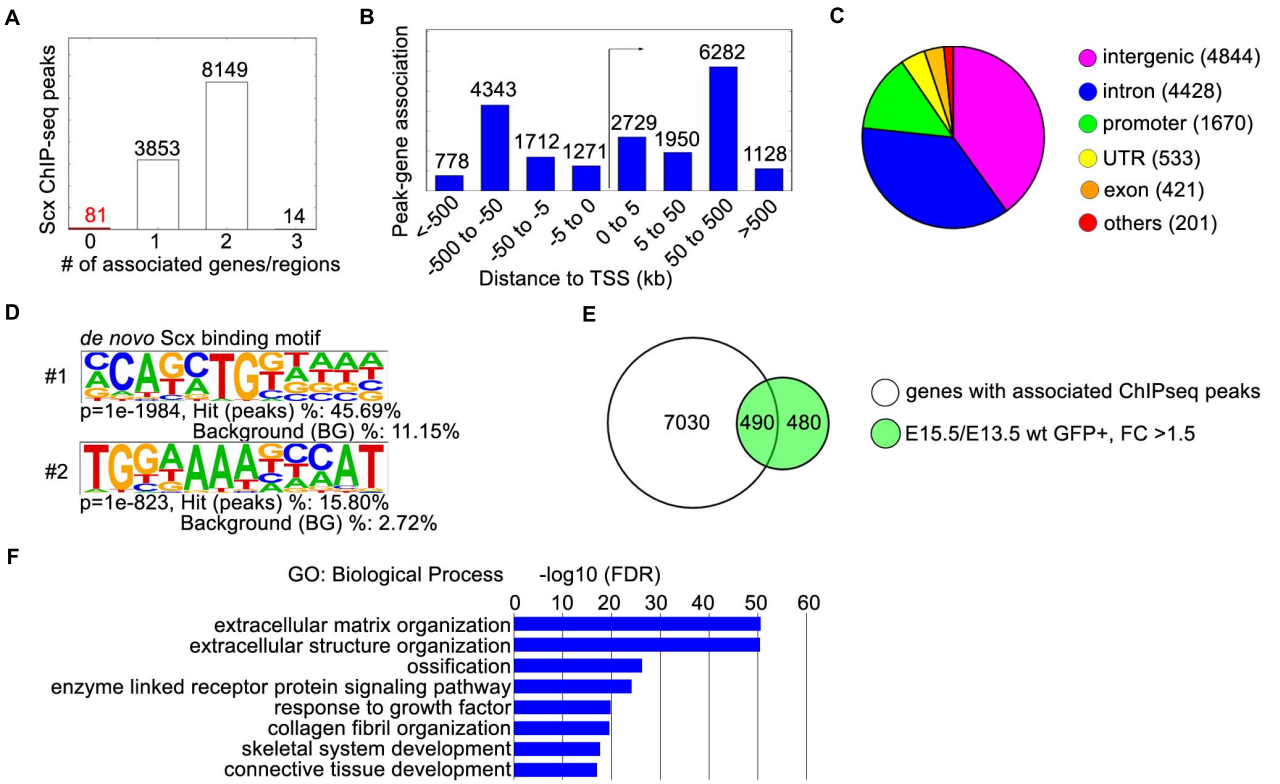

FIGURE 2 | ChIP-seq analysis of E13.5 $Scx^{Flag/Flag}$ forelimbs. **(A)** Peak-gene association analysis with the GREAT online tool (http://great.stanford.edu). The "basal plus extension" parameter was used to associate the ChIP-seq peaks to genes within 1,000 kb. The majority of peaks were associated with 1 or 2 genes. **(B)** Distribution of peak-gene associations by their distances to the transcription start site (TSS). **(C)** Distribution of ChIP-seq peaks by their locations. The majority of peaks are located in intronic (4428) or intergenic (4844) regions, while 1670 peaks were located in promoter regions. **(D)** The two most enriched Scx binding motifs from ChIP-seq peaks. **(E)** Comparison of 7520 genes with associated ChIP-seq peaks, with 970 genes that were up-regulated in GFP+ hindlimb cells from E13.5 to E15.5 by at least 1.5-fold. **(F)** Gene ontology analysis of the 490 differentially expressed genes with associated peaks from panel **(E)**. Representative GO terms are listed in the order of their *p*-values, with the most enriched GO term on top.

activity was detected in developing tendon tissues in the heterozygous and homozygous mutant mouse embryos, likely due to reporter gene silencing described previously in multiple other KOMP mouse lines (Kirov et al., 2015). To confirm that Scx function is lost in the $Scx^{-/-}$ embryos, we carried out *in situ* hybridization assay using a probe specific for the *Scx* coding sequence and found that *Scx* mRNA expression was completely absent in the $Scx^{-/-}$ embryos (**Figures 3B,C**).

We further characterized the phenotypes of the $Scx^{-/-}$ mutant mice. $Scx^{-/-}$ mice were born at Mendelian ratio, but with reduced body size and severely impaired limbs, with the autopod of both fore- and hind-limbs locked in a dorsal flexure (**Supplementary Figure 1**). All neonatal $Scx^{-/-}$ mutant mice exhibited severe hypoplasia of major limb and tail tendons (**Figures 3D–I**). Analysis of skeletal preparations showed that $Scx^{-/-}$ mutants lacked the deltoid tuberosity of the humerus in the forelimb and exhibited reduced size of the patella and the entheseal cartilage of the calcaneus in the hindlimb (**Supplementary Figures 2A–D**). In addition, the transverse processes of the lumbar vertebrae were reduced in the $Scx^{-/-}$ mutants (**Supplementary Figures 2E, F**). Using a previously reported Scx-GFP transgenic reporter (Pryce et al., 2007), we found that tendon differentiation and condensation in the developing limbs were disrupted by E15.5 in the homozygous mutant embryos (**Supplementary Figure 3**). The tendon and skeletal defects in these $Scx^{-/-}$ mice are similar to those reported previously in two other independent *Scx* mutant mouse lines (Murchison et al., 2007; Shukunami et al., 2018). Thus, this KOMP-generated *Scx* knockout mouse line is a valuable resource for the biomedical research community for further studies of Scx function *in vivo*.

Analysis of Scx-Dependent Transcriptome Expression Profiles During Early Tendon Cell Differentiation *in vivo*

We crossed the *Scx-GFP* transgenic reporter (Pryce et al., 2007) into the new $Scx^{+/-}$ mouse line and then intercrossed $Scx^{+/-}$; *Scx-GFP* mice for analysis of transcriptomic effects of Scx during early tendon cell differentiation. Scx-GFP^{+} cells were isolated by FACS from freshly dissected forelimb tissues from E15.5 wildtype, $Scx^{+/-}$, and $Scx^{-/-}$ mutant embryos for RNA-seq

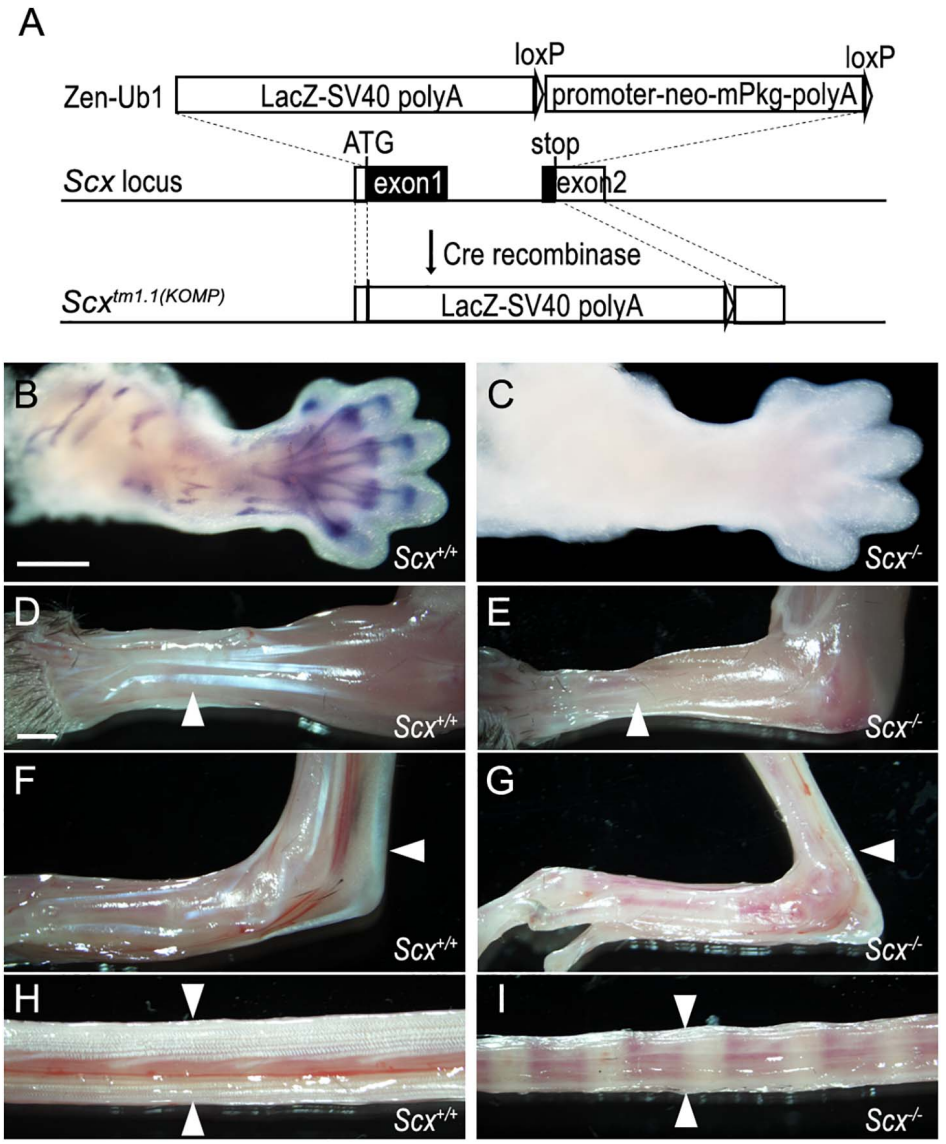

FIGURE 3 | Characterization of a *Scx* null mutant mouse strain. **(A)** Schematic diagram and strategy of generating *Scx* null mutant allele. A VelociGene ZEN-Ub1 LacZ reporter cassette was inserted after the endogenous *Scx* ATG codon, by homologous recombination, and replaced the entire *Scx* coding sequence plus a 56 bp 3′ UTR sequence. **(B,C)** *In situ* hybridization on E13.5 $Scx^{-/-}$ mutant and control forelimbs, with an anti-sense RNA probe against the protein coding region of the *Scx* mRNAs. **(D–I)** Whole mount view of tendons in forelimb **(D,E)**, hindlimb **(F,G)**, and tail **(H,I)** from $Scx^{-/-}$ mutant **(E,G,I)** and control littermates **(D,F,H)** at P21. White arrowheads point to extensor digitorium communis in panels **(D,E)**, Achilles tendons in panels **(F,G)**, and tail tendons in panels **(H,I)**. Scale bar is 500 μm in panel **(B)** and 1000 μm in panel **(D)**.

analysis. Analysis of the RNA-seq results from three $Scx^{-/-}$ embryos and three control littermates identified 68 genes that exhibited significant changes in expression levels (FDR < 0.05) in the forelimb Scx-GFP^{+} cells in E15.5 $Scx^{-/-}$ embryos compared with their control littermates (**Figures 4A–D**). Comparison of the Scx-dependent differentially expressed genes with the Scx ChIP-seq data revealed that 32 of the significantly down-regulated genes were associated with Scx occupancy in the tendon progenitor cells (**Figure 4E** and **Table 1**). These genes are likely critical direct target genes mediating Scx function in tendon formation and early tendon cell differentiation. Indeed, GO analysis of this gene group showed that "tendon development," "tendon cell differentiation," "keratan sulfate biosynthesis," and "ECM organization" are among the most significantly enriched biological processes (**Figure 4F**). The most significantly down-regulated Scx target genes in the E15.5 $Scx^{-/-}$ forelimb tendon cells include *Fmod*, *Tnmd*, *Kera*, and *Col11a1* (**Figure 4C** and **Table 1**), of which each plays important roles in tendon cell differentiation and/or collagen fibrillogenesis (Svensson et al., 1999; Pellegata et al., 2000; Docheva et al., 2005; Kilts et al., 2009; Wenstrup et al., 2011; Sun et al., 2020) but only *Tnmd* has previously been identified as a Scx transcriptional target gene

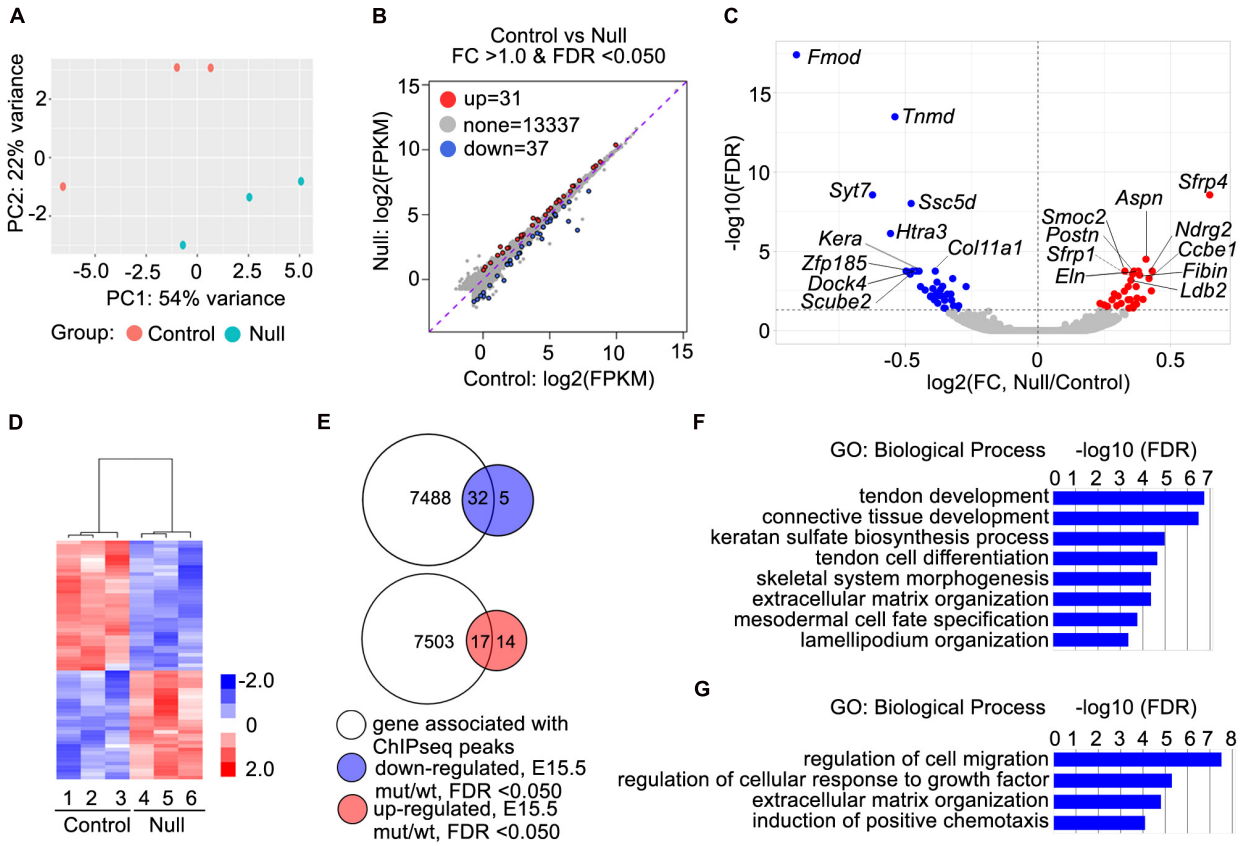

FIGURE 4 | RNA-seq data analysis and identification of candidate Scx direct target genes. **(A)** Principal component plot displaying the three *Scx*$^{-/-}$ and three control samples along PC1 and PC2, which account for 54 and 22%, respectively, of the variability within the RNA-seq dataset. **(B)** MA plot displaying differential expression profiles of the *Scx*$^{-/-}$ and control samples. Up-regulated genes are marked in red whereas down-regulated genes are marked in blue. **(C)** Volcano plot displaying the $\log_2$ fold change against the $\log_{10}$ value of the FDR adjusted *P* value. Up-regulated genes are shown in red while down-regulated genes shown in blue. Top 10 down-regulated and top 10 upregulated genes are marked by with symbol. **(D)** Heatmap showing hierarchical clustering on the 68 differentially expressed genes. The z-score scale bar represents relative expression+/- 2SD from the mean. **(E)** Comparisons of 7520 genes with associated Scx binding peaks with 37 down-regulated genes in *Scx*$^{-/-}$ samples at E15.5 and 31 up-regulated genes in *Scx*$^{-/-}$ samples at E15.5 **(B)**. **(F,G)** Gene ontology analyses of 32 down-regulated genes associated with Scx-binding peaks and 17 up-regulated genes associated with Scx-binding peaks, respectively. Representative GO terms are listed in the order of their *P* values, with the most enriched GO term on top.

(Li et al., 2015; Shukunami et al., 2018). The Scx-dependent target genes also include three genes encoding transcription factors, *Mkx*, *Six2*, and *Eya1* (**Table 1**). Mkx function is required for tendon fibril growth and tendon homeostasis (Ito et al., 2010; Liu et al., 2010, 2019; Suzuki et al., 2016).

Analysis of RNA-seq data also revealed 31 genes that were significantly up-regulated in the Scx-GFP^{+} forelimb cells of E15.5 *Scx*$^{-/-}$ embryos compared with control littermates (**Figures 4B–D**). Among these, 17 genes were associated with Scx ChIP-seq peaks in the tendon progenitor cells (**Figure 4E** and **Table 2**). GO analysis of this group of genes showed that many of these, including *Ccbe1*, *Cxcl12*, *Epha3*, *Fgf10*, *Igf1*, *Ldb2*, *Postn*, *Smoc2*, and *Surf1*, are involved in "regulation of cell migration" (**Figure 4G**). In addition, *Surf1*, *Postn*, *Smoc2*, *Eln*, and *Nid2* are involved in regulation of "extracellular matrix organization," whereas *Cxcl12* and *Fgf10* have been implicated in "induction of chemotaxis" (**Figure 4G** and **Table 2**). Taken together, Scx regulates early tendon cell differentiation by controlling the expression of multiple ECM components as well as signaling pathways controlling cell behavior.

Multiple Scx Target Genes Exhibited Specific Scx-Dependent Expression During Tendon Differentiation

We further analyzed the patterns of expression of the top 10 down-regulated genes in the E15.5 *Scx*$^{-/-}$ embryos from the RNA-seq data. Whole mount *in situ* hybridization analyses showed that the *Fmod, Htra3, Kera, Ssc5d, Tnmd,* and *Zfp185* genes each exhibited highly specific patterns of expression in the developing tendon tissues in E14.5 wildtype embryos and their expression in the developing limb tendons was dramatically reduced in the *Scx*$^{-/-}$ littermates (**Figures 5A–L**). Furthermore, quantitative real-time RT-PCR analysis revealed that expression of each of these genes was already significantly reduced in the Scx-GFP^{+} forelimb mesenchyme cells in *Scx*$^{-/-}$ embryos by E13.5, in comparison with their control littermates (**Figure 5M**). Among

TABLE 1 | Genes with associated Scx-binding peaks and down-regulated in *Scx*$^{-/-}$ tendon cells at E15.

Gene symbol	Scx-binding peaks (numbers indicate distance to TSS, in bp)							
Adgrg2	−184004							
Aqp1	−90524*	−41742	−3597	−3169	+2103			
C1qtnf3	−229323*	−79453	−75909	−23517	−11848	−3835*	−623*	
Ccdc85a	+114267	+118157						
Ccdc88a	−13517	−2700	−1					
Chst5	+5231	+5847						
Cilp2	+9479							
Col11a1	−170353	−98636	+34903	+35353				
Col22a1	+106886							
Cyr61	+931							
Dock4	+210357	+248137	+250413	+256430	+256533	+295104	+342939	+343124
Enpp2	+114774							
Eya1	−375541	−112658	−47591	+52976	+165834	+173401	+378637	+382083
Fat3	−425380	−329482	−140752	−895	+33046	+230423	+246601	+348404*
Fmod	−95614	−58501	−23204	−26				
Htra3	+57656	+70290*						
Kera	+5138	+12293	+17683	+19969				
Mkx	−231675*	−227917*	−83259	−33399				
Mtcl1	+20857	+32469	+84844	+214107				
Naalad2	+4887							
Olfml2b	−38976	−5227	+7772	+11134	+57278	+74224		
Plch1	+27008	+268469	+357217					
Rflnb	−132608*	−97812*	−71599	−15311	−14423	−14271	−55	
Scube2	+14689	+30597						
Six2	−247206	−242150	−218515	−205193	−193527	−173342	−164957	−135585
Ssc5d	−776							
St8sia1	+18010	+26582	+26704	+149719*				
Syt7	−69362	−7436	+14213	+39584*				
Thbs4	−37977	−33745	+62949	+155236*				
Tmem44	+14520	+71219						
Tnmd	−90582	−20742						
Zfp185	−423							

**Peak located in neighboring gene.*

those, *Fmod* and *Tnmd* have been reported to play important roles in tendon development whereas *Kera* plays crucial roles in other connective tissues including the cornea (Svensson et al., 1999; Pellegata et al., 2000; Docheva et al., 2005; Kilts et al., 2009). *Htra3* and *Zfp185* exhibited specific expression in the developing tendons, similar to *Tnmd*, whereas *Ssc5d* exhibited a similar pattern of expression as *Fmod* in both tendon cells and in joint cells (**Figure 5**). Further *in situ* hybridization analysis of serial transverse sections through the digit, metacarpal, and zeugopod regions of the E15.5 forelimb samples confirmed the specificity of expression of *Htra3*, *Zfp185*, and *Tnmd* throughout the differentiating tendon cells (**Supplementary Figure 4**). Examination of the Scx ChIP-seq profiles associated with these genes showed high quality enrichment of Scx binding at the basal promoter regions of *Fmod*, *Ssc5d*, and *Zfp185* whereas Scx binding was also specifically enriched at distal regulatory elements associated with *Fmod*, *Kera*, *Htra3*, and *Tnmd* (**Figure 6**). Whereas the roles of *Htra3*, *Ssc5d*, and *Zfp185* in tendon development remain unknown, our finding that they are direct Scx targets that exhibit Scx-dependent activation during early tendon differentiation suggests that they play crucial roles downstream of Scx in tendon development.

DISCUSSION

Previous genetic studies have identified Scx as the most crucial transcriptional regulator of tendon development as well as tendon homeostasis and repair (Murchison et al., 2007; Yoshimoto et al., 2017; Shukunami et al., 2018; Gumucio et al., 2020). Mice lacking Scx exhibited loss or severe disruption of force-transmitting tendons throughout the body as well as defects in entheseal development (Murchison et al., 2007; Killian and Thomopoulos, 2016; Yoshimoto et al., 2017). However, the molecular mechanisms mediating Scx function in tendon development is not well understood and very few Scx target genes in tendon cells have been identified. The lack of large scale identification of direct target genes of Scx in tendon development

TABLE 2 | Genes with associated Scx-binding peaks and upregulated in *Scx*$^{-/-}$ tendon cells at E15.5.

Gene symbol	Scx-binding peaks (numbers indicate distance to TSS, in bp)							
Adgrb3	−746	+600918*						
Aspn	−37162*	+1353	+3527					
Ccbe1	−112895	+57507*	+192663*	+210538*				
Cxcl12	−311414	−222186	−200466	−83159	−63138	+18174	+139363	+248065
Dio2	+329510							
Eln	−153983*	−148138	−70385					
Epha3	+7097	+244725	+250929	+307693	+576357	+747465	+779839	+779948
Fgf10	−237483	+195887						
Fibin	−50132	−50030	−48436	−29864	+124	+267	+9459	+13190
Igf1	−206628	−183042	−182419	−148	+1161	+187057	+188639	
Ldb2	−322438*	−123018	−15277	+214796				
Lingo2	−801973*	−15799	+145957					
Nid2	+66867*							
Postn	−10601	+127772	+129401	+226369	+297040	+304008		
Prg4	−339455*	−294031*	−251594	−149528	−106405	−23787		
Smoc2	−48448	+34969	+91272*	+217732	+231118	+327987	+385193*	
Sulf1	−513097	−254232	−111144	+194				

**Peak located in neighboring gene.*

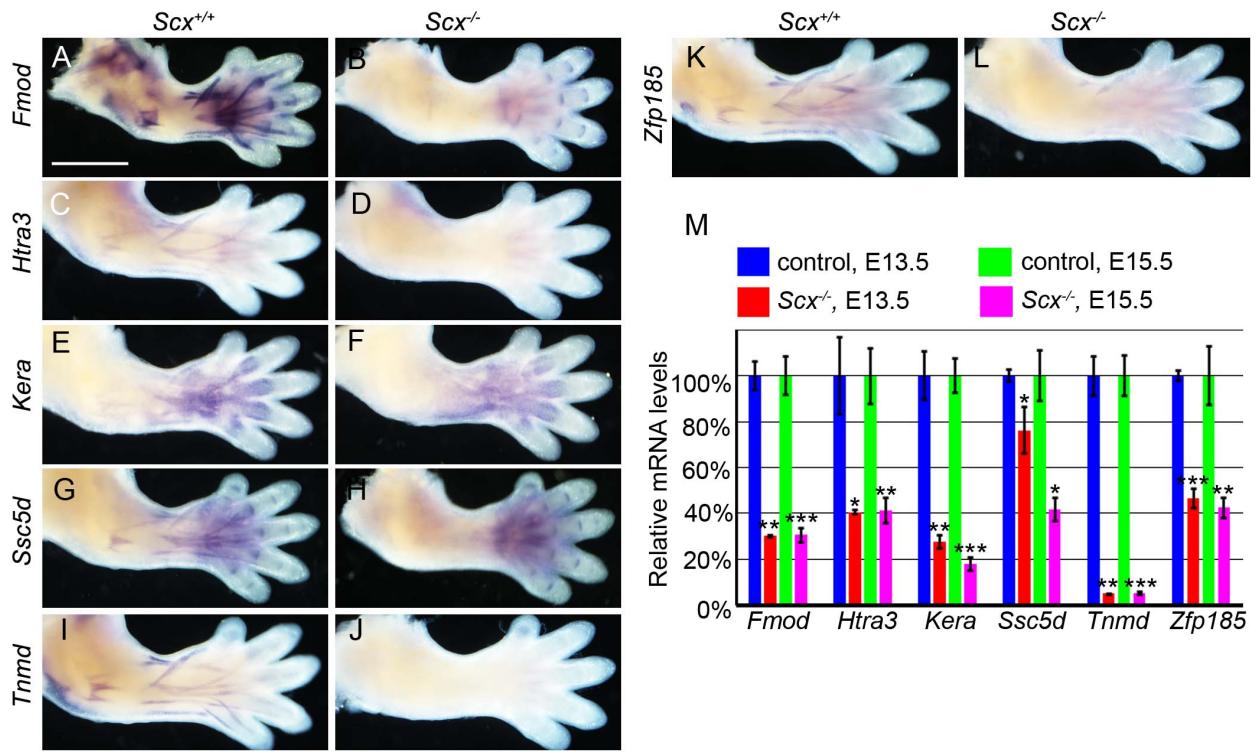

FIGURE 5 | Characterization of candidate genes from ChIP-seq and RNA-seq. **(A–L)** Whole mount *in situ* hybridization of six candidate genes in E14.5 *Scx*$^{-/-}$ mutant **(B,D,F,H,J,L)** and control **(A,C,E,G,I,K)** forelimbs. Expression of *Fmod, Kera, Ssc5d,* and *Zfp185* was dramatically reduced in *Scx*$^{-/-}$ mutant limbs **(B,F,H,L)**, while expression of *Htra3* and *Tnmd* were nearly completely absent in *Scx*$^{-/-}$ mutant **(D,J)**. Expression of *Fmod* and *Ssc5d* persisted in digit ligaments in the mutant limbs **(B,H)**. **(M)** Quantitative RT-PCR analysis of expression of the six candidate genes in *Scx*$^{-/-}$ mutant and control forelimb samples at E13.5 and E15.5. All genes were significantly reduced in *Scx*$^{-/-}$ mutants at both stages, compared with control littermates. *$p < 0.05$, **$p < 0.01$, ***$p < 0.001$.

is largely due to the lack of a reliable specific antibody for mapping genome-wide Scx binding in tendon cells *in vivo*. Scx belongs to the class II bHLH family of transcription factors, of which many have been shown to bind to an E-box (CANNTG) motif (Cserjesi et al., 1995; Massari and Murre, 2000). However, this short redundant sequence can be found throughout the

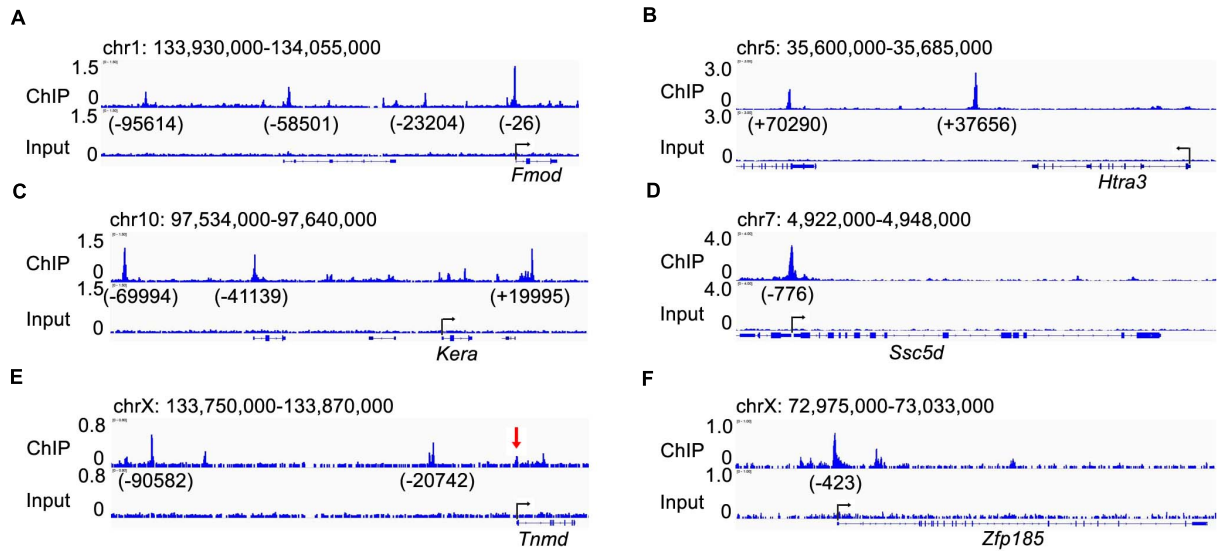

FIGURE 6 | Visualization of the Scx-binding peaks associated with the candidate Scx direct target genes. **(A–F)** genome browser views of genomic regions containing, *Fmod* **(A)**, *Htra3* **(B)**, *Kera* **(C)**, *Ssc5d* **(D)**, *Tnmd* **(E)**, and *Zfp185* **(F)** genes. Numbers under each peak indicate the distance to the transcription start site (TSS) the marked gene. The red arrow in panel **(E)** point to a Scx-binding peak at the Tnmd gene promoter region that is recognizable upon careful examination but was below the FDR < 0.01 threshold for identifying genome-wide Scx binding sites in our ChIP-seq data analysis.

genome. Thus, previous studies of Scx-mediated transcriptional regulation of putative target genes primarily relied on *in vitro* biochemical assays including electrophoresis mobility shift assay of recombinant Scx protein binding to E-box containing promoter sequences and promoter reporter assays in cell transfection studies (Lejard et al., 2007; Shukunami et al., 2018; Paterson et al., 2020), and more recently ChIP-qPCR assays of candidate promoter regions (Paterson et al., 2020). In this study, we have generated Scx^{Flag} mice and demonstrate that this new mouse line enables direct analysis of endogenous Scx protein function in the normal developmental and physiological context. Whereas we have used this mouse line for genome-wide mapping of Scx binding sites in early developing limb tendon tissues, this mouse line will provide a valuable tool for direct analysis of Scx function in many developmental and disease processes where Scx plays a role.

Our ChIP-seq analysis identified 12,097 high quality Scx binding sites in the E13.5 mouse forelimb, with the most highly enriched *de novo* motif identified as 5′ CAG/TA/CTG 3′. Whereas previous *in vitro* studies have shown Scx binding to various E-boxes including CACGTG in the *Col1a1* promoter (Lejard et al., 2007), CAGGTG in the *Col2a1* promoter (Furumatsu et al., 2010), and CAAATG and CAGATG in the *Tnmd* promoter (Li et al., 2015), direct comparative EMSA analysis of Scx binding to five distinct E-box containing elements from the mouse *Tnmd* promoter region showed that Scx preferentially bound to CAGATG and CATCTG, but not the others (Shukunami et al., 2018). Thus, the consensus Scx binding motif from our ChIP-seq data matches perfectly with the EMSA-determined preferential Scx binding motif, which affirms our genome-wide mapped Scx-binding sites. Whereas several *in vitro* studies have repeatedly demonstrated Scx binding to the *Tnmd* promoter regions and Scx activated expression of *Tnmd* promoter-reporter constructs in co-transfected cells (Li et al., 2015; Shukunami et al., 2018), our ChIP-seq results showed that endogenous Scx binding was primarily enriched at two upstream locations at about 20 and 90 kb, respectively, from the *Tnmd* TSS (**Figure 6E**). A minor Scx binding peak was detected at the *Tnmd* basal promoter region (**Figure 6E**), which is enriched over 4-fold over the input but the FDR value, at 0.025, was below the stringent threshold (4-fold enrichment over input and FDR < 0.01) used for identifying the genome-wide Scx binding peaks in our analysis. It is possible that Scx binding to both the distal enhancers and the promoter region to synergistically activate *Tnmd* gene expression in tenocytes.

Whereas previous studies have shown that activation of *Tnmd* expression during tendon development depends on Scx function and that Tnmd plays crucial roles in tenocyte proliferation and maturation, *Tnmd* null mice exhibited a much milder tendon phenotype than $Scx^{-/-}$ mice (Docheva et al., 2005; Murchison et al., 2007; Yoshimoto et al., 2017; Shukunami et al., 2018). Our ChIP-seq and RNA-seq results demonstrate that Scx directly regulates expression of a large number of genes during early tendon development, including activation of expression of many tendon cell-specific genes. In particular, we validated *Fmod, Htra3, Ssc5d,* and *Zfp185* as new direct target genes that dependent on Scx for their expression in the differentiating tendon cells. *Fmod*-deficient mice exhibited defects in tendon collagen fibrillogenesis (Chakravarti, 2002), but the roles of *Htra3*, *Ssc5d*, and *Zfp185* in tendon development are unknown. *Htra3* encodes a serine peptidase that cleaves proteoglycans, thus may function in ECM remodeling (Nie et al., 2003; Glaza et al., 2015). *Ssc5d* (*scavenger receptor cysteine rich family member with 5 domains*) has been implicated in playing a role at the interface between adaptive and innate immunity and in placental

function (Goncalves et al., 2009). *Zfp185* encodes LIM domain type zinc finger protein (Heiss et al., 1997; Zhang et al., 2016). Whereas the Zfp185 protein was originally hypothesized to reside in the cell nucleus, subsequent *in vitro* cell biological studies suggested that Zfp185 binds to F-actin and may be involved in modulating dynamics of actin filaments (Wang et al., 2008; Zhang et al., 2016). Thus, these gene products have diverse cellular functions and loss of their expression during early tendon cell differentiation in the $Scx^{-/-}$ embryos likely contributed to the severe disruption of tendon condensation phenotype.

Whereas our ChIP-seq analysis identified more than 12,000 high quality Scx-binding regions associated with over 7,500 genes in the embryonic forelimb tissues, our RNA-seq analysis uncovered a relatively small number of genes that exhibited significant differential expression in the Scx-GFP^{+} forelimb tendon cells between E15.5 $Scx^{-/-}$ and control littermates. These results suggest that Scx participates in the regulation of a large number of genes during early tendon development, but other factors likely partly compensate for Scx function in the $Scx^{-/-}$ mice. Nevertheless, the differential gene expression profiles uncovered by our RNA-seq data provide new insights into the molecular mechanisms underlying Scx-mediated regulation of tendon formation. It has been shown that the tendon microfibrils are highly disorganized in the $Scx^{-/-}$ mouse embryos (Murchison et al., 2007). We found that expression of *Col11a1* was among the most down-regulated genes in the E15.5 $Scx^{-/-}$ forelimb tendon cells. Recent studies have shown that ColXI, the gene product of *Col11a1*, plays an essential role in tendon fibril assembly and organization (Wenstrup et al., 2011; Sun et al., 2020). Mice with tendon-specific disruption of *Col11a1* in the Scx-expressing lineages exhibited abnormal tendon fibril structure, smaller fibril diameter and disrupted fibril alignment (Sun et al., 2020). Thus, activation of *Col11a1* expression in the differentiating tenocytes is likely an important part of Scx function in tendon formation. In addition to regulating tendon ECM organization and fibrillogenesis, Scx plays a crucial role in regulating tendon cell morphology and organization (Murchison et al., 2007). Whereas wildtype tenocytes develop a complex network of cytoplasmic extensions that engulf the collagen fibril bundles during tendon fibrillogenesis, the tenocytes in $Scx^{-/-}$ mouse embryos exhibited much reduced and less complex cytoplasmic extensions (Murchison et al., 2007). We found that *Dock4*, encoding a key regulator of filapodia and lamellipodia protrusions (Hiramoto et al., 2006; Abraham et al., 2015), was among the top downregulated genes in the E15.5 tendon cells. As tenocyte cytoplasmic extensions likely also involve spatially regulated changes of the actin cytoskeleton, our finding of significant down-regulation of *Zfp185*, *Ccdc85a* and *Ccdc88a*, which all encode actin binding proteins, in the tendon cells in E15.5 $Scx^{-/-}$ embryos suggests that Scx regulates expression of multiple cytoplasmic proteins to control tenocyte morphology and organization. Moreover, to maintain the stretched tenocyte morphology with a complex network of cytoplasmic extensions during tendon growth and elongation likely requires cell membrane repair mechanisms to maintain plasma membrane integrity. In $Scx^{-/-}$ mice tendon rudiments were detected in the embryonic tail but tail tendon was completely absent in 2-week-old mutant mice due to increased apoptosis (Murchison et al., 2007). Among the most significantly downregulated genes in the $Scx^{-/-}$ tendon cells in our RNA-seq data is *Syt7* (**Figure 4C**), which encodes a transmembrane protein with a crucial role in maintenance of plasma membrane integrity and repair via regulating lysosomal exocytosis (Chakrabarti et al., 2003). Further studies will be needed to investigate whether Syt7 plays an important role in Scx-mediated tenocyte differentiation and maintenance. Furthermore, it has been shown that Scx function is required for proper organization of tendon sheath such as the endotenon and that Epha4-expressing endotenon cells were detected intermixed with tenocytes in the limb tendons in $Scx^{-/-}$ embryos (Murchison et al., 2007). Our RNA-seq data showed that expression of *Epha3* was significantly increased in the limb tendon cell in E15.5 $Scx^{-/-}$ embryos. It is possible that the increased *Epha3* expression in the tenocytes resulted in disruption of the Eph-Efn signaling involved in regulation of tendon sheath formation.

Whereas *Scx* is expressed in all tendon progenitor cells and throughout of tendon development (Schweitzer et al., 2001; Brent et al., 2003), only a subset of tendon tissues were significantly disrupted in $Scx^{-/-}$ mice (Murchison et al., 2007). Huang et al. (2019) demonstrated that Scx function is required for recruitment of mesenchymal progenitor cells into the initially formed tendon rudiments during the growth and elongation of the limbs and tail (Huang et al., 2019). Remarkably, lineage-specific genetic analysis and cell transplantation assays demonstrated that Scx function is exclusively required in the recruited mesenchymal cells, but not in the recruiting tendon, for the recruitment and integration of the mesenchymal progenitor cells during tendon elongation (Huang et al., 2019). The molecular mechanism acting downstream of Scx in mediating the tendon cell recruitment and elongation is currently unknown. Although our RNA-seq data show significant changes in expression of several signaling molecules involved in regulation of cell migration and/or chemotaxis in the $Scx^{-/-}$ Scx-GFP^{+} forelimb cells, it is not clear whether and how some of these molecules may mediate Scx function in tendon cell recruitment. Further analysis of the detailed spatiotemporal patterns of expression of these genes during tendon elongation and/or single-cell transcriptomic profiling combined with lineage-specific functional studies will help resolve the underlying molecular mechanism.

In a recent report, Gumucio et al. (2020) performed RNA-seq analysis to identify genes and signaling pathways that respond differently to mechanical overloads in the plantaris tendons in adult mice due to conditional inactivation of *Scx* (Gumucio et al., 2020). We compared our RNA-seq results from embryonic tendon cells with their RNA-seq results from the adult tenocytes and found that there were a number of overlapping genes in both the down-regulated and up-regulated groups of Scx-dependent differentially expressed genes. In particular, the *Fmod*, *Kera*, *Ssc5d*, *Tnmd,* and *Zfp185* genes were significantly down-regulated in the adult *Scx*-deficient mutant tendon tissues. These genes likely play important roles in tendon cell differentiation at both embryonic and adult stages. Thus, further elucidation of the molecular mechanisms of tendon development will facilitate

investigation of adult tendon cell behaviors during injuries and regeneration and contribute ultimately to improvement in strategies for tendon therapies. In this regard, our ChIP-seq and RNA-seq datasets provide a rich resource for aiding the design of new studies of the molecular and cellular mechanisms of tendon development and repair.

DATA AVAILABILITY STATEMENT

ChIP-seq and RNA-seq data was deposited in the NCBI GEO database under the accession number(s) GSE173428.

ETHICS STATEMENT

The animal study was reviewed and approved by Cincinnati Children's Research Foundation Institutional Animal Care and Use Committee (IACUC).

AUTHOR CONTRIBUTIONS

HL, YL, and RJ conceptualized and designed the research. HWL helped revise the research design and data analysis during the manuscript revision. HL and JX performed the research. HL, JX, YL, HWL, and RJ analyzed the data and critically revised the manuscript. HL and RJ wrote the manuscript. All authors approved the final manuscript and agreed to be accountable for all aspects of the work in ensuring that questions related to the accuracy or integrity of any part of the work are appropriately investigated and resolved.

FUNDING

This research was supported by Cincinnati Children's Hospital Medical Center institutional funds to RJ and Cincinnati Children's Research Foundation Trustee Award to HWL.

ACKNOWLEDGMENTS

The *Scx*$^{tm1.1(KOMP)Vlcg/+}$ mouse strain used for this research project was created from ES cell clone 14378A-H1, generated by Regeneron Pharmaceuticals, Inc., and made into live mice by the KOMP Repository (www.KOMP.org) and the Mouse Biology Program (www.mousebiology.org) at the University of California Davis. We thank Ronen Schweitzer at Shriners Hospitals for Children (Portland, Oregon) for providing the *Scx-GFP* transgenic mouse strain. We thank the Transgenic Animal and Genome Editing Core facility at Cincinnati Children's Hospital Medical Center for assistance with the generation of the *Scx*^{Flag} mouse strain.

SUPPLEMENTARY MATERIAL

The Supplementary Material for this article can be found online at: https://www.frontiersin.org/articles/10.3389/fcell.2021.654397/full#supplementary-material

REFERENCES

Abraham, S., Scarcia, M., Bagshaw, R. D., McMahon, K., Grant, G., Harvey, T., et al. (2015). A Rac/Cdc42 exchange factor complex promotes formation of lateral filopodia and blood vessel lumen morphogenesis. *Nat. Commun.* 6:7286. doi: 10.1038/ncomms8286

Birch, H. L., Thorpe, C. T., and Rumian, A. P. (2013). Specialisation of extracellular matrix for function in tendons and ligaments. *Muscles Ligaments Tendons J.* 3, 12–22. doi: 10.11138/mltj/2013.3.1.012

Brent, A. E., Schweitzer, R., and Tabin, C. J. (2003). A somitic compartment of tendon progenitors. *Cell* 113, 235–248.

Chakrabarti, S., Kobayashi, K. S., Flavell, R. A., Marks, C. B., Miyake, K., Liston, D. R., et al. (2003). Impaired membrane resealing and autoimmune myositis in synaptotagmin VII-deficient mice. *J. Cell Biol.* 162, 543–549. doi: 10.1083/jcb.200305131

Chakravarti, S. (2002). Functions of lumican and fibromodulin: lessons from knockout mice. *Glycoconj J.* 19, 287–293. doi: 10.1023/A:1025348417078

Chen, J., Bardes, E. E., Aronow, B. J., and Jegga, A. G. (2009). ToppGene Suite for gene list enrichment analysis and candidate gene prioritization. *Nucleic Acids Res.* 37, 305–311. doi: 10.1093/nar/gkp427

Cong, L., Ran, F. A., Cox, D., Lin, S., Barretto, R., Habib, N., et al. (2013). Multiplex genome engineering using CRISPR/Cas systems. *Science* 339, 819–823. doi: 10.1126/science.1231143

Cserjesi, P., Brown, D., Ligon, K. L., Lyons, G. E., Copeland, N. G., Gilbert, D. J., et al. (1995). Scleraxis: a basic helix-loop-helix protein that prefigures skeletal formation during mouse embryogenesis. *Development* 121, 1099–1110.

Davis, M. E., Gumucio, J. P., Sugg, K. B., Bedi, A., and Mendias, C. L. (2013). MMP inhibition as a potential method to augment the healing of skeletal muscle and tendon extracellular matrix. *J. Appl. Physiol.* 115, 884–891. doi: 10.1152/japplphysiol.00137.2013

Delgado Caceres, M., Pfeifer, C. G., and Docheva, D. (2018). Understanding tendons: lessons from transgenic mouse models. *Stem Cells Dev.* 27, 1161–1174. doi: 10.1089/scd.2018.0121

Dobin, A., Davis, C. A., Schlesinger, F., Drenkow, J., Zaleski, C., Jha, S., et al. (2013). STAR: ultrafast universal RNA-seq aligner. *Bioinformatics* 29, 15–21. doi: 10.1093/bioinformatics/bts635

Docheva, D., Hunziker, E. B., Fassler, R., and Brandau, O. (2005). Tenomodulin is necessary for tenocyte proliferation and tendon maturation. *Mol. Cell. Biol.* 25, 699–705. doi: 10.1128/MCB.25.2.699-705.2005

Dourte, L. M., Pathmanathan, L., Mienaltowski, M. J., Jawad, A. F., Birk, D. E., and Soslowsky, L. J. (2013). Mechanical, compositional, and structural properties of the mouse patellar tendon with changes in biglycan gene expression. *J. Orthop. Res.* 31, 1430–1437. doi: 10.1002/jor.22372

Dunkman, A. A., Buckley, M. R., Mienaltowski, M. J., Adams, S. M., Thomas, S. J., Kumar, A., et al. (2014). The injury response of aged tendons in the absence of biglycan and decorin. *Matrix Biol.* 35, 232–238. doi: 10.1016/j.matbio.2013.10.008

Furumatsu, T., Shukunami, C., Amemiya-Kudo, M., Shimano, H., and Ozaki, T. (2010). Scleraxis and E47 cooperatively regulate the Sox9-dependent transcription. *Int. J. Biochem. Cell. Biol.* 42, 148–156. doi: 10.1016/j.biocel.2009.10.003

Glaza, P., Osipiuk, J., Wenta, T., Zurawa-Janicka, D., Jarzab, M., Lesner, A., et al. (2015). Structural and functional analysis of human HtrA3 protease and its subdomains. *PLoS One* 10:e0131142. doi: 10.1371/journal.pone.0131142

Goncalves, C. M., Castro, M. A., Henriques, T., Oliveira, M. I., Pinheiro, H. C., Oliveira, C., et al. (2009). Molecular cloning and analysis of SSc5D, a new member of the scavenger receptor cysteine-rich superfamily. *Mol. Immunol.* 46, 2585–2596. doi: 10.1016/j.molimm.2009.05.006

Guerquin, M. J., Charvet, B., Nourissat, G., Havis, E., Ronsin, O., Bonnin, M. A., et al. (2013). Transcription factor EGR1 directs tendon differentiation and

promotes tendon repair. *J. Clin. Invest.* 123, 3564–3576. doi: 10.1172/JCI67521

Gumucio, J. P., Schonk, M. M., Kharaz, Y. A., Comerford, E., and Mendias, C. L. (2020). Scleraxis is required for the growth of adult tendons in response to mechanical loading. *JCI Insight* 5:e138295. doi: 10.1172/jci.insight.138295

Hasson, P. (2011). "Soft" tissue patterning: muscles and tendons of the limb take their form. *Dev. Dyn.* 240, 1100–1107. doi: 10.1002/dvdy.22608

Havis, E., Bonnin, M. A., Esteves de Lima, J., Charvet, B., Milet, C., and Duprez, D. (2016). TGFbeta and FGF promote tendon progenitor fate and act downstream of muscle contraction to regulate tendon differentiation during chick limb development. *Development* 143, 3839–3851. doi: 10.1242/dev.136242

Heinz, S., Benner, C., Spann, N., Bertolino, E., Lin, Y. C., Laslo, P., et al. (2010). Simple combinations of lineage-determining transcription factors prime cis-regulatory elements required for macrophage and B cell identities. *Mol. Cell.* 38, 576–589. doi: 10.1016/j.molcel.2010.05.004

Heiss, N. S., Gloeckner, G., Bachner, D., Kioschis, P., Klauck, S. M., Hinzmann, B., et al. (1997). Genomic structure of a novel LIM domain gene (ZNF185) in Xq28 and comparisons with the orthologous murine transcript. *Genomics* 43, 329–338. doi: 10.1006/geno.1997.4810

Hiramoto, K., Negishi, M., and Katoh, H. (2006). Dock4 is regulated by RhoG and promotes Rac-dependent cell migration. *Exp. Cell Res.* 312, 4205–4216. doi: 10.1016/j.yexcr.2006.09.006

Huang, A. H., Watson, S. S., Wang, L., Baker, B. M., Akiyama, H., Brigande, J. V., et al. (2019). Requirement for scleraxis in the recruitment of mesenchymal progenitors during embryonic tendon elongation. *Development* 146:dev182782. doi: 10.1242/dev.182782

Ito, Y., Toriuchi, N., Yoshitaka, T., Ueno-Kudoh, H., Sato, T., Yokoyama, S., et al. (2010). The Mohawk homeobox gene is a critical regulator of tendon differentiation. *Proc. Natl. Acad. Sci. U S A* 107, 10538–10542. doi: 10.1073/pnas.1000525107

Killian, M. L., and Thomopoulos, S. (2016). Scleraxis is required for the development of a functional tendon enthesis. *FASEB J.* 30, 301–311. doi: 10.1096/fj.14-258236

Kilts, T., Ameye, L., Syed-Picard, F., Ono, M., Berendsen, A. D., Oldberg, A., et al. (2009). Potential roles for the small leucine-rich proteoglycans biglycan and fibromodulin in ectopic ossification of tendon induced by exercise and in modulating rotarod performance. *Scand J. Med. Sci. Sports* 19, 536–546. doi: 10.1111/j.1600-0838.2009.00909.x

Kirov, J. V., Adkisson, M., Nava, A. J., Cipollone, A., Willis, B., Engelhard, E. K., et al. (2015). Reporter gene silencing in targeted mouse mutants is associated with promoter CpG Island Methylation. *PLoS One* 10:e0134155. doi: 10.1371/journal.pone.0134155

Klein-Hessling, S., Muhammad, K., Klein, M., Pusch, T., Rudolf, R., Floter, J., et al. (2017). NFATc1 controls the cytotoxicity of CD8(+) T cells. *Nat. Commun.* 8:511. doi: 10.1038/s41467-017-00612-6

Kuo, C. K., Petersen, B. C., and Tuan, R. S. (2008). Spatiotemporal protein distribution of TGF-betas, their receptors, and extracellular matrix molecules during embryonic tendon development. *Dev. Dyn.* 237, 1477–1489. doi: 10.1002/dvdy.21547

Lejard, V., Blais, F., Guerquin, M. J., Bonnet, A., Bonnin, M. A., Havis, E., et al. (2011). EGR1 and EGR2 involvement in vertebrate tendon differentiation. *J. Biol. Chem.* 286, 5855–5867. doi: 10.1074/jbc.M110.153106

Lejard, V., Brideau, G., Blais, F., Salingcarnboriboon, R., Wagner, G., Roehrl, M. H., et al. (2007). Scleraxis and NFATc regulate the expression of the pro-alpha1(I) collagen gene in tendon fibroblasts. *J. Biol. Chem.* 282, 17665–17675. doi: 10.1074/jbc.M610113200

Li, Y., Ramcharan, M., Zhou, Z., Leong, D. J., Akinbiyi, T., Majeska, R. J., et al. (2015). The role of scleraxis in fate determination of mesenchymal stem cells for tenocyte differentiation. *Sci. Rep.* 5:13149. doi: 10.1038/srep13149

Liao, Y., Smyth, G. K., and Shi, W. (2014). featureCounts: an efficient general purpose program for assigning sequence reads to genomic features. *Bioinformatics* 30, 923–930. doi: 10.1093/bioinformatics/btt656

Liu, H., Lan, Y., Xu, J., Chang, C. F., Brugmann, S. A., and Jiang, R. (2013). Odd-skipped related-1 controls neural crest chondrogenesis during tongue development. *Proc. Natl. Acad. Sci. U S A* 110, 18555–18560. doi: 10.1073/pnas.1306495110

Liu, H., Xu, J., and Jiang, R. (2019). Mkx-Deficient mice exhibit hedgehog signaling-dependent ectopic ossification in the achilles tendons. *J. Bone Miner Res.* 34, 557–569. doi: 10.1002/jbmr.3630

Liu, H., Xu, J., Liu, C. F., Lan, Y., Wylie, C., and Jiang, R. (2015). Whole transcriptome expression profiling of mouse limb tendon development by using RNA-seq. *J. Orthop. Res.* 33, 840–848. doi: 10.1002/jor.22886

Liu, W., Watson, S. S., Lan, Y., Keene, D. R., Ovitt, C. E., Liu, H., et al. (2010). The atypical homeodomain transcription factor Mohawk controls tendon morphogenesis. *Mol. Cell. Biol.* 30, 4797–4807. doi: 10.1128/MCB.00207-10

Love, M. I., Huber, W., and Anders, S. (2014). Moderated estimation of fold change and dispersion for RNA-seq data with DESeq2. *Genome Biol.* 15:550. doi: 10.1186/s13059-014-0550-8

Massari, M. E., and Murre, C. (2000). Helix-loop-helix proteins: regulators of transcription in eucaryotic organisms. *Mol. Cell. Biol.* 20, 429–440. doi: 10.1128/mcb.20.2.429-440.2000

McLean, C. Y., Bristor, D., Hiller, M., Clarke, S. L., Schaar, B. T., Lowe, C. B., et al. (2010). GREAT improves functional interpretation of cis-regulatory regions. *Nat. Biotechnol.* 28, 495–501. doi: 10.1038/nbt.1630

Murchison, N. D., Price, B. A., Conner, D. A., Keene, D. R., Olson, E. N., Tabin, C. J., et al. (2007). Regulation of tendon differentiation by scleraxis distinguishes force-transmitting tendons from muscle-anchoring tendons. *Development* 134, 2697–2708. doi: 10.1242/dev.001933

Nie, G. Y., Hampton, A., Li, Y., Findlay, J. K., and Salamonsen, L. A. (2003). Identification and cloning of two isoforms of human high-temperature requirement factor A3 (HtrA3), characterization of its genomic structure and comparison of its tissue distribution with HtrA1 and HtrA2. *Biochem. J.* 371, 39–48. doi: 10.1042/BJ20021569

Nourissat, G., Berenbaum, F., and Duprez, D. (2015). Tendon injury: from biology to tendon repair. *Nat. Rev. Rheumatol.* 11, 223–233. doi: 10.1038/nrrheum.2015.26

Paterson, Y. Z., Evans, N., Kan, S., Cribbs, A., Henson, F. M. D., and Guest, D. J. (2020). The transcription factor scleraxis differentially regulates gene expression in tenocytes isolated at different developmental stages. *Mech. Dev.* 163:103635. doi: 10.1016/j.mod.2020.103635

Pellegata, N. S., Dieguez-Lucena, J. L., Joensuu, T., Lau, S., Montgomery, K. T., Krahe, R., et al. (2000). Mutations in KERA, encoding keratocan, cause cornea plana. *Nat. Genet.* 25, 91–95. doi: 10.1038/75664

Pryce, B. A., Brent, A. E., Murchison, N. D., Tabin, C. J., and Schweitzer, R. (2007). Generation of transgenic tendon reporters, ScxGFP and ScxAP, using regulatory elements of the scleraxis gene. *Dev. Dyn.* 236, 1677–1682. doi: 10.1002/dvdy.21179

Pryce, B. A., Watson, S. S., Murchison, N. D., Staverosky, J. A., Dunker, N., and Schweitzer, R. (2009). Recruitment and maintenance of tendon progenitors by TGFbeta signaling are essential for tendon formation. *Development* 136, 1351–1361. doi: 10.1242/dev.027342

Risso, D., Ngai, J., Speed, T. P., and Dudoit, S. (2014). Normalization of RNA-seq data using factor analysis of control genes or samples. *Nat. Biotechnol.* 32, 896–902. doi: 10.1038/nbt.2931

Robinson, M. D., McCarthy, D. J., and Smyth, G. K. (2010). edgeR: a Bioconductor package for differential expression analysis of digital gene expression data. *Bioinformatics* 26, 139–140. doi: 10.1093/bioinformatics/btp616

Schweitzer, R., Chyung, J. H., Murtaugh, L. C., Brent, A. E., Rosen, V., Olson, E. N., et al. (2001). Analysis of the tendon cell fate using Scleraxis, a specific marker for tendons and ligaments. *Development* 128, 3855–3866.

Scott, M. A., and Hu, Y. C. (2019). Generation of CRISPR-edited rodents using a Piezo-Driven Zygote injection technique. *Methods Mol. Biol.* 1874, 169–178. doi: 10.1007/978-1-4939-8831-0_9

Shukunami, C., Takimoto, A., Nishizaki, Y., Yoshimoto, Y., Tanaka, S., Miura, S., et al. (2018). Scleraxis is a transcriptional activator that regulates the expression of Tenomodulin, a marker of mature tenocytes and ligamentocytes. *Sci. Rep.* 8:3155. doi: 10.1038/s41598-018-21194-3

Shukunami, C., Takimoto, A., Oro, M., and Hiraki, Y. (2006). Scleraxis positively regulates the expression of tenomodulin, a differentiation marker of tenocytes. *Dev. Biol.* 298, 234–247. doi: 10.1016/j.ydbio.2006.06.036

Sun, M., Luo, E. Y., Adams, S. M., Adams, T., Ye, Y., Shetye, S. S., et al. (2020). Collagen XI regulates the acquisition of collagen fibril structure, organization and functional properties in tendon. *Matrix Biol.* 94, 77–94. doi: 10.1016/j.matbio.2020.09.001

Suzuki, H., Ito, Y., Shinohara, M., Yamashita, S., Ichinose, S., Kishida, A., et al. (2016). Gene targeting of the transcription factor Mohawk in rats causes heterotopic ossification of Achilles tendon via failed tenogenesis. *Proc. Natl. Acad. Sci. U S A* 113, 7840–7845. doi: 10.1073/pnas.1522054113

Svensson, L., Aszodi, A., Reinholt, F. P., Fassler, R., Heinegard, D., and Oldberg, A. (1999). Fibromodulin-null mice have abnormal collagen fibrils, tissue organization, and altered lumican deposition in tendon. *J. Biol. Chem.* 274, 9636–9647. doi: 10.1074/jbc.274.14.9636

Wang, N., Zheng, Q., Zhang, J. S., and Zhao, Y. (2008). Molecular cloning and characterization of a novel mouse actin-binding protein Zfp185. *J. Mol. Histol.* 39, 295–302. doi: 10.1007/s10735-008-9165-2

Watson, S. S., Riordan, T. J., Pryce, B. A., and Schweitzer, R. (2009). Tendons and muscles of the mouse forelimb during embryonic development. *Dev. Dyn.* 238, 693–700. doi: 10.1002/dvdy.21866

Wenstrup, R. J., Smith, S. M., Florer, J. B., Zhang, G., Beason, D. P., Seegmiller, R. E., et al. (2011). Regulation of collagen fibril nucleation and initial fibril assembly involves coordinate interactions with collagens V and XI in developing tendon. *J. Biol. Chem.* 286, 20455–20465. doi: 10.1074/jbc.M111.223693

Xu, J., Liu, H., Lan, Y., Park, J. S., and Jiang, R. (2020). Genome-wide identification of Foxf2 target genes in palate development. *J. Dent. Res.* 99, 463–471. doi: 10.1177/0022034520904018

Xu, J., Liu, H., Park, J. S., Lan, Y., and Jiang, R. (2014). Osr1 acts downstream of and interacts synergistically with Six2 to maintain nephron progenitor cells during kidney organogenesis. *Development* 141, 1442–1452. doi: 10.1242/dev.103283

Yang, G., Rothrauff, B. B., and Tuan, R. S. (2013). Tendon and ligament regeneration and repair: clinical relevance and developmental paradigm. *Birth Defects Res. C Embryo Today* 99, 203–222. doi: 10.1002/bdrc.21041

Yoshimoto, Y., Takimoto, A., Watanabe, H., Hiraki, Y., Kondoh, G., and Shukunami, C. (2017). Scleraxis is required for maturation of tissue domains for proper integration of the musculoskeletal system. *Sci. Rep.* 7:45010. doi: 10.1038/srep45010

Yu, H. B., Yurieva, M., Balachander, A., Foo, I., Leong, X., Zelante, T., et al. (2015). NFATc2 mediates epigenetic modification of dendritic cell cytokine and chemokine responses to dectin-1 stimulation. *Nucleic Acids Res.* 43, 836–847. doi: 10.1093/nar/gku1369

Zhang, Y., Lan, H., Shao, Q., Wang, R., Chen, H., Tang, H., et al. (2016). An A20/AN1-type zinc finger protein modulates gibberellins and abscisic acid contents and increases sensitivity to abiotic stress in rice (Oryza sativa). *J. Exp. Bot.* 67, 315–326. doi: 10.1093/jxb/erv464

Conflict of Interest: The authors declare that the research was conducted in the absence of any commercial or financial relationships that could be construed as a potential conflict of interest.

frontiers in Cell and Developmental Biology

REVIEW
published: 04 June 2021
doi: 10.3389/fcell.2021.657621

Interplay of Forces and the Immune Response for Functional Tendon Regeneration

Yuwei Yang[1,2], Yicong Wu[1,2], Ke Zhou[1,2], Dongmei Wu[1,2], Xudong Yao[1,2], Boon Chin Heng[3], Jing Zhou[1,2], Hua Liu[1,2] and Hongwei Ouyang[1,2,4,5]**

[1] Dr. Li Dak Sum & Yip Yio Chin Center for Stem Cells and Regenerative Medicine, and Department of Orthopedic Surgery of The Second Affiliated Hospital, Zhejiang University School of Medicine, Hangzhou, China, [2] Zhejiang University-University of Edinburgh Institute, Zhejiang University School of Medicine, and Key Laboratory of Tissue Engineering and Regenerative Medicine of Zhejiang Province, Zhejiang University School of Medicine, Hangzhou, China, [3] Central Laboratories, School of Stomatology, Peking University, Beijing, China, [4] Department of Sports Medicine, Zhejiang University School of Medicine, Hangzhou, China, [5] China Orthopedic Regenerative Medicine Group (CORMed), Hangzhou, China

Tendon injury commonly occurs during sports activity, which may cause interruption or rapid decline in athletic career. Tensile strength, as one aspect of tendon biomechanical properties, is the main parameter of tendon function. Tendon injury will induce an immune response and cause the loss of tensile strength. Regulation of mechanical forces during tendon healing also changes immune response to improve regeneration. Here, the effects of internal/external forces and immune response on tendon regeneration are reviewed. The interaction between immune response and internal/external forces during tendon regeneration is critically examined and compared, in relation to other tissues. In conclusion, it is essential to maintain a fine balance between internal/external forces and immune response, to optimize tendon functional regeneration.

Keywords: tendon regeneration, biomechanical properties, immune response, stem cells, forces

OPEN ACCESS

Edited by:
Qiang Wu,
Macau University of Science and Technology, China

Reviewed by:
Chunming Wang,
University of Macau, China
Xing-xing Fan,
Macau University of Science and Technology, China

****Correspondence:***
Hua Liu
liuhua@zju.edu.cn
Hongwei Ouyang
hwoy@zju.edu.cn

Specialty section:
This article was submitted to Stem Cell Research, a section of the journal Frontiers in Cell and Developmental Biology

Received: *23 January 2021*
Accepted: *26 April 2021*
Published: *04 June 2021*

Citation:
Yang Y, Wu Y, Zhou K, Wu D, Yao X, Heng BC, Zhou J, Liu H and Ouyang H (2021) Interplay of Forces and the Immune Response for Functional Tendon Regeneration. Front. Cell Dev. Biol. 9:657621. doi: 10.3389/fcell.2021.657621

INTRODUCTION

Tendon is a key component of the musculoskeletal system, which physically connects muscle with bone and transmits mechanical forces from muscle to bone. The significant role of tendon tissue in human locomotion is determined by its function and position. However, tendon is easily injured due to unconscious overuse and has limited healing and regenerative capacity. This is best illustrated by a study related to the National Basketball Association, whereby more than a third of players ended their careers prematurely, or were unable to regain their top performance after Achilles tendon rupture, due to deterioration of tendon mechanical properties (Lemme et al., 2019). It was also shown that 38.4% of professional football players suffered subsequent re-injury after their first Achilles tendon injury (Ekstrand et al., 2020). Clinically, biomechanical properties, particularly tendon tensile strength, are often related to the extent of tendon repair (Frankewycz et al., 2018; Feichtinger et al., 2019). It is well-known that tendon injury always induces an immune response, which may further lead to further loss of tensile strength, making the repaired tendon susceptible to repeated injuries. Inflammation is an important driver of tendon healing, but persistent inflammation causes tendon fibrosis and other matrix changes (Dakin et al., 2014). Therefore, delineating the relationship between immune response and tensile strength is crucial

for optimizing tendon regeneration. Besides, external tensions including physiotherapy (Evans and Thompson, 1993) and biomaterials (Sawadkar et al., 2020) providing mechanical support can regulate inflammation. In this review, we will critically examine the effects of internal/external forces and immune responses, particularly the interplay of internal/external forces and the immune response on tendon regeneration.

CONTRIBUTION OF NORMAL TENDON STRUCTURAL BASIS TO TENDON BIOMECHANICS

The key of tendon biomechanics is tensile strength (Wu et al., 2018). Tensile strength reflects the maximum tensile load that tendon is capable of enduring, and it is closely related to elastic modulus, which is an important index to evaluate tendon repair effect. In clinical studies, the elastic modulus of human Achilles tendon is over 300 kPa, which will decrease to 3–200 kPa after Achilles tendon rupture (Chen et al., 2013). For tendons at other sites, the average tensile strength of tendons with tendinitis was significantly reduced by three times compared with healthy tendons (Dirrichs et al., 2016). In the locomotor system, the average elastic modulus of healthy muscle, which also belongs to soft tissue, is only 20 kPa (Nordez and Hug, 2010), which is 15-fold lower than that of tendon (Feng et al., 2018). The average Young's modulus of skin is between 4.5 and 8 kPa (Pailler-Mattei et al., 2008), which is far less than the mean value of tendon. In contrast, compared with the hard tissue, the average modulus of elasticity of cartilage is 500 kPa (Wilusz et al., 2013), which is higher than that of tendon. This is mainly related to the different ways to undergo mechanical stress in soft and hard tissue; that is, the soft tissues mainly undergo mechanical tension, and the hard tissues mainly undergo mechanical compression. Hence, in the case of the same way to undergo mechanical stress, the tensile strength of tendon is much higher than that of other soft tissues. Those are why tensile strength is considered the key characteristic biomechanical parameter of tendon. The excellent tensile strength of tendon depends on the normal tendon structural basis.

Tendon is a type of sparsely vascularized soft tissue (Lehner et al., 2016), with abundant extracellular matrix (ECM), but sparsely populated with a few cell types (**Figure 1**). Tendon ECM contains collagen, elastin, proteoglycan, glycoprotein, and other macromolecules (Thorpe and Screen, 2016). Collagen is the major component of tendon, which accounts for 60–85% of tendon dry weight (Monti and Miyagi, 2015). On day 14 of chicken embryo development, tendon structure begins to be established by pre-fibrils (Birk et al., 1989). In this stage, tendon shows a weak capability to transmit force, which means the beginning of limb movement (McBride et al., 1988). Collagen fibrils are aggregated into collagen fibers after day 17 or 18 of chicken embryo development (Birk and Zycband, 1994). In this stage, it shows a mechanical characteristic of mature tendon (McBride et al., 1988). The collagen fibers are the basis of the excellent biomechanical properties of tendon by functioning as tensile-resistant fibers (Screen et al., 2015). By spreading the tension throughout the entire tendon rather than just a small part of the tissue, tensile strength is enhanced (Kannus, 2000).

Elastin is one type of non-collagenous matrix molecule within tendon that plays an essential role in tendon biomechanical properties. In tendon, elastin forms a three-dimensional crisscross network and links adjacent collagen fascicles. The elastin network appears in developing tendons in the embryo between days 7.5 and 8 (Hurle et al., 1994). It can help collagen fibers transfer mechanical forces and protect them from excessive shear (Hill et al., 2020) through close physical linkage with adjacent collagen fibrils. Additionally, the elastin network envelops and protects cells (Pang et al., 2017). Besides elastin, various proteoglycans, glycoproteins, and other molecules also play important roles in regulating collagen fibrillogenesis. These provide non-covalent interactions by being integrated within the collagen fibrils (Birk et al., 1989) and help resist collagen fibril sliding, which enhances tendon viscoelasticity and decreases failure loads (Redaelli et al., 2003; Robinson et al., 2017), thus ensuring good tendon biomechanical properties. Taken together, the orderly and complex structure of tendon ECM is the basis of the excellent biomechanical properties of tendon, and this relationship has been established during embryonic development.

There are two main cell types in tendon, tenocytes, and tendon stem cells. Tenocytes are active in synthesizing and secreting collagen (Kannus, 2000). The tenocyte gap junctions are also considered as essential mediators of mechanosensitive responses (Maeda et al., 2012; Wu et al., 2018) that regulate tendon ECM synthesis and degradation (Young et al., 2009). Tendon stem cells are known as tendon stem/progenitor cells (TSPCs) or tendon-derived stem cell (TDSCs), which are functionally similar to mesenchymal stem cells (MSCs) (Docheva et al., 2015). TSPCs possess the capacities of self-renewal, clonogenicity (Bi et al., 2007), and differentiation (Magne and Bougault, 2015). These cells also contribute to biomechanical properties of embryonic tendon by their actin cytoskeleton network. Between days 8 and 11, actin cytoskeleton network related to high cell density and contact shows a similar spatial structure as collagen fibers, which is considered to provide tendon with biomechanical force (Schiele et al., 2015). The actin cytoskeleton network of cells in tendon can provide more than 20% elastic modulus (Schiele et al., 2015). In contrast, the contribution of myocytes to the elastic modulus of muscle tissue is 13–21% (Collinsworth et al., 2002), and chondrocytes, together with their ECM, provides about 12% of Young's modulus of cartilage (Alexopoulos et al., 2003). These findings suggest that although the tendon is mainly composed of ECM, the cells in tendon also affect tendon mechanics to a certain extent. Compared with other tissues in the locomotor system, tendon cells have a greater impact on tissue mechanics, which also suggests that we need to pay more attention to the metabolic activities of cells in the tendon in the process of tendon functional regeneration.

In adult injured tendon, histological results revealed that collagen are often in a disorganized state. The population of tenocytes is increased compared with normal tendon (Li and Hua, 2016) and TSPCs trended toward chondrogenic and osteogenic differentiation (Docheva et al., 2015). For this reason,

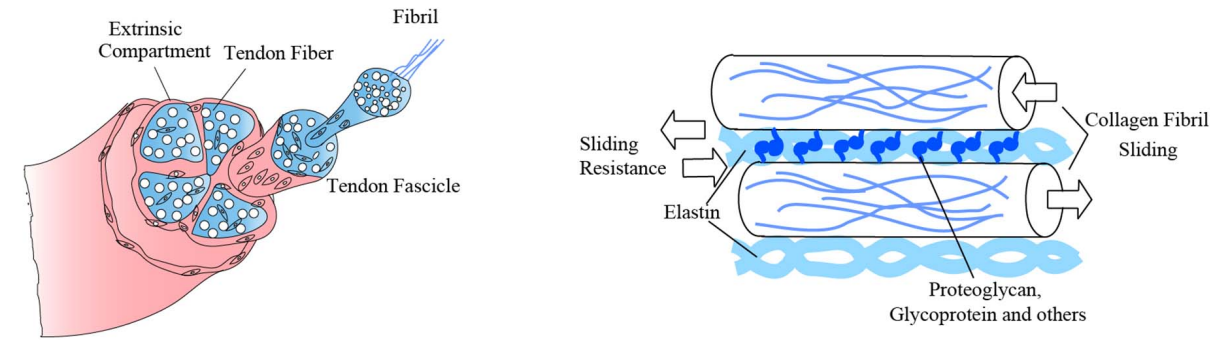

FIGURE 1 | The biomechanics of different components of tendon matrix ensure tensile strength of the whole tendon. **(A)** The main component of tendon is collagen. The base of tendon tissue is collagen fibers, which consist of collagen fibrils. **(B)** The tendon matrix components, collagen fibrils, elastin fibrils, proteoglycan, glycoprotein, and other macromolecules, combine with each other to provide micromechanics. These micromechanics interact and give rise to the macro-mechanics of tendon, which enable its biomechanical function.

more effective therapies should be developed in the future to enable tendon to achieve better regenerative effects, as close to the normal state as possible. At the cellular level, the ultimate goal of tendon regeneration is the normalization of cell number and ECM structure, as a basis for functional recovery of injured tendons.

INFLAMMATION IN THE PROCESS OF TENDON DISEASES REGULATES TENDON BIOMECHANICS

The deterioration of tensile strength is mostly due to disordered tendon matrix caused by a failed healing response in tendon diseases (Maffulli et al., 2010). There are three different pathogenesis of tendon diseases—genetic diseases, tendinopathy, and tendon rupture (Gaut and Duprez, 2016). Tendinopathy and tendon rupture are caused by external factors. Tendinopathy is a typical tendon disease, mostly manifesting after minor injury under long-term repeated overstress of tendon collagen fibers, which leads to chronic inflammation (Longo et al., 2009). In this process, inflammation does not subside and apoptotic cells fail to be cleared. With the stimulation of inflammation, tenocytes show high expression of stromal fibroblast activation markers to develop fibrosis (Dakin et al., 2018). Tendon rupture results from instantaneous overloading of external force or clinical operation. Compared with chronic inflammation, inflammation caused by rupture is more acute (Klatte-Schulz et al., 2018). Both tendinopathy and rupture can induce heterotopic ossification in tendon because of inflammation (Łęgosz et al., 2018). It has also been shown that tendon heterotopic ossification developing after rupture or tendinopathy will further decrease tensile strength, with calcium deposition in the tendon matrix and disordered collagen arrangement (Zhang et al., 2016). Furthermore, it has been demonstrated that, without the participation of the immune response, structural changes in tendon matrix induced by other environmental cues such as high glucose (Wu et al., 2017) contributes to the loss of tensile strength in tendon (Guney et al., 2015).

During inflammation, fibroblasts are recruited by immune cells to alter collagen arrangement, leading to negative changes in tensile strength (Best et al., 2019). At some time, suppression of macrophages can also cause increase of tensile strength because of high TGF-β3/TGF-β1 ratio similar to that in fetuses (De La Durantaye et al., 2014). This means that inflammation is actually one of the key factors that influence tendon functional regeneration by improving tensile strength. Furthermore, mechanosensitive proteins are usually influenced by the immune response, taking part in tendon regeneration. Take, for example, cystic fibrosis transmembrane conductance regulator (CFTR), one type of tension-mediated activation channel, which has been identified to be mechanosensitive under regenerative conditions in tendon (Liu et al., 2017). A further study confirmed that the anti-inflammatory molecule annexin A1 is a promising target of CFTR (Liu et al., 2018). This means that immune response takes part in the healing pathway involving some mechanosensitive genes or proteins that promote tendon regeneration.

IMMUNE RESPONSE DRIVES TENDON REPAIR

Inflammation is the main inducer of biomechanical decline in the process of tendon diseases; however, it is also one part of immune response that drives tendon repair. The tendon repair process can be extrinsic or intrinsic (Ingraham et al., 2003). The intrinsic repair process usually occurs during the fetal period in mammals (al-Qattan et al., 1993) or non-mammalian vertebrates (Andarawis-Puri et al., 2015) with minimal inflammatory cell infiltration and fibrosis (Ehrlich et al., 2005; Menzies et al., 2016). The extrinsic repair occurs in adult tendon, accompanied by inflammation (Koob and Summers, 2002). During intrinsic repair, the injury site has low ratio of TGF-β1/TGF-β3, which

is opposite to extrinsic repair (Ferguson and O'Kane, 2004). During extrinsic repair, excessive inflammatory response causes disruption of tendon ECM homeostasis, resulting in fibrosis and adhesive scar formation (Wu et al., 2019). Fibrosis and adhesive scar formation cause loss of biomechanical properties, which make these an extremely serious problem. During this process, fibroblasts proliferate and migrate from the epitenon and endotenon into the injured area, together with immune cell infiltration.

In general, with extrinsic repair of tendon, there are three stages involving wound healing, inflammation, proliferation, and rebuilding (Hope and Saxby, 2007; **Figure 2**). The changes in cell population and morphology and the compositions of matrices and molecules in peritendinous and intratendinous tissues are taken as the boundary standard of these three stages (Docheva et al., 2015). Firstly, the inflammatory stage is the most responsive stage after tendon injury. In this stage, there are significant inflammatory infiltrations of mast cells (Alim et al., 2017) and macrophages (Millar et al., 2010), with pro-inflammatory cytokines being present (Millar et al., 2008), as a result of platelet aggregation. Macrophages are the primary cells involved during the inflammatory stage, leading the direction of tendon healing. They release cytokines to trigger further inflammation (Hudgens et al., 2016). Mast cells are related to angiogenesis (Jetten et al., 2014) and pro-inflammatory response to tendon cells (Chisari et al., 2020), which can not only promote wound healing but also lead to decrease of the synthesis and degradation (Behzad et al., 2013) of tendon matrix. In this process, tendon cells will also respond to the inflammatory environment, regulate the production of type I collagen, and affect macrophage polarization through intercellular communication (Stolk et al., 2017). During the second stage, stromal fibroblasts are recruited and proliferate, in response to some cytokines such as interleukin (IL)-1β (Dakin et al., 2018) produced by inflammatory cells. At the same time, angiogenesis can also be observed (Oshiro et al., 2003). It is worth mentioning that in the injured tendon, the ratio of type I to type III collagen is lower than the native tendon (Williams et al., 1980). The reason is that the production of type III collagen increases because of the rapid proliferation of stromal fibroblasts. The rebuilding stage begins at this time point. At this stage, the synthesis of type I collagen is predominant, instead of type III collagen, and the organized collagen fibrils is progressively arranged into bundles. However, the ratio will not return to the normal level as before. Finally, fibrosis and excessive angiogenesis will result in further development into tendonitis. Apart from that, a few studies have reported that adaptive immune responses also exist after tendon injury. In the early inflammatory response, macrophages and dendritic cells present antigens, and dendritic cells allow rapid accumulation of T cells and B cells. Accordingly, a peak in the number of dendritic cells and $CD4^+$ T cells can be observed after 2 weeks of injury, while the number of B cells and $CD8^+$ T cells increases with time (Blomgran et al., 2016; Noah et al., 2020). During this process, $CD4^+$ T lymphocytes lead to an increase in fibronectin around tendon, providing a scaffold for the subsequent formation of adhesions, thereby reducing the mechanical properties of tendons (Wojciak and Crossan, 1993). It has been shown that the use of corticosteroids during the adaptive immune response of tendon healing reduces the number of $CD8a^+$ cytotoxic T cells, improving tendon healing (Blomgran et al., 2017). Although studies of innate and adaptive immune responses during tendon healing has been a lot, there is still much that remains to be studied, especially the specific effects of adaptive immunity on the tendon matrix structure.

Nevertheless, the immune response is more about playing a positive role in promoting tendon regeneration, particularly with the involvement of activated macrophages (Millar et al., 2017) and related cytokines (Gelberman et al., 2017). There are two main types of macrophages, M1 and M2. M1 macrophages exert a pro-inflammatory role during the early repair phase, yet M2 macrophages are able to exert anti-inflammatory effects to improve regeneration (Mauro et al., 2016). As a result, compared with M1 macrophages, more attention is paid to M2 macrophages, due to their more significant role in tendon regeneration. Recently, M2 macrophages are found to be able to accelerate regenerative responses in tendon healing (Chamberlain et al., 2019). Several recent therapeutic approaches

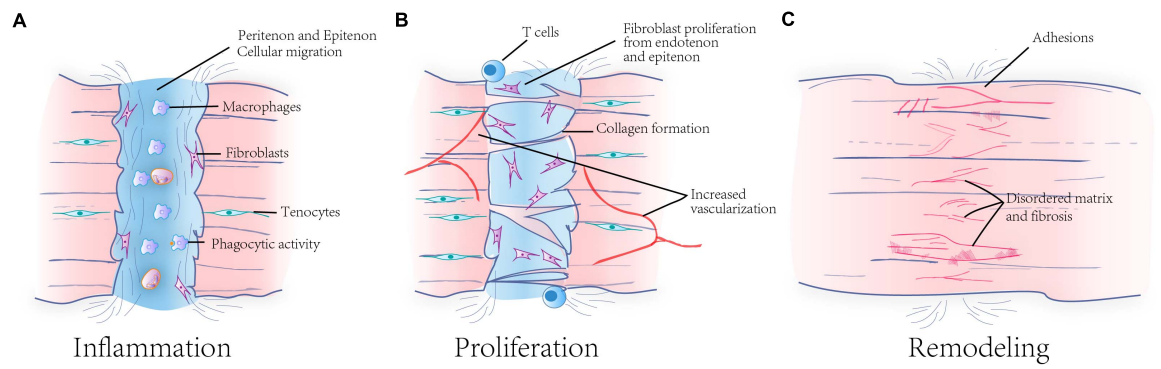

FIGURE 2 | Three phases of tendon healing and the matrix changes during the healing process. Tendon healing goes through three phases, including inflammation **(A)**, proliferation **(B)**, and remodeling **(C)**. In the inflammation phase, immune cells and fibroblasts from peritenon and epitenon migrate into injured position. In the proliferation phase, fibroblasts proliferate and angiogenesis occurs in this time. In the remodeling phase, repaired tendon has disordered matrix. The injured tendon finally forms tendon fibrosis and adhesion.

targeting macrophages have also shown that increasing the proportion of M2-type macrophages during tendon healing improves tendon biomechanical performance (Sunwoo et al., 2020). Moreover, inflammatory factors and cytokines are considered to indirectly regulate immune cells like macrophages during tendon scarless healing (Gelberman et al., 2017; Best et al., 2019). For adaptive immunity, a specialized T cell population is also present in tendons, which shows CD4 and CD8 double-negative. This population secretes IL-22 and potentially mediates tendon-to-bone healing (Sherlock et al., 2012; Abraham et al., 2017).

Furthermore, biomaterials can be applied to regulate the inflammatory response to promote tendon healing. In this regard, the main consideration is given to the bacteriostatic effect, biocompatibility, and modulation of immune cells of biomaterials. The bacteriostatic effect and biocompatibility of biomaterials are the most intensively considered aspects in tissue engineering. A study of biomaterials commonly used in tissue engineering has shown that hyaluronic acid has a significantly higher bacteriostatic effect than type I collagen and PLGA. Type I collagen has better biocompatibility in tendons, but *Staphylococcus aureus* can still establish itself in collagen scaffolds with high concentration. However, PLGA is less biocompatible and generates an acidic environment at the implantation site, which induces inflammatory reactions (Carlson et al., 2004). In addition, the new silk scaffolds used for tendon repair can enhance the maturation of dendritic cells and induce the generation of early immunity (Musson et al., 2015). Therefore, the selection of an appropriate biomaterial is very important for tendon repair. The modulation of immune cells by biomaterials has been extensively studied. The effects of biomaterials on macrophage polarization in tendon repair have been summarized; that is, biomaterials with ECM coatings, hydrophilic surfaces, and nanometer sizes can induce macrophage activation (Lin et al., 2018), whereas in recent years, other properties of biomaterials have also been shown to regulate macrophages. Magnetic materials, for example, have been shown to induce macrophage to M2 transition (Vinhas et al., 2020). The fiber arrangement of biomaterials also influences the polarization of macrophages to promote tendon repair (Schoenenberger et al., 2020).

INTERPLAY OF THE IMMUNE RESPONSE AND FORCES IMPROVES TENDON REGENERATION

In the regeneration of other tissues, such as cartilage and bone, the relationship between forces and immune response after injury has been characterized (Guilak et al., 2008; Raghunathan et al., 2017) and their interaction influences the regenerative effect. It has been demonstrated that external stimulation of cartilage are associated with inflammation and exert a profound influence on cartilage regeneration (Chen M. et al., 2018). Physical stimulation also causes sensitive response of pro-inflammatory mediators around injury areas (Fahy et al., 2019). These findings directly validate the potential influence of external forces on inflammation. Inflammation also facilitates the recovery of mechanical properties as well. One type of transcriptional regulator induced by immune cells is a mediator of the crosstalk between IL-4 and mechanical-induced signaling pathways, which suppresses the degradation of cartilage matrix (He et al., 2019). As we can see from this study, the interplay of immune response and forces improves cartilage healing. In view of its good prospect for clinical applications in other tissue regeneration therapies, it is worthwhile considering studying it in tendon.

The tune-up of the immune response and forces in tendon could be described in two parts (**Figure 3**). Firstly, the influence of immune response on tensile strength, and secondly, the influence of external forces on immune response. On one hand, immune response influences tensile strength, as mentioned above. On the other hand, cyclic stretching or overloading tends to trigger strong immune responses that will exacerbate tendinopathy (Chen Q. et al., 2018; Schoenenberger et al., 2018). Specifically, microinjuries of collagen fibrils resulting from overloaded stretch that eventually deform to 10–15% (Chen Q. et al., 2018) can also significantly reduce cell viability within tendons, while microinjuries that accumulate within tendon collagen fibrils ultimately activate immune responses (Stauber et al., 2020), increase expression of inflammatory markers, and lead to degradation of the tendon matrix (Thorpe et al., 2015). Cyclic stretching on tendon fibroblasts also produces a significant elevation in the expression of the inflammatory-related factor leukotriene B4 (Li et al., 2004). In an *in vivo* experiment, cyclic loading at low strength also caused an increase in the number of inflammatory macrophages at the tendon-to-bone healing after anterior cruciate ligament (ACL) reconstruction (Brophy et al., 2011). This implies the influence of mechanical loading on tendon-to-bone healing after clinical ACL reconstruction surgery. It also supported the idea that the use of anti-inflammatory drugs in the presence of cyclic stretching also leads to the development of tendinopathy (Li et al., 2004). This suggests that anti-inflammatory drugs are not able to suppress the immune response caused by cyclic stretching. Besides, there are currently no exact control and preventive methods for the inflammatory response resulting from such cyclic stretching or overloading. However, on the positive side, appropriate external forces also play a role in tendon regeneration. In one treatment modality, in order to restore normal ECM structure, tendons have been shown to respond to external tensile loading during healing (Freedman et al., 2018). Recently, dynamic stretching and substrates with mechanical property gradients have been reported to promote the differentiation of stem cells into tenocytes (Liu et al., 2017) and increase matrix production by differentiated tenocytes (Deng et al., 2014). Additionally, a multi-scale computational model for investigating the relationship between loading and tendon healing has been built (Chen K. et al., 2018). This model shows that the magnitude and application time of loading are crucial to tendon healing and regulation of collagen synthesis (Packer et al., 2014). Besides, the immune response is also regulated by stretch similar to biomechanics or mechanical loading provided by biomaterials or mechanical devices in tendon regeneration. In a recent study, mechanical loading appears to regulate M1 phase of

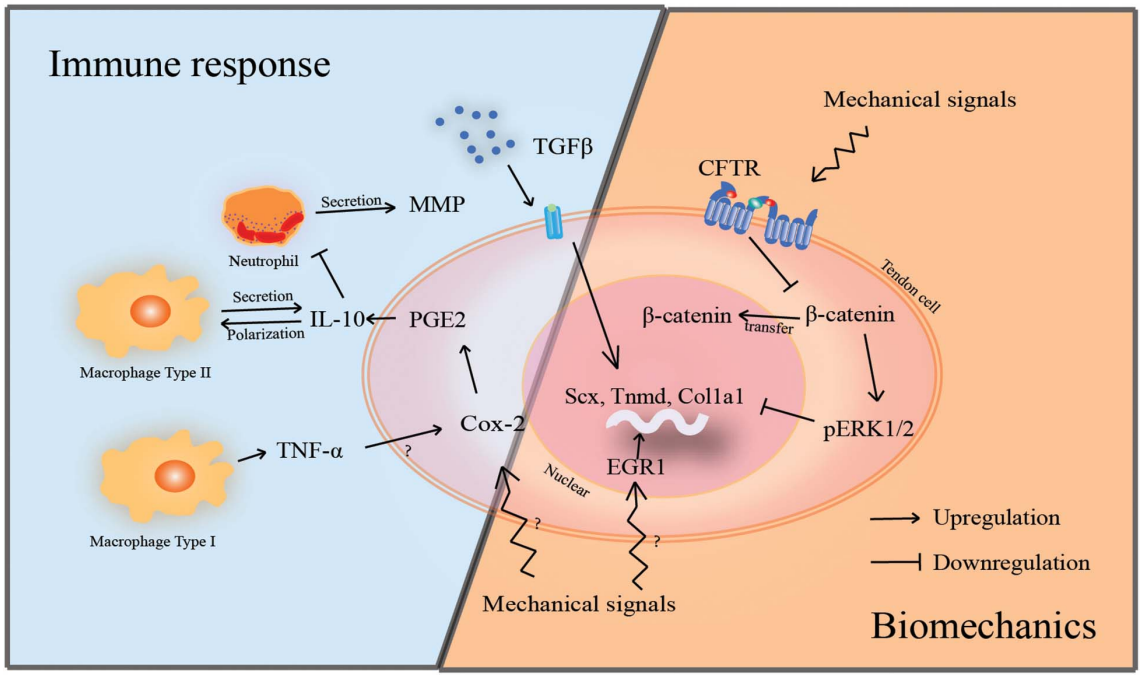

FIGURE 3 | Both mechanical signals and immune response can regulate tendon cells and further influence tendon regeneration. Inflammation and mechanical signals can control the tenogenic differentiation by regulating the transcription of tendon markers in tendon cells. Some cytokines and mechanical signals have the same targets, indicating a kind of potential co-regulation pathway. However, most mechanosensitive proteins are unknown, and the inflammation process still needs a deeper understanding. In that, it is necessary to figure out the mechanism of the balance between biomechanics and immune response during tendon regeneration.

inflammation, which improves tendon regeneration (Blomgran et al., 2016). Mechanosensitive proteins or genes contribute to immune responses during the tendon healing process as well. One mechanosensitive transcription factor, known as early growth response-1 (EGR1), plays a key role in the inflammatory response (Soo et al., 2006), and overexpression of EGR1 has been demonstrated to promote tendon healing (Gaut et al., 2016). This indicates the potential value of mechanosensitive protein in the regulation of immune response. As known, the properties of biomaterials such as tension within the fibers can modulate tendon healing capacity (Brammer et al., 2012; Zhang et al., 2017). Furthermore, whether the effects of the immune response on tendon healing can be modulated by biomaterials is an intriguing topic. To investigate that, a study showed that highly aligned fibers mitigate adverse tendon fibroblast response to paracrine signals or secreted pro-inflammatory cytokines of macrophages, by means of changing the matrix topography (Schoenenberger et al., 2018), and in this case, macrophages also showed a trend to M2-like polarization (Schoenenberger et al., 2020). This means that biomimetic scaffolds will regulate tendon resident cells' response to inflammation and even affect the development of inflammation through the force between scaffold fibers.

The interplay between forces and immune response has been widely observed in animal models and clinical trials. Because forces are more easily controllable, most applications are based on mechanical regulation. For example, biomechanics provided by biomaterial scaffold fibers can regulate inflammatory activation in rat tendons (Schoenenberger et al., 2020). In clinical trials, strength training provides stretch forces that mitigate the detrimental effects of inflammation (Lee et al., 2012; Hoogvliet et al., 2013). The complex relationship between forces and inflammation during the process of tendon healing suggests a delicate balance that modulates tendon functional regeneration. However, the mechanisms by which tendon tissues maintain the fine balance between their mechanosensitive components and the immune response are still largely unknown. Generally speaking, we should analyze the molecular mechanisms and interactions of such interplay and fine balance to realize the future potential of tendon functional regeneration.

CONCLUSION

Immune responses in tendon healing have been studied for decades (Sharma and Maffulli, 2005). The participation of immune components is already well-known, but we still lack a systematic and widely accepted understanding of the mechanistic pathway of the tendon healing process and its negative result—tendon diseases. As a result, tendon diseases remain an intractable clinical problem. The imbalanced anabolic–catabolic responses during the development of inflammation results in matrix degradation and disordered structure, which impairs

tendon tensile strength. Moreover, the recovery of normal tendon biomechanical properties and matrix is the basis of tendon functional regeneration. However, the contribution of collagen, elastin, and other macromolecular components to tendon biomechanics remains a systematical extrapolation. The limited knowledge and poor understanding of tendon biomechanical properties and matrix leads to limitations on tendon healing. On the other hand, the effects of mechanics is well-recognized at the cellular level, as mentioned above, but it is not deep enough to further improve tendon healing *in vivo* by way of external forces because the suitable range of external forces is still unclear. Even though a large number of studies on its positive effects has been carried out in animal models and clinical trials, there are few papers at the clinical level that explore the mechanisms of moderate loading on tendon healing. Currently, our knowledge of mechanosensitive proteins and genes is still developing. In conclusion, the deficiency of studies on the interplay between tendon immune response and internal/external forces is one of the limiting factors that hinder tendon functional regeneration.

Taken together, it is necessary to consider both the immune response and internal/external forces to achieve a better understanding of the mechanisms by which these contribute to tendon functional regeneration. The level of immune response is one of the key factors that determine the recovery of tendon internal forces. Additionally, mechanical changes caused by the exertion of internal or external forces on the tendon also modulate the immune response during tendon healing. It is hypothesized that tendon functional regeneration may be achieved by tuning up the immune response and internal/external forces.

AUTHOR CONTRIBUTIONS

YY, BH, and HL: conception, design, and manuscript writing. YW and XY: conception and design. KZ and DW: collection and assembly of data. JZ: manuscript writing. HO: conception, design, and final approval of manuscript. All authors contributed to the article and approved the submitted version.

FUNDING

This work was supported by the National Key R&D Program of China (2017YFA0104900).

REFERENCES

Abraham, A. C., Shah, S. A., and Thomopoulos, S. (2017). Targeting inflammation in rotator cuff tendon degeneration and repair. *Tech. Shoulder Elb. Surg.* 18, 84–90. doi: 10.1097/BTE.0000000000000124

al-Qattan, M. M., Posnick, J. C., Lin, K. Y., and Thorner, P. (1993). Fetal tendon healing: development of an experimental model. *Plast. Reconstr. Surg.* 92, 1155–1160; discussion 1161.

Alexopoulos, L. G., Haider, M. A., Vail, T. P., and Guilak, F. (2003). Alterations in the mechanical properties of the human chondrocyte pericellular matrix with osteoarthritis. *J. Biomech. Eng.* 125, 323–333. doi: 10.1115/1.1579047

Alim, M. A., Ackermann, P. W., Eliasson, P., Blomgran, P., Kristiansson, P., Pejler, G., et al. (2017). Increased mast cell degranulation and co-localization of mast cells with the NMDA receptor-1 during healing after Achilles tendon rupture. *Cell Tissue Res.* 370, 451–460. doi: 10.1007/s00441-017-2684-y

Andarawis-Puri, N., Flatow, E. L., and Soslowsky, L. J. (2015). Tendon basic science: development, repair, regeneration, and healing. *J. Orthop. Res.* 33, 780–784. doi: 10.1002/jor.22869

Behzad, H., Sharma, A., Mousavizadeh, R., Lu, A., and Scott, A. (2013). Mast cells exert pro-inflammatory effects of relevance to the pathophyisology of tendinopathy. *Arthritis Res. Ther.* 15:R184. doi: 10.1186/ar4374

Best, K. T., Lee, F. K., Knapp, E., Awad, H. A., and Loiselle, A. E. (2019). Deletion of NFKB1 enhances canonical NF-κB signaling and increases macrophage and myofibroblast content during tendon healing. *Sci. Rep.* 9:10926. doi: 10.1038/s41598-019-47461-5

Bi, Y., Ehirchiou, D., Kilts, T. M., Inkson, C. A., Embree, M. C., Sonoyama, W., et al. (2007). Identification of tendon stem/progenitor cells and the role of the extracellular matrix in their niche. *Nat. Med.* 13, 1219–1227. doi: 10.1038/nm1630

Birk, D. E., Southern, J. F., Zycband, E. I., Fallon, J. T., and Trelstad, R. L. (1989). Collagen fibril bundles: a branching assembly unit in tendon morphogenesis. *Development* 107, 437–443.

Birk, D. E., and Zycband, E. (1994). Assembly of the tendon extracellular matrix during development. *J. Anat.* 184, 457–463.

Blomgran, P., Blomgran, R., Ernerudh, J., and Aspenberg, P. (2016). A possible link between loading, inflammation and healing: immune cell populations during tendon healing in the rat. *Sci. Rep.* 6:29824. doi: 10.1038/srep29824

Blomgran, P., Hammerman, M., and Aspenberg, P. (2017). Systemic corticosteroids improve tendon healing when given after the early inflammatory phase. *Sci. Rep.* 7:12468. doi: 10.1038/s41598-017-12657-0

Brammer, K. S., Frandsen, C. J., and Jin, S. (2012). TiO2 nanotubes for bone regeneration. *Trends Biotechnol.* 30, 315–322. doi: 10.1016/j.tibtech.2012.02.005

Brophy, R. H., Kovacevic, D., Imhauser, C. W., Stasiak, M., Bedi, A., Fox, A. J. S., et al. (2011). Effect of short-duration low-magnitude cyclic loading versus immobilization on tendon-bone healing after ACL reconstruction in a rat model. *J. Bone Joint. Surg. Ser. A* 93, 381–393. doi: 10.2106/JBJS.I.00933

Carlson, G. A., Dragoo, J. L., Samimi, B., Bruckner, D. A., Bernard, G. W., Hedrick, M., et al. (2004). Bacteriostatic properties of biomatrices against common orthopaedic pathogens. *Biochem. Biophys. Res. Commun.* 321, 472–478. doi: 10.1016/j.bbrc.2004.06.165

Chamberlain, C. S., Clements, A. E. B., Kink, J. A., Choi, U., Baer, G. S., Halanski, M. A., et al. (2019). Extracellular vesicle-educated macrophages promote early achilles tendon healing. *Stem Cells* 37, 652–662. doi: 10.1002/stem.2988

Chen, K., Hu, X., Blemker, S. S., and Holmes, J. W. (2018). Multiscale computational model of Achilles tendon wound healing: untangling the effects of repair and loading. *PLoS Comput. Biol.* 14:1006652. doi: 10.1371/journal.pcbi.1006652

Chen, M., Guo, W., Gao, S., Hao, C., Shen, S., Zhang, Z., et al. (2018). Biomechanical stimulus based strategies for meniscus tissue engineering and regeneration. *Tissue Eng. Part B Rev.* 24, 392–402. doi: 10.1089/ten.teb.2017.0508

Chen, Q., Zhou, J., Zhang, B., Chen, Z., Luo, Q., and Song, G. (2018). Cyclic stretching exacerbates tendinitis by enhancing NLRP3 inflammasome activity via F-Actin depolymerization. *Inflammation* 41, 1731–1743. doi: 10.1007/s10753-018-0816-5

Chen, X. M., Cui, L. G., He, P., Shen, W. W., Qian, Y. J., and Wang, J. R. (2013). Shear wave elastographic characterization of normal and torn Achilles tendons: a pilot study. *J. Ultrasound Med.* 32, 449–455. doi: 10.7863/jum.2013.32.3.449

Chisari, E., Rehak, L., Khan, W. S., and Maffulli, N. (2020). The role of the immune system in tendon healing: a systematic review. *Br. Med. Bull.* 133, 49–64. doi: 10.1093/bmb/ldz040

Collinsworth, A. M., Zhang, S., Kraus, W. E., and Truskey, G. A. (2002). Apparent elastic modulus and hysteresis of skeletal muscle cells throughout

differentiation. *Am. J. Physiol. Cell Physiol.* 283, 1219–1227. doi: 10.1152/ajpcell.00502.2001

Dakin, S. G., Dudhia, J., and Smith, R. K. W. (2014). Resolving an inflammatory concept: the importance of inflammation and resolution in tendinopathy. *Vet. Immunol. Immunopathol.* 158, 121–127. doi: 10.1016/j.vetimm.2014.01.007

Dakin, S. G., Newton, J., Martinez, F. O., Hedley, R., Gwilym, S., Jones, N., et al. (2018). Chronic inflammation is a feature of Achilles tendinopathy and rupture. *Br. J. Sports Med.* 52, 359–367. doi: 10.1136/bjsports-2017-098161

De La Durantaye, M., Piette, A. B., Van Rooijen, N., and Frenette, J. (2014). Macrophage depletion reduces cell proliferation and extracellular matrix accumulation but increases the ultimate tensile strength of injured Achilles tendons. *J. Orthop. Res.* 32, 279–285. doi: 10.1002/jor.22504

Deng, D., Wang, W., Wang, B., Zhang, P., Zhou, G., Zhang, W. J., et al. (2014). Repair of Achilles tendon defect with autologous ASCs engineered tendon in a rabbit model. *Biomaterials* 35, 8801–8809. doi: 10.1016/j.biomaterials.2014.06.058

Dirrichs, T., Quack, V., Gatz, M., Tingart, M., Kuhl, C. K., and Schrading, S. (2016). Shear Wave elastography (SWE) for the evaluation of patients with tendinopathies. *Acad. Radiol.* 23, 1204–1213. doi: 10.1016/j.acra.2016.05.012

Docheva, D., Müller, S. A., Majewski, M., and Evans, C. H. (2015). Biologics for tendon repair. *Adv. Drug Deliv. Rev.* 84, 222–239. doi: 10.1016/j.addr.2014.11.015

Ehrlich, H. P., Lambert, P. A., Saggers, G. C., Myers, R. L., and Hauck, R. M. (2005). Dynamic changes appearing in collagen fibers during intrinsic tendon repair. *Ann. Plast. Surg.* 54, 201–206. doi: 10.1097/01.sap.0000141380.52782.db

Ekstrand, J., Krutsch, W., Spreco, A., van Zoest, W., Roberts, C., Meyer, T., et al. (2020). Time before return to play for the most common injuries in professional football: a 16-year follow-up of the UEFA Elite Club Injury Study. *Br. J. Sports Med.* 54, 421–426. doi: 10.1136/bjsports-2019-100666

Evans, R. B., and Thompson, D. E. (1993). The application of force to the healing tendon. *J. Hand Ther. Off. J. Am. Soc. Hand Ther.* 6, 266–284. doi: 10.1016/s0894-1130(12)80328-0

Fahy, N., Menzel, U., Alini, M., and Stoddart, M. J. (2019). Shear and dynamic compression modulates the inflammatory phenotype of human monocytes in vitro. *Front. Immunol.* 10:383. doi: 10.3389/fimmu.2019.00383

Feichtinger, X., Monforte, X., Keibl, C., Hercher, D., Schanda, J., Teuschl, A. H., et al. (2019). Substantial biomechanical improvement by extracorporeal shockwave therapy after surgical repair of rodent chronic rotator cuff tears. *Am. J. Sports Med.* 47, 2158–2166. doi: 10.1177/0363546519854760

Feng, Y. N., Li, Y. P., Liu, C. L., and Zhang, Z. J. (2018). Assessing the elastic properties of skeletal muscle and tendon using shearwave ultrasound elastography and MyotonPRO. *Sci. Rep.* 8:17064. doi: 10.1038/s41598-018-34719-7

Ferguson, M. W. J., and O'Kane, S. (2004). Scar-free healing: from embryonic mechanism to adult therapeutic intervention. *Philos. Trans. R. Soc. B Biol. Sci.* 359, 839–850. doi: 10.1098/rstb.2004.1475

Frankewycz, B., Penz, A., Weber, J., da Silva, N. P., Freimoser, F., Bell, R., et al. (2018). Achilles tendon elastic properties remain decreased in long term after rupture. *Knee Surg. Sports Traumatol. Arthrosc.* 26, 2080–2087. doi: 10.1007/s00167-017-4791-4

Freedman, B. R., Rodriguez, A. B., Leiphart, R. J., Newton, J. B., Ban, E., Sarver, J. J., et al. (2018). Dynamic loading and tendon healing affect multiscale tendon properties and ECM stress transmission. *Sci. Rep.* 8:10854. doi: 10.1038/s41598-018-29060-y

Gaut, L., and Duprez, D. (2016). Tendon development and diseases. *Wiley Interdiscip. Rev. Dev. Biol.* 5, 5–23. doi: 10.1002/wdev.201

Gaut, L., Robert, N., Delalande, A., Bonnin, M. A., Pichon, C., and Duprez, D. (2016). EGR1 regulates transcription downstream of mechanical signals during tendon formation and healing. *PLoS One* 11:0166237. doi: 10.1371/journal.pone.0166237

Gelberman, R. H., Linderman, S. W., Jayaram, R., Dikina, A. D., Sakiyama-Elbert, S., Alsberg, E., et al. (2017). Combined administration of ASCs and BMP-12 promotes an M2 macrophage phenotype and enhances tendon healing. *Clin. Orthop. Relat. Res.* 475, 2318–2331. doi: 10.1007/s11999-017-5369-7

Guilak, F., Fermor, B., Keefe, F. J., Kraus, V. B., Olson, S. A., Pisetsky, D. S., et al. (2008). The role of biomechanics and inflammation in cartilage injury and repair. *Clin. Orthop. Relat. Res.* 23, 1–7. doi: 10.1038/jid.2014.371

Guney, A., Vatansever, F., Karaman, I., Kafadar, I. H., Oner, M., and Turk, C. Y. (2015). Biomechanical properties of achilles tendon in diabetic vs non-diabetic patients. *Exp. Clin. Endocrinol. Diabetes* 123, 428–432. doi: 10.1055/s-0035-1549889

He, Z., Leong, D. J., Xu, L., Hardin, J. A., Majeska, R. J., Schaffler, M. B., et al. (2019). CITED2 mediates the cross-talk between mechanical loading and IL-4 to promote chondroprotection. *Ann. N. Y. Acad. Sci.* 1442, 128–137. doi: 10.1111/nyas.14021

Hill, J. R., Eekhoff, J. D., Brophy, R. H., and Lake, S. P. (2020). Elastic fibers in orthopedics: form and function in tendons and ligaments, clinical implications, and future directions. *J. Orthop. Res.* 38, 2305–2317. doi: 10.1002/jor.24695

Hoogvliet, P., Randsdorp, M. S., Dingemanse, R., Koes, B. W., and Huisstede, B. M. A. (2013). Does effectiveness of exercise therapy and mobilization techniques offer guidance for the treatment of lateral and medial epicondylitis? A systematic review. *Br. J. Sports Med.* 47, 1112–1119. doi: 10.1136/bjsports-2012-091990

Hope, M., and Saxby, T. S. (2007). Tendon healing. *Foot Ankle Clin.* 12, 553–567. doi: 10.1016/j.fcl.2007.07.003

Hudgens, J. L., Sugg, K. B., Grekin, J. A., Gumucio, J. P., Bedi, A., and Mendias, C. L. (2016). Platelet-Rich plasma activates proinflammatory signaling pathways and induces oxidative stress in tendon fibroblasts. *Am. J. Sports Med.* 44, 1931–1940. doi: 10.1177/0363546516637176

Hurle, J. M., Corson, G., Daniels, K., Reiter, R. S., Sakai, L. Y., and Solursh, M. (1994). Elastin exhibits a distinctive temporal and spatial pattern of distribution in the developing chick limb in association with the establishment of the cartilaginous skeleton. *J. Cell Sci.* 107, 2623–2634.

Ingraham, J. M., Hauck, R. M., and Ehrlich, H. P. (2003). Is the tendon embryogenesis process resurrected during tendon healing? *Plast. Reconstr. Surg.* 112, 844–854. doi: 10.1097/01.PRS.0000070180.62037.FC

Jetten, N., Verbruggen, S., Gijbels, M. J., Post, M. J., De Winther, M. P. J., and Donners, M. M. P. C. (2014). Anti-inflammatory M2, but not pro-inflammatory M1 macrophages promote angiogenesis in vivo. *Angiogenesis* 17, 109–118. doi: 10.1007/s10456-013-9381-6

Kannus, P. (2000). Structure of the tendon connective tissue. *Scand. J. Med. Sci. Sport* 10, 312–320.

Klatte-Schulz, F., Minkwitz, S., Schmock, A., Bormann, N., Kurtoglu, A., Tsitsilonis, S., et al. (2018). Different achilles tendon pathologies show distinct histological and molecular characteristics. *Int. J. Mol. Sci.* 19:404. doi: 10.3390/ijms19020404

Koob, T. J., and Summers, A. P. (2002). Tendon–bridging the gap. *Comp. Biochem. Physiol. A Mol. Integr. Physiol.* 133, 905–909. doi: 10.1016/S1095-6433(02)00255-6

Lee, B. G., Cho, N. S., and Rhee, Y. G. (2012). Effect of two rehabilitation protocols on range of motion and healing rates after arthroscopic rotator cuff repair: aggressive versus limited early passive exercises. *Arthrosc. J. Arthrosc. Relat. Surg.* 28, 34–42. doi: 10.1016/j.arthro.2011.07.012

Łęgosz, P., Drela, K., Pulik, Ł, Sarzyńska, S., and Małdyk, P. (2018). Challenges of heterotopic ossification—Molecular background and current treatment strategies. *Clin. Exp. Pharmacol. Physiol.* 45, 1229–1235. doi: 10.1111/1440-1681.13025

Lehner, C., Gehwolf, R., Ek, J., Korntner, S., Bauer, H., Bauer, H.-C., et al. (2016). The blood-tendon barrier: identification and characterisation of a novel tissue barrier in tendon blood vessels. *Eur. Cells Mater.* 31, 296–311. doi: 10.22203/ecm.v031a19

Lemme, N. J., Li, N. Y., Kleiner, J. E., Tan, S., DeFroda, S. F., and Owens, B. D. (2019). Epidemiology and video analysis of achilles tendon ruptures in the national basketball association. *Am. J. Sports Med.* 47, 2360–2366. doi: 10.1177/0363546519858609

Li, H. Y., and Hua, Y. H. (2016). Achilles tendinopathy: current concepts about the basic science and clinical treatments. *Biomed Res. Int.* 2016:6492597. doi: 10.1155/2016/6492597

Li, Z., Yang, G., Khan, M., Stone, D., Woo, S. L. Y., and Wang, J. H. C. (2004). Inflammatory response of human tendon fibroblasts, to cyclic mechanical stretching. *Am. J. Sports Med.* 32, 435–440. doi: 10.1177/0095399703258680

Lin, J., Zhou, W., Han, S., Bunpetch, V., Zhao, K., Liu, C., et al. (2018). Cell-material interactions in tendon tissue engineering. *Acta Biomater.* 70, 1–11. doi: 10.1016/j.actbio.2018.01.012

Liu, Y., Feng, L., Wang, H., Wang, Y., Chan, H.-C., Jiang, X., et al. (2018). Identification of an anti-inflammation protein, annexin A1, in tendon derived stem cells (TDSCs) of cystic fibrosis mice: a comparative proteomic analysis. *Proteomics Clin. Appl.* 12:1700162. doi: 10.1002/prca.201700162

Liu, Y., Xu, J., Xu, L., Wu, T., Sun, Y., Lee, Y.-W., et al. (2017). Cystic fibrosis transmembrane conductance regulator mediates tenogenic differentiation of tendon-derived stem cells and tendon repair: accelerating tendon injury healing by intervening in its downstream signaling. *FASEB J. Off. Publ. Fed. Am. Soc. Exp. Biol.* 31, 3800–3815. doi: 10.1096/fj.201601181R

Longo, U. G., Ronga, M., and Maffulli, N. (2009). Achilles tendinopathy. *Sports Med. Arthrosc.* 17, 112–126. doi: 10.1097/JSA.0000000000000185

Maeda, E., Ye, S., Wang, W., Bader, D. L., Knight, M. M., and Lee, D. A. (2012). Gap junction permeability between tenocytes within tendon fascicles is suppressed by tensile loading. *Biomech. Model. Mechanobiol.* 11, 439–447. doi: 10.1007/s10237-011-0323-1

Maffulli, N., Longo, U. G., and Denaro, V. (2010). Novel approaches for the management of tendinopathy. *J. Bone Joint Surg. Ser. A* 92, 2604–2613. doi: 10.2106/JBJS.I.01744

Magne, D., and Bougault, C. (2015). What understanding tendon cell differentiation can teach us about pathological tendon ossification. *Histol. Histopathol.* 30, 901–910. doi: 10.14670/HH-11-614

Mauro, A., Russo, V., Di Marcantonio, L., Berardinelli, P., Martelli, A., Muttini, A., et al. (2016). M1 and M2 macrophage recruitment during tendon regeneration induced by amniotic epithelial cell allotransplantation in ovine. *Res. Vet. Sci.* 105, 92–102. doi: 10.1016/j.rvsc.2016.01.014

McBride, D. J., Trelstad, R. L., and Silver, F. H. (1988). Structural and mechanical assessment of developing chick tendon. *Int. J. Biol. Macromol.* 10, 194–200. doi: 10.1016/0141-8130(88)90048-7

Menzies, N. A., Gomez, G. B., Bozzani, F., Chatterjee, S., Foster, N., Baena, I. G., et al. (2016). Cost-effectiveness and resource implications of aggressive action on tuberculosis in China, India, and South Africa: a combined analysis of nine models. *Lancet Glob. Heal.* 4, e816–e826. doi: 10.1016/S2214-109X(16)30265-0

Millar, N. L., Hueber, A. J., Reilly, J. H., Xu, Y., Fazzi, U. G., Murrell, G. A. C., et al. (2010). Inflammation is present in early human tendinopathy. *Am. J. Sports Med.* 38, 2085–2091. doi: 10.1177/0363546510372613

Millar, N. L., Murrell, G. A. C., and Mcinnes, I. B. (2017). Inflammatory mechanisms in tendinopathy - towards translation. *Nat. Rev. Rheumatol.* 13, 110–122. doi: 10.1038/nrrheum.2016.213

Millar, N. L., Wei, A. Q., Molloy, T. J., Bonar, F., and Murrell, G. A. C. (2008). Cytokines and apoptosis in supraspinatus tendinopathy. *Clin. Orthop. Relat. Res.* 466, 1569–1576. doi: 10.1007/s11999-008-0265-9

Monti, E., and Miyagi, T. (2015). Structure and function of mammalian sialidases. *Top. Curr. Chem.* 366, 185–208. doi: 10.1007/128_2012_328

Musson, D. S., Naot, D., Chhana, A., Matthews, B. G., McIntosh, J. D., Lin, S. T. C., et al. (2015). In vitro evaluation of a novel non-mulberry silk scaffold for use in tendon regeneration. *Tissue Eng. Part A* 21, 1539–1551. doi: 10.1089/ten.tea.2014.0128

Noah, A. C., Li, T. M., Martinez, L. M., Wada, S., Swanson, J. B., Disser, N. P., et al. (2020). Adaptive and innate immune cell responses in tendons and lymph nodes after tendon injury and repair. *J. Appl. Physiol.* 128, 473–482. doi: 10.1152/japplphysiol.00682.2019

Nordez, A., and Hug, F. (2010). Muscle shear elastic modulus measured using supersonic shear imaging is highly related to muscle activity level. *J. Appl. Physiol.* 108, 1389–1394. doi: 10.1152/japplphysiol.01323.2009

Oshiro, W., Lou, J., Xing, X., Tu, Y., and Manske, P. R. (2003). Flexor tendon healing in the rat: a histologic and gene expression study. *J. Hand Surg. Am.* 28, 814–823. doi: 10.1053/S0363-5023(03)00366-6

Packer, J. D., Bedi, A., Fox, A. J., Gasinu, S., Imhauser, C. W., Stasiak, M., et al. (2014). Effect of immediate and delayed high-strain loading on tendon-to-bone healing after anterior cruciate ligament reconstruction. *J. Bone Joint Surg. Am. Vol.* 96, 770–777. doi: 10.2106/JBJS.L.01354

Pailler-Mattei, C., Bec, S., and Zahouani, H. (2008). In vivo measurements of the elastic mechanical properties of human skin by indentation tests. *Med. Eng. Phys.* 30, 599–606. doi: 10.1016/j.medengphy.2007.06.011

Pang, X., Wu, J. P., Allison, G. T., Xu, J., Rubenson, J., Zheng, M. H., et al. (2017). Three dimensional microstructural network of elastin, collagen, and cells in Achilles tendons. *J. Orthop. Res.* 35, 1203–1214. doi: 10.1002/jor.23240

Raghunathan, V. K., Thomasy, S. M., Strøm, P., Yañez-Soto, B., Garland, S. P., Sermeno, J., et al. (2017). Tissue and cellular biomechanics during corneal wound injury and repair. *Acta Biomater.* 58, 291–301. doi: 10.1016/j.actbio.2017.05.051

Redaelli, A., Vesentini, S., Soncini, M., Vena, P., Mantero, S., and Montevecchi, F. M. (2003). Possible role of decorin glycosaminoglycans in fibril to fibril force transfer in relative mature tendons - A computational study from molecular to microstructural level. *J. Biomech.* 36, 1555–1569. doi: 10.1016/S0021-9290(03)00133-7

Robinson, K. A., Sun, M., Barnum, C. E., Weiss, S. N., Huegel, J., Shetye, S. S., et al. (2017). Decorin and biglycan are necessary for maintaining collagen fibril structure, fiber realignment, and mechanical properties of mature tendons. *Matrix Biol.* 64, 81–93. doi: 10.1016/j.matbio.2017.08.004

Sawadkar, P., Player, D., Bozec, L., and Mudera, V. (2020). The mechanobiology of tendon fibroblasts under static and uniaxial cyclic load in a 3D tissue engineered model mimicking native extracellular matrix. *J. Tissue Eng. Regen. Med.* 14, 135–146. doi: 10.1002/term.2975

Schiele, N. R., von Flotow, F., Tochka, Z. L., Hockaday, L. A., Marturano, J. E., Thibodeau, J. J., et al. (2015). Actin cytoskeleton contributes to the elastic modulus of embryonic tendon during early development. *J. Orthop. Res.* 33, 874–881. doi: 10.1002/jor.22880

Schoenenberger, A. D., Foolen, J., Moor, P., Silvan, U., and Snedeker, J. G. (2018). Substrate fiber alignment mediates tendon cell response to inflammatory signaling. *Acta Biomater.* 71, 306–317. doi: 10.1016/j.actbio.2018.03.004

Schoenenberger, A. D., Tempfer, H., Lehner, C., Egloff, J., Mauracher, M., Bird, A., et al. (2020). Macromechanics and polycaprolactone fiber organization drive macrophage polarization and regulate inflammatory activation of tendon in vitro and in vivo. *Biomaterials* 249:120034. doi: 10.1016/j.biomaterials.2020.120034

Screen, H. R. C., Berk, D. E., Kadler, K. E., Ramirez, F., and Young, M. F. (2015). Tendon functional extracellular matrix. *J. Orthop. Res.* 33, 793–799. doi: 10.1002/jor.22818

Sharma, P., and Maffulli, N. (2005). Tendon injury and tendinopathy. *J. Bone Joint Surg.* 87, 187–202. doi: 10.2106/JBJS.D.01850

Sherlock, J. P., Joyce-Shaikh, B., Turner, S. P., Chao, C. C., Sathe, M., Grein, J., et al. (2012). IL-23 induces spondyloarthropathy by acting on ROR-γt+ CD3+ CD4- CD8- entheseal resident T cells. *Nat. Med.* 18, 1069–1076. doi: 10.1038/nm.2817

Soo, J. C., Min, J. K., Homer, R. J., Hye, R. K., Zhang, X., Lee, P. J., et al. (2006). Role of early growth response-1 (Egr-1) in interleukin-13-induced inflammation and remodeling. *J. Biol. Chem.* 281, 8161–8168. doi: 10.1074/jbc.M506770200

Stauber, T., Blache, U., and Snedeker, J. G. (2020). Tendon tissue microdamage and the limits of intrinsic repair. *Matrix Biol.* 85–86, 68–79. doi: 10.1016/j.matbio.2019.07.008

Stolk, M., Klatte-Schulz, F., Schmock, A., Minkwitz, S., Wildemann, B., and Seifert, M. (2017). New insights into tenocyte-immune cell interplay in an in vitro model of inflammation. *Sci. Rep.* 7:9801. doi: 10.1038/s41598-017-09875-x

Sunwoo, J. Y., Eliasberg, C. D., Carballo, C. B., and Rodeo, S. A. (2020). The role of the macrophage in tendinopathy and tendon healing. *J. Orthop. Res.* 38, 1666–1675. doi: 10.1002/jor.24667

Thorpe, C. T., Chaudhry, S., Lei, I. I., Varone, A., Riley, G. P., Birch, H. L., et al. (2015). Tendon overload results in alterations in cell shape and increased markers of inflammation and matrix degradation. *Scand. J. Med. Sci. Sport* 25, e381–e391. doi: 10.1111/sms.12333

Thorpe, C. T., and Screen, H. R. C. (2016). "Tendon structure and composition," in *Metabolic Influences on Risk for Tendon Disorders*, eds P. W. Ackermann and D. A. Hart (Cham: Springer International Publishing), 3–10. doi: 10.1007/978-3-319-33943-6_1

Vinhas, A., Rodrigues, M. T., Gonçalves, A. I., Reis, R. L., and Gomes, M. E. (2020). Magnetic responsive materials modulate the inflammatory profile of IL-1β conditioned tendon cells. *Acta Biomater.* 117, 235–245. doi: 10.1016/j.actbio.2020.09.028

Williams, I. F., Heaton, A., and McCullagh, K. G. (1980). Cell morphology and collagen types in equine tendon scar. *Res. Vet. Sci.* 28, 302–310. doi: 10.1016/s0034-5288(18)32713-9

Wilusz, R. E., Zauscher, S., and Guilak, F. (2013). Micromechanical mapping of early osteoarthritic changes in the pericellular matrix of human articular cartilage. *Osteoarthr. Cartil.* 21, 1895–1903. doi: 10.1016/j.joca.2013.08.026

Wojciak, B., and Crossan, J. F. (1993). The accumulation of inflammatory cells in synovial sheath and epitenon during adhesion formation in healing rat flexor tendons. *Clin. Exp. Immunol.* 93, 108–114. doi: 10.1111/j.1365-2249.1993.tb06505.x

Wu, J., Yuan, H., Li, L., Fan, K., Qian, S., and Li, B. (2018). Viscoelastic shear lag model to predict the micromechanical behavior of tendon under

dynamic tensile loading. *J. Theor. Biol.* 437, 202–213. doi: 10.1016/j.jtbi.2017.10.018

Wu, P. T., Su, W. R., Li, C. L., Hsieh, J. L., Ma, C. H., Wu, C. L., et al. (2019). Inhibition of cd44 induces apoptosis, inflammation, and matrix metalloproteinase expression in tendinopathy. *J. Biol. Chem.* 294, 20177–20184. doi: 10.1074/jbc.RA119.009675

Wu, Y.-F., Wang, H.-K., Chang, H.-W., Sun, J., Sun, J.-S., and Chao, Y.-H. (2017). High glucose alters tendon homeostasis through downregulation of the AMPK/Egr1 pathway. *Sci. Rep.* 7:44199. doi: 10.1038/srep44199

Young, N. J., Becker, D. L., Fleck, R. A., Goodship, A. E., and Patterson-Kane, J. C. (2009). Maturational alterations in gap junction expression and associated collagen synthesis in response to tendon function. *Matrix Biol.* 28, 311–323. doi: 10.1016/j.matbio.2009.05.002

Zhang, C., Wang, X., Zhang, E., Yang, L., Yuan, H., Tu, W., et al. (2017). An epigenetic bioactive composite scaffold with well-aligned nanofibers for functional tendon tissue engineering. *Acta Biomater.* 66, 141–156. doi: 10.1016/j.actbio.2017.09.036

Zhang, K., Asai, S., Hast, M. W., Liu, M., Usami, Y., Iwamoto, M., et al. (2016). Tendon mineralization is progressive and associated with deterioration of tendon biomechanical properties, and requires BMP-Smad signaling in the mouse Achilles tendon injury model. *Matrix Biol.* 52–54, 315–324. doi: 10.1016/j.matbio.2016.01.015

Conflict of Interest: The authors declare that the research was conducted in the absence of any commercial or financial relationships that could be construed as a potential conflict of interest.

frontiers in Cell and Developmental Biology

ORIGINAL RESEARCH
published: 18 June 2021
doi: 10.3389/fcell.2021.659389

Potential Mechanisms of the Impact of Hepatocyte Growth Factor Gene-Modified Tendon Stem Cells on Tendon Healing

Mingzhao Zhang†, Hengchen Liu†, Manyu Shi, Tingting Zhang, Wenjun Lu, Shulong Yang, Qingbo Cui and Zhaozhu Li**

Department of Pediatric Surgery, The Second Affiliated Hospital of Harbin Medical University, Harbin, China

OPEN ACCESS

Edited by:
Zi Yin,
Zhejiang University, China

Reviewed by:
Yun-feng Rui,
Southeast University, China
Fei Fang,
Columbia University Irving Medical Center, United States

***Correspondence:**
Zhaozhu Li
zhaozhu247@163.com
Qingbo Cui
cuiqingbocqb@163.com

†These authors have contributed equally to this work and share first authorship

Specialty section:
This article was submitted to Stem Cell Research, a section of the journal Frontiers in Cell and Developmental Biology

Received: *27 January 2021*
Accepted: *10 May 2021*
Published: *18 June 2021*

Citation:
Zhang M, Liu H, Shi M, Zhang T, Lu W, Yang S, Cui Q and Li Z (2021) Potential Mechanisms of the Impact of Hepatocyte Growth Factor Gene-Modified Tendon Stem Cells on Tendon Healing. Front. Cell Dev. Biol. 9:659389. doi: 10.3389/fcell.2021.659389

The therapeutic impact of stem cells is potentially largely attributable to secretion of exosomes and soluble factors. The present study evaluates the impact of hepatocyte growth factor (HGF)–expressing tendon stem cells (TSCs) on tendon healing in a rat model. Patellar tendon TSCs were isolated and underwent transfection with lentiviral vectors containing HGF or green fluorescent protein (GFP) genes. *In vivo*, immunohistochemistry of tendons sampled 1 week postsurgery demonstrated that all stem cell–treated groups exhibited higher numbers of $CD163^+$ M2 monocytes and IL-10^+ cells (anti-inflammatory), and lower numbers of $CCR7^+$ M1 monocytes and IL-6^+ as well as COX-2^+ cells (pro-inflammatory). Effects were most pronounced in the HGF-expressing TSCs (TSCs + HGF) treated group. Histology ± immunohistochemistry of tendons sampled 4 and 8 weeks postsurgery demonstrated that all stem cell–treated groups exhibited more ordered collagen fiber arrangement and lower levels of COLIII, α-SMA, TGF-β1, and fibronectin (proteins relevant to fibroscarring). Effects were most pronounced in the TSCs + HGF–treated group. For the *in vitro* study, isolated tendon fibroblasts pretreated with TGF-β1 to mimic the *in vivo* microenvironment of tendon injury were indirectly cocultured with TSCs, TSCs + GFP, or TSCs + HGF using a transwell system. Western blotting demonstrated that all stem cell types decreased TGF-β1-induced increases in fibroblast levels of COX-2, COLIII, and α-SMA, concomitant with decreased activation of major TGF-β1 signaling pathways (p38 MAPK, ERK1/2, but not Smad2/3). This effect was most pronounced for TSCs + HGF, which also decreased the TGF-β1-induced increase in activation of the Smad2/3 signaling pathway. The presence of specific inhibitors of these pathways during fibroblast TGF-β1 stimulation also attenuated increases in levels of COX-2, COLIII, and α-SMA. In conclusion, TSCs + HGF, which exhibit HGF overexpression, may promoting tendon healing via decreasing inflammation and fibrosis, perhaps partly via inhibiting TGF-β1-induced signaling. These findings identify a novel potential therapeutic strategy for tendon injuries, warranting additional research.

Keywords: tendon stem cells, hepatocyte growth factor, inflammation, fibrosis, tendon healing

INTRODUCTION

Tendon-related disorders and injuries are a common clinical challenge that may cause severe pain and decreased mobility; they have a significant negative impact on domains of function and quality of life and necessitate approximately 30 million surgeries per year (worldwide) (Wu et al., 2017; Rinoldi et al., 2019; Yu et al., 2020). Natural tendon healing is a slow and complex process due to tissue hypocellularity and hypovascularity (Kokubu et al., 2020). The initial response to injury is inflammation, which can result in local scar formation (Wang et al., 2019). This compromises tendon strength and elasticity, increasing the risk of damage in response to subsequent tension (Cui et al., 2011). Although current surgical and rehabilitative methods have achieved superior efficacy relative to those available in the past (Ricchetti et al., 2008; Wu et al., 2017), truly functional tendon healing remains an intractable problem requiring more advanced therapeutic strategies (Yu et al., 2020).

In recent years, the therapeutic application of tendon stem cells (TSCs) in the context of tendon injury has gradually attracted increasing attention. Such stem cells retain the potential for self-renewal and differentiation. Cumulative research demonstrates that TSCs exhibit potential in the context of tendon injury therapeutics (Zhang et al., 2011; Ni et al., 2012; Yang et al., 2017). The therapeutic effect of stem cells is attributable largely to the secretion of exosomes and soluble growth factors (Wang L. S. et al., 2017). Therefore, increasing stem cell production of beneficial cytokines and trophic factors such as IL-10, hepatocyte growth factor (HGF), and vascular endothelial growth factor (VEGF) may enhance their therapeutic paracrine wound-healing capacity (Ricchetti et al., 2008; Li et al., 2015; Wang L. S. et al., 2017; Yang et al., 2018).

The trophic factor HGF has important paracrine activities, including stimulation of cell proliferation, migration, and differentiation as well as exhibiting anti-inflammatory, anti-apoptotic and antifibrotic properties (Ricchetti et al., 2008; Wang L. S. et al., 2017). It also plays an important role in the repair of many key organs and tissues, including in the contexts of corneal injury (Omoto et al., 2017); inflammatory responses to traumatic oral ulcers (Wang X. et al., 2017); and fibrosis of the liver, kidney, and lung (Yi et al., 2014). One of our prior studies demonstrates that HGF is able to oppose

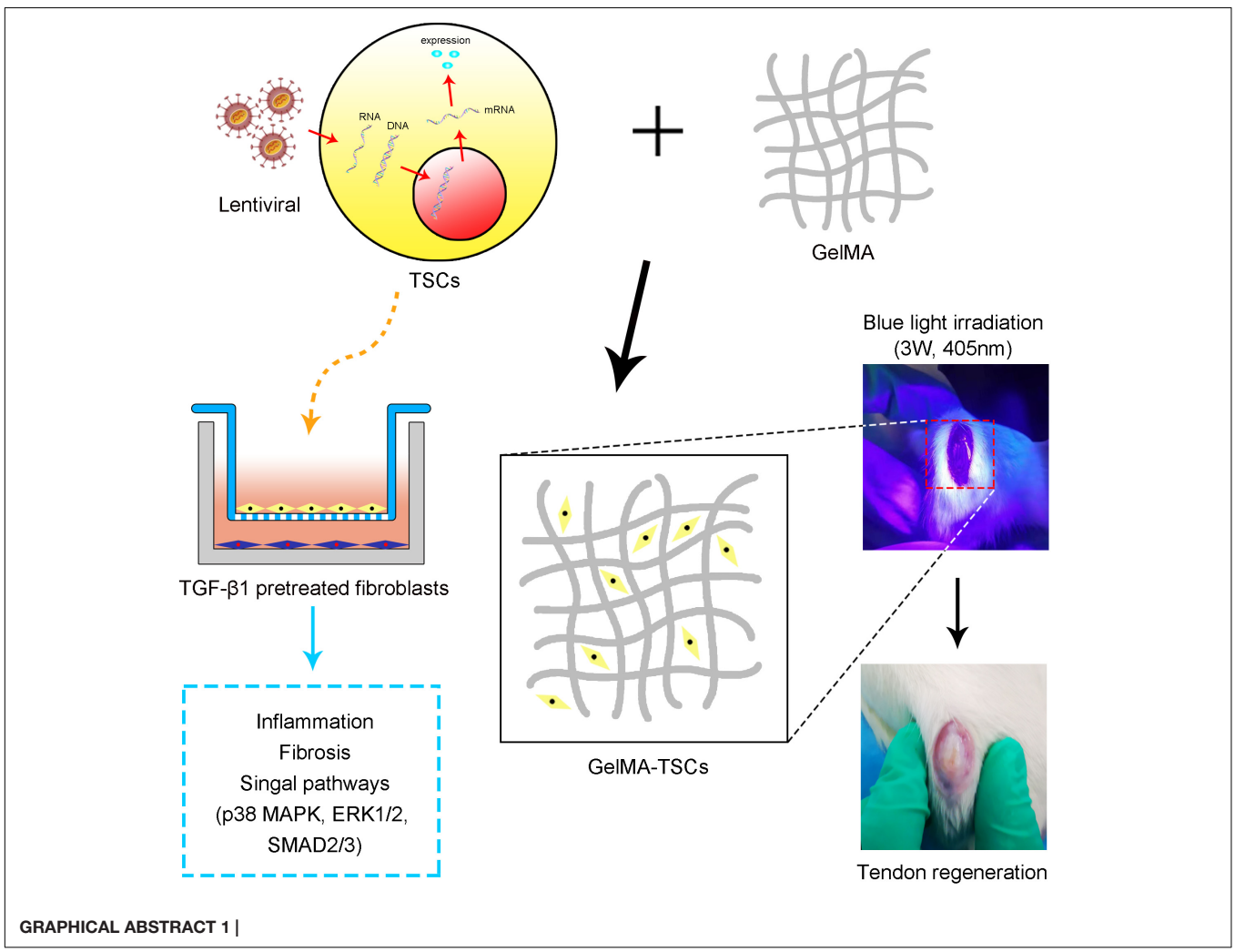

GRAPHICAL ABSTRACT 1 |

scar formation by inhibiting myofibroblast differentiation and excessive extracellular matrix (ECM) deposition (Cui et al., 2011). Although application of HGF is considered effective in treating tissue injury, sustained HGF delivery to the site of injury remains a major challenge (Li et al., 2015).

The present study investigates the potential of TSCs genetically modified to achieve HGF overexpression (TSCs + HGF) to enhance tendon healing (including partially elucidating underlying mechanisms). These novel results add to the body of literature concerning improved therapeutic tendon healing strategies.

MATERIALS AND METHODS

Isolation, Culture, and Identification of TSCs and Tendon Fibroblasts

Eight adult male Sprague–Dawley rats weighing between 180 and 200 g were used. Experimental protocols were approved by the Harbin Medical University Ethics Committee (No. Ky2018-135), and the experiment proceeded in accordance with institutional guidelines for the care and handling of laboratory animals. Isolation and identification of rat TSCs was performed as previously described (Zhang et al., 2020). Briefly, for flow cytometry, 4×10^6 cells from passages three to five were used to detect those positive for surface markers CD44 and CD90, and CD11b and CD106 were used as negative markers to exclude contamination by other cells. In addition, the multilineage differentiation capacity of TSCs was assessed via staining with Oil Red O (for adipogenic potential), Alizarin Red (for osteogenic potential), and Alcian Blue (for chondrogenic potential). Rat tendon fibroblast isolation and culture was performed as previously described (Fu et al., 2008; Chang et al., 2010). Passage three to five fibroblasts were used.

Lentiviral Transfection of TSCs

Lentiviral vectors expressing HGF (Lv-HGF, MOI = 20) and control lentiviral vectors expressing GFP (Lv-GFP, MOI = 20) were used to transfect TSCs (Hanbio, Shanghai, China); 5×10^5 cells were incubated in serum-free Dulbeccos' modified Eagle's medium (Gibco, Invitrogen, NY, Invitrogen Corporation, Grand Island, United States) containing lentiviral vectors and 6 μg/ml polybrene (Hanbio, Shanghai, China) for 24 h at 37°C in an atmosphere containing 5% CO_2. Thereafter, vector-containing medium was replaced with complete medium, and cells were cultured under identical conditions for a further 48 h. Successfully transfected cells were identified via fluorescence microscopy. Addition of 1 μg/ml puromycin (Thermo Fisher Scientific) for 2 to 3 days excluded untransfected cells. Expression of HGF by puromycin-resistant TSCs was further confirmed using fluorescence microscopy and Western blotting.

Surgical Tendon Injury and Experimental Intervention

A total of 75 adult male Sprague–Dawley rats weighing between 180 and 200 g underwent surgery using methods similar to those previously described (Shi et al., 2019). Briefly, a third of the central part of the patellar tendon (0.8 mm in width) was removed using a surgical blade, producing a central defect. Rats were randomly assigned to five intervention groups ($n = 15$ per group): (1) TSCs + HGF, (2) TSCs + GFP, (3) TSCs (untransfected control), (4) vehicle only control, and (5) untreated control. A total of 1×10^6 TSCs + HGF, TSCs + GFP, or TSCs were mixed with the vehicle, gelatin methacryloyl (GelMA) (EFL-GM-60; Suzhou Intelligent Manufacturing Research Institute, Suzhou, China). For treated groups, 30 μl of the cell-vehicle mixture was placed in the tendon defect and converted to a gel state via blue light irradiation (3 W, 405 nm) for 10–20 s with the light source placed at a distance of 3 cm from the defect. The entire remodeling process is shown in **Figure 1**. At 1, 4, and 8 weeks following surgery and intervention, tendon samples ($n = 5$ per time point) were collected from each group for histological evaluation and immunostaining.

Histology and Immunostaining

Patellar tendon samples were fixed in 4% formaldehyde and embedded in paraffin. Specimens from the 4- and 8-week time points were sectioned longitudinally into 5-μm slices and stained with hematoxylin and eosin (H&E). Immunohistochemistry was performed as described previously (Wang et al., 2019). Briefly, after deparaffinization and antigen retrieval, sections were incubated with 3% H_2O_2 for 15 min, and 5% normal goat serum was used to block non-specific binding sites. Sections were then incubated overnight at 4°C with the following antirat primary antibodies (all Abcam, Shanghai, China): mouse anticollagen III (COLIII; monoclonal; 1:200 dilution), rabbit anti-α-smooth muscle actin (α-SMA; polyclonal; 1:200 dilution), rabbit antitransforming growth factor-β1 (TGF-β1; polyclonal; 1:500 dilution), and mouse antifibronectin (monoclonal; 1:200 dilution). Sections were then incubated with horseradish peroxidase (HRP)-conjugated secondary antibodies (Zsjqbio, Beijing, China) for 30 min at room temperature. After addition of the HRP substrate 3,3′-diamniobenzidine (DAB) and hematoxylin staining, sections were dehydrated and mounted.

Specimens from the week 1 time point underwent immunostaining for inflammatory markers as described previously (Shi et al., 2019; Wang et al., 2019). Briefly, a cryomicrotome was used to produce serial 8-μm-thick sections. Sections were incubated with goat serum for 15 min at room temperature to block non-specific binding sites, followed by incubation overnight at 4°C with the following antirat primary antibodies: rabbit anti-CD163 (monoclonal; Abcam; 1:100 dilution), rabbit anti-C-C chemokine receptor type 7 (CCR7; polyclonal; Proteintech; 1:200 dilution), rat anti-IL-10; (monoclonal; Abcam; 1:100 dilution), mouse anti-IL-6 (monoclonal; Origene; 1:100 dilution), and rat anti-cyclooxygenase-2 (COX-2; monoclonal; Abcam; 1:100 dilution). Sections were then incubated for 60 min at room temperature, in the dark, with a species-appropriate secondary antibody (Proteintech; 1:200 dilution). Cell nuclei were stained using 4′,6-diamidino-2-phenylindole (DAPI; Beyotime, Shanghai, China) for 10 min at room temperature. Finally, images were acquired using a BX53

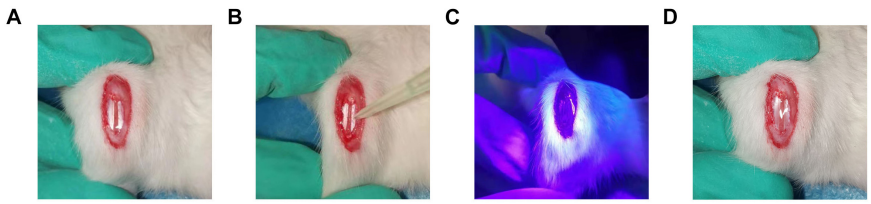

FIGURE 1 | Establishment of patellar tendon injury model. **(A)** The central third of the patellar tendon was removed, resulting in a tendon defect. **(B)** GelMA containing stem cells was infused into the Patellar tendon defect. **(C)** Radiation with a 405-nm light source for 10–20 s at a distance of 3 cm from the tendon defect. **(D)** Cross-linking to form the gel state.

microscope (Olympus, Japan) prior to analysis using ImageJ software.

Stem Cell Coculture With Tendon Fibroblasts

Fibroblasts were initially precultured in medium in the presence or absence (negative control) of 5 ng/ml TGF-β1 (PeproTech, Seoul, South Korea) for 24 h at 37°C in an atmosphere containing 5% CO_2. Then, stem cells (TSCs, TSCs + GFP, or TSCs + HGF) and tendon fibroblasts were cocultured in a transwell system (pore size: 0.4 mm) (Corning Inc., NY, United States) as described previously (Chen et al., 2018). Briefly, 1.5×10^5 tendon fibroblasts in 2 ml medium were seeded into the lower chamber of each well of a six-well transwell plate, and an equivalent number of stem cells in 1 ml medium were seeded into the corresponding upper chambers. Coculture proceeded for 24 h under incubation conditions identical to those described above. To study the impact of stem cell–released soluble factors on TGF-β1-induced signaling pathways (p38 MAPK, ERK1/2, and Smad2/3) and subsequent inflammation and fibrosis, lower-chamber fibroblasts were pretreated with 20 nM each of inhibitors of p38 MAPK (SB203580), ERK1/2 (PD98059), and Smad2/3 (SB431542) activation (all MedChemExpress, CA, United States) for 1 h at 37°C prior to addition of TGF-β1.

Protein Extraction and Western Blotting

Here, 5×10^5 treated fibroblasts per group were lysed using RIPA buffer (Beyotime, Shanghai, China). The lysate was centrifuged at 12,000 rpm for 20 min at 4°C to pellet debris, and the supernatant was collected. Total protein concentration was estimated using the bicinchoninic acid (BCA) assay (Beyotime, Shanghai, China). Per sample, 10 μg of total protein was electrophoretically separated on a 10% sodium dodecyl sulfate (SDS)-polyacrylamide gel, and protein spots were transferred to a polyvinylidene fluoride (PVDF) membrane. The membrane was incubated with 5% skim milk powder in TBST for 1 h at room temperature to block non-specific binding sites, followed by incubation overnight at 4°C in the presence of antirat primary antibodies: rat anti-COX-2 (monoclonal; Abcam; 1:1000 dilution), mouse anti-COLIII (monoclonal; Abcam; 1:1000 dilution), rabbit anti-α-SMA (polyclonal; Abcam; 1:1000 dilution), anti-p38 MAPK (monoclonal; Cell Signaling Technology; 1:1000 dilution), anti-phospho-p38 MAPK (monoclonal; Cell Signaling Technology; 1:1000 dilution), anti-ERK1/2 (monoclonal; Cell Signaling Technology; 1:1000 dilution), anti-phospho-ERK1/2 (monoclonal; Cell Signaling Technology; 1:2000 dilution), anti-Smad2/3 (monoclonal; Cell Signaling Technology; 1:1000 dilution), and anti-phospho-Smad2/3 (monoclonal; Cell Signaling Technology; 1:2000 dilution). The proteins COX-2, α-SMA, and ColIII were selected as proxies to study the effects of stem cells on TGF-β1-induced inflammation and fibrosis, and the proteins p38 MAPK, ERK1/2, and Smad2/3 are involved in signaling pathways downstream of TGF-β1 that may be impacted by stem cells. Finally, the membrane was incubated with HRP-conjugated secondary antibodies for 1 h at room temperature (Boster, Wuhan, China; 1:5000 dilution) prior to addition of DAB. The membrane was imaged using a chemiluminescence CCD imaging system (ChemiScope 6200T imager, Clinx Science Instruments Co. Ltd., Shanghai, China) and protein band gray values were analyzed using ImageJ software.

Statistical Analysis

All values are expressed as mean ± SD. Quantitative data across all groups were analyzed using one-way ANOVA followed by Tukey's test. A P-value < 0.05 was considered to be statistically significant.

RESULTS

Determination of TSC Phenotypes and Lentiviral Vector Transduction Efficiency

Flow cytometry demonstrated that isolated TSCs were $CD44^+$ $CD90^+$ $CD11b^-$ $CD106^-$ (**Figure 2A**). Microscopy demonstrated typical TSC spindle-shaped morphology (**Figure 2B**), and cells retained multilineage differentiation capacity (ability to differentiate into adipogenic, osteogenic, or chondrogenic precursors) (**Figure 2C**). After TSC lentiviral (Lv-HGF, Lv-GFP) transduction and puromy1cin screening, green fluorescence demonstrated successful transduction (**Figure 2D**), and Western blot assessment of transduction efficiency demonstrated higher HGF protein expression in the Lv-HGF (relative to the Lv-GFP) group, but no significant difference between the PBS-only and Lv-GFP groups (**Figures 2E,F**).

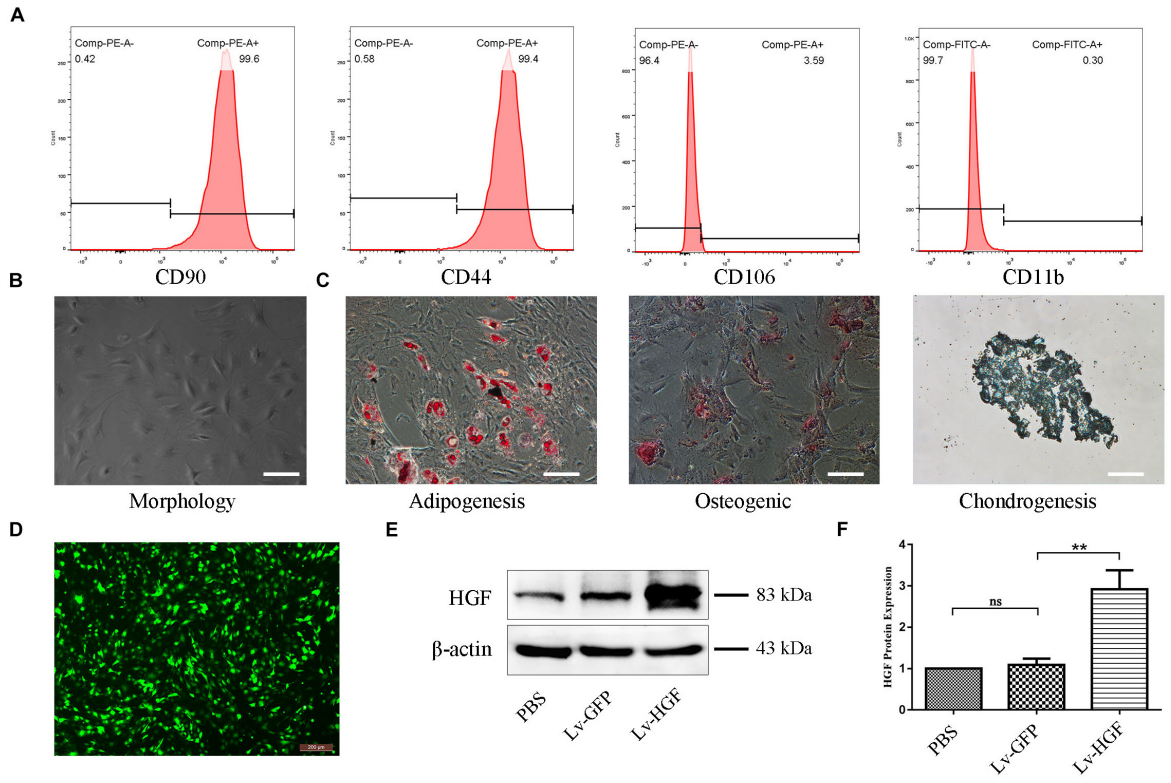

FIGURE 2 | Confirmation of TSC identity, differentiation capacity, and transduction efficiency. **(A)** Flow cytometric detection of cell surface markers, including CD90, CD44, CD106, and CD11b/c. **(B)** Typical TSC morphology. **(C)** Oil Red O, Alizarin Red, and Alcian Blue stains demonstrating TSC multilineage differentiation capacity. Scale bars: 100 μm. **(D)** Fluorescent photomicrograph demonstrating examples of TSC morphology after HGF transduction and puromycin screening. **(E,F)** Western blot confirming HGF protein expression by TSCs following transduction. Data are expressed as means ± SD of three independent experiments; $^{**}P < 0.01$.

Effect of TSCs + HGF on the Early Inflammatory Response

In tendon specimens collected at week 1 postsurgery, numbers of $CD163^+$ M2 macrophages (anti-inflammatory) within the defects of all stem cell–treated animals were elevated (relative to the vehicle-only and untreated control groups). This effect was most pronounced in the TSCs + HGF–treated group (**Figure 3A**), which also exhibited the lowest numbers of $CCR7^+$ M1 macrophages (pro-inflammatory) (**Figure 3B**). Furthermore, the TSCs + HGF group exhibited the most significantly elevated number of IL-10^+ (M2-favoring) and decreased number of IL-6^+ (M1-favoring) and COX-2^+ (prostaglandin synthesis-competent) cells, compared with other treatment groups (**Figures 3C–E**). Quantitative analysis results are shown in **Figure 3F**.

The TSCs + HGF Group Demonstrates Improves Tendon Healing via Regulation of Tendon Matrix Deposition

Staining of weeks 4 and 8 tendon specimens with H&E demonstrated that TSCs + HGF treatment group specimens exhibited more continuous and regular collagen fiber arrangement (relative to that of the TSCs or TSCs + GFP treatment groups) (**Figures 4A**, **5A**). Furthermore, all stem cell–treated groups exhibited decreased levels of the tendon matrix-influencing factors COLIII, α-SMA, TGF-β1, and fibronectin at weeks 4 and 8 postsurgery, and this effect was most pronounced in the TSCs + HGF group (**Figures 4B–E**, **5B–E**). Quantitative analysis results are shown in **Figures 4F**, **5F**.

Exposure to TGF-β1 Induces Inflammation and Fibrosis via Activation of Fibroblast p38 MAPK, ERK1/2, and Smad2/3 Signaling Pathways

Inhibitors of p38 MAPK, ERK1/2, and Smad2/3 activation were used to determine whether these signaling pathways are involved in TGF-β1-induced fibroblast functional changes. Western blots confirmed that TGF-β1-induced activation of p38 MAPK, ERK1/2, and Smad2/3 signaling pathways was indeed inhibited (**Figures 6A, C–E**). Functionally, inhibition of p38 MAPK and Smad2/3 signaling co-occurred with a significant decrease in TGF-β1-induced COX-2, COLIII, and α-SMA level elevation, and inhibition of ERK1/2 signaling co-occurred only with a significant decrease in TGF-β1-induced α-SMA and COLIII (but not COX-2) level elevation (**Figures 6B, F–H**). These findings

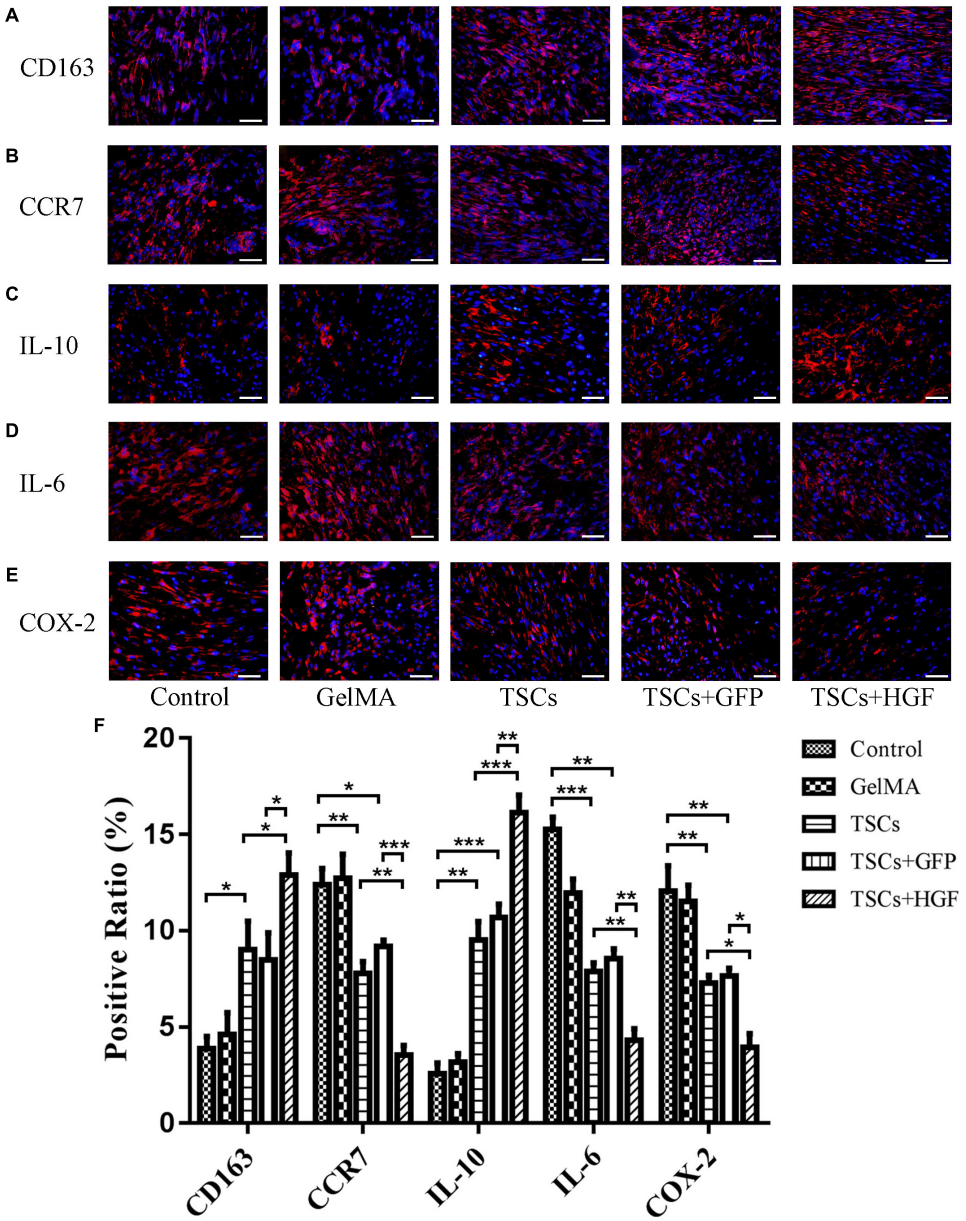

FIGURE 3 | Impact of TSCs + HGF on tendon inflammation. Immunohistochemical representative images of **(A)** CD163^{+} cells, **(B)** CCR7^{+} cells, **(C)** IL-10^{+} cells, **(D)** IL-6^{+} cells, and **(E)** COX-2^{+} cells at 1 week postoperative repair site. **(F)** Positive cell ratio of inflammation-related factors at 1 week (n = 5). Bars: 50 μm. Data are represented as mean ± SD. $^{*}P < 0.05$, $^{**}P < 0.01$, $^{***}P < 0.001$.

suggest that ERK1/2 signaling may be dispensable for TGF-β1-induced inflammation.

Coculture With TSCs + HGF Results in Decreased Levels of COX-2, α-SMA, COLIII, p-p38 MAPK, p-ERK1/2, and p-Smad2/3 in TGF-β1-Stimulated Fibroblasts

Following indirect coculture of stem cell groups with tendon fibroblasts (**Figure 7A**), Western blots demonstrated that TGF-β1 increased levels of COX-2, α-SMA, and COLIII, but that all stem cell groups mitigated this effect with the most pronounced impact by TSCs + HGF (**Figures 7B–E**). Furthermore, TGF-β1 significantly increased the proportion of phosphorylated p38 MAPK, ERK1/2, and Smad2/3 in fibroblasts, and coculture with TSCs or TSCs + GFP inhibited these increases for p38 MAPK and ERK1/2 only, and coculture with TSCs + HGF inhibited these increases for all three proteins (p38 MAPK, ERK1/2, and Smad2/3) (**Figures 8A–D**). The effects of TSCs + HGF were most pronounced (**Figure 8**). These findings suggest that all stem cell groups (but especially

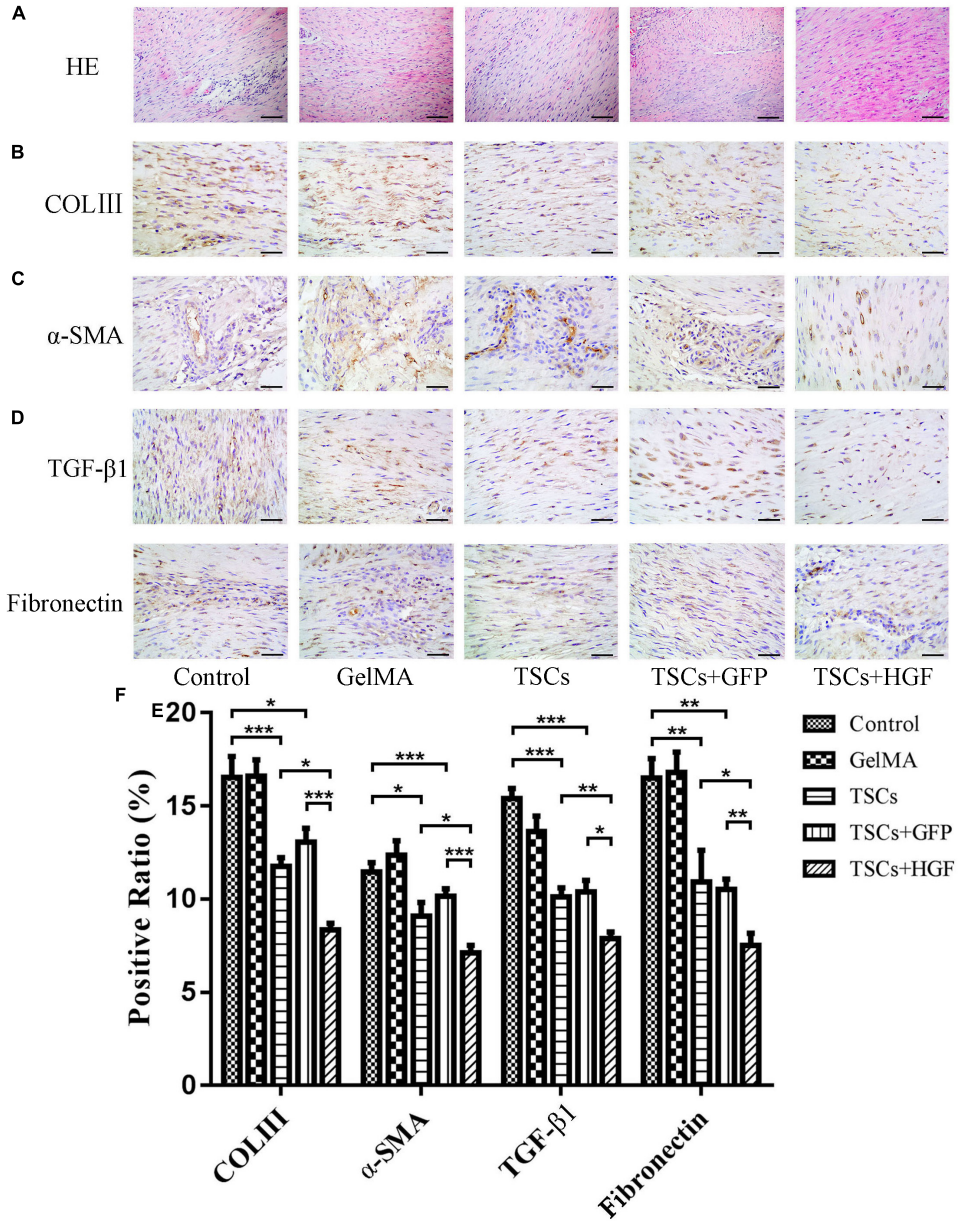

FIGURE 4 | Impact of treatment with TSCs expressing HGF (TSCs + HGF) on tendon levels of fibrosis-relevant proteins at 4 weeks postsurgery. **(A)** H&E stain of the tendon repair site. Immunohistochemical evaluation of **(B)** COLIII, **(C)** α-SMA, **(D)** TGF-β1, and **(E)** fibronectin patterns. **(F)** Quantitation of fibrosis-relevant proteins (n = 5). Bars: 50 μm. Data are represented as mean ± SD. $^{*}P < 0.05$, $^{**}P < 0.01$, $^{***}P < 0.001$.

TSCs + HGF) were able to decrease signaling downstream of TGF-β1 and that anti-inflammatory and antifibrotic stem cell effects may, thus, be at least partially mediated via this mechanism.

DISCUSSION

At present, accumulating evidence indicates that stem cells promote tissue healing mainly via paracrine mechanisms (Zhao et al., 2018). One important trophic factor with paracrine activity, HGF, exhibits a variety of functions, including promoting angiogenesis, regulating inflammation, inhibiting fibrosis, and promoting tissue regeneration (Wang L. S. et al., 2017). Our previous study also reveals that the use of exogenous HGF has a positive therapeutic effect on the formation of fibrosis and scar in tendon injury healing (Cui et al., 2011). We, therefore, hypothesized that tendon healing may be enhanced via sustained TSC expression of HGF.

Tendon healing occurs in three stages: inflammation, cell proliferation, and tissue remodeling. The present study initially examined the role of TSCs + HGF in regulating

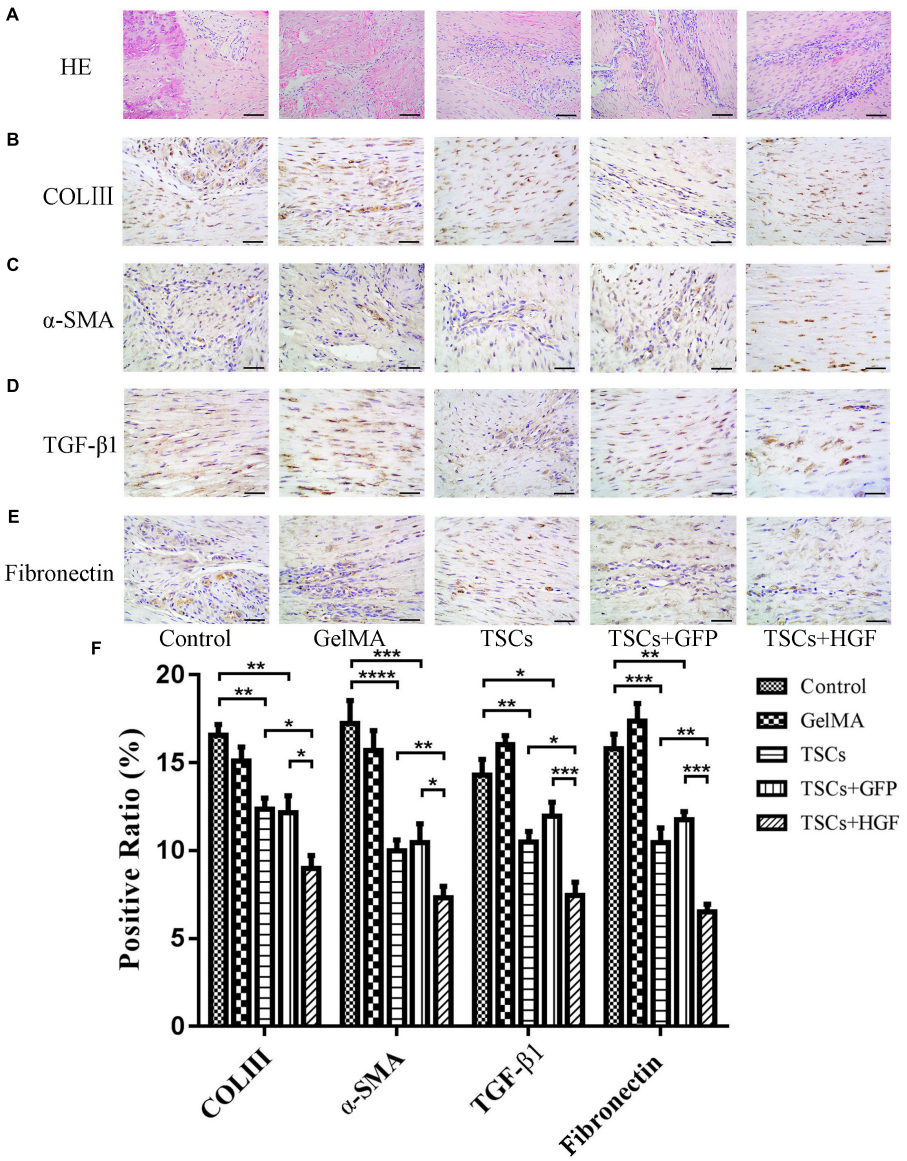

FIGURE 5 | Impact of treatment with TSCs expressing HGF (TSCs + HGF) on tendon levels of fibrosis-relevant proteins at 8 weeks postsurgery. **(A)** H&E stain of the tendon repair site. Immunohistochemical evaluation of **(B)** COLIII, **(C)** α-SMA, **(D)** TGF-β1, and **(E)** fibronectin patterns. **(F)** Quantitation of fibrosis-relevant proteins (n = 5). Bars: 50 μm. Data are represented as mean ± SD. $^{*}P < 0.05$, $^{**}P < 0.01$, $^{***}P < 0.001$.

the inflammatory response *in vivo*. During recent years, the importance of macrophages and various inflammatory mediators in tendon healing has become apparent, and it is now believed that "molecular inflammation" plays a key role in tendon pathophysiology (Sunwoo et al., 2020). Macrophages exist as functionally distinct phenotypes with differential roles during tendon healing (Sunwoo et al., 2020). Classically activated macrophages (M1) secrete pro-inflammatory cytokines early during the wound-healing process, and alternatively activated macrophages (M2) promote wound healing during the inflammatory response phase by means of producing anti-inflammatory factors and antagonizing M1 responses (Saleh et al., 2019). Although M1 macrophages can cause ECM degradation, inflammation, and apoptosis (Klinkert et al., 2017; Laplante et al., 2017; Dai et al., 2018), M2 macrophages can inhibit inflammation, prevent scar formation, and enhance tendon strength (Chamberlain et al., 2019). Switching macrophages from the M1 to the M2 phenotype after tendon injury can promote tendon healing (Manning et al., 2015). The present study demonstrates that treatment with TSCs + HGF significantly increases numbers of $CD163^{+}$ M2 macrophages and decreases numbers of $CCR7^{+}$ M1 macrophages (more so than treatment with either TSCs or TSCs + GFP) and that levels of M2-favoring IL-10 are highest, and those of M1-favoring factor IL-6 and pro-inflammatory factor COX-2 are lowest in the TSCs + HGF treatment group. These findings suggest that

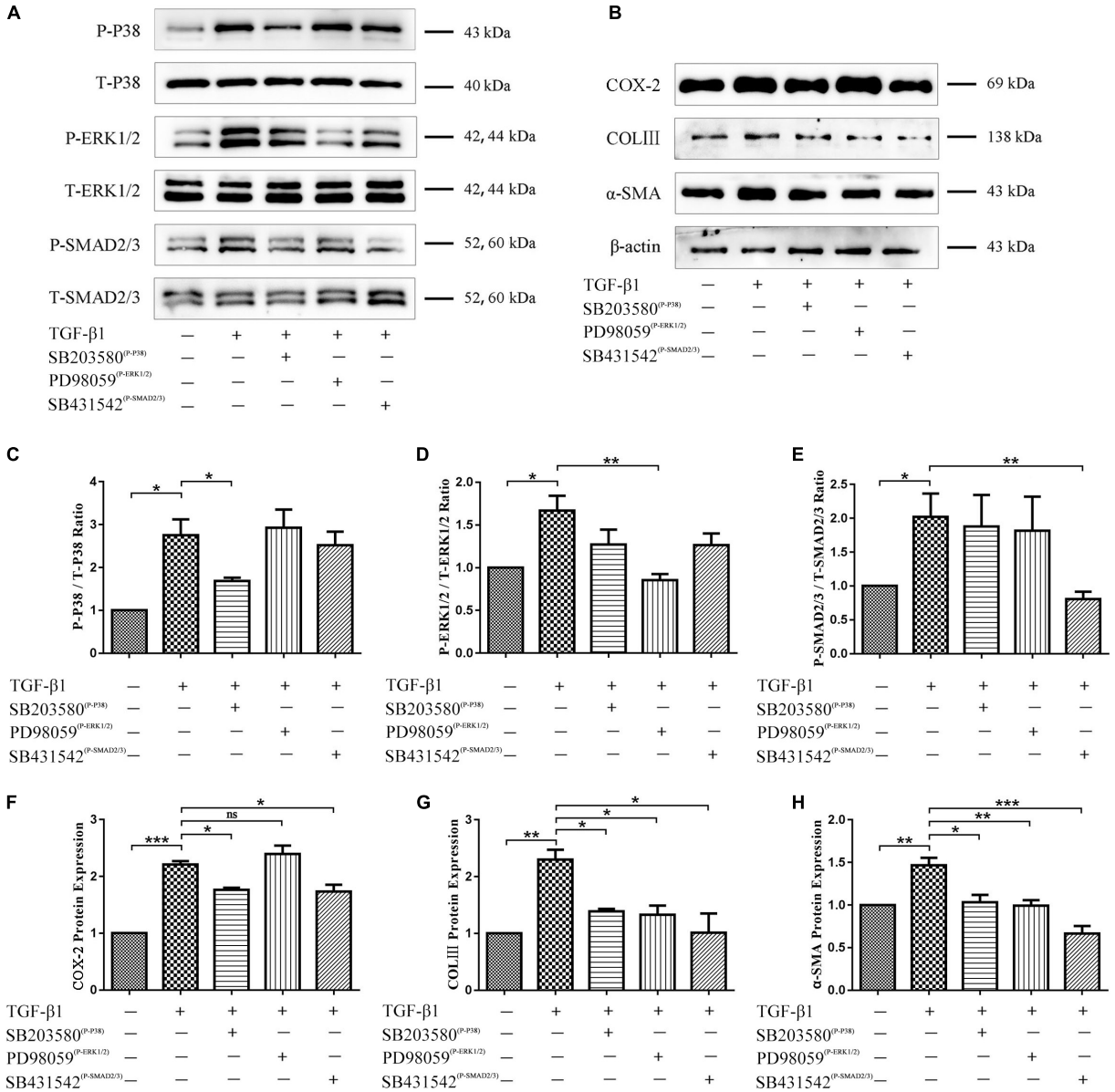

FIGURE 6 | Role of p38 MAPK, ERK1/2, and Smad2/3 signaling in TGF-β1-induced inflammatory and fibrotic fibroblast functions. **(A)** Western blots confirming inhibition of p38 MAPK, ERK1/2, and Smad2/3 signaling pathways by SB203580, PD98059, and SB431542. **(B)** Western blots demonstrating levels of COX-2, COLIII, and α-SMA after inhibition of p38 MAPK, ERK1/2, and Smad2/3 signaling pathways. Quantitation of **(C)** phospho-p38 MAPK, **(D)** phospho-ERK1/2, **(E)** phospho-Smad2/3, **(F)** COX-2, **(G)** COL III, **(H)** α-SMA proportions (n = 3). Data are represented as mean ± SD. *P < 0.05, **P < 0.01, ***P < 0.001.

TSCs + HGF have therapeutic potential to promote tendon healing via anti-inflammatory modulation of macrophages and associated cytokines.

However, inflammation is a double-edged sword. On the one hand, it prevents wound infection and can induce tissue healing; on the other hand, excessive inflammation can lead to scarring, thereby limiting tendon mobility and strength and increasing the risk of tendon reinjury (Wang et al., 2019). To investigate whether inhibiting inflammation is associated with decreased fibrosis and scar formation during tendon healing, the present study evaluated the expression of COLIII, α-SMA, TGF-β1, and fibronectin. Collagen is the major tendon constituent with parallelized COLI being the most abundant subtype. Indeed, COLI accounts for about 90% of normal tendon mass, and COLIII makes up less than 10% of this mass. A substantial increase in disorganized COLIII is typically observed in scar tissue, and decreases tendon strength while increasing the risk of reinjury (Liao et al., 2020). Previous studies demonstrate that increased COLIII expression is associated with scar formation and inferior tendon mechanical properties after healing (Matsumoto et al., 2002; Juneja et al., 2013). The present study demonstrates significantly lower COLIII levels in all stem

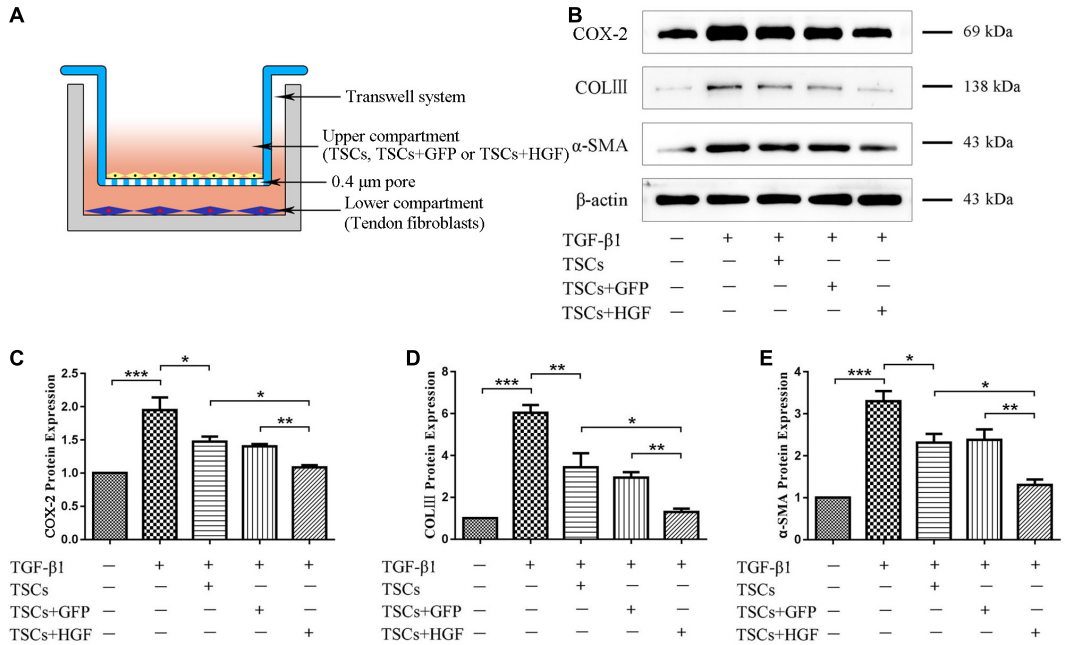

FIGURE 7 | TSC and tendon fibroblast coculture system and levels of fibroblast inflammatory and fibrotic proteins. **(A)** An indirect coculture model system. **(B)** WB images of COX-2, COLIII, and α-SMA. Quantitative analysis of **(C)** COX-2, **(D)** COL III, and **(E)** α-SMA (n = 3). Data are represented as mean ± SD. $^{*}P < 0.05$, $^{**}P < 0.01$, $^{***}P < 0.001$.

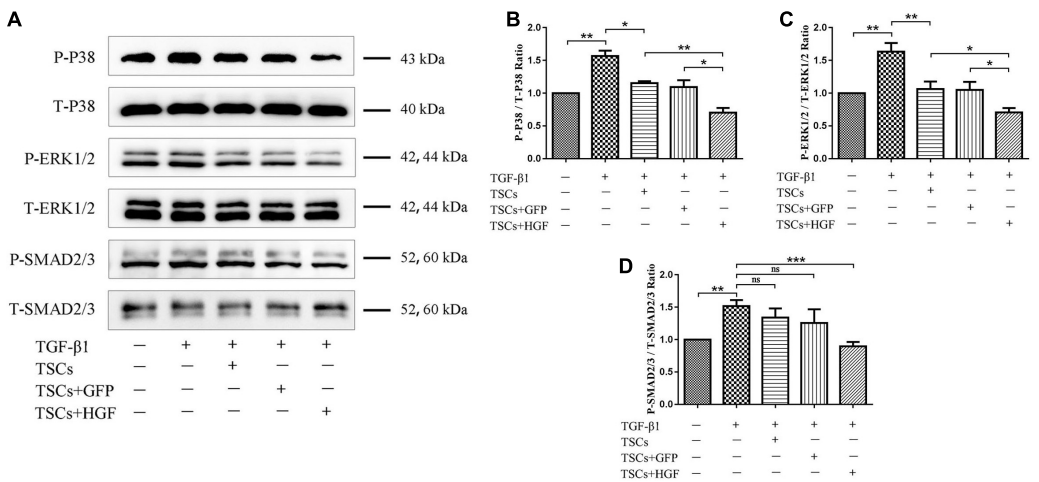

FIGURE 8 | Effect of coculture with TSCs on tendon fibroblast TGF-β1-induced signaling pathways. **(A)** Western blots demonstrating p38 MAPK, ERK1/2, and Smad2/3 protein levels. Quantitation of **(B)** phospho-p38 MAPK, **(C)** phospho-ERK1/2, and **(D)** phospho-Smad2/3 proportions (n = 3). Data are represented as mean ± SD. $^{*}P < 0.05$, $^{**}P < 0.01$, $^{***}P < 0.001$.

cell–treated groups but especially in the TSCs + HGF group, suggesting a positive effect of stem cells on tendon repair. We have previously demonstrated that inhibiting overexpression of the myofibroblast marker α-SMA restrains scar formation following tendon injury (Cui et al., 2011). The present study demonstrates that α-SMA levels in tendons sampled at weeks 4 and 8 postsurgery are significantly lower in all stem cell–treated groups, but especially in the TSCs + HGF group, suggesting inhibition of myofibroblast differentiation, which may contribute to decreased scar formation. In addition, the TSCs + HGF group demonstrates the lowest levels of TGF-β1 and fibronectin. Like inflammation, TGF-β1 can have context-dependent differential effects. Although it is important during the initial stages of tissue healing (contributing to scaffold formation for local tissue outgrowth), high levels of TGF-β1 during the later stages of wound healing can lead to scarring and impaired tissue function (James et al., 2008; Cui et al., 2011). Fibronectin exists largely as an ECM component of both embryonic and adult tissues; it is

also associated with the formation of scar tissue and adhesions after tendon injury and has a profound influence on wound-healing quality (Wang et al., 2019). The present findings suggest that TSCs + HGF may promote high-quality tendon healing (including inhibition of scar formation).

In recent years, GelMA has attracted attention in the domain of tissue engineering due to its excellent biological properties and experimenter ability to control its shape (including formation of three-dimensional structures) for personalized tissue repair (Yue et al., 2015; Shao et al., 2018). GelMA provides a degradable polymeric scaffold able to support cell attachment, infiltration, and proliferation; stem cell loading of GelMA has been widely explored for wound repair, and this material is proven to be an effective tissue engineering scaffold (Saleh et al., 2019; Lee et al., 2020; Luo et al., 2020). To the best of our knowledge, the present study is the first to apply TSC-loaded GelMA in a rat patellar tendon injury model. In our hands, GelMA photo-crosslinking stably attached the cell-loaded gel to the patellar tendon window defect, facilitating location-targeted cell therapy without the loss of cells. Thus, initial findings indicate that this may be a promising therapeutic strategy to enhance tendon healing.

The present study used a transwell coculture system to study the impact of TSCs + HGF on TGF-β1-induced tendon fibroblast function. As mentioned, TGF-β1 activity is implicated in fibrotic disorders and plays crucial roles in tissue healing and the pathogenesis of scarring and formation of adhesions (Yao et al., 2020). A large number of studies employ various strategies in an attempt to counter the more pathological effects of TGF-β1. For example, RelA/p65 inhibition prevents the formation of tendon adhesions by inhibiting TGF-β1-induced inflammation and cell proliferation (Chen et al., 2017); microRNA-21-3p gene-modified umbilical cord stem cell–derived exosomes inhibit tendon inflammation and adhesion formation by inhibiting TGF-β1-induced expression of COX-2, α-SMA, and COLIII (Yao et al., 2020); HGF can alleviate renal interstitial fibrosis via inhibiting the TGF-β1/SMAD pathway (Xu et al., 2018) and also regulates the activation of TGF-β1 in rat hepatocytes and hepatic stellate cells (Narmada et al., 2013); and we have previously demonstrated that HGF inhibits TGF-β1-induced fibrosis in a rat Achilles tendon injury model (Cui et al., 2011).Therefore, the present study pretreated tendon-derived fibroblasts with TGF-β1 to investigate whether the beneficial effects of stem cells on tendon healing may be associated with impacts on TGF-β1-induced pathways. Consistent with previous studies, TGF-β1 enhanced tendon fibroblast levels of inflammation and fibrosis indicators, including COX-2, α-SMA, and COLIII (Yao et al., 2020). Increased levels of α-SMA and COLIII likely indicate excessive deposition of ECM components: a pathological hallmark of fibrotic disorders. In addition, pro-inflammatory COX-2 is also associated with fibrosis and formation of adhesions after tendon injury (Chen et al., 2017; Yao et al., 2020). As hypothesized, all stem cell–exposed fibroblast groups, but especially the TSCs + HGF-exposed group, exhibited decreased TGF-β1-induced increases in indicator protein levels. These findings suggest that the beneficial effects of TSCs + HGF on tendon healing may be mediated in part via countering TGF-β1-induced functions. To further investigate the possibility that TSCs + HGF anti-inflammatory and antifibrotic effects are mediated via altered TGF-β1-induced signaling pathways, we studied stem cell impact on the major signal transduction pathways downstream of TGF-β1 (p38 MAPK, ERK1/2, and Smad2/3); these pathways are involved in cell proliferation, differentiation, development, inflammation, and apoptosis (Nuwormegbe et al., 2017). Coculture with TSCs + HGF most significantly inhibited TGF-β1-induced fibroblast increases in phosphorylated p38 MAPK, ERK1/2, and Smad2/3 protein levels, concomitant with a significant decrease in myofibroblast differentiation, and ECM synthesis. However, decreased ERK1/2 phosphorylation did not decrease levels of inflammatory indicators. These findings suggest that the antifibrotic effects of TSCs + HGF may be mediated via downmodulation of the p38 MAPK, ERK1/2, and Smad2/3 signaling pathways, and their anti-inflammatory effects may be mediated via downmodulation of the p38 MAPK and Smad2/3 (but not the ERK1/2) signaling pathways. Exposure to the other stem cell groups (TSCs and TSCs + GFP) also decreased fibroblast p38 MAPK and ERK1/2 (but not Smad2/3) pathway activation, suggesting that their therapeutic effects may be mediated via downmodulation of the p38 MAPK and ERK1/2 signaling pathways. Given that TSCs + HGF demonstrate the most pronounced effect on signaling pathway activation downmodulation, they may ultimately provide a more potent therapeutic effect than the other stem cell groups.

However, the present study suffers from several limitations. First, only a 1:1 coculture ratio of the two cell types was examined. Second, *in vitro* studies did not explore the impact of stem cells (including TSCs + HGF) on tenocytes. Third, the mechanism study of the effects of TSCs + HGF on immune cells is lacking. Finally, *in vivo* studies only show the histology by H&E staining, which may not completely detail the positive effect of TSCs + HGF on tendon repair. Further investigation may be required to prove this, including quantified histology scores, mechanical testing, and the size of collagen fibrils, among others. All these limitations are the bases and direction for further studies.

CONCLUSION

Taken together, findings of the present study demonstrate that increased HGF provision (by TSCs + HGF) inhibits inflammation and scar formation during tendon healing and suggest that inhibition of TGF-β1-induced p38 MAPK and Smad2/3 signaling may contribute to anti-inflammatory effects, while inhibition of TGF-β1-induced p38 MAPK, ERK1/2, and Smad2/3 signaling may contribute to antifibrotic effects. Thus, this study provides evidence supporting HGF-overexpression in TSCs possibly as a novel therapeutic strategy to enhance tendon healing. Additional future studies are warranted.

DATA AVAILABILITY STATEMENT

The raw data supporting the conclusions of this article will be made available by the authors, without undue reservation.

ETHICS STATEMENT

The animal study was reviewed and approved by the Harbin Medical University Ethics Committee.

AUTHOR CONTRIBUTIONS

MZ: experimental design, cytology experiments, animal experiments, data acquisition, data analysis, and manuscript writing. HL: cytology experiments, animal experiments, data acquisition, data analysis, and final approval of manuscript. TZ and MS: statistical analysis of the data and final approval of manuscript. WL and SY: experimental technical support and final approval of manuscript. QC and ZL: experimental design, text revision, and final approval of manuscript. All authors contributed to the article and approved the submitted version.

FUNDING

This study was supported by the National Natural Science Foundation of China (81871837 and 81572117) and the Specialized Research Fund for Doctoral Programs in Colleges and Universities of China (20132307110007).

ACKNOWLEDGMENTS

We would like to acknowledge the reviewers for their helpful comments on this manuscript.

REFERENCES

Chamberlain, C. S., Clements, A. E. B., Kink, J. A., Choi, U., Baer, G. S., Halanski, M. A., et al. (2019). Extracellular vesicle-educated macrophages promote early Achilles tendon healing. *Stem Cells* 37, 652–662. doi: 10.1002/stem.2988

Chang, C. H., Tsai, W. C., Lin, M. S., Hsu, Y. H., and Pang, J. H. (2010). The promoting effect of pentadecapeptide BPC 157 on tendon healing involves tendon outgrowth, cell survival, and cell migration. *J. Appl. Physiol.* 110, 774–780. doi: 10.1152/japplphysiol.00945.2010

Chen, S., Jiang, S., Zheng, W., Tu, B., Liu, S., Ruan, H., et al. (2017). RelA/p65 inhibition prevents tendon adhesion by modulating inflammation, cell proliferation, and apoptosis. *Cell Death Dis.* 8:e2710. doi: 10.1038/cddis.2017.135

Chen, X., Zhang, Y., Wang, W., Liu, Z., Meng, J., and Han, Z. (2018). Mesenchymal stem cells modified with heme oxygenase-1 have enhanced paracrine function and attenuate lipopolysaccharide-induced inflammatory and oxidative damage in pulmonary microvascular endothelial cells. *Cell. Physiol. Biochem.* 49, 101–122. doi: 10.1159/000492847

Cui, Q., Wang, Z., Jiang, D., Qu, L., Guo, J., and Li, Z. (2011). HGF inhibits TGF-β1-induced myofibroblast differentiation and ECM deposition via MMP-2 in Achilles tendon in rat. *Eur. J. Appl. Physiol.* 111, 1457–1463. doi: 10.1007/s00421-010-1764-4

Dai, M., Sui, B., Xue, Y., Liu, X., and Sun, J. (2018). Cartilage repair in degenerative osteoarthritis mediated by squid type II collagen via immunomodulating activation of M2 macrophages, inhibiting apoptosis and hypertrophy of chondrocytes. *Biomaterials* 180, 91–103. doi: 10.1016/j.biomaterials.2018.07.011

Fu, S. C., Cheuk, Y. C., Chan, K. M., Hung, L. K., and Wong, M. W. (2008). Is cultured tendon fibroblast a good model to study tendon healing? *J. Orthop. Res.* 26, 374–383. doi: 10.1002/jor.20483

James, R., Kesturu, G., Balian, G., and Chhabra, A. B. (2008). Tendon: biology, biomechanics, repair, growth factors, and evolving treatment options. *J. Hand Surg.* 33, 102–112. doi: 10.1016/j.jhsa.2007.09.007

Juneja, S. C., Schwarz, E. M., O'Keefe, R. J., and Awad, H. A. (2013). Cellular and molecular factors in fexor tendon repair and adhesions: a histological and gene expression analysis. *Connect. Tissue Res.* 54, 218–226. doi: 10.3109/03008207.2013.787418

Klinkert, K., Whelan, D., Clover, A. J. P., Leblond, A. L., Kumar, A. H. S., and Caplice, N. M. (2017). Selective M2 macrophage depletion leads to prolonged inflammation in surgical wounds. *Eur. Surg. Res.* 58, 109–120. doi: 10.1159/000451078

Kokubu, S., Inaki, R., Hoshi, K., and Hikita, A. (2020). Adipose-derived stem cells improve tendon repair and prevent ectopic ossification in tendinopathy by inhibiting inflammation and inducing neovascularization in the early stage of tendon healing. *Regen. Ther.* 14, 103–110. doi: 10.1016/j.reth.2019.12.003

Laplante, P., Brillant-Marquis, F., Brissette, M. J., Joannette-Pilon, B., Cayrol, R., Kokta, V., et al. (2017). MFG-E8 reprogramming of macrophages promotes wound healing by increased bFGF production and fbroblast functions. *J. Invest. Dermatol.* 137, 2005–2013. doi: 10.1016/j.jid.2017.04.030

Lee, K., Xue, Y., Lee, J., Kim, H. J., Liu, Y., Tebon, P., et al. (2020). A Patch of detachable hybrid microneedle depot for localized delivery of mesenchymal stem cells in regeneration therapy. *Adv. Funct. Mater.* 30:2000086. doi: 10.1002/adfm.202000086

Li, J., Zheng, C. Q., Li, Y., Yang, C., Lin, H., and Duan, H. G. (2015). Hepatocyte growth factor gene-modified mesenchymal stem cells augment sinonasal wound healing. *Stem Cells Dev.* 24, 1817–1830. doi: 10.1089/scd.2014.0521

Liao, X., Falcon, N. D., Mohammed, A. A., Paterson, Y. Z., Mayes, A. G., Guest, D. J., et al. (2020). Synthesis and formulation of four-arm PolyDMAEA-siRNA polyplex for transient downregulation of collagen type III gene expression in tgf-β1 stimulated tenocyte culture. *ACS Omega* 5, 1496–1505. doi: 10.1021/acsomega.9b03216

Luo, L., He, Y., Jin, L., Zhang, Y., Guastaldi, F. P., Albashari, A. A., et al. (2020). Application of bioactive hydrogels combined with dental pulp stem cells for the repair of large gap peripheral nerve injuries. *Bioact. Mater.* 6, 638–654. doi: 10.1016/j.bioactmat.2020.08.028

Manning, C. N., Martel, C., Sakiyama-Elbert, S. E., Silva, M. J., Shah, S., Gelberman, R. H., et al. (2015). Adipose-derived mesenchymal stromal cells modulate tendon fibroblast responses to macrophage-induced inflammation in vitro. *Stem Cell Res. Ther.* 6:74.

Matsumoto, F., Trudel, G., and Uhthof, H. K. (2002). High collagen type I and low collagen type III levels in knee joint contracture: an immunohistochemical study with histological correlate. *Acta Orthop. Scand.* 73, 335–343. doi: 10.1080/000164702320155365

Narmada, B. C., Chia, S. M., Tucker-Kellogg, L., and Yu, H. (2013). HGF regulates the activation of TGF-β1 in rat hepatocytes and hepatic stellate cells. *J. Cell. Physiol.* 228, 393–401. doi: 10.1002/jcp.24143

Ni, M., Lui, P. P. Y., Rui, Y. F., Lee, Y. W., Lee, Y. W., Tan, Q., et al. (2012). Tendon-derived stem cells (TDSCs) promote tendon repair in a rat patellar tendon window defect model. *J. Orthop. Res.* 30, 613–619. doi: 10.1002/jor.21559

Nuwormegbe, S. A., Sohn, J. H., and Kim, S. W. (2017). A PPAR – gamma agonist rosiglitazone suppresses fibrotic response in human pterygium fibroblasts by modulating the p38 MAPK pathway. *Invest. Ophthalmol. Vis. Sci.* 58, 5217–5226. doi: 10.1167/iovs.17-22203

Omoto, M., Suri, K., Amouzegar, A., Li, M., Katikireddy, K. R., Mittal, S. K., et al. (2017). Hepatocyte growth factor suppresses inflammation and promotes epithelium repair in corneal injury. *Mol. Ther.* 25, 1881–1888. doi: 10.1016/j.ymthe.2017.04.020

Ricchetti, E. T., Reddy, S. C., Ansorge, H. L., Zgonis, M. H., Van Kleunen, J. P., Liechty, K. W., et al. (2008). Effect of interleukin-10 overexpression on the properties of healing tendon in a murine patellar tendon model. *J. Hand Surg. Am.* 33, 1843–1852. doi: 10.1016/j.jhsa.2008.07.020

Rinoldi, C., Costantini, M., Kijeńska-Gawrońska, E., Testa, S., Fornetti, E., Heljak, M., et al. (2019). Tendon tissue engineering: effects of mechanical and

biochemical stimulation on stem cell alignment on cell-Laden Hydrogel Yarns. *Adv. Healthc. Mater.* 8:e1801218.

Saleh, B., Dhaliwal, H. K., Portillo-Lara, R., Shirzaei Sani, E., Abdi, R., Amiji, M. M., et al. (2019). Local immunomodulation using an adhesive hydrogel loaded with miRNA-laden nanoparticles promotes wound healing. *Small* 15:e1902232.

Shao, L., Gao, Q., Zhao, H., Xie, C., Fu, J., and Liu, Z. (2018). Fiber-based mini tissue with morphology-controllable GelMA microfibers. *Small* 14:1802187. doi: 10.1002/smll.201802187

Shi, Z., Wang, Q., and Jiang, D. (2019). Extracellular vesicles from bone marrow-derived multipotent mesenchymal stromal cells regulate inflammation and enhance tendon healing. *J. Transl. Med.* 17, 211–212.

Sunwoo, J. Y., Eliasberg, C. D., Carballo, C. B., and Rodeo, S. A. (2020). The role of the macrophage in tendinopathy and tendon healing. *J. Orthop. Res.* 38, 1666–1675. doi: 10.1002/jor.24667

Wang, L. S., Wang, H., Zhang, Q. L., Yang, Z. J., Kong, F. X., and Wu, C. T. (2017). Hepatocyte growth factor gene therapy for ischemic diseases and tissue regeneration. *Hum. Gene Ther.* 29, 413–423. doi: 10.1089/hum.2017.217

Wang, X., Tang, Y., Shen, R., Chen, J., Chen, G., Luo, G., et al. (2017). Hepatocyte growth factor (HGF) optimizes oral traumatic ulcer healing of mice by reducing inflammation. *Cytokinre* 99, 275–280. doi: 10.1016/j.cyto.2017.08.006

Wang, Y., He, G., Tang, H., Shi, Y., Kang, X., Lyu, J., et al. (2019). Aspirin inhibits inflammation and scar formation in the injury tendon healing through regulating JNK/STAT-3 signalling pathway. *Cell Prolif.* 52:e12650.

Wu, F., Nerlich, M., and Docheva, D. (2017). Tendon injuries: basic science and new repair proposals. *EFORT Open Rev.* 2, 332–342. doi: 10.1302/2058-5241.2.160075

Xu, J., Yu, T. T., Zhang, K., Li, M., Shi, H. J., Meng, X. J., et al. (2018). HGF alleviates renal interstitial fibrosis via inhibiting the TGF-β1/SMAD pathway. *Eur. Rev. Med. Pharmacol. Sci.* 22, 7621–7627.

Yang, Q. Q., Shao, Y. X., Zhang, L. Z., and Zhou, Y. L. (2018). Therapeutic strategies for flexor tendon healing by nanoparticle-mediated co-delivery of bFGF and VEGFA genes. *Colloids Surf. B Biointerfaces* 164, 165–176. doi: 10.1016/j.colsurfb.2018.01.031

Yang, Z., Cao, H., Gao, S., Yang, M., Lyu, J., and Tang, K. (2017). Effect of tendon stem cells in chitosan/β-glycerophosphate/collagen hydrogel on Achilles tendon healing in a rat model. *Med. Sci. Monit.* 23, 4633–4643. doi: 10.12659/msm.906747

Yao, Z., Li, J., Wang, X., Peng, S., Ning, J., Qian, Y., et al. (2020). MicroRNA-21-3p engineered umbilical cord stem cell-derived exosomes inhibit tendon adhesion. *J. Inflamm. Res.* 13, 303–316. doi: 10.2147/jir.s254879

Yi, X., Li, X., Zhou, Y., Ren, S., Wan, W., Feng, G., et al. (2014). Hepatocyte growth factor regulates the TGF-ß1 induced proliferation, differentiation and secretory function of cardiac fibroblasts. *Int. J. Mol. Med.* 34, 381–390. doi: 10.3892/ijmm.2014.1782

Yu, H., Cheng, J., Shi, W., Ren, B., Zhao, F., Shi, Y., et al. (2020). Bone marrow mesenchymal stem cells-derived exosomes promote tendon regeneration via facilitating the proliferation and migration of endogenous. *Acta Biomater.* 106, 328–341. doi: 10.1016/j.actbio.2020.01.051

Yue, K., Trujillo-de Santiago, G., Alvarez, M. M., Tamayol, A., Annabi, N., and Khademhosseini, A. (2015). Synthesis, properties, and biomedical applications of gelatin methacryloyl (GelMA) hydrogels. *Biomaterials* 73, 254–271. doi: 10.1016/j.biomaterials.2015.08.045

Zhang, J., Li, B., and Wang, J. H. (2011). The role of engineered tendon matrix in the stemness of tendon stem cells in vitro and the promotion of tendon-like tissue formation in vivo. *Biomaterials* 32, 6972–6981. doi: 10.1016/j.biomaterials.2011.05.088

Zhang, M., Liu, H., Cui, Q., Han, P., Yang, S., Shi, M., et al. (2020). Tendon stem cell-derived exosomes regulate inflammation and promote the high-quality healing of injured tendon. *Stem Cell Res. Ther.* 11:402.

Zhao, B., Li, X., Shi, X., Zhang, W., Wu, G., Wang, X., et al. (2018). Exosomal microRNAs derived from human amniotic epithelial cells accelerate wound healing by promoting the proliferationand migration of fibroblasts. *Stem Cells Int.* 2018:5420463.

Conflict of Interest: The authors declare that the research was conducted in the absence of any commercial or financial relationships that could be construed as a potential conflict of interest.

frontiers in Cell and Developmental Biology

REVIEW
published: 02 July 2021
doi: 10.3389/fcell.2021.687117

The Roles of MicroRNAs in Tendon Healing and Regeneration

Lingli Ding[1†], Min Wang[1†], Shengnan Qin[2] and Liangliang Xu[1*]*

[1] Lingnan Medical Research Center, The First Affiliated Hospital, Guangzhou University of Chinese Medicine, Guangzhou, China, [2] Department of Orthopaedics, Guangzhou Institute of Traumatic Surgery, Guangzhou Red Cross Hospital, Medical College, Jinan University, Guangzhou, China

Tendons connect the muscle abdomen of skeletal muscles to the bone, which transmits the force generated by the muscle abdomen contraction and pulls the bone into motion. Tendon injury is a common clinical condition occurring in certain populations, such as repeated tendon strains in athletes. And it can lead to substantial pain and loss of motor function, in severe cases, significant disability. Tendon healing and regeneration have attracted growing interests. Some treatments including growth factors, stem cell therapies and rehabilitation programs have been tried to improve tendon healing. However, the basic cellular biology and pathology of tendons are still not fully understood, and the management of tendon injury remains a considerable challenge. Regulating gene expression at post-transcriptional level, microRNA (miRNA) has been increasingly recognized as essential regulators in the biological processes of tendon healing and regeneration. A wide range of miRNAs in tendon injury have been shown to play vital roles in maintaining and regulating its physiological function, as well as regulating the tenogenic differentiation potential of stem cells. In this review, we show the summary of the latest information on the role of miRNAs in tendon healing and regeneration, and also discuss potentials for miRNA-directed diagnosis and therapy in tendon injuries and tendinopathy, which may provide new theoretical foundation for tenogenesis and tendon healing.

Keywords: microRNA, tendon healing, tendinopathy, tenogenesis, stem cells

OPEN ACCESS

Edited by:
Gang Li,
The Chinese University of Hong Kong, China

Reviewed by:
Erick Omar Hernandez-Ochoa, University of Maryland, Baltimore, United States
Laura N. Borodinsky, University of California, Davis, United States

***Correspondence:**
Shengnan Qin
qinqinsn@163.com
Liangliang Xu
xull-2016@gzucm.edu.cn

[†]These authors have contributed equally to this work and share first authorship

Specialty section:
This article was submitted to Stem Cell Research, a section of the journal Frontiers in Cell and Developmental Biology

Received: *29 March 2021*
Accepted: *11 June 2021*
Published: *02 July 2021*

Citation:
Ding L, Wang M, Qin S and Xu L (2021) The Roles of MicroRNAs in Tendon Healing and Regeneration. Front. Cell Dev. Biol. 9:687117. doi: 10.3389/fcell.2021.687117

INTRODUCTION

Tendon is a connective tissue composed of closely arranged bundles of parallel collagen fibers (Wang et al., 2012). It plays an important role in the skeletal muscle system. Tendons are located between muscles and bones and can cushion the pressure caused by the direct interaction between muscles and bones, thereby stabilizing the joints (Laurencin and Freeman, 2005; Thorpe and Screen, 2016). As a long-term pressure-bearing tissue, tendons are easy to form a variety of acute and chronic injuries (Khan et al., 1999). Since the beginning of this century, the global prevalence of tendon disease has been on the rise. Tendon disease is one of the most common diagnoses of people engaged in sports professions, accounting for 30% of the total number of injuries diagnosed (Millar et al., 2021). At the late stage of tendon healing, it is easy to form scar tissue with decreased strength. And it is easy to adhere to the surrounding tissue, which increases the risk of tendon injury again (Bruns et al., 2000; Sharma and Maffulli, 2005). On the other hand, there are fewer blood vessels and poor blood flow inside the tendon, which makes the tendon heal more slowly

(Whalen, 1951; Miyashita et al., 1997; Tempfer and Traweger, 2015; Nichols et al., 2019). The high frequency and slow healing of tendon injury not only seriously affects the normal life of patients, but also increases the social and economic burden. Therefore, how to promote tendon repair and regeneration is a great challenge in tissue engineering. miRNA is a small non-coding ribonucleic acid that participates in the regulation of cellular processes by inhibiting the translation and stability of messenger ribonucleic acid. Since the discovery of miRNA in the 1990s, people's understanding of miRNAs has been deepened (Lee et al., 1993; Di Leva et al., 2014), and its application has become more and more extensive. miRNAs play an important role in inflammation, cell cycle regulation, stress response, cell growth, differentiation, proliferation, apoptosis and migration etc. (Lee et al., 1993; Hata, 2013; Saliminejad et al., 2019), recent studies have shown that they also participate in tendon regeneration and repair.

Here, we briefly described the structure and function of tendon, and the biology of miRNA. Then the roles of miRNA in tendon repair and regeneration was summarized; and the potentials and challenges of miRNA-directed diagnosis and therapy in tendon injuries and tendinopathy were also discussed.

TENDON STRUCTURE

Tendon is a connective tissue rich in matrix, which is mainly composed of closely arranged bundles of parallel collagen fibers (Wang et al., 2012; Tsai et al., 2021). They are attached to muscles and bones, and stabilize joints by cushioning the pressure caused by direct interaction between muscles and bones (Laurencin and Freeman, 2005; Thorpe and Screen, 2016). The place where the tendon is inserted into the muscle is called the tendon joint, while the joint between the tendon and the bone is called the bone-tendon junction (O'Brien, 1997; Thorpe and Screen, 2016). The tendon, as a tissue that transmits and loads, transfers strength from the muscle to the bone and drives the joint movement by contracting the muscle (Wang, 2006; Voleti et al., 2012). There are usually no blood vessels inside the tendon, while there are blood vessels and nerves passing through the sheath around it (Kannus, 2000; Tempfer and Traweger, 2015).

Tendon is mainly composed of type I collagen (also known as collagen I, COL I), which contains a small amount of proteoglycans, glycoproteins and minor collagens (Voleti et al., 2012). The dry mass of human tendons accounts for about 30% of the total tendon mass, and the remaining 70% is water (Sharma and Maffulli, 2005). Type I collagen accounts for 65–80%, and elastin accounts for about 2% of the dry weight of tendons (Sharma and Maffulli, 2006). Collagen is mainly a helical structure formed by the intertwining of three chains (Voleti et al., 2012). It is constantly cross-linked to form the specific spatial structure of the tendon (Gaut and Duprez, 2016). The collagen fibers are considered to be the basic force transmission units of tendons, which are densely arranged in the extracellular matrix (ECM) and parallel to the bone-muscle axis (Nourissat et al., 2015). Among the tendon cells, tenoblasts and tenocytes accounts for about 90%, while the remaining 10% are mainly composed of chondrocytes, synovial cells, vascular endothelial cells and smooth muscle cells (Sharma and Maffulli, 2006; Wang, 2006).

Abbreviations: AMPK, adenosine 5′-monophosphate-activated protein kinase; BMSCs, bone marrow mesenchymal stem cells; COL 1, Type I Collagen; COL5A1, collagen type V α-1 chain; CUGBP2, CUG triplet repeat-binding protein 2; EC, endothelial cell; ECM, Extracellular Matrix; EGR-1, early growth response-1; FGF2, Fibroblast Growth Factor 2; HMGA2, high-mobility AT-hook 2; hTSPCs, human tendon-derived stem/progenitor cells; IRS1, insulin receptor substrate 1; KLF6, krüppel-like factor 6; miRBase, Microribonucleic Acid Database; miRNA/miR, microRNA; mRNA, messenger RNA; MSCs, mesenchymal stem cells; Nox4, NADPH oxidase 4; PPI, peptidyl-prolyl isomerase; pre-miRNA, miRNA precursor; RCT, rotator cuff tendon; RISC, RNA-induced silencing complex; ROCK1, Rho-associated coiled-coil protein kinase 1; Scx, scleraxis; Smad3, SMAD family member 3; TDSCs, tendon-derived stem cells; TGF-β, transforming growth factor-β; TNC, tenascin-C; TNMD, tenomodulin; TOB1, transducer of ERBB2, 1; TREM-1, triggering receptor expressed on myeloid cells-1; TSCs, tendon stem cells; Tsp-4, thrombospondin-4; TSPCs, tendon stem/progenitor cells; VEGFA, vascular endothelial growth factor-A; UTR, untranslated region.

MicroRNA Biology

Since the discovery of the first miRNA in 1993 and another miRNA let-7 7 years later (Lee et al., 1993; Reinhart et al., 2000; Di Leva et al., 2014), people's understanding of miRNA has been deepened for more than two decades, and the potential therapeutic effects of miRNA have been explored. According to the latest version of the microribonucleic acid database (miRBase) released in 2018, the human genome contains 1,917 annotated hairpin precursors and 2,654 mature sequences (Kozomara et al., 2019). miRNA is a class of endogenous non-coding RNA molecules with a length of about 22 nucleotides (Ambros et al., 2003; Ambros, 2004; Kabekkodu et al., 2018; Lu and Rothenberg, 2018). miRNA regulates gene expression mainly by binding to mRNA, which plays an important role in cell growth, differentiation, proliferation and apoptosis (Vasudevan et al., 2007; Sayed and Abdellatif, 2011). They are widely distributed in many tissues in the body which can be extracted from cells, tissues and body fluids (tears, urine, plasma and serum) (Lu and Rothenberg, 2018). Most of the miRNAs are transcribed by the ribonucleic acid polymerase II (Cai et al., 2004; Lee et al., 2004), but there is a small part of miRNAs that are associated with Alu repeats have been reported to be transcribed by Pol III (Borchert et al., 2006). The production of miRNA is initiated by the transcription of pri-miRNA in the nucleus. Before being transported to the cytoplasm, pri-miRNA is further processed by RNase III Drosha enzyme to form miRNA precursor (pre-miRNA). Then it is digested by another RNAse III enzyme Dicer, and binds with Argonaute protein to form RNA-induced silencing complex (RISC). After that, one of the double strands is degraded and the other forms a mature miRNA (Esteller, 2011; Di Leva et al., 2014; Koturbash et al., 2015; Vidigal and Ventura, 2015). Although the miRNAs do not encode proteins themselves, they could influence the transcription of mRNAs to regulate proteins expression (Selbach et al., 2008). The functions of miRNA are mainly divided into four aspects: (1) participate in epigenetic regulation of gene expression; (2) mRNA degradation; (3) post-transcriptional inhibition of target mRNA translation; (4) act as a ligand to bind to immune receptors and participate in inflammatory response (Carthew and Sontheimer, 2009; Fabbri et al., 2012; Lehmann et al., 2012;

Fritz et al., 2016; Kabekkodu et al., 2018). Therefore, exploring new means of treating diseases are made possible by targeting miRNAs to intervene in the activity of specific genes. This strategy is also beneficial for promoting tendon healing and regeneration which is linked to the roles of miRNAs in tendon.

MICRORNAS REGULATE TENDON HEALING

Tendon healing is characterized by scar formation, tissue disorder, and decreased mechanical properties (Andarawis-Puri et al., 2015). Tendon healing can be generally summarized as three stages: inflammatory response stage, proliferative repair stage and remodeling stage, and these three stages overlap each other (Strickland, 2000). Tendinopathy is a failed healing reaction, accompanied by haphazard proliferation of tendinocytes, intracellular abnormalities, destruction of collagen fibers, and subsequent increase in the non-collagen matrix (Longo et al., 2018). Many miRNAs have been shown to be involved in regulating the biological processes of tendon healing (Summarized in **Table 1**).

miRNAs Regulate Cellular Proliferation and Inflammation

Apoptosis of tendinocytes is accelerated within a few days after injury, followed by increased cell proliferation within 2–4 weeks, which activates molecular events to inhibit apoptosis (Wu et al., 2010). One study filtrated differentially expressed genes between diseased and normal tendons, and miR-499 was found to regulate CUGBP2 and MYB which are important regulators of cellular proliferation, apoptosis and differentiation (Cai et al., 2015). Inhibiting miRNA-205-5p could promote tendon-bone healing of rotator cuff tendon (RCT) through increasing cellular viability and proliferation (Xu et al., 2019).

It has been reported that inflammation is involved in the whole process of tissue repair, with both advantages and disadvantages (Eming et al., 2009). The expression levels of miRNAs that are inflammatory targets mediated by the JAK2/STAT3 pathway, such as miR-146a-5p, miR-193b-3p, etc., were significantly reduced in glenohumeral arthritis tendon (Thankam et al., 2018). The network analysis of genes associated with AMPK and TREM-1 signaling revealed miR-31-5p, miR-195-5p and other thirteen miRNAs might be interrelated with the pathogenesis of RCT injury patients (Thankam et al., 2019). Such knowledge has important implications for inflammatory response and proliferative repair stage of tendon healing.

miRNAs Regulate Tendon Adhesion

Despite advances in tendon repair and post-operative rehabilitation, tendon adhesion is still considered to be a challenging part of the repair process. The formation of adhesion during tendon healing is regulated by TGF-β, Smad3, p65, etc. (Katzel et al., 2011; Wu et al., 2016; Chen et al., 2017). Using miRNA therapy to modulate TGF-β expression holds great promise in preventing tendon adhesion formation (Chen et al., 2009). Overexpression of miR-29b down-regulated TGF-β1/Smad3 levels, and inhibited fibroblast growth, thereby enhanced tendon healing after rats Achilles tendon injury (Chen et al., 2014). Exosomes are rich in miRNAs, which act as important regulators of intercellular communication and play an irreplaceable role in inflammation, fibrogenesis, and tissue repair (Simeoli et al., 2017). Exosomal miR-21-5p secreted by bone marrow macrophages directly targets Smad7 and leads to increased proliferation and migration ability of tenocytes as well as fibrosis activity, providing a potential target for the prevention and treatment of tendon adhesion (Cui et al., 2019). In addition, a study has shown that human Umbilical Cord Stem Cell-Derived Exosomes may regulate p65 activity through the delivery of miR-21a-3p, and ultimately inhibit tendon adhesion (Yao et al., 2020).

These studies are promising for further research into tendon adhesion, and are critical to determine how to improve repair outcomes and identify new therapeutic strategies to promote tendon healing and prevent adhesion formation.

miRNAs Regulate Tendon Extracellular Matrix

Tenocytes produce ECM which participates in tendon injury repair to maintain tendons homeostasis. The matrix remodeling rate of pathological tendons is increased, which leads to the decrease of mechanical stability of tendons and more vulnerable to injury (Longo et al., 2018). ECM disrupted by matrix metalloproteinases is another mark for ECM remodeling occurring at the site of the lesion (Xue and Jackson, 2015). Seven miRNAs, including miR-145-5p, miR-151a-3p, miR-382-5p, miR-199a-5p, miR-21-5p, miR-125a-5p, and miR-498 were found to be highly active and are thought to mediate major biological processes related to tendon matrix body integrity, which may be associated with tendon-related pathology (Thankam et al., 2016). COL5A1 encodes the α1 chain of type V collagen which is a minor amount fibrillar collagen (Posthumus et al., 2011). In its 3′-untranslated region (3′-UTR), COL5A1 gene has a *Bst*UI restriction fragment length polymorphisms, which is associated with achilles tendon pathology and more specifically, chronic achilles tendinopathy (Mokone et al., 2006). miRNA can inhibit protein synthesis by binding to COL5A1 3′-UTR to regulate target mRNA stability and/or translation efficiency (Garzon et al., 2009). A functional miRNA site for miR-608 within the COL5A1 3′-UTR was identified, which has important implications for the understanding of the molecular basis of tendinopathy and other exercise-related phenotypes (Abrahams et al., 2013). miR-29a demonstrated a functional role in post-transcriptional regulation of collagen in murine and human (Millar et al., 2015).

miRNAs Regulate Tendon Homeostasis

Some studies have highlighted miRNAs involved in tendon homeostasis during developmental and healing processes. Skeletal muscle has intimate functional adaptations with tendon, and they are called as "tendon units" (Magnusson et al., 2008). miRNAs including miRNA-1, miRNA-133a, miRNA-133a* and miRNA-133b, which regulate striated muscle to mechanical loading, unloading and various disease

TABLE 1 | Summary of miRNAs in tendon tendinopathy.

miRNA	Targets	Models	Cells	Biological functions	References
miRNA-499	CUGBP2, MYB	Clinical samples of tendinopathy		Regulated cell proliferation, tenocyte apoptosis and differentiation	Cai et al., 2015
miR-205-5p	VEGFA		Rats BMSCs	involved in tendon-bone healing of RCT	Xu et al., 2019
miR-146a-5p, miR-193b-3p, etc.	JAK2/STAT3 and interconnecting pathways	Clinical Human biceps tendons		Linked to inflammation	Thankam et al., 2018
miR-31-5p, miR-195-5p, etc.	AMPK and TREM-1 signaling	Clinical Human rotator cuff tendon injuries		Associated with the pathogenesis of RCT injuries with fatty infiltration and inflammation	Thankam et al., 2019
miR-29b	TGF-β1/ Smad3	Achilles tendon injury rats		Inhibition of fibroblasts growth.	Chen et al., 2014
miR-21-5p	Smad7	tendon adhesion in mice	Tenocytes and fibroblasts	Controlling the fibrotic healing response	Cui et al., 2019
miR-337-3p	IRS1 and Nox4		Rat TSPCs	Alleviating ectopic ossification in rat tendinopathy	Geng et al., 2020
miR-21-3p	p65		HUMSC-Exos	tendon adhesion	Yao et al., 2020
miR-145-5p, miR-151a-3p, miR-382-5p, miR-199a-5p, miR-21-5p, miR-125a-5p, and miR-498	COL1A2, COL3A1, MMP9 and MMP2	Clinical human shoulder tendons		Associated with the integrity of tendon matrisome	Thankam et al., 2016
miR-608	COL5A1		HT1080 fibrosarcoma cells	Associated with the molecular basis of tendinopathy	Abrahams et al., 2013
miR-29a	IL-33/sST2	Superficial digital flexor tendon of horses	Human tenocytes	Facilitating tissue remodeling in the tendon after injury	Millar et al., 2015; Watts et al., 2017
miRNA-338, miRNA-381	Scx	Untrained adult rats under a single session of mechanical loading	Tendon fibroblast	Regulating development of limb tendons	Mendias et al., 2012
miR28-5p	p53 deacetylase sirtuin 3		Primary human tenocytes	Prevention of bim RNA Degradation	Poulsen et al., 2014
miR-148a-3p	KLF6		A co-culture system of tenocytes with ECs	Correlated with Tsp-4 levels and promoting angiogenesis	Ge et al., 2018
miR-210	VEGF, FGF2 and COL 1	Transected and repaired rats achilles tendons		*via* acceleration of angiogenesis	Usman et al., 2015

processes (McCarthy et al., 2009; McCarthy, 2011), are all increased in mechanically loaded tendons and TGF-β-treated fibroblasts (Mendias et al., 2012). Mechanosensitive miRNAs, including miR-338, and miR-381, may bind to the 3′-UTR of scleraxis (Scx), which is a key regulator of extremity tendon development (Mendias et al., 2012). miR-100, miR-378, miR-205, miR-21, miR-221, and miR-222 were shown to involve with the accommodation of ECM synthesis and cell proliferation. And the let-7 family (such as let-7a, let-7e, and let-7b) also plays significant role in adjusting postnatal tendon adaptation to mechanical loading and TGF-β treatment (Mendias et al., 2012). Overexpression of mechanical sensitive miR-337-3p mitigates ectopic ossification in rat tendinopathy model *via* targeting insulin receptor substrate 1 (IRS1) and NADPH oxidase 4 (Nox4) of tendon derived stem cells, which not only provides a new understanding of the molecular mechanism of heterotopic ossification in tendinopathy, but also emphasizes the significance of miR-337-3p as a recognized therapeutic target for the clinical treatment of tendinopathy (Geng et al., 2020). Tenocytes routinely encounter oxidative stress. High glucose combined with oxidative stress lead to the up-regulation of miR28-5p which directly down-regulates the expression of p53 deacetylase sirtuin 3, leading to the increase of p53 acetylation level (Poulsen et al., 2014).

Thrombospondin-4 (Tsp-4) is indispensable for muscle attachment and ECM assembly at muscle-tendon junctions (Subramanian and Schilling, 2014). Targeting Krüppel-like factor 6 (KLF6), miR-148a-3p could affect the expression of TSP-4 in tendonocytes, and is closely related with Tsp-4 levels in tendinopathy tissues, which also promoted endothelial cell (EC) angiogenesis (Ge et al., 2018). Single local injection of double stranded miR-210 accelerated neovascularization through upregulating the expression of VEGF, FGF2 and type I collagen (COL1), and induced a microenvironment conducive to rat Achilles tendon healing during the early phase (Usman et al., 2015). The formation of new capillaries through angiogenesis is the key to tendon healing. However, excessive or dysfunctional angiogenic responses may adversely affect the healing outcome.

Understanding the relationship between miRNAs and the biological elements of tendon development, tendon homeostasis, and healing is the first requirement to determine an effective treatment for tendinopathy.

MICRORNAS IN TENOGENIC DIFFERENTIATION

The aim of tendon regeneration is to restore its inherent structural and functional characteristics, which remains a great challenge (Andarawis-Puri et al., 2015). Stem cell-based therapy has become an important research direction in tissue engineering and regenerative medicine, especially for tendon and bone. Mesenchymal stem cells (MSCs) and tendon stem/progenitor cells (TSPCs) have received increasing attention toward tenogenic differentiation and tendon regeneration. MSCs are self-renewing, cultured and extended adult stem cells isolated from a variety of tissues with the ability of multipotent differentiation (Ferreira et al., 2018). TSPCs referred to as tendon-derived stem cells (TDSCs) or tendon stem cells (TSCs). These cells, residing in the fascicular matrix of tendon, also have self-renewal and multi-lineage differentiation ability, and might open a new field of tenogenesis and replacement of damaged tendons (Zhou et al., 2010). Current studies with respect to the effect of miRNAs

TABLE 2 | Summary of miRNAs in tenogenic differentiation (+).

miRNA	stem cells		Targets	Tenogenic differentiation	References
	Cell type	Tissue origin			
miR-140-5p	TSPCs	Human tendons	Pin1	(–)	Chen et al., 2015a
miR-29b-3p	MSCs and TSPCs	Human	TGF-β1 and COL1A1	(–)	Lu et al., 2017
miR-378a	TSPCs	Mice tail tendons	TGF-β2	(–)	Liu et al., 2019
miR124	TSPCs	Human Anterior Cruciate Ligament	EGR1	(–)	Wang et al., 2016
let-7	TSPCs	Human	HMGA2	(–)	Sun et al., 2020
miR-135a	TSPCs	Rat Achilles tendons	ROCK1	(–)	Chen et al., 2015b
miR-217	TSPCs	Human Achilles tendons	p16	(+)	Han et al., 2017
miR-218	BMSCs	Rats	TOB1	(+)	Gao et al., 2016

(+) and (–) represent promotion and inhibition, respectively.

known to be involved in tenogenesis were summarized in **Table 2**.

miRNAs Inhibit Tenogenic Differentiation

It is well known that TGF-β1 is produced by fibroblasts and can be upregulated in autosynthesis, and overproduction of TGF-β1 leads to excessive cell proliferation and matrix synthesis (Tomasek et al., 2002; Frangogiannis, 2020). Type I collagen (COL1), forming macromolecular networks, is the most abundant protein in the human body and provides strength and resiliency to tissues such as tendons, and ligaments (Rittié, 2017). miR-29b-3p has been reported to directly inhibit the expression of TGF-β1 and COL1, thereby forming a new regulatory feedback loop between H19 and TGF-β1 and inhibiting tendon differentiation (Lu et al., 2017). Transforming growth factor β2 (TGF-β2) is required for fetal tendon development in mice and had been shown to induce Scx expression in mouse and chick embryos (Pryce et al., 2009; Havis et al., 2016). Embedding in the sequence of this transcriptional regulator of oxidative energy metabolism is miR-378a, which is involved in metabolic pathways, mitochondrial energy homeostasis, and related biological processes such as muscle development, differentiation, and regeneration (Krist et al., 2015). In miR-378a knock-in transgenic mice and their TSPCs, miR-378a impaired tenogenic differentiation and tendon injury healing by inhibition collagen and ECM production *via* reducing TGF-β2 (Liu et al., 2019). Early growth response-1 (EGR-1) regulated specific differentiation of TSPCs into tenocytes and also induced the expression of tendon marker genes SCX, TNMD, TNC, and COL1 both *in vitro* and *in vivo* (Tao et al., 2015). Directly binding with EGR-1, miR-124 prevented collagen formation and tendon differentiation *via* suppressing EGR-1 expression (Wang et al., 2016). The high-mobility AT-hook 2 (HMGA2) mRNA transcript, involved in many cellular processes, contains seven complementary sites for let-7 binding in its 3′ -UTR and is known for its regulatory role in stem cell self-renewal and differentiation along with oncogenesis (Hammond and Sharpless, 2008). Recent studies have established that HMGA2 overexpression protected hTSPCs against H_2O_2-induced loss of stemness through autophagy activation, while increased HMGA2 silencing by the miRNA let-7 could induce hTSPC impairments, and thus plays a critical role in tendon homeostasis and regeneration (Sun et al., 2020). Rho-associated coiled-coil protein kinase 1 (ROCK1) plays vital roles in many aspects including cell morphology, mitosis, motility, and even

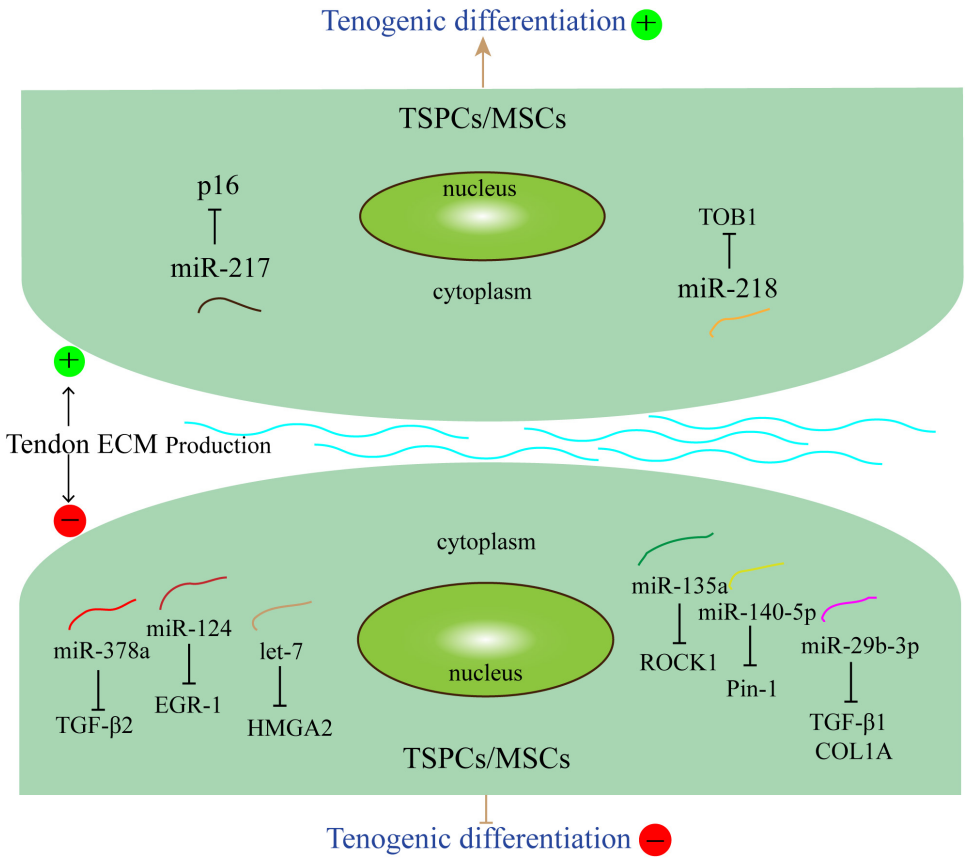

FIGURE 1 | miRNAs related to tenogenic differentiation. Several miRNAs, such as miR-140-5p, miR-29b-3p, miR-378a, miR124, let-7, and miR-135a could inhibit tenogenic differentiation. Other miRNAs, including miR-217 and miR-218 could promote tenogenic differentiation. The arrows and T-shaped lines point toward mechanisms that represent promotion and inhibition, respectively.

senescence (Julian and Olson, 2014; Guan et al., 2020). miR-135a which directly binded to the 3′-UTR of ROCK1, suppresses proliferation, migration and tenogenic differentiation of TSPCs (Chen et al., 2015b). miR-140-5p has been shown to delay the progression of human TSPCs senescence by targeting Pin1 which is a highly conserved peptidyl-prolyl isomerase (PPI) (Chen et al., 2015a). Therefore, Pin1 overexpression may increases tendon differentiation and inhibits senescence of TSPCs.

miRNAs Promote Tenogenic Differentiation

Aged TSPCs showed substantial upregulation of senescence marker $p16^{INK4A}$ (Kohler et al., 2013). Osteogenic and adipogenic differentiation capacity is significantly restored by $p16^{INK4A}$ knockdown in aging MSCs (Feng et al., 2014). Aged TSPCs showed decreased tenogenic differentiation capacity and upregulation of p16 which is a direct target of miR-217 (Han et al., 2017). Furthermore, TSPCs senescence may lead to defective self-renewal and altered fate (Zhou et al., 2010). TOB1 (Transducer of ERBB2, 1) is one of the TOB/B-cell translocation gene family. A study has suggested that the expression of TOB1 increased with aging during skeletal muscle development and the proliferative potential of myoblasts decreased with muscle development and aging (Yuan et al., 2011). What's more, TOB1 is a negative regulator of BMP/Smad signaling, which negatively regulates proliferation and differentiation of osteoblasts by inhibiting the activity of receptor-regulated Smad protein (Xiong et al., 2006). A study investigated that miR-218 was found to promote the role of BMSCs in tendon-bone healing by inhibiting TOB1 in a rat supraspinatus repair model (Gao et al., 2016).

These studies showed that miRNAs may affect the differentiation of tendon stem cells and mesenchymal stem cells through different pathways and mechanisms (**Figure 1**). Understanding the functional of miRNAs and their roles in physiological and pathological processes of tendons is crucial for the development of new therapies for tenogenic differentiation and repair.

CHALLENGES AND FUTURE PERSPECTIVES

miRNAs have been shown to regulate many potential genes related with tendon healing and tenogensis. There is great hope that tendon stem cell research could be applied to improve tendon injuries. TSPCs and MSCs are expected to be the mediums for tendon repair and regeneration, which is regulated by some director genes and a set of miRNAs coupled with some niche factors such as VEGF, TGF-β, ECM, oxidative stress, and mechanical stimuli, etc. Therefore, the study of these miRNAs may provide some potential targets for the diagnosis of tendon diseases and regeneration therapy in the future.

However, miRNAs reaching the target tendon is limited because of the poor pharmacokinetic properties of miRNAs, which means a need to produce adjuvant carrier systems that increase the stability of miRNAs. Future studies should identify how these miRNAs act on other stem cells and their extracellular microenvironments, and discover miRNAs which are responsible for tendon healing and tendon regeneration. And more importantly, future research should focus on finding the methods and approaches applicable to clinical practice.

AUTHOR CONTRIBUTIONS

LX and SQ conceived, designed, supervised, and commented on all the drafts of this manuscript. LD and MW contributed to the manuscript completion. All authors read and approved the final manuscript.

REFERENCES

Abrahams, Y., Laguette, M. J., Prince, S., and Collins, M. (2013). Polymorphisms within the COL5A1 3'-UTR that alters mRNA structure and the MIR608 gene are associated with Achilles tendinopathy. *Ann. Hum. Genet.* 77, 204–214. doi: 10.1111/ahg.12013

Ambros, V. (2004). The functions of animal microRNAs. *Nature* 431, 350–355. doi: 10.1038/nature02871

Ambros, V., Bartel, B., Bartel, D. P., Burge, C. B., Carrington, J. C., Chen, X., et al. (2003). A uniform system for microRNA annotation. *RNA* 9, 277–279. doi: 10.1261/rna.2183803

Andarawis-Puri, N., Flatow, E. L., and Soslowsky, L. J. (2015). Tendon basic science: development, repair, regeneration, and healing. *J. Orthop. Res.* 33, 780–784. doi: 10.1002/jor.22869

Borchert, G. M., Lanier, W., and Davidson, B. L. (2006). RNA polymerase III transcribes human microRNAs. *Nat. Struct. Mol. Biol.* 13, 1097–1101. doi: 10.1038/nsmb1167

Bruns, J., Kampen, J., Kahrs, J., and Plitz, W. (2000). Achilles tendon rupture: experimental results on spontaneous repair in a sheep-model. *Knee Surg. Sports Traumatol. Arthrosc.* 8, 364–369. doi: 10.1007/s001670000149

Cai, X., Cai, M., and Lou, L. (2015). Identification of differentially expressed genes and small molecule drugs for the treatment of tendinopathy using microarray analysis. *Mol. Med. Rep.* 11, 3047–3054. doi: 10.3892/mmr.2014.3081

Cai, X., Hagedorn, C. H., and Cullen, B. R. (2004). Human microRNAs are processed from capped, polyadenylated transcripts that can also function as mRNAs. *RNA* 10, 1957–1966. doi: 10.1261/rna.7135204

Carthew, R. W., and Sontheimer, E. J. (2009). Origins and mechanisms of miRNAs and siRNAs. *Cell* 136, 642–655. doi: 10.1016/j.cell.2009.01.035

Chen, C. H., Zhou, Y. L., Wu, Y. F., Cao, Y., Gao, J. S., and Tang, J. B. (2009). Effectiveness of microRNA in Down-regulation of TGF-beta gene expression in digital flexor tendons of chickens: in vitro and in vivo study. *J. Hand Surg. Am.* 34, 1777–1784.e1.

Chen, L., Liu, J., Tao, X., Wang, G., Wang, Q., and Liu, X. (2015a). The role of Pin1 protein in aging of human tendon stem/progenitor cells. *Biochem. Biophys. Res. Commun.* 464, 487–492. doi: 10.1016/j.bbrc.2015.06.163

Chen, L., Wang, G. D., Liu, J. P., Wang, H. S., Liu, X. M., Wang, Q., et al. (2015b). miR-135a modulates tendon stem/progenitor cell senescence via suppressing ROCK1. *Bone* 71, 210–216. doi: 10.1016/j.bone.2014.11.001

Chen, Q., Lu, H., and Yang, H. (2014). Chitosan inhibits fibroblasts growth in Achilles tendon via TGF-β1/Smad3 pathway by miR-29b. *Int. J. Clin. Exp. Pathol.* 7, 8462–8470.

Chen, S., Jiang, S., Zheng, W., Tu, B., Liu, S., Ruan, H., et al. (2017). RelA/p65 inhibition prevents tendon adhesion by modulating inflammation, cell proliferation, and apoptosis. *Cell Death Dis.* 8:e2710. doi: 10.1038/cddis.2017.135

Cui, H., He, Y., Chen, S., Zhang, D., Yu, Y., and Fan, C. (2019). Macrophage-derived miRNA-containing exosomes induce peritendinous fibrosis after

tendon injury through the miR-21-5p/Smad7 pathway. *Mol. Ther. Nucleic Acids* 14, 114–130. doi: 10.1016/j.omtn.2018.11.006

Di Leva, G., Garofalo, M., and Croce, C. M. (2014). MicroRNAs in cancer. *Ann. Rev. Pathol.* 9, 287–314.

Eming, S. A., Hammerschmidt, M., Krieg, T., and Roers, A. (2009). Interrelation of immunity and tissue repair or regeneration. *Semin. Cell Dev. Biol.* 20, 517–527. doi: 10.1016/j.semcdb.2009.04.009

Esteller, M. (2011). Non-coding RNAs in human disease. *Nat. Rev. Genet.* 12, 861–874.

Fabbri, M., Paone, A., Calore, F., Galli, R., Gaudio, E., Santhanam, R., et al. (2012). MicroRNAs bind to Toll-like receptors to induce prometastatic inflammatory response. *Proc. Natl. Acad. Sci. U.S.A.* 109, E2110–E2116.

Feng, X., Xing, J., Feng, G., Huang, D., Lu, X., Liu, S., et al. (2014). p16(INK4A) mediates age-related changes in mesenchymal stem cells derived from human dental pulp through the DNA damage and stress response. *Mech. Ageing Dev.* 14, 46–55. doi: 10.1016/j.mad.2014.09.004

Ferreira, J. R., Teixeira, G. Q., Santos, S. G., Barbosa, M. A., Almeida-Porada, G., and Gonçalves, R. M. (2018). Mesenchymal stromal cell secretome: influencing therapeutic potential by cellular pre-conditioning. *Front. Immunol.* 9:2837. doi: 10.3389/fimmu.2018.02837

Frangogiannis, N. (2020). Transforming growth factor-β in tissue fibrosis. *J. Exp. Med.* 217:e20190103.

Fritz, J. V., Heintz-Buschart, A., Ghosal, A., Wampach, L., Etheridge, A., Galas, D., et al. (2016). Sources and functions of extracellular small RNAs in human circulation. *Annu. Rev. Nutr.* 36, 301–336. doi: 10.1146/annurev-nutr-071715-050711

Gao, Y., Zhang, Y., Lu, Y., Wang, Y., Kou, X., Lou, Y., et al. (2016). TOB1 deficiency enhances the effect of bone marrow-derived mesenchymal stem cells on tendon-bone healing in a rat rotator cuff repair model. *Cell Physiol. Biochem.* 38, 319–329. doi: 10.1159/000438632

Garzon, R., Calin, G. A., and Croce, C. M. (2009). MicroRNAs in cancer. *Annu. Rev. Med.* 60, 167–179.

Gaut, L., and Duprez, D. (2016). Tendon development and diseases. *Wiley Interdiscip. Rev. Dev. Biol.* 5, 5–23. doi: 10.1002/wdev.201

Ge, H., Shrestha, A., Liu, C., Wu, P., and Cheng, B. (2018). MicroRNA 148a-3p promotes Thrombospondin-4 expression and enhances angiogenesis during tendinopathy development by inhibiting Krüppel-like factor 6. *Biochem. Biophys. Res. Commun.* 502, 276–282. doi: 10.1016/j.bbrc.2018.05.167

Geng, Y., Zhao, X., Xu, J., Zhang, X., Hu, G., Fu, S. C., et al. (2020). Overexpression of mechanical sensitive miR-337-3p alleviates ectopic ossification in rat tendinopathy model via targeting IRS1 and Nox4 of tendon-derived stem cells. *J. Mol. Cell Biol.* 12, 305–317. doi: 10.1093/jmcb/mjz030

Guan, X., Guan, X., Dong, C., and Jiao, Z. (2020). Rho GTPases and related signaling complexes in cell migration and invasion. *Exp. Cell. Res.* 388:111824. doi: 10.1016/j.yexcr.2020.111824

Hammond, S. M., and Sharpless, N. E. (2008). HMGA2, microRNAs, and stem cell aging. *Cell* 135, 1013–1016. doi: 10.1016/j.cell.2008.11.026

Han, W., Wang, B., Liu, J., and Chen, L. (2017). The p16/miR-217/EGR1 pathway modulates age-related tenogenic differentiation in tendon stem/progenitor cells. *Acta Biochim. Biophys. Sin. (Shanghai)* 49, 1015–1021. doi: 10.1093/abbs/gmx104

Hata, A. (2013). Functions of microRNAs in cardiovascular biology and disease. *Annu. Rev. Physiol.* 75, 69–93. doi: 10.1146/annurev-physiol-030212-183737

Havis, E., Bonnin, M. A., Esteves de Lima, J., Charvet, B., Milet, C., and Duprez, D. (2016). TGFβ and FGF promote tendon progenitor fate and act downstream of muscle contraction to regulate tendon differentiation during chick limb development. *Development* 143, 3839–3851.

Julian, L., and Olson, M. F. (2014). Rho-associated coiled-coil containing kinases (ROCK): structure, regulation, and functions. *Small GTPases* 5:e29846. doi: 10.4161/sgtp.29846

Kabekkodu, S. P., Shukla, V., Varghese, V. K., D' Souza, J., Chakrabarty, S., and Satyamoorthy, K. (2018). Clustered miRNAs and their role in biological functions and diseases. *Biol. Rev. Camb. Philos. Soc.* 93, 1955–1986. doi: 10.1111/brv.12428

Kannus, P. (2000). Structure of the tendon connective tissue. *Scand. J. Med. Sci. Sports* 10, 312–320. doi: 10.1034/j.1600-0838.2000.010006312.x

Katzel, E. B., Wolenski, M., Loiselle, A. E., Basile, P., Flick, L. M., Langstein, H. N., et al. (2011). Impact of Smad3 loss of function on scarring and adhesion formation during tendon healing. *J. Orthop. Res.* 29, 684–693. doi: 10.1002/jor.21235

Khan, K. M., Cook, J. L., Bonar, F., Harcourt, P., and Astrom, M. (1999). Histopathology of common tendinopathies. Update and implications for clinical management. *Sports Med.* 27, 393–408. doi: 10.2165/00007256-199927060-00004

Kohler, J., Popov, C., Klotz, B., Alberton, P., Prall, W. C., Haasters, F., et al. (2013). Uncovering the cellular and molecular changes in tendon stem/progenitor cells attributed to tendon aging and degeneration. *Aging Cell* 12, 988–999. doi: 10.1111/acel.12124

Koturbash, I., Tolleson, W. H., Guo, L., Yu, D., Chen, S., Hong, H., et al. (2015). microRNAs as pharmacogenomic biomarkers for drug efficacy and drug safety assessment. *Biomark. Med.* 9, 1153–1176. doi: 10.2217/bmm.15.89

Kozomara, A., Birgaoanu, M., and Griffiths-Jones, S. (2019). miRBase: from microRNA sequences to function. *Nucleic Acids Res.* 47, D155–D162.

Krist, B., Florczyk, U., Pietraszek-Gremplewicz, K., Józkowicz, A., and Dulak, J. (2015). The role of miR-378a in metabolism, angiogenesis, and muscle biology. *Int. J. Endocrinol.* 2015:281756.

Laurencin, C. T., and Freeman, J. W. (2005). Ligament tissue engineering: an evolutionary materials science approach. *Biomaterials* 26, 7530–7536. doi: 10.1016/j.biomaterials.2005.05.073

Lee, R. C., Feinbaum, R. L., and Ambros, V. (1993). The *C. elegans* heterochronic gene lin-4 encodes small RNAs with antisense complementarity to lin-14. *Cell* 75, 843–854. doi: 10.1016/0092-8674(93)90529-y

Lee, Y., Kim, M., Han, J., Yeom, K. H., Lee, S., Baek, S. H., et al. (2004). MicroRNA genes are transcribed by RNA polymerase II. *EMBO J.* 23, 4051–4060. doi: 10.1038/sj.emboj.7600385

Lehmann, S. M., Krüger, C., Park, B., Derkow, K., Rosenberger, K., Baumgart, J., et al. (2012). An unconventional role for miRNA: let-7 activates Toll-like receptor 7 and causes neurodegeneration. *Nat. Neurosci.* 15, 827–835. doi: 10.1038/nn.3113

Liu, Y., Feng, L., Xu, J., Yang, Z., Wu, T., Zhang, J., et al. (2019). MiR-378a suppresses tenogenic differentiation and tendon repair by targeting at TGF-β2. *Stem Cell Res Ther.* 10:108.

Longo, U. G., Ronga, M., and Maffulli, N. (2018). Achilles tendinopathy. *Sports Med. Arthrosc. Rev.* 26, 16–30.

Lu, T. X., and Rothenberg, M. E. (2018). MicroRNA. *J. Allergy Clin. Immunol.* 141, 1202–1207.

Lu, Y. F., Liu, Y., Fu, W. M., Xu, J., Wang, B., Sun, Y. X., et al. (2017). Long noncoding RNA H19 accelerates tenogenic differentiation and promotes tendon healing through targeting miR-29b-3p and activating TGF-β1 signaling. *FASEB J.* 31, 954–964. doi: 10.1096/fj.201600722r

Magnusson, S. P., Narici, M. V., Maganaris, C. N., and Kjaer, M. (2008). Human tendon behaviour and adaptation, in vivo. *J. Physiol.* 586, 71–81. doi: 10.1113/jphysiol.2007.139105

McCarthy, J. J. (2011). The MyomiR network in skeletal muscle plasticity. *Exerc. Sport Sci. Rev.* 39, 150–154. doi: 10.1097/jes.0b013e31821c01e1

McCarthy, J. J., Esser, K. A., Peterson, C. A., and Dupont-Versteegden, E. E. (2009). Evidence of MyomiR network regulation of beta-myosin heavy chain gene expression during skeletal muscle atrophy. *Physiol. Genomics* 39, 219–226. doi: 10.1152/physiolgenomics.00042.2009

Mendias, C. L., Gumucio, J. P., and Lynch, E. B. (2012). Mechanical loading and TGF-β change the expression of multiple miRNAs in tendon fibroblasts. *J. Appl. Physiol. (1985)* 113, 56–62. doi: 10.1152/japplphysiol.00301.2012

Millar, N. L., Gilchrist, D. S., Akbar, M., Reilly, J. H., Kerr, S. C., Campbell, A. L., et al. (2015). MicroRNA29a regulates IL-33-mediated tissue remodelling in tendon disease. *Nat. Commun.* 6:6774.

Millar, N. L., Silbernagel, K. G., Thorborg, K., Kirwan, P. D., Galatz, L. M., Abrams, G. D., et al. (2021). Tendinopathy. *Nat. Rev. Dis. Primers* 7:1. doi: 10.1002/9780470757987.ch1

Miyashita, H., Ochi, M., and Ikuta, Y. (1997). Histological and biomechanical observations of the rabbit patellar tendon after removal of its central one-third. *Arch. Orthop. Trauma Surg.* 116, 454–462. doi: 10.1007/s004020050162

Mokone, G. G., Schwellnus, M. P., Noakes, T. D., and Collins, M. (2006). The COL5A1 gene and Achilles tendon pathology. *Scand. J. Med. Sci. Sports* 16, 19–26. doi: 10.1111/j.1600-0838.2005.00439.x

Nichols, A. E. C., Best, K. T., and Loiselle, A. E. (2019). The cellular basis of fibrotic tendon healing: challenges and opportunities. *Transl. Res.* 209, 156–168. doi: 10.1016/j.trsl.2019.02.002

Nourissat, G., Berenbaum, F., and Duprez, D. (2015). Tendon injury: from biology to tendon repair. *Nat. Rev. Rheumatol.* 11, 223–233. doi: 10.1038/nrrheum.2015.26

O'Brien, M. (1997). Structure and metabolism of tendons. *Scand. J. Med. Sci. Sports* 7, 55–61. doi: 10.1111/j.1600-0838.1997.tb00119.x

Posthumus, M., Schwellnus, M. P., and Collins, M. (2011). The COL5A1 gene: a novel marker of endurance running performance. *Med. Sci. Sports Exerc.* 43, 584–589. doi: 10.1249/mss.0b013e3181f34f4d

Poulsen, R. C., Knowles, H. J., Carr, A. J., and Hulley, P. A. (2014). Cell differentiation versus cell death: extracellular glucose is a key determinant of cell fate following oxidative stress exposure. *Cell Death Dis.* 5:e1074. doi: 10.1038/cddis.2014.52

Pryce, B. A., Watson, S. S., Murchison, N. D., Staverosky, J. A., Dünker, N., and Schweitzer, R. (2009). Recruitment and maintenance of tendon progenitors by TGFbeta signaling are essential for tendon formation. *Development* 136, 1351–1361. doi: 10.1242/dev.027342

Reinhart, B. J., Slack, F. J., Basson, M., Pasquinelli, A. E., Bettinger, J. C., Rougvie, A. E., et al. (2000). The 21-nucleotide let-7 RNA regulates developmental timing in *Caenorhabditis elegans*. *Nature* 403, 901–906. doi: 10.1038/35002607

Rittié, L. (2017). Type I collagen purification from rat tail tendons. *Methods Mol. Biol.* 1627, 287–308. doi: 10.1007/978-1-4939-7113-8_19

Saliminejad, K., Khorram Khorshid, H. R., Soleymani Fard, S., and Ghaffari, S. H. (2019). An overview of microRNAs: biology, functions, therapeutics, and analysis methods. *J. Cell. Physiol.* 234, 5451–5465. doi: 10.1002/jcp.27486

Sayed, D., and Abdellatif, M. (2011). MicroRNAs in development and disease. *Physiol. Rev.* 91, 827–887.

Selbach, M., Schwanhäusser, B., Thierfelder, N., Fang, Z., Khanin, R., and Rajewsky, N. (2008). Widespread changes in protein synthesis induced by microRNAs. *Nature* 455, 58–63. doi: 10.1038/nature07228

Sharma, P., and Maffulli, N. (2005). Tendon injury and tendinopathy: healing and repair. *J. Bone Joint Surg. Am.* 87, 187–202. doi: 10.2106/00004623-200501000-00030

Sharma, P., and Maffulli, N. (2006). Biology of tendon injury: healing, modeling and remodeling. *J. Musculoskelet. Neuronal Interact.* 6, 181–190.

Simeoli, R., Montague, K., Jones, H. R., Castaldi, L., Chambers, D., Kelleher, J. H., et al. (2017). Exosomal cargo including microRNA regulates sensory neuron to macrophage communication after nerve trauma. *Nat. Commun.* 8:1778.

Strickland, J. W. (2000). Development of flexor tendon surgery: twenty-five years of progress. *J. Hand Surg. Am.* 25, 214–235. doi: 10.1053/jhsu.2000.jhsu25a0214

Subramanian, A., and Schilling, T. F. (2014). Thrombospondin-4 controls matrix assembly during development and repair of myotendinous junctions. *Elife* 3:e02372.

Sun, Y., Chen, H., Ye, H., Liang, W., Lam, K. K., Cheng, B., et al. (2020). Nudt21-mediated alternative polyadenylation of HMGA2 3'-UTR impairs stemness of human tendon stem cell. *Aging (Albany N. Y.)* 12, 18436–18452. doi: 10.18632/aging.103771

Tao, X., Liu, J., Chen, L., Zhou, Y., and Tang, K. (2015). EGR1 induces tenogenic differentiation of tendon stem cells and promotes rabbit rotator cuff repair. *Cell Physiol. Biochem.* 35, 699–709. doi: 10.1159/000369730

Tempfer, H., and Traweger, A. (2015). Tendon vasculature in health and disease. *Front. Physiol.* 6:330. doi: 10.3389/fphys.2015.00330

Thankam, F. G., Boosani, C. S., Dilisio, M. F., and Agrawal, D. K. (2018). MicroRNAs associated with inflammation in shoulder tendinopathy and glenohumeral arthritis. *Mol. Cell. Biochem.* 437, 81–97. doi: 10.1007/s11010-017-3097-7

Thankam, F. G., Boosani, C. S., Dilisio, M. F., Dietz, N. E., and Agrawal, D. K. (2016). MicroRNAs associated with shoulder tendon matrisome disorganization in glenohumeral arthritis. *PLoS One* 11:e0168077. doi: 10.1371/journal.pone.0168077

Thankam, F. G., Boosani, C. S., Dilisio, M. F., Gross, R. M., and Agrawal, D. K. (2019). Genes interconnecting AMPK and TREM-1 and associated microRNAs in rotator cuff tendon injury. *Mol Cell. Biochem* 454, 97–109. doi: 10.1007/s11010-018-3456-z

Thorpe, C. T., and Screen, H. R. (2016). Tendon structure and composition. *Adv. Exp. Med. Biol.* 920, 3–10. doi: 10.1007/978-3-319-33943-6_1

Tomasek, J. J., Gabbiani, G., Hinz, B., Chaponnier, C., and Brown, R. A. (2002). Myofibroblasts and mechano-regulation of connective tissue remodelling. *Nat. Rev. Mol. Cell Biol.* 3, 349–363. doi: 10.1038/nrm809

Tsai, S. L., Nödl, M. T., and Galloway, J. L. (2021). Bringing tendon biology to heel: leveraging mechanisms of tendon development, healing, and regeneration to advance therapeutic strategies. *Dev. Dyn.* 250, 393–413. doi: 10.1002/dvdy.269

Usman, M. A., Nakasa, T., Shoji, T., Kato, T., Kawanishi, Y., Hamanishi, M., et al. (2015). The effect of administration of double stranded MicroRNA-210 on acceleration of Achilles tendon healing in a rat model. *J. Orthop. Sci.* 20, 538–546. doi: 10.1007/s00776-015-0709-5

Vasudevan, S., Tong, Y., and Steitz, J. A. (2007). Switching from repression to activation: microRNAs can up-regulate translation. *Science* 318, 1931–1934. doi: 10.1126/science.1149460

Vidigal, J. A., and Ventura, A. (2015). The biological functions of miRNAs: lessons from in vivo studies. *Trends Cell Biol.* 25, 137–147. doi: 10.1016/j.tcb.2014.11.004

Voleti, P. B., Buckley, M. R., and Soslowsky, L. J. (2012). Tendon healing: repair and regeneration. *Annu. Rev. Biomed. Eng.* 14, 47–71.

Wang, B., Guo, J., Feng, L., Suen, C. W., Fu, W. M., Zhang, J. F., et al. (2016). MiR124 suppresses collagen formation of human tendon derived stem cells through targeting egr1. *Exp. Cell Res.* 347, 360–366. doi: 10.1016/j.yexcr.2016.08.018

Wang, J. H. (2006). Mechanobiology of tendon. *J. Biomech.* 39, 1563–1582. doi: 10.1016/j.jbiomech.2005.05.011

Wang, J. H., Guo, Q., and Li, B. (2012). Tendon biomechanics and mechanobiology–a minireview of basic concepts and recent advancements. *J. Hand Ther.* 25, 133–140; quiz141.

Watts, A. E., Millar, N. L., Platt, J., Kitson, S. M., Akbar, M., Rech, R., et al. (2017). MicroRNA29a treatment improves early tendon injury. *Mol. Ther.* 25, 2415–2426. doi: 10.1016/j.ymthe.2017.07.015

Whalen, W. P. (1951). Utilization of scar tissue in bridging tendon defects. *Ann. Surg.* 133, 567–571. doi: 10.1097/00000658-195113340-00019

Wu, Y. F., Chen, C. H., Cao, Y., Avanessian, B., Wang, X. T., and Tang, J. B. (2010). Molecular events of cellular apoptosis and proliferation in the early tendon healing period. *J. Hand Surg. Am.* 35, 2–10. doi: 10.1016/j.jhsa.2009.10.021

Wu, Y. F., Mao, W. F., Zhou, Y. L., Wang, X. T., Liu, P. Y., and Tang, J. B. (2016). Adeno-associated virus-2-mediated TGF-β1 microRNA transfection inhibits adhesion formation after digital flexor tendon injury. *Gene Ther.* 23, 167–175. doi: 10.1038/gt.2015.97

Xiong, B., Rui, Y., Zhang, M., Shi, K., Jia, S., Tian, T., et al. (2006). Tob1 controls dorsal development of zebrafish embryos by antagonizing maternal beta-catenin transcriptional activity. *Dev. Cell* 11, 225–238. doi: 10.1016/j.devcel.2006.06.012

Xu, Q., Sun, W. X., and Zhang, Z. F. (2019). High expression of VEGFA in MSCs promotes tendon-bone healing of rotator cuff tear via microRNA-205-5p. *Eur. Rev. Med .Pharmacol. Sci.* 23, 4081–4088.

Xue, M., and Jackson, C. J. (2015). Extracellular matrix reorganization during wound healing and its impact on abnormal scarring. *Adv. Wound Care (New Rochelle)* 4, 119–136. doi: 10.1089/wound.2013.0485

Yao, Z., Li, J., Wang, X., Peng, S., Ning, J., Qian, Y., et al. (2020). MicroRNA-21-3p engineered umbilical cord stem cell-derived exosomes inhibit tendon adhesion. *J. Inflamm. Res.* 13, 303–316. doi: 10.2147/jir.s254879

Yuan, J., Cao, J. Y., Tang, Z. L., Wang, N., and Li, K. (2011). Molecular characterization of Tob1 in muscle development in pigs. *Int. J. Mol. Sci.* 12, 4315–4326. doi: 10.3390/ijms12074315

Zhou, Z., Akinbiyi, T., Xu, L., Ramcharan, M., Leong, D. J., Ros, S. J., et al. (2010). Tendon-derived stem/progenitor cell aging: defective self-renewal and altered fate. *Aging Cell* 9, 911–915. doi: 10.1111/j.1474-9726.2010.00598.x

Conflict of Interest: The authors declare that the research was conducted in the absence of any commercial or financial relationships that could be construed as a potential conflict of interest.

frontiers in Cell and Developmental Biology

ORIGINAL RESEARCH
published: 12 July 2021
doi: 10.3389/fcell.2021.687856

Mechanical Overloading Induced-Activation of mTOR Signaling in Tendon Stem/Progenitor Cells Contributes to Tendinopathy Development

Daibang Nie[1,2†], Yiqin Zhou[2,3†], Wang Wang[1], Jianying Zhang[2] and James H.-C. Wang[2,4,5*]*

[1] Department of Immunology, College of Basic Medicine, Chongqing Medical University, Chongqing, China, [2] MechanoBiology Laboratory, Department of Orthopaedic Surgery, University of Pittsburgh, Pittsburgh, PA, United States, [3] Department of Orthopaedics, Shanghai Changzheng Hospital, Naval Medical University, Shanghai, China, [4] Department of Physical Medicine and Rehabilitation, University of Pittsburgh, Pittsburgh, PA, United States, [5] Department of Bioengineering, University of Pittsburgh, Pittsburgh, PA, United States

OPEN ACCESS

Edited by:
Zi Yin,
Zhejiang University, China

Reviewed by:
Yangwu Chen,
Zhejiang University, China
Ting-Wu Qin,
Sichuan University, China
Xudong Fu,
Zhejiang University, China

***Correspondence:**
Jianying Zhang
jianying@pitt.edu
James H.-C. Wang
wanghc@pitt.edu

[†] These authors have contributed equally to this work

Specialty section:
This article was submitted to Stem Cell Research, a section of the journal Frontiers in Cell and Developmental Biology

Received: 30 March 2021
Accepted: 18 June 2021
Published: 12 July 2021

Citation:
Nie D, Zhou Y, Wang W, Zhang J and Wang JH-C (2021) Mechanical Overloading Induced-Activation of mTOR Signaling in Tendon Stem/Progenitor Cells Contributes to Tendinopathy Development. Front. Cell Dev. Biol. 9:687856. doi: 10.3389/fcell.2021.687856

Despite the importance of mechanical loading in tendon homeostasis and pathophysiology, the molecular responses involved in the mechanotransduction in tendon cells remain unclear. In this study, we found that *in vitro* mechanical loading activated the mammalian target of rapamycin (mTOR) in rat patellar tendon stem/progenitor cells (TSCs) in a stretching magnitude-dependent manner. Application of rapamycin, a specific inhibitor of mTOR, attenuated the phosphorylation of S6 and 4E-BP1 and as such, largely inhibited the mechanical activation of mTOR. Moreover, rapamycin significantly decreased the proliferation and non-tenocyte differentiation of PTSCs as indicated by the reduced expression levels of LPL, PPARγ, SOX-9, collagen II, Runx-2, and osteocalcin genes. In the animal studies, mice subjected to intensive treadmill running (ITR) developed tendon degeneration, as evidenced by the formation of round-shaped cells, accumulation of proteoglycans, and expression of SOX-9 and collagen II proteins. However, daily injections of rapamycin in ITR mice reduced all these tendon degenerative changes. Collectively, these findings suggest that mechanical loading activates the mTOR signaling in TSCs, and rapamycin may be used to prevent tendinopathy development by blocking non-tenocyte differentiation due to mechanical over-activation of mTOR in TSCs.

Keywords: mechanical loading, treadmill running, tendon stem cells, mTOR, rapamycin

INTRODUCTION

Tendons are connective tissues that transmit mechanical force (i.e., muscle contraction) to bone to enable joint movement. While a physiological level of mechanical loading is necessary to maintain tendon homeostasis, excessive loading makes tendon tissues susceptible to the development of tendinopathy which is characterized by inflammation and/or degeneration (Maffulli et al., 1998). Tendinopathy is especially prevalent in both occupational and athletic settings that involve repetitive motions (Cook and Purdam, 2009; Zhang and Wang, 2010c) and represents a major healthcare problem in the US.

Like other connective tissues, tendons contain stem/progenitor cells (Bi et al., 2007; Zhang and Wang, 2010a). These tendon stem cells (TSCs) possess common adult stem cell characteristics, and they play a crucial role in tendon development, homeostasis, and repair (Popov et al., 2015; Zhang et al., 2019). We showed that excessive mechanical loading can cause aberrant differentiation of TSCs (Zhang and Wang, 2010b). Others also showed that mechanical loading increases bone morphogenetic protein-2 (BMP-2) expression in TSCs, which in turn promoted osteogenic differentiation of TSCs (Rui et al., 2011). Also, repetitive mechanical loading induces high levels of prostaglandin E2 (PGE_2) production in tendons, which may induce the differentiation of TSCs into non-tenocytes (Zhang and Wang, 2010c). Years of research have generally concluded that excessive mechanical loading might lead to the development of degenerative tendinopathy commonly seen in clinical settings (Soslowsky et al., 2000; Glazebrook et al., 2008; Abraham et al., 2011; Ng et al., 2011; Zhang and Wang, 2013).

As a central controller of organ growth and development, the mammalian target of rapamycin (mTOR) has been linked to mechanical overloading-induced hypertrophy in the skeletal muscles as well as chondrogenesis (Goodman et al., 2010; Guan et al., 2014; Yoon, 2017). mTOR functions as a master sensor of growth factors, stress, energy status, oxygen, and nutrients, and is involved in a number of major cellular processes. Previous studies showed that rapamycin, a specific inhibitor of mTOR, suppresses the differentiation of human mesenchymal stem cells and primary mouse bone marrow stromal cells to osteoblasts (Singha et al., 2008; Pantovic et al., 2013). A recent study has shown that repetitive mechanical stretching of human tendon cells activates mTOR pathway and increases mRNA translation and collagen synthesis (Mousavizadeh et al., 2020). However, mTOR signaling in TSCs under various mechanical loading conditions remains unclear. In this study, we investigated whether mechanical loading could activate the mTOR signaling in TSCs and explored whether inhibiting mTOR by rapamycin could prevent tendinopathy development due to mechanical overloading placed on the tendon.

MATERIALS AND METHODS

Isolation of Patellar TSCs (PTSCs) and Cell Culture

PTSCs were isolated from the patellar tendons of Sprague-Dawley rats (female, 5 months, Jackson Lab, Bar Harbor, ME) as previously described (Zhang and Wang, 2010a). The protocol for use of the rats was approved by the IACUC of the University of Pittsburgh. Briefly, tendon sheaths from the patellar tendons were removed to obtain the core portions of the tendons. Tendon samples were then minced into small pieces and each 100 mg wet tissue sample was digested in 1 ml phosphate buffered saline (PBS) containing 3 mg collagenase type I (GIBCO, Grand Island, NY, United States) and 4 mg dispase (GIBCO, Grand Island, NY, United States) at 37°C for 1 hr. After centrifugation at 3,500 rpm/min for 15 min to remove the enzymes, the cells were cultured in a growth medium containing DMEM (Lonza, Walkersville, MD, United States) supplemented with 20% fetal bovine serum (FBS; Atlanta Biologicals, Lawrenceville, GA, United States), 100 U/ml penicillin and 100 μg/ml streptomycin (Atlanta Biologicals, Lawrenceville, GA, United States). In all culture experiments, PTSCs at passage 2 or 3 were used.

Cell Stretching Experiments

We used a uniaxial cell stretching system we had developed previously to investigate the mechanobiological response of rat PTSCs *in vitro* (Wang and Grood, 2000). After PTSCs were seeded in silicone dishes at a density of 4×10^5/dish and cultured in growth medium (DMEM + 10% FBS) overnight, cyclic stretching at 4 and 8% at 0.5 Hz was applied to silicone dishes for 2 h. Control PTSCs without stretching were cultured in the silicone dishes with the same medium. Similar stretching experiments were also done in serum-free medium. A total of three dishes for each loading condition and control were used, respectively, and the experiment was performed in triplicates. After the end of the cell stretching experiments, PTSCs were collected for Western analysis and qRT-PCR.

Cell Proliferation Assay

CCK-8 assays were performed to assess the PTSC proliferation according to the manufacturer's instruction (Sigma, St. Louis, MO, United States). Briefly, 1×10^3 cells/well were plated in 96-well plates in 100 μl growth medium and incubated at 37°C for 24 h to allow attachment. The medium was then replaced with fresh DMEM supplemented with 10% FBS, plus the addition of 500 nM rapamycin (Sigma, St. Louis, MO, United States). After 72 h, 10 μl of CCK-8 was added into each well and incubated at 37°C for 2 h. Finally, the absorbance was recorded at 450 nm using a microplate reader (SpectraMax M5, Molecular Devices, CA, United States).

In vitro Differentiation Experiments

The multi-differentiation potential of the PTSCs was tested *in vitro* for adipogenesis, chondrogenesis, and osteogenesis. PTSCs were seeded in a 6-well plate at a density of 2.4×10^5 cells/well and incubated overnight to allow cell attachment. The next day, the media were changed to the respective differentiation cocktails with or without 500 nM rapamycin. Commercially available differentiation cocktails used were StemPro® Adipogenesis, Osteogenesis, and Chondrogenesis Differentiation Kits (Life Technologies, Carlsbad, CA, United States). After 14 days, the adipogenesis was evaluated using Oil Red O staining assay, the chondrogenesis was detected using Alcian blue staining assay, and the osteogenesis was assessed by Alizarin Red S assay (Zhang and Wang, 2010a). All the stained cells were imaged with an inverted microscope (Nikon eclipse, TE2000-U, United States).

Mouse Treadmill Running Experiments

C57BL/6J mice (female, 3 months old, Jackson Lab, Bar Harbor, ME) were divided into four groups with 6 mice per group. The mice in group 1 were allowed regular cage activities (Cage). The mice in group 2 received a daily IP

injection of rapamycin (5 mg/kg body weight) for 12 weeks (Cage + Rapa). The mice in group 3 were subjected to the intensive treadmill running (ITR) at 15 m/min for 3 h/day, 5 days/week for 12 weeks. The mice in group 4 received daily IP injection of rapamycin, with the same dosage as in group 2 (ITR + Rapa), and ran the same ITR. All mice were sacrificed after 12 weeks of experiments. The patellar tendon tissues were harvested from these mice and processed for histochemical and immunohistochemical analyses.

Histochemical and Immunohistochemical Analyses on Mouse Tendon Tissue Sections

Each mouse patellar tendon was dissected from the knee and collected without skin. The tissue samples were fixed with 4% paraformaldehyde overnight at room temperature, washed three times with PBS, and then soaked in 30% sucrose in PBS at 4°C overnight. The treated tissue samples were embedded in O.C.T compound (Sakura Finetek United States Inc., Torrance, CA, United States) in disposable molds and frozen at −80°C. Then, cryostat sectioning was performed at −25°C to obtain about 8 μm thick tissue section slides, which were left at room temperature overnight. The tissue slides were collected and numbered continuously from the surface to the inside. Consecutive tissue slides were used for H&E, Safranin O and Fast Green, and Masson trichrome staining. Thus, three tissue slides that were numbered 10, 20, 30 in each patellar tendon were stained with H&E, and another three tissue sections numbered 11, 21, 31 in each patellar tendon were stained with Safranin O and Fast Green. In addition, three tissue sections numbered 12, 22, 32 in each patellar tendon were stained with Masson trichrome kit (Sigma-Aldrich, Cat# HT15) according to the standard protocols.

For immunostaining, the section slides with the same number ID from each group were then incubated with rabbit anti-collagen II antibody (1:500, Abcam Cat# ab34712) overnight at 4°C. For SOX-9 staining, the tissue sections were further treated with 0.1% Triton X-100 for 30 min at room temperature, washed with PBS three times, and then the sections were incubated overnight at 4°C with rabbit anti-SOX-9 antibody (1:500, Millipore, Cat# AB5535). The next morning, the tissue sections were washed 3 times with PBS and incubated at room temperature for 2 h with Cy3-conjugated goat anti-rabbit IgG antibody (1:500, Millipore, Cat# AP132C). Finally, the total cell numbers in the tendon tissue sections were analyzed by staining with 4.6-diamidino-2-phenylindole (DAPI), and the stained results were determined under a fluorescent microscope (Nikon, Eclipse TE2000U, United States).

Quantitative Real-Time RT-PCR (qRT-PCR)

Total RNA was extracted from PTSCs using RNeasy Mini Kit (Qiagen, Valencia, CA, United States). First-strand cDNA was synthesized in a 20 μl reaction from 1 μg total RNA by reverse transcription with SuperScript II (Invitrogen, Carlsbad, CA, United States). The conditions for the cDNA synthesis were 65°C for 5 min and cooling 1 min at 4°C, then 42°C for 50 min and 72°C for 15 min. The qRT-PCR was carried out using QIAGEN QuantiTect SYBR Green PCR Kit (Qiagen, Valencia, CA, United States). Rat-specific primers used for RT-PCR were: PPARγ: 5′-GCCTGCGTCCCCGCCTTAT-3′ (forward), 5′-GCCTGCGTCCCCGCCTTAT-3′ (reverse); LPL: 5′-CTTAAGTGGAAGAACGACTCCTACT-3′ (forward), 5′-GTCATGGCATTTCACAAACACTGCCA-3′ (reverse) (Mello et al., 2008); SOX-9: 5′- AGCGACAACTTTACCAG-3′ (forward), 5′-GGAAAACAGAGAACGAAAC-3′ (reverse); Collagen II: 5′-GGCTTAGGGCAGAGAGAGAAG-3′ (forward), 5′-TGGACAGTAGACGGAGGAAAGTC-3′ (reverse) (Rafiei and Ashrafizadeh, 2018); Runx-2: 5′-CCGCACGACAACCGCACCAT-3′ (forward), 5′-CGCTCCGCTTC-3′ (reverse) (Yoshida et al., 2004); and Osteocalcin: 5′-AAAGCCCAGCGACTCT-3′ (forward), 5′-CTAAACGGTGGTGCCATAGAT-3′ (reverse) (Rafiei and Ashrafizadeh, 2018). GAPDH was used as an internal control. All primers were synthesized by Invitrogen (Carlsbad, CA, United States). After an initial denaturation for 10 min at 95°C, PCR was performed for 30 cycles for GAPDH, and 40 cycles for LPL, PPARγ, SOX-9, collagen II, Runx-2, and osteocalcin, with each cycle consisting of denaturation for 50 s at 95°C, followed by annealing for 30 s at 58°C for all the genes. At least three independent experiments were performed to obtain relative expression levels of each gene. Data were analyzed by the $2^{-\Delta\Delta Ct}$ method (Livak and Schmittgen, 2001). The gene expression levels of the treatment groups were normalized to that of the control group for each of the three experiments.

Western Blot Analysis

Cell lysates were prepared in RIPA buffer using standard procedures provided by the manufacturer (Sigma, St. Louis, MO, United States). The protein concentrations were measured using a BCA Protein Assay Kit (Thermo Fisher Scientific, Pittsburgh, PA, United States) to ensure equal loading. Loading buffer was added to 30 μg protein, and samples were heated at 100 °C for 5 min before separated on 4–20% SDS-PAGE gels, then transferred onto PVDF membranes (Bio-Rad, Hercules, CA, United States). Protein blots were blocked with 5% Non-Fat dry milk (Bio-Rad, Hercules, CA, United States) at room temperature for 1 h. Antibodies used were p-S6 (Cell Signaling Technology, Cat# 4858), S6 (1:1,000, Cell Signaling Technology, Cat# 2317), p-4EBP1 (1:1,000, Cell Signaling Technology Cat# 2855), 4EBP1 (1:1,000, Cell Signaling Technology, Cat# 9644), and β-actin (1:10,000, Abcam, Cat# ab8226). The next day, the blots were washed three times with 0.1% Tween 20-containing PBS buffer (PBS-T) buffer, then incubated with the corresponding secondary antibodies (1:15,000, LI-COR Biosciences) for 1 h at room temperature. Following another three washes with PBS-T buffer, visualization of the protein bands of the blots was realized with the LiCoR Odyssey imager (LI-COR Biosciences, Lincoln, NE, United States), and semi-quantification of the protein bands was done using the software provided by the LiCoR Odyssey imager.

Semi-Quantification of Histochemical and Immunohistochemical Staining Results

Semi-quantification was performed to quantify the extent of cell marker staining in tendon tissue sections. Three tissue sections/mouse from 6 mice/group with a total of 18 tissue sections were stained. The positive staining in the sections was identified under the microscope and analyzed using SPOT imaging software (Diagnostic Instruments, Inc., Sterling Heights, MI). The proportion of positive staining from histochemical staining was determined by dividing the positively stained area by the total area viewed under the microscope. For immunohistochemical staining, the proportion of positive staining was calculated by dividing the positively stained cell numbers by the total cell numbers. The mean value from all 18-tissue section staining results represented the final percentage of positive staining.

Statistical Analysis

All data were represented by the mean and standard deviation (mean ± SD). One-way analysis of variance (ANOVA) was used for statistical data analysis. For multiple comparisons, the Fisher's LSD *post hoc* test was performed. All statistical tests were done using GraphPad Prism 7 (GraphPad Software, San Diego, CA). Differences with a $p < 0.05$ were considered statistically significant.

RESULTS

Mechanical Loading Activates the mTOR Signaling in PTSCs *in vitro*

To investigate whether mechanical loading could activate mTOR signaling in PTSCs, we isolated TSCs from the rat patellar tendons. These PTSCs were subjected to different levels of cyclic stretching to mimic normal (4%) and excessive (8%) mechanical loads on tendon tissue. We found that both 4 and 8% stretching increased the expression of phospho-S6, compared to the control PTSCs cultured in the same medium but without stretching (**Figure 1A**). Such an increase in mTOR signaling activity appeared to be positively correlated to the magnitude of mechanical stretching (**Figure 1B**). However, the addition of rapamycin resulted in decreased p-S6/S6, and p-4E-BP1/4E-BP1, suggesting rapamycin inhibited loading-induced activation of the mTOR (**Figure 1** and **Supplementary Figure 1**). This indicates that mechanical loading activates mTOR signaling in a loading magnitude-dependent manner, and such mechanical activation of mTOR can be inhibited by rapamycin treatment.

Mechanical Activation of mTOR Is Independent of FBS *in vitro*

Given the role of mTOR as a master sensor of cellular conditions including stress and metabolic substrates, we determined whether those nutrient factors in FBS could affect mechanical loading-induced mTOR activation. We cultured PTSCs in medium without FBS and subjected them to 4 or 8% stretching. Quantification of Western blot results showed that the increase in the ratio of p-S6/S6 protein levels under 4 and 8% stretching without FBS in medium (**Figures 1C,D**) was similar to that when the cells were stretched at 4 and 8% with the presence of FBS (**Figures 1A,B**). The results suggest that mechanical loading-induced mTOR activation is likely independent of those factors (e.g., growth factors and nutrients) in FBS.

Rapamycin Decreases PTSC Proliferation and Differentiation *in vitro*

To determine the effect of rapamycin on PTSC proliferation and differentiation, we utilized rat PTSCs under normal culture conditions. We found that the treatment of rapamycin for 72 h significantly reduced PTSC proliferation compared to the control **(Figures 2A,B,I)**. PTSCs treated with 500 nM of rapamycin maintained good viability in the rapamycin treated group, with slight morphological changes compared to the control group (**Figures 2A,B**). Next, we cultured rat PTSCs in three separate differentiation media to test their potentials to undergo adipogenesis, chondrogenesis, and osteogenesis. PTSCs in the control group without rapamycin were able to differentiate into adipocytes, chondrocytes, and osteocytes, as shown by the staining of Oil Red O, Alcian blue, and Alizarin Red S assay, respectively (**Figures 2C,E,G**). However, the presence of rapamycin (500 nM) in the osteogenic, adipogenic, or chondrogenic induction media markedly reduced the extent of TSC differentiation (**Figures 2D,F,H**). These results were also supported by gene expression results of those differentiation markers: PPARγ and LPL for adipogenesis, SOX-9 and collagen II for chondrogenesis, and Runx-2 and osteocalcin for osteogenesis (**Figures 2J–O**).

Rapamycin Blocks Mechanical Overloading-Induced Non-tenocyte Differentiation of PTSCs

Next, we tested whether rapamycin could rescue mechanical loading induced non-tenocyte differentiation of PTSCs in an *in vitro* cell stretching model. We cultured cells in a normal culture medium (DMEM plus 10% FBS) and subjected cells to 4 or 8% stretching. We found that after stretching, the expression of the tenocyte-related gene collagen I was up-regulated in PTSCs (**Figure 3A**). Although rapamycin appeared to decrease collagen I expression induced by 4% stretching, there was no significant difference between the 4% stretching group and the 4% stretching plus rapamycin treated group (**Figure 3A**). There was also no significant difference in non-tenocyte-related gene expression in PTSCs between these two groups. However, rapamycin significantly decreased 8% stretching-induced collagen I levels in PTSCs (**Figure 3A**). Furthermore, 8% stretching of PTSCs significantly increased the expression of non-tenocyte-related genes, including LPL for adipocytes (**Figure 3B**), collagen II for chondrocytes (**Figure 3C**), and Runx-2 for osteocytes (**Figure 3D**), as compared to the control group. Finally, the

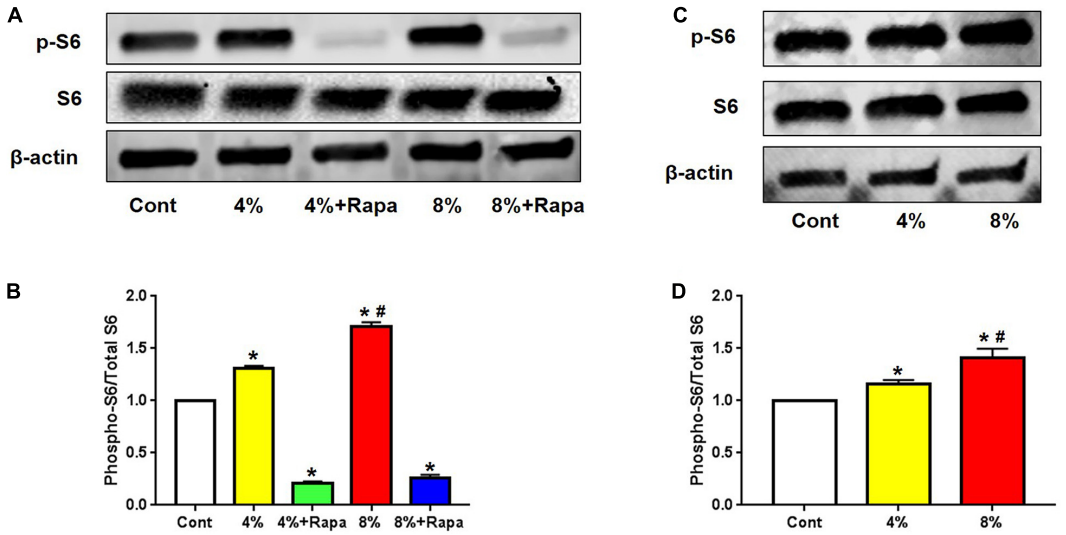

FIGURE 1 | Mechanical loading activates mTOR in a stretching magnitude-dependent manner and rapamycin abolishes the loading-induced activation. Western blot analysis shows higher levels of p-S6 in 4 and 8% stretched PTSCs. The addition of rapamycin to the culture medium largely blocks this effect **(A)**. Quantification of the Western blot results shows that 4 and 8% stretching significantly increase p-S6 levels, but rapamycin negates this effect **(B)**. Western blot analysis of p-S6 levels in PTSCs subjected to 4 and 8% mechanical stretching and cultured in medium without FBS shows that p-S6 levels are higher in stretched cells than the control cells **(C)**. Quantification of the Western blot results confirms these findings **(D)**. Control (Cont): PTSCs cultured under the same culture conditions as other groups but without stretching. Note that * denotes 4 and 8% compared to control, # denotes 8% + Rapa compared to 8% stretch in **(B)**, * denotes 4 and 8% compared to control, # denotes 8% compared to 4% stretch in **(D)** ($n = 3$, and values are mean ± SD. $^{*}p < 0.05$, $^{\#}p < 0.05$).

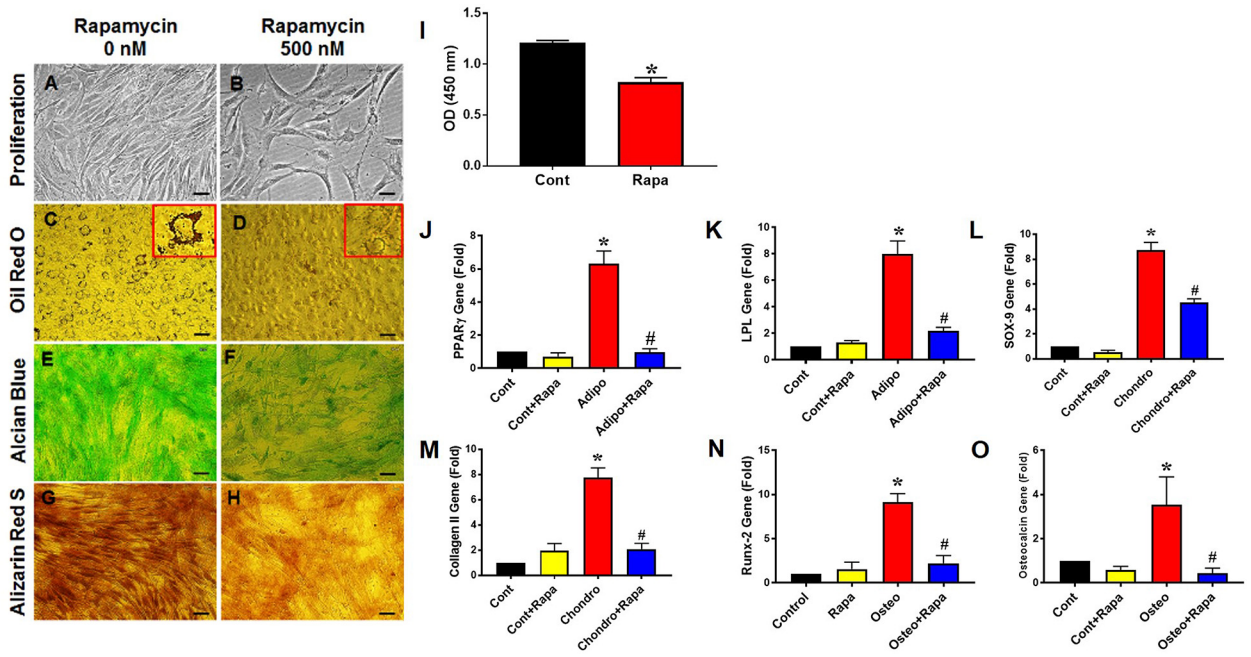

FIGURE 2 | Rapamycin inhibits PTSC proliferation and differentiation *in vitro*. Rapamycin at the dose 500 nM significantly reduces PTSC proliferation (**I**; see also decreased cell density in **B** compared to **A**). Similarly, rapamycin inhibits PTSC differentiation in the adipogenic (**C,D**; see large amounts of lipid droplets in the inset of **C** but not in **D**), chondrogenic **(E,F)**, and osteogenic **(G,H)** induction media. Moreover, the rapamycin treatment inhibits the expression of marker genes: PPARγ **(J)** and LPL **(K)** for adipocytes, SOX-9 **(L)** and collagen II **(M)** for chondrocytes, and Runx-2 **(N)** and osteocalcin **(O)** for osteocytes. Note that * denotes treatments compared to control, # denotes comparison between each differentiation medium treatment + Rapa with each medium treatment alone ($n = 3$, and values are mean ± SD. $^{*}p < 0.05$, $^{\#}p < 0.05$). Black bars: 50 μm.

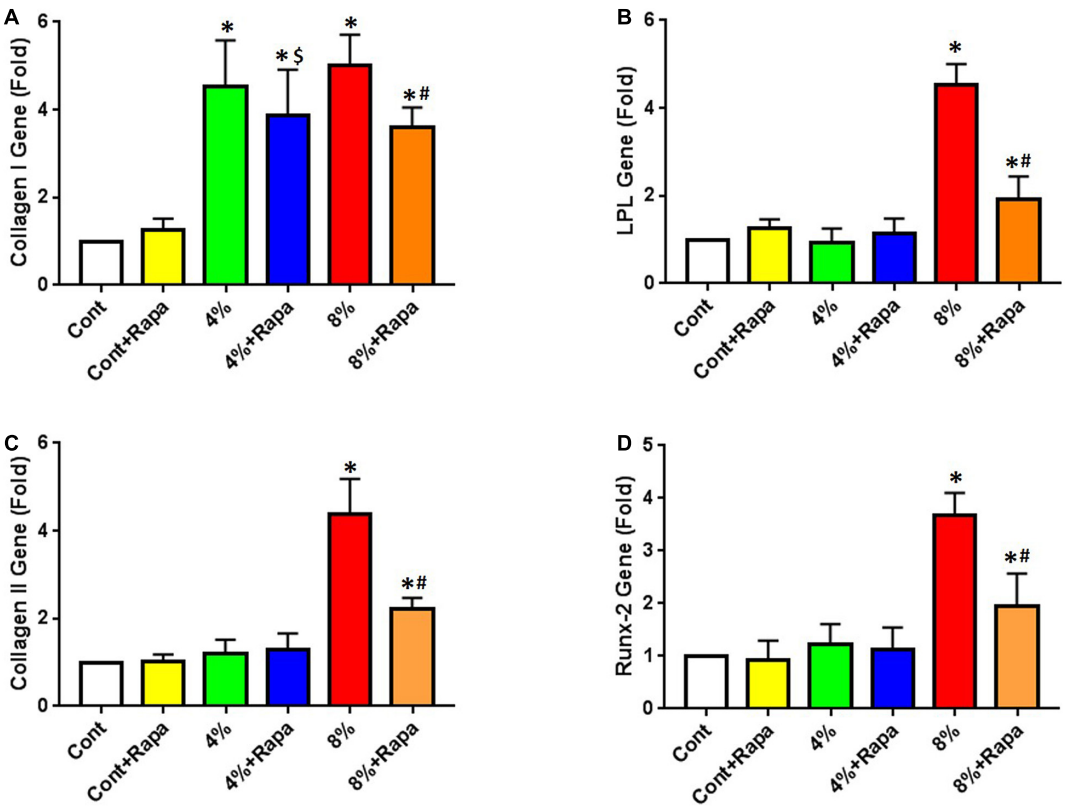

FIGURE 3 | Rapamycin inhibits non-tenocyte differentiation of PTSCs induced by mechanical stretching. Rapamycin does not significantly decrease the collagen I expression induced by 4% stretching (4% + Rapa vs. 4%), but it does decrease the collagen I expression at 8% stretching (8% + Rapa vs. 8%) **(A)**. Moreover, rapamycin treatment significantly reduces the expression of non-tenocyte related genes induced by 8% stretching, including LPL for adipocytes **(B)**, collagen II for chondrocytes **(C)**, and Runx-2 for osteocytes **(D)**. Under 4% stretching, however, rapamycin does not cause changes in the expression of these non-tenocyte genes **(B–D)**. Note that * denotes 4 and 8% compared to control, $ denotes 4% + Rapa compared to 4%, and # denotes 8% + Rapa compared to 8% ($n = 3$, and values are mean ± SD. $^{*}p < 0.05$, $^{\#}p < 0.05$).

addition of rapamycin significantly reduced the expression of all three non-tenocyte marker genes.

Rapamycin Inhibits ITR-Induced Tendon Degeneration *in vivo*

Furthermore, we tested whether rapamycin could rescue mechanical loading induced tendon degeneration in an ITR mouse model. Histochemical analysis showed that the mouse tendon cells in the cage group exhibited an elongated morphology (**Figures 4A–C**, white arrows in **Figure 4C**) and rapamycin injection group (**Figures 4D–F**, white arrows in **Figure 4F**). However, the majority of the patellar tendon cells changed into a round shape after mice were subjected to an ITR regimen for 12 weeks (**Figures 4G–I**, yellow arrows in **Figure 4I**). This morphological alteration was, however, blocked by rapamycin injections (**Figures 4J–L**). Semi-quantification of the results indicated that more than 55% of the cells in ITR tendons were round-shaped cells, but only less than 10% cells were round-shaped in the rapamycin treated ITR tendons (**Figure 4M**).

Similar findings were obtained with the Safranin O and Fast Green staining. Tendon cells in cage control mice (**Figures 5A–C**) and rapamycin injection mice (**Figures 5D–F**) displayed a normal appearance with an elongated shape (**Figures 5A–F**, white arrows in **Figures 5C,F**). However, tendons under the ITR condition were positively stained with Safranin O, indicating that non-tenocyte differentiation of PTSCs likely took place (red in **Figures 5G–I**, yellow arrows in **Figure 5I**) and as a result, proteoglycans were accumulated in the tendon matrix. Such tendon degeneration due to ITR was effectively prevented by rapamycin injections, with the corresponding tendon tissues showing a lack of Safranin O staining (**Figures 5J–L**). Semi-quantification of the staining results showed that more than 32% of the tendon cells in ITR tendons were positively stained with Safranin O, but less than 5% of the tendon cells in rapamycin treated ITR tendons were positively stained (**Figure 5M**).

Additionally, Masson trichrome (MT) staining results showed that the mechanical overloading by ITR caused degenerative changes in tendon tissue, as evidenced by the loose, disorganized connective tissue that was strongly stained blue (**Figure 6C**). However, the cage control tendons (**Figure 6A**) and rapamycin injection only tendons (**Figure 6B**), which consist of normally dense connective tissues (mainly tight collagen fiber bundles), were largely stained red (**Figures 6A,B,E**). Rapamycin injection reduced degenerative changes in ITR tendons as shown by the

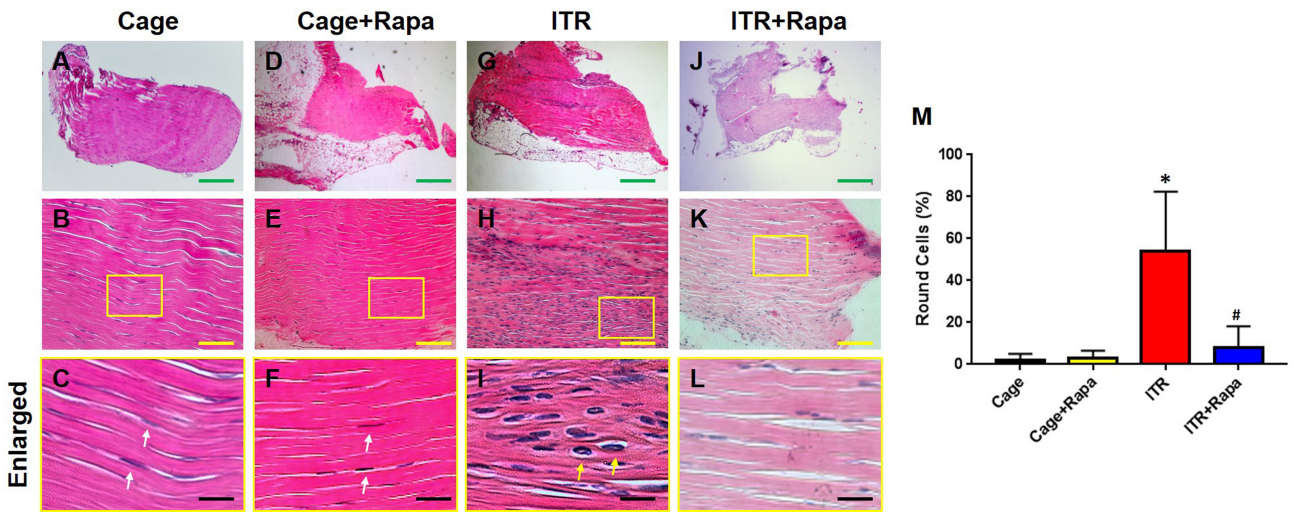

FIGURE 4 | Rapamycin blocks the ITR-induced cellular morphological changes in mouse patellar tendons. H&E staining shows the normal elongated shape of the tendon cells in cage control **(A–C)** and rapamycin injected mouse tendons (**D–F**, white arrows in **C,F**). Many round shape cells are present in ITR tendons (**G-I**; yellow arrows in **I**). With rapamycin injection prior to ITR, markedly fewer round shaped cells are shown in the tendon tissues **(J–L)**. Semi-quantification analysis indicates that more than 55% of the cells in ITR tendon, but less than 10% of the cells in ITR + Rapa treated tendons are round **(M)**. Note that * denotes ITR compared to control, # denotes ITR + Rapa compared to ITR (*$p < 0.05$, $^{\#}p < 0.05$). Green bar: 500 μm; Yellow bars: 100 μm; Black bars: 25 μm.

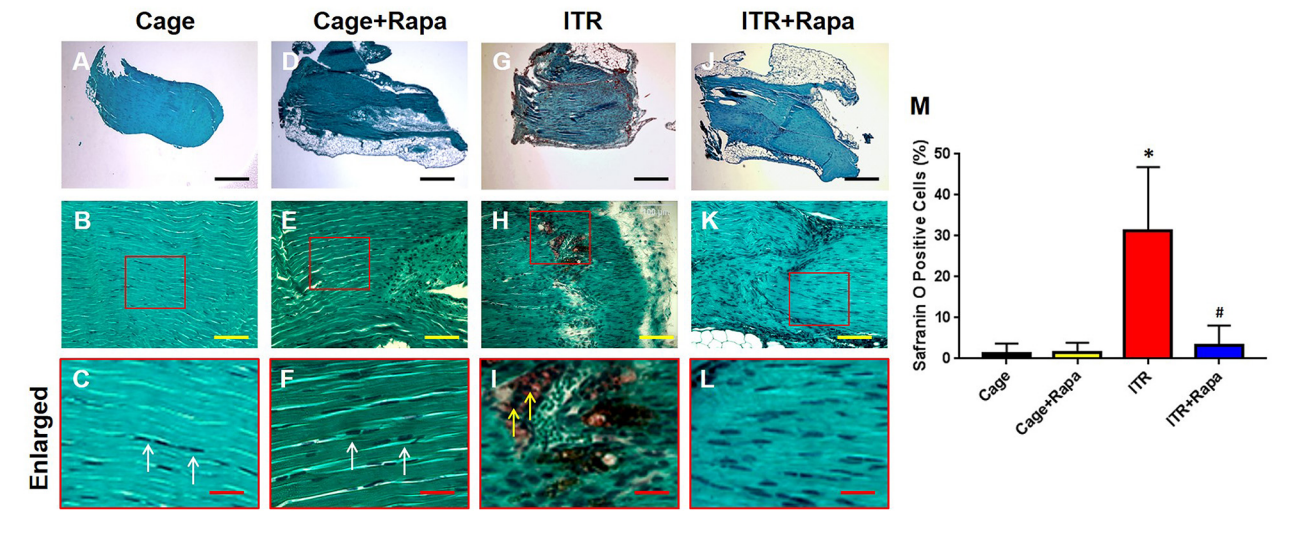

FIGURE 5 | Rapamycin inhibits ITR-induced degenerative changes in mouse tendons. Histochemical analysis by Safranin O and Fast Green staining shows tendon cells in elongated shape in collagen tissues from tendons of the cage control (**A–C**, white arrows in **C**) and tendons with rapamycin injections (**D–F**, white arrows in **F**). However, many round-shaped cells are positively stained with Safranin O in tendons of the ITR group (red in **G,H,I**; yellow arrows in **I**). Rapamycin injection blocks the ITR-induced degenerative changes in the tendons **(J–L)**. Semi-quantification analysis indicates that more than 30% of the cells in ITR tendon are positively stained with Safranin O, but less than 7% of the cells in ITR + Rapa treated tendons are positively stained with Safranin O **(M)**. Note that * denotes ITR compared to control, # denotes ITR + Rapa compared to ITR (*$p < 0.05$, $^{\#}p < 0.05$). Black bars: 500 μm; Yellow bars: 100 μm; Red bars: 25 μm.

decrease in the loose, degenerative tendinous tissues and the increase in the dense, normal-like tendinous tissues (**Figure 6D**). These results were also supported by semi-quantification analysis (**Figure 6E**).

Furthermore, immunostaining confirmed tendinopathy-like changes with high percentages of the tendon cells from the ITR group positively stained with SOX-9 (**Figures 7A–H,Q**) and collagen II (**Figures 7I–P,R**). These non-tenocyte markers were undetected within tendon tissues collected from cage mice (**Figures 7A,B,I,J**) and rapamycin injection only mice (**Figures 7C,D,K,L**). Thus, rapamycin effectively inhibited the ITR-induced upregulation of SOX-9 expression in the mouse tendons, as evidenced by limited numbers of cells positively stained with these markers in the ITR + Rapa group (**Figures 7G,H,Q**). Similarly, enhanced collagen type II expression in the tendon tissues by ITR was reverted by rapamycin treatment (**Figures 7O,P,R**).

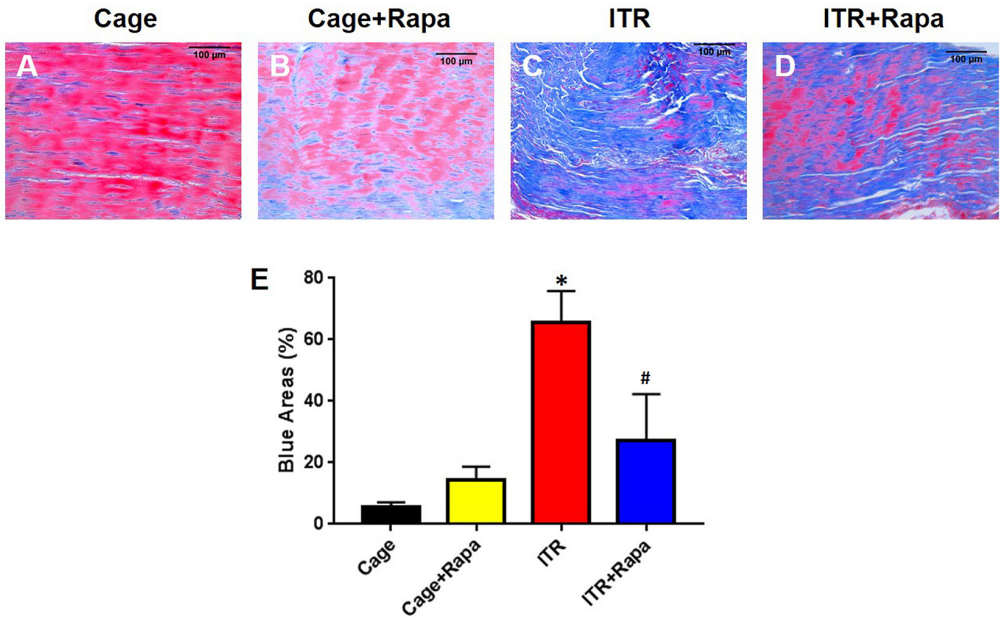

FIGURE 6 | Rapamycin reduces ITR-induced tendon tissue degeneration. Masson trichrome staining results indicate that the collagen fascicles in the patellar tendons of cage control mice are dense connective tissues, which are well organized, and positively stained with Biebrich scarlet-acid fuchsin (red in **A**). Similar results are found in the tendon tissues of the mice treated with rapamycin injection daily for 12 weeks **(B)**. However, in ITR mouse tendons, loose and disorganized connective tissues are present and positively stained with aniline blue **(C)**. Finally, rapamycin injection reduces the degenerative changes in mouse tendons induced by ITR, as shown by decreased blue area and increased the red area **(D)**. Semi-quantification analysis confirms these findings **(E)**. Note that * denotes ITR compared to control, # denotes ITR + Rapa compared to ITR ($^{*}p < 0.05$, $^{\#}p < 0.05$). Black bars: 100 μm.

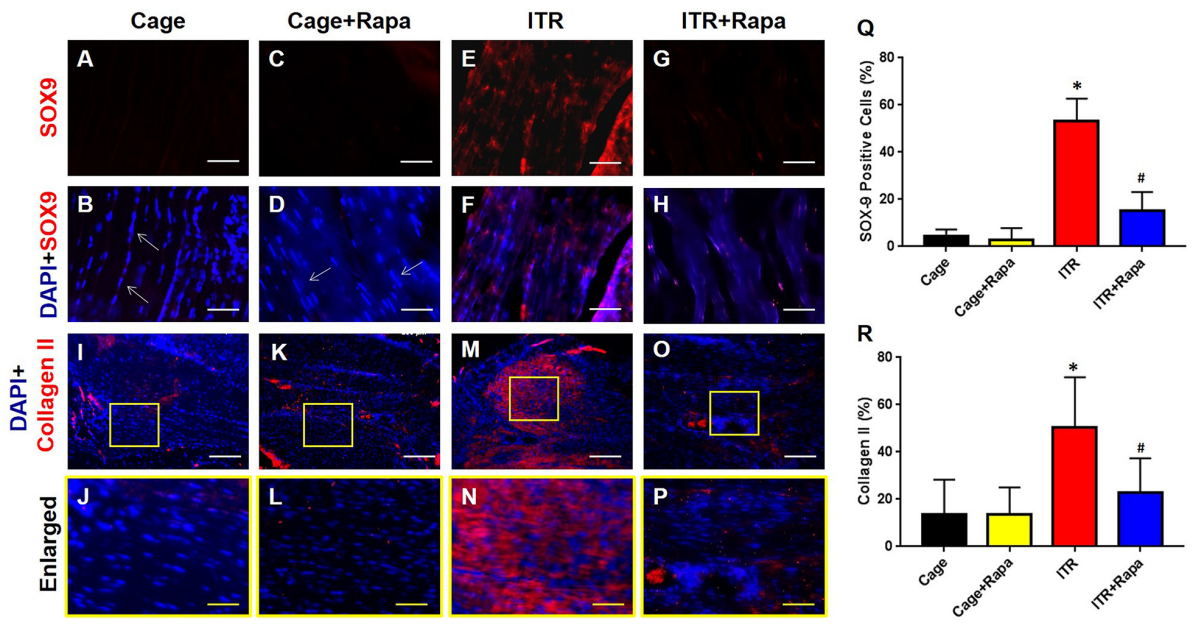

FIGURE 7 | Rapamycin blocks ITR-induced SOX-9 and collagen II expression in mouse tendons. The cells of cage control tendons **(A,B,I,J)** and tendons from the rapamycin injection group **(C,D,K,L)** exhibit an elongated shape with negative SOX-9 staining (white arrows in **B,D**) and minimal levels of collagen II staining **(K,L)**. However, many cells are positively stained with SOX-9 (red cells in **E,F**) and collagen II (red cells in **M,N**) in tendons of the ITR group. Rapamycin injection blocks the ITR-induced degenerative changes in the tendon, as evidenced by markedly fewer cells positively stained with SOX-9 **(G,H)** or collagen II **(O,P)**. Semi-quantification analysis indicates that more than 55% of the cells in ITR tendons are positively stained either with SOX-9 **(Q)** or with collagen II **(R)**. Note that * denotes ITR compared to cage control, # denotes ITR + Rapa compared to ITR ($^{*}p < 0.05$, $^{\#}p < 0.05$). White bars: 200 μm; Yellow bars: 25 μm.

DISCUSSION

Mechanical loading is well recognized for its importance in tendon development, tendon injury healing, and pathology, but tendon mechanotransduction is still poorly understood and represents a key area in tendon research. In this report, we show that mechanical loading activated mTOR signaling in PTSCs, and that treatment with rapamycin suppressed cell proliferation and differentiation *in vitro* and ITR-induced tendon degeneration *in vivo*. Based on the findings from the *in vitro* study, we suggest that mTOR signaling in PTSCs plays a critical role in the development of degenerative tendinopathy due to mechanical overloading in ITR mice, and that as a specific inhibitor of mTOR, rapamycin may be used to prevent tendinopathy development.

Previous studies showed that mechanical stimulation can lead to the activation of the mTOR pathway in human periodontal ligament fibroblasts and human tendon cells (Blawat et al., 2020; Mousavizadeh et al., 2020). Research has shown that mTOR signaling may be necessary for an increase in protein synthesis and resulting hypertrophic tissue in response to mechanical loads (Goodman, 2019). Also, the activation of mTOR signaling is sufficient to induce an increase in muscle protein synthesis and muscle fiber hypertrophy (Goodman et al., 2010). In addition, mechanical activation of mTOR is required for cell proliferation, chondrogenesis, and cartilage growth during bone development (Guan et al., 2014). This study focused on assessing the effect of mTOR activation on PTSCs during normal and excessive mechanical loading, with results suggesting that mTOR activation of PTSCs may be dependent upon the mechanical load (4 vs. 8%), and that mechanical loading itself may result in cellular stress that mTOR is able to sense in tendon tissue.

Excessive mechanical loading is known to cause catabolic changes in tendons and induce differentiation of TSCs into non-tenocytes, which may lead to the development of degenerative tendinopathy frequently seen in clinical settings (Zhang et al., 2010; Zhang and Wang, 2010b; Abraham et al., 2011; Zhang and Wang, 2013). In this study, mechanical over-stretching of PTSCs *in vitro* at 8% caused an increase in non-tenocyte differentiation, including adipogenesis, chondrogenesis, and osteogenesis. However, rapamycin reduced the expression of these non-tenocyte genes. Based on these results, we assessed the preventative potential of the classic mTOR antagonist rapamycin in the prevention of tendinopathy development due to excessive mechanical loading. Indeed, daily injections of rapamycin in mice block the formation of degenerative changes in ITR tendons.

Elevated expression of SOX-9 and collagen II in tendons were observed in mice subjected to ITR, which matched similar results observed in clinical specimens of excessive mechanical loading-induced tendinopathy (Rui et al., 2012). In our data, the presence of these markers was greatly reduced in the tendon tissues treated with rapamycin prior to ITR, suggesting that mTOR signaling due to mechanical loading conditions on tendon cells regulates the expression of these non-tendinous tissue markers, and hence mechanical activation of mTOR may play a crucial role in the development of tendinopathy.

An important observation in this study was with Masson trichrome (MT) staining. Normal cage tendons were stained red, whereas ITR tendons were stained blue. The results are consistent with previous reports that loose, immature, or degenerative connective tissues are stained blue, whereas normal tendon consisting of dense connective tissues (mainly collagen type I) are stained red with MT staining (Martinello et al., 2015; Bastiani et al., 2018). The reason for such a difference in color may be that dye penetration is easier in loose connective tissue than in the normal dense connective tissue (Bastiani et al., 2018). Using MT staining, this study was able to confirm that rapamycin injection decreased the extent of connective tissue disorganization and degeneration in the ITR tendons.

There are a few limitations in this study. First, the detailed upstream and downstream signaling components involved in the mTOR response to mechanical loading were not determined. mTOR signaling has been correlated with the formation of muscle ossification, which was shown to be negatively regulated by PI3Kα (Valer et al., 2019). Therefore, while this study focused on the effects of rapamycin/mTOR signaling on PTSCs *in vitro* and tendons *in vivo* due to mechanical overloading, future studies are warranted to investigate detailed mTOR signaling pathways under mechanical loading conditions. Second, mTOR is known to be linked to aging-associated tendon disorders (Wilkinson et al., 2012; Zaseck et al., 2016), and future studies may include mice of different ages in the ITR model to further elucidate the role of mTOR and the effects of rapamycin in the development of tendinopathy. Third, it is known that mTOR exists in two complexes, namely mTORC1 and mTORC2. mTORC1 regulates protein translation, autophagy, among other functions, and is mediated by S6K1, 4E-BP1, and others. On other hand, mTORC2 is considered mainly as a downstream effector of IGF-1 signaling pathway (Kennedy and Lamming, 2016). Since this study showed increased phosphorylation of S6 and 4E-BP1, it is likely that mechanical loading activated mTORC1 pathway. However, the existing data from this study are not sufficient yet to show that mTORC1 actually mediates mechanical overloading-induced non-tenocyte differentiation of PTSCs. Future research is warranted to determine respective roles of mTORC1 and mTORC2 in the non-tenocyte differentiation of PTSCs and development of tendinopathy due to mechanical overloading conditions.

Fourth, this study mainly utilized histochemical and immunohistochemical analyses to determine the results of ITR-induced tendon degeneration and the protective effects of rapamycin injections. However, other methodologies such as TEM and mechanical testing of tendon are highly desirable to show changes in structural and mechanical properties of the tendon due to mechanical loading and rapamycin treatment. Finally, while the identity of cell type, or PTSCs, in our *in vitro* study was clearly defined, it is not certain what exact types of cells were involved in the differentiation of these cells into chondrocyte-like cells, judged by the round cell shape and expression of those chondrogenic markers (proteoglycan accumulation, and expression of SOX-9 and collagen II proteins). However, PTSCs should be part of the tendon cell population because, unlike terminally differentiated "tenocytes," these

stem/progenitor cells possess multi-differentiation potential (Zhang and Wang, 2010a). Other stem/progenitor cells from paratenon (Zhang et al., 2021) could also be part of the cells that undergo non-tenocyte differentiation in response to mechanical overloading-induced tendon injury.

In conclusion, this study showed that mechanical loading activates mTOR signaling in PTSCs, and rapamycin treatment reduces non-tenocyte differentiation *in vitro*. Moreover, injections of rapamycin decreased the tendon's degenerative changes in mice subjected to ITR. These findings suggest that rapamycin may be used as a therapeutic option to prevent the development of tendinopathy due to mechanical overloading placed on the tendon.

DATA AVAILABILITY STATEMENT

The original contributions presented in the study are included in the article/**Supplementary Material**, further inquiries can be directed to the corresponding author/s.

ETHICS STATEMENT

The animal study was reviewed and approved by the Ethics Committee of the University of Pittsburgh.

AUTHOR CONTRIBUTIONS

DN, YZ, and JZ contributed to the cell culture experiments, animal experiments, data acquisition, and analysis. DN and WW drafted the manuscript. JZ took part in the experimental design and manuscript revision. JW conceived the study, supervised experiments, and data analysis, and revised the manuscript. All authors read and approved the final manuscript.

FUNDING

This work was supported in part by NIHRO1AR065949 (JW).

ACKNOWLEDGMENTS

We thank Dr. Bhavani P. Thampatty for assistance in the preparation of this manuscript.

SUPPLEMENTARY MATERIAL

The Supplementary Material for this article can be found online at: https://www.frontiersin.org/articles/10.3389/fcell.2021.687856/full#supplementary-material

Supplementary Figure 1 | Rapamycin inhibits the phosphorylation of both S6 and 4E-BP1.

REFERENCES

Abraham, T., Fong, G., and Scott, A. (2011). Second harmonic generation analysis of early Achilles tendinosis in response to in vivo mechanical loading. *BMC Musculoskelet. Disord.* 12:26. doi: 10.1186/1471-2474-12-26

Bastiani, G., Corte, F. D., Brass, K. E., Cantarelli, C., Dau, S., Kommers, G. D., et al. (2018). Histochemistry of equine damaged tendons, ligaments and articular cartilage. *Acta Sci. Vet.* 146:1612.

Bi, Y., Ehirchiou, D., Kilts, T. M., Inkson, C. A., Embree, M. C., Sonoyama, W., et al. (2007). Identification of tendon stem/progenitor cells and the role of the extracellular matrix in their niche. *Nat. Med.* 13, 1219–1227. doi: 10.1038/nm1630

Blawat, K., Mayr, A., Hardt, M., Kirschneck, C., Nokhbehsaim, M., Behl, C., et al. (2020). Regulation of Autophagic Signaling by Mechanical Loading and Inflammation in Human PDL Fibroblasts. *Int. J. Mol. Sci.* 21:9446. doi: 10.3390/ijms21249446

Cook, J. L., and Purdam, C. R. (2009). Is tendon pathology a continuum? . *Br. J. Sports Med.* 43, 409–416. doi: 10.1136/bjsm.2008.051193

Glazebrook, M. A., Wright, J. R. Jr., Langman, M., Stanish, W. D., and Lee, J. M. (2008). Histological analysis of achilles tendons in an overuse rat model. *J. Orthop. Res.* 26, 840–846. doi: 10.1002/jor.20546

Goodman, C. A. (2019). Role of mTORC1 in mechanically induced increases in translation and skeletal muscle mass. *J. Appl. Physiol.* 127, 581–590. doi: 10.1152/japplphysiol.01011.2018

Goodman, C. A., Miu, M. H., Frey, J. W., Mabrey, D. M., Lincoln, H. C., Ge, Y., et al. (2010). A phosphatidylinositol 3-kinase/protein kinase B-independent activation of mammalian target of rapamycin signaling is sufficient to induce skeletal muscle hypertrophy. *Mol. Biol. Cell* 21, 3258–3268. doi: 10.1091/mbc.E10-05-0454

Guan, Y., Yang, X., Yang, W., Charbonneau, C., and Chen, Q. (2014). Mechanical activation of mammalian target of rapamycin pathway is required for cartilage development. *FASEB J.* 28, 4470–4481. doi: 10.1096/fj.14-252783

Kennedy, B. K., and Lamming, D. W. (2016). The mechanistic target of rapamycin: the grand conducTOR of metabolism and aging. *Cell Metab.* 23, 990–1003. doi: 10.1016/j.cmet.2016.05.009

Livak, K. J., and Schmittgen, T. D. (2001). Analysis of relative gene expression data using real-time quantitative PCR and the 2(-Delta Delta C(T)) Method. *Methods* 25, 402–408. doi: 10.1006/meth.2001.1262

Maffulli, N., Khan, K. M., and Puddu, G. (1998). Overuse tendon conditions: time to change a confusing terminology. *Arthroscopy* 14, 840–843. doi: 10.1016/s0749-8063(98)70021-0

Martinello, T., Pascoli, F., Caporale, G., Perazzi, A., Iacopetti, I., and Patruno, M. (2015). Might the Masson trichrome stain be considered a useful method for categorizing experimental tendon lesions? *Histol. Histopathol.* 30, 963–969. doi: 10.14670/HH-11-601

Mello, T., Nakatsuka, A., Fears, S., Davis, W., Tsukamoto, H., Bosron, W. F., et al. (2008). Expression of carboxylesterase and lipase genes in rat liver cell-types. *Biochem. Biophys. Res. Commun.* 374, 460–464. doi: 10.1016/j.bbrc.2008.07.024

Mousavizadeh, R., Hojabrpour, P., Eltit, F., McDonald, P. C., Dedhar, S., McCormack, R. G., et al. (2020). β1 integrin. *ILK and mTOR regulate collagen synthesis in mechanically loaded tendon cells. Sci. Rep.* 10:12644. doi: 10.1038/s41598-020-69267-6

Ng, G. Y., Chung, P. Y., Wang, J. S., and Cheung, R. T. (2011). Enforced bipedal downhill running induces Achilles tendinosis in rats. *Connect. Tissue Res.* 52, 466–471. doi: 10.3109/03008207.2011.562334

Pantovic, A., Krstic, A., Janjetovic, K., Kocic, J., Harhaji-Trajkovic, L., Bugarski, D., et al. (2013). Coordinated time-dependent modulation of AMPK/Akt/mTOR signaling and autophagy controls osteogenic differentiation of human mesenchymal stem cells. *Bone* 52, 524–531. doi: 10.1016/j.bone.2012.10.024

Popov, C., Burggraf, M., Kreja, L., Ignatius, A., Schieker, M., and Docheva, D. (2015). Mechanical stimulation of human tendon stem/progenitor cells results in upregulation of matrix proteins, integrins and MMPs, and activation of p38 and ERK1/2 kinases. *BMC Mol. Biol.* 16:6. doi: 10.1186/s12867-015-0036-6

Rafiei, H., and Ashrafizadeh, M. (2018). Expression of collagen Type II and osteocalcin genes in mesenchymal stem cells from rats treated with lead acetate II. *Iranian. J. Toxicol.* 12, 35–40. doi: 10.32598/ijt.12.5.540.1

Rui, Y. F., Lui, P. P., Ni, M., Chan, L. S., Lee, Y. W., and Chan, K. M. (2011). Mechanical loading increased BMP-2 expression which promoted osteogenic differentiation of tendon-derived stem cells. *J. Orthop. Res.* 29, 390–396. doi: 10.1002/jor.21218

Rui, Y. F., Lui, P. P., Rolf, C. G., Wong, Y. M., Lee, Y. W., and Chan, K. M. (2012). Expression of chondro-osteogenic BMPs in clinical samples of patellar tendinopathy. *Knee Surg. Sports Traumatol. Arthrosc.* 20, 1409–1417. doi: 10.1007/s00167-011-1685-8

Singha, U. K., Jiang, Y., Yu, S., Luo, M., Lu, Y., Zhang, J., et al. (2008). Rapamycin inhibits osteoblast proliferation and differentiation in MC3T3-E1 cells and primary mouse bone marrow stromal cells. *J. Cell. Biochem.* 103, 434–446. doi: 10.1002/jcb.21411

Soslowsky, L. J., Thomopoulos, S., Tun, S., Flanagan, C. L., Keefer, C. C., Mastaw, J., et al. (2000). Neer Award 1999. Overuse activity injures the supraspinatus tendon in an animal model: a histologic and biomechanical study. *J. Shoulder Elbow Surg.* 9, 79–84.

Valer, J. A., Sánchez-de-Diego, C., Gámez, B., Mishina, Y., Rosa, J. L., and Ventura, F. (2019). Inhibition of phosphatidylinositol 3-kinase α (PI3Kα) prevents heterotopic ossification. *EMBO. Mol. Med.* 11:e10567. doi: 10.15252/emmm.201910567

Wang, J. H., and Grood, E. S. (2000). The strain magnitude and contact guidance determine orientation response of fibroblasts to cyclic substrate strains. *Connect. Tissue Res.* 41, 29–36. doi: 10.3109/03008200009005639

Wilkinson, J. E., Burmeister, L., Brooks, S. V., Chan, C. C., Friedline, S., Harrison, D. E., et al. (2012). Rapamycin slows aging in mice. *Aging Cell* 11, 675–682. doi: 10.1111/j.1474-9726.2012.00832.x

Yoon, M. S. (2017). mTOR as a key regulator in maintaining skeletal muscle mass. *Front. Physiol.* 8:788. doi: 10.3389/fphys.2017.00788

Yoshida, C. A., Yamamoto, H., Fujita, T., Furuichi, T., Ito, K., Inoue, K., et al. (2004). Runx2 and Runx3 are essential for chondrocyte maturation, and Runx2 regulates limb growth through induction of Indian hedgehog. *Genes Dev.* 18, 952–963. doi: 10.1101/gad.1174704

Zaseck, L. W., Miller, R. A., and Brooks, S. V. (2016). Rapamycin attenuates age-associated changes in tibialis anterior tendon viscoelastic properties. *J. Gerontol. A Biol. Sci. Med. Sci.* 71, 858–865. doi: 10.1093/gerona/glv307

Zhang, C., Zhu, J., Zhou, Y., Thampatty, B. P., and Wang, J. H. (2019). Tendon stem/progenitor cells and their interactions with extracellular matrix and mechanical loading. *Stem Cells Int.* 2019:3674647. doi: 10.1155/2019/3674647

Zhang, J., Li, F., Williamson, K. M., Tan, S., Scott, D., Onishi, K., et al. (2021). Characterization of the structure, vascularity, and stem/progenitor cell populations in porcine Achilles tendon (PAT). *Cell Tissue Res.* 384, 367–387. doi: 10.1007/s00441-020-03379-3

Zhang, J., Pan, T., Liu, Y., and Wang, J. H. (2010). Mouse treadmill running enhances tendons by expanding the pool of tendon stem cells (TSCs) and TSC-related cellular production of collagen. *J. Orthop. Res.* 28, 1178–1183. doi: 10.1002/jor.21123

Zhang, J., and Wang, J. H. (2010a). Characterization of differential properties of rabbit tendon stem cells and tenocytes. *BMC Musculoskelet. Disord.* 11:10. doi: 10.1186/1471-2474-11-10

Zhang, J., and Wang, J. H. (2010b). Mechanobiological response of tendon stem cells: implications of tendon homeostasis and pathogenesis of tendinopathy. *J. Orthop. Res.* 28, 639–643. doi: 10.1002/jor.21046

Zhang, J., and Wang, J. H. (2010c). Production of PGE(2) increases in tendons subjected to repetitive mechanical loading and induces differentiation of tendon stem cells into non-tenocytes. *J. Orthop. Res.* 28, 198–203. doi: 10.1002/jor.20962

Zhang, J., and Wang, J. H. (2013). The effects of mechanical loading on tendons–an in vivo and in vitro model study. *PLoS One* 8:e71740. doi: 10.1371/journal.pone.0071740

Conflict of Interest: The authors declare that the research was conducted in the absence of any commercial or financial relationships that could be construed as a potential conflict of interest.

frontiers in Cell and Developmental Biology

ORIGINAL RESEARCH
published: 16 July 2021
doi: 10.3389/fcell.2021.682719

Type II Collagen Sponges Facilitate Tendon Stem/Progenitor Cells to Adopt More Chondrogenic Phenotypes and Promote the Regeneration of Fibrocartilage-Like Tissues in a Rabbit Partial Patellectomy Model

*Wen Wang[1,2†], Shengnan Qin[1†], Peiliang He[1,2], Wei Mao[1,2], Liang Chen[1,2], Xing Hua[3], Jinli Zhang[1], Xifeng Xiong[1], Zhihe Liu[1], Pengzhen Wang[1], Qingqi Meng[1], Fei Dong[1], Aiguo Li[1,2], Honghui Chen[1] and Jiake Xu[4]**

[1] Department of Orthopedics, Guangzhou Institute of Traumatic Surgery, Guangzhou Red Cross Hospital, Medical College, Jinan University, Guangzhou, China, [2] Department of Clinical Medicine, Guizhou Medical University, Guiyang, China, [3] Department of Pathology, Guangzhou Red Cross Hospital, Medical College, Jinan University, Guangzhou, China, [4] School of Biomedical Sciences, The University of Western Australia, Perth, WA, Australia

Objective: Fibrocartilage transition zone (FC) is difficult to regenerate after surgical re-attachment of tendon to bone. Here, we investigated whether type II collagen-sponges (CII-sponges) facilitated tendon stem/progenitor cells (TSPCs) to adopt chondrogenic phenotypes and further observed if this material could increase the FC areas in bone-tendon junction (BTJ) injury model.

Methods: CII-sponges were made as we previously described. The appearance and pore structure of CII-sponges were photographed by camera and microscopies. The viability, proliferation, and differentiation of TSPCs were examined by LIVE/DEAD assay, alamarBlue, and PKH67 *in vitro* tracking. Subsequently, TSPCs were seeded in CII-sponges, Matrigel or monolayer, and induced under chondrogenic medium for 7 or 14 days before being harvested for qPCR or being transplanted into nude mice to examine the chondrogenesis of TSPCs. Lastly, partial patellectomy (PP) was applied to establish the BTJ injury model. CII-sponges were interposed between the patellar fragment and tendon, and histological examination was used to assess the FC regeneration at BTJ after surgery at 8 weeks.

Results: CII-sponges were like sponges with interconnected pores. TSPCs could adhere, proliferate, and differentiate in this CII-sponge up to 14 days at least. Both qPCR and immunostaining data showed that compared with TSPCs cultured in monolayer or Matrigel, cells in CII-sponges group adopted more chondrogenic phenotypes with an overall increase of chondrocyte-related genes and proteins. Furthermore, in PP injured model, much more new formed cartilage-like tissues could be observed in CII-sponges

OPEN ACCESS

Edited by:
Zi Yin,
Zhejiang University, China

Reviewed by:
Antonio Giordano,
Temple University, United States
Wenguo Cui,
Shanghai Jiao Tong University, China
Song Zhao,
Shanghai Jiao Tong University, China

***Correspondence:**
Jiake Xu
jiake.xu@uwa.edu.au

† These authors have contributed equally to this work

Specialty section:
This article was submitted to Stem Cell Research, a section of the journal Frontiers in Cell and Developmental Biology

Received: *19 March 2021*
Accepted: *15 June 2021*
Published: *16 July 2021*

Citation:
Wang W, Qin S, He P, Mao W, Chen L, Hua X, Zhang J, Xiong X, Liu Z, Wang P, Meng Q, Dong F, Li A, Chen H and Xu J (2021) Type II Collagen Sponges Facilitate Tendon Stem/Progenitor Cells to Adopt More Chondrogenic Phenotypes and Promote the Regeneration of Fibrocartilage-Like Tissues in a Rabbit Partial Patellectomy Model. Front. Cell Dev. Biol. 9:682719. doi: 10.3389/fcell.2021.682719

group, evidenced by a large amount of positive proteoglycan expression and typical oval or round chondrocytes in this area.

Conclusion: Our study showed that CII-sponges facilitated the TSPCs to differentiate toward chondrocytes and increased the area of FCs, which suggests that CII-sponges are meaningful for the reconstruction of FC at bone tendon junction. However, the link between the two phenomena requires further research and validation.

Keywords: tendon stem and progenitor cells, type II collagen sponges, fibrocartilage transition zones, bone tendon junction, chondrogenesis

INTRODUCTION

Fibrocartilage transition zone (FC) is the structure of bone tendon junction. Surgical reattachment of tendon to bone often fails due to the lack of regeneration of this specialised structure, thereby presenting difficulty for tendon to bone healing. It is reported that many factors, like mechanical loading, extracellular matrix, and biological factors (Wong et al., 2004; Lui P. et al., 2010; Hu et al., 2015; Leung et al., 2015), may contribute to better healing outcome at the junction between tendon graft and bone. However, it is important to note that the new-formation of cartilaginous tissues between the two completely different or inhomogeneous tissues is a key process even though these tissues function as intermediate in endochondral ossification and disappear with time during healing eventually. It is confirmed that the reconstruction from patellar tendon to cartilage was much easier to that from tendon to the remaining patellar in partial patellectomy model (Lu et al., 2008). Several studies have also demonstrated that cartilaginous tissues formed between tendon graft and bone, resembling the natural transition zone in ACL reconstruction surgery (Yamakado et al., 2002; Lim et al., 2004; Park et al., 2018). Many studies reported better healing outcomes with the appearance of chondrocyte-like cells between tendon graft and tendon (Grassman et al., 2002; Wang et al., 2010, 2014; Hu et al., 2015; Lu et al., 2015, 2016; Song et al., 2017). Wong et al. (2009) showed that articular cartilage interposed in patellar tendon and the remaining patellar could result in more FC than direct repair at all time points, and hence stronger mechanical strength recovery. These findings suggest that the formation of cartilage interface by different means could be an effective way to promote the regeneration of native FC and hence be beneficial to the reconstruction of bone tendon junction.

Considering that the implication of cartilaginous interfaces for regeneration of bone tendon junction, it is important to induce stem/progenitor cells from either bone marrow or tendon to differentiate toward chondrocytes or fibrochondrocytes after tendon reconnected to bone tissues. Our previous study showed that tendon stem/progenitor cells (TSPCs) were differentiated toward fibrochondrocytes under classical chondrogenic induction medium, so TSPCs could be candidate for the seed cells for bone tendon junction repair (Qin et al., 2020). However, in our previous study, only a proportion of TSPCs after induction differentiated, and the reason for this might be due to the fact that chondrocytes in monolayer 2D culture dedifferentiate to a less specialised fibroblastic phenotype and produce less cartilage extracellular matrix (ECM). The ECM on which stem cells grow has been proved to play a particularly important role in controlling cell differentiation fate (Badylak, 2005; Evans et al., 2010). Type II collagen is the main component of articular cartilage of knee, and scaffolds made of type II collagen have been proved to direct stem cells toward chondrocytes and promote the repair of cartilage defect (Chen et al., 2011). Compared to monolayer, chondrocytes grown in 3D porous collagen sponges can maintain the expression of chondrocyte-specific genes as well as the production of cartilage-specific ECM (Yates et al., 2005).

The aim of this study is to induce TSPCs to adopt more chondrogenic phenotype, we chose cross-linked type II collagen-sponges (CII-sponges) which we previously homemade to provide a three-dimensional environment for TSPCs and further observed the role of this material in the regeneration of FCs at bone-tendon junction (BTJ). The CII-sponges have been proved to be beneficial to the new formation of cartilage-like tissues at the site of full-thickness articular cartilage defect as evidenced by positive proteoglycan staining and positive type II collagen staining (Chen et al., 2011). Here, we observed the chondrogenic differentiation of TSPCs in the pellet culture system. We also assessed the growth of cells that were seeded in our homemade CII-sponges and further investigated the role of CII-sponges in directing TSPCs toward chondrocytes or fibrochondrocytes. Finally, the regeneration of FCs at injured bone tendon junctions was evaluated. We show that CII-sponges effectively directed TSPCs differentiation toward fibrochondrocytes, and also could increase the formation of fibrocartilage-like tissues at the BTJ.

MATERIALS AND METHODS

Cell Culture

The TSPCs were isolated from human tendon as previously described (Qin et al., 2020). Cells at passage 6 were employed to do experiments.

Immunocytochemistry Staining

To observe the chondrogenic proteins expression of human TSPCs, cells were harvested and seeded in coverslips. Cells were fixed using 4% paraformaldehyde for 10 min at room temperature before the immunocytochemistry (ICC) procedure. The samples were incubated with PBS containing 0.25% Triton X-100 to permeabilise the cells. In order to block unspecific binding of the

antibodies, cells were incubated with 1% BSA in PBS for 30 min, and then incubate cells with the diluted primary antibodies, including Collagen I, Collagen II, Sox9, and Aggrecan, in 1% BSA in PBS for overnight at 4°C. Subsequently were incubated the cells in 0.3% H_2O_2 to block the endogenous peroxidase, and then applied to the secondary antibodies for 1 h at room temperature. Finally, the samples were developed with chromogen for 3 min at room temperature, rinsed with in running tap water for 5 min and counterstained with haematoxylin.

The Chondrogenic Induction of Tendon Stem Cells in Pellet Culture System

To assess the chondrogenic differentiation potential of TSPCs we isolated, classical pellet culture system was used. TSPCs (passage 6) were centrifuged and then cultured in chondrogenic induction medium which is LG-DMEM with 10% FBS and containing 10^{-7} M dexamethasone, 40 μg/ml proline, 100 μg/ml pyruvate, 50 μg ascorbate-2-phosphate (all from Sigma-Aldrich), and 1:100 diluted ITS + premix (6.25 mg/ml insulin, 6.25 mg/ml transferrin, 1.25 mg/ml bovine serum albumin, 5.35 mg/ml linoleic acid, and 6.25 mg/ml selenous acid) (Becton Dickinson, Franklin Lakes, NJ, United States) as well as TGF-β3/BMP-2 (10 ng/ml TGF-β3 and 50 ng/ml BMP-2). After 21 days, pellets were harvested to be fixed and embedded in order to observe the expression of proteins mentioned above using by immunohistochemistry staining.

The Preparation of CII-Sponges

Type II collagen was extracted as previously described (Chen et al., 2011). Type II collagen protein was extracted from the hyaline cartilage of knees from pigs. Firstly, the hyaline cartilage was peeled off and cut into pieces. Secondly, type II collagen fibres were dissolved with acetic acid solution containing pepsin into solution and centrifuged in order to remove those undissolved cartilage tissues. Thirdly, the supernatant with type II collagen was mixed with NaCl solution in a way collagens dissolved into acetic acid can be salted out. Subsequently, these salted-out collagens were re-dissolved in acetic acid to get the purified collagen solution. Finally, this purified collagen solution were re-adjusted by dialysing with distilled water to PH 5.5.

In order to get CII-sponges, two steps were applied. First, the purified collagen solution per well was poured into 24-well plate in every 0.5 ml solution per well, and after freeze-drying by vacuum freeze-dryer (PINPAI, United States), sponge-like materials were obtained. Secondly, due to the fact that collagen sponges we got in the last step would be dissolved in water easily, the collagen sponges needed to be cross-linked before being used as scaffolds. In order to get cross-linked CII-sponges, these CII-sponges were further cross-linked with EDC/NHS as we previously described (Qin et al., 2010).

Pore Structure of CII-Sponges

The appearance of the CII-sponges was photographed by camera, and the pore structure and porosity of the CII-sponges were observed by laser confocal electron microscopy (LCM), scanning electron microscopy (SEM), and bright field microscopy (BFM). For LCM, collagen has autofluorescence, thereby producing a bright green fluorescence in sponges with the excitation wavelength of 488 nm and the emission wavelength of 520 nm using the Confocal microscope, so the pore diameter in the same layer could be seen. For SEM examination, the samples were air dried, sputter-coated with gold and the pore structure could be observed. The samples were also observed by microscopy under BFM.

TSPCs Seeded in Monolayer, Matrigel, or CII-Sponges

TSPCs were seeded in monolayer, Matrigel, or CII-sponges for 7 or 14 days with or without chondrogenic induction. For monolayer, 10^6 TSPCs were seeded in 10 cm culture dish. For Matrigel, 10^6 TSPCs were collected and resuspended in 0.2 ml medium, and then mixed with 0.2 ml Matrigel. After several seconds, Matrigel could form gel-like scaffold. For CII-sponges, 10^6 cells were resuspended in 0.5 ml medium and then seeded in 2.5 cm^2 CII sponge. Matrigel- or CII sponge-cells compounds were then cultured in 24 well plates.

The Viability of TSPCs Seeded in CII-Sponges

LIVE/DEAD assay was used to check the cell viability of TSPCs after 14 days culture. TSPCs at passage 6 were harvested and approximately 10^6 cells were seeded in each 2.5 cm^2 CII-sponges. After 3-day culture, the sponges were changed to a new dish in order to rule out the cells which did not adhere to the materials. Meanwhile, the culture medium was changed to chondrogenic medium. Cells viability was checked by LIVE/DEAD assay (ThermoFisher, United States) in the process of chondrogenic induction, and live/dead cells after 14-day induction were photographed by immunofluorescence microscope. The sponges with cells were washed once by PBS in order to remove the serum in culture medium, and then 1 ml PBS with 2 μl Calcein AM and 0.4 μl EthD-1 was added in each sponges. Meanwhile, one drop of NucBlue™ Live ReadyProbes™ Reagents (ThermoFisher, United States) was added per 1 ml PBS to distinguish the nuclei in cells. After 30 min incubation at room temperature, live cells could retain the polyanionic dye calcein AM well, thereby producing a bright green fluorescence at the excitation/emission wavelength ∼495/∼515 nm. At the same time, EthD-1 could enter dead cells and produce an intense strong red fluorescence by binding to nucleic acids at the excitation/emission wavelength ∼495/∼635 nm. NucBlue™ Live cell stain was excited by UV light, emitting blue fluorescence at the excitation/emission wavelength ∼360/∼460 nm.

AlamarBlue Cell Viability Regent (ThermoFisher, United States) was used to monitor the proliferation of TSPCs seeded in CII-sponges without compromising cell health. The viability of TSPCs seeded in CII-sponges was measured at day 1, 3, 7, and 14, respectively. To assay for viability, the pre-mixed alamarBlue reagent were added with the completed medium to cells, incubated for 2 h, and absorbance values were measured using a plate reader (BioTek, United States).

In vitro Tracking of TSPCs Seeded in CII-Sponges

PKH67 kit is for general cell membrane labelling, and can be applied to label and track cells over an extended period of time *in vitro*, with no apparent toxic effects. Due to the fact that non-dividing cells remain brightly labelled with membrane intercalating dyes and the same stem cell could not proliferate and differentiate simultaneously, we examined the labelled cells remaining in CII-sponges with or without chondrogenic induction *in vitro*. TSPCs were labelled with PKH67 according to manufacturers' protocol, and seeded in CII-sponges. The collagen sponges seeded with cells were cultured in completed medium for 7 days, and then would continue to be cultured in completed medium or induced with chondrogenic medium for further 14 days. TSPCs labelled with PKH67 would be observed with fluorescence microscopes at day 7 and 21.

q-PCR

Cells were seeded in monolayer, Matrigel, and CII-sponges and continued to be cultured in completed medium for 7 days. Subsequently, cells were cultured in chondrogenic medium or completed medium for 7 or 14 days. Total RNA was extracted using TRIzol^{TM}, and cDNA was synthesised using 500 ng RNA with PrimeScript RT master Mix (Takara, China) according to manufacturer's instruction. The resulting cDNA was then used for real-time PCR with PowerUP^{TM} SYBR^{TM} Green Master Mix (ThermoFisher, United States) by Analytik Jena qTOWER^{G}. The conditions for PCR were as follow: 50°C for 2 min, 95°C for 5 min, followed by 40 cycles of (95°C for 15 s, 60°C for 60°C 1 min) with a melt curve stage of (95°C for 15 s, 60°C for 1 min, 95°C for 15 s). The primers used were as follow: Col1α1 (Forward: 5′-CAGCCGCTTCACCTACAGC-3′, Reverse: 5′-TTTTGTATTCAATCACTGTCTTGCC-3′), Sox 9 (Forward: 5′-TACGACTGGACGCTGGTGCC-3′ and Reverse: 5′-CCGTTCTTCACCGACTTCCTCC-3′), Col2α1 (Forward: 5′-GGCAATAGCAGGTTCACGTACA-3′ and Reverse: 5′-CGATAACAGTCTTGCCCCACTT-3′), Aggrecan (Forward: 5′-AAGTATCATCAGTCCCAGAATCTAGCA-3′ and Reverse: 5′-TTGGTGGAGACGTAAGGTGC-3′), and GAPDH (Forward: 5′-CGTAAAGACCTCTATGCCAACA-3′ and Reverse: 5′-CGGACTCATCGTACTCCTGCT-3′). The relative mRNA levels of all genes were normalised to housekeeping gene GAPDH and calculated using $2^{-\Delta\Delta CT}$ method.

Heterotopic Chondrogenesis of TSPCs *in vivo*

The chondrogenic characteristics of TSPCs seeded in monolayer, Matrigel, or CII-sponges were observed *in vivo*. For monolayer, 10^6 TSPCs were cultured in completed medium for 7 days in 10 cm dish. Meanwhile, 10^6 TSPCs were seeded in Matrigel or collagen II sponge and also cultured in completed medium for 7 days. Cells in monolayer culture were then centrifuged to form a pellet due to the fact that cells without scaffolds were not able to be transplanted subcutaneously into the dorsal surface of immunocompromised nude mice. Cells in all of three groups were then induced by chondrogenic medium for 14 days *in vitro* before being transplanted. These transplants were harvested after 4 weeks, and proteoglycan or some proteins were further observed by histology examination.

Partial Patellectomy Model

Twelve mature female New Zealand White rabbits (16 weeks old) underwent partial patellectomy and surgical reconstruction between the patella and patellar tendon using a previously established protocol (Wang et al., 2007). Briefly, with the animal under general anaesthesia with sodium pentobarbital, and the distal one-third of the patella as well as its fibrocartilage zone to the patellar tendon were removed. The patellar tendon was then directly sutured to the remaining proximal patella via the two holes drilled longitudinally through patella, with non-absorbable suture. CII-sponges were then interposed between patellar and patellar tendon. Direct repair was set as a control group. The operated knee joint was then immobilised for up to 4 weeks. Animals were kept individually in metal cages and fed with standard rabbit diet and water *ad libitum*. After 8 weeks, the animals were euthanised with an overdose of sodium pentobarbital, and the patellar and patellar tendon (PPT) complexes of the operated were harvested and prepared for histology examination. This study was approved by the Animal Research Ethics Committee of the Guangzhou Red Cross Hospital Ethics Committee (Approval No. 2018-002-01).

Histology Examination

All samples, including pellet formed *in vitro*, and transplants harvested from nude mice and PPT complexes from rabbits, were immediately fixed in 10% neural formalin for 3 days, and subsequently PPT complexes were decalcified by 10% formic acid for more than 1 month. Samples were finally embedded in paraffin and sliced up at 5 μm. The sections were stained with Safranin O/Fast Green.

Immunohistochemical (IHC) staining were used to detect the expression of proteins, including Collagen I and II, Sox9, and Aggrecan (All from Abcam, United States), in continuous sections. The IHC staining was performed using a Mouse and Rabbit Specific HRP/DAB detection IHC kit (from ZSGB-BIO, China) according to manufacturer's protocol. Briefly, deparaffinize and rehydrate the paraffin-embedded sections. Wash the slides in TBS plus 0.025% Triton-X100. After blocking with blocking solution of the kit, apple primary antibodies diluted in TBS with 1% BSA and allow the sections to incubate overnight at 4°C. Wash twice, and then block non-specific background staining. Apple biotinylated goat anti-rabbit/mouse antibody supplied with the kit and incubate for 15 min at room temperature. Apply streptavidin biotin peroxidase and incubate for 10 min at RT. Rinse four times, and add DAB substrate for less than 3 min to develop colour. Wash three times in buffer and apply H&E counterstain, dehydrate, and tissue clear. Meanwhile, in order to quantify the proteoglycan and proteins expression, the positive area of proteoglycan and all of proteins were analysed by ImageProPlus. To be more specific, the positive areas of proteoglycan (red) and proteins (brown) were counted by Image ProPlus, and the percentage of positive areas were normalised to the total areas of transplant from nude mice.

Statistical Analysis

All data were presented as mean ± SD, and all reported representative data were from at least three independent experiments. All statistical analyses were performed with one-way AVONA analysis by PRISM 8. $p \leqq 0.05$ was considered as statistically significant. ns, represented as no significance; * represented as $P < 0.05$, ** represented as $P < 0.01$, and *** represented as $P < 0.001$.

RESULTS

Chondrocyte-Related Protein Expression of TSPCs and Chondrogenic Differentiation of TSPCs in Pellet Culture

In order to determine whether TSPCs express chondrogenic differentiation proteins, Sox 9, collagen I, collagen II, and aggrecan expressions were investigated by ICC staining firstly. Strong expressions of collagen I in TSPCs were observed, while no expression of chondrocyte-specific proteins, including Sox 9, collagen II, and aggrecan, could be detected (**Figure 1A**).

Given we found that TSPCs differentiated toward fibrochondrocytes in monolayer culture, we chose the pellet culture system, a classic evaluation model for chondrogenesis of MSCs *in vitro*, to assess the chondrogenic differentiation potential of TSPCs from human tendon. IHC staining showed that after chondrogenic induction in pellet culture, Collagen I, a protein that was identified as the unique phenotype of TSPCs (Bi et al., 2007) and also as the fibroblast-specific protein, was still strongly expressed. However, aggrecan and type II collagen were weakly expressed, whereas Sox 9 was little expressed (**Figure 1B**).

The Characterisation of CII-Sponges and Cell Viability as Well as *in vitro* Differentiation Tracking of TSPCs

CII-sponges we homemade looks like a porous sponge (**Figure 2A**). The pore structure of CII-sponges was examined by the LCM, the SEM, and BFM (**Figure 2B**). After layered scanning of LCM, aperture size in the same layer could be seen, and in our previous paper the size was 92.17 ± 29.55 μm (Qin et al., 2010), which was believed the appropriate pore size for chondrocytes growth (Nehrer et al., 1997; Zhang et al., 2014). SEM showed that CII-sponges had the film-like structures which are beneficial to cell adhesion and proliferation, and BF showed that this collagen sponge had similar aperture size and a large number of pores, which can be helpful to nutrient exchange. We also confirmed whether TSPCs could survive in this homemade collagen sponges after a period of culture *in vitro* (**Figure 2C**). The viability of TSPCs adhere to collagen scaffolds was assessed by LIVE/DEAD assay. It could be seen that the number of dead cells was decreased in a time manner, and more than 90% of the total cells were alive (Green), and a few of dead cells (red) could also be found after 14 days culture *in vitro*. AlamarBlue was used to track the proliferation of TSPCs adhere to CII-sponges, cells could proliferate well in the CII-sponges evidenced by the

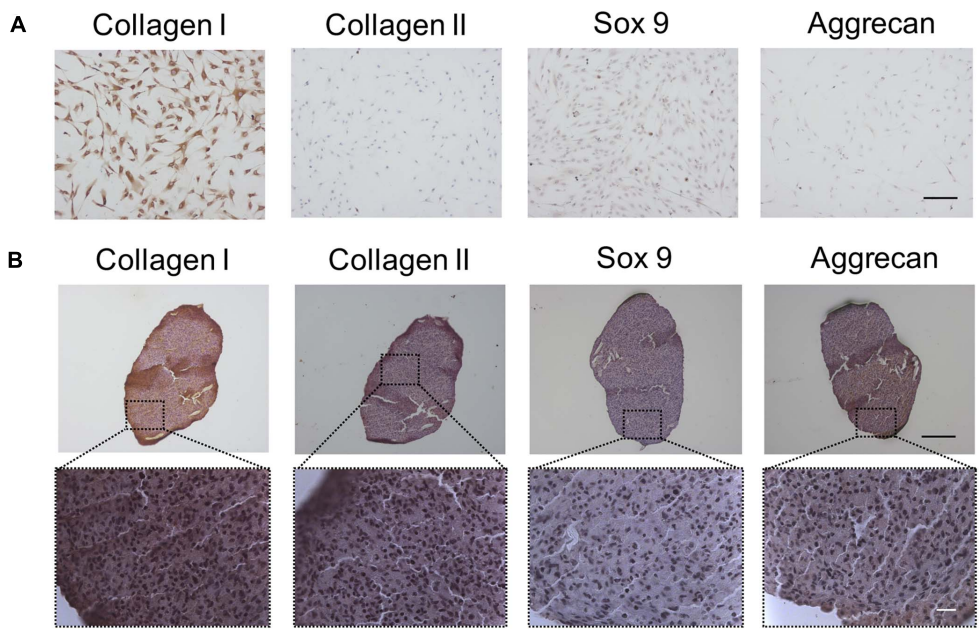

FIGURE 1 | The fibrochondrocytes-related proteins expression of TSPCs by ICC or IHC staining. **(A)** TSPCs were cultured in completed medium in monolayer for 24 h, scale bar 200 μm. **(B)** TSPCs were induced in chondrogenic medium in pellet culture for 21 days, and continous slices were used to detect these proteins expression. Scale bar 100 μm (top) and 20 μm (bottom).

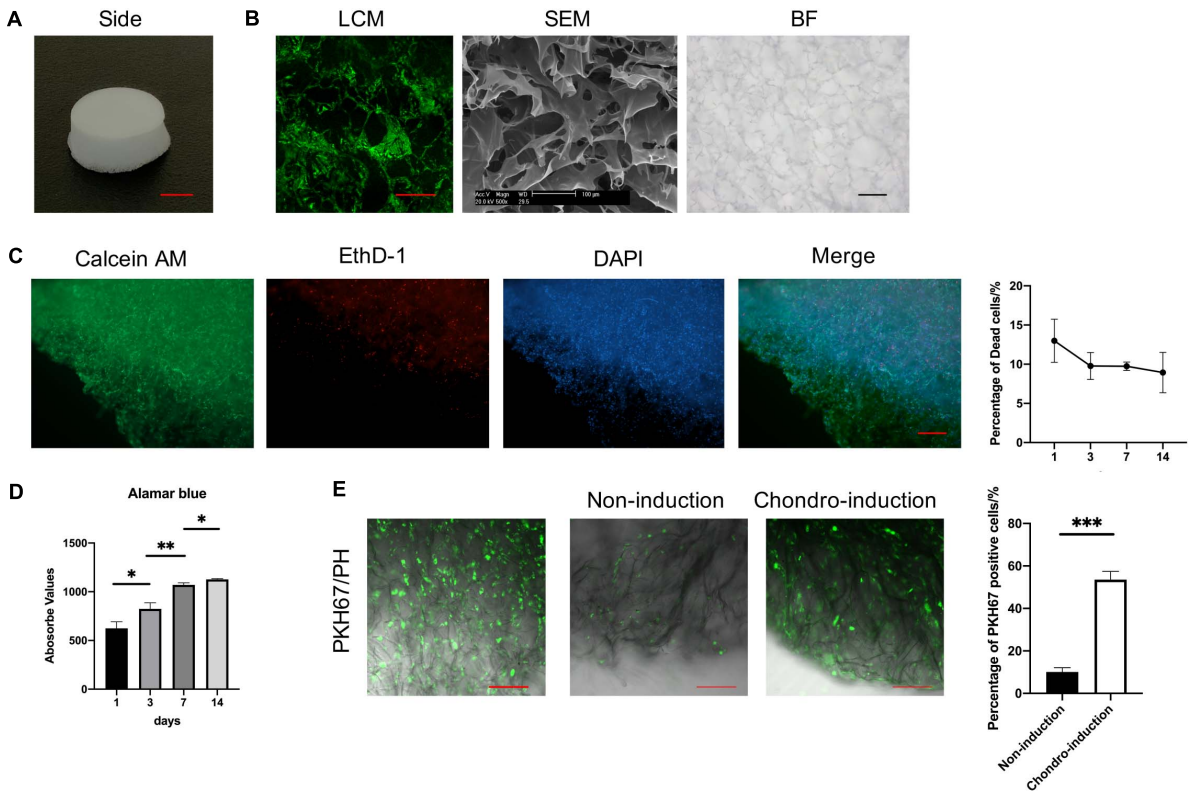

FIGURE 2 | The characterisation of CII-sponges. **(A)** The appearance of CII-sponges, scale bar 0.5 cm. **(B)** The pore structure of CII-sponges scanned by laser confocal (LCM), scanning electricity (SEM), and bright field (BF) Microscopes, scale bar 200 μm (LCM), 100 μm (SEM), and 200 μm (BF). **(C)** The cell viability of TSPCs seeded in CII-sponges was detected by LIVE/DEAD assay, live cells (Green), dead cells (Red), and Nuclei (Blue), scale bar 200 μm. The percentage of dead cells in total cells at day 1, 3, 7, and 14 were analysed by Image ProPlus. **(D)** AlamarBlue detected the proliferation of TSPCs cultured in CII-sponges. **(E)** *In vitro* tracking of TSPCs labelled with PKH67 in CII-sponges. Scale 100 μm. The percentage of PKH67 positive cells with or without chondrogenic induction was qualified by Image ProPlus. * represented as $p \leqq 0.05$, ** represented as $p \leqq 0.01$, and *** represented as $p \leqq 0.001$.

viability of cells enhanced over time (**Figure 2D**). In order to track the differentiation of TSPCs seeded in scaffolds, PKH67 was applied for labelling and tracking TSPCs (**Figure 2E**). Through multi-layer scanning using LCM, CII-sponges, and cells labelled with PKH67 could be observed at the same time through different channels. Cells labelled with PKH67 could produce green fluorescence, and CII-sponges were like as fibres by phase contrast (PH). After 7-day culture, cells adhere to materials could be found by green fluorescence. However, there was a difference in the number of cells with green fluorescence after a further 14-day culture with or without chondrogenic induction. A decrease in fluorescence was found in cells that continue to be cultured in completed medium, while a relatively slow decrease was found in cells under chondrogenic medium. More cells producing fluorescence could be seen in chondrogenic induction group than those in non-induction group.

Chondrogenic Genes Expression of TSPCs in CII-Sponges

To assess the chondrogenic differentiation of TSPCs in CII-sponges *in vitro*, we detected the chondrogenic differentiation-related genes expression of TSPCs after 7- or 14-days culture with or without chondrogenic induction. Cells cultured in monolayer or Matrigel were as control (**Figure 3**).

Results found that when TSPCs were cultured *in vitro* for 7 days with or without chondrogenic induction, CII-sponges could overall induce TSPCs to differentiate toward chondrogenic lineage. To be more specific, CII-sponges showed upregulated chondrocyte-specific genes expression, including Sox 9 and aggrecan, but downregulated Col1α1 significantly in comparation to Matrigel and monolayer culture. There was no significant difference in col2α1 expressions in three groups with or without induction.

When turned to 14 days culture, we could see that the trends of four genes were overall similar with 7 days culture under completed medium. However, different trends were seen when cells were cultured under chondrogenic medium. The trends of Aggrecan and col2α1 in all of three groups remained similar with 7-day induction. However, the expression of Sox 9 and Col1α1 both in CII-sponges and in Matrigel decreased significantly compared with that in monolayer culture.

However, it is worthy to mention that once TSPCs were cultured under chondrogenic medium either for 7 or 14 days, Col1α1 mRNA levels increased in all of three groups compared with those without induction, indicating that chondrogenic medium could not reverse the fibrochondrogenic differentiation

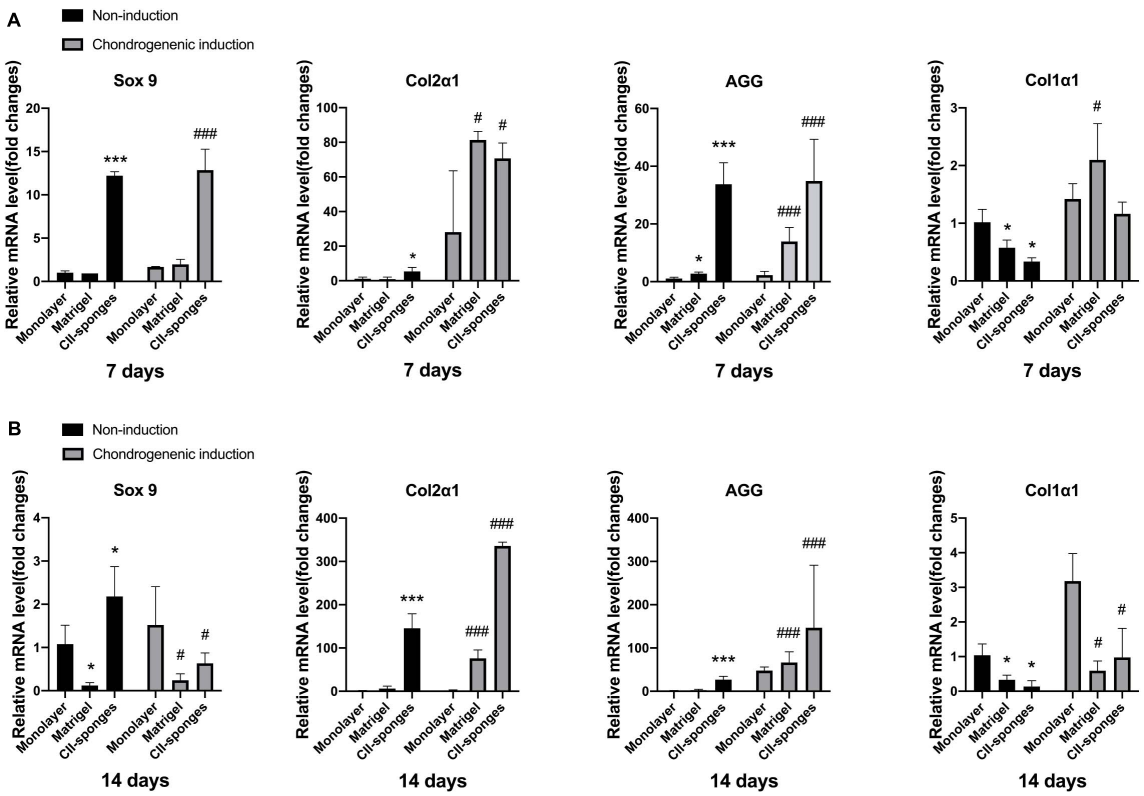

FIGURE 3 | The fibrochondrocytes related genes expression with or without chondrogenic induction. **(A)** The mRNA levels of chondrogenic genes, including Sox 9, Col2α1 and AGG, and fibroblastic gene, Col1α1, in TSPCs seeded in monolayer, Matrigel, or CII-sponges for 7 days with or without chondrogenic induction. **(B)** The mRNA levels of chondrogenic genes, including Sox 9, Col2α1 and AGG, and fibroblastic gene, Col1α1, in TSPCs seeded in monolayer, Matrigel, or CII-sponges for 14 days with or without chondrogenic induction. * or # represented $p \leqq 0.05$, and *** or ### represented $p \leqq 0.001$.

of TSPCs *in vitro*, which is consistent with our previous published data (Qin et al., 2020).

The Chondrogenic Differentiation of TSPCs *in vivo*

To further evaluate the role of CII-sponges in the chondrogenic differentiation of TSPCs *in vivo*, cells were seeded in CII-sponges or Matrigel or in pellet formed by cells in monolayer culture and then induced in chondrogenic medium for 14 days before being transplanted subcutaneously into immunocompromised mice. Safranin O/Fast Green staining was applied to observe cells and proteoglycan expression in formed tissues (**Figure 4A**). After 5 weeks *in vivo*, a lot of cells could be found in all of three groups, while expression of proteoglycan showed huge differences, and the expression of proteoglycan in CII-sponges groups increased significantly in comparison with that in both monolayer and Matrigel groups (**Figure 4B**). Cells in both Matrigel and CII-sponges expressed a good deal of proteoglycan (red), but those cultured in monolayer expressed weakly, mostly around cells. It is worth noting that there was a significant difference in cell morphology in CII-sponges compared with the other two groups in magnified photographs. Cells with CII-sponges showed round or oval shape (black arrows), which were more like fibrochondrocytes or chondrocytes, whereas cells in the other two groups still exhibited shutter or long morphology (red arrows), which were more like fibroblasts.

Immunohistochemical staining was also used to confirm the expression of chondrogenic differentiation related proteins, including collagen I and II, Sox 9, and Aggrecan (**Figure 4C**), and the collagen II, Sox 9 and aggrecan proteins levels in CII-sponges group increased sigificantly in comparison with those in both monolayer and Matrigel groups, while no significant difference in collagen I protein expression in all of three groups (**Figure 4D**). In all of three groups, strongly positive type I collagen staining could be seen. However, only CII-sponges could induce chondrogenic proteins expression of TSPCs *in vivo*, as evidenced by strong positive type II collagen staining as well as positive Sox 9 and aggrecan staining. Although there was only a small amount of expression of Sox 9 and aggrecan staining around cells in CII-sponges under magnified field by microscopy, none could be found in monolayer or Matrigel groups.

Histological Evaluation of the Regeneration of Fibrocartilage Transition Zones at BTJ

To further examined if CII-sponges could promote the regeneration of FCs after surgical re-attachment of tendon and

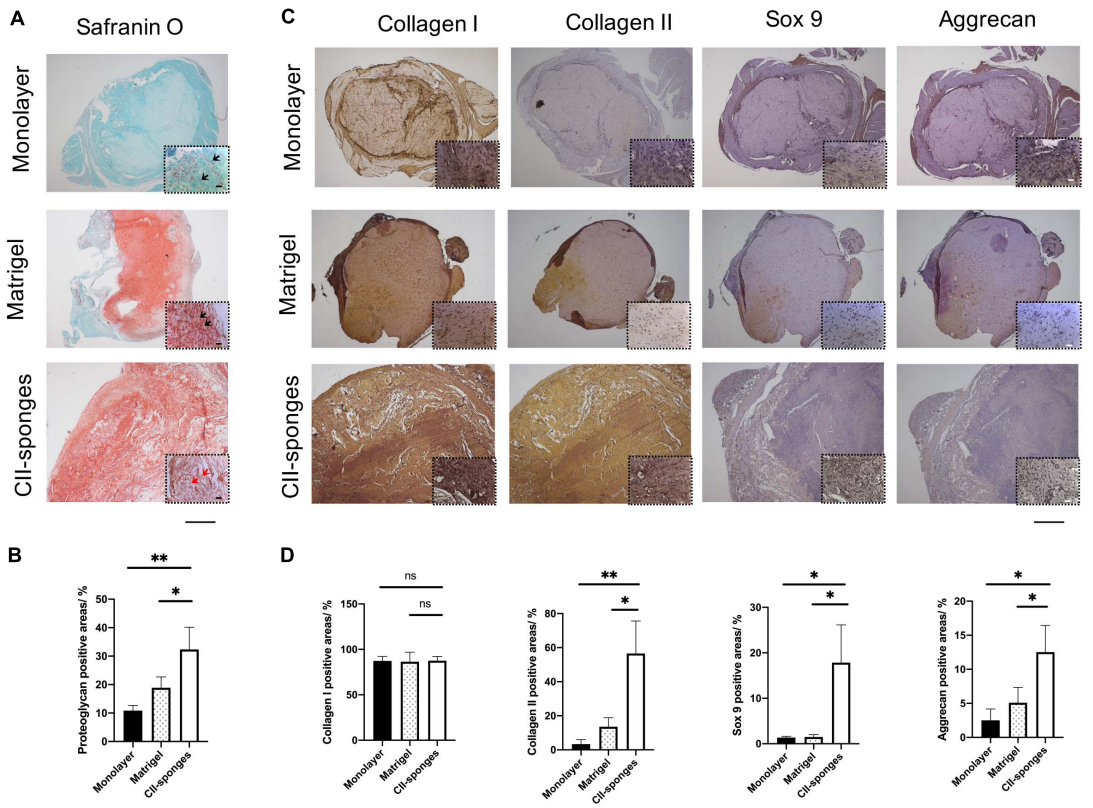

FIGURE 4 | Histological evaluation of the chondrogenic differentiation of TSPCs seeded in Monolayer, Matrigel, or CII-sponges. **(A)** Safranin O/Fast Green staining were applied to observe cells and proteoglycan expression in formed tissues. Scale bar 200 μm and scale bar 20 μm (The magnified photos in dot lines). **(B)** The proteoglycan positive areas were measured by Image ProPlus. ns, represented as no significance; * represented as $P < 0.05$, ** represented as $P < 0.01$, and *** represented as $P < 0.001$. **(C)** Immunohistochemistry staining was also used to confirm the expression of chondrogenic differentiation related proteins, including type I and type II collagen, Sox 9, and aggrecan, in continuous slices. Scale bar 200 μm and scale bar 20 μm (The magnified photos in dot lines). **(D)** The positive areas of these above proteins were quantified by Image ProPlus. ns, represented as no significance; * represented as $p \leqq 0.05$ and ** represented as $p \leqq 0.01$.

bone, histological staining, H&E, and Safranin O, was performed (**Figure 5**). Based on H&E staining and Safranin O/Fast Green staining, obvious tissue integration was found at BTJ after 8 weeks in both groups. In the control group, more indirect insertion-like structures (also called fibrous entheses) formed at the junction as evidenced by the fact that tendon tissues reconnected with bone directly and most of fibroblast-like cells could be found in the surrounding (black arrows) (**Figure 5A**). A small new formed cartilage could be observed at BTJ evidenced by positive proteoglycan staining by Safranin O/Fast Green staining and round or oval chondrocyte-like cells (red arrows and blue arrows) could be seen in this new-formed cartilage (**Figure 5A**). However, in CII-sponges group, fibrocartilaginous entheses formed, characterised by four gradual transition zones, including bone, a large amount of cartilage-like tissues, and tendon, where typical chondrocyte-like cells (black, red, and blue arrows) could be found in these three areas (**Figure 5A**). Cartilage-like tissues expressions were qualified by measuring the areas of positive proteoglycan in Safranin O/Fast green staining using Image ProPlus, which showed the positive area of proteoglycan in CII-sponges group was significantly larger than that in control group, $^{***}p \leqq 0.001$ (**Figure 5B**).

DISCUSSION

New fibrocartilage zone formation is one of the most important indicators of good BTJ reconstruction (Wong et al., 2004; Zhang M. et al., 2019; Zhang Y. et al., 2019; Shi et al., 2020). It is well known that the regeneration of fibrocartilage is a slow and difficult process after tendon reattached to bone. It is reported that the mechanical strength of BTJ repair without FCs formed was only one-tenth of that of native patellar-patellar tendon junction (Lui P. et al., 2010). Although it is believed that cartilage-like tissue formation or the presence of chondrocytes at the BTJ is an intermediate process for the regeneration of FCs (Lui P.P. et al., 2010), it cannot be denied that this process is the most important one for better BTJ healing. Lu et al. (2008) confirmed that the cartilage to tendon was superior to bone to tendon healing, which might be due to the fusion of cartilage to tendon is much easier than that of bone to tendon. It is reasonable to believe that the key to promote the regeneration of FCs is to promote the chondrogenesis of MSCs migrated from bone or tendon and hence to promote the new formation of cartilage-like tissue at the early healing stage. Indeed, Wong et al. (2004, 2009) have already demonstrated that interposition of autologous articular cartilage

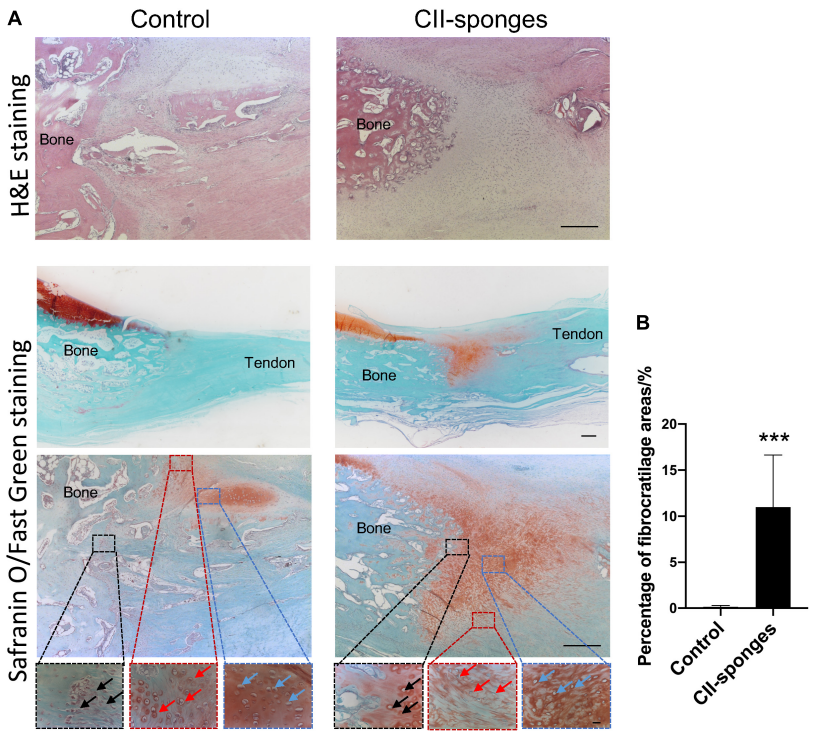

FIGURE 5 | Histological evaluation of the regeneration of fibrocartilage transition zones at BTJ. **(A)** The regeneration of fibrocartilage transition zones at patellar-patellar tendon junction after partial patellectomy was evaluated by histology staining, H&E, Scale bar 200 μm. The whole bone tendon junction, the positive proteoglycan expression areas (red) and the morphology of the cells at the BTJ were observed by Safranin O/Fast Green staining, Scale bar 500 μm (top), Scale bar 200 μm (middle) and Scale bar 20 μm (bottom). In order to observe the morphology of the cells at the fibrocartilage zones, three different regions (Dotted boxes) at BTJ were chosen. To be more specific, in the control group the black box indicated the junction between tendon and bone tissues, fibroblast-like cells could be seen (black arrow), the red box suggested the junction between bone and new formed cartilage, chondrocyte-like cells were found (red arrow), and the blue box represented the new formed cartilage, typical chondrocytes could be observed (blue arrow). In the CII-sponge group, the black box indicated the junction between the bone and new formed cartilage, the red box suggested the junction between the tendon and new formed cartilage, and the blue box represented the new formed cartilage. The chondrocytes could be found in all of these three different areas, and indicated by black, red and blue arrows, respectively. **(B)** Quantification of proteoglycan positive areas in Safranin O staining by Image ProPlus. *** represented as $p \leqq 0.001$.

or allogenic chondrocyte pellet could improve FC regeneration using the partial patellectomy rabbit model. All of these findings suggest that promoting the chondrogenesis of stem cells and hence new cartilage formation at BTJ is not only a key process but also one of the effective means for better reconstruction of BTJ.

We previously found that TSPCs differentiated to fibrochondrocytes under chondrogenic induction, in this study we further examined if CII-sponges we made would guide TSPCs to adopt chondrogenic phenotypes and eventually promote the formation of fibrocartilage tissues. Data showed that CII-sponges with good porosity and good cell compatible were beneficial for chondrogenesis of TSPCs *in vitro* or *in vivo*. Moreover, interposition of CII-sponges at the BTJ improved the fibrocartilage formation in the rabbit PP model.

Pellet culture system is the most classical culture system used to assess the chondrogenic differentiation of stem cells. Although most of studies on tendon stem cells have confirmed that tendon stem cells had the chondrogenic potential in pellet culture system, but these reports generally only detect the expression of proteoglycan by safranin O staining or alcian blue staining (Bi et al., 2007; Rui et al., 2010; Zhang and Wang, 2010). There was only a little amount of expression around cells in most studies, and no further observation into cartilage differentiation indicators, such as collagen I/II, aggrecan and other chondrocyte-related proteins was conducted. In our previous study, we found that tendon stem cells in a monolayer culture differentiated to fibrocartilage cells rather than chondrocytes by detecting expression of collagen I and II, Sox 9, and tenascin C. Similar results were found in this study when TSPCs were cultured in the 3-D environment. Even though the mRNA level of Col1α1 was downregulated when TSPCs were seeded in Matrigel or CII-sponges, strong expression of collagen I could be found, as evidenced by IHC staining.

Collagen scaffolds are usually manufactured for surgical and dental purposes or cell culture matrices. The porous collagen sponges provide a highly biocompatible environment for cells due to their high porosity and interconnected pores. Porosity and pore sizes have been demonstrated to regulate cellular behaviours (Loh and Choong, 2013; Zhang et al.,

2014), like adhesion and ingrowth. This high biocompatibility makes collagen sponges perfect implantable medical products and scaffolds for *in vitro* testing systems. In our study, the porosity of CII-sponges we made was over 99% porous, and interconnected, round, or elongated pores could be seen (Qin et al., 2010). Good porosity and the interconnected pores are important in diffusing nutrients and gases as well as removing metabolic waste. Pore size of scaffolds can also influence cellular attachment, morphology, and differentiation (Matsiko et al., 2015). For chondrocytes, pores of 50–300 μm are usually recognised as the suitable sizes for stimulating stem cell chondrogenesis and cartilage regeneration (Nehrer et al., 1997; Zhang et al., 2014). Pore size of CII-sponges we made was approximately 92.17 ± 29.55 μm (Qin et al., 2010). CII-sponges could also facilitate the adhesion of TSPCs, evidenced by a large proportion of live cells and a few dead cells found after 14-day culture. AlamarBlue confirmed that cells adhered to CII-sponges also remained a stable viability over time. PKH67 *in vitro* tracking data showed that under chondrogenic induction, more cells expressed green fluorescence compared with those without induction.

Many studies believed that the differentiation lineage of stem cells could be directed by the composition of the extracellular matrix (Badylak, 2005; Evans et al., 2010). For example, Bosnakovski et al. (2006) have found that type II collagen hydrogels significantly induced chondrogenic differentiation of bone marrow mesenchymal stem cells compared to type I collagen hydrogels or alginate gels. Buma et al. (2003) compared the role of type I and type II collagen matrices for the repair of full-thickness articular cartilage defects and found that type I collagen were superior to guide progenitor cells from a subchondral origin into the defect areas whereas type II collagen matrices were better in directing stem cells into a chondrocyte phenotype. In our study, we found that CII-sponges have the capability of promoting the differentiation of TSPCs down the chondrogenic lineage as evidenced by gene expression *in vitro*. Chondrocyte-related genes, including Sox 9, the early marker of chondrogenesis, as well as col2α1 and aggrecan, the late markers, were all upregulated by CII-sponges with or without chondrogenic induction at both time points. However, Matrigel did not show similar effects, with only col2α1 and aggrecan upregulated after 14-day chondrogenic induction. Meanwhile, compared with monolayer groups, the expression of fibroblastic marker, col1a1, decreased overall in both Matrigel groups and CII-sponges groups, with only slightly increased in Matrigel groups after 7-day chondrogenic induction. This might confirm the hypothesis that stem cell differentiation could be driven by the matrices specific to a particular tissue.

Type II collagen predominantly composed of articular cartilage, thus a scaffold made with type II collagen might be suitable for cartilage-tissues formation by directing MSCs differentiation toward chondrocytes. Chen et al. (2011) observed the role of type II collagen sponge materials on promoting cartilage repair using MRI combined with histology. Funayama et al. (2008) indicated that type II collagen gel was suitable for injection into cartilage defects and offered a useful scaffold during chondrocyte transplantation.

Immunohistology observations from *in vivo* data revealed that CII-sponges promoted the proteoglycans deposit as well as the expression of chondrogenic specific markers, including Sox 9, aggrecan, and type II collagen, whereas Matrigel only induced a little of these three markers expression, despite of a large amount of proteoglycans deposit similar as CII-sponges.

Noticeably, compared with non-induction groups, the mRNA and protein levels of fibroblastic marker, type I collagen, increased in all of three groups after chondrogenic induction. This is consistent with our previous results which found TSPCs differentiate to fibrochondrocytes rather than chondrocytes. Type I collagen is one of the most important protein to distinguish these two cells. Although CII-sponges and Matrigel downregulated the mRNA level of col1a1 with or without induction, IHC staining showed that type I collagen protein deposits could be found in both scaffolds. This might indicate that TSPCs differentiate toward fibrocartilage cells under chondrogenic induction when they were cultured in two-dimensional monolayer culture system or in three-dimensional scaffolds.

Cartilage-like tissues could be found during healing at BTJ injured model in CII-sponges group. Although, it is reported that endochondral ossification occur subsequently and these cartilaginous tissues disappear eventually during healing (Lui P.P. et al., 2010). The presence of chondrocytes at the BTJ was commonly associated with better healing. In our study, CII-sponges facilitated the formation of cartilage-like tissues with obvious four transition zones and abundant of proteoglycan expression. This continuous change in tissue composition from tendon to bone is presumed to aid in the efficient transfer of load between the two materials. However, no obvious fibres inserted to bone were found in CII-sponges group. The reason for this may be the time point we chose, and collagen fibres occurred in a relatively late time point, like at 18 or 24 weeks, and then sharpey's fibres formed.

In conclusion, we found that CII-sponges we made facilitated TSPCs to adopt more chondrocyte phenotype *in vitro* and *in vivo* and meanwhile promoted the regeneration of fibrocartilage-like tissues in the BTJ injured model. This CII-sponges might well be suitable for the reconstruction of FC at BTJ.

DATA AVAILABILITY STATEMENT

The original contributions presented in the study are included in the article/supplementary material, further inquiries can be directed to the corresponding author/s.

ETHICS STATEMENT

The animal study was reviewed and approved by Guangzhou Red Cross Hospital Ethics Committee.

AUTHOR CONTRIBUTIONS

SQ and JX drafted the manuscript. SQ, WW, PH, WM, LC, JZ, XX, ZL, PW, QM, and FD performed the experiments. SQ analysed the data. AL, HC, and XH contributed the experiment instruments and analysis tools. SQ and JX conceived and designed the experiments. All authors contributed to the article and approved the submitted version.

FUNDING

This work was supported by grants from the National Natural Science Foundation of China (Nos. 30973067 and 81228013), Guangzhou Science and Technology Program Key Project (No. 201704020145), Guangzhou Municipal Science and Technology Project (No. 202002030049), and Guangzhou General Guidance Project (No. 20181A010020).

REFERENCES

Badylak, S. F. (2005). Regenerative medicine and developmental biology: the role of the extracellular matrix. *Anat. Rec. B New Anat.* 287, 36–41. doi: 10.1002/ar.b.20081

Bi, Y., Ehirchiou, D., Kilts, T. M., Inkson, C. A., Embree, M. C., Sonoyama, W., et al. (2007). Identification of tendon stem/progenitor cells and the role of the extracellular matrix in their niche. *Nat. Med.* 13, 1219–1227. doi: 10.1038/nm1630

Bosnakovski, D., Mizuno, M., Kim, G., Takagi, S., Okumura, M., and Fujinaga, T. (2006). Chondrogenic differentiation of bovine bone marrow mesenchymal stem cells (MSCs) in different hydrogels: influence of collagen type II extracellular matrix on MSC chondrogenesis. *Biotechnol. Bioeng.* 93, 1152–1163. doi: 10.1002/bit.20828

Buma, P., Pieper, J. S., van Tienen, T., Van Susante, J. L., van der Kraan, P. M., Veerkamp, J. H., et al. (2003). Cross-linked type I and type II collagenous matrices for the repair of full-thickness articular cartilage defects–a study in rabbits. *Biomaterials* 24, 3255–3263. doi: 10.1016/s0142-9612(03)00143-1

Chen, H., Yang, X., Liao, Y., Zeng, X., Liang, P., Kang, N., et al. (2011). MRI and histologic analysis of collagen type II sponge on repairing the cartilage defects of rabbit knee joints. *J. Biomed. Mater. Res. B Appl. Biomater.* 96, 267–275. doi: 10.1002/jbm.b.31762

Evans, N. D., Gentleman, E., Chen, X., Roberts, C. J., Polak, J. M., and Stevens, M. M. (2010). Extracellular matrix-mediated osteogenic differentiation of murine embryonic stem cells. *Biomaterials* 31, 3244–3252. doi: 10.1016/j.biomaterials.2010.01.039

Funayama, A., Niki, Y., Matsumoto, H., Maeno, S., Yatabe, T., Morioka, H., et al. (2008). Repair of full-thickness articular cartilage defects using injectable type II collagen gel embedded with cultured chondrocytes in a rabbit model. *J. Orthop. Sci.* 13, 225–232. doi: 10.1007/s00776-008-1220-z

Grassman, S. R., Mcdonald, D. B., Thornton, G. M., Shrive, N. G., and Frank, C. B. (2002). Early healing processes of free tendon grafts within bone tunnels is bone-specific: a morphological study in a rabbit model. *Knee* 9, 21–26. doi: 10.1016/s0968-0160(01)00128-4

Hu, J., Zhang, T., Xu, D., Qu, J., Qin, L., Zhou, J., et al. (2015). Combined magnetic fields accelerate bone-tendon junction injury healing through osteogenesis. *Scand. J. Med. Sci. Sports* 25, 398–405. doi: 10.1111/sms.12251

Leung, K. S., Chong, W. S., Chow, D. H., Zhang, P., Cheung, W. H., Wong, M. W., et al. (2015). A comparative study on the biomechanical and histological properties of bone-to-bone, bone-to-tendon, and tendon-to-tendon healing: an achilles tendon-calcaneus model in goats. *Am. J. Sports Med.* 43, 1413–1421. doi: 10.1177/0363546515576904

Lim, J. K., Hui, J., Li, L., Thambyah, A., Goh, J., and Lee, E. H. (2004). Enhancement of tendon graft osteointegration using mesenchymal stem cells in a rabbit model of anterior cruciate ligament reconstruction. *Arthroscopy* 20, 899–910. doi: 10.1016/s0749-8063(04)00653-x

Loh, Q. L., and Choong, C. (2013). Three-dimensional scaffolds for tissue engineering applications: role of porosity and pore size. *Tissue Eng. Part B Rev.* 19, 485–502. doi: 10.1089/ten.teb.2012.0437

Lu, H., Liu, F., Chen, H., Chen, C., Qu, J., Xu, D., et al. (2016). The effect of low-intensity pulsed ultrasound on bone-tendon junction healing: initiating after inflammation stage. *J. Orthop. Res.* 34, 1697–1706. doi: 10.1002/jor.23180

Lu, H., Qin, L., Lee, K., Wong, W., Chan, K., and Leung, K. (2008). Healing compared between bone to tendon and cartilage to tendon in a partial inferior patellectomy model in rabbits. *Clin. J. Sport Med.* 18, 62–69. doi: 10.1097/jsm.0b013e31815c24ba

Lu, H., Zheng, C., Wang, Z., Chen, C., Chen, H., and Hu, J. (2015). Effects of low-intensity pulsed ultrasound on new trabecular bone during bone-tendon junction healing in a rabbit model: a synchrotron radiation micro-CT study. *PLoS One* 10:e0124724. doi: 10.1371/journal.pone.0124724

Lui, P., Zhang, P., Chan, K., and Qin, L. (2010). Biology and augmentation of tendon-bone insertion repair. *J. Orthop. Surg. Res.* 5:59. doi: 10.1186/1749-799x-5-59

Lui, P. P., Ho, G., Shum, W. T., Lee, Y. W., Ho, P. Y., Lo, W. N., et al. (2010). Inferior tendon graft to bone tunnel healing at the tibia compared to that at the femur after anterior cruciate ligament reconstruction. *J. Orthop. Sci.* 15, 389–401. doi: 10.1007/s00776-010-1460-6

Matsiko, A., Gleeson, J. P., and O'brien, F. J. (2015). Scaffold mean pore size influences mesenchymal stem cell chondrogenic differentiation and matrix deposition. *Tissue Eng. Part A* 21, 486–497. doi: 10.1089/ten.tea.2013.0545

Nehrer, S., Breinan, H. A., Ramappa, A., Young, G., Shortkroff, S., Louie, L. K., et al. (1997). Matrix collagen type and pore size influence behaviour of seeded canine chondrocytes. *Biomaterials* 18, 769–776. doi: 10.1016/s0142-9612(97)00001-x

Park, S. H., Choi, Y. J., Moon, S. W., Lee, B. H., Shim, J. H., Cho, D. W., et al. (2018). Three-dimensional bio-printed scaffold sleeves with mesenchymal stem cells for enhancement of tendon-to-bone healing in anterior cruciate ligament reconstruction using soft-tissue tendon graft. *Arthroscopy* 34, 166–179. doi: 10.1016/j.arthro.2017.04.016

Qin, S., Chen, H., Yang, X., Kang, N., Tan, J., Liang, P., et al. (2010). Characteristics of EDC/NHS-crosslinked collagen type II matrix. *Orthop. J. China* 18, 1014–1018.

Qin, S., Wang, W., Liu, Z., Hua, X., Fu, S., Dong, F., et al. (2020). Fibrochondrogenic differentiation potential of tendon-derived stem/progenitor cells from human patellar tendon. *J. Orthop. Transl.* 22, 101–108. doi: 10.1016/j.jot.2019.08.006

Rui, Y. F., Lui, P. P., Li, G., Fu, S. C., Lee, Y. W., and Chan, K. M. (2010). Isolation and characterization of multipotent rat tendon-derived stem cells. *Tissue Eng. Part A* 16, 1549–1558. doi: 10.1089/ten.tea.2009.0529

Shi, Y., Kang, X., Wang, Y., Bian, X., He, G., Zhou, M., et al. (2020). Exosomes derived from bone marrow stromal cells (BMSCs) enhance tendon-bone healing by regulating macrophage polarization. *Med. Sci. Monit.* 26:e923328.

Song, F., Jiang, D., Wang, T., Wang, Y., Chen, F., Xu, G., et al. (2017). Mechanical loading improves tendon-bone healing in a rabbit anterior cruciate ligament reconstruction model by promoting proliferation and matrix formation of mesenchymal stem cells and tendon cells. *Cell. Physiol. Biochem.* 41, 875–889. doi: 10.1159/000460005

Wang, L., Gao, W., Xiong, K., Hu, K., Liu, X., and He, H. (2014). VEGF and BFGF expression and histological characteristics of the bone-tendon junction during acute injury healing. *J. Sports Sci. Med.* 13, 15–21.

Wang, L., Qin, L., Cheung, W. H., Lu, H. B., Yang, X. H., Leung, K. S., et al. (2010). A delayed bone-tendon junction healing model established for potential treatment of related sports injuries. *Br. J. Sports Med.* 44, 114–120. doi: 10.1136/bjsm.2008.048041

Wang, W., Chen, H. H., Yang, X. H., Xu, G., Chan, K. M., and Qin, L. (2007). Postoperative programmed muscle tension augmented osteotendinous junction repair. *Int. J. Sports Med.* 28, 691–696. doi: 10.1055/s-2007-964864

Wong, M. W., Qin, L., Lee, K. M., and Leung, K. S. (2009). Articular cartilage increases transition zone regeneration in bone-tendon junction healing. *Clin. Orthop. Relat. Res.* 467, 1092–1100. doi: 10.1007/s11999-008-0606-8

Wong, M. W., Qin, L., Tai, J. K., Lee, S. K., Leung, K. S., and Chan, K. M. (2004). Engineered allogeneic chondrocyte pellet for reconstruction of fibrocartilage zone at bone-tendon junction–a preliminary histological observation. *J. Biomed. Mater. Res. B Appl. Biomater.* 70, 362–367. doi: 10.1002/jbm.b.30049

Yamakado, K., Kitaoka, K., Yamada, H., Hashiba, K., Nakamura, R., and Tomita, K. (2002). The influence of mechanical stress on graft healing in a bone tunnel. *Arthroscopy* 18, 82–90. doi: 10.1053/jars.2002.25966

Yates, K. E., Allemann, F., and Glowacki, J. (2005). Phenotypic analysis of bovine chondrocytes cultured in 3D collagen sponges: effect of serum substitutes. *Cell Tissue Bank.* 6, 45–54. doi: 10.1007/s10561-005-5810-0

Zhang, J., and Wang, J. H. (2010). Characterization of differential properties of rabbit tendon stem cells and tenocytes. *BMC Musculoskelet. Disord.* 11:10. doi: 10.1186/1471-2474-11-10

Zhang, M., Zhen, J., Zhang, X., Yang, Z., Zhang, L., Hao, D., et al. (2019). Effect of autologous platelet-rich plasma and gelatin sponge for tendon-to-bone healing after rabbit anterior cruciate ligament reconstruction. *Arthroscopy* 35, 1486–1497. doi: 10.1016/j.arthro.2018.11.014

Zhang, Q., Lu, H., Kawazoe, N., and Chen, G. (2014). Pore size effect of collagen scaffolds on cartilage regeneration. *Acta Biomater.* 10, 2005–2013. doi: 10.1016/j.actbio.2013.12.042

Zhang, Y., Yu, J., Zhang, J., and Hua, Y. (2019). Simvastatin With PRP promotes chondrogenesis of bone marrow stem cells in vitro and wounded rat achilles tendon-bone interface healing in vivo. *Am. J. Sports Med.* 47, 729–739. doi: 10.1177/0363546518819108

Conflict of Interest: The authors declare that the research was conducted in the absence of any commercial or financial relationships that could be construed as a potential conflict of interest.

Advantages of publishing in Frontiers

OPEN ACCESS
Articles are free to read for greatest visibility and readership

FAST PUBLICATION
Around 90 days from submission to decision

HIGH QUALITY PEER-REVIEW
Rigorous, collaborative, and constructive peer-review

TRANSPARENT PEER-REVIEW
Editors and reviewers acknowledged by name on published articles

Frontiers
Avenue du Tribunal-Fédéral 34
1005 Lausanne | Switzerland

Visit us: www.frontiersin.org
Contact us: frontiersin.org/about/contact

REPRODUCIBILITY OF RESEARCH
Support open data and methods to enhance research reproducibility

DIGITAL PUBLISHING
Articles designed for optimal readership across devices

FOLLOW US
@frontiersin

IMPACT METRICS
Advanced article metrics track visibility across digital media

EXTENSIVE PROMOTION
Marketing and promotion of impactful research

LOOP RESEARCH NETWORK
Our network increases your article's readership